Abstract and Applied Analysis

Advances in Nonlinear Complexity Analysis for Partial Differential Equations

Guest Editors: Zhengde Dai, Qianshun S. Chang, Lan Xu, Syed Tauseef Mohyud-Din, Hafez Tari, and Peicheng Zhu

Advances in Nonlinear Complexity Analysis for Partial Differential Equations

Abstract and Applied Analysis

Advances in Nonlinear Complexity Analysis for Partial Differential Equations

Guest Editors: Zhengde Dai, Qianshun S. Chang, Lan Xu, Syed Tauseef Mohyud-Din, Hafez Tari, and Peicheng Zhu

Editorial Board

Contents

Advances in Nonlinear Complexity Analysis for Partial Differential Equations, Zhengde Dai, Qianshun S. Chang, Lan Xu, Syed Tauseef Mohyud-Din, Hafez Tari, and Peicheng Zhu
Volume 2013, Article ID 585716, 1 page

Stability for the Kirchhoff Plates Equations with Viscoelastic Boundary Conditions in Noncylindrical Domains, Jum-Ran Kang
Volume 2013, Article ID 420803, 12 pages

Combined Exp-Function Ansatz Method and Applications, Gui Mu, Jun Liu, Zhengde Dai, and Xi Liu
Volume 2013, Article ID 234319, 3 pages

A Local Fractional Variational Iteration Method for Laplace Equation within Local Fractional Operators, Yong-Ju Yang, Dumitru Baleanu, and Xiao-Jun Yang
Volume 2013, Article ID 202650, 6 pages

Pullback Attractors for Nonautonomous 2D-Navier-Stokes Models with Variable Delays, Xiaoli Liu and Yejuan Wang
Volume 2013, Article ID 425031, 10 pages

Continuum Modeling and Control of Large Nonuniform Wireless Networks via Nonlinear Partial Differential Equations, Yang Zhang, Edwin K. P. Chong, Jan Hannig, and Donald Estep
Volume 2013, Article ID 262581, 16 pages

Shock in the Yarn during Unwinding from Packages, Stanislav Praček, Klemen Možina, and Franci Sluga
Volume 2013, Article ID 972941, 6 pages

Exponential Attractor for Coupled Ginzburg-Landau Equations Describing Bose-Einstein Condensates and Nonlinear Optical Waveguides and Cavities, Gui Mu and Jun Liu
Volume 2013, Article ID 390476, 8 pages

Allee-Effect-Induced Instability in a Reaction-Diffusion Predator-Prey Model, Weiming Wang, Yongli Cai, Yanuo Zhu, and Zhengguang Guo
Volume 2013, Article ID 487810, 10 pages

Various Heteroclinic Solutions for the Coupled Schrödinger-Boussinesq Equation, Murong Jiang and Zhengde Dai
Volume 2013, Article ID 158140, 5 pages

Variational Iteration Method for the Magnetohydrodynamic Flow over a Nonlinear Stretching Sheet, Lan Xu and Eric W. M. Lee
Volume 2013, Article ID 573782, 5 pages

Adaptive Wavelet Precise Integration Method for Nonlinear Black-Scholes Model Based on Variational Iteration Method, Huahong Yan
Volume 2013, Article ID 735919, 6 pages

A Lotka-Volterra Competition Model with Cross-Diffusion, Wenyan Chen and Ya Chen
Volume 2013, Article ID 624352, 5 pages

Analysis of Stability of Traveling Wave for Kadomtsev-Petviashvili Equation, Jun Liu, Xi Liu, Gui Mu, Chunyan Zhu, and Jie Fu
Volume 2013, Article ID 230871, 3 pages

The Multisoliton Solutions for the $(2 + 1)$**-Dimensional Sawada-Kotera Equation**, Zhenhui Xu, Hanlin Chen, and Wei Chen
Volume 2013, Article ID 767254, 5 pages

Symmetry Reduced and New Exact Nontraveling Wave Solutions of (2+1)-Dimensional Potential Boiti-Leon-Manna-Pempinelli Equation, Chen Han-Lin and Xian Da-Quan
Volume 2013, Article ID 784134, 5 pages

Construction of Target Controllable Image Segmentation Model Based on Homotopy Perturbation Technology, Shu-Li Mei
Volume 2013, Article ID 131207, 8 pages

A Novel Method for Solving KdV Equation Based on Reproducing Kernel Hilbert Space Method, Mustafa Inc, Ali Akgül, and Adem Kiliçman
Volume 2013, Article ID 578942, 11 pages

Saddle-Node Heteroclinic Orbit and Exact Nontraveling Wave Solutions for (2+1)D KdV-Burgers Equation, Da-Quan Xian
Volume 2013, Article ID 696074, 7 pages

Homotopy Perturbation Method for Fractional Gas Dynamics Equation Using Sumudu Transform, Jagdev Singh, Devendra Kumar, and A. Kılıçman
Volume 2013, Article ID 934060, 8 pages

Complex Dynamics of a Diffusive Holling-Tanner Predator-Prey Model with the Allee Effect, Zongmin Yue, Xiaoqin Wang, and Haifeng Liu
Volume 2013, Article ID 270191, 12 pages

Nonlinear Response of Strong Nonlinear System Arisen in Polymer Cushion, Jun Wang, Li-xin Lu, Huan-xin Jiang, and Yong Zhu
Volume 2013, Article ID 891914, 3 pages

Exact Solutions of ϕ^4 **Equation Using Lie Symmetry Approach along with the Simplest Equation and Exp-Function Methods**, Hossein Jafari, Nematollah Kadkhoda, and Chaudry Masood Khalique
Volume 2012, Article ID 350287, 7 pages

Local Fractional Fourier Series with Application to Wave Equation in Fractal Vibrating String, Ming-Sheng Hu, Ravi P. Agarwal, and Xiao-Jun Yang
Volume 2012, Article ID 567401, 15 pages

Soliton Solutions for the Wick-Type Stochastic KP Equation, Y. F. Guo, L. M. Ling, and D. L. Li
Volume 2012, Article ID 327682, 9 pages

Comment on "Variational Iteration Method for Fractional Calculus Using He's Polynomials", Ji-Huan He
Volume 2012, Article ID 964974, 2 pages

Analysis of the Nonlinear Structural-Acoustic Resonant Frequencies of a Rectangular Tube with a Flexible End Using Harmonic Balance and Homotopy Perturbation Methods, Y. Y. Lee
Volume 2012, Article ID 391584, 13 pages

Exact Travelling Wave Solutions for Isothermal Magnetostatic Atmospheres by Fan Subequation Method, Hossein Jafari, Maryam Ghorbani, and Chaudry Masood Khalique
Volume 2012, Article ID 962789, 11 pages

Hindawi Publishing Corporation
Abstract and Applied Analysis
Volume 2013, Article ID 585716, 1 page
http://dx.doi.org/10.1155/2013/585716

Editorial

Advances in Nonlinear Complexity Analysis for Partial Differential Equations

Zhengde Dai,[1] Qianshun S. Chang,[2] Lan Xu,[3] Syed Tauseef Mohyud-Din,[4] Hafez Tari,[5] and Peicheng Zhu[6]

[1] *School of Mathematics and Statistics, Yunnan University, Kunming 650091, China*
[2] *Institute of Applied Mathematics and System Sciences, Academy of Sciences of China, Beijing 100080, China*
[3] *National Engineering Laboratory for Modern Silk, Soochow University, Suzhou 215123, China*
[4] *Department of Mathematics, HITEC University, Taxila Cantt, Pakistan*
[5] *Department of Mechanical Engineering, Ohio State University, Columbus, OH 43210, USA*
[6] *Department of Mathematics, University of the Basque Country (UPV/EHU) and IKERBASQUE, Basque Foundation for Science, 48011 Bilbao, Spain*

Correspondence should be addressed to Zhengde Dai; zhddai2004@yahoo.com.cn

Received 19 August 2013; Accepted 19 August 2013

Nonlinear Partial Differential Equations (NPDE) including integrable, nearintegrable, and nonintegrable systems arise from a number of physical, chemical, biological, and life sciences. The complexity analysis of solutions for NPDE is a very important subject in nonlinear science all the time. In recent years, this research field has taken many new advances. The purpose of this special issue is to highlight some recent researches carried out on the asymptotical behavior analysis of solution with initial boundary value problem, spatiotemporal feature analysis, variety analysis of dynamics, stochastic behavior analysis, numerical simulation and analysis, and so forth.

We have received 81 submissions to the special issue which were rigorously reviewed by up to 8 reviewers as well as by at least one of the guest editors; all the manuscripts had 2 reviewers. As a result, 27 manuscripts are accepted. In these articles, the most new results in the research field of nonlinear complexity of solutions are obtained. We hope that this special issue can lead to both theoretical insight and practical applications in nonlinear complexity analysis for NPDE.

Acknowledgments

We would like to thank the authors of all the contributions, the reviewers for their useful and timely comments on the papers submitted to this issue.

Zhengde Dai
Qianshun S. Chang
Lan Xu
Syed Tauseef Mohyud-Din
Hafez Tari
Peicheng Zhu

Hindawi Publishing Corporation
Abstract and Applied Analysis
Volume 2013, Article ID 420803, 12 pages
http://dx.doi.org/10.1155/2013/420803

Research Article

Stability for the Kirchhoff Plates Equations with Viscoelastic Boundary Conditions in Noncylindrical Domains

Jum-Ran Kang

Department of Mathematics, Dong-A University, Saha-Ku, Busan 604-714, Republic of Korea

Correspondence should be addressed to Jum-Ran Kang; pointegg@hanmail.net

Received 18 September 2012; Accepted 15 May 2013

Academic Editor: Zhengde Dai

We study Kirchhoff plates equations with viscoelastic boundary conditions in a noncylindrical domain. This work is devoted to proving the global existence, uniqueness of solutions, and decay of the energy of solutions for Kirchhoff plates equations in a noncylindrical domain.

1. Introduction

Let Ω be an open bounded domain of $\mathbb{R}^2$ containing the origin and having C^2 boundary. Let $\gamma : [0,\infty[\to \mathbb{R}$ be a continuously differentiable function. Consider the family of subdomains $\{\Omega_t\}_{0\le t<\infty}$ of $\mathbb{R}^2$ given by

$$\Omega_t = T(\Omega), \quad T: y \in \Omega \longrightarrow x = \gamma(t)\, y, \tag{1}$$

whose boundaries are denoted by Γ_t, and let $\widehat{Q}$ be the noncylindrical domain of $\mathbb{R}^3$ given by

$$\widehat{Q} = \bigcup_{0\le t<\infty} \Omega_t \times \{t\} \tag{2}$$

with boundary

$$\widehat{\Sigma} = \bigcup_{0\le t<\infty} \Gamma_t \times \{t\}. \tag{3}$$

In this paper, we consider the following Kirchhoff plates equations with viscoelastic boundary conditions:

$$u'' + \Delta^2 u = 0 \quad \text{in } \Omega_t \times (0,\infty), \tag{4}$$

$$u = \frac{\partial u}{\partial \nu} = 0 \quad \text{on } \Gamma_{0,t} \times (0,\infty), \tag{5}$$

$$-u + \int_0^t g_1(t-s)\, \mathscr{B}_2 u(s)\, ds = 0 \quad \text{on } \Gamma_{1,t} \times (0,\infty), \tag{6}$$

$$\frac{\partial u}{\partial \nu} + \int_0^t g_2(t-s)\, \mathscr{B}_1 u(s)\, ds = 0 \quad \text{on } \Gamma_{1,t} \times (0,\infty), \tag{7}$$

$$u(0,x) = u_0(x), \quad u'(0,x) = u_1(x) \quad \text{in } \Omega_0, \tag{8}$$

where $\nu = (\nu_1, \nu_2)$ is the unit normal at $(\sigma, t) \in \widehat{\Sigma}$ directed towards the exterior of $\widehat{Q}$. We divide the boundary into two parts:

$$\Gamma_t = \Gamma_{0,t} \cup \Gamma_{1,t} \quad \text{with } \overline{\Gamma}_{0,t} \cap \overline{\Gamma}_{1,t} = \emptyset,\ \Gamma_{0,t} \neq \emptyset. \tag{9}$$

We are denoting by $\mathscr{B}_1$ and $\mathscr{B}_2$ the following differential operators:

$$\mathscr{B}_1 u = \Delta u + (1-\mu) B_1 u, \qquad \mathscr{B}_2 u = \frac{\partial \Delta u}{\partial \nu} + (1-\mu)\frac{\partial B_2 u}{\partial \eta}, \tag{10}$$

where B_1 and B_2 are given by

$$\begin{aligned} B_1 u &= 2\nu_1\nu_2 u_{x_1x_2} - \nu_1^2 u_{x_2x_2} - \nu_2^2 u_{x_1x_1}, \\ B_2 u &= \left(\nu_1^2 - \nu_2^2\right) u_{x_1x_2} + \nu_1\nu_2 \left(u_{x_2x_2} - u_{x_1x_1}\right), \end{aligned} \tag{11}$$

and the constant μ, $0 < \mu < 1/2$, represents Poisson's ratio. From the physics point of view, system (4) describes the small transversal vibrations of a thin plate with a moving boundary device. The integral equations (6) and (7) describe the memory effects which can be caused, for example, by the interaction with another viscoelastic element. The relaxation functions $g_1, g_2 \in C^1(0,\infty)$ are positive and nondecreasing.

The uniform stabilization of plates equations with linear or nonlinear boundary feedback in cylindrical domain was investigated by several authors; see for example [1–3] among others. The uniform decay for viscoelastic plates with memory was studied by [4, 5] and the references therein. Santos et al. [6] studied the asymptotic behavior of the solutions of a nonlinear wave equation of Kirchhoff type with boundary condition of memory type. Santos and Junior [7] investigated the stability of solutions for Kirchhoff plate equations with boundary memory condition. Park and Kang [8] studied the exponential decay for the Kirchhoff plate equations with nonlinear dissipation and boundary memory condition. They proved that the energy decays uniformly exponentially or algebraically with the same rate of decay as the relaxation functions. But the existence of solutions and decay of energy for the Kirchhoff plate equations with viscoelastic boundary conditions in noncylindrical domain are not studied yet. In a moving domain, the transverse deflection $u(x,t)$ of the thin plate which changes its configuration at each instant of time increases its deformation and hence increases its tension. Moreover, the horizontal movement of the boundary yields nonlinear terms involving derivatives in the space variables. To control these nonlinearities, we add in the boundary a memory type. This term will play an important role in the dissipative nature of the problem.

In [9–17], the authors considered the global existence and the uniform decay of solution in noncylindrical domains. Dal Passo and Ughi [15] investigated a certain class of parabolic equations in noncylindrical domains. Benabidallah and Ferreira [9] proved the existence of solutions for the nonlinear beam equation in noncylindrical domains. Santos et al. [17] studied the global solvability and asymptotic behavior for the nonlinear coupled system of viscoelastic waves with memory in noncylindrical domains. Park and Kang [14] investigated the global existence and stability for von Karman equations with memory in noncylindrical domains. Motivated by these results, we prove the exponential decay of the energy to the Kirchhoff plate equations with viscoelastic boundary conditions in noncylindrical domains.

This paper is organized as follows. In Section 2, we recall notations and hypotheses. In Section 3, we prove the existence and uniqueness of solutions by employing Faedo-Galerkin's method. In Section 4, we establish the exponential decay rate of the solution.

2. Notations and Hypotheses

We begin this section introducing notations and some hypotheses. Throughout this paper we use standard functional spaces and denote that $\|\cdot\|_p$, $\|\cdot\|_{p,t}$ are $L^p(\Omega)$ norm and $L^p(\Omega_t)$ norm. We define the inner product

$$(u,v)=\int_\Omega u(x)\,v(x)\,dx,\qquad (u,v)_t=\int_{\Omega_t} u(x)\,v(x)\,dx. \tag{12}$$

Also, let us assume that there exists $x_0\in\mathbb{R}^2$ such that

$$\begin{gathered}\Gamma_{0,t}=\{x\in\Gamma_t : \nu(x)\cdot(x-x_0)\le 0\},\\ \Gamma_{1,t}=\{x\in\Gamma : \nu(x)\cdot(x-x_0)>0\}.\end{gathered} \tag{13}$$

The method used to prove the result of existence and uniqueness is based on the transformation of our problem into another initial boundary value problem defined over a cylindrical domain whose sections are not time dependent. This is done using a suitable change of variable. Then we show the existence and uniqueness for this new problem. Our existence result on noncylindrical domains will follow by using the inverse transformation. That is, by using the diffeomorphism

$$\tau:\widehat{Q}\longrightarrow Q,\quad (x,t)\in\Omega_t\times\{t\}\longrightarrow(y,t)=\left(\frac{x}{\gamma(t)},t\right) \tag{14}$$

and $\tau^{-1}: Q\to\widehat{Q}$ defined by

$$\tau^{-1}(y,t)=(x,t)=(\gamma(t)\,y,t). \tag{15}$$

For each function u we denote by v the function

$$v(y,t)=u\circ\tau^{-1}(y,t)=u(x,t), \tag{16}$$

the initial boundary value problem (4)–(8) becomes

$$v''+\gamma^{-4}\Delta^2 v+A(t)\,v+b(y,t)\cdot\nabla v+c(y,t)\cdot\nabla v'=0 \quad \text{in } \Omega\times(0,\infty), \tag{17}$$

$$v=\frac{\partial v}{\partial \nu}=0\quad \text{on } \Gamma_0\times(0,\infty), \tag{18}$$

$$-v+\int_0^t g_1(t-s)\,\gamma^{-2}(s)\,\mathscr{B}_2 v(s)\,ds=0\quad \text{on } \Gamma_1\times(0,\infty), \tag{19}$$

$$\frac{\partial v}{\partial \nu}+\int_0^t g_2(t-s)\,\gamma^{-2}(s)\,\mathscr{B}_1 v(s)\,ds=0\quad \text{on } \Gamma_1\times(0,\infty), \tag{20}$$

$$v(y,0)=v_0(y),\quad v'(y,0)=v_1(y)\quad \text{in } \Omega, \tag{21}$$

where

$$\begin{gathered}A(t)\,v=\sum_{i,j=1}^{2}\partial_{y_i}\left(a_{ij}\partial_{y_j}v\right),\\ a_{ij}=\left(\gamma'\gamma^{-1}\right)^2 y_i y_j\quad (i,j=1,2),\\ b(y,t)=-\gamma^{-2}\left(\gamma''\gamma+(\gamma')^2\right)y,\\ c(y,t)=-2\gamma'\gamma^{-1}y.\end{gathered} \tag{22}$$

The above method was introduced by Dal Passo and Ughi [15] for studying a certain class of parabolic equations in noncylindrical domains. This idea was used in [11, 13, 14, 16, 17].

We will use (19) and (20) to estimate the values $\mathscr{B}_1$ and $\mathscr{B}_2$ on Γ_1. Denoting by

$$(g * v)(t) = \int_0^t g(t-s)\, v(s)\, ds \tag{23}$$

the convolution product operator and differentiating (19) and (20) we arrive at the following Volterra equations:

$$\begin{aligned} \frac{\mathscr{B}_2 v}{\gamma^2} + \frac{1}{g_1(0)} g_1' * \frac{\mathscr{B}_2 v}{\gamma^2} &= \frac{1}{g_1(0)} v', \\ \frac{\mathscr{B}_1 v}{\gamma^2} + \frac{1}{g_2(0)} g_2' * \frac{\mathscr{B}_1 v}{\gamma^2} &= -\frac{1}{g_2(0)} \frac{\partial v'}{\partial \nu}. \end{aligned} \tag{24}$$

Applying Volterra's inverse operator, we get

$$\begin{aligned} \frac{\mathscr{B}_2 v}{\gamma^2} &= \frac{1}{g_1(0)} \left\{ v' + k_1 * v' \right\}, \\ \frac{\mathscr{B}_1 v}{\gamma^2} &= -\frac{1}{g_2(0)} \left\{ \frac{\partial v'}{\partial \nu} + k_2 * \frac{\partial v'}{\partial \nu} \right\}, \end{aligned} \tag{25}$$

where the resolvent kernels of $-g_i'/g_i(0)$ satisfy

$$k_i + \frac{1}{g_i(0)} g_i' * k_i = -\frac{1}{g_i(0)} g_i', \quad \forall i = 1, 2. \tag{26}$$

Denoting by $\tau_1 = 1/g_1(0)$ and $\tau_2 = 1/g_2(0)$, we obtain

$$\frac{\mathscr{B}_2 v}{\gamma^2} = \tau_1 \left\{ v' + k_1(0)\, v - k_1(t)\, v_0 + k_1' * v \right\}, \tag{27}$$

$$\begin{aligned} \frac{\mathscr{B}_1 v}{\gamma^2} = -\tau_2 \Bigg\{ & \frac{\partial v'}{\partial \nu} + k_2(0) \frac{\partial v}{\partial \nu} \\ & - k_2(t) \frac{\partial v_0}{\partial \nu} + k_2' * \frac{\partial v}{\partial \nu} \Bigg\}. \end{aligned} \tag{28}$$

Therefore, we use (27) and (28) instead of the boundary conditions (19) and (20).

Let us define the bilinear form $a(\cdot,\cdot)$ as follows:

$$\begin{aligned} a(w, v) = {} & w_{x_1x_1} v_{x_1x_1} + w_{x_2x_2} v_{x_2x_2} \\ & + \mu \left(w_{x_1x_1} v_{x_2x_2} + w_{x_2x_2} v_{x_1x_1} \right) \\ & + 2(1-\mu)\, w_{x_1x_2} v_{x_1x_2}. \end{aligned} \tag{29}$$

Since $\Gamma_0 \neq \emptyset$ we know that $\int_\Omega a(v,v)dy$ is equivalent to the $H^2(\Omega)$ norm, that is,

$$c_0 \|v\|^2_{H^2(\Omega)} \le \int_\Omega a(v,v)\, dy \le C_0 \|v\|^2_{H^2(\Omega)}, \tag{30}$$

where c_0 and C_0 are generic positive constants.

Let us denote that

$$\begin{aligned} (g \circ v)(t) &:= \int_0^t g(t-s)\,(v(t) - v(s))\, ds, \\ (g \square v)(t) &:= \int_0^t g(t-s)\, |v(t) - v(s)|^2 ds. \end{aligned} \tag{31}$$

The following lemma states an important property of the convolution operator.

Lemma 1. *For $g, v \in C^1([0,\infty) : \mathbb{R})$ one has*

$$\begin{aligned} (g * v)\, v' = {} & -\frac{1}{2} g(t)\, |v(t)|^2 + \frac{1}{2} g' \square v \\ & - \frac{1}{2} \frac{d}{dt} \left[g \square v - \left(\int_0^t g(s)\, ds \right) |v|^2 \right]. \end{aligned} \tag{32}$$

The proof of this lemma follows by differentiating the term $g \square v$.

We state the following lemma which will be useful in what follows.

Lemma 2 (see [7]). *Let w and v be functions in $H^4(\Omega) \cap H_0^2(\Omega)$. Then one has*

$$\begin{aligned} \int_\Omega \left(\Delta^2 w \right) v\, dy = {} & \int_\Omega a(w, v)\, dy \\ & + \int_{\Gamma_1} \left\{ (\mathscr{B}_2 w)\, v - (\mathscr{B}_1 w) \frac{\partial v}{\partial \nu} \right\} d\Gamma. \end{aligned} \tag{33}$$

Lemma 3 (see [18]). *Suppose that $f \in L^2(\Omega)$, $g \in H^{1/2}(\Gamma_1)$, and $h \in H^{3/2}(\Gamma_1)$; then, any solution of*

$$\begin{aligned} \int_\Omega a(v, w)\, dy = {} & \int_\Omega f w\, dy + \int_{\Gamma_1} g w\, d\Gamma \\ & + \int_{\Gamma_1} h \frac{\partial w}{\partial \nu} d\Gamma, \quad \forall w \in H_0^2(\Omega) \end{aligned} \tag{34}$$

satisfies $v \in H^4(\Omega)$ and also

$$\begin{aligned} \Delta^2 v = f, \quad v = \frac{\partial v}{\partial \nu} = 0 \quad \text{on } \Gamma_0, \\ \mathscr{B}_1 v = h, \quad \mathscr{B}_2 v = g \quad \text{on } \Gamma_1. \end{aligned} \tag{35}$$

To show the existence of solution, we will use the following hypotheses:

$$\gamma' \le 0, \qquad \gamma \in L^\infty(0,\infty), \qquad \inf_{0 \le t < \infty} \gamma(t) = \gamma_0 > 0, \tag{36}$$

$$\gamma' \in W^{2,\infty}(0,\infty) \cap W^{2,1}(0,\infty), \tag{37}$$

$$0 < \max_{0 \le t < \infty} \left| \gamma'(t) \right| \gamma(t) \le \frac{1}{\sqrt{2 c_1 c_0^{-1} M d}}, \tag{38}$$

where $d = \operatorname{diam}(\Omega)$, $M = \operatorname{meas}(\Omega)$, and c_0 is a positive imbedding constant such that $\|\nabla v\|^2 \le c_1 \|\Delta v\|^2$, for all $v \in H_0^2(\Omega)$.

3. Existence and Regularity

In this section we will study the existence and regularity of solutions for system (4)–(8).

The well posedness of system (17)–(21) is given by the following theorem.

Theorem 4. *Let $k_i \in C^2(\mathbb{R}^+)$ be such that*

$$k_i, -k_i', k_i'' \geq 0. \tag{39}$$

The function γ satisfies that

$$\left|\gamma'(t)\right| \gamma^{-1}(t) < \min\left\{1, -\frac{k_i'(t)}{2}\right\}. \tag{40}$$

If $(v_0, v_1) \in (H^4(\Omega) \cap H_0^2(\Omega)) \times H_0^2(\Omega)$ satisfy the compatibility condition

$$\mathscr{B}_2 v_0 - \tau_1 \gamma^2(0) v_1 = 0, \qquad \mathscr{B}_1 v_0 + \tau_2 \gamma^2(0) \frac{\partial v_1}{\partial \nu} \quad \text{on } \Gamma_1 \tag{41}$$

then there exists only one solution for system (17)–(21) *satisfying*

$$\begin{gathered} v \in L^\infty\left(0, T; H^4(\Omega) \cap H_0^2(\Omega)\right), \\ v' \in L^\infty\left(0, T; H_0^2(\Omega)\right), \quad v'' \in L^\infty\left(0, T; L^2(\Omega)\right). \end{gathered} \tag{42}$$

Proof. The main idea is to use the Galerkin method. To do this let us denote by B the operator

$$Bw = \Delta^2 w, \qquad D(B) = H_0^2(\Omega) \cap H^4(\Omega). \tag{43}$$

It is well known that B is a positive self-adjoint operator in the Hilbert space $L^2(\Omega)$ for which there exist sequences $\{w_n\}_{n\in\mathbb{N}}$ and $\{\lambda_n\}_{n\in\mathbb{N}}$ of eigenfunctions and eigenvalues of B such that the set of linear combinations of $\{w_n\}_{n\in\mathbb{N}}$ is dense in $D(B)$ and $\lambda_1 < \lambda_2 \leq \cdots \leq \lambda_n \to \infty$ as $n \to \infty$. Let us define

$$v_{0m} = \sum_{j=1}^{m} \left(v_0, w_j\right) w_j, \qquad v_{1m} = \sum_{j=1}^{m} \left(v_1, w_j\right) w_j. \tag{44}$$

Note that for any $(v_0, v_1) \in D(B) \times H_0^2(\Omega)$, we have $v_{0m} \to v_0$ strong in $D(B)$ and $v_{1m} \to v_1$ strong in $H_0^2(\Omega)$.

Let us denote by V_m the space generated by $w_1, w_2, \ldots, w_m$. Standard results on ordinary differential equations guarantee that there exists only one local solution

$$v_m(t) = \sum_{j=1}^{m} g_{jm}(t) w_j, \tag{45}$$

of the approximate system

$$\begin{aligned} &\int_\Omega v_m'' w_j\, dy + \gamma^{-4} \int_\Omega a\left(v_m, w_j\right) dy + \int_\Omega A(t) v_m w_j\, dy \\ &\quad + \int_\Omega c(y,t) \cdot \nabla v_m' w_j\, dy + \int_\Omega b(y,t) \cdot \nabla v_m w_j\, dy \\ &= -\tau_1 \gamma^{-2} \int_{\Gamma_1} \left\{v_m' + k_1(0) v_m - k_1(t) v_{0m} + k_1' * v_m\right\} w_j\, d\Gamma \\ &\quad - \tau_2 \gamma^{-2} \int_{\Gamma_1} \left\{\frac{\partial v_m'}{\partial \nu} + k_2(0) \frac{\partial v_m}{\partial \nu} - k_2(t) \frac{\partial v_{0m}}{\partial \nu} \right. \\ &\quad \left. + k_2' * \frac{\partial v_m}{\partial \nu}\right\} \frac{w_j}{\partial \nu} d\Gamma \quad (j = 1, 2, \ldots, m), \end{aligned} \tag{46}$$

$$v_m(x, 0) = v_{0m}, \quad v_m'(x, 0) = v_{1m}. \tag{47}$$

By standard methods for differential equations, we prove the existence of solutions to the approximate equation (46) on some interval $[0, t_m)$. Then, this solution can be extended to the whole interval $[0, T]$, for all $T > 0$, by using the following first estimate.

The First Estimate. Multiplying (46) by $g_{jm}'(t)$, summing up the product result $j = 1, 2, \ldots, m$, and making some calculations using Lemma 1, we get

$$\begin{aligned} &\frac{1}{2} \frac{d}{dt} \left[\int_\Omega \left|v_m'\right|^2 dy + \gamma^{-4} \int_\Omega a\left(v_m, v_m\right) dy \right. \\ &\qquad + \tau_1 \gamma^{-2} \int_{\Gamma_1} \left(k_1(t) \left|v_m\right|^2 - k_1' \square v_m\right) d\Gamma \\ &\qquad \left. + \tau_2 \gamma^{-2} \int_{\Gamma_1} \left(k_2(t) \left|\frac{\partial v_m}{\partial \nu}\right|^2 - k_2' \square \frac{\partial v_m}{\partial \nu}\right) d\Gamma \right] \\ &\quad + 2\gamma^{-5} \gamma' \int_\Omega a\left(v_m, v_m\right) dy \\ &\quad + \tau_1 \gamma^{-3} \gamma' \int_{\Gamma_1} \left(k_1(t) \left|v_m\right|^2 - k_1' \square v_m\right) d\Gamma \\ &\quad + \tau_2 \gamma^{-3} \gamma' \int_{\Gamma_1} \left(k_2(t) \left|\frac{\partial v_m}{\partial \nu}\right|^2 - k_2' \square \frac{\partial v_m}{\partial \nu}\right) d\Gamma \\ &= -\int_\Omega A(t) v_m v_m'\, dy - \int_\Omega c(y,t) \cdot \nabla v_m' v_m'\, dy \\ &\quad - \int_\Omega b(y,t) \cdot \nabla v_m v_m'\, dy \\ &\quad - \tau_1 \gamma^{-2} \int_{\Gamma_1} \left(\left|v_m'\right|^2 - k_1(t) v_{0m} v_m' - \frac{1}{2} k_1'(t) \left|v_m\right|^2 \right. \\ &\qquad \left. + \frac{1}{2} k_1'' \square v_m\right) d\Gamma \\ &\quad - \tau_2 \gamma^{-2} \int_{\Gamma_1} \left(\left|\frac{\partial v_m'}{\partial \nu}\right|^2 - k_2(t) \frac{\partial v_{0m}}{\partial \nu} \frac{\partial v_m'}{\partial \nu} \right. \\ &\qquad \left. - \frac{1}{2} k_2'(t) \left|\frac{\partial v_m}{\partial \nu}\right|^2 + \frac{1}{2} k_2'' \square \frac{\partial v_m}{\partial \nu}\right) d\Gamma. \end{aligned} \tag{48}$$

Now we will estimate terms of the right-hand side of (48). From the hypotheses on γ and Green's formula, we get

$$\begin{aligned} &-\int_\Omega A(t) v_m v_m'\, dy \\ &\quad = -\int_\Omega \sum_{i,j=1}^{2} \partial_{y_i} \left(a_{ij} \partial_{y_j} v_m\right) v_m'\, dy \\ &\quad = \int_\Omega \sum_{i,j=1}^{2} \left(a_{ij} \partial_{y_j} v_m\right) \partial_{y_i} v_m'\, dy \end{aligned}$$

$$= \int_\Omega \sum_{i,j=1}^{2} \left(\gamma'\gamma^{-1}\right)^2 y_i y_j \partial_{y_j} v_m \partial_{y_i} v'_m \, dy$$

$$= \frac{d}{dt} \int_\Omega \frac{1}{2} \left(\gamma'\gamma^{-1}\right)^2 \left|\nabla v_m \cdot y\right|^2 dy$$

$$- \left(\gamma'\gamma^{-1}\right) \left[\gamma''\gamma^{-1} - \left(\gamma'\gamma^{-1}\right)^2\right] \left\|\nabla v_m \cdot y\right\|_2^2,$$

$$\int_\Omega c(y,t) \cdot \nabla v'_m v'_m \, dy$$

$$= -\int_\Omega 2\gamma'\gamma^{-1} y \cdot \nabla v'_m v'_m \, dy$$

$$= -\int_\Omega \gamma'\gamma^{-1} y \cdot \nabla \left|v'_m\right|^2 dy = 2\gamma'\gamma^{-1} \left\|v'_m\right\|_2^2,$$

$$- \int_\Omega b(y,t) \cdot \nabla v_m v'_m \, dy$$

$$= \int_\Omega \gamma^{-2} \left(\gamma''\gamma + \left(\gamma'\right)^2\right) y \cdot \nabla v_m v'_m \, dy$$

$$\leq \left(\frac{\left|\gamma''\gamma^{-1}\right| + \left|\gamma'\gamma^{-1}\right|^2}{2}\right) \left(\left\|y \cdot \nabla v_m\right\|_2^2 + \left\|v'_m\right\|_2^2\right)$$

$$\leq C_1 \left(\left\|\nabla v_m\right\|_2^2 + \left\|v'_m\right\|_2^2\right). \tag{49}$$

Young's inequality yields

$$\int_{\Gamma_1} k_1(t) v_{0m} v'_m \, d\Gamma \leq \frac{1}{2} \int_{\Gamma_1} \left|v'_m\right|^2 d\Gamma + \frac{k_1^2(t)}{2} \int_{\Gamma_1} \left|v_{0m}\right|^2 d\Gamma,$$

$$\int_{\Gamma_1} k_2(t) \frac{\partial v_{0m}}{\partial \nu} \frac{\partial v'_m}{\partial \nu} d\Gamma$$

$$\leq \frac{1}{2} \int_{\Gamma_1} \left|\frac{\partial v'_m}{\partial \nu}\right|^2 d\Gamma + \frac{k_2^2(t)}{2} \int_{\Gamma_1} \left|\frac{\partial v_{0m}}{\partial \nu}\right|^2 d\Gamma. \tag{50}$$

Replacing the above calculations in (48) and using our assumptions $k_i, -k'_i, k''_i \geq 0$ and (30), we have

$$\frac{1}{2}\frac{d}{dt} \left[\left\|v'_m\right\|_2^2 + \gamma^{-4} \int_\Omega a(v_m, v_m)\, dy - \left(\gamma'\gamma^{-1}\right)^2 \left\|\nabla v_m \cdot y\right\|_2^2\right.$$

$$+ \tau_1 \gamma^{-2} \int_{\Gamma_1} \left(k_1(t) \left|v_m\right|^2 - k'_1 \Box v_m\right) d\Gamma$$

$$\left. + \tau_2 \gamma^{-2} \int_{\Gamma_1} \left(k_2(t) \left|\frac{\partial v_m}{\partial \nu}\right|^2 - k'_2 \Box \frac{\partial v_m}{\partial \nu}\right) d\Gamma\right]$$

$$\leq C_2 \left[\left\|v'_m\right\|_2^2 + \int_\Omega a(v_m, v_m)\, dy\right.$$

$$+ \int_{\Gamma_1} \left(k_1(t) \left|v_m\right|^2 - k'_1 \Box v_m\right) d\Gamma$$

$$\left. + \int_{\Gamma_1} \left(k_2(t) \left|\frac{\partial v_m}{\partial \nu}\right|^2 - k'_2 \Box \frac{\partial v_m}{\partial \nu}\right) d\Gamma\right]$$

$$+ \frac{\tau_1 \gamma^{-2}}{2} k_1^2(t) \int_{\Gamma_1} \left|v_{0m}\right|^2 d\Gamma + \frac{\tau_2 \gamma^{-2}}{2} k_2^2(t) \int_{\Gamma_1} \left|\frac{\partial v_{0m}}{\partial \nu}\right|^2 d\Gamma. \tag{51}$$

From our choice of v_{0m} and v_{1m} and integrating (51) over $(0,t)$ with $t \in (0, t_m)$, we obtain

$$\left\|v'_m\right\|_2^2 + \gamma^{-4} \int_\Omega a(v_m, v_m)\, dy - \left(\gamma'\gamma^{-1}\right)^2 \left\|\nabla v_m \cdot y\right\|_2^2$$

$$+ \tau_1 \gamma^{-2} \int_{\Gamma_1} \left(k_1(t) \left|v_m\right|^2 - k'_1 \Box v_m\right) d\Gamma$$

$$+ \tau_2 \gamma^{-2} \int_{\Gamma_1} \left(k_2(t) \left|\frac{\partial v_m}{\partial \nu}\right|^2 - k'_2 \Box \frac{\partial v_m}{\partial \nu}\right) d\Gamma$$

$$\leq C_3 \int_0^t \left[\left\|v'_m(s)\right\|_2^2 + \int_\Omega a(v_m(s), v_m(s))\, dy\right.$$

$$+ \int_{\Gamma_1} \left(k_1(s) \left|v_m(s)\right|^2 - \left(k'_1 \Box v_m\right)(s)\right) d\Gamma$$

$$\left. + \int_{\Gamma_1} \left(k_2(s) \left|\frac{\partial v_m(s)}{\partial \nu}\right|^2 - \left(k'_2 \Box \frac{\partial v_m}{\partial \nu}\right)(s)\right) d\Gamma\right] ds$$

$$+ C_4. \tag{52}$$

We observe that, from (30) and (38),

$$\left(\gamma'\gamma^{-1}\right)^2 \left\|\nabla v_m \cdot y\right\|_2^2 \leq \left(\gamma'\gamma^{-1}\right)^2 M d^2 \left\|\nabla v_m\right\|_2^2$$

$$\leq \left(\gamma'\gamma^{-1}\right)^2 c_1 c_0^{-1} M d^2 \int_\Omega a(v_m, v_m)\, dy$$

$$\leq \frac{\gamma^{-4}}{2} \int_\Omega a(v_m, v_m)\, dy, \tag{53}$$

for all $t \geq 0$. Hence, by Gronwall's lemma we get

$$\left\|v'_m\right\|_2^2 + \int_\Omega a(v_m, v_m)\, dy + \int_{\Gamma_1} \left(k_1(t) \left|v_m\right|^2 - k'_1 \Box v_m\right) d\Gamma$$

$$+ \int_{\Gamma_1} \left(k_2(t) \left|\frac{\partial v_m}{\partial \nu}\right|^2 - k'_2 \Box \frac{\partial v_m}{\partial \nu}\right) d\Gamma \leq C_5, \tag{54}$$

where C_5 is a positive constant which is independent of m and t.

The Second Estimate. First of all, we are going to estimate $v''_m(0)$ in $L^2(\Omega)$-norm. Letting $t \to 0^+$ in (46), multiplying the result by $g''_{jm}(0)$, and using the compatibility condition (41), we have

$$\left\|v''_m(0)\right\|_2^2 \le C_6. \tag{55}$$

Now, differentiating (46) with respect to t, we obtain

$$\begin{aligned}
&\int_\Omega v'''_m w_j\,dy + \gamma^{-4}\int_\Omega a\left(v'_m, w_j\right)dy \\
&- 4\gamma^{-5}\gamma'\int_\Omega a\left(v_m, w_j\right)dy \\
=& -\int_\Omega \frac{d}{dt}\left[A(t)v_m\right]w_j\,dy - \int_\Omega \frac{d}{dt}\left[c(y,t)\cdot\nabla v'_m\right]w_j\,dy \\
&- \int_\Omega \frac{d}{dt}\left[b(y,t)\cdot\nabla v_m\right]w_j\,dy \\
&- \tau_1\gamma^{-2}\int_{\Gamma_1}\left\{v''_m + k_1(0)v'_m + k'_1 * v'_m\right\}w_j\,d\Gamma \\
&- \tau_2\gamma^{-2}\int_{\Gamma_1}\left\{\frac{\partial v''_m}{\partial\nu} + k_2(0)\frac{\partial v'_m}{\partial\nu} + k'_2 * \frac{\partial v'_m}{\partial\nu}\right\}\frac{w_j}{\partial\nu}d\Gamma \\
&+ 2\tau_1\gamma^{-3}\gamma'\int_{\Gamma_1}\left\{v'_m + k_1(0)v_m - k_1(t)v_{0m}\right. \\
&\qquad\left. + k'_1 * v_m\right\}w_j\,d\Gamma \\
&+ 2\tau_2\gamma^{-3}\gamma'\int_{\Gamma_1}\left\{\frac{\partial v'_m}{\partial\nu} + k_2(0)\frac{\partial v_m}{\partial\nu} - k_2(t)\frac{\partial v_{0m}}{\partial\nu}\right. \\
&\qquad\left. + k'_2 * \frac{\partial v_m}{\partial\nu}\right\}\frac{w_j}{\partial\nu}d\Gamma.
\end{aligned} \tag{56}$$

Multiplying (56) by $g''_{jm}(t)$, summing up the product result in j, and using Lemma 1, we have

$$\begin{aligned}
&\frac{1}{2}\frac{d}{dt}\left[\left\|v''_m\right\|_2^2 + \gamma^{-4}\int_\Omega a\left(v'_m, v'_m\right)dy\right. \\
&\quad - 8\gamma^{-5}\gamma'\int_\Omega a\left(v_m, v'_m\right)dy \\
&\quad + \tau_1\gamma^{-2}\int_{\Gamma_1}\left(k_1(t)\left|v'_m\right|^2 - k'_1\square v'_m\right)d\Gamma \\
&\quad\left. + \tau_2\gamma^{-2}\int_{\Gamma_1}\left(k_2(t)\left|\frac{\partial v'_m}{\partial\nu}\right|^2 - k'_2\square\frac{\partial v'_m}{\partial\nu}\right)d\Gamma\right] \\
&+ 6\gamma^{-5}\gamma'\int_\Omega a\left(v'_m, v'_m\right)dy \\
&+ 4\gamma^{-4}\left(\gamma''\gamma^{-1} - 5\left(\gamma'\gamma^{-1}\right)^2\right)\int_\Omega a\left(v_m, v'_m\right)dy \\
&+ \tau_1\gamma^{-3}\gamma'\int_{\Gamma_1}\left(k_1(t)\left|v'_m\right|^2 - k'_1\square v'_m\right)d\Gamma \\
&+ \tau_2\gamma^{-3}\gamma'\int_{\Gamma_1}\left(k_2(t)\left|\frac{\partial v'_m}{\partial\nu}\right|^2 - k'_2\square\frac{\partial v'_m}{\partial\nu}\right)d\Gamma \\
=& -\int_\Omega \frac{d}{dt}\left[A(t)v_m\right]v''_m\,dy - \int_\Omega \frac{d}{dt}\left[c(y,t)\cdot\nabla v'_m\right]v''_m\,dy \\
&- \int_\Omega \frac{d}{dt}\left[b(y,t)\cdot\nabla v_m\right]v''_m\,dy \\
&- \tau_1\gamma^{-2}\int_{\Gamma_1}\left(\left|v''_m\right|^2 + \frac{1}{2}k''_1\square v'_m - \frac{1}{2}k'_1(t)\left|v'_m\right|^2\right)d\Gamma \\
&- \tau_2\gamma^{-2}\int_{\Gamma_1}\left(\left|\frac{\partial v''_m}{\partial\nu}\right|^2 + \frac{1}{2}k''_2\square\frac{\partial v'_m}{\partial\nu} - \frac{1}{2}k'_2(t)\left|\frac{\partial v'_m}{\partial\nu}\right|^2\right)d\Gamma \\
&+ 2\tau_1\gamma^{-3}\gamma'\int_{\Gamma_1}\left\{v'_m + k_1(0)v_m - k_1(t)v_{0m}\right. \\
&\qquad\left. + k'_1 * v_m\right\}v''_m\,d\Gamma \\
&+ 2\tau_2\gamma^{-3}\gamma'\int_{\Gamma_1}\left\{\frac{\partial v'_m}{\partial\nu} + k_2(0)\frac{\partial v_m}{\partial\nu} - k_2(t)\frac{\partial v_{0m}}{\partial\nu}\right. \\
&\qquad\left. + k'_2 * \frac{\partial v_m}{\partial\nu}\right\}\frac{v''_m}{\partial\nu}d\Gamma.
\end{aligned} \tag{57}$$

Now we will estimate terms of the right-hand side of (57). From the hypotheses on γ and Green's formula, we get

$$\begin{aligned}
&-\int_\Omega \frac{d}{dt}\left[A(t)v_m\right]v''_m\,dy \\
&= -\int_\Omega \frac{d}{dt}\left[\sum_{i,j=1}^{2}\partial_{y_i}\left(\left(\gamma'\gamma^{-1}\right)^2 y_i y_j \partial_{y_j} v_m\right)\right]v''_m\,dy \\
&= -\int_\Omega\left[\sum_{i,j=1}^{2}\partial_{y_i}\left(2\gamma'\gamma^{-1}\left(\gamma''\gamma^{-1} - \left(\gamma'\gamma^{-1}\right)^2\right)y_i y_j\partial_{y_j}v_m\right.\right. \\
&\qquad\left.\left. + \left(\gamma'\gamma^{-1}\right)^2 y_i y_j \partial_{y_j} v'_m\right)\right]v''_m\,dy \\
&= -\int_\Omega\left[\sum_{i,j=1}^{2}\partial_{y_i}\left(2\gamma'\gamma^{-1}\left(\gamma''\gamma^{-1} - \left(\gamma'\gamma^{-1}\right)^2\right)\right.\right. \\
&\qquad\left.\left. \times y_i y_j \partial_{y_j} v_m\right)\right]v''_m\,dy \\
&\quad + \int_\Omega\sum_{i,j=1}^{2}\left(\gamma'\gamma^{-1}\right)^2 y_i y_j \partial_{y_j} v'_m \partial_{y_i} v''_m\,dy
\end{aligned}$$

$$
\begin{aligned}
&= -\int_\Omega \left[\sum_{i,j=1}^{2} \partial_{y_i}\left(2\gamma'\gamma^{-1}\left(\gamma''\gamma^{-1}-\left(\gamma'\gamma^{-1}\right)^2\right)y_i y_j \partial_{y_j} v_m\right)\right] v_m'' \, dy \\
&\quad + \frac{d}{dt}\int_\Omega \frac{1}{2}\left(\gamma'\gamma^{-1}\right)^2 \left|\nabla v_m' \cdot y\right|^2 dy \\
&\quad - \left(\gamma'\gamma^{-1}\right)\left[\gamma''\gamma^{-1} - \left(\gamma'\gamma^{-1}\right)^2\right] \left\|\nabla v_m' \cdot y\right\|_2^2,
\end{aligned} \tag{58}
$$

$$
\begin{aligned}
&- \int_\Omega \frac{d}{dt}\left[c(y,t)\cdot \nabla v_m'\right] v_m'' \, dy \\
&\quad = \int_\Omega \frac{d}{dt}\left[2\gamma'\gamma^{-1} y \cdot \nabla v_m'\right] v_m'' \, dy \\
&\quad = \int_\Omega \left[2\left(\gamma''\gamma^{-1} - \left(\gamma'\gamma^{-1}\right)^2\right) y \cdot \nabla v_m' \right. \\
&\qquad\qquad \left. + 2\gamma'\gamma^{-1} y \cdot \nabla v_m''\right] v_m'' \, dy \\
&\quad = \int_\Omega \left[2\left(\gamma''\gamma^{-1} - \left(\gamma'\gamma^{-1}\right)^2\right) y \cdot \nabla v_m'\right] v_m'' \, dy \\
&\qquad + \int_\Omega \gamma'\gamma^{-1} y \cdot \nabla |v_m''|^2 \, dy \\
&\quad \le \left(\left|\gamma''\gamma^{-1}\right| + \left|\gamma'\gamma^{-1}\right|^2\right)\left(\left\|y\cdot\nabla v_m'\right\|_2^2 + \left\|v_m''\right\|_2^2\right) \\
&\qquad - 2\gamma'\gamma^{-1}\left\|v_m''\right\|_2^2,
\end{aligned} \tag{59}
$$

$$
\begin{aligned}
&- \int_\Omega \frac{d}{dt}\left[b(y,t)\cdot \nabla v_m\right] v_m'' \, dy \\
&\quad = \int_\Omega \frac{d}{dt}\left[\left(\gamma''\gamma^{-1} + \left(\gamma'\gamma^{-1}\right)^2\right) y \cdot \nabla v_m\right] v_m'' \, dy \\
&= \int_\Omega \frac{d}{dt}\left[\gamma''\gamma^{-1} + \left(\gamma'\gamma^{-1}\right)^2\right] y \cdot \nabla v_m v_m'' \, dy \\
&\quad + \int_\Omega \left(\gamma''\gamma^{-1} + \left(\gamma'\gamma^{-1}\right)^2\right) y \cdot \nabla v_m' v_m'' \, dy \\
&\le C_7\left(\left\|y\cdot\nabla v_m\right\|_2^2 + \left\|y\cdot\nabla v_m'\right\|_2^2 + \left\|v_m''\right\|_2^2\right).
\end{aligned} \tag{60}
$$

We know that

$$
\begin{aligned}
\left(k_1' * v_m\right)(t) = {} & \int_0^t k_1'(t-s)\left(v_m(s) - v_m(t)\right) ds \\
& + k_1(t) v_m(t) - k_1(0) v_m(t).
\end{aligned} \tag{61}
$$

By using Hölder's inequality and our assumption $k_1' \le 0$, we note that

$$
\begin{aligned}
&\left\|\int_0^t k_1'(t-s)\left(v(t)-v(s)\right) ds\right\|_{\Gamma_1}^2 \\
&\le \left(\int_0^t k_1'(s)\, ds\right)\int_{\Gamma_1}\int_0^t k_1'(t-s)\left(v(t)-v(s)\right)^2 ds\, d\Gamma \\
&\le \int_{\Gamma_1} k_1(0)\left|k_1'\right| \Box v \, d\Gamma
\end{aligned} \tag{62}
$$

and, hence, by applying Young's inequality, we obtain

$$
\begin{aligned}
&\left|2\tau_1\gamma^{-3}\gamma'\int_{\Gamma_1}\left\{v_m' + k_1(0) v_m - k_1(t) v_{0m} + k_1' * v_m\right\} v_m'' \, d\Gamma\right| \\
&\quad \le \tau_1\gamma^{-3}\left|\gamma'\right|\int_{\Gamma_1}\left|v_m''\right|^2 d\Gamma + \tau_1\gamma^{-3}\left|\gamma'\right| \\
&\qquad \times \int_{\Gamma_1}\left(\left|v_m'\right|^2 + k_1^2(t)\left|v_{0m}\right|^2 + k_1(0)\left|k_1'\right|\Box v_m \right. \\
&\qquad\qquad \left. + k_1^2(t)\left|v_m\right|^2\right) d\Gamma.
\end{aligned} \tag{63}
$$

By the same argument of (63), we can obtain the similar estimate

$$
\begin{aligned}
&\left|2\tau_2\gamma^{-3}\gamma'\int_{\Gamma_1}\left\{\frac{\partial v_m'}{\partial\nu} + k_2(0)\frac{\partial v_m}{\partial\nu}\right.\right. \\
&\qquad\qquad \left.\left. - k_2(t)\frac{\partial v_{0m}}{\partial\nu} + k_2' * \frac{\partial v_m}{\partial\nu}\right\}\frac{v_m''}{\partial\nu} d\Gamma\right| \\
&\quad \le \tau_2\gamma^{-3}\left|\gamma'\right|\int_{\Gamma_1}\left|\frac{v_m''}{\partial\nu}\right|^2 d\Gamma + \tau_2\gamma^{-3}\left|\gamma'\right| \\
&\qquad \times \int_{\Gamma_1}\left(\left|\frac{v_m'}{\partial\nu}\right|^2 + k_2^2(t)\left|\frac{\partial v_{0m}}{\partial\nu}\right|^2\right. \\
&\qquad\qquad \left. + k_2(0)\left|k_2'\right|\Box\frac{\partial v_m}{\partial\nu} + k_2^2(t)\left|\frac{\partial v_m}{\partial\nu}\right|^2\right) d\Gamma.
\end{aligned} \tag{64}
$$

Applying (58)–(64) to (57) and using the first estimate (54) and our assumptions $k_i, -k_i', k_i'' \ge 0$ and $|\gamma'|\gamma^{-1} < \min\{1, -(k_i'/2)\}$, we have

$$
\begin{aligned}
&\frac{1}{2}\frac{d}{dt}\left[\left\|v_m''\right\|_2^2 + \gamma^{-4}\int_\Omega a\left(v_m', v_m'\right) dy - \left(\gamma'\gamma^{-1}\right)^2\left\|\nabla v_m' \cdot y\right\|_2^2\right. \\
&\qquad - 8\gamma^{-5}\gamma'\int_\Omega a\left(v_m, v_m'\right) dy \\
&\qquad + \tau_1\gamma^{-2}\int_{\Gamma_1}\left(k_1(t)\left|v_m'\right|^2 - k_1'\Box v_m'\right) d\Gamma \\
&\qquad \left. + \tau_2\gamma^{-2}\int_{\Gamma_1}\left(k_2(t)\left|\frac{\partial v_m'}{\partial\nu}\right|^2 - k_2'\Box\frac{\partial v_m'}{\partial\nu}\right) d\Gamma\right]
\end{aligned}
$$

$$
\begin{aligned}
&\le C_8 \left[\left\| v_m'' \right\|_2^2 + \int_\Omega a\left(v_m', v_m'\right) dy + \int_\Omega a\left(v_m, v_m'\right) dy \right.\\
&\qquad + \int_{\Gamma_1} \left(k_1(t) \left| v_m' \right|^2 - k_1' \square v_m' \right) d\Gamma \\
&\qquad \left. + \int_{\Gamma_1} \left(k_2(t) \left| \frac{\partial v_m'}{\partial \nu} \right|^2 - k_2' \square \frac{\partial v_m'}{\partial \nu} \right) d\Gamma \right] \\
&\quad + \tau_1 \gamma^{-3} \left| \gamma' \right| \int_{\Gamma_1} k_1^2(t) \left| v_{0m} \right|^2 d\Gamma \\
&\quad + \tau_2 \gamma^{-3} \left| \gamma' \right| \int_{\Gamma_1} k_2^2(t) \left| \frac{\partial v_{0m}}{\partial \nu} \right|^2 d\Gamma + C_9.
\end{aligned} \tag{65}
$$

From (55) and our choice of v_{0m} and v_{1m} and integrating (65) over $(0, t)$ with $t \in (0, t_m)$, we obtain

$$
\begin{aligned}
&\left\| v_m'' \right\|_2^2 + \gamma^{-4} \int_\Omega a\left(v_m', v_m'\right) dy - \left(\gamma' \gamma^{-1}\right)^2 \left\| \nabla v_m' \cdot y \right\|_2^2 \\
&\quad - 8 \gamma^{-5} \gamma' \int_\Omega a\left(v_m, v_m'\right) dy \\
&\quad + \tau_1 \gamma^{-2} \int_{\Gamma_1} \left(k_1(t) \left| v_m' \right|^2 - k_1' \square v_m' \right) d\Gamma \\
&\quad + \tau_2 \gamma^{-2} \int_{\Gamma_1} \left(k_2(t) \left| \frac{\partial v_m'}{\partial \nu} \right|^2 - k_2' \square \frac{\partial v_m'}{\partial \nu} \right) d\Gamma \\
&\le 2C_8 \int_0^t \left[\left\| v_m''(s) \right\|_2^2 + \int_\Omega a\left(v_m'(s), v_m'(s)\right) dy \right.\\
&\qquad + \int_\Omega a\left(v_m(s), v_m'(s)\right) dy \\
&\qquad + \int_{\Gamma_1} \left(k_1(s) \left| v_m'(s) \right|^2 - \left(k_1' \square v_m'\right)(s) \right) d\Gamma \\
&\qquad \left. + \int_{\Gamma_1} \left(k_2(s) \left| \frac{\partial v_m'(s)}{\partial \nu} \right|^2 - \left(k_2' \square \frac{\partial v_m'}{\partial \nu} \right)(s) \right) d\Gamma \right] ds \\
&\quad + C_{10}.
\end{aligned} \tag{66}
$$

Using the same arguments as for (53), we get

$$
\left(\gamma' \gamma^{-1}\right)^2 \left\| \nabla v_m' \cdot y \right\|_2^2 < \frac{\gamma^{-4}}{2} \int_\Omega a\left(v_m', v_m'\right) dy, \tag{67}
$$

for all $t \ge 0$. Therefore, by Gronwall's lemma, we obtain

$$
\begin{aligned}
&\left\| v_m'' \right\|_2^2 + \int_\Omega a\left(v_m', v_m'\right) dy + \int_{\Gamma_1} \left(k_1(t) \left| v_m' \right|^2 - k_1' \square v_m' \right) d\Gamma \\
&\quad + \int_{\Gamma_1} \left(k_2(t) \left| \frac{\partial v_m'}{\partial \nu} \right|^2 - k_2' \square \frac{\partial v_m'}{\partial \nu} \right) d\Gamma \le C_{11},
\end{aligned} \tag{68}
$$

where C_{11} is a positive constant which is independent of m and t.

According to (54) and (68), we get

$$
\{v_m\} \text{ is bounded in } L^\infty\left(0, T; H_0^2(\Omega)\right), \tag{69}
$$

$$
\{v_m'\} \text{ is bounded in } L^\infty\left(0, T; H_0^2(\Omega)\right), \tag{70}
$$

$$
\{v_m''\} \text{ is bounded in } L^\infty\left(0, T; L^2(\Omega)\right). \tag{71}
$$

From (69) to (71), there exists a subsequence of $\{v_m\}$, which we still denote by $\{v_m\}$, such that

$$
v_m \longrightarrow v \text{ weak star in } L^\infty\left(0, T; H_0^2(\Omega)\right), \tag{72}
$$

$$
v_m' \longrightarrow v' \text{ weak star in } L^\infty\left(0, T; H_0^2(\Omega)\right), \tag{73}
$$

$$
v_m'' \longrightarrow v'' \text{ weak star in } L^\infty\left(0, T; L^2(\Omega)\right). \tag{74}
$$

Letting $m \to \infty$ in (46) and using (72)–(74), we obtain

$$
\begin{aligned}
&\int_\Omega a(v, w)\, dy \\
&\quad = -\gamma^4 \int_\Omega v'' w\, dy - \gamma^4 \int_\Omega A(t) v w\, dy \\
&\qquad - \gamma^4 \int_\Omega c(y, t) \cdot \nabla v' w\, dy \\
&\qquad - \gamma^4 \int_\Omega b(y, t) \cdot \nabla v w\, dy \\
&\qquad - \tau_1 \gamma^2 \int_{\Gamma_1} \left\{ v' + k_1(0) v - k_1(t) v_0 + k_1' * v \right\} w\, d\Gamma \\
&\qquad - \tau_2 \gamma^2 \int_{\Gamma_1} \left\{ \frac{\partial v'}{\partial \nu} + k_2(0) \frac{\partial v}{\partial \nu} - k_2(t) \frac{\partial v_0}{\partial \nu} \right.\\
&\qquad\qquad \left. + k_2' * \frac{\partial v}{\partial \nu} \right\} \frac{\partial w}{\partial \nu} d\Gamma
\end{aligned} \tag{75}
$$

for any $w \in H_0^2(\Omega)$. From Lemma 3 we obtain that $v \in L^\infty(0, T; H^4(\Omega))$. The uniqueness of solutions follows by using standard arguments. □

Theorem 5. *Under the hypotheses of Theorem 4, let $u_0 \in H_0^2(\Omega_0) \cap H^4(\Omega_0)$, $u_1 \in H_0^2(\Omega_0)$. Then there exists a unique solution u of the problem* (4)–(8) *satisfying*

$$
\begin{aligned}
u &\in L^\infty\left(0, \infty; H_0^2(\Omega_t) \cap H^4(\Omega_t)\right), \\
u' &\in L^\infty\left(0, \infty; H_0^2(\Omega_t)\right), \\
u'' &\in L^\infty\left(0, \infty; L^2(\Omega_t)\right).
\end{aligned} \tag{76}
$$

Proof. This idea was used in [11, 13, 14, 16, 17]. To show the existence in noncylindrical domains, we return to our original problem in the noncylindrical domains by using the change variable given in (14) by $(y, t) = \tau(x, t)$, $(x, t) \in \widehat{Q}$.

Let v be the solution obtained from Theorem 4 and u defined by (16); then u belongs to the class

$$\begin{aligned} u &\in L^{\infty}\left(0,\infty; H_0^2(\Omega_t)\cap H^4(\Omega_t)\right),\\ u' &\in L^{\infty}\left(0,\infty; H_0^2(\Omega_t)\right),\\ u'' &\in L^{\infty}\left(0,\infty; L^2(\Omega_t)\right). \end{aligned} \tag{77}$$

Denoting by

$$u(x,t) = v(y,t) = (v\circ\tau)(x,t), \tag{78}$$

then from (15) it is easy to see that u satisfies (4)–(8) in the sense of $L^{\infty}(0,\infty;L^2(\Omega_t))$. If u_1, u_2 are two solutions obtained through the diffeomorphism τ given by (14), then $v_1 = v_2$, so $u_1 = u_2$. Thus the proof of Theorem 5 is completed. □

4. Exponential Decay

In this section, we show that the solution of system (4)–(8) decays exponentially. First of all, we introduce the useful lemma for a noncylindrical domain.

Lemma 6 (see [11, 12]). *Let $G(\cdot,\cdot)$ be the smooth function defined in $\Omega_t\times[0,\infty[$. Then*

$$\begin{aligned} \frac{d}{dt}\int_{\Omega_t} G(x,t)\,dx &= \int_{\Omega_t}\frac{d}{dt}G(x,t)\,dx\\ &\quad + \gamma'\gamma^{-1}\int_{\Gamma_t} G(x,t)(x\cdot\overline{\nu})\,d\Gamma, \end{aligned} \tag{79}$$

where $\overline{\nu}$ is the x-component of the unit normal exterior ν.

By the same argument of (27) and (28), it can be written as

$$\mathscr{B}_2 u = \tau_1\left\{u' + k_1(0)u - k_1(t)u_0 + k_1' * u\right\}, \tag{80}$$

$$\mathscr{B}_1 u = -\tau_2\left\{\frac{\partial u'}{\partial\nu} + k_2(0)\frac{\partial u}{\partial\nu} - k_2(t)\frac{\partial u_0}{\partial\nu} + k_2' * \frac{\partial u}{\partial\nu}\right\}. \tag{81}$$

We use (80) and (81) instead of the boundary conditions (6) and (7).

We will use the following lemma.

Lemma 7 (see [4]). *For every $u\in H^4(\Omega)$ and for every $\mu\in\mathbb{R}$, one has*

$$\begin{aligned} &\int_{\Omega_t}(m\cdot\nabla u)\Delta^2 u\,dx\\ &= \int_{\Omega_t} a(u,u)\,dx + \frac{1}{2}\int_{\Gamma_t}(m\cdot\nu)\,a(u,u)\,d\Gamma\\ &\quad + \int_{\Gamma_t}\left[(\mathscr{B}_2 u)(m\cdot\nabla u) - (\mathscr{B}_1 u)\frac{\partial}{\partial\nu}(m\cdot\nabla u)\right]d\Gamma. \end{aligned} \tag{82}$$

Now, we define the energy of problem (4)–(8) by

$$\begin{aligned} E(t) = \frac{1}{2}\Bigg[&\left\|u'\right\|_{2,t}^2 + \int_{\Omega_t} a(u,u)\,dx\\ &+ \tau_1\int_{\Gamma_{1,t}}\left(k_1(t)|u|^2 - k_1'\square u\right)d\Gamma\\ &+\tau_2\int_{\Gamma_{1,t}}\left(k_2(t)\left|\frac{\partial u}{\partial\nu}\right|^2 - k_2'\square\frac{\partial u}{\partial\nu}\right)d\Gamma\Bigg]. \end{aligned} \tag{83}$$

We observe that $E(t)$ is a positive function. Using Lemmas 6 and 1, we have

$$\begin{aligned} E'(t) \le{}& \frac{\gamma'\gamma^{-1}}{2}\int_{\Gamma_{1,t}}\left[\left|u'\right|^2 + a(u,u)\right](x\cdot\overline{\nu})\,d\Gamma\\ &- \frac{\tau_1}{2}\int_{\Gamma_{1,t}}\left|u'\right|^2 d\Gamma + \frac{\tau_1}{2}k_1^2(t)\int_{\Gamma_{1,t}}\left|u_0\right|^2 d\Gamma\\ &+ \frac{\tau_1}{2}k_1'(t)\int_{\Gamma_{1,t}}|u|^2 d\Gamma - \frac{\tau_1}{2}\int_{\Gamma_{1,t}}k_1''\square u\,d\Gamma\\ &- \frac{\tau_2}{2}\int_{\Gamma_{1,t}}\left|\frac{\partial u'}{\partial\nu}\right|^2 d\Gamma + \frac{\tau_2}{2}k_2^2(t)\int_{\Gamma_{1,t}}\left|\frac{\partial u_0}{\partial\nu}\right|^2 d\Gamma\\ &+ \frac{\tau_2}{2}k_2'(t)\int_{\Gamma_{1,t}}\left|\frac{\partial u}{\partial\nu}\right|^2 d\Gamma - \frac{\tau_2}{2}\int_{\Gamma_{1,t}}k_2''\square\frac{\partial u}{\partial\nu}d\Gamma. \end{aligned} \tag{84}$$

Let us consider the following functional:

$$\psi(t) = \int_{\Omega_t}(m\cdot\nabla u)\,u'\,dx. \tag{85}$$

The following lemma plays an important role for the construction of the Lyapunov functional.

Lemma 8. *Let one suppose that the initial data $(u_0,u_1)\in(H^4(\Omega_0)\cap H_0^2(\Omega_0))\times H_0^2(\Omega_0)$ and satisfies the compatibility condition* (41)*. Then the solution of system* (4)–(8) *satisfies*

$$\begin{aligned} \psi'(t) \le{}& \frac{1}{2}\int_{\Gamma_{1,t}}(m\cdot\nu)\left|u'\right|^2 d\Gamma - \int_{\Omega_t}\left|u'\right|^2 dx\\ &- \int_{\Omega_t} a(u,u)\,dx - \frac{1}{2}\int_{\Gamma_{1,t}}(m\cdot\nu)\,a(u,u)\,d\Gamma\\ &- \int_{\Gamma_{1,t}}\left[(\mathscr{B}_2 u)(m\cdot\nabla u) - (\mathscr{B}_1 u)\frac{\partial}{\partial\nu}(m\cdot\nabla u)\right]d\Gamma\\ &+ \gamma'\gamma^{-1}\int_{\Gamma_{1,t}}(m\cdot\nabla u)\,u'(x\cdot\overline{\nu})\,d\Gamma. \end{aligned} \tag{86}$$

Proof. Differentiating ψ and using (4) and Lemmas 6 and 7, we get

$$\begin{aligned}\psi'(t) = & \int_{\Omega_t}\left(m\cdot\nabla u'\right)u'dx + \int_{\Omega_t}(m\cdot\nabla u)u''dx \\ & + \gamma'\gamma^{-1}\int_{\Gamma_{1,t}}(m\cdot\nabla u)u'(x\cdot\overline{\nu})d\Gamma \\ = & \frac{1}{2}\int_{\Gamma_{1,t}}(m\cdot\nu)\left|u'\right|^2 d\Gamma - \int_{\Omega_t}\left|u'\right|^2 dx \\ & - \int_{\Omega_t}a(u,u)dx - \frac{1}{2}\int_{\Gamma_t}(m\cdot\nu)a(u,u)d\Gamma \\ & - \int_{\Gamma_t}\left[(\mathscr{B}_2 u)(m\cdot\nabla u) - (\mathscr{B}_1 u)\frac{\partial}{\partial\nu}(m\cdot\nabla u)\right]d\Gamma \\ & + \gamma'\gamma^{-1}\int_{\Gamma_t}(m\cdot\nabla u)u'(x\cdot\overline{\nu})d\Gamma.\end{aligned} \tag{87}$$

Let us next examine the integrals over $\Gamma_{0,t}$ in (87). Since $u = \partial u/\partial\nu = 0$ on $\Gamma_{0,t}$, we have

$$\begin{gathered}B_1 u = B_2 u = \nabla u = 0 \quad \text{on } \Gamma_{0,t}, \\ u_{x_1} = \frac{\partial u}{\partial\nu}\nu_1, \qquad u_{x_2} = \frac{\partial u}{\partial\nu}\nu_2,\end{gathered} \tag{88}$$

and hence

$$\begin{aligned}\int_{\Gamma_{0,t}}(\mathscr{B}_1 u)\frac{\partial}{\partial\nu}(m\cdot\nabla u)d\Gamma = & \int_{\Gamma_{0,t}}\Delta u(m\cdot\nu)\frac{\partial^2 u}{\partial\nu^2}d\Gamma \\ = & \int_{\Gamma_{0,t}}(m\cdot\nu)|\Delta u|^2 d\Gamma,\end{aligned} \tag{89}$$

$$\int_{\Gamma_{0,t}}(m\cdot\nu)a(u,u)d\Gamma = \int_{\Gamma_{0,t}}(m\cdot\nu)|\Delta u|^2 d\Gamma. \tag{90}$$

Therefore, from (87)–(90) we have

$$\begin{aligned}\psi'(t) = & \frac{1}{2}\int_{\Gamma_{1,t}}(m\cdot\nu)\left|u'\right|^2 d\Gamma - \int_{\Omega_t}\left|u'\right|^2 dx - \int_{\Omega_t}a(u,u)dx \\ & + \frac{1}{2}\int_{\Gamma_{0,t}}(m\cdot\nu)|\Delta u|^2 d\Gamma \\ & - \frac{1}{2}\int_{\Gamma_{1,t}}(m\cdot\nu)a(u,u)d\Gamma - \int_{\Gamma_{1,t}}(\mathscr{B}_2 u)(m\cdot\nabla u)d\Gamma \\ & + \int_{\Gamma_{1,t}}(\mathscr{B}_1 u)\frac{\partial}{\partial\nu}(m\cdot\nabla u)d\Gamma \\ & + \gamma'\gamma^{-1}\int_{\Gamma_{1,t}}(m\cdot\nabla u)u'(x\cdot\overline{\nu})d\Gamma.\end{aligned} \tag{91}$$

Noting that $m\cdot\nu \le 0$ on $\Gamma_{0,t}$ follows from (91), we have the conclusion of the lemma. □

Let us introduce the Lyapunov functional

$$\mathscr{L}(t) = NE(t) + \psi(t), \tag{92}$$

with $N > 0$. Using Young's inequality and choosing $N > 0$ sufficiently large, we see that

$$q_0 E(t) \le \mathscr{L}(t) \le q_1 E(t) \tag{93}$$

for q_0 and q_1 are positive constants. We will show later that the functional $\mathscr{L}$ satisfies the inequality of the following result.

Lemma 9 (see [7]). *Let f be a real positive function of class C^1. If there exist positive constants p_0, p_1, and p_2 such that*

$$f'(t) \le -p_0 f(t) + p_1 e^{-p_2 t} \tag{94}$$

then there exist positive constants p and c such that

$$f(t) \le (f(0) + c)e^{-pt}. \tag{95}$$

Finally, we will show the main result of this section.

Theorem 10. *Assume that there exist positive constants β_1 and β_2 such that*

$$\begin{gathered}k_i(0) > 0, \quad k_i'(t) \le -\beta_1 k_i(t), \\ k_i''(t) \ge -\beta_2 k_i'(t), \quad i = 1,2.\end{gathered} \tag{96}$$

If $(u_0, u_1) \in H_0^2(\Omega_0)\times L^2(\Omega_0)$ then there exist constants $\omega, C > 0$ such that

$$E(t) \le CE(0)e^{-\omega t}, \quad \forall t \ge 0. \tag{97}$$

Proof. From (84) and Lemma 8 we have

$$\begin{aligned}\mathscr{L}'(t) \le & \frac{\gamma'\gamma^{-1}N}{2}\int_{\Gamma_{1,t}}\left[\left|u'\right|^2 + a(u,u)\right](x\cdot\overline{\nu})d\Gamma \\ & - \frac{\tau_1 N}{2}\int_{\Gamma_{1,t}}\left|u'\right|^2 d\Gamma + \frac{\tau_1 N}{2}k_1^2(t)\int_{\Gamma_{1,t}}\left|u_0\right|^2 d\Gamma \\ & + \frac{\tau_1 N}{2}k_1'(t)\int_{\Gamma_{1,t}}|u|^2 d\Gamma - \frac{\tau_1 N}{2}\int_{\Gamma_{1,t}}k_1''\Box u d\Gamma \\ & - \frac{\tau_2 N}{2}\int_{\Gamma_{1,t}}\left|\frac{\partial u'}{\partial\nu}\right|^2 d\Gamma \\ & + \frac{\tau_2 N}{2}k_2^2(t)\int_{\Gamma_{1,t}}\left|\frac{\partial u_0}{\partial\nu}\right|^2 d\Gamma \\ & + \frac{\tau_2 N}{2}k_2'(t)\int_{\Gamma_{1,t}}\left|\frac{\partial u}{\partial\nu}\right|^2 d\Gamma \\ & - \frac{\tau_2 N}{2}\int_{\Gamma_{1,t}}k_2''\Box\frac{\partial u}{\partial\nu}d\Gamma \\ & + \frac{1}{2}\int_{\Gamma_{1,t}}(m\cdot\nu)\left|u'\right|^2 d\Gamma\end{aligned}$$

$$
\begin{aligned}
&- \int_{\Omega_t} \left|u'\right|^2 dx - \int_{\Omega_t} a(u,u)\,dx \\
&- \frac{1}{2}\int_{\Gamma_{1,t}} (m\cdot\nu)\, a(u,u)\, d\Gamma \\
&- \int_{\Gamma_{1,t}} \left[(\mathscr{B}_2 u)(m\cdot\nabla u) - (\mathscr{B}_1 u)\frac{\partial}{\partial\nu}(m\cdot\nabla u)\right] d\Gamma \\
&+ \gamma'\gamma^{-1} \int_{\Gamma_{1,t}} (m\cdot\nabla u)\, u'\,(x\cdot\overline{\nu})\, d\Gamma.
\end{aligned} \tag{98}
$$

Since the boundary conditions (80) and (81) can be written as

$$
\begin{aligned}
\mathscr{B}_2 u &= \tau_1 \left\{ u' + k_1(t)\,u - k_1(t)\,u_0 - k_1' \circ u \right\}, \\
\mathscr{B}_1 u &= -\tau_2 \left\{ \frac{\partial u'}{\partial\nu} + k_2(t)\frac{\partial u}{\partial\nu} - k_2(t)\frac{\partial u_0}{\partial\nu} - k_2' \circ \frac{\partial u}{\partial\nu} \right\},
\end{aligned} \tag{99}
$$

by using Young's inequality we obtain

$$
\begin{aligned}
\left| -\int_{\Gamma_{1,t}} (\mathscr{B}_2 u)(m\cdot\nabla u)\, d\Gamma \right| \le{}& \frac{\tau_1}{2\epsilon}\int_{\Gamma_{1,t}} \left|u'\right|^2 d\Gamma \\
&+ \frac{\tau_1}{2\epsilon} k_1^2(t) \int_{\Gamma_{1,t}} |u|^2 d\Gamma \\
&+ \frac{\tau_1}{2\epsilon} k_1^2(t) \int_{\Gamma_{1,t}} \left|u_0\right|^2 d\Gamma \\
&+ \frac{\tau_1}{2\epsilon} \int_{\Gamma_{1,t}} k_1(0) \left|k_1'\right| \Box u\, d\Gamma \\
&+ \frac{\epsilon}{2}\int_{\Gamma_{1,t}} |m\cdot\nabla u|^2 d\Gamma,
\end{aligned} \tag{100}
$$

$$
\begin{aligned}
\left| \int_{\Gamma_{1,t}} (\mathscr{B}_1 u)\frac{\partial}{\partial\nu}(m\cdot\nabla u)\, d\Gamma \right| \le{}& \frac{\tau_2}{2\epsilon}\int_{\Gamma_{1,t}} \left|\frac{\partial u'}{\partial\nu}\right|^2 d\Gamma \\
&+ \frac{\tau_2}{2\epsilon} k_2^2(t) \int_{\Gamma_{1,t}} \left|\frac{\partial u}{\partial\nu}\right|^2 d\Gamma \\
&+ \frac{\tau_2}{2\epsilon} k_2^2(t) \int_{\Gamma_{1,t}} \left|\frac{\partial u_0}{\partial\nu}\right|^2 d\Gamma \\
&+ \frac{\tau_2}{2\epsilon} \int_{\Gamma_{1,t}} k_2(0) \left|k_2'\right| \Box \frac{\partial u}{\partial\nu} d\Gamma \\
&+ \frac{\epsilon}{2}\int_{\Gamma_{1,t}} \left|\frac{\partial}{\partial\nu}(m\cdot\nabla u)\right|^2 d\Gamma,
\end{aligned} \tag{101}
$$

where ϵ is a positive constant. Since the bilinear form $a(u,u)$ is strictly coercive, using the trace theory and the fact $m\cdot\nu \ge \delta_0$ on $\Gamma_{1,t}$, we get

$$
\begin{aligned}
&\int_{\Gamma_{1,t}} |m\cdot\nabla u|^2 d\Gamma + \int_{\Gamma_{1,t}} \left|\frac{\partial}{\partial\nu}(m\cdot\nabla u)\right|^2 d\Gamma \\
&\quad \le \lambda_0 \int_{\Omega_t} a(u,u)\,dx + \frac{\lambda_0}{\delta_0}\int_{\Gamma_{1,t}} (m\cdot\nu)\, a(u,u)\, d\Gamma,
\end{aligned} \tag{102}
$$

where λ_0 is a constant depending on Ω and μ. Substituting inequalities (100)–(102) into (98) we have

$$
\begin{aligned}
\mathscr{L}'(t) \le{}& \frac{\gamma'\gamma^{-1}N}{2}\int_{\Gamma_{1,t}} \left[\left|u'\right|^2 + a(u,u)\right](x\cdot\overline{\nu})\, d\Gamma \\
&- \frac{\tau_1 N}{2}\int_{\Gamma_{1,t}} \left|u'\right|^2 d\Gamma + \frac{\tau_1 N}{2} k_1^2(t)\int_{\Gamma_{1,t}} \left|u_0\right|^2 d\Gamma \\
&- \frac{\tau_1\beta_1 N}{2} k_1(t) \int_{\Gamma_{1,t}} |u|^2 d\Gamma + \frac{\tau_1\beta_2 N}{2}\int_{\Gamma_{1,t}} k_1' \Box u\, d\Gamma \\
&- \frac{\tau_2 N}{2}\int_{\Gamma_{1,t}} \left|\frac{\partial u'}{\partial\nu}\right|^2 d\Gamma \\
&+ \frac{\tau_2 N}{2} k_2^2(t) \int_{\Gamma_{1,t}} \left|\frac{\partial u_0}{\partial\nu}\right|^2 d\Gamma \\
&- \frac{\tau_2\beta_1 N}{2} k_2(t) \int_{\Gamma_{1,t}} \left|\frac{\partial u}{\partial\nu}\right|^2 d\Gamma \\
&+ \frac{\tau_2\beta_2 N}{2}\int_{\Gamma_{1,t}} k_2' \Box \frac{\partial u}{\partial\nu} d\Gamma \\
&- \int_{\Omega_t} \left|u'\right|^2 dx - \left(1 - \frac{\epsilon\lambda_0}{2}\right)\int_{\Omega_t} a(u,u)\,dx \\
&- \left(\frac{1}{2} - \frac{\epsilon\lambda_0}{2\delta_0}\right)\int_{\Gamma_{1,t}} (m\cdot\nu)\, a(u,u)\, d\Gamma \\
&+ \frac{1}{2}\int_{\Gamma_{1,t}} (m\cdot\nu)\left|u'\right|^2 d\Gamma + \frac{\tau_1}{2\epsilon}\int_{\Gamma_{1,t}} \left|u'\right|^2 d\Gamma \\
&+ \frac{\tau_1}{2\epsilon} k_1^2(t)\int_{\Gamma_{1,t}} |u|^2 d\Gamma + \frac{\tau_1}{2\epsilon} k_1^2(t)\int_{\Gamma_{1,t}} \left|u_0\right|^2 d\Gamma \\
&+ \frac{\tau_1}{2\epsilon}\int_{\Gamma_{1,t}} k_1(0)\left|k_1'\right| \Box u\, d\Gamma + \frac{\tau_2}{2\epsilon}\int_{\Gamma_{1,t}} \left|\frac{\partial u'}{\partial\nu}\right|^2 d\Gamma \\
&+ \frac{\tau_2}{2\epsilon} k_2^2(t)\int_{\Gamma_{1,t}} \left|\frac{\partial u}{\partial\nu}\right|^2 d\Gamma + \frac{\tau_2}{2\epsilon} k_2^2(t)\int_{\Gamma_{1,t}} \left|\frac{\partial u_0}{\partial\nu}\right|^2 d\Gamma \\
&+ \frac{\tau_2}{2\epsilon}\int_{\Gamma_{1,t}} k_2(0)\left|k_2'\right| \Box \frac{\partial u}{\partial\nu} d\Gamma \\
&+ \gamma'\gamma^{-1}\int_{\Gamma_{1,t}} (m\cdot\nabla u)\, u'\,(x\cdot\overline{\nu})\, d\Gamma.
\end{aligned} \tag{103}
$$

First, choose $\epsilon > 0$ sufficiently small such that

$$1 - \frac{\epsilon\lambda_0}{2} > 0, \quad \frac{1}{2} - \frac{\epsilon\lambda_0}{2\delta_0} > 0. \tag{104}$$

Then, choosing N large enough, we have

$$\mathscr{L}'(t) \le -c_2 E(t) + c_3 K^2(t) E(0), \tag{105}$$

where $c_2, c_3 > 0$ and $K(t) = k_1(t) + k_2(t)$. From (93), (96), and (105), we obtain

$$\mathscr{L}'(t) \le -\frac{c_2}{q_1}\mathscr{L}(t) + c_4 c_3 E(0) e^{-2\beta_1 t} \text{ for some } c_4 > 0. \tag{106}$$

By Lemma 9, there exist positive constants c_5 and c_6 such that

$$\mathscr{L}(t) \le (\mathscr{L}(0) + c_5 E(0)) e^{-c_6 t}, \quad \forall t \ge 0. \tag{107}$$

Using (93), we conclude that

$$E(t) \le CE(0) e^{-\omega t}, \quad \forall t \ge 0 \tag{108}$$

for some positive constants C and ω. □

Acknowledgment

This research was supported by the Basic Science Research Program through the National Research Foundation of Korea (NRF) funded by the Ministry of Education, Science and Technology (2012R1A1A3011630).

References

[1] V. Komornik, "On the nonlinear boundary stabilization of Kirchhoff plates," *Nonlinear Differential Equations and Applications*, vol. 1, no. 4, pp. 323–337, 1994.

[2] J. E. Lagnese, *Boundary Stabilization of Thin Plates*, vol. 10, Society for Industrial and Applied Mathematics (SIAM), Philadelphia, Pa, USA, 1989.

[3] I. Lasiecka, "Exponential decay rates for the solutions of Euler-Bernoulli equations with boundary dissipation occurring in the moments only," *Journal of Differential Equations*, vol. 95, no. 1, pp. 169–182, 1992.

[4] J. E. Lagnese, "Asymptotic energy estimates for Kirchhoff plates subject to weak viscoelastic damping," in *Control and Estimation of Distributed Parameter Systems*, vol. 91 of *International Series of Numerical Mathematics*, pp. 211–236, Birkhäuser, Basel, Switzerland, 1989.

[5] J. E. Muñoz Rivera, E. C. Lapa, and R. Barreto, "Decay rates for viscoelastic plates with memory," *Journal of Elasticity*, vol. 44, no. 1, pp. 61–87, 1996.

[6] M. L. Santos, J. Ferreira, D. C. Pereira, and C. A. Raposo, "Global existence and stability for wave equation of Kirchhoff type with memory condition at the boundary," *Nonlinear Analysis. Theory, Methods & Applications*, vol. 54, no. 5, pp. 959–976, 2003.

[7] M. L. Santos and F. Junior, "A boundary condition with memory for Kirchhoff plates equations," *Applied Mathematics and Computation*, vol. 148, no. 2, pp. 475–496, 2004.

[8] J. Y. Park and J. R. Kang, "A boundary condition with memory for the Kirchhoff plate equations with non-linear dissipation," *Mathematical Methods in the Applied Sciences*, vol. 29, no. 3, pp. 267–280, 2006.

[9] R. Benabidallah and J. Ferreira, "Asymptotic behaviour for the nonlinear beam equation in noncylindrical domains," *Communications in Applied Analysis*, vol. 6, no. 2, pp. 219–234, 2002.

[10] M. M. Cavalcanti, V. N. Domingos Cavalcanti, J. Ferreira, and R. Benabidallah, "On global solvability and asymptotic behaviour of a mixed problem for a nonlinear degenerate Kirchhoff model in moving domains," *Bulletin of the Belgian Mathematical Society*, vol. 10, no. 2, pp. 179–196, 2003.

[11] J. Ferreira, M. L. Santos, and M. P. Matos, "Stability for the beam equation with memory in non-cylindrical domains," *Mathematical Methods in the Applied Sciences*, vol. 27, no. 13, pp. 1493–1506, 2004.

[12] J. Ferreira, M. L. Santos, M. P. Matos, and W. D. Bastos, "Exponential decay for Kirchhoff wave equation with nonlocal condition in a noncylindrical domain," *Mathematical and Computer Modelling*, vol. 39, no. 11-12, pp. 1285–1295, 2004.

[13] T. G. Ha and J. Y. Park, "Global existence and uniform decay of a damped Klein-Gordon equation in a noncylindrical domain," *Nonlinear Analysis. Theory, Methods & Applications*, vol. 74, no. 2, pp. 577–584, 2011.

[14] J. Y. Park and J. R. Kang, "Global existence and stability for a von Karman equations with memory in noncylindrical domains," *Journal of Mathematical Physics*, vol. 50, no. 11, Article ID 112701, 13 pages, 2009.

[15] R. Dal Passo and M. Ughi, "Problème de Dirichlet pour une classe d'équations paraboliques non linéaires dégénérées dans des ouverts non cylindriques," *Comptes Rendus des Séances de l'Académie des Sciences*, vol. 308, no. 19, pp. 555–558, 1989.

[16] M. L. Santos, J. Ferreira, and C. A. Raposo, "Existence and uniform decay for a nonlinear beam equation with nonlinearity of Kirchhoff type in domains with moving boundary," *Abstract and Applied Analysis*, no. 8, pp. 901–919, 2005.

[17] M. L. Santos, M. P. C. Rocha, and P. L. O. Braga, "Global solvability and asymptotic behavior for a nonlinear coupled system of viscoelastic waves with memory in a noncylindrical domain," *Journal of Mathematical Analysis and Applications*, vol. 325, no. 2, pp. 1077–1094, 2007.

[18] J. L. Lions and E. Magenes, *Non-Homogeneous Boundary Value Problems and Applications. Vol. I*, Springer, New York, NY, USA, 1972.

Hindawi Publishing Corporation
Abstract and Applied Analysis
Volume 2013, Article ID 234319, 3 pages
http://dx.doi.org/10.1155/2013/234319

Research Article

Combined Exp-Function Ansatz Method and Applications

Gui Mu,[1] Jun Liu,[1] Zhengde Dai,[2] and Xi Liu[3]

[1] *College of Mathematics and Information Science, Qujing Normal University, Qujing 655011, China*
[2] *School of Mathematics and Statics, Yunnan University, Kunming 650091, China*
[3] *School of Information Science and Engineering, Yunnan University, Kunming 650091, China*

Correspondence should be addressed to Zhengde Dai; zhddai2004@yahoo.com.cn

Received 3 November 2012; Accepted 20 May 2013

Academic Editor: Syed Tauseef Mohyud-Din

Our aim is to present a combined Exp-function ansatz method. This method replaces the traditional assumptions of multisolitons by a combination of the hyperbolic functions and triangle functions in Hirota bilinear forms of nonlinear evolution equation. Using this method, we can obtain many new type analytical solutions of various nonlinear evolution equations including multisoliton solutions as well as breath-like solitons solutions. These solutions will exhibit interesting dynamic diversity.

1. Introduction

Up to now, many kinds of integrable nonlinear partial differential equations have been discovered, such as nonlinear Schrodinger equation, KdV equation, Sine-Gordon equation, KP, BKP, coupled KP, and Toda lattice and Toda molecule equations. All of these equations can be transformed into bilinear forms by some special transformations including rational transformation, logarithmic transformation, and bilogarithmic transformation [1]. Once we get the bilinear forms of these equations, one can construct directly their N-soliton solutions following Hirota's basic assumptions. In addition, bilinear forms can be utilized to construct the other kinds of solutions. Lou [2–6] has constructed many localized structures by a variable separation method, and the author of [1] has obtained determinants and pfaffians solutions using the bilinear forms. Recently, Dai et al. [7] proposed the three-wave method for nonlinear evolution equations (NEE). Meanwhile, some fractional differential equations and local fractional equations are studied extensively using different methods [8–10]. Analytical solutions for nonlinear partial differential equations are discussed systematically in [11]. Motivated by the above considerations, we investigate another ansatz and present "combined Exp-function ansatz method" as follows.

Consider a (2 + 1)-dimensional nonlinear evolution equation of the general form

$$F\left(u, u_t, u_x, u_y, \ldots\right) = 0, \tag{1}$$

where F is a polynomial of $u(x, y, t)$ and its derivatives. With the help of rational transformation, logarithmic transformation, and bilogarithmic transformation, for a KdV-type bilinear equation, it has just one dependent variable f. We next consider a bilinear equation of the form

$$G\left(D_t, D_x, D_y, \ldots\right) f \cdot f = 0, \tag{2}$$

where G is a general polynomial in D_t, D_x, D_y, where the D-operator is defined by

$$\begin{aligned} &D_x^m D_t^n F(x, y, t) \cdot G(x, y, t) \\ &\quad = \left(\frac{\partial}{\partial x} - \frac{\partial}{\partial x'}\right)^m \left(\frac{\partial}{\partial t} - \frac{\partial}{\partial t'}\right)^n \\ &\quad \times F(x, y, t)\, G\left(x', y', t'\right)\Big|_{x'=x, y'=y, t'=t}. \end{aligned} \tag{3}$$

Traditionally, one obtains N-soliton solutions with the assumption

$$f = \sum_{\mu=0,1} \exp\left(\sum_{i>j}^{N} A_{ij}\mu_i\mu_j + \sum_{i=1}^{n} \mu_i \xi_i\right). \tag{4}$$

Here, instead of the above assumption, the function f is assumed in terms of cosh functions and cos functions

$$f = \sum_{i=1}^{m} a_i \left(\exp\left(\xi_i\right) + \exp\left(-\xi_i\right)\right) + \sum_{j=1}^{n} b_i \left(\exp\left(i\xi_j\right) + \exp\left(-i\xi_j\right)\right), \tag{5}$$

or equivalently

$$f = 2\sum_{i=1}^{m} a_i \cosh\left(\xi_i\right) + 2\sum_{j=1}^{m} b_i \cos\left(\eta_j\right), \tag{6}$$

where $\xi_i = k_i x + l_i y + c_i t$ and $\eta_i = d_i x + e_i y + f_i t$. In (5), it is seen that real and complex variables coexist in Exp-function; hence, this method is called combined Exp-function ansatz method. To derive analytic expression, we can take the following procedure in detail: inserting (5) into (2), then equating the coefficients of the same kind terms to zero, and subsequently solving the resulting algebraic equations to determine the relationship between variables k_i, $l_i \ldots$ with the help of symbolic computation software such as Maple. In (5), cosh functions are responsible for energy localization, but cosine functions take into account periodic effect in real physical background. If cosh functions and cosine functions coexist, the intensity of periodic effect depends on the scale distance between the coefficients a_i and b_j. When all of the coefficients of cosine functions b_j are equal to zero, (5) corresponds to multisoliton of (1).

2. Application to $(2 + 1)$-Dimensional NLEE Equation

In this section, firstly, we study the $(2 + 1)$-dimensional nonlinear evolution equation

$$u_{xxxy} + 3u_y u_{xx} + 3u_x u_{xy} + 2u_{yt} = 0. \tag{7}$$

In [12], Bekir has studied its Painlevé property. By the independent variable transformation $u = 2(\ln\varphi)_{xx}$, (7) is reduced to Hirota bilinear form

$$\left(D_y D_t + D_x^3 D_y\right)\varphi\cdot\varphi = 0. \tag{8}$$

Firstly, we obtain N-soliton with the aid of Hirota method. To get one-soliton solution, we assume that

$$\phi = 1 + e^{k_1 x + l_1 y + c_1 t}. \tag{9}$$

Inserting (9) into (8), then one-soliton solution can be derived as

$$u(x,t) = \frac{2k_1 e^{k_1 x + l_1 y - k_1^3 t}}{1 + e^{k_1 x + l_1 y - k_1^3 t}}. \tag{10}$$

For the two-soliton solutions, substituting

$$\phi = 1 + e^{k_1 x + l_1 y + c_1 t} + e^{k_2 x + l_2 y + c_2 t} + a_{12} e^{k_1 x + l_1 y + c_1 t + k_2 x + l_2 y + c_2 t} \tag{11}$$

into (8) and solving for the phase shift a_{12}, one can find the two-soliton solutions explicitly. The higher level soliton solutions can be obtained in a parallel manner. Next, we will show how the combined Exp-function ansatz method is used to construct new exact solution of nonlinear evolution equation. In fact, the basic procedure is similar to N-soliton procedure. For simplification, we only present the case for the parameters $m = 2$ and $n = 1$ in (5) to explain our method. That is, we assume in the following form that

$$\varphi = \cosh\left(k_1 x + l_1 y + c_1 t\right) + \cos\left(k_2 x + l_2 y + c_2 t\right) + a_3 \cosh\left(k_3 x + l_3 y + c_3 t\right). \tag{12}$$

Substituting (12) into (8), we have

$$\begin{gathered} c_1 = -k_3^3\left(-1 + 3l_3^2 - 6l_3^2 a_3^2 + 3l_3^4 a_3^2\right), \\ c_2 = k_3^3 l_3\left(1 - a_3^2\right)\left(l_3^2 - 2l_3^2 a_3^2 + a_3^4 l_3^2 - 3\right), \\ c_3 = k_3^3\left(-1 + 3l_3^2 - 6l_3^2 a_3^2 + 3a_3^4 l_3^2\right), \\ k_1 = -k_3, \qquad k_2 = l_3 k_3\left(1 - a_3^2\right), \\ l_2 = 1, \qquad l_1 = l_3, \end{gathered} \tag{13}$$

where l_3, a_3, and k_3 are free parameters. This case leads to a breath-kink solitary solution

$$\begin{aligned} u(x,t) = {} & (2(k_1 \sin(k_1 x + l_1 y + c_1 t) \\ & - k_2 \sin(k_2 x + l_2 y + c_2 t) \\ & + a_3 k_3 \sin(k_3 x + l_3 y + c_3 t))) \\ & \times (\cosh(k_1 x + l_1 y + c_1 t) + \cos(k_2 x + l_2 y + c_2 t) \\ & + a_3 \cosh(k_3 x + l_3 y + c_3 t))^{-1}. \end{aligned} \tag{14}$$

The dynamics of this family of solutions will breathe periodically in the process of propagation of the soliton resulting from cosine function. In order to explain the university of our method, next, we continue to consider the $(2 + 1)$-dimensional AKNS equation

$$4u_{xt} + u_{xxxy} + 8u_x u_{xy} + 4u_y u_{xx} = 0. \tag{15}$$

Taking the transformation $u = (\ln\varphi)_x$, (15) leads to multibilinear form

$$\begin{gathered} \left(4D_x D_t + D_x^3 D_y\right)\varphi\cdot\varphi = 0, \\ D_x(\ln f)_{xx}\cdot(\ln f)_{xy} = 0. \end{gathered} \tag{16}$$

According to the one-soliton assumption, the one-soliton solution of $(2 + 1)$-dimensional AKNS equation is derived as

$$u(x,t) = \frac{k_1 e^{k_1 x + l_1 y - (1/4) l_1 {k_1}^2 t}}{1 + e^{k_1 x + l_1 y - (1/4) l_1 {k_1}^2 t}}. \tag{17}$$

For the two-soliton solutions which can be obtained following the assumption in (16)

$$\varphi = 1 + e^{k_1x+l_1y+c_1t} + e^{k_2x+l_2y+c_2t} + a_{12}e^{k_1x+l_1y+c_1t+k_2x+l_2y+c_2t}, \tag{18}$$

we have

$$a_{12} = \frac{(k_1 - k_2)\left(l_2k_1^2 + 2l_1k_1k_2 - 2l_2k_1k_2 - l_1k_2^2\right)}{(k_1 + k_2)\left(l_2k_1^2 + 2l_1k_1k_2 + 2l_2k_1k_2 + l_1k_2^2\right)}. \tag{19}$$

In addition,

$$l_1k_2 - l_2k_1 = 0. \tag{20}$$

Thus, we found the two-soliton solutions explicitly

$$\begin{aligned} u(x,t) = {} & \Big(k_1e^{k_1x+l_1y-(1/4)l_1k_1{}^2t} + k_2e^{k_2x+l_2y-(1/4)l_2k_2{}^2t} \\ & +a_{12}(k_1+k_2)\,e^{k_1x+l_1y-(1/4)l_1k_1{}^2t+k_2x+l_2y-(1/4)l_2k_2{}^2t}\Big) \\ & \times\Big(1 + e^{k_1x+l_1y-(1/4)l_1k_1{}^2t} + e^{k_2x+l_2y-(1/4)l_2k_2{}^2t} \\ & +a_{12}e^{k_1x+l_1y-(1/4)l_1k_1{}^2t+k_2x+l_2y-(1/4)l_2k_2{}^2t}\Big)^{-1}. \end{aligned} \tag{21}$$

Similarly, the higher order soliton solutions can be examined in a parallel manner. Finally, following the procedure of combined Exp-function ansatz method, the two periodic solutions of AKNS equation can be obtained by setting $m = 2$ and $n = 1$in (5) in the following form:

$$\varphi = \cos\left(kx + ly + \left(2k^2l - c\right)t\right) + \cos\left(kx + ly + ct\right), \tag{22}$$

where l and k are free parameters. This case leads to a family of double periodic solutions as

$$\begin{aligned} u(x,t) = {} & \Big(-k\sin\left(kx + ly + \left(2k^2l - c\right)t\right) \\ & +k\sin\left(kx + ly + ct\right)\Big) \\ & \times\Big(\cos\left(kx + ly + \left(2k^2l - c\right)t\right) \\ & + \cos\left(kx + ly + ct\right)\Big)^{-1}. \end{aligned} \tag{23}$$

The above solutions are given out for the first time in the literature.

3. Conclusions

Generally, N-soliton solution can be constructed after one obtains multilinear form of nonlinear evolution equations according to Hirota method. In this paper, we proposed a different ansatz method which is composed of complex and real exponential functions. This method allows us to construct multiple kinds of solutions, such as N-soliton solutions and breath-type solitary solutions. By taking two (2 + 1)-dimensional nonlinear evolution equations as examples, it is shown that this method is effective and direct for constructing new exact solutions of nonlinear integrable partial differential equations.

Acknowledgments

The work was supported by the Chinese Natural Science Foundation Grant no. 11061028, Yunnan NSF Grant no. 2010CD086, and Qujin Normal University NSF Grant no. 2010QN018.

References

[1] R. Hirota, *The Direct Method in Soliton Theory*, vol. 155 of *Cambridge Tracts in Mathematics*, Cambridge University Press, Cambridge, UK, 2004.

[2] S.-Y. Lou, "Searching for higher-dimensional integrable models from lower ones via Painlevé analysis," *Physical Review Letters*, vol. 80, no. 23, pp. 5027–5031, 1998.

[3] S.-Y. Lou, "Dromions, dromion lattice, breathers and instantons of the Davey-Stewartson equation," *Physica Scripta*, vol. 65, no. 1, pp. 7–12, 2002.

[4] S.-Y. Lou, "On the coherent structures of the Nizhnik-Novikov-Veselov equation," *Physics Letters A*, vol. 277, no. 2, pp. 94–100, 2000.

[5] S.-Y. Lou and H.-Y. Ruan, "Revisitation of the localized excitations of the (2 + 1)-dimensional KdV equation," *Journal of Physics. A. Mathematical and General*, vol. 34, no. 2, pp. 305–316, 2001.

[6] S.-Y. Lou, J. Lin, and X.-Y. Tang, "Painlevé integrability and multi-dromion solutions of the 2 + 1 dimensional AKNS system," *The European Physical Journal. B. Condensed Matter Physics*, vol. 22, no. 4, pp. 473–478, 2001.

[7] Z. D. Dai, C. J. Wang, S. Q. Lin, D. L. Li, and G. Mu, "The three-wave method for nonlinear evolution equations," *Nonlinear Science Letters A*, vol. 1, no. 1, pp. 77–82, 2010.

[8] H. Jafari and H. Tajadodi, "He's variational iteration method for solving fractional Riccati differential equation," *International Journal of Differential Equations*, vol. 2012, Article ID 764738, 8 pages, 2010.

[9] K. Li, J. Peng, and J. Jia, "Cauchy problems for fractional differential equations with Riemann-Liouville fractional derivatives," *Journal of Functional Analysis*, vol. 263, no. 2, pp. 476–510, 2012.

[10] J. J. Mohan and G. V. S. R. Deekshitulu, "Fractional order difference equations," *International Journal of Differential Equations*, vol. 2012, Article ID 780619, 11 pages, 2012.

[11] R. Ellahi and A. Zeeshan, *Analytical Solutions for Nonlinear Partial Differential Equations*, LAMBERT Academic Publishing GmbH, Saarbrücken, Germany, 2012, http://www.amazon.com/Analytical-Solutions-non-Linear-Differential-Equations/dp/3846524158.

[12] A. Bekir, "Painlevé test for some (2 + 1)-dimensional nonlinear equations," *Chaos, Solitons and Fractals*, vol. 32, no. 2, pp. 449–455, 2007.

Hindawi Publishing Corporation
Abstract and Applied Analysis
Volume 2013, Article ID 202650, 6 pages
http://dx.doi.org/10.1155/2013/202650

Research Article

A Local Fractional Variational Iteration Method for Laplace Equation within Local Fractional Operators

Yong-Ju Yang,[1] Dumitru Baleanu,[2,3,4] and Xiao-Jun Yang[5,6]

[1] *School of Mathematics and Statistics, Nanyang Normal University, Nanyang 4730 61, China*
[2] *Department of Mathematics and Computer Sciences, Faculty of Arts and Sciences, Çankaya University, 06530 Ankara, Turkey*
[3] *Department of Chemical and Materials Engineering, Faculty of Engineering, King Abdulaziz University, P.O. Box 80204, Jeddah 21589, Saudi Arabia*
[4] *Institute of Space Sciences, Magurele, RO-077125 Bucharest, Romania*
[5] *Institute of Software Science, Zhengzhou Normal University, Zhengzhou 450044, China*
[6] *Department of Mathematics and Mechanics, China University of Mining and Technology, Xuzhou 221008, China*

Correspondence should be addressed to Xiao-Jun Yang; dyangxiaojun@163.com

Received 15 November 2012; Accepted 27 February 2013

Academic Editor: Syed Tauseef Mohyud-Din

The local fractional variational iteration method for local fractional Laplace equation is investigated in this paper. The operators are described in the sense of local fractional operators. The obtained results reveal that the method is very effective.

1. Introduction

As it is known, the partial differential equations [1, 2] and fractional differential equations [3–5] appear in many areas of science and engineering. As a result, various kinds of analytical methods and numerical methods were developed [6–8]. For example, the variational iteration method [9–15] was applied to solve differential equations [16–18], integral equations [19], and numerous applications to different nonlinear equations in physics and engineering. Also, the fractional variational iteration method [20–23] and the fractional complex transform [24–27] were discussed recently. The efficient techniques have successfully addressed a wide class of nonlinear problems for differential equations; see [28–36] and the references therein. We notice that the developed methods are very convenient, efficient, and accurate.

Recently, the local fractional variational iteration method [37] is derived from local fractional operators [38–48]. The method, which accurately computes the solutions in a local fractional series form or in an exact form, presents interest to applied sciences for problems where the other methods cannot be applied properly.

In this paper, we investigate the application of local fractional variational iteration method for solving the local fractional Laplace equations [49] with the different fractal conditions.

This paper is organized as follows.

In Section 2, the basic mathematical tools are reviewed. Section 3 presents briefly the local fractional variational iteration method based on local fractional variational for fractal Lagrange multipliers. Section 4 presents solutions to the local fractional Laplace equations with differential fractal conditions.

2. Mathematical Fundamentals

In this section, we present few mathematical fundamentals of local fractional calculus and introduce the basic notions of local fractional continuity, local fractional derivative, and local fractional integral of nondifferential functions.

2.1. Local Fractional Continuity

Lemma 1 (see [42]). *Let F be a subset of the real line and a fractal. If $f : (F, d) \to (\Omega', d')$ is a bi-Lipschitz mapping, then there is, for constants $\rho, \tau > 0$ and $F \subset R$,*

$$\rho^s H^s(F) \le H^s(f(F)) \le \tau^s H^s(F) \tag{1}$$

such that for all $x_1, x_2 \in F$,

$$\rho^\alpha |x_1 - x_2|^\alpha \le |f(x_1) - f(x_2)| \le \tau^\alpha |x_1 - x_2|^\alpha. \tag{2}$$

As a direct result of Lemma 1, one has [42]

$$|f(x_1) - f(x_2)| \le \tau^\alpha |x_1 - x_2|^\alpha \tag{3}$$

such that

$$|f(x_1) - f(x_2)| < \varepsilon^\alpha, \tag{4}$$

where α is fractal dimension of F.

Suppose that there is [38–43]

$$|f(x) - f(x_0)| < \varepsilon^\alpha \tag{5}$$

with $|x - x_0| < \delta$, for ε, $\delta > 0$ and $\varepsilon, \delta \in R$, then $f(x)$ is called local fractional continuous at $x = x_0$ and it is denoted by

$$\lim_{x \to x_0} f(x) = f(x_0). \tag{6}$$

Suppose that the function $f(x)$ is satisfied the condition (5) *for $x \in (a, b)$, and hence it is called a local fractional continuous on the interval (a, b), denoted by*

$$f(x) \in C_\alpha(a, b). \tag{7}$$

2.2. Local Fractional Derivatives and Integrals. Suppose that $f(x) \in C_\alpha(a, b)$, then the local fractional derivative of $f(x)$ of order α at $x = x_0$ is given by [37–43]

$$\begin{aligned} D_x^{(\alpha)} f(x_0) = f^{(\alpha)}(x_0) &= \left.\frac{d^\alpha f(x)}{dx^\alpha}\right|_{x=x_0} \\ &= \lim_{x \to x_0} \frac{\Delta^\alpha (f(x) - f(x_0))}{(x - x_0)^\alpha}, \end{aligned} \tag{8}$$

where $\Delta^\alpha(f(x) - f(x_0)) \cong \Gamma(1 + \alpha)\Delta(f(x) - f(x_0))$.

There is [38–40]

$$f(x) \in D_x^{(\alpha)}(a, b) \tag{9}$$

if

$$f^{(\alpha)}(x) = D_x^{(\alpha)} f(x) \tag{10}$$

for any $x \in (a, b)$.

Local fractional derivative of high order is written in the form [38–40]

$$f^{(k\alpha)}(x) = \overbrace{D_x^{(\alpha)} \cdots D_x^{(\alpha)}}^{k\text{ times}} f(x), \tag{11}$$

and local fractional partial derivative of high order is [38–40]

$$\frac{\partial^{k\alpha}}{\partial x^{k\alpha}} f(x) = \overbrace{\frac{\partial^\alpha}{\partial x^\alpha} \cdots \frac{\partial^\alpha}{\partial x^\alpha}}^{k\text{ times}} f(x). \tag{12}$$

Let a function $f(x)$ satisfy the condition (7). Local fractional integral of $f(x)$ of order α in the interval $[a, b]$ is given by [37–43]

$$\begin{aligned} {}_aI_b^{(\alpha)} f(x) &= \frac{1}{\Gamma(1 + \alpha)} \int_a^b f(t)(dt)^\alpha \\ &= \frac{1}{\Gamma(1 + \alpha)} \lim_{\Delta t \to 0} \sum_{j=0}^{j=N-1} f(t_j)(\Delta t_j)^\alpha, \end{aligned} \tag{13}$$

where $\Delta t_j = t_{j+1} - t_j$, $\Delta t = \max\{\Delta t_1, \Delta t_2, \Delta t_j, \ldots\}$, and $[t_j, t_{j+1}]$, $j = 0, \ldots, N - 1$, $t_0 = a$, $t_N = b$, is a partition of the interval $[a, b]$. For other definition of local fractional derivative, see [44–48].

There exists [38–40]

$$f(x) \in I_x^{(\alpha)}(a, b) \tag{14}$$

if

$$f^{(\alpha)}(x) = {}_aI_x^{(\alpha)} f(x) \tag{15}$$

for any $x \in (a, b)$.

Local fractional multiple integrals of $f(x)$ is written in the form [40]

$${}_{x_0}I_x^{(k\alpha)} f(x) = \overbrace{{}_{x_0}I_x^{(\alpha)} \cdots {}_{x_0}I_x^{(\alpha)}}^{k\text{ times}} f(x) \tag{16}$$

if (7) is valid for $x \in (a, b)$.

3. Local Fractional Variational Iteration Method

In this section, we introduce the local fractional variational iteration method derived from the local fractional variational approach for fractal Lagrange multipliers [40].

Let us consider the local fractional variational approach in the one-dimensional case through the following local fractional functional, which reads [40]

$$I(y) = {}_aI_b^{(\alpha)} f(x, y(x), y^{(\alpha)}(x)), \tag{17}$$

where $y^{(\alpha)}(x)$ is taken in local fractional differential operator and $a \le x \le b$.

The local fractional variational derivative is given by [40]

$$\delta^\alpha I = {}_aI_b^{(\alpha)} \left\{ \left(\frac{\partial f}{\partial y} - \frac{d^\alpha}{dx^\alpha} \left(\frac{\partial f}{\partial y^{(\alpha)}} \right) \right) \eta(x) \right\}, \tag{18}$$

where δ^α is local fractional variation signal and $\eta(a) = \eta(b) = 0$.

The nonlinear local fractional equation reads as

$$L_\alpha u + N_\alpha u = 0, \tag{19}$$

where L_α and N_α are linear and nonlinear local fractional operators, respectively.

Local fractional variational iteration algorithm can be written as [37]

$$u_{n+1}(t) = u_n(t) + {}_{t_0}I_t^{(\alpha)} \{\xi^\alpha [L_\alpha u_n(s) + N_\alpha u_n(s)]\}. \tag{20}$$

Here, we can construct a correction functional as follows [37]:

$$u_{n+1}(t) = u_n(t) + {}_{t_0}I_t^{(\alpha)} \{\xi^\alpha [L_\alpha u_n(s) + N_\alpha \tilde{u}_n(s)]\}, \tag{21}$$

where $\tilde{u}_n$ is considered as a restricted local fractional variation and ξ^α is a fractal Lagrange multiplier; that is, $\delta^\alpha \tilde{u}_n = 0$ [37, 40].

Having determined the fractal Lagrangian multipliers, the successive approximations u_{n+1}, $n \geq 0$, of the solution u will be readily obtained upon using any selective fractal function u_0. Consequently, we have the solution

$$u = \lim_{n\to\infty} u_n. \tag{22}$$

Here, this technology is called the local fractional variational method [37]. We notice that the classical variation is recovered in case of local fractional variation when the fractal dimension is equal to 1. Besides, the convergence of local fractional variational process and its algorithms were taken into account [37].

4. Solutions to Local Fractional Laplace Equation in Fractal Timespace

The local fractional Laplace equation (see [38–40] and the references therein) is one of the important differential equations with local fractional derivatives. In the following, we consider solutions to local fractional Laplace equations in fractal timespace.

Case 1. Let us start with local fractional Laplace equation given by

$$\frac{\partial^{2\alpha} T(x,t)}{\partial t^{2\alpha}} + \frac{\partial^{2\alpha} T(x,t)}{\partial x^{2\alpha}} = 0 \tag{23}$$

and subject to the fractal value conditions

$$\frac{\partial^\alpha}{\partial t^\alpha} T(x,0) = 0, \quad T(x,0) = -E_\alpha(x^\alpha). \tag{24}$$

A corrected local fractional functional for (24) reads as

$$\begin{aligned} u_{n+1}(x,t) &= u_n(x,t) \\ &\quad + {}_0I_t^{(\alpha)} \left\{ \frac{\lambda^\alpha}{\Gamma(1+\alpha)} \left(\frac{\partial^{2\alpha} T_n(x,\tau)}{\partial \tau^{2\alpha}} + \frac{\partial^{2\alpha} T_n(x,\tau)}{\partial x^{2\alpha}} \right) \right\}. \end{aligned} \tag{25}$$

Taking into account the properties of the local fractional derivative, we obtain

$$\begin{aligned} \delta^\alpha u_{n+1}(x,t) &= \delta^\alpha u_n(x,t) \\ &\quad + \delta^\alpha {}_0I_t^{(\alpha)} \left\{ \frac{\lambda^\alpha}{\Gamma(1+\alpha)} \left(\frac{\partial^{2\alpha} T_n(x,\tau)}{\partial \tau^{2\alpha}} + \frac{\partial^{2\alpha} T_n(x,\tau)}{\partial x^{2\alpha}} \right) \right\}. \end{aligned} \tag{26}$$

Hence, from (25)-(26) we get

$$\begin{aligned} \delta^\alpha u_{n+1}(x,t) &= \delta^\alpha u_n(x,t) + \frac{\lambda^\alpha}{\Gamma(1+\alpha)} \delta^\alpha u_n^{(\alpha)}(x,t) \Big|_{\tau=t} \\ &\quad - \left[\frac{\lambda^\alpha}{\Gamma(1+\alpha)} \right]^{(\alpha)} \delta^\alpha u_n(x,t) \Big|_{\tau=t} \\ &\quad - (\delta^\alpha u_n(x,\tau))\, {}_0I_t^{(\alpha)} \left(\frac{\lambda^\alpha}{\Gamma(1+\alpha)} \right)^{(2\alpha)} \\ &= \delta^\alpha u_n(x,t) + \frac{\lambda^\alpha}{\Gamma(1+\alpha)} \delta^\alpha u_n^{(\alpha)} \Big|_{\tau=t} \\ &\quad - \left(\frac{\lambda^\alpha}{\Gamma(1+\alpha)} \right)^{(\alpha)} \delta^\alpha u_n(x,t) \Big|_{\tau=t} \\ &\quad + (\delta^\alpha u_n(x,\tau))\, {}_0I_t^{(\alpha)} \left(\frac{\lambda^\alpha}{\Gamma(1+\alpha)} \right)^{(2\alpha)} = 0. \end{aligned} \tag{27}$$

As a result, from (27) we can derive

$$\begin{gathered} \left(\frac{\lambda^\alpha}{\Gamma(1+\alpha)} \right)^{(2\alpha)} = 0, \qquad \frac{\lambda^\alpha}{\Gamma(1+\alpha)} \Big|_{\tau=t} = 0, \\ \left(\frac{\lambda^\alpha}{\Gamma(1+\alpha)} \right)^{(\alpha)} = 1. \end{gathered} \tag{28}$$

We have $\lambda = \tau - t$ such that the fractal Lagrange multiplier reads as

$$\frac{\lambda^\alpha}{\Gamma(1+\alpha)} = \frac{(\tau - t)^\alpha}{\Gamma(1+\alpha)}. \tag{29}$$

From (24) we take the initial value, which reads as

$$u_0(x,t) = -E_\alpha(x^\alpha). \tag{30}$$

By using (25) we structure a local fractional iteration procedure as

$$\begin{aligned} u_{n+1}(x,t) &= u_n(x,t) \\ &\quad + {}_0I_t^{(\alpha)} \left\{ \frac{(\tau - t)^\alpha}{\Gamma(1+\alpha)} \left(\frac{\partial^{2\alpha} T_n(x,\tau)}{\partial \tau^{2\alpha}} + \frac{\partial^{2\alpha} T_n(x,\tau)}{\partial x^{2\alpha}} \right) \right\}. \end{aligned} \tag{31}$$

Hence, we can derive the first approximation term as

$$\begin{aligned} u_1(x,t) &= u_0(x,t) \\ &\quad + {}_0I_t^{(\alpha)}\left\{\frac{(\tau-t)^\alpha}{\Gamma(1+\alpha)}\left(\frac{\partial^{2\alpha}T_0(x,\tau)}{\partial\tau^{2\alpha}}+\frac{\partial^{2\alpha}T_0(x,\tau)}{\partial x^{2\alpha}}\right)\right\} \\ &= -E_\alpha(x^\alpha) + {}_0I_t^{(\alpha)}\left\{\frac{(\tau-t)^\alpha}{\Gamma(1+\alpha)}(-E_\alpha(x^\alpha))\right\} \\ &= E_\alpha(x^\alpha)\left(-1+\frac{t^{2\alpha}}{\Gamma(1+2\alpha)}\right). \end{aligned} \tag{32}$$

The second approximation can be calculated in the similar way, which is

$$\begin{aligned} u_2(x,t) &= u_1(x,t) \\ &\quad + {}_0I_t^{(\alpha)}\left\{\frac{(\tau-t)^\alpha}{\Gamma(1+\alpha)}\left(\frac{\partial^{2\alpha}T_1(x,\tau)}{\partial\tau^{2\alpha}}+\frac{\partial^{2\alpha}T_1(x,\tau)}{\partial x^{2\alpha}}\right)\right\} \\ &= E_\alpha(x^\alpha)\left(-1+\frac{t^{2\alpha}}{\Gamma(1+2\alpha)}\right) \\ &\quad + {}_0I_t^{(\alpha)}\left\{\frac{(\tau-t)^\alpha}{\Gamma(1+\alpha)}\left(\frac{t^{2\alpha}E_\alpha(x^\alpha)}{\Gamma(1+2\alpha)}\right)\right\} \\ &= E_\alpha(x^\alpha)\left(-1+\frac{t^{2\alpha}}{\Gamma(1+2\alpha)}-\frac{t^{4\alpha}}{\Gamma(1+4\alpha)}\right). \end{aligned} \tag{33}$$

Proceeding in this manner, we get

$$u_n(x,t) = E_\alpha(x^\alpha)\left(\sum_{k=0}^{n}(-1)^k\frac{t^{2k\alpha}}{\Gamma(1+2k\alpha)}\right). \tag{34}$$

Thus, the final solution reads as

$$\begin{aligned} u(x,t) &= \lim_{n\to\infty} u_n(x,t) \\ &= E_\alpha(x^\alpha)\left(\sum_{k=0}^{\infty}(-1)^k\frac{t^{2k\alpha}}{\Gamma(1+2k\alpha)}\right) \\ &= -E_\alpha(x^\alpha)\cos_\alpha(t^\alpha). \end{aligned} \tag{35}$$

Case 2. Consider the local fractional Laplace equation as

$$\frac{\partial^{2\alpha}T(x,t)}{\partial t^{2\alpha}}+\frac{\partial^{2\alpha}T(x,t)}{\partial x^{2\alpha}}=0 \tag{36}$$

subject to fractal value conditions given by

$$\frac{\partial^\alpha}{\partial t^\alpha}T(x,0) = -E_\alpha(x^\alpha), \quad T(x,0)=0. \tag{37}$$

Now we can structure the same local fractional iteration procedure (31).

By using (36)-(37) we take an initial value as

$$u_0(x,t) = -\frac{t^\alpha E_\alpha(x^\alpha)}{\Gamma(1+\alpha)}. \tag{38}$$

The first approximation term reads as

$$\begin{aligned} u_1(x,t) &= u_0(x,t) \\ &\quad + {}_0I_t^{(\alpha)}\left\{\frac{(\tau-t)^\alpha}{\Gamma(1+\alpha)}\left(\frac{\partial^{2\alpha}T_0(x,\tau)}{\partial\tau^{2\alpha}}+\frac{\partial^{2\alpha}T_0(x,\tau)}{\partial x^{2\alpha}}\right)\right\} \\ &= -\frac{t^\alpha E_\alpha(x^\alpha)}{\Gamma(1+\alpha)} + {}_0I_t^{(\alpha)}\left\{\frac{(\tau-t)^\alpha}{\Gamma(1+\alpha)}\left(-\frac{t^\alpha E_\alpha(x^\alpha)}{\Gamma(1+\alpha)}\right)\right\} \\ &= -\frac{t^\alpha E_\alpha(x^\alpha)}{\Gamma(1+\alpha)} + \frac{t^{3\alpha}E_\alpha(x^\alpha)}{\Gamma(1+3\alpha)}. \end{aligned} \tag{39}$$

In the same manner, the second approximation is given by

$$\begin{aligned} u_2(x,t) &= u_1(x,t) \\ &\quad + {}_0I_t^{(\alpha)}\left\{\frac{(\tau-t)^\alpha}{\Gamma(1+\alpha)}\left(\frac{\partial^{2\alpha}T_1(x,\tau)}{\partial\tau^{2\alpha}}+\frac{\partial^{2\alpha}T_1(x,\tau)}{\partial x^{2\alpha}}\right)\right\} \\ &= -\frac{t^\alpha E_\alpha(x^\alpha)}{\Gamma(1+\alpha)} + \frac{t^{3\alpha}E_\alpha(x^\alpha)}{\Gamma(1+3\alpha)} \\ &\quad + {}_0I_t^{(\alpha)}\left\{\frac{(\tau-t)^\alpha}{\Gamma(1+\alpha)}\left(\frac{t^{3\alpha}E_\alpha(x^\alpha)}{\Gamma(1+3\alpha)}\right)\right\} \\ &= -\frac{t^\alpha E_\alpha(x^\alpha)}{\Gamma(1+\alpha)} + \frac{t^{3\alpha}E_\alpha(x^\alpha)}{\Gamma(1+3\alpha)} - \frac{t^{5\alpha}E_\alpha(x^\alpha)}{\Gamma(1+5\alpha)}. \end{aligned} \tag{40}$$

Finally, we can obtain the local fractional series solution as follows:

$$u_n(x,t) = E_\alpha(x^\alpha)\left(\sum_{k=0}^{n}(-1)^k\frac{t^{(2k+1)\alpha}}{\Gamma(1+(2k+1)\alpha)}\right). \tag{41}$$

Thus, the expression of the final solution is given by

$$\begin{aligned} u(x,t) &= \lim_{n\to\infty} u_n(x,t) \\ &= E_\alpha(x^\alpha)\left(\sum_{i=0}^{\infty}(-1)^k\frac{t^{(2k+1)\alpha}}{\Gamma(1+(2k+1)\alpha)}\right) \\ &= -E_\alpha(x^\alpha)\sin_\alpha(t^\alpha). \end{aligned} \tag{42}$$

As is known, the Mittag-Leffler function in fractal space can be written in the form

$$\begin{aligned} &\left|E_\alpha(x^\alpha)-E_\alpha(x_0^\alpha)\right| \le E_\alpha(x_0^\alpha)\left|x-x_0\right|^\alpha < \varepsilon^\alpha, \\ &\left|\sin_\alpha(t^\alpha)-\sin_\alpha(t_0^\alpha)\right| < \left|\cos_\alpha(x_0^\alpha)\right|\left|t-t_0\right|^\alpha < \varepsilon^\alpha. \end{aligned} \tag{43}$$

Hence, the fractal dimensions of both $E_\alpha(x^\alpha)$ and $\cos_\alpha(t^\alpha)$ are equal to α.

5. Conclusions

Local fractional calculus is set up on fractals and the local fractional variational iteration method is derived from local fractional calculus. This new technique is efficient for the applied scientists to process these differential and integral equations with the local fractional operators. The variational iteration method [9–19, 27] is derived from fractional calculus and classical calculus; the fractional variational iteration method [20–22, 27] is derived from the modified fractional derivative, while the local fractional variational iteration method [37] is derived from the local fractional calculus [37–43]. Other methods for local fractional ordinary and partial differential equations were considered in [27].

In this paper, two outstanding examples of applications of the local fractional variational iteration method to the local fractional Laplace equations are investigated in detail. The reliable obtained results are complementary with the ones presented in the literature.

References

[1] R. D. Driver, *Ordinary and Delay Differential Equations*, Springer, Berlin, Germany, 1977.

[2] A. M. Wazwaz, *Partial Differential Equations: Methods and Applications*, Balkema Publishers, Leiden, The Netherlands, 2002.

[3] I. Podlubny, *Fractional Differential Equations*, Academic Press, New York, NY, USA, 1999.

[4] R. Hilfer, *Applications of Fractional Calculus in Physics*, World Scientific Publishing, Singapore, 2000.

[5] A. A. Kilbas, H. M. Srivastava, and J. J. Trujillo, *Theory and Applications of Fractional Differential Equations*, Elsevier, Amsterdam, The Netherlands, 2006.

[6] G. Adomian, *Solving Frontier Problems of Physics: The Decomposition Method*, Kluwer Academic Publishers, Boston, Mass, USA, 1994.

[7] D. Baleanu, K. Diethelm, E. Scalas, and J. J. Trujillo, *Fractional Calculus Models and Numerical Methods*, vol. 3 of *Series on Complexity, Nonlinearity and Chaos*, World Scientific Publishing, 2012.

[8] A.-M. Wazwaz, *A First Course in Integral Equations*, World Scientific Publishing, Singapore, 1997.

[9] J.-H. He, "Variational iteration method for autonomous ordinary differential systems," *Applied Mathematics and Computation*, vol. 114, no. 2-3, pp. 115–123, 2000.

[10] J.-H. He, "Variational approach for nonlinear oscillators," *Chaos, Solitons & Fractals*, vol. 34, no. 5, pp. 1430–1439, 2007.

[11] J. H. He, "Variational iteration method—a kind of non-linear analytical technique: some examples," *International Journal of Non-Linear Mechanics*, vol. 34, no. 4, pp. 699–708, 1999.

[12] J. H. He, "Comment on variational iteration method for fractional calculus using He's polynomials," *Abstract and Applied Analysis*, vol. 2012, Article ID 964974, 2 pages, 2012.

[13] S. T. Mohyud-Din, M. A. Noor, K. I. Noor, and M. M. Hosseini, "Solution of singular equation by He's variational iteration method," *International Journal of Nonlinear Sciences and Numerical Simulation*, vol. 11, no. 2, pp. 81–86, 2010.

[14] J.-H. He, "Some asymptotic methods for strongly nonlinear equations," *International Journal of Modern Physics B*, vol. 20, no. 10, pp. 1141–1199, 2006.

[15] J. H. He, G. C. Wu, and F. Austin, "The variational iteration method which should be followed," *Nonlinear Science Letters A*, vol. 1, no. 1, pp. 1–30, 2010.

[16] M. Tatari and M. Dehghan, "He's variational iteration method for computing a control parameter in a semi-linear inverse parabolic equation," *Chaos, Solitons & Fractals*, vol. 33, no. 2, pp. 671–677, 2007.

[17] S. Momani and S. Abuasad, "Application of He's variational iteration method to Helmholtz equation," *Chaos, Solitons & Fractals*, vol. 27, no. 5, pp. 1119–1123, 2006.

[18] Z. M. Odibat and S. Momani, "Application of variational iteration method to nonlinear differential equations of fractional order," *International Journal of Nonlinear Sciences and Numerical Simulation*, vol. 7, no. 1, pp. 27–34, 2006.

[19] L. Xu, "Variational iteration method for solving integral equations," *Computers & Mathematics with Applications*, vol. 54, no. 7-8, pp. 1071–1078, 2007.

[20] J.-H. He, "A short remark on fractional variational iteration method," *Physics Letters A*, vol. 375, no. 38, pp. 3362–3364, 2011.

[21] G.-c. Wu and E. W. M. Lee, "Fractional variational iteration method and its application," *Physics Letters A*, vol. 374, no. 25, pp. 2506–2509, 2010.

[22] Y. Khan, N. Faraz, A. Yildirim, and Q. Wu, "Fractional variational iteration method for fractional initial-boundary value problems arising in the application of nonlinear science," *Computers & Mathematics with Applications*, vol. 62, no. 5, pp. 2273–2278, 2011.

[23] J.-H. He, S. K. Elagan, and Z. B. Li, "Geometrical explanation of the fractional complex transform and derivative chain rule for fractional calculus," *Physics Letters A*, vol. 376, no. 4, pp. 257–259, 2012.

[24] Z. B. Li and J. H. He, "Application of the fractional complex transform to fractional differential equations," *Nonlinear Science Letters A*, vol. 2, no. 3, pp. 121–126, 2011.

[25] Z. B. Li, W. H. Zhu, and J. H. He, "Exact solutions of time-fractional heat conduction equation by the fractional complex transform," *Thermal Science*, vol. 16, no. 2, pp. 335–338, 2012.

[26] Q. L. Wang, J. H. He, and Z. B. Li, "Fractional model for heat conduction in polar bear hairs," *Thermal Science*, vol. 16, no. 2, pp. 339–342, 2012.

[27] J. H. He, "Asymptotic methods for solitary solutions and compactons," *Abstract and Applied Analysis*, vol. 2012, Article ID 916793, 130 pages, 2012.

[28] S. T. Mohyud-Din, A. Yildirim, and G. Demirli, "Analytical solution of wave system in R^n with coupling controllers," *International Journal of Numerical Methods for Heat & Fluid Flow*, vol. 21, no. 2, pp. 198–205, 2011.

[29] S. T. Mohyud-Din, A. Yıldırım, and S. Sarıaydın, "Numerical soliton solution of the Kaup-Kupershmidt equation," *International Journal of Numerical Methods for Heat & Fluid Flow*, vol. 21, no. 3-4, pp. 272–281, 2011.

[30] S. T. Mohyud-Din, A. Yıldırım, and S. A. Sezer, "Numerical soliton solutions of improved Boussinesq equation," *International Journal of Numerical Methods for Heat & Fluid Flow*, vol. 21, no. 6-7, pp. 822–827, 2011.

[31] M. A. Abdou, A. A. Soliman, and S. T. El-Basyony, "New application of Exp-function method for improved Boussinesq equation," *Physics Letters A*, vol. 369, no. 5-6, pp. 469–475, 2007.

[32] S. A. El-Wakil, M. A. Madkour, and M. A. Abdou, "Application of Exp-function method for nonlinear evolution equations with variable coefficients," *Physics Letters A*, vol. 369, no. 1-2, pp. 62–69, 2007.

[33] J. H. He, "An elementary introduction to recently developed asymptotic methods and nanomechanics in textile engineering," *International Journal of Modern Physics B*, vol. 22, no. 21, pp. 3487–3578, 2008.

[34] S. T. Mohyud-Din, M. A. Noor, and K. I. Noor, "Some relatively new techniques for nonlinear problems," *Mathematical Problems in Engineering*, vol. 2009, Article ID 234849, 25 pages, 2009.

[35] W.-X. Ma, H. Wu, and J. He, "Partial differential equations possessing Frobenius integrable decompositions," *Physics Letters A*, vol. 364, no. 1, pp. 29–32, 2007.

[36] W. X. Ma and Y. You, "Rational solutions of the Toda lattice equation in Casoratian form," *Chaos, Solitons and Fractals*, vol. 22, no. 2, pp. 395–406, 2004.

[37] X. J. Yang and D. Baleanu, "Fractal heat conduction problem solved by local fractional variation iteration method," *Thermal Science*, 2012.

[38] X. J. Yang, "Local fractional integral transforms," *Progress in Nonlinear Science*, vol. 4, pp. 1–225, 2011.

[39] X. J. Yang, *Local Fractional Functional Analysis and Its Applications*, Asian Academic Publisher, Hong Kong, 2011.

[40] X. J. Yang, *Advanced Local Fractional Calculus and Its Applications*, World Science Publisher, New York, NY, USA, 2012.

[41] W. P. Zhong, X. J. Yang, and F. Gao, "A Cauchy problem for some local fractional abstract differential equation with fractal conditions," *Journal of Applied Functional Analysis*, vol. 8, no. 1, pp. 92–99, 2013.

[42] M. S. Hu, R. P. Agarwal, and X. J. Yang, "Local fractional Fourier series with application to wave equation in fractal vibrating string," *Abstract and Applied Analysis*, vol. 2012, Article ID 567401, 15 pages, 2012.

[43] M. S. Hu, D. Baleanu, and X. J. Yang, "One-phase problems for discontinuous heat transfer in fractal media," *Mathematical Problems in Engineering*, vol. 2013, Article ID 358473, 3 pages, 2013.

[44] K. M. Kolwankar and A. D. Gangal, "Fractional differentiability of nowhere differentiable functions and dimensions," *Chaos*, vol. 6, no. 4, pp. 505–513, 1996.

[45] J. H. He, "A new fractal derivation," *Thermal Science*, vol. 15, pp. S145–S147, 2011.

[46] W. Chen, "Time-space fabric underlying anomalous diffusion," *Chaos, Solitons & Fractals*, vol. 28, no. 4, pp. 923–929, 2006.

[47] J. Fan and J. H. He, "Biomimic design of multi-scale fabric with efficient heat transfer property," *Thermal Science*, vol. 16, no. 5, pp. 1349–1352, 2012.

[48] J. Fan and J. H. He, "Fractal derivative model for air permeability in hierarchic porous media," *Abstract and Applied Analysis*, vol. 2012, Article ID 354701, 7 pages, 2012.

[49] A. Liangprom and K. Nonlaopon, "On the convolution equation related to the diamond Klein-Gordon operator," *Abstract and Applied Analysis*, vol. 2011, Article ID 908491, 16 pages, 2011.

Hindawi Publishing Corporation
Abstract and Applied Analysis
Volume 2013, Article ID 425031, 10 pages
http://dx.doi.org/10.1155/2013/425031

Research Article

Pullback Attractors for Nonautonomous 2D-Navier-Stokes Models with Variable Delays

Xiaoli Liu and Yejuan Wang

School of Mathematics and Statistics, Lanzhou University, Lanzhou 730000, China

Correspondence should be addressed to Yejuan Wang; wangyj@lzu.edu.cn

Received 5 January 2013; Accepted 30 March 2013

Academic Editor: de Dai

Using a method based on the concept of the Kuratowski measure of the noncompactness of a bounded set as well as some new estimates of the equicontinuity of the solutions, we prove the existence of a unique pullback attractor in higher regularity space for the multivalued process associated with the nonautonomous 2D-Navier-Stokes model with delays and without the uniqueness of solutions.

1. Introduction

It is well known that the Navier-Stokes equations are very important in the understanding of fluids motion and turbulence. These equations have been studied extensively over the last decades (see [1–3], and the references cited therein). Recently, Caraballo and Real [4] considered global attractors for functional Navier-Stokes models with the uniqueness of solutions and for the delay, so that a wide range of hereditary characteristics (constant or variable delay, distributed delay, etc.) can be treated in a unified way. Very recently, Marín-Rubio and Real [5] used the theory of multivalued dynamical system to establish the existence of attractors for the 2D-Navier-Stokes model with delays, when the forcing term containing the delay is sublinear and only continuous.

For the study of asymptotic behavior for functional partial differential equations without the uniqueness of solutions, as far as we know, not many papers have been published. However, some results in the finite dimensional context can be found in [6, 7] (see also [8–10] for some preliminary and interesting results on the structure of the attractors for ordinary differential delay systems).

The pullback attractor is a possible approach to define an "attractor" for the nonautonomous dynamical systems, the long time behavior of nonautonomous dynamical systems is an interesting and challenging problem; see, for example, [11–19], and so forth. The purpose of our current paper is to study existence of pullback attractors for the following functional Navier-Stokes problem:

$$\begin{gathered}
\frac{\partial u}{\partial t}-\nu\Delta u+\sum_{i=1}^{2}u_i\frac{\partial u}{\partial x_i} \\
= f\left(t,u\left(t-\rho\left(t\right)\right)\right)-\nabla p+g\left(t\right)\quad \text{in } (\tau,+\infty)\times\Omega, \\
\operatorname{div} u=0\quad \text{in } (\tau,+\infty)\times\Omega, \\
u=0\quad \text{on } (\tau,+\infty)\times\Gamma, \\
u\left(\tau+t,x\right)=\phi\left(t,x\right),\quad t\in[-h,0],\ x\in\Omega,
\end{gathered}\tag{1}$$

where $\Omega\subset\mathbb{R}^2$ is an open bounded set with regular boundary Γ, $\nu>0$ is the kinematic viscosity, u is the velocity field of the fluid, p is the pressure, $\tau\in\mathbb{R}$ is the initial time, g is a nondelayed external force field, f is another external force term and contains some memory effects during a fixed interval of time of length $h>0$, ρ is an adequate given delay function, and ϕ the initial datum on the interval $[-h,0]$.

Using the technique of measure of noncompactness, noting that all norms on finite dimensional spaces are equivalent, we apply the new method to check the pullback ω-limit compactness given in [20] and then get the existence of the pullback attractors in C_V.

We consider the following usual abstract spaces:

$$\mathscr{V} = \left\{u \in \left(C_0^{\infty}(\Omega)\right)^2 : \operatorname{div} u = 0\right\}, \quad (2)$$

where H = the closure of $\mathscr{V}$ in $(L^2(\Omega))^2$ with norm $|\cdot|$ and inner product $(\cdot,\cdot)$, where for $u, v \in (L^2(\Omega))^2$,

$$(u, v) = \sum_{j=1}^{2} \int_{\Omega} u_j(x) v_j(x)\, dx, \quad (3)$$

where V = the closure of $\mathscr{V}$ in $(H_0^1(\Omega))^2$ with norm $\|\cdot\|$ and associated scalar product $((\cdot,\cdot))$, where for $u, v \in (H_0^1(\Omega))^2$,

$$((u, v)) = \sum_{i,j=1}^{2} \int_{\Omega} \frac{\partial u_j}{\partial x_i} \frac{\partial v_j}{\partial x_i} dx. \quad (4)$$

Note that $V \subset H \equiv H' \subset V'$, where the injections are dense and compact. We will use $\|\cdot\|_*$ for the norm in V' and $\langle\cdot,\cdot\rangle$ for the duality pairing between V and V'.

Define the trilinear form b on $V \times V \times V$ by

$$b(u, v, w) = \sum_{i,j=1}^{2} \int_{\Omega} u_i \frac{\partial v_j}{\partial x_i} w_j dx, \quad \forall u, v, w \in V. \quad (5)$$

Now, let us establish some assumptions for (1).

We assume that the given delay function satisfies $\rho \in C^1(\mathbb{R}; [0, h])$, and there exists a constant ρ_* satisfying

$$\rho'(t) \leqslant \rho_* < 1, \quad \forall t \in \mathbb{R}. \quad (6)$$

Furthermore, we suppose that f and g satisfy the following assumptions:

(H1) $f(\cdot, v) : \mathbb{R} \to H$ is measurable for all $v \in H$,

(H2) $f(t, \cdot) : H \to H$ is continuous for all $t \in \mathbb{R}$,

(H3) there exist positive constants k_1, k_2 such that for any $v \in H$,

$$\left|f(t, v)\right|^2 \leqslant k_1^2 + k_2^2 |v|^2, \quad \forall t \in \mathbb{R}, \quad (7)$$

(H4) there exists a fixed $\delta_0 > 0$ such that for any $\delta \in (0, \delta_0)$, the external force $g \in L^2_{\mathrm{loc}}(\mathbb{R}; H)$ satisfies

$$\int_{-\infty}^{t} \left|g(r)\right|^2 e^{\delta r} dr < \infty, \quad \forall t \in \mathbb{R}. \quad (8)$$

Set $A : V \to V'$ as $\langle Au, v\rangle = ((u, v))$, $B : V \times V \to V'$ by $\langle B(u, v), w\rangle = b(u, v, w)$, for all $u, v, w \in V$. Denote by P the corresponding orthogonal projection $P : (L^2(\Omega))^2 \to H$. We further set $A := -P\Delta$. The Stokes operator A is self-adjoint and positive from $D(A) = V \cap (H^2(\Omega))^2$ to H. The inverse operator is compact. Excluding the pressure, the system (1) can be written in the form

$$\begin{aligned} &\frac{d}{dt} u(t) + \nu A u(t) + B(u(t), u(t)) \\ &\quad = f(t, u(t - \rho(t))) + g(t) \quad \text{in } \mathscr{D}'\left(\tau, +\infty; V'\right), \\ &\quad u(\tau + t) = \phi(t), \quad t \in [-h, 0], \ x \in \Omega. \end{aligned} \quad (9)$$

2. Preliminaries

Let X be a complete metric space with metric $d_X(\cdot,\cdot)$, and denote by $\mathscr{P}(X)$ the class of nonempty subsets of X. As usual, let us denote by $H_X^*(\cdot,\cdot)$ the Hausdorff semidistance between A and B, which are defined by

$$H_X^*(A, B) = \sup_{a \in A} \operatorname{dist}_X(a, B), \quad (10)$$

where $\operatorname{dist}_X(a, B) = \inf_{b \in B} d_X(a, b)$. Finally, denote by $\mathscr{N}(A, r)$ the open neighborhood $\{y \in X \mid \operatorname{dist}_X(y, A) < r\}$ of radius $r > 0$ of a subset A of a Banach space X.

Definition 1. A family of mappings $U(t, \tau) : X \to \mathscr{P}(X)$, $t \geqslant \tau$, $\tau \in \mathbb{R}$ is called to be a multivalued process (MVP in short) if it satisfies

(1) $U(\tau, \tau)x = \{x\}$, for all $\tau \in \mathbb{R}$, $x \in X$;

(2) $U(t, s)U(s, \tau)x = U(t, \tau)x$, for all $t \geqslant s \geqslant \tau$, $\tau \in \mathbb{R}$, $x \in X$.

Let $\mathscr{D}$ be a nonempty class of parameterized sets $\mathscr{D} = \{D(t)\}_{t \in \mathbb{R}} \subset \mathscr{P}(X)$.

Definition 2. Let $\{U(t, \tau)\}$ be a multivalued process on X. One says that $\{U(t, \tau)\}$ is

(1) pullback $\mathscr{D}$-dissipative, if there exists a family $\mathscr{Q} = \{Q(t)\}_{t \in \mathbb{R}} \in \mathscr{D}$, so that for any $\mathscr{B} = \{B(t)\}_{t \in \mathbb{R}} \in \mathscr{D}$ and each $t \in \mathbb{R}$, there exists a $t_0 = t_0(\mathscr{B}, t) \in \mathbb{R}^+$ such that

$$U(t, t - s) B(t - s) \subset Q(t), \quad \forall s \geqslant t_0; \quad (11)$$

(2) pullback $\mathscr{D}$-limit-set compact with respect to each $t \in \mathbb{R}$, if for any $\mathscr{B} = \{B(t)\}_{t \in \mathbb{R}} \in \mathscr{D}$ and $\varepsilon > 0$, there exists a $t_1 = t_1(\mathscr{B}, t, \varepsilon) \in \mathbb{R}^+$ such that

$$k\left(\bigcup_{s \geqslant t_1} U(t, t - s) B(t - s)\right) \leqslant \varepsilon, \quad (12)$$

where k is the Kuratowski measure of noncompactness.

Definition 3. A family of nonempty compact subsets $\mathscr{A} = \{A(t)\}_{t \in \mathbb{R}} \subset \mathscr{P}(X)$ is called to be a pullback $\mathscr{D}$-attractor for the multivalued process $\{U(t, \tau)\}$, if it satisfies

(1) $\mathscr{A} = \{A(t)\}_{t \in \mathbb{R}}$ is invariant; that is,

$$U(t, \tau) A(\tau) = A(t), \quad \forall t \geqslant \tau, \ \tau \in \mathbb{R}, \quad (13)$$

(2) $\mathscr{A}$ is pullback $\mathscr{D}$-attracting; that is, for every $\mathscr{B} \in \mathscr{D}$ and any fixed $t \in \mathbb{R}$,

$$\lim_{s \to +\infty} H_X^*(U(t, t - s) B(t - s), A(t)) = 0. \quad (14)$$

Let X, Y be two Banach spaces, and let X^*, Y^* be their dual spaces, respectively. We also assume that X is a dense subspace of Y, the injection $i : X \hookrightarrow Y$ is continuous, and its adjoint $i^* : Y^* \hookrightarrow X^*$ is densely injective.

Theorem 4 (see [21, 22]). *Let X, Y be two Banach spaces satisfy the previous assumptions, and let $\{U(t,\tau)\}$ be a multivalued process on X and Y, respectively. Assume that $\{U(t,\tau)\}$ is upper semicontinuous or weak upper semicontinuous on Y. If for fixed $t \geqslant \tau$, $\tau \in \mathbb{R}$, $U(t,\tau)$ maps compact subsets of X into bounded subsets of $\mathscr{P}(X)$, then $U(t,\tau)$ is norm-to-weak upper semicontinuous on X.*

By slightly modifying the arguments of Theorem 3.4 and Remark 3.9 in [21], we have the following.

Theorem 5. *Let X be a Banach space, and let $\{U(t,\tau)\}$ be a multivalued process on X. Also let $U(t,\tau)x$ be norm-to-weak upper semicontinuous in x for fixed $t \geqslant \tau$, $\tau \in \mathbb{R}$; that is, if $x_n \to x$, then for any $y_n \in U(t,\tau)x_n$, there exist a subsequence $y_{n_k} \in U(t,\tau)x_{n_k}$ and a $y \in U(t,\tau)x$ such that $y_{n_k} \rightharpoonup y$ (weak convergence). Then the multivalued process $\{U(t,\tau)\}$ possesses a pullback $\mathscr{D}$-attractor $\mathscr{A} = \{A(t)\}_{t\in\mathbb{R}}$ in X given by*

$$\begin{aligned} A(t) &= \omega_t(Q) \\ &= \bigcap_{T\in\mathbb{R}^+} \overline{\bigcup_{s\geqslant T} U(t,t-s)Q(t-s)} \subset Q(t) \end{aligned} \tag{15}$$

if and only if $\{U(t,\tau)\}$ is pullback $\mathscr{D}$-dissipative and pullback $\mathscr{D}$-limit-set compact with respect to each $t \in \mathbb{R}$, where $\mathscr{Q} = \{Q(t)\}_{t\in\mathbb{R}} \in \mathscr{D}$ is pullback $\mathscr{D}$-absorbing for the multivalued process $\{U(t,\tau)\}$.

A multivalued process $\{U(t,\tau)\}$ is said to be pullback $\mathscr{D}$-asymptotically upper-semicompact in X if for each fixed $t \in \mathbb{R}$, any $\mathscr{B} = \{B(t)\}_{t\in\mathbb{R}} \in \mathscr{D}$, any sequence $\{T_n\}$ with $T_n \to +\infty$, $\{x_n\}$ with $x_n \in B(t-T_n)$, and any $\{y_n\}$ with $y_n \in U(t,t-T_n)x_n$; this last sequence $\{y_n\}$ is relatively compact in X.

Remark 6. Let $\{U(t,\tau)\}$ be a multivalued process on X. Then $\{U(t,\tau)\}$ is pullback $\mathscr{D}$-asymptotically upper-semicompact if and only if $\{U(t,\tau)\}$ is pullback $\mathscr{D}$-limit-set compact; see [21].

Let X be a Banach space, and let $h > 0$ be a given positive number (the delay time). Denote by C_X the Banach space $C([-h,0];X)$ endowed with the norm

$$\|\phi\|_{C_X} = \sup_{\theta\in[-h,0]} \|\phi(\theta)\|_X. \tag{16}$$

Let us consider $\mathscr{D}_{C_X}$ a class of sets parameterized in time, $\mathscr{D} = \{D(t)\}_{t\in\mathbb{R}} \subset \mathscr{P}(C_X)$. To study the pullback $\mathscr{D}$-limit-set compactness of the multivalued process on C_X, we need the following result from [20].

Theorem 7. *Let $\{U(t,\tau)\}$ be a multivalued process on C_X. Suppose that for each $t \in \mathbb{R}$, any $\mathscr{B} \in \mathscr{D}_{C_X}$ and $\varepsilon > 0$, there exist $\tau_0 = \tau_0(t,\mathscr{B},\varepsilon) > 0$, a finite dimensional subspace X_1 of X, and a $\delta > 0$ such that*

(1) *for each fixed $\theta \in [-h,0]$,*

$$\left\| \bigcup_{s\geqslant\tau_0} \bigcup_{u_t(\cdot)\in U(t,t-s)B(t-s)} Pu(t+\theta) \right\|_X \text{ is bounded;} \tag{17}$$

(2) *for all $s \geqslant \tau_0$, $u_t(\cdot) \in U(t,t-s)B(t-s)$, $\theta_1,\theta_2 \in [-h,0]$ with $|\theta_2-\theta_1| < \delta$,*

$$\|P(u(t+\theta_1) - u(t+\theta_2))\|_X < \varepsilon; \tag{18}$$

(3) *for all $s \geqslant \tau_0$, $u_t(\cdot) \in U(t,t-s)B(t-s)$,*

$$\sup_{\theta\in[-h,0]} \|(I-P)u(t+\theta)\|_X < \varepsilon, \tag{19}$$

where $P : X \to X_1$ is the canonical projector. Then $\{U(t,\tau)\}$ is pullback $\mathscr{D}$-limit-set compact in C_X with respect to each $t \in \mathbb{R}$.

3. Existence of an Absorbing Family of Sets in C_V

By the classical Faedo-Galerkin scheme and compactness method, analogous to the arguments in [5], we have the following.

Theorem 8. *Let one consider $\phi \in C_H$, $g \in L^2_{\text{loc}}(\mathbb{R};H)$, and assume that $f : \mathbb{R}\times H \to H$ satisfies the hypotheses $(H1)$–$(H3)$. Then, for each $\tau \in \mathbb{R}$,*

(a) *there exists a weak solution u to problem (9) satisfying*

$$u \in C([\tau-h,T];H) \cap L^\infty(\tau,T;H) \cap L^2(\tau,T;V) \quad \forall T \geqslant \tau; \tag{20}$$

(b) *if $\phi \in C_V$, then there exists a strong solution u to problem (9); that is,*

$$u \in C([\tau-h,T];V) \cap L^\infty(\tau,T;V) \cap L^2(\tau,T;D(A)), \quad \forall T \geqslant \tau. \tag{21}$$

Given $T > \tau$ and $u : [\tau-h,T) \to H$, for each $t \in [\tau,T)$, we denote by u_t the function defined on $[-h,0]$ by the relation $u_t(s) = u(t+s)$, $s \in [-h,0]$. We also denote $C_H = C([-h,0];H)$ and $C_V = C([-h,0];V)$. Let C be the arbitrary positive constants, which may be different from line to line and even in the same line.

Thanks to Theorem 8, we can define a multivalued process $(C_V, \{U(\cdot,\cdot)\})$ as

$$\begin{aligned} U(t,\tau)(\phi) = \{&u_t(\cdot;\tau,\phi) \mid u(\cdot) \text{ is a strong solution of} \\ &(9) \text{ with initial datum } \phi \in C_V\}. \end{aligned} \tag{22}$$

We first need a priori estimates for the solution u of (9) in the space C_H and a necessary bound on the term $\int_{t-1}^t e^{\alpha r}\| u(r) \|^2 dr$, which will be very useful in our analysis; it relates the absorption property for the multivalued process $\{U(t,\tau)\}$ on C_V.

Lemma 9. *In addition to the assumptions $(H1)$–$(H4)$, assume that*

$$k_2^2 < \left(\frac{\nu\lambda_1}{2}\right)^2 (1-\rho_*) \tag{23}$$

holds true. Then

$$\|u_t\|_{C_H}^2 \leqslant \left(1 + \frac{2k_2^2 e^{\alpha h}}{\nu\lambda_1(1-\rho_*)\alpha}\right) e^{\alpha(\tau-t+h)}\|\phi\|_{C_H}^2 + \frac{2k_1^2}{\nu\lambda_1\alpha} + \frac{e^{-\alpha(t-h)}}{2\varepsilon_2}\int_{-\infty}^{t} e^{\alpha s}|g(s)|^2 ds, \quad \forall t \geqslant \tau + h, \tag{24}$$

$$\nu\int_{t-1}^{t} e^{\alpha r}\|u(r)\|^2 dr \leqslant Ce^{\alpha\tau}\|\phi\|_{C_H}^2 + Ce^{\alpha t} + C\int_{-\infty}^{t} e^{\alpha r}|g(r)|^2 dr, \quad \forall t \geqslant \tau + h + 1, \tag{25}$$

provided that $\alpha > 0$ is small enough.

Proof. By the energy inequality and the Poincaré inequality, we have

$$\frac{d}{dt}|u(t)|^2 + \nu\lambda_1|u(t)|^2 + \nu\|u(t)\|^2 \leqslant 2\left(f\left(t, u(t-\rho(t))\right), u(t)\right) + 2\left(g(t), u(t)\right). \tag{26}$$

We fixed two positive parameters ε_1 and ε_2 to be chosen later on. Then by (H3) and Young's inequality, we can deduce that

$$\begin{aligned} \left|\left(f\left(t, u(t-\rho(t))\right), u(t)\right)\right| &\leqslant \left|f\left(t, u(t-\rho(t))\right)\right| |u(t)| \\ &\leqslant \varepsilon_1|u(t)|^2 + \frac{k_1^2 + k_2^2|u(t-\rho(t))|^2}{4\varepsilon_1}, \\ \left|g(t), u(t)\right| &\leqslant \varepsilon_2|u(t)|^2 + \frac{1}{4\varepsilon_2}|g(t)|^2. \end{aligned} \tag{27}$$

Therefore,

$$\frac{d}{dt}|u(t)|^2 + \nu\|u(t)\|^2 \leqslant \left(2\varepsilon_1 + 2\varepsilon_2 - \nu\lambda_1\right)|u(t)|^2 + \frac{k_1^2 + k_2^2|u(t-\rho(t))|^2}{2\varepsilon_1} + \frac{|g(t)|^2}{2\varepsilon_2}. \tag{28}$$

Let $\alpha > 0$ to be determined later on. Then it follows that

$$\begin{aligned} \frac{d}{dt}\left(e^{\alpha t}|u(t)|^2\right) &= \alpha e^{\alpha t}|u(t)|^2 + e^{\alpha t}\frac{d}{dt}|u(t)|^2 \\ &\leqslant \left(\alpha + 2\varepsilon_1 + 2\varepsilon_2 - \nu\lambda_1\right)e^{\alpha t}|u(t)|^2 + \frac{e^{\alpha t}k_1^2}{2\varepsilon_1} + \frac{e^{\alpha t}k_2^2|u(t-\rho(t))|^2}{2\varepsilon_1} + \frac{e^{\alpha t}|g(t)|^2}{2\varepsilon_2}. \end{aligned} \tag{29}$$

Integrating between τ and t $(\geqslant \tau)$, we have

$$\begin{aligned} e^{\alpha t}|u(t)|^2 \leqslant{}& e^{\alpha\tau}|u(\tau)|^2 + \left(\alpha + 2\varepsilon_1 + 2\varepsilon_2 - \nu\lambda_1\right)\int_{\tau}^{t} e^{\alpha s}|u(s)|^2 ds + \frac{k_1^2}{2\varepsilon_1}\int_{\tau}^{t} e^{\alpha s} ds \\ &+ \frac{k_2^2}{2\varepsilon_1}\int_{\tau}^{t} e^{\alpha s}|u(s-\rho(s))|^2 ds + \frac{1}{2\varepsilon_2}\int_{\tau}^{t} e^{\alpha s}|g(s)|^2 ds. \end{aligned} \tag{30}$$

Let $r = s - \rho(s)$; note that $\rho(s) \in [0, h]$ and $1/(1-\rho'(s)) \leqslant 1/(1-\rho_*)$ for all $s \in \mathbb{R}$. Hence,

$$\begin{aligned} \frac{k_2^2}{2\varepsilon_1}\int_{\tau}^{t} e^{\alpha s}|u(s-\rho(s))|^2 ds &\leqslant \frac{k_2^2}{2\varepsilon_1}\frac{1}{1-\rho_*}\int_{\tau-h}^{t} e^{\alpha(r+h)}|u(r)|^2 dr \\ &\leqslant \frac{k_2^2 e^{\alpha h}}{2\varepsilon_1(1-\rho_*)} \times \left(\int_{\tau-h}^{\tau} e^{\alpha r}|u(r)|^2 dr + \int_{\tau}^{t} e^{\alpha r}|u(r)|^2 dr\right) \\ &\leqslant \frac{k_2^2 e^{\alpha(h+\tau)}\|\phi\|_{C_H}^2}{2\varepsilon_1(1-\rho_*)\alpha} + \frac{k_2^2 e^{\alpha h}}{2\varepsilon_1(1-\rho_*)}\int_{\tau}^{t} e^{\alpha r}|u(r)|^2 dr. \end{aligned} \tag{31}$$

Combining (30) and (31) together, we get

$$\begin{aligned} e^{\alpha t}|u(t)|^2 \leqslant{}& \left(1 + \frac{k_2^2 e^{\alpha h}}{2\varepsilon_1(1-\rho_*)\alpha}\right)e^{\alpha\tau}\|\phi\|_{C_H}^2 + \frac{k_1^2 e^{\alpha t}}{2\varepsilon_1\alpha} + \frac{1}{2\varepsilon_2}\int_{-\infty}^{t} e^{\alpha s}|g(s)|^2 ds \\ &+ \left(\alpha + 2\varepsilon_1 + 2\varepsilon_2 - \nu\lambda_1 + \frac{k_2^2 e^{\alpha h}}{2\varepsilon_1(1-\rho_*)}\right) \times \int_{\tau}^{t} e^{\alpha s}|u(s)|^2 ds. \end{aligned} \tag{32}$$

Let $\varepsilon_1 = \nu\lambda_1/4$ and using (23), so we can choose positive constants α and ε_2 small enough such that $\alpha + 2\varepsilon_1 + 2\varepsilon_2 - \nu\lambda_1 + (k_2^2 e^{\alpha h}/2\varepsilon_1(1-\rho_*)) < 0$ and $\alpha < \delta_0$ (where δ_0 is given in the assumption (H4)). Then, it follows that

$$e^{\alpha t}|u(t)|^2 \leqslant \left(1 + \frac{2k_2^2 e^{\alpha h}}{\nu\lambda_1(1-\rho_*)\alpha}\right) e^{\alpha\tau}\|\phi\|_{C_H}^2 + \frac{2k_1^2 e^{\alpha t}}{\nu\lambda_1\alpha} + \frac{1}{2\varepsilon_2}\int_{-\infty}^{t} e^{\alpha s}|g(s)|^2 ds. \tag{33}$$

Setting now $t+\theta$ instead of t (where $\theta \in [-h, 0]$), multiplying by $e^{-\alpha(t+\theta)}$, it holds

$$\begin{aligned}|u(t+\theta)|^2 &\leqslant \left(1 + \frac{2k_2^2 e^{\alpha h}}{\nu\lambda_1(1-\rho_*)\alpha}\right) e^{\alpha(\tau-t-\theta)}\|\phi\|_{C_H}^2 \\ &\quad + \frac{2k_1^2}{\nu\lambda_1\alpha} + \frac{e^{-\alpha(t+\theta)}}{2\varepsilon_2}\int_{-\infty}^{t+\theta} e^{\alpha s}|g(s)|^2 ds \\ &\leqslant \left(1 + \frac{2k_2^2 e^{\alpha h}}{\nu\lambda_1(1-\rho_*)\alpha}\right) e^{\alpha(\tau-t+h)}\|\phi\|_{C_H}^2 \\ &\quad + \frac{2k_1^2}{\nu\lambda_1\alpha} + \frac{e^{-\alpha(t-h)}}{2\varepsilon_2}\int_{-\infty}^{t} e^{\alpha s}|g(s)|^2 ds.\end{aligned} \tag{34}$$

Note that $\| u_t \|_{C_H}^2 = \sup_{\theta\in[-h,0]}|u(t+\theta)|^2$, thus the conclusion (24) follows immediately from (34).

Finally, we will obtain the bound on the term $\nu\int_{t-1}^{t} e^{\alpha r}\| u(r) \|^2 dr$. It follows from (28) that

$$\begin{aligned}\nu e^{\alpha t}\|u(t)\|^2 &\leqslant (2\varepsilon_1 + 2\varepsilon_2 - \nu\lambda_1) e^{\alpha t}|u(t)|^2 \\ &\quad + \frac{k_1^2 e^{\alpha t}}{2\varepsilon_1} + \frac{k_2^2 e^{\alpha t}|u(t-\rho(t))|^2}{2\varepsilon_1} \\ &\quad + \frac{e^{\alpha t}|g(t)|^2}{2\varepsilon_2} + \alpha e^{\alpha t}|u(t)|^2 \\ &\quad - \frac{d}{dt}\left(e^{\alpha t}|u(t)|^2\right).\end{aligned} \tag{35}$$

Integrating from $t-1$ to t, we have

$$\begin{aligned}&\nu\int_{t-1}^{t} e^{\alpha r}\|u(r)\|^2 dr \\ &\quad\leqslant (\alpha + 2\varepsilon_1 + 2\varepsilon_2 - \nu\lambda_1)\int_{t-1}^{t} e^{\alpha r}|u(r)|^2 dr \\ &\qquad + \frac{k_1^2}{2\varepsilon_1}\int_{t-1}^{t} e^{\alpha r} dr \\ &\qquad + \frac{k_2^2}{2\varepsilon_1}\int_{t-1}^{t} e^{\alpha r}|u(r-\rho(r))|^2 dr \\ &\qquad + \frac{1}{2\varepsilon_2}\int_{t-1}^{t} e^{\alpha r}|g(r)|^2 dr \\ &\qquad + e^{\alpha(t-1)}|u(t-1)|^2.\end{aligned} \tag{36}$$

Similar to the arguments of (31), we can deduce that

$$\begin{aligned}&\frac{k_2^2}{2\varepsilon_1}\int_{t-1}^{t} e^{\alpha r}|u(r-\rho(r))|^2 dr \\ &\quad\leqslant \frac{k_2^2}{2\varepsilon_1}\frac{1}{1-\rho_*}\int_{t-1-h}^{t} e^{\alpha(r+h)}|u(r)|^2 dr \\ &\quad\leqslant \frac{k_2^2 e^{\alpha h}}{2\varepsilon_1(1-\rho_*)} \\ &\qquad\times\left(\int_{t-1-h}^{t-1} e^{\alpha r}|u(r)|^2 dr + \int_{t-1}^{t} e^{\alpha r}|u(r)|^2 dr\right) \\ &\quad\leqslant \frac{k_2^2 e^{\alpha(h+t-1)}\|u_{t-1}\|_{C_H}^2}{2\varepsilon_1(1-\rho_*)\alpha} \\ &\qquad + \frac{k_2^2 e^{\alpha h}}{2\varepsilon_1(1-\rho_*)}\int_{t-1}^{t} e^{\alpha r}|u(r)|^2 dr.\end{aligned} \tag{37}$$

Recall that $\varepsilon_1 = \nu\lambda_1/4$ and $\alpha + 2\varepsilon_1 + 2\varepsilon_2 - \nu\lambda_1 + (k_2^2 e^{\alpha h}/2\varepsilon_1(1-\rho_*)) < 0$. By (24) and (36)-(37), we have (25) as desired, and thus the proof of this lemma is completed. □

By slightly modifying the proof of Lemma 1.1 in [23], we have the following result.

Lemma 10. *Let $t \in \mathbb{R}$ be given arbitrarily. Let g, h, and y be three positive locally integrable functions on $(-\infty, t]$ such that y' is locally integrable on $(-\infty, t]$, which satisfy that*

$$\begin{gathered}\frac{dy}{ds} \leqslant gy + h \quad \text{for } s \leqslant t, \\ \int_{t-1}^{t} g(s)\,ds \leqslant a_1, \qquad \int_{t-1}^{t} h(s)\,ds \leqslant a_2, \\ \int_{t-1}^{t} y(s)\,ds \leqslant a_3,\end{gathered} \tag{38}$$

where a_1, a_2, and a_3 are positive constants. Then

$$y(t) \leqslant \exp(a_1)(a_3 + a_2). \tag{39}$$

Now we state and prove the main result in this section.

Theorem 11. *Suppose in addition to the hypotheses in Lemma 9, assume that*

$$\lim_{t\to-\infty}\int_{-\infty}^{t} e^{-\gamma(t-r)}|g(r)|^2 dr < \infty \quad \forall\gamma > 0 \tag{40}$$

holds true. Then the multivalued process $\{U(t,\tau)\}$ on C_V is pullback $\mathscr{D}$-dissipative.

Proof. We take the inner product of (9) with $Au(t)$, we obtain

$$\begin{aligned}&\frac{1}{2}\frac{d}{dt}\|u(t)\|^2 + \nu|Au(t)|^2 + (B(u(t), u(t)), Au(t)) \\ &\quad = (f(t, u(t-\rho(t))), Au(t)) + (g(t), Au(t)).\end{aligned} \tag{41}$$

Now we evaluate the terms, using (H3) and Young's inequality, and we arrive to

$$\begin{aligned}&\left|\left(f\left(t,u\left(t-\rho\left(t\right)\right)\right),Au\left(t\right)\right)\right|+\left|\left(g\left(t\right),Au\left(t\right)\right)\right|\\&\quad\leqslant\frac{\nu}{2}\left|Au\left(t\right)\right|^2+\frac{\left|f\left(t,u\left(t-\rho\left(t\right)\right)\right)\right|^2}{\nu}+\frac{\left|g\left(t\right)\right|^2}{\nu}\\&\quad\leqslant\frac{\nu}{2}\left|Au\left(t\right)\right|^2+\frac{k_1^2+k_2^2\left\|u_t\right\|_{C_H}^2}{\nu}+\frac{\left|g\left(t\right)\right|^2}{\nu}.\end{aligned}\tag{42}$$

Next,

$$\begin{aligned}&\left|\left(B\left(u\left(t\right),u\left(t\right)\right),Au\left(t\right)\right)\right|\\&\quad\leqslant C_1\left|u\left(t\right)\right|^{1/2}\left\|u\left(t\right)\right\|\left|Au\left(t\right)\right|^{3/2}\\&\quad\leqslant\frac{\nu}{4}\left|Au\left(t\right)\right|^2+\frac{C_2}{\nu^3}\left|u\left(t\right)\right|^2\|u(t)\|^4.\end{aligned}\tag{43}$$

Thanks to (41)–(43) and the fact that $\|\varphi\|^2\leqslant\lambda_1^{-1}|A\varphi|^2$ for $\varphi\in D(A)$, we can deduce that

$$\begin{aligned}&\frac{d}{dt}\|u(t)\|^2+\frac{\nu\lambda_1}{2}\|u(t)\|^2\\&\quad\leqslant\frac{2k_1^2+2k_2^2\left\|u_t\right\|_{C_H}^2}{\nu}+\frac{2\left|g\left(t\right)\right|^2}{\nu}\\&\qquad+\frac{2C_2}{\nu^3}\left|u\left(t\right)\right|^2\|u(t)\|^4,\end{aligned}\tag{44}$$

and consequently,

$$\begin{aligned}&\frac{d}{dt}\left(e^{\alpha t}\|u(t)\|^2\right)+\left(\frac{\nu\lambda_1}{2}-\alpha\right)e^{\alpha t}\|u(t)\|^2\\&\quad\leqslant\frac{2k_1^2+2k_2^2\left\|u_t\right\|_{C_H}^2}{\nu}e^{\alpha t}+\frac{2\left|g\left(t\right)\right|^2}{\nu}e^{\alpha t}\\&\qquad+\frac{2C_2e^{\alpha t}}{\nu^3}\left|u\left(t\right)\right|^2\|u(t)\|^4.\end{aligned}\tag{45}$$

Since $\varepsilon_1=\nu\lambda_1/4$ and $\alpha+2\varepsilon_1+2\varepsilon_2-\nu\lambda_1+(k_2^2e^{\alpha h}/2\varepsilon_1(1-\rho_*))<0$, it is easy to see that $(\nu\lambda_1/2)-\alpha>0$. Then

$$\begin{aligned}&\frac{d}{dt}\left(e^{\alpha t}\left\|u\left(t\right)\right\|^2\right)\\&\quad\leqslant\frac{2k_1^2+2k_2^2\left\|u_t\right\|_{C_H}^2}{\nu}e^{\alpha t}+\frac{2\left|g\left(t\right)\right|^2}{\nu}e^{\alpha t}\\&\qquad+\frac{2C_2}{\nu^3}\left|u\left(t\right)\right|^2\|u(t)\|^2\|u(t)\|^2e^{\alpha t}.\end{aligned}\tag{46}$$

Let $t\in\mathbb{R}$ be given arbitrarily and taking τ such that $t\geqslant\tau+h+1$. In order to apply Lemma 10, in view of (24), now we firstly obtain

$$\begin{aligned}&\int_{t-1}^{t}\left(\frac{2k_1^2+2k_2^2\left\|u_r\right\|_{C_H}^2}{\nu}e^{\alpha r}+\frac{2\left|g\left(r\right)\right|^2}{\nu}e^{\alpha r}\right)dr\\&\quad\leqslant\int_{t-1}^{t}\frac{2k_1^2+2k_2^2\left\|u_r\right\|_{C_H}^2}{\nu}e^{\alpha r}dr\\&\qquad+\int_{t-1}^{t}\frac{2\left|g\left(r\right)\right|^2}{\nu}e^{\alpha r}dr\\&\quad\leqslant Ce^{\alpha t}+Ce^{\alpha\tau}\|\phi\|_{C_H}^2+C\int_{-\infty}^{t}e^{\alpha r}\left|g\left(r\right)\right|^2dr.\end{aligned}\tag{47}$$

Then, it follows from (24) and (25) that

$$\begin{aligned}&\frac{2C_2}{\nu^3}\int_{t-1}^{t}\left|u\left(r\right)\right|^2\|u(r)\|^2dr\\&\quad\leqslant\frac{2C_2}{\nu^3}\int_{t-1}^{t}\left\|u_r\right\|_{C_H}^2\|u(r)\|^2dr\\&\quad\leqslant\frac{2C_2}{\nu^3}\int_{t-1}^{t}\left(1+\frac{2k_2^2e^{\alpha h}}{\nu\lambda_1\left(1-\rho_*\right)\alpha}\right)e^{\alpha(\tau-r+h)}\\&\qquad\times\|\phi\|_{C_H}^2\|u(r)\|^2dr\\&\qquad+\frac{4C_2k_1^2}{\nu^4\lambda_1\alpha}\int_{t-1}^{t}\|u(r)\|^2dr\\&\qquad+\frac{2C_2}{\nu^3}\int_{t-1}^{t}\left(\frac{e^{-\alpha(r-h)}}{2\varepsilon_2}\|u(r)\|^2\int_{-\infty}^{r}e^{\alpha s}\left|g\left(s\right)\right|^2ds\right)dr\\&\quad\leqslant Ce^{2\alpha\tau}e^{-2\alpha t}\|\phi\|_{C_H}^2+C\\&\qquad+Ce^{-\alpha t}\int_{-\infty}^{t}e^{\alpha r}\left|g\left(r\right)\right|^2dr+Ce^{\alpha\tau}e^{-\alpha t}\|\phi\|_{C_H}^2\\&\qquad+Ce^{\alpha\tau}e^{-2\alpha t}\|\phi\|_{C_H}^2\int_{-\infty}^{t}e^{\alpha r}\left|g\left(r\right)\right|^2dr\\&\qquad+Ce^{-2\alpha t}\left(\int_{-\infty}^{t}e^{\alpha r}\left|g\left(r\right)\right|^2dr\right)^2.\end{aligned}\tag{48}$$

Combining (25) and (47)-(48) together, by Lemma 10, we can conclude that

$$\|u(t)\|^2\leqslant\left(a_3+a_2\right)e^{a_1}\quad\forall t\geqslant\tau+h+1,\tag{49}$$

where

$$\begin{aligned}
a_3 &= Ce^{\alpha\tau}\|\phi\|_{C_H}^2 + Ce^{\alpha t} + C\int_{-\infty}^{t} e^{\alpha r}|g(r)|^2 dr,\\
a_2 &= Ce^{\alpha t} + Ce^{\alpha\tau}\|\phi\|_{C_H}^2 + C\int_{-\infty}^{t} e^{\alpha r}|g(r)|^2 dr,\\
a_1 &= Ce^{2\alpha\tau}e^{-2\alpha t}\|\phi\|_{C_H}^2 + C\\
&\quad + Ce^{-\alpha t}\int_{-\infty}^{t} e^{\alpha r}|g(r)|^2 dr + Ce^{\alpha\tau}e^{-\alpha t}\|\phi\|_{C_H}^2\\
&\quad + Ce^{\alpha\tau}e^{-2\alpha t}\|\phi\|_{C_H}^2\int_{-\infty}^{t} e^{\alpha r}|g(r)|^2 dr\\
&\quad + Ce^{-2\alpha t}\left(\int_{-\infty}^{t} e^{\alpha r}|g(r)|^2 dr\right)^2.
\end{aligned} \tag{50}$$

Therefore, if we take τ such that $t \geqslant \tau + 1 + 2h$, then similar to the above mentioned, we get

$$\|u_t\|_{C_V}^2 = \sup_{\theta\in[-h,0]} \|u(t+\theta)\|^2 \leqslant (a_3 + a_2)e^{a_1}. \tag{51}$$

We denote by $\mathscr{R}$ the set of all functions $r : \mathbb{R} \to (0, +\infty)$ such that

$$\lim_{t\to-\infty} r^2(t) = 0, \tag{52}$$

and denote by $\mathscr{D}_{C_V}$ the class of all families $\mathscr{D} = \{D(t)\}_{t\in\mathbb{R}} \subset \mathscr{P}(C_V)$ such that $D(t) \subset \overline{\mathscr{N}}(0, r_{\mathscr{D}}(t))$, for some $r_{\mathscr{D}} \in \mathscr{R}$, where $\mathscr{P}(C_V)$ denotes the family of all nonempty subsets of C_V and $\overline{\mathscr{N}}(0, r_{\mathscr{D}}(t))$ denotes the closed ball in C_V centered at zero with radius $r_{\mathscr{D}}(t)$.

Denote by $R(t)$ the nonnegative number given for each $t \in \mathbb{R}$ by

$$\begin{aligned}
(R(t))^2 &= \left(Ce^{\alpha t} + C\int_{-\infty}^{t} e^{\alpha r}|g(r)|^2 dr\right)\\
&\quad\times \exp\Bigg(Ce^{-\alpha t}\int_{-\infty}^{t} e^{\alpha r}|g(r)|^2 dr\\
&\qquad + Ce^{-2\alpha t}\left(\int_{-\infty}^{t} e^{\alpha r}|g(r)|^2 dr\right)^2\Bigg),
\end{aligned} \tag{53}$$

and consider the family of closed balls $\mathscr{Q} = \{Q(t)\}_{t\in\mathbb{R}}$ in C_V defined by

$$Q(t) = \left\{\psi \in C_V : \|\psi\|_{C_V} \leqslant R(t)\right\}. \tag{54}$$

It is straightforward to check that $\mathscr{Q} \in \mathscr{D}_{C_V}$, and moreover, by (51) and (52), the family of $\mathscr{Q}$ is pullback $\mathscr{D}$-absorbing for the multivalued process $\{U(t,\tau)\}$ on C_V.

The proof of Theorem 11 is completed. □

4. Existence of the Pullback Attractors in C_V

Theorem 12. *Suppose in addition to the hypotheses in Theorem 11 that $g \in C(\mathbb{R}; H)$. Then there exists a unique pullback $\mathscr{D}$-attractor $\{A_{C_V}(t)\}_{t\in R}$ for the multivalued process $\{U(t,\tau)\}$ in C_V.*

Proof. Since A^{-1} is a continuous compact operator in H, by the classical spectral theory, there exist a sequence $\{\lambda_j\}_{j=1}^{\infty}$,

$$0 < \lambda_1 \leqslant \lambda_2 \leqslant \cdots \leqslant \lambda_j \leqslant \cdots, \quad \lambda_j \longrightarrow +\infty, \text{ as } j \longrightarrow +\infty, \tag{55}$$

and a family of elements $\{w_j\}_{j=1}^{\infty}$ of $D(A)$ which are orthonormal in H such that

$$Aw_j = \lambda_j w_j \quad \forall j \in \mathbb{N}. \tag{56}$$

Let $V_m = \operatorname{span}\{w_1, \dots, w_m\}$ in V and $P_m : V \to V_m$ be an orthogonal projector.

Let $u = u_1 + u_2$, where $u_1 = P_m u$ and $u_2 = (I - P_m)u$. We decompose (9) as follows:

$$\begin{aligned}
&\frac{\partial u_2(t)}{\partial t} + \nu A u_2(t) + B(u(t), u(t)) - P_m B(u_1(t), u_1(t))\\
&\quad = f(t, u(t-\rho(t)))\\
&\qquad - P_m f(t, u_1(t-\rho(t))) + (I - P_m)g(t),\\
&u_2(\tau + t) = (I - P_m)\phi(t), \quad t \in [-h, 0],
\end{aligned} \tag{57}$$

$$\begin{aligned}
&\frac{\partial u_1(t)}{\partial t} + \nu A u_1(t) + P_m B(u_1(t), u_1(t))\\
&\quad = P_m f(t, u_1(t-\rho(t))) + P_m g(t),\\
&u_1(\tau + t) = P_m\phi(t), \quad t \in [-h, 0].
\end{aligned} \tag{58}$$

We divide the proof into three steps.

(1) For every fixed $t \in \mathbb{R}$, any $\mathscr{B} = \{B(t)\}_{t\in\mathbb{R}} \in \mathscr{D}_{C_V}$ and $\varepsilon > 0$, we observe that for any $T \geqslant t - s$ with $s \geqslant 0$,

$$\begin{aligned}
&U(T, t-s)(\phi)\\
&\quad = \{u_T(\cdot; t-s, \phi) \mid u(\cdot) \text{ is a strong solution}\\
&\qquad \text{of (9) with } \phi \in B(t-s)\}.
\end{aligned} \tag{59}$$

Taking the inner product in H of (57) with $Au_2 = A(I - P_m)u$, we get

$$\begin{aligned}
&\frac{1}{2}\frac{d}{dT}\|u_2(T)\|^2 + \nu|Au_2(T)|^2\\
&\quad \leqslant |(f(T, u(T-\rho(T))), Au_2(T))|\\
&\qquad + |(P_m f(T, u_1(T-\rho(T))), Au_2(T))|\\
&\qquad + |(B(u(T), u(T)), Au_2(T))|\\
&\qquad + |(P_m B(u_1(T), u_1(T)), Au_2(T))|\\
&\qquad + |((I - P_m)g(T), Au_2(T))|.
\end{aligned} \tag{60}$$

By (H3) and Young's inequality, we have

$$\begin{aligned}
&|(f(T, u(T-\rho(T))), Au_2(T))| + |(g(T), Au_2(T))|\\
&\quad \leqslant \frac{\nu}{8}|Au_2(T)|^2 + C + C\|u_T\|_{C_H}^2 + C|g(T)|^2.
\end{aligned} \tag{61}$$

To estimate $(B(u(T),u(T)),Au_2(T))$, we recall some inequalities [19]:

$$|\varphi|_{(L^\infty(\Omega))^2} \leqslant C_3 \|\varphi\| \left(1+\log\frac{|A\varphi|^2}{\lambda_1\|\varphi\|^2}\right)^{1/2} \quad \forall\varphi\in D(A), \tag{62}$$

and thus

$$\begin{aligned} |B(u,v)| &\leqslant C_4 |(u\cdot\nabla)v| \leqslant C_4|u|_{L^\infty(\Omega)}\|v\| \\ &\leqslant C_4C_3\|u\|\|v\|\left(1+\log\frac{|Au|^2}{\lambda_1\|u\|^2}\right)^{1/2}. \end{aligned} \tag{63}$$

Note that $|Au_1|^2 \leqslant \lambda_m\|u_1\|^2$, and set $L = 1+\log(\lambda_{m+1}/\lambda_1)$. Then by Young's inequality, we can deduce that

$$\begin{aligned} &\left|(B(u(T),u(T)),Au_2(T))\right| \\ &\quad\leqslant \left|(B(u_2(T),u_1(T)+u_2(T)),Au_2(T))\right| \\ &\qquad+\left|(B(u_1(T),u_1(T)+u_2(T)),Au_2(T))\right| \\ &\quad\leqslant C_1\left|u_2(T)\right|^{1/2}\left|Au_2(T)\right|^{3/2} \\ &\qquad\times(\|u_1(T)\|+\|u_2(T)\|) \\ &\qquad+C_3C_4L^{1/2}\|u_1(T)\|\left|Au_2(T)\right| \\ &\qquad\times(\|u_1(T)\|+\|u_2(T)\|) \\ &\quad\leqslant \frac{\nu}{8}\left|Au_2(T)\right|^2+C|u(T)|^2\|u(T)\|^4+C\|u(T)\|^4. \end{aligned} \tag{64}$$

By (60)–(64) and Poincaré inequality, we obtain

$$\begin{aligned} &\frac{d}{dT}\|u_2(T)\|^2+\nu\lambda_{m+1}\|u_2(T)\|^2 \\ &\quad\leqslant C+C\|u_T\|^2_{C_H}+C|g(T)|^2 \\ &\qquad+C|u(T)|^2\|u(T)\|^4+C\|u(T)\|^4. \end{aligned} \tag{65}$$

Applying the Gronwall's lemma in the interval $[t-s,t+\theta]$, it yields

$$\begin{aligned} &\|u_2(t+\theta)\|^2 \\ &\leqslant \|u_2(t-s)\|^2 e^{-\nu\lambda_{m+1}(\theta+s)} \\ &\quad+C\int_{t-s}^{t+\theta} e^{-\nu\lambda_{m+1}(t+\theta-r)} \\ &\qquad\times\left(1+\|u_r\|^2_{C_H}+|g(r)|^2+|u(r)|^2\|u(r)\|^4+\|u(r)\|^4\right)dr. \end{aligned} \tag{66}$$

Let $\varepsilon>0$ be given arbitrarily. Note that $g\in C(\mathbb{R};H)$, then we can take $m+1$ large enough such that for any fixed $\eta>0$,

$$C\int_{t-h-\eta}^{t+\theta} e^{-\nu\lambda_{m+1}(t+\theta-r)}|g(r)|^2dr \leqslant \frac{C}{\nu\lambda_{m+1}} < \frac{\varepsilon}{4}, \tag{67}$$

$$\begin{aligned} &\sup_{\theta\in[-h,0]} C\int_{-\infty}^{t-h-\eta} e^{-\nu\lambda_{m+1}(t+\theta-r)}|g(r)|^2dr \\ &\quad\leqslant C\int_{-\infty}^{t-h-\eta} e^{-\nu\lambda_{m+1}(t-h-r)}|g(r)|^2dr \\ &\quad\leqslant Ce^{-\nu\lambda_{m+1}(t-h)} \\ &\qquad\times\left(\int_{t-h-\eta-1}^{t-h-\eta} e^{\nu\lambda_{m+1}r}|g(r)|^2dr\right. \\ &\qquad\qquad\left.+\int_{t-h-\eta-2}^{t-h-\eta-1} e^{\nu\lambda_{m+1}r}|g(r)|^2dr+\cdots\right) \\ &\quad\leqslant Ce^{-\nu\lambda_{m+1}(t-h)} \\ &\qquad\times\left(e^{(\nu\lambda_{m+1}-\alpha)(t-h-\eta)}+e^{(\nu\lambda_{m+1}-\alpha)(t-h-\eta-1)}+\cdots\right) \\ &\qquad\times\int_{-\infty}^{t} e^{\alpha r}|g(r)|^2dr \\ &\quad\leqslant \frac{Ce^{-\nu\lambda_{m+1}\eta}e^{-\alpha(t-h-\eta)}}{1-e^{-(\nu\lambda_{m+1}-\alpha)}}\int_{-\infty}^{t} e^{\alpha r}|g(r)|^2dr \\ &\quad< \frac{\varepsilon}{4}. \end{aligned} \tag{68}$$

Combining (67) and (68) together, we can get for $m+1$ large enough,

$$\sup_{\theta\in[-h,0]} C\int_{-\infty}^{t+\theta} e^{-\nu\lambda_{m+1}(t+\theta-r)}|g(r)|^2dr < \frac{\varepsilon}{2}. \tag{69}$$

On the other hand, thanks to Lemma 9 and Theorem 11, we can deduce that when $m+1$ and s are large enough,

$$\begin{aligned} &\sup_{\theta\in[-h,0]} \|u_2(t-s)\|^2 e^{-\nu\lambda_{m+1}(\theta+s)} \\ &\quad\leqslant \|u_2(t-s)\|^2 e^{-\nu\lambda_{m+1}(s-h)} < \frac{\varepsilon}{4}, \\ &\sup_{\theta\in[-h,0]} C\int_{t-s}^{t+\theta} e^{-\nu\lambda_{m+1}(t+\theta-r)} \\ &\qquad\times\left(C+\|u_r\|^2_{C_H}+|u(r)|^2\|u(r)\|^4+\|u(r)\|^4\right)dr \\ &\quad< \frac{\varepsilon}{4}. \end{aligned} \tag{70}$$

Thanks to (69) and (70), it follows from (66) that when $m+1$ and s are large enough,

$$\begin{aligned}
&\|u_{2t}\|_{C_V}^2 \\
&= \sup_{\theta\in[-h,0]} \|u_2(t+\theta)\|^2 \\
&\leqslant \sup_{\theta\in[-h,0]} \|u_2(t-s)\|^2 e^{-\nu\lambda_{m+1}(\theta+s)} \\
&\quad + \sup_{\theta\in[-h,0]} C \int_{t-s}^{t+\theta} e^{-\nu\lambda_{m+1}(t+\theta-r)} \\
&\qquad \times \left(C + \|u_r\|_{C_H}^2 + |g(r)|^2 + |u(r)|^2\|u(r)\|^4 \right. \\
&\qquad \left. + \|u(r)\|^4 \right) dr \\
&< \varepsilon.
\end{aligned} \tag{71}$$

(2) Now we consider the ordinary functional differential system (58) and check the condition (2) in Theorem 7. Note that $|Au_1|^2 \leqslant \lambda_m \| u_1 \|^2 \leqslant \lambda_m^2 |u_1|^2$. Without generality, we assume that $\theta_1, \theta_2 \in [-h, 0]$ with $0 < \theta_1 - \theta_2 < 1$. Hence

$$\begin{aligned}
&\|u_1(t+\theta_1) - u_1(t+\theta_2)\| \\
&\leqslant \sqrt{\lambda_m} |u_1(t+\theta_1) - u_1(t+\theta_2)| \\
&\leqslant \sqrt{\lambda_m} \int_{t+\theta_2}^{t+\theta_1} \left| \frac{du_1(T)}{dT} \right| dT \\
&\leqslant \sqrt{\lambda_m} \int_{t+\theta_2}^{t+\theta_1} \left(\nu |Au_1(T)| + |B(u_1(T), u_1(T))| \right. \\
&\qquad \left. + |f(T, u_1(T-\rho(T)))| + |P_m g(T)| \right) dT.
\end{aligned} \tag{72}$$

Notice that

$$|B(u_1, u_1)| \leqslant C|Au_1| \|u_1\| \leqslant C\sqrt{\lambda_m}\|u_1\|^2 \leqslant C\lambda_m^{3/2}|u_1|^2. \tag{73}$$

Then, it follows from (H3), (H4), and (24) that

$$\begin{aligned}
&\int_{t+\theta_2}^{t+\theta_1} \left(|Au_1(T)| + |B(u_1(T), u_1(T))| \right) dT \\
&\leqslant C \int_{t+\theta_2}^{t+\theta_1} |u_1(T)| dT + C \int_{t+\theta_2}^{t+\theta_1} |u_1(T)|^2 dT \\
&\leqslant C \int_{t+\theta_2}^{t+\theta_1} |u_1(T)|^2 dT + C(\theta_1 - \theta_2) \\
&\leqslant C\left(e^{-\alpha\theta_2} - e^{-\alpha\theta_1}\right) + C(\theta_1 - \theta_2) \\
&\quad + C\left(e^{-\alpha\theta_2} - e^{-\alpha\theta_1}\right) e^{-\alpha t} \int_{-\infty}^{t} e^{\alpha r} |g(r)|^2 dr, \\
&\int_{t+\theta_2}^{t+\theta_1} |f(T, u_1(T-\rho(T)))| dT \\
&\leqslant \int_{t+\theta_2}^{t+\theta_1} \left(|f(T, u_1(T-\rho(T)))|^2 + C \right) dT \\
&\leqslant \int_{t+\theta_2}^{t+\theta_1} \left(k_2^2 \|u_{1T}\|_{C_H}^2 + C \right) dT \\
&\leqslant C\left(e^{-\alpha\theta_2} - e^{-\alpha\theta_1}\right) + C(\theta_1 - \theta_2) \\
&\quad + C\left(e^{-\alpha\theta_2} - e^{-\alpha\theta_1}\right) e^{-\alpha t} \int_{-\infty}^{t} e^{\alpha r} |g(r)|^2 dr.
\end{aligned} \tag{74}$$

Since $g \in C(\mathbb{R}; H)$ and t is fixed,

$$\int_{t+\theta_2}^{t+\theta_1} |P_m g(T)| dT \leqslant C(\theta_1 - \theta_2). \tag{75}$$

Equations (74)–(75) imply that the condition (2) in Theorem 7 is proved.

(3) Invoking Theorem 7, in view of the previous arguments and Theorem 11, we can see that the multivalued process $\{U(t,\tau)\}$ is pullback $\mathscr{D}$-limit-set compact and pullback $\mathscr{D}$-dissipative in C_V.

In order to get the existence of pullback $\mathscr{D}$-attractors, by the proof of Theorem 3.2 in [21], now we only need to show the negative invariance of $\{A_{C_V}(t)\}_{t\in\mathbb{R}}$, where

$$\begin{aligned}
A_{C_V}(t) &= \omega_t(\mathcal{Q}) \\
&= \bigcap_{T\in\mathbb{R}^+} \overline{\bigcup_{s\geqslant T} U(t, t-s) Q(t-s)}, \quad \forall t \in \mathbb{R},
\end{aligned} \tag{76}$$

and $\mathcal{Q} = \{Q(t)\}_{t\in\mathbb{R}} \in \mathscr{D}_{C_V}$ is a pullback $\mathscr{D}$-absorbing set of $\{U(t,\tau)\}$ in C_V.

Let $y \in A_{C_V}(t)$. Then there exist sequences $s_n \in \mathbb{R}^+$, $s_n \to +\infty$ $(n \to \infty)$, $x_n \in Q(t-s_n)$, and $y_n \in U(t, t-s_n)x_n$ such that

$$y_n \longrightarrow y \quad \text{in } C_V \text{ as } n \longrightarrow \infty. \tag{77}$$

On the other hand, for n sufficiently large,

$$y_n \in U(t, t-s_n) x_n = U(t,\tau) U(\tau, t-s_n) x_n. \tag{78}$$

Then by the pullback $\mathscr{D}$-limit-set compactness of the multivalued process $\{U(t,\tau)\}$, there is a subsequence of $\tilde{x}_n \in U(\tau, t-s_n)x_n = U(\tau, \tau-(\tau+s_n-t))x_n$, which we still relabel as $\tilde{x}_n$ such that $y_n \in U(t,\tau)\tilde{x}_n$ and

$$\tilde{x}_n \longrightarrow x \quad \text{in } C_V \text{ as } n \longrightarrow \infty. \tag{79}$$

Clearly, $x \in A_{C_V}(\tau)$.

We observe that y_n is bounded in C_V for n sufficiently large. Then by slightly modifying the proof of the existence of solutions (see [16] for details), in view of Theorem 2.11 in [21], we can see that

$$y_n(\cdot) \rightharpoonup u(\cdot + t, \tau, x) \quad \text{in } L^2([-h, 0]; V). \tag{80}$$

This together with (77)–(79), we can deduce that $y \in U(t,\tau)x \subset U(t,\tau)A_{C_V}(\tau)$, and thus the proof of Theorem 12 is finished. □

Acknowledgments

This research was supported by the National Natural Science Foundation of China under Grant no. 10801066 and the Fundamental Research Funds for the Central Universities under Grant no. lzujbky-2011-47 and no. lzujbky-2012-k26. The Project was sponsored by the Scientific Research Foundation for the Returned Overseas Chinese Scholars, State Education Ministry.

References

[1] P. Constantin and C. Foias, *Navier-Stokes Equations*, The University of Chicago Press, Chicago, Ill, USA, 1988.

[2] P. Marín-Rubio and J. C. Robinson, "Attractors for the stochastic 3D Navier-Stokes equations," *Stochastics and Dynamics*, vol. 3, no. 3, pp. 279–297, 2003.

[3] R. Temam, *Navier-Stokes Equations: Theory and Numerical Analysis*, vol. 2, North-Holland, Amsterdam, The Netherlands, 2nd edition, 1979.

[4] T. Caraballo and J. Real, "Attractors for 2D-Navier-Stokes models with delays," *Journal of Differential Equations*, vol. 205, no. 2, pp. 271–297, 2004.

[5] P. Marín-Rubio and J. Real, "Pullback attractors for 2D-Navier-Stokes equations with delays in continuous and sub-linear operators," *Discrete and Continuous Dynamical Systems A*, vol. 26, no. 3, pp. 989–1006, 2010.

[6] T. Caraballo, P. Marín-Rubio, and J. Valero, "Autonomous and non-autonomous attractors for differential equations with delays," *Journal of Differential Equations*, vol. 208, no. 1, pp. 9–41, 2005.

[7] T. Caraballo, P. Marín-Rubio, and J. Valero, "Attractors for differential equations with unbounded delays," *Journal of Differential Equations*, vol. 239, no. 2, pp. 311–342, 2007.

[8] J. K. Hale and S. M. Verduyn-Lunel, *Introduction to Functional Differential Equations*, Springer, Berlin, Germany, 1993.

[9] J. Mallet-Paret and G. R. Sell, "Systems of differential delay equations: floquet multipliers and discrete Lyapunov functions," *Journal of Differential Equations*, vol. 125, no. 2, pp. 385–440, 1996.

[10] J. Mallet-Paret and G. R. Sell, "The Poincaré-Bendixson theorem for monotone cyclic feedback systems with delay," *Journal of Differential Equations*, vol. 125, no. 2, pp. 441–489, 1996.

[11] T. Caraballo, M. J. Garrido-Atienza, B. Schmalfuß, and J. Valero, "Non-autonomous and random attractors for delay random semilinear equations without uniqueness," *Discrete and Continuous Dynamical Systems A*, vol. 21, no. 2, pp. 415–443, 2008.

[12] T. Caraballo and P. E. Kloeden, "Non-autonomous attractor for integro-differential evolution equations," *Discrete and Continuous Dynamical Systems S*, vol. 2, no. 1, pp. 17–36, 2009.

[13] T. Caraballo, P. E. Kloeden, and J. Real, "Pullback and forward attractors for a damped wave equation with delays," *Stochastics and Dynamics*, vol. 4, no. 3, pp. 405–423, 2004.

[14] T. Caraballo, G. Łukaszewicz, and J. Real, "Pullback attractors for asymptotically compact non-autonomous dynamical systems," *Nonlinear Analysis: Theory, Methods and Applications A*, vol. 64, no. 3, pp. 484–498, 2006.

[15] D. N. Cheban, P. E. Kloeden, and B. Schmalfuß, "The relationship between pullback, forward and global attractors of nonautonomous dynamical systems," *Nonlinear Dynamics and Systems Theory*, vol. 2, no. 2, pp. 9–28, 2002.

[16] V. V. Chepyzhov and M. I. Vishik, *Attractors for Equations of Mathematical Physics*, vol. 49, American Mathematical Society, Providence, RI, USA, 2002.

[17] P. E. Kloeden and B. Schmalfuß, "Asymptotic behaviour of nonautonomous difference inclusions," *Systems & Control Letters*, vol. 33, no. 4, pp. 275–280, 1998.

[18] P. E. Kloeden and J. A. Langa, "Flattening, squeezing and the existence of random attractors," *Proceedings of the Royal Society of London A*, vol. 463, no. 2077, pp. 163–181, 2007.

[19] Y. Wang, C. Zhong, and S. Zhou, "Pullback attractors of nonautonomous dynamical systems," *Discrete and Continuous Dynamical Systems A*, vol. 16, no. 3, pp. 587–614, 2006.

[20] Y. J. Wang and P. E. Kloeden, "The uniform attractor of a multi-valued process generated by reaction-diffusion delay equations on an unbounded domain ," *Discrete and Continuous Dynamical Systems A*. In press.

[21] Y. Wang and S. Zhou, "Kernel sections on multi-valued processes with application to the nonlinear reaction-diffusion equations in unbounded domains," *Quarterly of Applied Mathematics*, vol. 67, no. 2, pp. 343–378, 2009.

[22] C.-K. Zhong, M.-H. Yang, and C.-Y. Sun, "The existence of global attractors for the norm-to-weak continuous semigroup and application to the nonlinear reaction-diffusion equations," *Journal of Differential Equations*, vol. 223, no. 2, pp. 367–399, 2006.

[23] R. Temam, *Infinite Dimensional Dynamical Systems in Mechanics and Physics*, Springer, New York, NY, USA, 1988.

Hindawi Publishing Corporation
Abstract and Applied Analysis
Volume 2013, Article ID 262581, 16 pages
http://dx.doi.org/10.1155/2013/262581

Research Article

Continuum Modeling and Control of Large Nonuniform Wireless Networks via Nonlinear Partial Differential Equations

Yang Zhang,[1] Edwin K. P. Chong,[1] Jan Hannig,[2] and Donald Estep[3]

[1] *Department of Electrical and Computer Engineering, Colorado State University, Fort Collins, CO 80523-1373, USA*
[2] *Department of Statistics and Operation Research, The University of North Carolina at Chapel Hill, Chapel Hill, NC 27599-3260, USA*
[3] *Department of Statistics, Colorado State University, Fort Collins, CO 80523-1373, USA*

Correspondence should be addressed to Yang Zhang; yang.zhang@colostate.edu

Received 4 January 2013; Revised 27 February 2013; Accepted 8 March 2013

Academic Editor: Lan Xu

We introduce a continuum modeling method to approximate a class of large wireless networks by nonlinear partial differential equations (PDEs). This method is based on the convergence of a sequence of underlying Markov chains of the network indexed by N, the number of nodes in the network. As N goes to infinity, the sequence converges to a continuum limit, which is the solution of a certain nonlinear PDE. We first describe PDE models for networks with uniformly located nodes and then generalize to networks with nonuniformly located, and possibly mobile, nodes. Based on the PDE models, we develop a method to control the transmissions in nonuniform networks so that the continuum limit is invariant under perturbations in node locations. This enables the networks to maintain stable global characteristics in the presence of varying node locations.

1. Introduction

This paper is concerned with modeling and control of large stochastic networks via nonlinear partial differential equations (PDEs). Recently, we introduced a continuum modeling method for large wireless networks modeled by a certain class of Markov chains. We start with a family of networks indexed by N, the number of nodes, and a related sequence of Markov chains. Under appropriate conditions, the sequence of Markov chains converges in a certain sense to a continuum limit, which is the solution of a nonlinear PDE, as N goes to infinity. Therefore we can use the limiting PDE to approximate the large network [1–5]. This result assumed uniform networks, that is, networks with immobile and uniformly located nodes. Moreover, the model assumes that the nodes have a *fixed* transmission range in the sense that they communicate (exchange data and interfere) only with their immediate neighbors.

The work in this paper builds on the above method. We consider nonuniform networks, that is, networks with nonuniformly located and possibly mobile nodes. We also consider nodes with more general transmission ranges; that is, they may communicate with neighbors further away than immediate ones. For such networks, a natural problem would be to find their continuum limits (the limiting PDEs). A less obvious but more interesting problem concerns the control of nonuniform networks. For example, suppose that a uniform network with certain transmissions achieves a steady state that is desirable in terms of global traffic distribution (e.g., load is well balanced over the network). Further suppose that we want the network to maintain such global characteristics if the nodes are no longer at their original uniform locations. Then the problem is to control the transmissions in the network such that its continuum limit remains invariant.

We address these problems as follows. First, we present a more general network model than that in the existing results [1, 2] and derive its limiting PDEs in the setting of uniform node locations. This generalization is necessary for the discussion of the control of nonuniform networks later. Second, through transformation between uniform and nonuniform node locations, we derive limiting PDEs for nonuniform networks. Finally, by comparing the limiting PDEs of corresponding uniform and nonuniform networks, we develop a method to control the transmissions of nonuniform networks so that the continuum limit is invariant under node locations. In other words, we can maintain a stable global characteristic for nonuniform networks.

The remainder of the paper is organized as follows. First, to describe and contextualize our contribution in this paper, we provide in Section 2 the existing results on continuum modeling of uniform networks. Next, we present the main results of the paper in Section 3; in Section 3.1, we introduce a more general network model and derive its limiting PDEs; in Section 3.2, we derive limiting PDEs for nonuniform and possibly mobile networks; and in Section 3.3, we present a control method for nonuniform networks so that the continuum limit is invariant under node locations. Then we present some numerical examples in Section 4 and conclude the paper in Section 5.

2. Existing Results on Continuum Modeling of Stochastic Networks

This section is devoted to reviewing our continuum modeling method [1, 2] for stochastic networks whose nodes are uniformly located and have a *fixed* transmission range. The study of nonuniform networks in this paper builds on this result. We first describe the network model and then present the result on the convergence of its underlying Markov chain to its continuum limit, which is the solution of a limiting PDE. We discuss some related literature on stochastic network modeling at the end of this section.

We will generalize this modeling method to uniform networks with more general transmission ranges in Section 3.1 and to nonuniform networks in Section 3.2.

2.1. Network Model. Consider a compact, convex Euclidean domain $\mathscr{D} \subset \mathbb{R}^J$ representing a spatial region, with dimension J. In practice, J is typically either 1 or 2. However, our analysis in this paper applies to general J, though our examples are for $J = 1, 2$. Next, consider N points $V_N = \{v_N(1), \dots, v_N(N)\}$ in $\mathscr{D}$ that form a uniform grid. We refer to these points as grid points and denote the distance between any two neighboring grid points by ds_N.

Now consider a network of N wireless sensor nodes over $\mathscr{D}$, where the nodes are labeled by $n = 1, \dots, N$. By a uniform network we mean that node n is located at the grid point $v_N(n) \in V_N$, where $n = 1, \dots, N$. We focus on uniform networks in this section.

The sensor nodes generate, according to a probability distribution, data messages that need to be communicated to the *destination nodes* located on the boundary of $\mathscr{D}$, which represent specialized devices that collect the sensor data. The sensor nodes also serve as relays for routing messages to the destination nodes. Each sensor node has the capacity to store messages in a *queue* and is capable of either transmitting or receiving messages to or from its *immediate* neighbors. In other words, it has a fixed *1-step* transmission range. (We will generalize to further steps of transmission range later in Section 3.1.) At each time instant $k = 0, 1, \dots$, each sensor node probabilistically decides to be a transmitter or receiver, but not both. This simplified rule of transmission allows for a relatively simple representation. We illustrate such a uniform network over a two-dimensional (2D) domain in Figure 1(a).

In this network, communication between nodes is interference limited because all nodes share the same wireless channel. We assume a simple collision protocol: a transmission from a transmitter to an immediate neighboring receiver is successful if and only if none of the other immediate neighbors of the receiver is a transmitter, as illustrated in Figure 1(b). This is the case presented in [1]. (Later, in Section 3.1, when we consider further transmission ranges, interference will occur between not only immediate neighbors, but also neighbors further apart.) In a successful transmission, *one* message is transmitted from the transmitter to the receiver.

We assume that the probability that a node decides to be a transmitter is a function of its normalized queue length (normalized by an "averaging" parameter M). That is, at time k, node n decides to be a transmitter with probability $W(n, X_{N,M}(k,n)/M)$, where $X_{N,M}(k,n)$ is the queue length of node n at time k, and W is a given function.

The queue lengths $X_{N,M}(k) = [X_{N,M}(k,1), \dots, X_{N,M}(k,N)]^\top \in \mathbb{R}^N$ (the superscript $\top$ represents transpose) form a Markov chain whose evolution is given by

$$X_{N,M}(k+1) = X_{N,M}(k) + F_N\left(\frac{X_{N,M}(k)}{M, U_N(k)}\right). \tag{1}$$

Here, the $U_N(k)$ are i.i.d. random vectors that do not depend on the state $X_{N,M}(k)$, and F_N is a given function. As a concrete example, below we present the expression of (1) for a particular network.

For the sake of explanation, we simplify the problem further and consider a 1D domain (2D networks will be treated in the next section). Here, N sensor nodes are uniformly located in an interval $\mathscr{D} \subset \mathbb{R}$ and labeled by $n = 1, \dots, N$. The destination nodes are located on the boundary of $\mathscr{D}$, labeled by $n = 0$ and $n = N + 1$.

We assume that if node n is a transmitter at a certain time instant, it randomly chooses to transmit one message to the right or the left immediate neighbor with probability $P_r(n)$ and $P_l(n)$, respectively, where $P_r(n) + P_l(n) \le 1$. In contrast to strict equality, the inequality here allows for a more general stochastic model of transmission: after a sensor node randomly decides to transmit over the wireless channel, there is still a positive probability that the message is not transferred to its intended receiver (what might be called an "outage").

The special destination nodes at the boundaries of the domain do not have queues; they simply receive any message transmitted to them and never themselves transmit anything. We illustrate the time evolution of the queues in the network in Figure 1(c).

For the particular network introduced above, we have the following expression for $U_N(k)$ in (1)

$$U_N(k) = [(k,1), \dots, Q(k,N), T(k,1), \dots, T(k,N), G(k,1), \dots, G(k,N)]^\top, \tag{2}$$

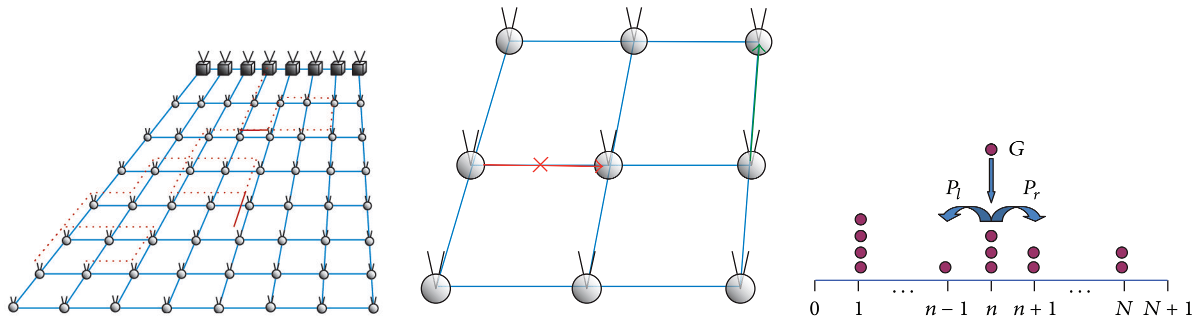

(a) (b) (c)

Figure 1: (a) An illustration of a uniform wireless sensor network over a 2D domain. Destination nodes are located at the far edge. We show the possible path of a message originating from a node located in the left-front region. (b) An illustration of the collision protocol: reception at a node fails when one of its other neighbors transmits (regardless of the intended receiver). (c) An illustration of the time evolution of the queues in the 1D network model.

which is a random vector comprising independent random variables: $Q(k,n)$ are uniform random variables on $[0,1]$ used to determine if the node is a transmitter or not; $T(k,n)$ are ternary random variables used to determine the direction in which a message is passed, which take values R, L, and S (representing transmitting to the right, the left, and neither, resp.) with probabilities $P_r(n)$, $P_l(n)$, and $1-(P_r(n)+P_l(n))$, respectively; and $G(k,n)$ are the number of messages generated at node n at time k. We model $G(k,n)$ by independent Poisson random variables with mean $g(n)$ and call $g(n)$ the incoming traffic to the network.

For a generic $x=[x_1,\dots,x_N]^\top \in \mathbb{R}^N$, the nth component of $F_N(x,U_N(k))$, where $n=1,\dots,N$, is

$$
\begin{aligned}
&1+G(k,n) \\
&\quad \text{if } Q(k,x_{n-1}) < W(n-1,x_{n-1}), \quad T(k,n-1)=R, \\
&\qquad Q(k,x_n) > W(n,x_n), \quad Q(k,x_{n+1}) > W(n+1,x_{n+1}); \\
&\quad \text{or } Q(k,x_{n+1}) < W(n+1,x_{n+1}), \quad T(k,n+1)=L, \\
&\qquad Q(k,x_n) > W(n,x_n), \quad Q(k,x_{n-1}) > W(n-1,x_{n-1}) \\
&-1+G(k,n) \\
&\quad \text{if } Q(k,x_n) < W(n,x_n), \ T(k,n)=L, \\
&\qquad Q(k,x_{n-1}) > W(n-1,x_{n-1}), \\
&\qquad Q(k,x_{n-2}) > W(n-2,x_{n-2}); \\
&\quad \text{or } Q(k,x_n) < W(n,x_n), T(k,n)=R, \\
&\qquad Q(k,x_{n+1}) > W(n+1,x_{n+1}), \\
&\qquad Q(k,x_{n+2}) > W(n+2,x_{n+2}) \\
&G(k,n) \quad \text{otherwise,}
\end{aligned}
\tag{3}
$$

where x_n with $n \le 0$ or $n \ge N+1$ are defined to be zero, and W is the function that specifies the probability that a node decides to be a transmitter, as defined earlier. Here, the three possible values of F_N correspond to the three events that, at time k, node n successfully receives one message, successfully transmits one message, and does neither of the above, respectively. The inequalities and equations on the right describe conditions under which these three events occur: for example, $Q(k,x_{n-1}) < W(n-1,x_{n-1})$ corresponds to the choice of node $n-1$ to be a transmitter at time k, $T(k,n-1)=R$ corresponds to its choice to transmit to the right, and so on.

We assume that $W(n,y) = \min(1,y)$. (We will use this assumption throughout the paper.) Under this assumption, the probability that a node is a transmitter increases linearly with its queue length, up to a maximum value of 1 when the normalized queue length exceeds 1. In general, we would naturally adopt a W function that is increasing in the queue length, so that nodes with more data are more likely to transmit. Here, we assume this function to be linear purely for the sake of simplicity. We could have used a more complicated increasing function. However, doing so complicates the derivation of the resulting PDE and does not serve any insightful purpose.

2.2. Continuum Limit of the Markov Chain. Next, we present in Theorem 2 a result on the convergence of the Markov chain (1) to its continuum limit, which is the solution of a PDE. Based on this theorem, we can approximate the network introduced above by the limiting PDE. We stress that this theorem is not limited to the particular network model above but holds for uniform networks in a more general setting, which we will introduce later in Section 3.1.

The Markov chain model (1) is related to a deterministic difference equation. We set

$$f_N(x) = EF_N(x,U_N(k)), \quad x \in \mathbb{R}^N, \tag{4}$$

and define $x_{N,M}(k) = [x_{N,M}(k,1),\dots,x_{N,M}(k,N)]^\top \in \mathbb{R}^N$ by

$$
\begin{aligned}
x_{N,M}(k+1) &= x_{N,M}(k) + \frac{1}{M} f_N(x_{N,M}(k)), \\
x_{N,M}(0) &= \frac{X_{N,M}(0)}{M} \quad \text{a.s.}
\end{aligned}
\tag{5}
$$

("a.s." is short for "almost surely").

Example 1. For the 1D 1-step network model in Section 2.1, it follows from (3) (with the particular choice of $W(n, y) = \min(1, y)$) that, for $x = [x_1, \ldots, x_N]^\top \in [0,1]^N$, the nth component of $f_N(x)$ in its corresponding deterministic difference equation (5), where $n = 1, \ldots, N$, is (after some tedious algebra, as described in [3])

$$\begin{aligned}&(1 - x_n)\left[P_r(n-1)\,x_{n-1}\,(1 - x_{n+1})\right.\\&\qquad\left.+P_l(n+1)\,x_{n+1}\,(1 - x_{n-1})\right]\\&\quad - x_n\left[P_r(n)\,(1 - x_{n+1})\,(1 - x_{n+2})\right.\\&\qquad\left.+P_l(n)\,(1 - x_{n-1})\,(1 - x_{n-2})\right] + g(n),\end{aligned} \tag{6}$$

where x_n with $n \le 0$ or $n \ge N + 1$ are defined to be zero.

We now construct the PDE whose solution describes the limiting behavior of the Markov chain.

For any continuous function $w : \mathscr{D} \to \mathbb{R}$, let y_N be the vector in $\mathbb{R}^N$ composed of the values of w at the grid points $v_N(n)$; that is, $y_N = [w(v_N(1)), \ldots, w(v_N(N))]^\top$. Given a point $s \in \mathscr{D}$, we let $\{s_N\} \subset \mathscr{D}$ be any sequence of grid points $s_N \in V_N$ such that as $N \to \infty$, $s_N \to s$. Let $f_N(y_N, s_N)$ be the component of the vector $f_N(y_N)$ corresponding to the location s_N; that is, if $s_N = v_N(n) \in V_N$, then $f_N(y_N, s_N)$ is the nth component of $f_N(y_N)$.

Assume that there exists a function f such that as $N \to \infty$, given s in the interior of $\mathscr{D}$, for any sequence of grid points $s_N \to s$,

$$\frac{f_N(y_N, s_N)}{ds_N^2} \longrightarrow f\left(s_N, w(s_N), \nabla w(s_N), \nabla^2 w(s_N)\right). \tag{7}$$

Here, $\nabla^i w$ represents all the ith order derivatives of w, where $i = 1, 2$. These assumptions are technical conditions on the asymptotic behavior of the sequence of functions $\{f_N\}$ that insure that $f_N(y_N, s_N)$ is asymptotically close to an expression that looks like the right-hand side of a time-dependent PDE. Such conditions are familiar in the context of PDE limits of Brownian motion. Checking these conditions often amounts to a simple algebraic exercise.

Assume that there exists a unique function $z : [0, T] \times \mathscr{D} \to \mathbb{R}$ that solves the limiting PDE

$$\dot{z}(t, s) = f\left(s, z(t, s), \nabla z(t, s), \nabla^2 z(t, s)\right), \tag{8}$$

with boundary condition $z(t, s) = 0$ and initial condition $z(0, s) = z_0(s)$. Throughout the paper we assume that $X_{N,M}(0, n)/M = z_0(v_N(n))$ a.s. for each n. We call $X_{N,M}(0)$ the initial state of the network.

Establishing existence and uniqueness for the resulting nonlinear models is a difficult problem in theoretical analysis of partial differential equations in general. The techniques are heavily dependent on the particular form of f. Therefore, as is common with numerical analysis, we assume that this has been established. Below, limiting PDE of the network is a nonlinear diffusion-convection problem. Existence and uniqueness for such problems for "small" data and short times can be established under general conditions. Key ingredients are coercivity, which will hold as long as z is bounded away from 1, and diffusion dominance, which will also hold as long as z is bounded above.

We now present a convergence theorem from [1], which states that the Markov chain $X_{N,M}(k)$ converges uniformly to the solution z of its limiting PDE, as $N \to \infty$ and $M \to \infty$ in a *dependent* way. By this we mean that we set M to be a function of N, written M_N, such that $M_N \to \infty$ as $N \to \infty$. Then we can treat $X_{N,M}$ as sequences of the *single* index N, written X_N. We apply such changes of notation throughout the rest of the paper *whenever* M is treated as a function of N. Define the time step

$$dt_N = \frac{ds_N^2}{M_N} \tag{9}$$

and the total number of time steps $K_N = \lfloor T/dt_N \rfloor$.

Theorem 2. *Almost surely, there exist a sequence $\{\gamma_N\}$, $c_0 < \infty$, N_0, and $\widehat{M}_1 < \widehat{M}_2 < \widehat{M}_3, \ldots$, such that as $N \to \infty$, $\gamma_N \to 0$, and for each $N \ge N_0$ and each $M_N \ge \widehat{M}_N$,*

$$\max_{\substack{k=0,\ldots,K_N\\ n=1,\ldots,N}} \left| \frac{X_N(k, n)}{M_N} - z\left(kdt_N, v_N(n)\right) \right| < c_0 \gamma_N. \tag{10}$$

Hence we can approximate the Markov chain by its continuum limit, the limiting PDE solution, and the accuracy of the approximation increases with N.

Example 3. As a concrete example, we now construct the limiting PDE for the 1D 1-step network model in Section 2.1. To satisfy the conditions on f_N introduced above, we make further assumptions to the network model. We assume that there are functions p_r and p_l from $\mathscr{D}$ to $\mathbb{R}$ such that

$$P_r(n) = p_r(v_N(n)), \qquad P_l(n) = p_l(v_N(n)); \tag{11}$$

and further that

$$p_r(s) = \frac{1}{2} + c_r(s)\, ds_N, \qquad p_l(s) = \frac{1}{2} + c_l(s)\, ds_N, \tag{12}$$

where c_r and c_l are functions from $\mathscr{D}$ to $\mathbb{R}$. Let $c = c_l - c_r$. We call c the convection.

In order to guarantee that the number of messages entering the system from outside over finite time intervals remains finite throughout the limiting process, we set the incoming traffic

$$g(n) = M g_p(v_N(n))\, dt_N. \tag{13}$$

We call g_p the incoming traffic function. Assume that c_l, c_r, and g_p are in $\mathscr{C}^1$.

By these assumptions, it follows from (6) that the limiting PDE (8) for the 1D 1-step network is as follows:

$$\dot{z} = \frac{1}{2}\frac{\partial}{\partial s}\left((1 - z)(1 + 3z)\frac{\partial z}{\partial s}\right) + \frac{\partial}{\partial s}\left(cz(1 - z)^2\right) + g_p, \tag{14}$$

with boundary condition $z = 0$. The detailed derivation for this PDE was presented in [3].

This is a nonlinear diffusion-convection PDE. Note that the computations needed to obtain this require tedious but elementary algebraic manipulations. For this purpose, we found it helpful to use the symbolic tools in Matlab. A comparison of this PDE and the simulation of the corresponding network is provide in Section 4.1.1.

2.3. The Related Literature. The modeling and analysis of stochastic networks is a large field of research and much of the previous contributions share goals with our continuum modeling method.

The analysis for establishing our continuum modeling result used Kushner's ordinary differential equation (ODE) method [6], which is closely related to the line of research called stochastic approximation. This line of research was started by Robbins and Monro [7] and Kiefer and Wolfowitz [8] in the early 1950s and widely used in many areas (see, e.g., [9, 10], for surveys). These results do not study the "large-system" limit in the same sense as our method, and the limits of the system they study are ODEs instead of PDEs. Markov chains modeling's various systems have also been shown by other endeavors to converge to ODEs [11, 12], abstract Cauchy problems [13], or other stochastic processes [6, 14]. These results use methods different from Kushner's but share with it the principle idea in weak convergence theory [6, 14, 15].

There are a variety of other analysis methods for large systems taking completely different approaches. For example, the well-cited work of Gupta and Kumar [16], followed by many others (e.g., [17, 18]), derives scaling laws of network performance parameters (e.g., throughput); many efforts based on mean field theory [19–22] or on the theory of large deviations [23–25] study the limit of the so-called empirical (or occupancy) measure or distribution. These approaches differ from our work because they do not study the spatiotemporal characteristics of the system.

There do exist numerous continuum models in a wide spectrum of areas that formulate spatiotemporal phenomena (e.g., [26–29]), many of which use PDEs. All these works differ from our continuum limit method both by the properties of the system being studied and the analytic approaches. In addition, most of them study distributions of limiting processes that are random, while our limiting functions themselves are deterministic.

There is a vast literature on the convergence of a large variety of network models different from ours, to fluid and diffusion limits [30–35]. Unlike our work, this field of research focuses primarily on networks with a fixed number of nodes.

There are well-established mathematical tools to solve PDEs, which include analytical methods, such as the method of characteristics, integral transforms [36], and asymptotic methods [37], and numerical methods such as the finite element method [38] and the finite difference method [39]. The continuum model allows us to use these tools to greatly reduce computation time. The limiting PDEs for the networks in this paper can be solved by computer software packages in Matlab or Comsol that use numerical methods.

3. Main Results

3.1. Continuum Models of Uniform Networks. We introduced the wireless sensor network model in a simple setting in Section 2.1. In this subsection, we consider uniform networks in a more general setting where the network nodes have more general transmission ranges and derive their limiting PDEs. Such generalization is necessary for the control of nonuniform networks to be possible (explained in Section 3.3.1). We consider nonuniform networks in Section 3.2.

3.1.1. A More General Network Model. Recall that in Section 2.1 we introduced 1-step networks where the sensor nodes communicate (exchange data and interfere) with their immediate neighbors. We now consider L-step networks where the nodes communicate with their communicating neighbors, which can be further away than the immediate ones. To be specific, at each time instant, a transmitter tries to transmit a message to one of its communicating neighbors; a receiver may receive a message from one of its communicating neighbors. Interference also occurs among communicating neighbors: a transmission from a transmitter to a receiver (one of the communicating neighbors of the transmitter) is successful if and only if none of the other communicating neighbors of the receiver is a transmitter.

For an L-step network, we call the positive integer L its *communication range* and assume that it determines the communicating neighbors as follows.

In a 1D L-step network of N nodes, communicating neighbors of the node at $s \in V_N \subset \mathbb{R}$ are the nodes at $s \pm l ds_N$, where $1 \le l \le L$.

In 2D networks, we consider two types of communicating neighbors. In a 2-D L-step network of N nodes, for a node at $s = (s_1, s_2) \in V_N \subset \mathbb{R}^2$, its communicating neighbors are the nodes at

$$(s_1 \pm l_1 ds_N, s_2 \pm l_2 ds_N), \tag{15}$$

where

(i) for Type I networks, $0 \le l_1,\ l_2 \le L$, $l_1 + l_2 > 0$, and $l_1 l_2 = 0$;

(ii) for Type II networks, $0 \le l_1,\ l_2 \le L$ and $l_1 + l_2 > 0$.

We illustrate the two types of definition of communicating neighbors for 2-D 1-step networks in Figure 2.

We assume the use of directional antennas and power control to accommodate such routing schemes. Here we consider two types of communicating neighbors because they may correspond to two types of routing schemes, and one may be a better model than the other for networks with different design choices. For example, a Type-II network may offer higher rate in propagating information to the destination nodes at the boundaries but at the same time may require more complex directional antennas and power control to implement.

Next we derive the limiting PDEs for this more general network model.

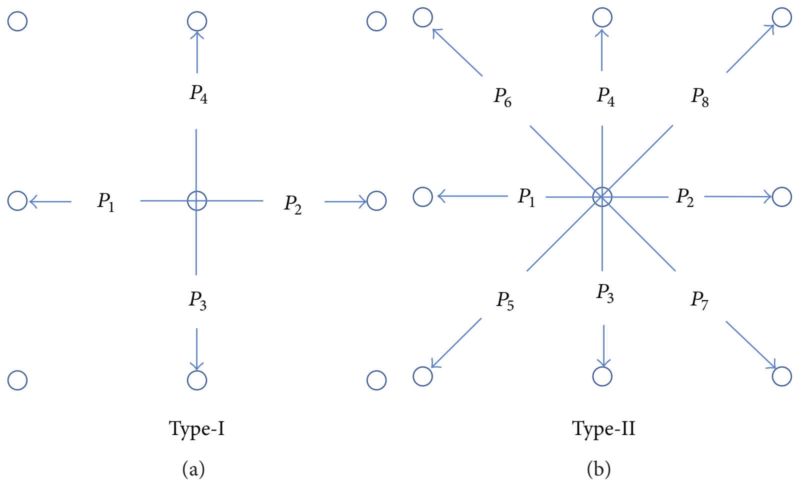

FIGURE 2: The two types of communicating neighbors of 2D 1-step networks. The nodes pointed by the arrows are the communicating neighbors of the node in the center. The labels on the arrows are probabilities of transmitting to the pointed communicating neighbors.

3.1.2. Limiting PDEs for Uniform Networks. The network model above can again be written as (1), for which Theorem 2 still holds.

We assume that if, at time k, node n is a transmitter, it randomly chooses to transmit a message to its ith communicating neighbor with probability $P_i(k,n)$, where the possible values of i depend on the number of its communicating neighbors. Note that here P_i depends on k, that is, is time variant, which generalizes the case in Section 2.1. Correspondingly, we now assume that

$$P_i(k,n) = p_i\left(kdt_N, v_N(n)\right); \tag{16}$$

that

$$p_i(t,s) = b_i(t,s) + c_i(t,s)\,ds_N, \tag{17}$$

where b_i and c_i are $\mathscr{C}^1$ functions from $[0,T]\times\mathscr{D}$ to $\mathbb{R}$. We call p_i the *direction function*. We have assumed above that the probabilities P_i of the direction of transmission are the values of the continuous functions p_i at the grid points, respectively. This may correspond to stochastic routing schemes where nodes in close vicinity behave similarly based on some local information that they share or to those with an underlying network-wide directional configuration that are continuous in space, designed to relay messages to destination nodes at known locations.

For a JD L-step network, let $\lambda_{(J,L)}$ be the number of the communicating neighbors of its nodes that are away from the boundaries. We have that

$$\lambda_{(J,L)} := \begin{cases} 2LJ, & \text{for Type-I networks;} \\ (1+2L)^J - 1, & \text{for Type-II networks.} \end{cases} \tag{18}$$

We assume that the communicating neighbors of each node are indexed according only to their *relative* locations with respect to the node. For example, if we call the left immediate neighbor of *any* node its 1st neighbor, then the left immediate neighbor of *all* nodes must be their 1st neighbor, respectively. That is, for a node at $v_N(n)$, if we denote by $v_N(n,i)$ the location of its ith communicating neighbor, then $v_N(n) - v_N(n,i)$ depends on i, but not on n.

We present below the limiting PDE in the sense of Theorem 2 for an arbitrary J-D L-step network with both Type-I and II communicating neighbors. The PDE is derived in a way similar to that of (14) for the 1-D 1-step network in Section 2, which involves writing down the expression of the corresponding Markov chain (1) and then the difference equation (5), except that we now have to consider transmission to and interference from more neighbors instead of only the two immediate ones, requiring more arduous, but still elementary, algebraic manipulation. We omit the algebraic details here.

Let $\{e_1,\dots,e_J\}$ be the standard basis of $\mathbb{R}^J$; that is, e_j is the element of $\mathbb{R}^J$ with the jth entry being 1 and other entries 0. Define

$$\begin{aligned} b^{(j)} &= \sum_i^{\lambda_{(J,L)}} \frac{\left(\left(v_N(n,i) - v_N(n)\right)^\top e_j\right)^2 b_i}{2}, \\ c^{(j)} &= \sum_i^{\lambda_{(J,L)}} \left(v_N(n,i) - v_N(n)\right)^\top e_j c_i. \end{aligned} \tag{19}$$

Then the limiting PDE for a J-D L-step network is

$$\begin{aligned} \dot{z} = \sum_{j=1}^{J} \Bigg(& b^{(j)} \frac{\partial}{\partial s_j}\left(\left(1 + \left(\lambda_{(J,L)} + 1\right) z\right)(1-z)^{(\lambda_{(J,L)}-1)} \frac{\partial z}{\partial s_j}\right) \\ & + 2(1-z)^{(\lambda_{(J,L)}-1)} \frac{\partial z}{\partial s_j}\frac{\partial b^{(j)}}{\partial s_j} + z(1-z)^{\lambda_{(J,L)}} \frac{\partial^2 b^{(j)}}{\partial s_j^2} \\ & + \frac{\partial}{\partial s_j}\left(c^{(j)} z (1-z)^{\lambda_{(J,L)}}\right)\Bigg) + g_p, \end{aligned} \tag{20}$$

with boundary condition $z(t,s)=0$. This general PDE works for both Type-I and II communicating neighbors, provided that $\lambda_{(J,L)}$ is calculated with (18) accordingly. We will present some concrete examples of the PDEs and the corresponding network models in Section 4.1.

3.2. Continuum Models of Nonuniform Networks. In this subsection we extend the continuum models to nonuniform and mobile networks. First we introduce the transformation function, which is the mapping between the node locations of uniform and nonuniform networks. Then, through the transformation function, we derive the continuum limits of nonuniform and mobile networks with given trajectories and transmissions. We consider the domain $\mathscr{D} \subset \mathbb{R}^J$ and a fixed time interval $[0, T]$.

3.2.1. Location Transformation Function. For networks with the design of uniform node placement, there may be small perturbations to the uniform grid because of imperfect implementation or landscape limitation; some sensor networks may have nodes with moderate mobility. The study of nonuniform networks here is motivated by the need for modeling these networks. Again we assume the use of directional antennas and power control to preserve the neighborhood structure in the nonuniform or mobile networks.

Consider a nonuniform and possibly mobile network with N nodes indexed by $n = 1, \dots, N$ over $\mathscr{D}$. The nodes no longer are located at the grid points V_N and possibly change their locations at each time step k.

We denote by $\widetilde{v}_N(k, n)$ the location of node n of the nonuniform network at time k. Let $\widetilde{v}_N(k) = [\widetilde{v}_N(k,1), \dots, \widetilde{v}_N(k, N)]$ and $\widetilde{V}_N = [\widetilde{v}_N(0), \dots, \widetilde{v}_N(K_N)]$. Assume that there exists a smooth *transformation function* $\phi(t, s) : [0, T] \times \mathscr{D} \to \mathscr{D}$ such that, for each k and n,

$$\widetilde{v}_N(k, n) = \phi\left(kdt_N, v_N(n)\right), \tag{21}$$

and, for each t_o, $\phi(t_o, \cdot)$ is bijective. Hence ϕ is the mapping between the nonuniform node locations and uniform grid points.

Note that, for mobile networks, by assuming that $\phi(t_o, \cdot)$ is bijective for each t_o, we focus on a subset of all possible node movements, which simplifies the problem. This restricts the mobility of nodes but is still a reasonable model in many practical scenarios, for example, in sensor networks where each node collects environmental data from its designated area and moves in a small neighborhood of, instead of arbitrarily far away from, their original locations.

Since $\phi(t_o, \cdot)$ is bijective, its inverse with respect to s exists and we denote it by $\eta : [0, T] \times \mathscr{D} \to \mathscr{D}$; that is, for each t and s,

$$\eta\left(t, \phi(t, s)\right) = s. \tag{22}$$

Throughout the paper we assume fixed nodes on the boundary; that is, $\phi(t, s) = s$ for s on the boundary of $\mathscr{D}$.

For *given* N and $\widetilde{V}_N$, a transformation function ϕ can be constructed using some interpolation scheme. Note that ϕ is not unique because of the freedom we have in choosing different schemes. Let ϕ_j and η_j be the jth components of ϕ and η, respectively, where $j = 1, \dots, J$. For the rest of the paper, we assume that for $i \neq j$,

$$\frac{\partial \phi_j}{\partial s_i} = 0. \tag{23}$$

Then equivalently, for $i \neq j$, $(\partial \eta_j / \partial s_i) = 0$. This assumption can be achieved by choosing a proper interpolation scheme, and it simplifies the analysis below.

On the other hand, a *given* ϕ, by (21), specifies a sequence $\{\widetilde{V}_N\}$ of nonuniform node locations indexed by N. We study the continuum limit of a *sequence* of nonuniform networks associated with such $\{\widetilde{V}_N\}$; that is, for each N, the N-node nonuniform network has node locations $\widetilde{V}_N$.

3.2.2. Continuum Limits of Mirroring Networks. For an N-node network (uniform or nonuniform), we define its *transmission-interference rule* to be

(i) the probability that node m sends a message to node n at time k;

(ii) the fact of whether nodes m and n interfere at time k,

for $m, n = 1, \dots, N$ and $k = 0, 1, \dots, K_N$. The transmission-interference rule specifies how the nodes in a network interact with each other at each time step. At each time step, each node chooses to be a transmitter with a certain probability; if it chooses to be a transmitter, it then chooses one of its communicating neighbors to send a message to. The first component of this definition is determined by the probabilities of the above choices of *all* the nodes at *all* the time steps. The second component of this definition is determined by the neighborhood structure of the network at each time step; that is, which nodes are the communicating neighbors of each node (so that they interfere with it) at each time step.

For each N, write $X_N = [X_N(0), \dots, X_N(K_N)]$. Then we can describe a network during $[0, T]$ entirely by its states X_N. Define the *network behavior* of a network X_N to be the combination of its initial state $X_N(0)$, transmission-interference rule, and incoming traffic $g(n)$. Two sequences $\{X_N\}$ and $\{\widetilde{X}_N\}$ of networks indexed by the number N of nodes, with different node locations in general, are said to *mirror* each other if, for each N, X_N and $\widetilde{X}_N$ have the same network behavior. We state in the following theorem the relationship between the continuum limits of mirroring networks.

Theorem 4. *Suppose that a sequence $\{\widetilde{X}_N\}$ of networks has node locations specified by a given transformation function ϕ with inverse η. If $\{\widetilde{X}_N\}$ mirrors a sequence $\{X_N\}$ of uniform networks, then $\{X_N\}$ converges to a function $q(t, s)$ on $[0, T] \times \mathscr{D}$ in the sense of Theorem 2 if and only if $\{\widetilde{X}_N\}$ converges to*

$$u(t, s) := q\left(t, \eta(t, s)\right), \tag{24}$$

in the sense that almost surely there exist a sequence $\{\gamma_N\}$, $c_0 < \infty$, N_0, and $\widehat{M}_1 < \widehat{M}_2 < \widehat{M}_3, \dots$, such that as $N \to \infty$, $\gamma_N \to 0$, and for each $N \geq N_0$ and each $M_N \geq \widehat{M}_N$,

$$\max_{\substack{k=0,\dots,K_N \\ n=1,\dots,N}} \left| \frac{\widetilde{X}_N(k, n)}{M_N} - u\left(kdt_N, \widetilde{v}_N(k, n)\right) \right| < c_0 \gamma_N, \tag{25}$$

where $\widetilde{v}_N(k, n)$ is the location of node n at time k in $\widetilde{X}_N$.

Proof. "⇒": Since $\{X_N\}$ and $\{\widetilde{X}_N\}$ mirror each other, they would converge to the same continuum limit on a uniform grid. Therefore, by Theorem 2, almost surely, there exist a sequence $\{\gamma_N\}$, $c_0 < \infty$, N_0, and $\widehat{M}_1 < \widehat{M}_2 < \widehat{M}_3, \ldots$, such that as $N \to \infty$, $\gamma_N \to 0$, and for each $N \ge N_0$ and each $M_N \ge \widehat{M}_N$,

$$\max_{\substack{k=0,\ldots,K_N \\ n=1,\ldots,N}} \left| \frac{\widetilde{X}_N(k,n)}{M_N} - q\left(kdt_N, v_N(n)\right) \right| < c_0 \gamma_N. \tag{26}$$

We note that

$$\begin{aligned} q\left(kdt_N, v_N(n)\right) &= u\left(kdt_N, \phi\left(kdt_N, v_N(n)\right)\right) \\ &= u\left(kdt_N, \widetilde{v}_N(k,n)\right), \end{aligned} \tag{27}$$

where the first equality follows from (22) and (24), and the second from (21). Then (26) is equivalent to (25).

"⇐": Done analogously in the opposite direction. □

3.2.3. Sensitivity of Uniform Continuum Models to Location Perturbation. In networks with nodes not necessarily at, but close to, the uniform grid points, we can use *uniform* continuum models to approximate nonuniform networks, that is, treat them as uniform while deriving limiting PDEs. Then a certain approximation error arises from ignoring nonuniformity. If we treat such nonuniformities as perturbations to the uniform models, the above theorem enables us to analyze the error *sensitivity* of these models with respect to such perturbation.

Consider a sequence $\{\widetilde{X}_N\}$ of nonuniform networks with node locations specified by the transformation function ϕ with inverse η. Suppose that we ignore the nonuniformity and approximate $\{\widetilde{X}_N\}$ by the continuum limit q of the sequence $\{X_N\}$ of uniform networks that mirrors $\{\widetilde{X}_N\}$. We now characterize the maximum approximation error

$$\varepsilon_N := \max_{\substack{k=0,\ldots,K_N \\ n=1,\ldots,N}} \left| \frac{\widetilde{X}_N(k,n)}{M_N} - q\left(kdt_N, \widetilde{v}_N(k,n)\right) \right| \tag{28}$$

by ϕ in the following proposition.

Proposition 5. *Almost surely, there exist a sequence $\{\gamma_N\}$, c_0, $c_1 < \infty$, N_0, and $\widehat{M}_1 < \widehat{M}_2 < \widehat{M}_3, \ldots$, such that as $N \to \infty$, $\gamma_N \to 0$, and for each $N \ge N_0$ and each $M_N \ge \widehat{M}_N$,*

$$\begin{aligned} \varepsilon_N \le c_0\gamma_N &+ \sup_{(t,s)} \left| q_s(t,s) \right| \sup_{(t,s)} \left| \eta(t,s) - s \right| \\ &+ c_1 \sup_{(t,s)} \left(\eta(t,s) - s\right)^2. \end{aligned} \tag{29}$$

Proof. We have, from the triangle inequality, that

$$\begin{aligned} \varepsilon_N \le \max_{k,n} \Bigg(&\left| \frac{\widetilde{X}_N(k,n)}{M_N} - u\left(kdt_N, \widetilde{v}_N(k,n)\right) \right| \\ &+ \left| u\left(kdt_N, \widetilde{v}_N(k,n)\right) - q\left(kdt_N, \widetilde{v}_N(k,n)\right) \right| \Bigg) \\ \le \max_{k,n} &\left| \frac{\widetilde{X}_N(k,n)}{M_N} - u\left(kdt_N, \widetilde{v}_N(k,n)\right) \right| \\ &+ \sup_{(t,s)\in[0,T]\times\mathscr{D}} \left| u(t,s) - q(t,s) \right|, \end{aligned} \tag{30}$$

where u is defined by (24).

By Theorem 4, almost surely, there exist a sequence $\{\gamma_N\}$, $c_0 < \infty$, N_0, and $\widehat{M}_1 < \widehat{M}_2 < \widehat{M}_3, \ldots$, such that as $N \to \infty$, $\gamma_N \to 0$, and for each $N \ge N_0$ and each $M_N \ge \widehat{M}_N$, the first term above is smaller than $c_0\gamma_N$.

The second term represents the error caused by location perturbation. By (24) and Taylor's theorem, there exists $c_1 < \infty$ such that

$$\begin{aligned} u(t,s) - q(t,s) &= q\left(t, \eta(t,s)\right) - q(t,s) \\ &\le q_s(t,s)\left(\eta(t,s) - s\right) + c_1\left(\eta(t,s) - s\right)^2. \end{aligned} \tag{31}$$

Therefore we have that

$$\begin{aligned} \sup_{(t,s)} \left| u(t,s) - q(t,s) \right| \le \sup_{(t,s)} &\left| q_s(t,s) \right| \sup_{(t,s)} \left| \eta(t,s) - s \right| \\ &+ c_1 \sup_{(t,s)} \left(\eta(t,s) - s\right)^2. \end{aligned} \tag{32}$$

By (30) this completes the proof. □

This proposition states that, for fixed q and for N and M_N sufficiently large, ε_N is dominated by the supremum location perturbation $\sup_{(t,s)}|\eta(t,s) - s|$, when it is close to 0. We note that by definition $\sup_{(t,s)}|\eta(t,s) - s| = \sup_{(t,s)}|\phi(t,s) - s|$. In the case where $\widetilde{X}_N$ are uniform; that is, $\eta(t,s) = \phi(t,s) = s$, the last two terms on the right-hand side of (29) vanish.

3.2.4. Limiting PDEs for Nonuniform Networks. Consider a sequence $\{\widetilde{X}_N\}$ of networks with *given* network behavior and with node locations specified by a given transformation function ϕ with inverse η. If a sequence $\{X_N\}$ of uniform networks mirrors $\{\widetilde{X}_N\}$, from this given network behavior, we can find the continuum limit q of $\{X_N\}$ by constructing its limiting PDE as in Section 3.1.2. Suppose that this PDE has the form

$$\dot{q}(t,s) = Q\left(s, q(t,s), \frac{\partial q}{\partial s_j}(t,s), \frac{\partial^2 q}{\partial s_j^2}(t,s)\right), \tag{33}$$

with initial condition $q(0,s) = q_0(s)$, where $j = 1, \ldots, J$, $t \in [0,T]$, and $s = (s_1, \ldots, s_J) \in \mathscr{D}$. By Theorem 4, we have that the continuum limit $u(t,s)$ of $\{\widetilde{X}_N\}$ satisfies (24).

However, in general, we can only solve (33) numerically instead of analytically. In fact, all the limiting PDEs in this paper are solved by software using numerical methods. In this case we cannot find the closed-form expression of u from q using (24). Instead, we derive a PDE that u satisfies so that we can solve it numerically.

Suppose that $u(t,s)$ solves the PDE

$$\dot{u}(t,s) = \Gamma\left(s, u(t,s), \frac{\partial u}{\partial s_j}(t,s), \frac{\partial^2 u}{\partial s_j^2}(t,s)\right), \tag{34}$$

with initial condition $u(0,s) = u_0(s)$, where $j = 1,\ldots,J$ and $(t,s) \in [0,T] \times \mathscr{D}$. We now find Γ from the known PDE (33).

By (23), (24), and the chain rule,

$$\frac{\partial u}{\partial s_j}(t,s) = \frac{\partial \eta_j}{\partial s_j}(t,s)\frac{\partial q}{\partial s_j}(t,\eta(t,s)). \tag{35}$$

By (23), the product rule, and the chain rule,

$$\begin{aligned}\frac{\partial^2 u}{\partial s_j^2}(t,s) &= \frac{\partial^2 \eta_j}{\partial s_j^2}(t,s)\frac{\partial q}{\partial s_j}(t,\eta(t,s)) \\ &\quad + \left(\frac{\partial \eta_j}{\partial s_j}(t,s)\right)^2 \frac{\partial^2 q}{\partial s_j^2}(t,\eta(t,s)).\end{aligned} \tag{36}$$

Note that, without assumption (23), the expression of the derivatives above would be much more complex. Then by (24), (33), and (34) we have

$$\begin{aligned}&\Gamma\left(s, u(t,s), \frac{\partial u}{\partial s_j}(t,s), \frac{\partial^2 u}{\partial s_j^2}(t,s)\right) \\ &= Q\left(\eta(t,s), u(t,s), \frac{(\partial u/\partial s_j)(t,s)}{(\partial \eta_j/\partial s_j)(t,s)}, \frac{(\partial^2 u/\partial s_j^2)(t,s)}{((\partial \eta_j/\partial s_j)(t,s))^2}, \right. \\ &\qquad \left. -\frac{(\partial^2 \eta_j/\partial s_j^2)(t,s)(\partial u/\partial s_j)(t,s)}{((\partial \eta_j/\partial s_j)(t,s))^3}\right),\end{aligned} \tag{37}$$

where $u_0(s) = q_0(\eta(0,s))$. Hence we find the limiting PDE (34) of $\{\widetilde{X}_N\}$.

We present a concrete numerical example of the nonuniform network and its continuum limit later in Section 4.2.

3.3. Control of Nonuniform Networks. The global characteristic of the network is determined by the transmission-interference rule defined in Section 3.2.2 and is described by its limiting PDE. The transmission-interference rule depends entirely on the transmission range L and the probabilities P_i, which in turn by (16) depends on the direction function p_i. On the other hand, L and p_i also determine the limiting PDE of a sequence of networks. Therefore we can *control* the transmission-interference rule to obtain the desired limiting PDE, and hence the desired global characteristic of the network, by changing L and p_i.

For uniform networks, this procedure is straightforward because L and p_i relate directly to the form and coefficients of the limiting PDE. For example, for the 1D 1-step network in Section 2.2 with limiting PDE (14), increasing the convection c results in a greater bias of the PDE solution to the left side of the domain. (A numerical example of this network is provided in Section 4.1.1.)

We now study this kind of control for nonuniform and possibly mobile networks. For such networks, we have to take into account the varying node locations in order to still achieve certain global characteristics. The goal is to develop a control method so that the continuum limit is invariant under node locations and mobility, that is, remains the same as a reference, which is the continuum limit of the sequence of corresponding uniform networks with a certain transmission-interference rule. We then say the sequence has a location-invariant continuum limit.

We illustrate this idea in Figure 3. The plus signs in both figures represent the queues of a certain uniform network at a certain time. The solid lines in both figures represent the continuum limit (the limiting PDE solution) of the same uniform network at the same time. Thus they resemble each other. On the left, the diamonds represent the queues of a nonuniform network with the same transmission-interference rule as the uniform network, but no longer resembling the continuum limit because of the changes in node locations. On the right, the circles represent the queues of a second nonuniform network with the same node locations as the first nonuniform network, but under some control over its transmission-interference rule, therefore resembling the continuum limit of the uniform network. In other words, location invariance in the second nonuniform network has been achieved by network control. Apparently, for this particular network, such a control scheme has to be able to direct more (and the right amount of) data traffic to the right-hand side. In what follows, we describe how this can be done by properly increasing the probabilities of the nodes transmitting to the right through the use of the limiting PDEs.

Throughout the paper we assume no control over node location or motion.

3.3.1. Transmission-Interference Rule for Location Invariance. Consider a sequence $\{\widetilde{X}_N\}$ of nonuniform networks whose node locations are specified by a given transformation function ϕ with inverse η and a sequence $\{\widehat{X}_N\}$ of uniform networks with *given* transmission-interference rule and continuum limit u. We want to control the transmission-interference rule of $\{\widetilde{X}_N\}$ so that it also converges to u, that is, obtains the location-invariant continuum limit.

Again we do not assume a known closed-form expression of u. Instead, assume that $u(t,s)$ solves (34), except that Γ is now *given*.

Define

$$q(t,s) = u(t,\phi(t,s)). \tag{38}$$

Suppose that a sequence $\{X_N\}$ of uniform networks has continuum limit $q(t,s)$. By Theorem 4, for $\{\widetilde{X}_N\}$ to converge to this desired $u(t,s)$, it suffices that $\{\widetilde{X}_N\}$ mirrors $\{X_N\}$. Therefore all we have to do is to specify the transmission-interference rule of $\{X_N\}$ to $\{\widetilde{X}_N\}$. Next we find this transmission-interference rule.

Suppose that $q(t,s)$ solves (33), except that Q is now *unknown*. Again using the product rule and the chain rule as

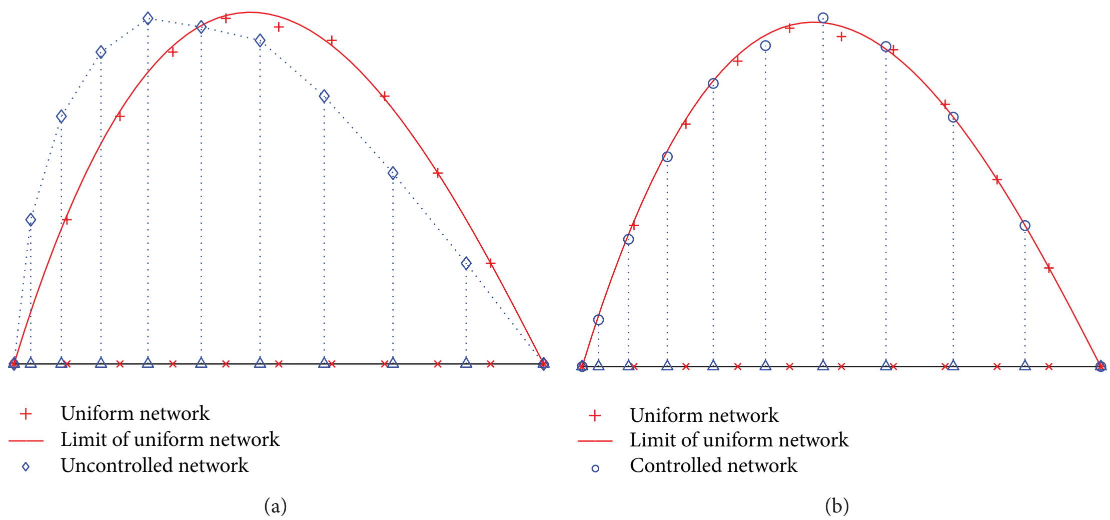

FIGURE 3: An illustration of control of nonuniform networks. On the x-axis, the $\times$ marks are the uniform grid, and the Δ marks are the nonuniform node locations.

we did in Section 3.2.4, by (33), (34), and (38), we have that

$$Q\left(s, q(t,s), \frac{\partial q}{\partial s_j}(t,s), \frac{\partial^2 q}{\partial s_j^2}(t,s)\right) = \Gamma\left(\phi(t,s), q(t,s), \frac{(\partial q/\partial s_j)(t,s)}{(\partial \phi_j/\partial s_j)(t,s)}, \frac{(\partial^2 q/\partial s_j^2)(t,s)}{((\partial \phi_j/\partial s_j)(t,s))^2} - \frac{(\partial^2 \phi_j/\partial s_j^2)(t,s)(\partial q/\partial s_j)(t,s)}{((\partial \phi_j/\partial s_j)(t,s))^3}\right), \tag{39}$$

and $q_0(s) = u_0(\phi(0,s))$, where $j = 1, \dots, J$.

Since $q(t,s)$ is the continuum limit of a sequence of uniform networks, (33) must be a case of (20), the general limiting PDE. Therefore we can replace the left-hand side of (39) by the right-hand side of (20) and get

$$\begin{aligned}\sum_{j=1}^{J}\Bigg(b^{(j)}(t,s)\frac{\partial}{\partial s_j}\Bigg(&(1+(\lambda_{(J,L)}+1)z(t,s)) \\ &\times(1-z(t,s))^{(\lambda_{(J,L)}-1)}\frac{\partial z}{\partial s_j}(t,s)\Bigg) \\ &+2(1-z(t,s))^{(\lambda_{(J,L)}-1)}\frac{\partial z}{\partial s_j}(t,s)\frac{\partial b^{(j)}}{\partial s_j}(t,s) \\ &+z(t,s)(1-z(t,s))^{\lambda_{(J,L)}}\frac{\partial^2 b^{(j)}}{\partial s_j^2}(t,s) \\ &+\frac{\partial}{\partial s_j}\left(c^{(j)}(t,s)z(t,s)(1-z(t,s))^{\lambda_{(J,L)}}\right)\Bigg)+g_p(t,s) \\ = \Gamma\Bigg(\phi(t,s), q(t,s), &\frac{(\partial q/\partial s_j)(t,s)}{(\partial \phi_j/\partial s_j)(t,s)}, \frac{(\partial^2 q/\partial s_j^2)(t,s)}{((\partial \phi_j/\partial s_j)(t,s))^2} - \frac{(\partial^2 \phi_j/\partial s_j^2)(t,s)(\partial q/\partial s_j)(t,s)}{((\partial \phi_j/\partial s_j)(t,s))^3}\Bigg).\end{aligned} \tag{40}$$

We call this the *comparison equation*. If we can solve it for L, p_l, and g_p, our goal is accomplished because they determine the network behavior, which includes the transmission-interference rule, for each N-node uniform network in the mirroring sequence $\{X_N\}$. If we assign the same transmission-interference rule to $\{\widetilde{X}_N\}$, then it has the location-invariant continuum limit $u(t,s)$.

We note a constraint for (40): by (16), for each i, p_i has to be sufficiently small such that, for each k and n,

$$P_i(k,n) \in [0,1], \qquad \sum_i P_i(k,n) \in [0,1]. \tag{41}$$

In turn by (17), b_i and c_i have to be sufficiently small for (41) to hold. By further observing (18) and (19), it follows that the transmission range L has to be sufficiently large. For this reason, it is necessary to generalize from 1-step to L-step transmission range, as we did in Section 3.1. Note that with this constraint, (40) is still underdetermined. Such freedom gives us a class of transmission-interference rules to assign to $\{\widetilde{X}_N\}$ instead of just one.

One way to solve (40) is this. Suppose that we have chosen L sufficiently large. Since (34) is now given, we know the numerical form of u and in turn that of q by (38). For fixed t_o, we put $q(t_o,s)$ in (40). For each j, if we fix $b^{(j)}(t_o,s)$, then we can solve (40), which is now an ordinary differential equation (ODE), for $c^{(j)}(t_o,s)$. Similarly, fixing $c^{(j)}(t_o,s)$ makes (40) an ODE that we can solve for $b^{(j)}(t_o,s)$. Then by (19) we can further choose b_i and c_i and further determine p_i by (17). Thus we have found P_i by (16), which together with L determines the transmission-interference rule.

3.3.2. Distributed Control Using Local Information. The control method presented above is centralized in the sense that it requires knowledge of the transformation function ϕ over $\mathscr{D}$. This assumes that each node knows the location of all other nodes. However, this is generally not the case in practice, especially for networks without a central control unit. In this subsection we present a distributed version of our control method, where only the locations of nearby nodes are needed for each node to determine its transmission-interference rule. We can do this because all the information needed to solve the comparison equation (40) can be approximated locally at each node.

The derivatives of ϕ in (40) can be approximated from the locations of neighboring nodes using a certain finite difference method. For example, in the 1-D case, we can use the following approximation:

$$\frac{\partial \phi}{\partial s}(t,s) \approx \frac{\phi\left(kdt_N, v_N(n+1)\right) - \phi\left(kdt_N, v_N(n-1)\right)}{2ds_N} = \frac{\tilde{v}_N(k,n+1) - \tilde{v}_N(k,n-1)}{2ds_N}, \tag{42}$$

where $t = kdt_N$ and $s \in [v_N(n-1), v_N(n+1))$. Note that we can also use the location information of further neighbors to get a more accurate approximation of $\partial\phi/\partial s$. The trade-off between locality and accuracy can be flexibly adjusted.

The ODE for $b^{(j)}$ or $c^{(j)}$ can also be solved based on local information using numerical procedures such as Euler's method [40].

We present two concrete examples of network control in 1D and 2D case, in Sections 4.3.1 and 4.3.2, respectively.

4. Numerical Examples

We now present numerical examples for continuum model of uniform networks, continuum model of nonuniform networks, and control of nonuniform networks in Sections 4.1, 4.2, and 4.3, respectively.

4.1. Examples of Uniform Networks

4.1.1. 1D Example. We discussed the 1D 1-step network as a running example through Section 2 and derived its limiting PDE (14). We now run Monte Carlo simulation for such a net work and compare the simulation result with the limiting PDE solution. (Simulations and PDEs presented in this paper are run and solved using Matlab.) We set the spatial domain $\mathscr{D} = [-1,1]$. We set the number of nodes $N = 50$ and the normalizing parameter $M = 5000$. We set the initial condition of the limiting PDE $z_0(s) = r_1 e^{-s^2}$, where $r_1 > 0$ is a constant, so that initially the nodes in the middle have messages to transmit, while those near the boundaries have very few. We set the incoming traffic function $g_p(s) = r_2 e^{-s^2}$, where

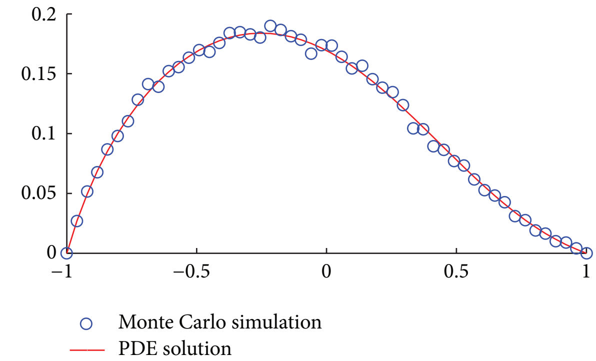

Figure 4: The Monte Carlo simulation and the PDE solution of a 1D 1-step network.

$r_2 > 0$ is a constant determining the total load of the network, so that the nodes in the middle generate more messages than those near the boundaries. We set the diffusion function $b = 1/2$ and the convection function $c = 2$, so that each node transmits to the left with a higher probability than to the right; that is, more data traffic in the network is routed to the left. In Figure 4, we show the PDE solution and the simulation result at time $t = 1$ s, where the x-axis denotes the node location and y-axis denotes the normalized queue length. As we can see, the PDE well resembles the network.

4.1.2. 2D Examples. We consider 2-D 1-step networks with the two types of communicating neighbors separately (as illustrated in Figure 2).

Type I Communicating Neighbors. For 2D 1-step networks of Type I communicating neighbors, we define the probabilities P_i of transmitting to the 4 communicating neighbors as in Figure 2. This is the same as the 2D network studied in [1].

The limiting PDE for this network is as follows:

$$\dot{z} = \sum_{j=1}^{2}\left(b^{(j)}\frac{\partial}{\partial s_j}\left((1+5z)(1-z)^3\frac{\partial z}{\partial s_j}\right) + 2(1-z)^3\frac{\partial z}{\partial s_j}\frac{\partial b^{(j)}}{\partial s_j} + z(1-z)^4\frac{\partial^2 b^{(j)}}{\partial s_j^2} + \frac{\partial}{\partial s_j}\left(c^{(j)}z(1-z)^4\right)\right) + g_p, \tag{43}$$

where $b^{(1)} = (b_1+b_2)/2$, $b^{(2)} = (b_3+b_4)/2$, $c^{(1)} = c_1 - c_2$, $c^{(2)} = c_3 - c_4$, and $(s_1,s_2) \in \mathscr{D}$. (As mentioned in Section 3.1.2, we omit the detailed algebraic derivation.)

We consider such a network over the spatial domain $D = [-1,1]\times[-1,1]$. We set the number of nodes $N = 80 \times 80$

and the normalizing parameter $M = 80^3$. We set the initial condition

$$z_0(s) = r_1 e^{-4((s_1+0.65)^2+(s_2+0.75)^2)} + r_2 e^{-3((s_1-0.75)^2+(s_2-0.85)^2)} + r_3 e^{-2((s_1-0.75)^2+(s_2+0.75)^2)} + r_4 e^{-3((s_1+0.85)^2+(s_2-0.75)^2)}, \tag{44}$$

where the constants $r_1, \ldots, r_4 > 0$, so that initially the nodes near $(-0.65, -0.75)$, $(0.75, 0.85)$, $(0.75, -0.75)$, and $(-0.85, 0.75)$ have more messages to transmit than those far away from these points. We set the incoming traffic function

$$z_0(s) = r_5 e^{-4((s_1+0.65)^2+(s_2+0.75)^2)} + r_6 e^{-3((s_1-0.75)^2+(s_2-0.85)^2)} + r_7 e^{-2((s_1-0.75)^2+(s_2+0.75)^2)} + r_8 e^{-3((s_1+0.85)^2+(s_2-0.75)^2)}, \tag{45}$$

where the constants $r_5, \ldots, r_8 > 0$, so that the nodes near $(-0.65, -0.75)$, $(0.75, 0.85)$, $(0.75, -0.75)$, and $(-0.85, 0.75)$ generate more messages to transmit than those far away from these points. This may correspond to four information sources at these four points that generate different rate of data traffic. Set the diffusion functions $b_i = 1/4$, where $i = 1, \ldots, 4$, and the convection functions $c_1 = 0$, $c_2 = 1$, $c_3 = 0.1$, and $c_4 = -0.1$. Hence $b^{(1)} = b^{(2)} = 1/4$, $c^{(1)} = -1$, and $c^{(2)} = 0.2$, so that more data traffic in the network is routed to the south and the east. In Figure 5, we show the contour of the PDE solution and the simulation result at $t = 0.1$ s. We can again see the resemblance.

Type II Communicating Neighbors. For 2-D 1-step networks of Type II communicating neighbors, we define the probabilities P_i of transmitting to the 8 communicating neighbors as in Figure 2. The limiting PDE is as follows:

$$\dot{z} = \sum_{j=1}^{2} \left(b^{(j)} \frac{\partial}{\partial s_j} \left((1+9z)(1-z)^7 \frac{\partial z}{\partial s_j} \right) + 2(1-z)^7 \frac{\partial z}{\partial s_j} \frac{\partial b^{(j)}}{\partial s_j} + z(1-z)^8 \frac{\partial^2 b^{(j)}}{\partial s_j^2} + \frac{\partial}{\partial s_j} \left(c^{(j)} z (1-z)^8 \right) \right) + g_p, \tag{46}$$

where $b^{(1)} = \sum_{l=1,2,5,\ldots,8} (b_l/2)$, $b^{(2)} = \sum_{l=3,4,5,\ldots,8} (b_l/2)$, $c^{(1)} = c_1 - c_2 + c_5 - c_7 + c_6 - c_8$, and $c^{(2)} = c_3 - c_4 + c_5 - c_6 + c_7 - c_8$.

Again the spatial domain $D = [-1, 1] \times [-1, 1]$. We set the number of nodes $N = 80 \times 80$ and the normalizing parameter $M = 80^3$. We set the initial condition

$$z_0(s) = r_1 e^{-4((s_1+0.55)^2+(s_2+0.55)^2)} + r_2 e^{(s_1-0.55)^2+(s_2-0.55)^2}, \tag{47}$$

where the constants $r_1, r_2 > 0$, so that initially the nodes near $(-0.55, -0.55)$ and $(0.55, 0.55)$ have more messages to transmit than those far away from these two points. We set the incoming incoming traffic function

$$g_p(s) = r_3 e^{-4((s_1+0.55)^2+(s_2+0.55)^2)} + r_4 e^{(s_1-0.55)^2+(s_2-0.55)^2}, \tag{48}$$

where the constants $r_3, r_4 > 0$, so that the nodes near $(-0.55, -0.55)$ and $(0.55, 0.55)$ generate more messages to transmit than those far away from these two points. This may correspond to two information sources at these two points that generate different rates of data traffic. In Figure 6, we show the contours of the PDE solution and the simulation results with the diffusion functions $b_i = 1/8$, for $i = 1, \ldots, 8$, and convection functions $c_1 = 1$, $c_2 = 2$, $c_3 = 3$, $c_4 = 4$, $c_5 = -1$, $c_6 = -2$, $c_7 = -3$, and $c_8 = -4$. Hence $b^{(1)} = b^{(1)} = 3/8$, $c^{(1)} = 3$, and $c^{(2)} = 1$, so that more data traffic in the network is routed to the west and the south.

The reader can verify that the two PDEs (43) and (46) above are special cases of (20).

4.2. Example of Nonuniform Network. We illustrate a 2-D nonuniform network $\widetilde{X}_N$, its continuum limit $u(t, s)$, and the continuum limit $q(t, s)$ of its mirroring uniform network in Figure 7. The spatial domain $D = [-1, 1] \times [-1, 1]$. We assume that the mirroring uniform network is a 2D 1-step network of Type-I communicating neighbors. Therefore q satisfies the limiting PDE (43). For the mirroring uniform network, we set the initial condition $q_0(s) = l_1 e^{-(s_1^2+s_2^2)}$, and incoming traffic $g_p(s) = l_2 e^{-(s_1^2+s_2^2)}$ where the constants $l_1, l_2 > 0$; we set the diffusion functions $b_i = 1/4$ and the convection functions $c_i = 0$, for $i = 1, \ldots, 4$. The inverse transformation function here is set to be $\eta_j(s) = (s_j + 1)^2/2 - 1$ for $j = 1, 2$. (Notice that this satisfies (23)) Therefore the continuum limit u of the nonuniform network $\widetilde{X}_N$ is $u(t, s) = q(t, \eta(s))$.

4.3. Examples of Control of Nonuniform Networks

4.3.1. 1D Example. Let the domain $\mathscr{D} = [-1, 1]$. Let $u(t, s)$ be the continuum limit of a sequence $\{\widehat{X}_N\}$ of 1-D 1-step uniform networks with transmission range $\widehat{L} = 1$, the diffusion function $\widehat{b} = 1/2$, the convection function $\widehat{c} = 0$, and a given incoming traffic function $\widehat{g}_p$ for all $(t, s) \in [0, T] \times \mathscr{D}$. A given transformation function ϕ specifies the node locations of a sequence $\{\widetilde{X}_N\}$ of nonuniform networks. We show how to find the transmission-interference rule for $\{\widetilde{X}_N\}$ to converge to $u(t, s)$. As the continuum limit of this particular 1-D 1-step network, $u(t, s)$ solves the PDE

$$\dot{u} = \frac{\partial}{\partial s} \left(\frac{1}{2} (1-u)(1+3u) \frac{\partial u}{\partial s} \right) + g_p, \tag{49}$$

with boundary condition $u(t, s) = 0$ and initial condition $u(0, s) = u_0(s)$. This is a special case of (14).

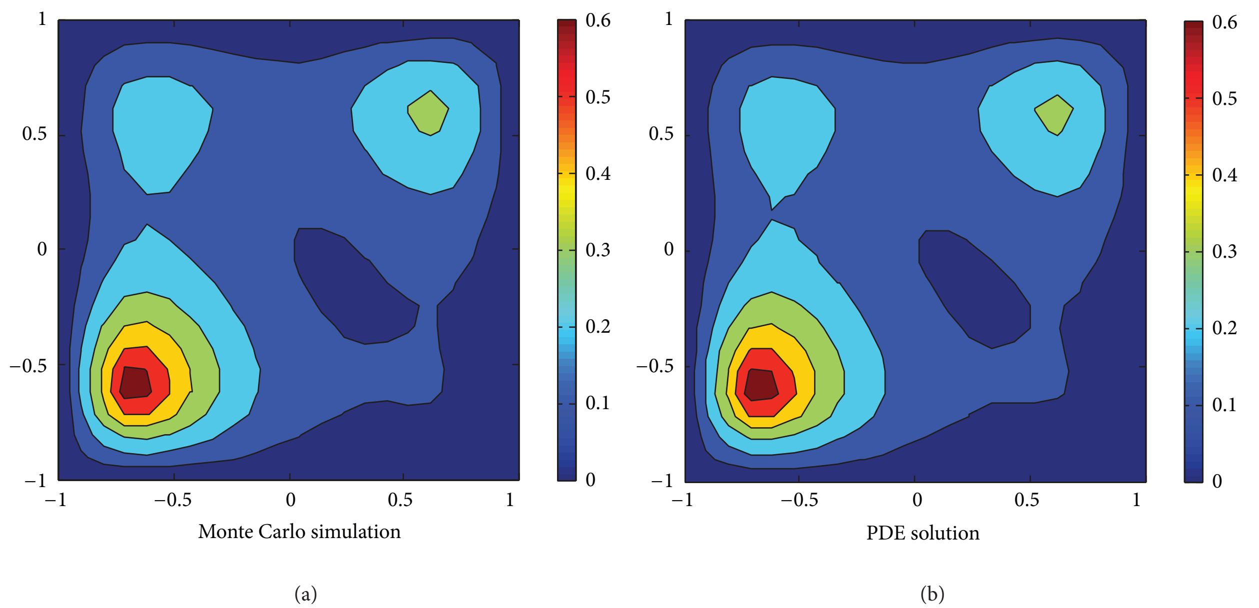

FIGURE 5: The Monte Carlo simulation and the PDE solution of a 2D 1-step network of Type I communicating neighbors.

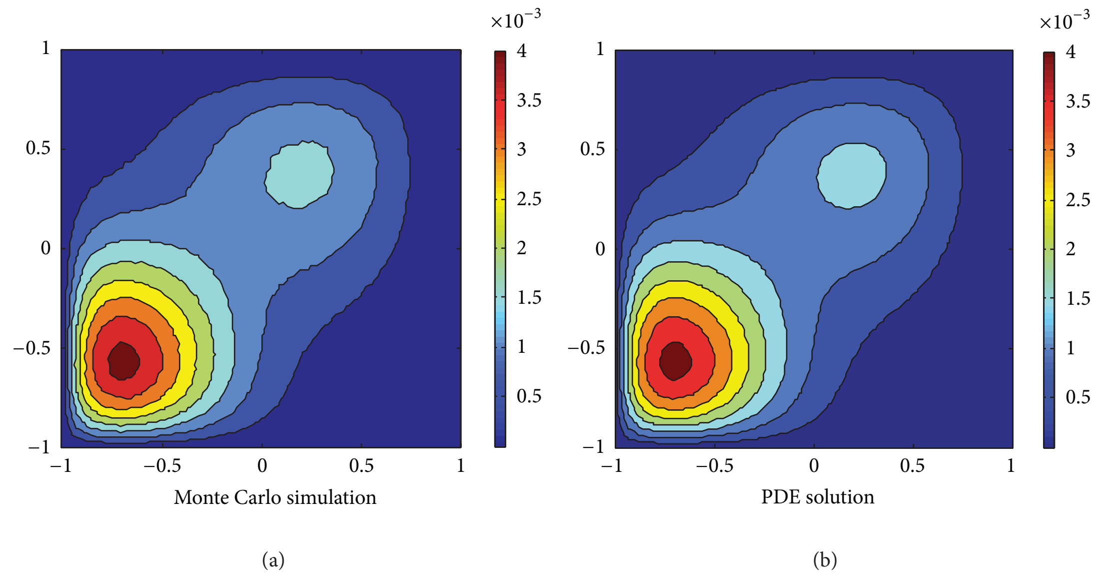

FIGURE 6: The Monte Carlo simulation and the PDE solution of a 2D 1-step network of Type II communicating neighbors.

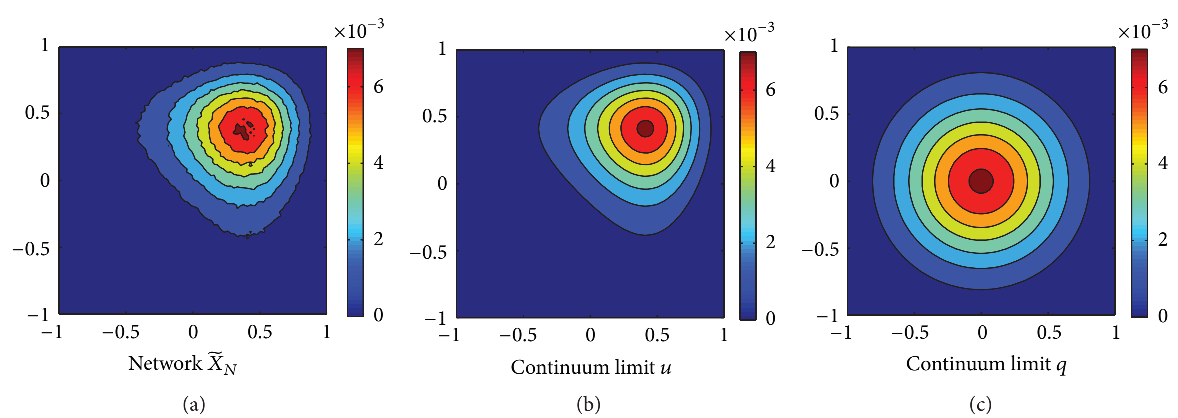

FIGURE 7: A nonuniform network, its limiting PDE solution, and the limiting PDE solution of its mirroring uniform network.

In this case $\lambda_{(J,L)} = 2L$. Let $\theta = 1/(2(\partial\phi/\partial s)^2)$. Then the comparison equation (40) becomes

$$\begin{aligned} & b^{(1)}\frac{\partial}{\partial s}\left((1+(2L+1)q)(1-q)^{(2L-1)}\frac{\partial q}{\partial s}\right) \\ &\quad + 2(1-q)^{(2L-1)}\frac{\partial q}{\partial s}\frac{\partial b^{(1)}}{\partial s} + q(1-q)^{2L}\frac{\partial^2}{\partial s^2}b^{(1)} \\ &\quad + \frac{\partial}{\partial s}\left(c^{(1)}q(1-q)^{2L}\right) + \widehat{g}_p \\ &= \theta(1-q)(1+3q)\frac{\partial^2 q}{\partial s^2} + 2(1-3q)\theta\left(\frac{\partial q}{\partial s}\right)^2 \\ &\quad + \frac{1}{2}(1-q)(1+3q)\frac{\partial\theta}{\partial s}\frac{\partial q}{\partial s} + g_p(\phi), \end{aligned} \tag{50}$$

where q is the continuum limit of the mirroring sequence $\{X_N\}$ of $\{\widetilde{X}_N\}$.

We assume that $\widehat{g}_p(s) = g_p(\phi(t,s))$, which corresponds to the assumption that the continuum limit of the incoming traffic is invariant under node locations and mobility. This assumption is feasible in a large class of networks where traffic load depends directly on actual physical location. For example, in a wireless sensor network that detects environmental events such as a forest fire, the event-triggered data traffic depends on the distribution of heat rather than the node locations.

Suppose that we set

$$b^{(1)} = \theta. \tag{51}$$

Since q is known to be the solution of (49), (50) has now become a first-order linear ODE for $c^{(1)}$.

We can use Euler's method to solve this ODE based on local information. For fixed t_o, suppose the ODE is written in the form $\Phi(t_o, s, c^{(1)}) = dc^{(1)}/ds$. We first choose $c^{(1)}(t_o, s(1))$ such that $P_i(k_o, 1)$ satisfies (41), where $t_o = k_o dt_N$. Then we can approximate $c^{(j)}(t_o, s(n))$ by $\widehat{c}(t_o, n)$, where $\widehat{c}(t_o, 1) = c^{(j)}(t_o, s(1))$, and $\widehat{c}(t_o, n+1) = \widehat{c}(t_o, n) + \Phi(t_o, s(n), \widehat{c}(t_o, n))ds_N$, for $n = 1, \ldots, N$.

With this given ϕ, the transmission range L of the mobile network has to be greater or equal to 2 for (41) to hold. We choose $L = 2$. Then any b_i, c_i, where $i = 1, 2$, that satisfy (50) and (51) will give us the desired transmission-interference rule of networks in $\{X_N\}$ and, hence, that of $\{\widetilde{X}_N\}$.

We simulate a 51-node controlled mobile network $\widetilde{X}_N$ in the sequence $\{\widetilde{X}_N\}$ that mirrors $\{X_N\}$, whose node locations are specified by this given ϕ. In Figure 8, we compare the simulation result with the continuum limit of $\{\widehat{X}_N\}$, at $t = 1$ s. We set the initial condition $z_0(s) = r_1 e^{-s^2}$ and the incoming traffic function $g_p(s) = r_2 e^{-s^2}$, where the constants $r_1, r_2 > 0$. As we can see, the global characteristic of $\widetilde{X}_N$ resembles $u(t,s)$, the continuum limit of $\{\widehat{X}_N\}$.

4.3.2. 2D Example. Let the domain $\mathscr{D} = [-1,1]\times[-1,1]$. Let $u(t,s)$ be the continuum limit of a sequence $\{\widehat{X}_N\}$ of 2-D 1-step uniform networks of Type-II communicating neighbors with transmission range $\widehat{L} = 1$, the diffusion functions $\widehat{b}_i(t,s) = 1/8$, for $i = 1,\ldots,8$, the convection functions $\widehat{c}^{(j)} = 0$, for $j = 1,2$, and given incoming traffic function $\widehat{g}_p$ for all $(t,s) \in [0,T]\times\mathscr{D}$. Again denote the given transformation function that specifies the node locations of $\{\widetilde{X}_N\}$ by $\phi(t,s)$.

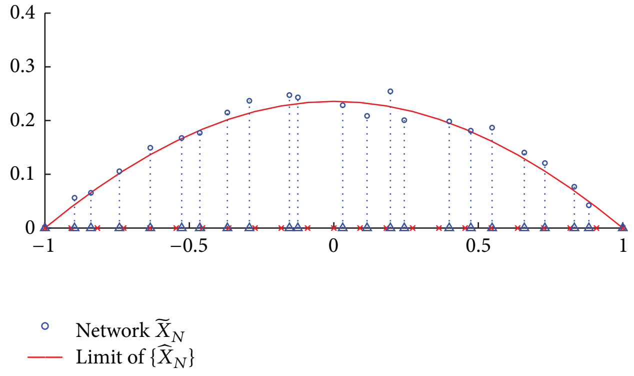

Figure 8: The comparison of the 1D controlled network and the location-invariant continuum limit at $t = 1$ s. On the x-axis, the $\times$ marks are the uniform grid, and the Δ marks are the nonuniform node locations.

As the continuum limit of this particular 1D 1-step network, $u(t,s)$ solves the PDE

$$\dot{u} = \frac{3}{8}\sum_{j=1}^{2}\frac{\partial}{\partial s_j}\left((1+9u)(1-u)^7\frac{\partial u}{\partial s_j}\right) + \widehat{g}_p, \tag{52}$$

with boundary condition $u(t,s) = 0$ and initial condition $u(0,s) = u_0(s)$. This is a special case of (46).

Let $\theta_j = 1/(2(\partial\phi_j/\partial s_j)^2)$. Then the comparison equation (40) becomes

$$\begin{aligned} & \sum_{j=1}^{2}\left(b^{(j)}\frac{\partial}{\partial s}\left((1+(\lambda_{(2,L)}+1)q)(1-q)^{(\lambda_{(2,L)}-1)}\frac{\partial q}{\partial s}\right)\right. \\ &\quad + 2(1-q)^{(\lambda_{(2,L)}-1)}\frac{\partial q}{\partial s}\frac{\partial \widehat{b}_j}{\partial s_j} \\ &\quad \left. + q(1-q)^{\lambda_{(2,L)}}\frac{\partial^2 b^{(j)}}{\partial s^2} + \frac{\partial}{\partial s}\left(c^{(j)}q(1-q)^{\lambda_{(2,L)}}\right)\right) + \widehat{g}_p \\ &= \sum_{j=1}^{2}\left(\frac{3}{4}(1-q)^7(1+9q)\theta_j\frac{\partial^2 q}{\partial x_j^2}\right. \\ &\quad + \frac{3}{8}(1-q)^7(1+9q)\frac{\partial\theta_j}{\partial x_j}\frac{\partial q}{\partial x_j} \\ &\quad \left. + \frac{3}{2}(1-36q)(1-q)^6\theta_j\left(\frac{\partial q}{\partial x_j}\right)^2\right) + g_p(\phi), \end{aligned} \tag{53}$$

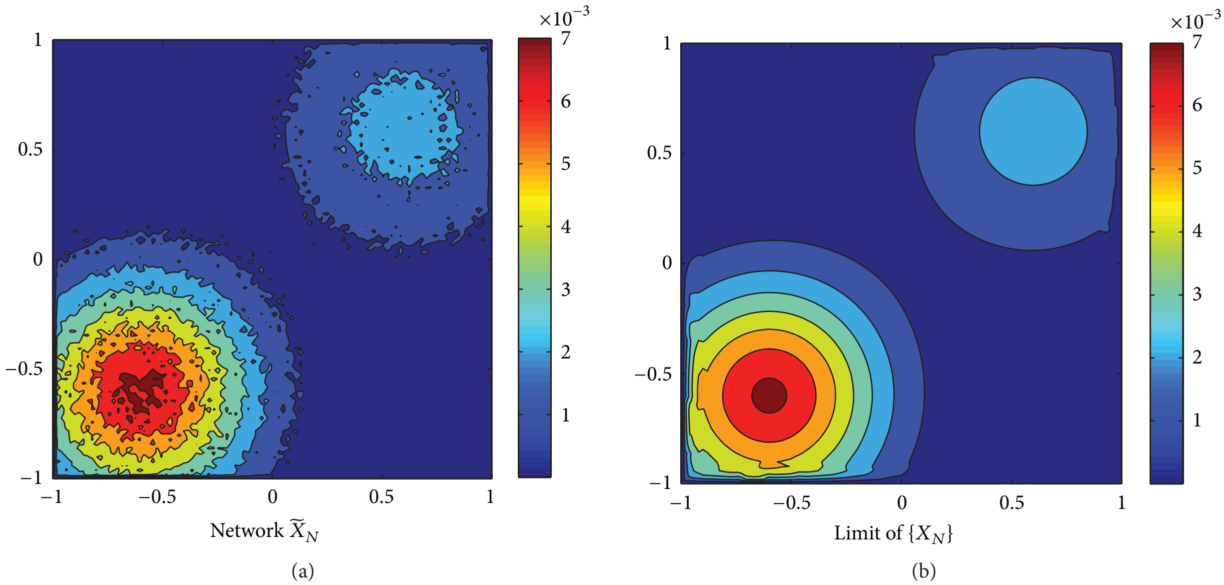

FIGURE 9: The comparison of the 2D controlled network and the location-invariant continuum limit at $t = 1$ s.

where q is the continuum limit of the mirroring sequence $\{X_N\}$ of $\{\widetilde{X}_N\}$. Assume that $\widehat{g}_p(t,s) = g_p(\phi(t,s))$ and

$$b^{(j)} = \theta_j. \tag{54}$$

Since q is known to be the solution of (52), we have two first-order linear ODEs of $c^{(j)}$, where $j = 1, 2$.

For this given ϕ, $L = 2$ is sufficient for (41) to hold. Then any $b_i, c_i, l = 1, 2$ that satisfy (53) and (54) will give us the desired transmission-interference rule for $\{X_N\}$ and, hence, $\{\widetilde{X}_N\}$.

We simulate a (100×100)-node controlled mobile network $\widetilde{X}_N$ in the sequence $\{\widetilde{X}_N\}$ that mirrors $\{X_N\}$, whose node locations are specified by ϕ. In Figure 9, we compare the simulation result with the continuum limit of $\{\widehat{X}_N\}$, at $t = 1s$. We set the initial condition

$$\begin{aligned} z_0(s) = {} & r_1 e^{-4((s_1+0.6)^2+(s_2+0.6)^2)} \\ & + r_2 e^{-3((s_1-0.6)^2+(s_2-0.6)^2)} \end{aligned} \tag{55}$$

and the incoming traffic function

$$\begin{aligned} g_p(s) = {} & r_3 e^{-4((s_1+0.6)^2+(s_2+0.6)^2)} \\ & + r_4 e^{-3((s_1-0.6)^2+(s_2-0.6)^2)}, \end{aligned} \tag{56}$$

where the constants $r_1, \ldots, r_4 > 0$. Again, the global characteristic of $\widetilde{X}_N$ resembles $u(t,s)$, the continuum limit of $\{\widehat{X}_N\}$.

5. Conclusion

In this paper we study the modeling of nonuniform and possibly mobile networks via nonlinear PDEs and develop a distributed method to control their transmission-interference rules to maintain certain global characteristics. We demonstrate our method with a family of wireless sensor networks. Our method can be extended to other network models. The freedom in the control method mentioned in Section 3.3 can also be further exploited to improve the network performance.

Acknowledgments

Yang Zhang and Edwin K. P. Chong's research was supported in part by NSF under ECCS-0700559 and ONR under Grant N00014-08-1-110. Jan Hannig's research was supported in part by NSF under Grant nos 1007543 and 1016441. Donald Estep's work was supported in part by the Defense Threat Reduction Agency (HDTRA1-09-1-0036), Department of Energy (DE-FG02-04ER25620, DE-FG02-05ER25699, DE-FC02-07ER54909, DE-SC0001724, DE-SC0005304, and INL00120133), Lawrence Livermore National Laboratory (B573139, B584647, and B590495), the National Aeronautics and Space Administration (NNG04GH63G), the National Institutes of Health (5R01GM096192-02), the National Science Foundation (DMS-0107832, DMS-0715135, DGE-0221595003, MSPA-CSE-0434354, ECCS-0700559, DMS-1016268, and DMS-FRG-1065046), and Idaho National Laboratory (00069249, 00115474). A preliminary version of parts of the work of this paper was presented at the 49th Annual Allerton Conference on Communication, Control, and Computing, 2011.

References

[1] Y. Zhang, E. K. P. Chong, J. Hannig, and D. J. Estep, "Continuum limits of Markov chains with application to network modeling," http://arxiv.org/abs/1106.4288.

[2] Y. Zhang, E. K. P. Chong, J. Hannig, and D. Estep, "On continuum limits of markov chains and network modeling," in *Proceedings of the 49th IEEE Conference on Decision and Control (CDC '10)*, pp. 6779–6784, Atlanta, Ga, USA, December 2010.

[3] E. K. P. Chong, D. Estep, and J. Hannig, "Continuum modeling of large networks," *International Journal of Numerical Modelling*, vol. 21, no. 3, pp. 169–186, 2008.

[4] N. J. Burch, *Continuum modeling of stochastic wireless sensor networks [M.S. thesis]*, Colorado State University, 2008.

[5] N. Burch, E. Chong, D. Estep, and J. Hannig, "Analysis of routing protocols and interference-limited communication in large wireless networks," *Journal of Engineering Mathematics*, pp. 1–17, 2012.

[6] H. J. Kushner, *Approximation and Weak Convergence Methods for Random Processes, with Applications to Stochastic Systems Theory*, MIT Press Series in Signal Processing, Optimization, and Control, 6, MIT Press, Cambridge, Mass, USA, 1984.

[7] H. Robbins and S. Monro, "A stochastic approximation method," *Annals of Mathematical Statistics*, vol. 22, pp. 400–407, 1951.

[8] J. Kiefer and J. Wolfowitz, "Stochastic estimation of the maximum of a regression function," *Annals of Mathematical Statistics*, vol. 23, pp. 462–466, 1952.

[9] M. Benaïm, "Dynamics of stochastic approximation algorithms," in *Séminaire de Probabilités, XXXIII*, vol. 1709 of *Lecture Notes in Mathematics*, pp. 1–68, Springer, Berlin, Germany, 1999.

[10] T. L. Lai, "Stochastic approximation," *The Annals of Statistics*, vol. 31, no. 2, pp. 391–406, 2003.

[11] T. G. Kurtz, "Solutions of ordinary differential equations as limits of pure jump Markov processes," *Journal of Applied Probability*, vol. 7, pp. 49–58, 1970.

[12] R. W. R. Darling, "Fluid limits of pure jump Markov processes: a practical guide," http://arxiv.org/abs/math/0210109.

[13] R. McVinish and P. Pollett, "The deterministic limit of heterogeneous density dependent Markov chains," submitted to *Annals of Applied Probability*.

[14] S. N. Ethier and T. G. Kurtz, *Markov Processes: Characterization and Convergence*, Wiley Series in Probability and Mathematical Statistics: Probability and Mathematical Statistics, John Wiley & Sons Inc., New York, NY, USA, 1986.

[15] P. Billingsley, *Convergence of Probability Measures*, Wiley Series in Probability and Statistics: Probability and Statistics, John Wiley & Sons, New York, NY, USA, 2nd edition, 1999.

[16] P. Gupta and P. R. Kumar, "The capacity of wireless networks," *IEEE Transactions on Information Theory*, vol. 46, no. 2, pp. 388–404, 2000.

[17] M. Grossglauser and D. N. C. Tse, "Mobility increases the capacity of ad hoc wireless networks," *IEEE/ACM Transactions on Networking*, vol. 10, no. 4, pp. 477–486, 2002.

[18] J. D. Herdtner and E. K. P. Chong, "Throughput-storage tradeoff in ad hoc networks," in *Proceedings of the 24th Annual Joint Conference of the IEEE Computer and Communications Societies (INFOCOM '05)*, vol. 4, pp. 2536–2542, March 2005.

[19] M. Benaïm and J.-Y. L. Boudec, "A class of mean field interaction models for computer and communication systems," *Performance Evaluation*, pp. 11–12, 2008.

[20] P. E. Caines, "Bode lecture: mean field stochastic control," in *Proceedings of the 48th IEEE Conference on Decision and Control*, Shanghai, China, 2009.

[21] D. A. Dawson, J. Tang, and Y. Q. Zhao, "Balancing queues by mean field interaction," *Queueing Systems*, vol. 49, no. 3-4, pp. 335–361, 2005.

[22] C. Graham and P. Robert, "Self-adaptive congestion control for multiclass intermittent connections in a communication network," *Queueing Systems*, vol. 69, no. 3-4, pp. 237–257, 2011.

[23] C. S. Chang, "Sample path large deviations and intree networks," *Queueing Systems*, vol. 20, no. 1-2, pp. 7–36, 1995.

[24] N. G. Duffield, "A large deviation analysis of errors in measurement based admission control to buffered and bufferless resources," *Queueing Systems*, vol. 34, no. 1-4, pp. 131–168, 2000.

[25] S. Ahn and J. Jeon, "Analysis of $G/D/1$ queueing systems with inputs satisfying large deviation principle under weak* topology," *Queueing Systems*, vol. 40, no. 3, pp. 295–311, 2002.

[26] D. Blount, "Law of large numbers in the supremum norm for a chemical reaction with diffusion," *The Annals of Applied Probability*, vol. 2, no. 1, pp. 131–141, 1992.

[27] C.-f. Huang and H. Pagès, "Optimal consumption and portfolio policies with an infinite horizon: existence and convergence," *The Annals of Applied Probability*, vol. 2, no. 1, pp. 36–64, 1992.

[28] G.-L. Xu and S. E. Shreve, "A duality method for optimal consumption and investment under short-selling prohibition. II. Constant market coefficients," *The Annals of Applied Probability*, vol. 2, no. 2, pp. 314–328, 1992.

[29] M. Burger, P. A. Markowich, and J.-F. Pietschmann, "Continuous limit of a crowd motion and herding model: analysis and numerical simulations," *Kinetic and Related Models*, vol. 4, no. 4, pp. 1025–1047, 2011.

[30] H. Chen and W. Whitt, "Diffusion approximations for open queueing networks with service interruptions," *Queueing Systems*, vol. 13, no. 4, pp. 335–359, 1993.

[31] J. M. Harrison and V. Nguyen, "Brownian models of multiclass queueing networks: current status and open problems," *Queueing Systems*, vol. 13, no. 1–3, pp. 5–40, 1993.

[32] H. Chen, O. Kella, and G. Weiss, "Fluid approximations for a processor-sharing queue," *Queueing Systems*, vol. 27, no. 1-2, pp. 99–125, 1997.

[33] R.-R. Chen and S. Meyn, "Value iteration and optimization of multiclass queueing networks," *Queueing Systems*, vol. 32, no. 1–3, pp. 65–97, 1999.

[34] R. C. Hampshire, M. Harchol-Balter, and W. A. Massey, "Fluid and diffusion limits for transient sojourn times of processor sharing queues with time varying rates," *Queueing Systems*, vol. 53, no. 1-2, pp. 19–30, 2006.

[35] F. J. Piera, R. R. Mazumdar, and F. M. Guillemin, "Existence and characterization of product-form invariant distributions for state-dependent stochastic networks in the heavy-traffic diffusion limit," *Queueing Systems*, vol. 58, no. 1, pp. 3–27, 2008.

[36] R. B. Guenther and J. W. Lee, *Partial Differential Equations of Mathematical Physics and Integral Equations*, Dover, Mineola, NY, USA, 1996.

[37] J.-H. He, "Asymptotic Methods for Solitary Solutions and Compactons," *Abstract and Applied Analysis*, vol. 2012, Article ID 916793, 130 pages, 2012.

[38] G. R. Liu and S. S. Quek, *The Finite Element Method: A Practical Course*, Butterworth-Heinemann, 2003.

[39] A. R. Mitchell and D. F. Griffiths, *The Finite Difference Method in Partial Differential Equations*, John Wiley & Sons, Chichester, UK, 1980.

[40] J. C. Robinson, *An Introduction to Ordinary Differential Equations*, Cambridge University Press, Cambridge, UK, 2004.

Hindawi Publishing Corporation
Abstract and Applied Analysis
Volume 2013, Article ID 972941, 6 pages
http://dx.doi.org/10.1155/2013/972941

Research Article

Shock in the Yarn during Unwinding from Packages

Stanislav Praček, Klemen Možina, and Franci Sluga

Department of Textiles, NTF, University of Ljubljana, Snežniška 5, 1000 Ljubljana, Slovenia

Correspondence should be addressed to Stanislav Praček; stane.pracek@ntf.uni-lj.si

Received 14 December 2012; Revised 18 January 2013; Accepted 4 February 2013

Academic Editor: Lan Xu

Tension in the yarn and its oscillations during the over-end unwinding of the yarn from stationary packages depend on the unwinding speed, the shape and the winding type of the package, the air drag coefficient, and also the coefficient of friction between the yarn and the package. The yarn does not leave the surface package immediately at the unwinding point. Instead, it first slides on the surface and then lifts off to form the balloon. The problem of simulating the unwinding process can be split into two smaller subproblems: the first task is to describe the motion of the yarn in the balloon; the second one is to solve the sliding motion. In spite of the seemingly complex form of the equations, they can be partially analytically solved as we show in the paper.

1. Introduction

During the yarn unwinding from a stationary package, the yarn slides on the surface of the package before it lifts off to form a balloon. The point where the yarn begins to slide is known as the unwinding point, while the point where the yarn lifts off from the surface is known as the lift-off point. On this section of the yarn, that is, between the unwinding point and the lift-off point, the tension in the yarn drops from its value in the balloon (at the lift-off point) to its residual value, defined as the tension of the yarn inside the package. The equations of motion which govern the motion of the yarn are known: we have established them in Section 2 of this paper. They can be partially analytically solved, as we show in the following. The theory of yarn unwinding off a package and the balloon theory had a quick development in the fifties because of Padfield's work [1, 2]. She fixed Mack equations for the balloon [3] so that they take into account the Coriolis system force. She found the results for a single balloon as it unwinds from a cylindrical package. The same theory was later used to calculate the parameters for multiple consecutive balloons with a nonzero unwinding angle and a cylindrical, conical, or empty package [1]. Kothari and Leaf derived motion equations that include the effect of the gravity force and air resistance force tangential component [4, 5]. Using extensive numerical methods for cylindrical and conical packages they showed that these effects can be ignored. Recently Fraser used the motion theory to show that the time dependence can be excluded from motion equations in a mathematical correct way [6, 7]. He derived movable boundary conditions for packages with small winding angle. Fraser also determined that the tension inside and the radius of a balloon are smaller for an elastic yarn. Using simple physics He recently introduced different nanophenomena in nanotextile that are the newest additions to the theory of electrospinning [8, 9].

2. The Equation of Motion for Yarn

The problem of yarn motion on the package surface during the unwinding can be treated in analogy with the motion of the yarn forming the balloon between the lift-off point and the eyelet, through which the yarn is being pulled.

The yarn is being withdrawn with velocity V through an eyelet, where we also fix the origin O of our coordinate system (Figure 1). The yarn is rotating aroun the z-axis with an angular velocity ω. At the lift-off point Lp, the yarn lifts from the package and forms a balloon. At the unwinding point Up, the yarn starts to slide on the surface of the package. Angle ϕ is the winding angle of the yarn on the package.

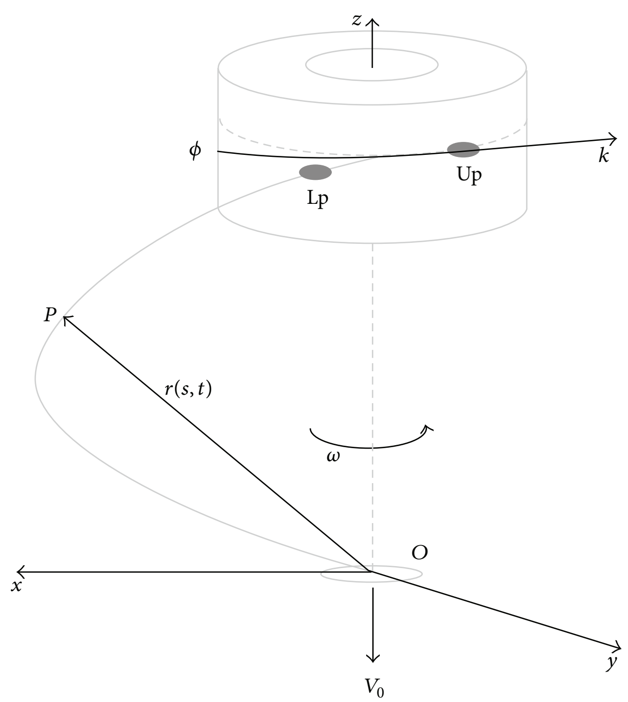

Figure 1: Mechanical setup in over-end yarn unwinding from cylindrical package.

The general equation of motion for the yarn was derived and justified in one of the previous works [10]:

$$\rho\left(D^2 r + 2\omega \times Dr + \omega \times (\omega \times r) + \dot{\omega} \times r\right) = \frac{\partial}{\partial s}\left(T \frac{\partial r}{\partial s}\right) + f. \quad (1)$$

The position vector r points from the origin of the coordinate system to a chosen point along the yarn, ρ is the linear density of the yarn mass, ω is the angular velocity vector of the spinning coordinate system in which the yarn is being described and which points along the z-axis, D is the operator of the total time derivative which follows the motion of the point inside the spinning coordinate system, $D = \partial/\partial t|_{r,\theta,z} - V\partial/\partial s$, T is the mechanical tension, and f is the linear density of external forces.

3. Friction between the Yarn and the Package Surface

There is a friction between the package and the yarn which is sliding on its surface before it lifts off to form the balloon. The yarn is exerting a normal force on the package (i.e., a force perpendicular to the package surface, thus in radial direction). This force is not known a priori, but must be determined as part of the solution to the full problem. The simplest expression of the friction law states that the friction force is proportional to the normal component of the force. The coefficient of proportionality is known as the coefficient of friction μ. The friction force points in the direction opposite to the yarn motion.

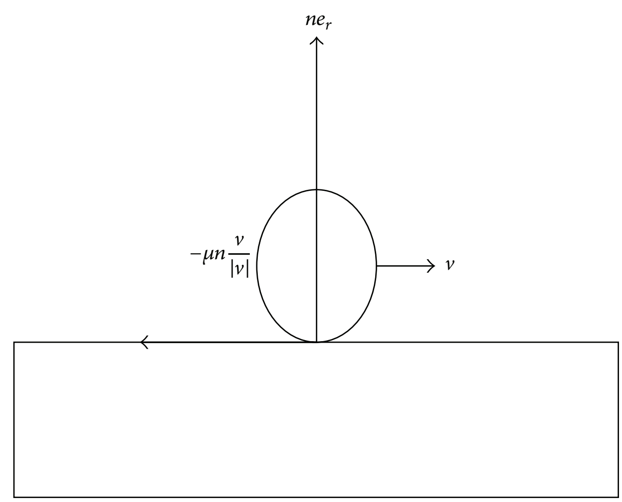

Figure 2: The force of friction between the package surface and the yarn.

The quantity f in (1) therefore has two components: the radial force of the package on the yarn (which is equal in magnitude to the force of the yarn on the package, in accordance with Newton's law of reciprocal action) and the friction force proper (Figure 2):

$$f = ne_r - \mu n \frac{v}{|v|}. \quad (2)$$

Here n is the linear density of the normal component of the force between the yarn and the surface, e_r is the unit vector in the radial direction, and $v/|v|$ is the unit vector in the direction of the yarn.

When the yarn slides on the surface, it thus experiences the normal force ne_r and the friction force $-\mu n\, v/|v|$.

The friction law is at best a rough approximation to a more complex real behavior. In reality, the coefficient of friction depends in a complicated way on the sliding velocity [11–16], and it is different at various points of the package surface since the package is seldom fully homogenous. We thus take μ to be some average coefficient of friction which one can determine empirically [17].

4. Quasi-Stationary Approximation

Equation (1) is generally valid and describes an arbitrary motion of the yarn, even in cases when the conditions are rapidly changing, for example, near the package edges. Near the package edge the winding angle suddenly changes, therefore the motion of the yarn on the package surface and in the part of the balloon near the lift-off point becomes very complex. Near the edges, undesired events can occur: the yarn can fall off the package or a layer of the yarn collapses. The description of such transient effects is beyond the validity of our simplified model, since one should accurately model the behavior of the yarn also in the layers forming the package bulk. For example, the residual forces of the yarn in the package would also play a role [18].

Strictly speaking, the yarn undergoes sliding motion on the package surface only when the unwinding point is at a certain distance away from the package edges. In such circumstances, the conditions are quasi-stationary: in the rotating coordinate frame the yarn only slowly changes its form. For this reason, in the first approximation the time dependence can be fully described by time-variable boundary conditions, while the time-derivative terms in the equation of motion can be neglected:

$$\rho\left(V^2\frac{\partial^2 r}{\partial s^2} - 2V\omega \times \frac{\partial r}{\partial s} + \omega \times (\omega \times r)\right) = \frac{\partial}{\partial s}\left(T\frac{\partial r}{\partial s}\right) + f. \tag{3}$$

5. The Equation of Motion for the Yarn on the Package: Simplification to a Two-Dimensional Problem

When the yarn slides on the package surface, its motion effectively occurs within a two-dimensional subspace. This fact can be taken into account in (3) in order to simplify the problem to a two-dimensional problem which can be handled more easily. It turns out that in the case of sliding motion on the cylindrical package, the problem can be solved to a large extent using analytical techniques. Analytical solutions allow for a more direct understanding of the relation between the different quantities. For this reason, we will henceforth assume that the package is cylindrical, and we will determine the analytical solution.

The radius vector to a point on the surface of a cylinder can be expressed as (compare with equation (17) in [10])

$$r(s) = ce_r(\theta(s)) + z(s)\,e_z. \tag{4}$$

The quantity c is the constant distance of the point r from the package axis. It is equal to the radius of the layer which is being unwound. The unit vector e_z points along the direction of the package axis, and the unit vector e_r points in the radial direction with the polar angle $\theta(s)$ (see Figure 3). There are two unknowns in this expression, $\theta(s)$ and $z(s)$, while the third $[r(s)]$ drops out since it is constant on the surface. The motion of the yarn has thus been translated to a two-dimensional problem. This ansatz will be used in (4) to find a simplified equation of motion.

The arc-length derivatives of the radius vector are computed using the relations (18) from [10] to obtain

$$\begin{aligned} r'(s) &= c\theta'(s)\,e_\theta + z'(s)\,e_z, \\ r''(s) &= c\theta''(s) - c\left[\theta'(s)\right]^2 e_r + z''(s)\,e_z, \end{aligned} \tag{5}$$

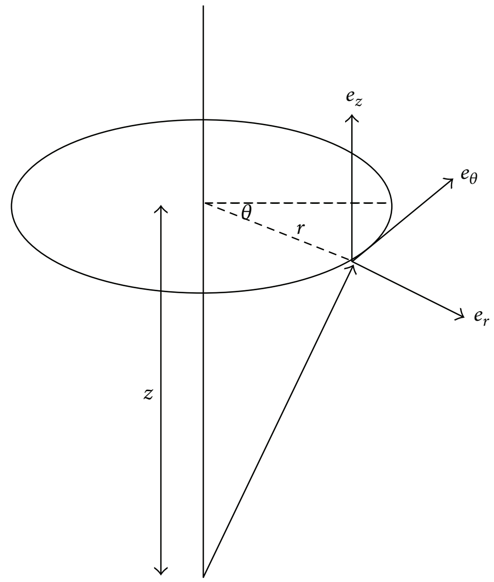

Figure 3: The cylindrical coordinate system.

where the dashes indicate the arc-length derivative. We then obtain

$$\begin{aligned} &\frac{\partial}{\partial s}\left(T\frac{\partial r}{\partial s}\right) \\ &= \frac{\partial T}{\partial s}\frac{\partial r}{\partial s} + T\frac{\partial^2 r}{\partial s^2} \\ &= T'\left(c\theta' e_\theta + z' e_z\right) + T\left(c\theta'' e_\theta - c\left(\theta'\right)^2 e_r + z'' e_z\right) \\ &= -cT\left(\theta'\right)^2 e_r + c\left(T'\theta' + T\theta''\right)e_\theta + \left(T'z' + Tz''\right)e_z. \end{aligned} \tag{6}$$

We also need the relations

$$\begin{aligned} \omega \times r' &= -c\omega\theta'(s)\,e_r, \\ \omega \times (\omega \times r) &= -\omega^2 c e_r \end{aligned} \tag{7}$$

which can be derived using a simple calculation of the vector products.

Equation (3) may then be decomposed along its different components:

$$(r)\ \rho\left(-cV^2\left(\theta'\right)^2 + 2Vc\omega\theta' - \omega^2 c\right) = -cT\left(\theta'\right)^2 + f_r, \tag{8}$$

$$(\theta)\ \rho\left(cV^2\theta''\right) = cT\theta'' + cT\theta' + f_\theta, \tag{9}$$

$$(z)\ \rho\left(V^2 z''\right) = Tz'' + Tz' + f_z. \tag{10}$$

The quantities f_r, f_θ, and f_z are the components of the linear density of the external force (2). The first one is simply $f_r = n$, while the other two still need to be determined. The velocity of the yarn in the quasi-stationary approximation is (see equation (23) in [10], where we substitute $v_{\mathrm{rel}} = 0$)

$$v = -Vt + \omega \times r = c\left(\omega - V\theta'\right)e_\theta - z'Ve_z. \tag{11}$$

This expression can then be used to derive the unit vector in the direction of the yarn velocity:

$$\frac{v}{|v|} = \frac{1}{\sqrt{c^2(\omega - V\theta')^2 + z'^2V^2}} \left[c\left(\omega - V\theta'\right)e_\theta - z'Ve_z\right], \tag{12}$$

from which then finally follow the two components of the linear density of the force:

$$f_\theta = \frac{-\mu nc\left(\omega - V\theta'\right)}{\sqrt{c^2(\omega - V\theta')^2 + z'^2V^2}},$$
$$f_z = \frac{\mu nz'V}{\sqrt{c^2(\omega - V\theta')^2 + z'^2V^2}}. \tag{13}$$

Equations (8)–(10) and (13) are the simplified equations of motions that we required. At first they appear more complex than the vector expressions (2) and (3), since they are expressed component by component. Nevertheless, they are indeed simpler: the unknown functions are θ, z, n_θ, n_z, and T, but we have managed to eliminate r and n_r. In this part of the paper we will show that the function T can equally be eliminated.

6. Partial Analytical Solution

Equation (9) from the previous section is multiplied by $c\theta'$, (10) by z'; they are then added together and reorganized to read

$$\begin{aligned}\rho V^2\left(c^2\theta'\theta'' + z'z''\right) &= T\left(c^2\theta'\theta'' + z'z''\right) \\ &\quad + T'\left(c^2\theta'^2 + z'^2\right) + c\theta' f_\theta + z' f_z.\end{aligned} \tag{14}$$

In this equation, ρ is the linear density of the yarn, V the unwinding velocity, c the package radius, T the tension in the yarn, f the linear density of the force of friction, and the position of the point is given in the cylindrical coordinate system ($r\theta z$). The dash after a symbol denotes the operation of taking the derivative with respect to the arc length s. Now we take into account the condition of nonextensibility, which states that the extension of yarn may be neglected. For motion on the package surface, this condition (equation (34) in [10]) can be expressed as

$$c^2\theta'^2 + z'^2 = 1. \tag{15}$$

Taking a derivative of this equation, we obtain

$$c^2\theta'\theta'' + z'z'' = 0. \tag{16}$$

Inserting (15) and (16) into (14), we end up with

$$T' = -c\theta' f_\theta - z' f_z. \tag{17}$$

In this equation we insert the expressions for the components of the linear density of the force

$$f_\theta = \frac{-\mu nc\left(\omega - V\theta'\right)}{\sqrt{c^2(\omega - V\theta')^2 + z'^2V^2}},$$
$$f_z = \frac{\mu nz'V}{\sqrt{c^2(\omega - V\theta')^2 + z'^2V^2}} \tag{18}$$

and we obtain

$$\begin{aligned}T' &= \frac{\mu n\left(c^2\theta'\left(\omega - V\theta'\right) - z'^2V\right)}{\sqrt{c^2(\omega - V\theta')^2 + z'^2V^2}} \\ &= \frac{\mu n\left(c^2\omega\theta' - V\right)}{\sqrt{c^2(\omega - V\theta')^2 + z'^2V^2}}.\end{aligned} \tag{19}$$

To obtain the last expression we have used (15). The n from this equation is evaluated and inserted in the expression for f_θ in (18):

$$f_\theta = cT'\frac{V\theta' - \omega}{c^2\omega\theta' - V}. \tag{20}$$

This is then used in

$$\rho cV^2\theta'' = cT\theta'' + cT'\theta' + f_\theta \tag{21}$$

to obtain

$$\left(\rho V^2 - T\right)\theta'' = T'\theta' + \frac{V\theta' - \omega}{c^2\omega\theta' - V}T' = \omega T'\frac{c^2\theta'^2 - 1}{c^2\omega\theta' - V}. \tag{22}$$

We rewrite this equation as

$$\frac{c\omega}{V}\frac{T'}{\rho V^2 - T} = c\theta''\left[\frac{\left(c^2\omega/V\right)\theta' - 1}{c^2\theta'^2 - 1}\right]. \tag{23}$$

After introducing the dimensionless angular velocity $\Omega = c\omega/V$ and a new variable $\chi = c\theta$, the equation takes a more clear expression:

$$\Omega\frac{T'}{\rho V^2 - T} = \chi''\left[\frac{1 - \Omega\chi'}{1 - \chi'^2}\right]. \tag{24}$$

The quantity $\chi' = c\theta'$ is always smaller than 1 when the yarn slides on the package surface, since the length of one loop of yarn on the package is at least $2\pi c$. A simple consideration (and the help of Figure 4) can convince us that the derivative χ' is related with the tangential direction of the yarn on the package surface. In fact, one has $\chi' = \cos\phi$. Using a similar consideration one can also establish that $z' = \tan\phi$.

Equation (24) can be integrated analytically. The left hand side is the derivative of the function $-\Omega\ln|T - \rho V^2|$, while the right hand side is the derivate of the function $((\Omega-1)/2)\ln|1-\chi''| + ((\Omega+1)/2)\ln|1+\chi''|$.

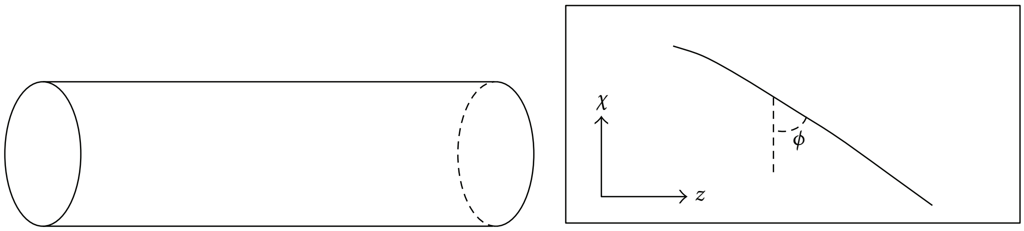

(a) (b)

Figure 4: (a) The surface of the cylinder is cut along the long edge and the surface is flattened. (b) The flattened surface is a plane with axes z and χ. The angle ϕ is the angle of the yarn in the $(z\chi)$ plane.

As can be easily verified, we thus obtain

$$
\begin{aligned}
&-\Omega \ln\left|T-\rho V^2\right| \frac{(\Omega-1)}{2} \ln\left|1-\chi'\right| \\
&\quad+\frac{(\Omega+1)}{2} \ln\left|1+\chi'\right| + \text{const.}
\end{aligned} \tag{25}
$$

The tension T is always larger than the quantity ρV^2, which is twice the linear density of the kinetic energy which the yarn has because of it being pulled through the eyelet [19, 20]. We have also already established that $\chi' < 1$. For this reason, all quantities between the absolute value brackets are positive, thus the brackets do not need to be written.

Exponentiating the expression we had obtained and rearranging it slightly, we obtain

$$
T-\rho V^2 = K\left[\left(1-c\theta'\right)^{((1-\Omega)/2\Omega)}\left(1+c\theta'\right)^{-((1+\Omega)/2\Omega)}\right], \tag{26}
$$

where K is an integration constant. It can be determined by considering the behavior at the lift-off point. If the winding angle is Φ, then the change of the arc length s by $2\pi c/\cos\Phi$ (i.e., the length of one loop) corresponds to a change of θ by 2π.

Therefore at the lift-off point θ' is equal to $\cos\Phi/c$, and finally $\chi'(\mathrm{Od}) = \cos\Phi$. (The winding angle Φ is by definition equal to the angle of the yarn in the $(z\chi)$ plane, therefore this result is in full agreement with the expression $\chi' = \cos\phi$ which we had established before.) In this point the tension in the yarn is equal to the residual tension of the yarn inside the package, T_{res}. If both expressions are used in (26), we obtain

$$
T_{\text{res}}-\rho V^2 = K\left[(1-\cos\Phi)^{((1-\Omega)/2\Omega)}(1+\cos\Phi)^{-((1+\Omega)/2\Omega)}\right]. \tag{27}
$$

Equation (26) may therefore be written as

$$
\begin{aligned}
&\frac{T-\rho V^2}{T_{\text{res}}-\rho V^2} \\
&\quad=\left[\left(\frac{1-c\theta'}{1-\cos|\Phi|}\right)^{((1-\Omega)/2\Omega)}\left(\frac{1+c\theta'}{1+\cos|\Phi|}\right)^{-((1+\Omega)/2\Omega)}\right].
\end{aligned} \tag{28}
$$

In parallel cylindrical package with dense parallel winding, the dimensionless angular velocity $\Omega = c\omega/V$ is approximately equal to 1. Setting $\Omega = 1$ in (26) we obtain

$$
T-\rho V^2 = \frac{K}{1+c\theta'}. \tag{29}
$$

This result had already been established by Fraser et al. [6], but our equation (26) holds in general. In cross-wound package one namely has

$$
\Omega = \frac{\cos\Phi}{1-\sin\Phi}, \tag{30}
$$

where Φ is the winding angle at the point where the yarn is currently being unwound. This implies that in cross-wound packages, the dimensionless angular velocity is not equal to one, but it is larger than 1 during the unwinding in the backward direction ($\Phi > 1$) and smaller than 1 during the unwinding in the forward direction ($\Phi < 1$).

In the section of yarn which slides on the surface and experiences friction from the lower layers, the tension decreases from the value at the lift-off point to the residual value. At the same time, the angle ϕ increases from its value at the unwinding point to the value of Φ at the lift-off point. The relation between these two phenomena is given precisely by (28).

Equation (19) can be rewritten as

$$
\begin{aligned}
T' &= \frac{\mu n\left(V\Omega\cos\phi - V\right)}{\sqrt{V^2(\Omega-\cos\phi)^2 + V^2\tan^2\phi}} \\
&= \frac{\mu n\left(\Omega\cos\phi - 1\right)}{\sqrt{(\Omega-\cos\phi)^2 + \tan^2\phi}}.
\end{aligned} \tag{31}
$$

Using the approximation of $\Omega = 1$ and $\cos\phi \sim 1-\phi^2/2$, $\tan\phi \sim \phi$, we obtain

$$
T' \approx \frac{-\mu n\phi}{2}. \tag{32}
$$

The decrease of the tension along the yarn is proportional to the coefficient of friction, as expected. The larger the coefficient of friction is, the shorter is the sliding segment of the yarn. The derivative is also proportional to the angle ϕ, thus the decrease is larger near the lift-off point where ϕ is large, but smaller at the unwinding point where in the case of dense parallel winding the angle ϕ is almost equal to zero.

7. Conclusion

We have shown how the equation of motion on the package surface can be obtained from the general equation of yarn motion by considering the force of friction. The external force has two components: the normal force of the package surface and the force of friction. We have described the conditions for the validity of the quasi-stationary approximation which was then used to simplify the equation of motion to a two-dimensional problem. We have also shown that the simplification of the equation of motion for the sliding motion of the yarn to a two-dimensional problem makes it possible to establish the main conclusions analytically. We have shown how the section of the yarn which slides on the package surface makes it possible that the tension in the yarn reduces to its residual yarn and how this is related to the form of the sliding yarn. More accurate solutions of the problem can, however, only be obtained using a full numerical solution of the equations using the shooting method [6, 19, 20]. Another very interesting approach for solving the equation of motion for the yarn would be the use of the methods described by Ji-Huan He. The analytical solution can be obtained using the variational iteration method or the homotopy perturbation method reviewed in [8, 21, 22].

References

[1] D. G. Padfield, "The motion and tension of an unwinding thread," *Proceedings of the Royal Society A*, vol. 245, no. 1242, pp. 382–407, 1958.

[2] D. G. Padfield, "A note on the fluctuations of tension during unwinding," *Journal of the Textile Institute Proceedings*, vol. 47, no. 5, pp. 301–308, 1956.

[3] A. E. de Barr and H. Catling, *Manual of Cotton Spinning*, vol. 5, Butterworth, Oxford, UK, 1976.

[4] V. K. Kothari and G. A. V. Leaf, "The unwinding of yarns from packages. Part I: the theory of yarn-unwinding," *Journal of the Textile Institute*, vol. 70, no. 3, pp. 89–95, 1979.

[5] V. K. Kothari and G. A. V. Leaf, "The unwinding of yarns from packages. Part II: unwinding from cylindrical packages," *Journal of the Textile Institute*, vol. 70, no. 5, pp. 172–183, 1979.

[6] W. B. Fraser, T. K. Ghosh, and S. K. Batra, "On unwinding yarn from cylindrical package," *Proceedings of the Royal Society A*, vol. 436, no. 1898, pp. 479–498, 1992.

[7] W. B. Fraser, "Effect of yarn elasticity on an unwinding balloon," *Journal of the Textile Institute*, vol. 83, no. 4, pp. 603–613, 1992.

[8] J.-H. He, "An elementary introduction to recently developed asymptotic methods and nanomechanics in textile engineering," *International Journal of Modern Physics B*, vol. 22, no. 21, pp. 3487–3578, 2008.

[9] S. Q. Wang, J.-H. He, and L. Xu, "Non-ionic surfactants for enhancing electrospinability and for the preparation of electrospun nanofibers," *Polymer International*, vol. 57, no. 9, pp. 1079–1082, 2008.

[10] S. Praček, "Theory of string motion in the textile process of yarn unwinding," *International Journal of Nonlinear Sciences and Numerical Simulation*, vol. 8, no. 3, pp. 451–460, 2007.

[11] J. Strnad, *Fizika, Prvi Del: Mehanika, Toplota*, DMFA, Ljubljana, Slovenia, 1995.

[12] J. A. Roberson and C. T. Crowe, *Engineering Fluid Dynamics*, Druga Izdaja, Houghton Mifflin Company, Boston, Mass, USA, 1980.

[13] S. Pahor, *Uvod v Analiticno Mehaniko*, DMFA, Ljubljana, Slovenia, 1995.

[14] J. N. Bronštejn and K. A. Semendjajev, *Matematični Priročnik*, Tehniška založba Slovenije, Ljubljana, Slovenia, 1994.

[15] T. K. Ghosh, S. K. Batra, and A. S. Murthy, "Dynamic analysis of yarn unwinding from cylindrical packages. Part I: parametric studies of the two-region problem," *Textile Research Journal*, vol. 71, no. 9, pp. 771–778, 2001.

[16] T. K. Ghosh, S. K. Batra, and X. Murthy, "Dynamic analysis of yarn unwinding from cylindrical packages. Part II: the three-region analysis," *Textile Research Journal*, vol. 71, no. 10, pp. 855–861, 2001.

[17] R. Wu, J. Yu, C. D. Rahn, and B. C. Goswami, "Measuring yarn/package friction during over-end unwinding," *Textile Research Journal*, vol. 70, no. 4, pp. 321–327, 2000.

[18] J. D. Clark, W. B. Fraser, and D. M. Stump, "Modelling of tension in yarn package unwinding," *Journal of Engineering Mathematics*, vol. 40, no. 1, pp. 59–75, 2001.

[19] X. M. Kong, *Steady state unwinding of yarn from cylindrical packages: theory and experiment [Ph.D. thesis]*, Clemson University, Clemson, SC, USA, 1997.

[20] X. M. Kong, C. D. Rahn, and B. C. Goswami, "Steady-state unwinding of yarn from cyclindrical packages," *Textile Research Journal*, vol. 69, no. 4, pp. 292–306, 1999.

[21] J.-H. He, "Some asymptotic methods for strongly nonlinear equations," *International Journal of Modern Physics B*, vol. 20, no. 10, pp. 1141–1199, 2006.

[22] J.-H. He, "Asimptotic methods for solitary solutions and compactons," *Abstract and Applied Analysis*, vol. 2012, Article ID 916793, 130 pages, 2012.

Hindawi Publishing Corporation
Abstract and Applied Analysis
Volume 2013, Article ID 390476, 8 pages
http://dx.doi.org/10.1155/2013/390476

Research Article

Exponential Attractor for Coupled Ginzburg-Landau Equations Describing Bose-Einstein Condensates and Nonlinear Optical Waveguides and Cavities

Gui Mu and Jun Liu

College of Mathematics and Information Science, Qujing Normal University, Qujing, Yunnan 655011, China

Correspondence should be addressed to Jun Liu; liujunxei@126.com

Received 4 February 2013; Accepted 6 March 2013

Academic Editor: de Dai

The existence of the exponential attractors for coupled Ginzburg-Landau equations describing Bose-Einstein condensates and nonlinear optical waveguides and cavities with periodic initial boundary is obtained by showing Lipschitz continuity and the squeezing property.

1. Introduction

Inertial set was introduced (see [1–5]) in order to overcome some of the theoretical difficulties that are associated with inertial manifolds. An inertial set, by definition, contains the global attractor and attracts all trajectories at a uniform exponential rate. Consequently, it contains the slow transients as well as the global attractor. In the theory of dynamical systems the slow transients correspond to slowly converging stable manifolds that are in some sense close to central manifolds. Numerical simulations of infinite dimensional dynamical systems often capture both slow transients and parts of the attractor. After a large but finite time the state of the system obtained from the numerical calculation may often be at a finite distance from the global attractor but at an infinitesimal distance to the inertial set. In this sense, we propose to call the inertial set an exponential attractor to be consistent with the physical intuition [5].

An exponential attractor is an exponentially attracting compact set with finite fractal dimension that is positively invariant under the forward semiflow. The notion of exponential attractors was introduced by Eden et al. [3] and has been shown to be one of the very important notions in the study of long time behavior of solutions to nonlinear diffusion equations [6]. The easiest way of obtaining an exponential attractor is by taking the intersection of an absorbing set with an inertial manifold.

In the area of hyperbolic evolutionary equations, the existence of exponential attractors has been proved for many equations. In this paper, we will prove the existence of exponential attractor for coupled Ginzburg-Landau equations

$$\begin{gathered} iu_t + \gamma_2 \Delta u + i\gamma u + \left(\sigma_1 + i\sigma_2 |u|^2\right)|u|^2 u + v = 0, \\ iv_t + \gamma_2 \Delta u + \left(i\Gamma - \chi\right) v + u = 0, \end{gathered} \tag{1}$$

with the periodic boundary conditions

$$u(x,t) = u(x+D,t), \qquad v(x,t) = v(x+D,t), \qquad x \in R, \quad t > 0, \tag{2}$$

and initial value

$$u(x,0) = u_0(x), \quad v(x,0) = v_0(x), \quad x \in R. \tag{3}$$

Its physical realizations include systems from nonlinear optics and a double-cigar-shaped Bose-Einstein condensate with a negative scattering length. In particular, in the case of the optical systems, u and v are amplitudes of electromagnetic waves in two cores of the system, the evolutional variable t is either time or propagation distance in the dual-core optical fiber, and x is the transverse coordinate in the cavity or the reduced time in the application to the fibers [7].

This paper is organized as follows. In Section 2, we give a description of preliminaries with existence of exponential attractor and the properties of solutions and bounded absorbing sets of (1). In Section 3, the existence of the exponential attractor in V_2 type exponential attractor is proved. In Section 4, we give some conclusions for this paper.

2. Preliminaries

Let V_1, V_2 be two Hilbert spaces, and let V_2 be dense in V_1 and compactly imbedded into V_1. Let $S(t)_{t\geq 0}$ be a continuous map from V_1, V_2 into itself. We study

$$\frac{du}{dt} + Au + g(u) = f(x), \quad t > 0, \ x \in \Omega, \tag{4}$$

$$u(x, 0) = u_0(x), \tag{5}$$

Dirichlet problem or periodic boundary problem, (6)

where Ω is a bounded open set in R^n, $\partial\Omega$ is smooth, and A is a positive self-adjoint operator with a compact inverse. Letting $\{w_i\}_{i=1}^{\infty}$ denote the complete set of eigenvectors of A, the corresponding eigenvalues are

$$0 \leq \lambda_1 < \lambda_1 \cdots \lambda_i < \cdots \longrightarrow +\infty. \tag{7}$$

We assume that the nonlinear semigroup $S(t)_{t\geq 0}$ defined in (4)–(6) possesses a compact attractor $\mathbf{B}$ of (V_2, V_1)-type; namely, there exists a compact set $\mathbf{B}$ in V_1, and $\mathbf{B}$ attracts all bounded subsets in V_2 and is invariant under the action of $S(t)_{t\geq 0}$.

Let C be a compact subset of V_2. $S(t)_{t\geq 0}$ leaves the set C invariant and set

$$\mathbf{B} = \bigcap_{s\geq 0} \overline{\bigcup_{t\geq s} S(t)_{t\geq 0} C}, \tag{8}$$

that is, for $S(t)_{t\geq 0}$ on C, $\mathbf{B}$ is the global attractor.

Definition 1. A compact set M is called an exponential attractors for $S(t)_{t\geq 0}, C$ if

(i) $\mathbf{B} \subseteq M \subseteq C$;

(ii) $S(t)M \subseteq M$, for every $t \geq 0$;

(iii) M has finite fractal dimension $d_F < \infty$;

(iv) There exist constants c_1 and c_2 such that

$$\operatorname{dist}_{v_2}(S(t)C, M) \leq c_1 \exp(-c_2 t), \quad \forall t > 0, \tag{9}$$

where

$$\operatorname{dist}_{v_2}(A, D) = \sup_{x\in A} \inf_{y\in D} \|x - y\|_{V_2}. \tag{10}$$

Definition 2. If there exists a bounded function $l(t)$ independent u and v such that

$$\|S(t)u - S(t)v\|_{V_2} \leq l(t)\|u - v\|_{V_2}, \tag{11}$$

for every $u, v \in C$, then we say $S(t)$ is Lipschitz continuous in C and $l(t)$ is Lipschitz constant for $S(t)$ in C.

Definition 3. A continuous semigroup $S(t)_{t\geq 0}$ is said to satisfy the squeezing property on C if there exists $t_* > 0$ such that $S(t_*)$ satisfies the following.

For every $\delta \in (0, (1/8))$, there exists an orthogonal projection P_{N_0} of rank equal to N_0 such that for every u and v in C if

$$\left\|P_{N_0}(S(t_*)u - S(t_*)v)\right\|_{v_2} \leq \left\|Q_{N_0}(S(t_*)u - S(t_*)v)\right\|_{v_2} \tag{12}$$

holds, then we also have

$$\|S(t_*)u - S(t_*)v\|_{v_2} \leq \delta\|u - v\|_{v_2}, \tag{13}$$

where $Q_{N_0} = I - P_{N_0}$.

Theorem 4 (see [3]). *Suppose (4)–(6) satisfy the following conditions.*

(1) *There exist nonlinear semigroup $S(t)_{t\geq 0}$ and a compact attractor $\mathbf{B}$.*

(2) *There exists a compact set $\mathbf{C}$ in V_2 which is positively invariant for $S(t)_{t\geq 0}$.*

(3) *$S(t)_{t\geq 0}$ is Lipschitz continuous and is squeezing in C.*

Then (4)–(6) admit an exponential attractor M in V_2 for $S(t)_{t\geq 0}$ and

$$M = \bigcup_{0\leq t\leq t_*} S(t)M_*, \tag{14}$$

where

$$M_* = \mathbf{B} \bigcup \left(\bigcup_{j=1}^{\infty} \bigcup_{k=1}^{\infty} S(t_*)^j \left(E^{(k)}\right) \right). \tag{15}$$

Moreover,

$$\begin{gathered} d_F(M) \leq 1 + CN_0, \\ \operatorname{dist}_{V_2}(S(t)B, M) \leq C_0 \exp(-C_1 t), \end{gathered} \tag{16}$$

where N_0, $E(k)$ are defined as in [4], C, C_0, C_1 are the constants independent of B, and t_* is a positive constant.

Proposition 5. *There exists $t_0(B_0)$ such that*

$$B^* = \overline{\bigcup_{0\leq t\leq t_0} S(t)B_0} \tag{17}$$

is a compact positively invariant set in V_1 and is absorbing set for all bounded subsets in V_2, where B_0 is a closed absorbing set in V_2 for $S(t)_{t\geq 0}$.

Proposition 6. *Let B_0, B_1 be bounded and closed absorbing sets for (4)–(6) in (V_2, V_1), respectively. Then there exists a compact attractor A^* of (V_2, V_1)-type. For the proof of Proposition 5 and Proposition 6, we refer the reader to [5].*

Denoting by $|\cdot|_{L^p}$ the norm in $L^p(0, L)$, $1 \leq p \leq \infty$, for simplicity, we denote by $|\cdot|_0$ and $|\cdot|_\infty$ the norm in the case

$p = 2$ and $p = \infty$, respectively. Suppose that $H = L^2(0, L)$, $E_i = H^i(0, L) \times H^i(0, L)$ $(i = 1, 2)$, where $H^i(0, L)$ is a Hilbert space for the scalar product

$$((\cdot,\cdot))_{H^i} = (\cdot,\cdot) + \sum_{j=1}^{i} \left(D^j\cdot, D^j\cdot\right), \quad D = \frac{\partial}{\partial x}. \tag{18}$$

The norm of E_i is defined by $\|(u, v)\|_{E_i}^2 = \|u\|_{H^i}^2 + \|v\|_{H^i}^2$.

We now establish some time-uniform a priori estimates on (u, v) in E_1 and E_2, respectively.

Lemma 7. *Assume that $(u_0, v_0) \in E_1$; then*

$$\|(u, v)\|_{E_1}^2 \le c\left\|(u_0, v_0)\right\|_{E_1}^2 e^{-\delta_1 t} + c_1. \tag{19}$$

Thus there exists $t_1 = t_1(R) > 0$ such that

$$\|(u, v)\|_{E_1}^2 \le c_2, \qquad t \ge t_1, \tag{20}$$

whenever $\|(u_0, v_0)\|_{E_1} \le R$.

Lemma 8. *Assume that $(u_0, v_0) \in E_2$; then*

$$\|(u, v)\|_{E_2}^2 \le c\left\|(u_0, v_0)\right\|_{E_2}^2 e^{-\delta_2 t} + c_3. \tag{21}$$

Thus there exists $t_2 = t_2(R) > 0$ such that

$$\|(u, v)\|_{E_2}^2 \le c_4, \quad t \ge t_2, \tag{22}$$

whenever $\|(u_0, v_0)\|_{E_2} \le R$.

Theorem 9. *Assume that all the parameters of (1) are positive. For (u_0, v_0) given in E_i $(i = 1, 2)$, there exists a unique solution*

$$(u, v) \in L^\infty\left(R_+, E_i\right). \tag{23}$$

And also

$$(u, v) \in \mathscr{C}\left(R_+, E_1\right), \quad \forall \left(u_0, v_0\right) \in E_1. \tag{24}$$

Furthermore, the solution operator of the system is a continuous semigroup $S(t)$ on E_1 which possesses bounded absorbing sets $B_i \subset E_i$, for $i = 1, 2$.

Thus, we observe that Lemmas 7 and 8 show that there exists constant k depending only on the data that the balls

$$\begin{aligned} B_1 &= \left\{(u, v) \in E_1, \|u\|_{H_1} + \|v\|_{H_1} \le k\right\}, \\ B_2 &= \left\{(u, v) \in E_2, \|u\|_{H_2} + \|v\|_{H_2} \le k\right\} \end{aligned} \tag{25}$$

are bounded absorbing sets for $S(t)$ in E_1 and E_2, respectively:

Let

$$V_1 = E_1, \qquad V_2 = E_2, \qquad B = \overline{\bigcup_{t\ge0} S(t)\, B_2}, \tag{26}$$

then B is a compact invariant subset in V_2; we know that semigroup $S(t)$ defined by problem (31)–(34) possesses a V_2-type compact attractor. According to Theorem 4, we need only to show the Lipschitz continuity and the squeezing property of the dynamical system $S(t)$ in B, respectively. That is what we proceed to do in the following sections.

3. Exponential Attractor in V_2 for Problem (1)-(2)

In this section, we show the existence of the exponential attractor in V_2 for problem (1)-(2). In order to prove the Lipschitz continuity and the squeezing property, we need to extend Hölder inequality

$$\int_\Omega \left|u(x)\, u_2(x)\cdots u_k(x)\right| d_x \le \prod_{j=1}^{k}\left\|u_j\right\|_{L^{p_j}}, \tag{27}$$

where $\sum_{j=1}^{k}(1/p_j) = 1$, $p_j > 1$ and Gagliardo-Nirenberg (G-N) inequality

$$\left\|\nabla^j u\right\|_p \le c\left\|\nabla^m u\right\|_r^a \|u\|_q^{1-a}, \tag{28}$$

where

$$\begin{gathered} \frac{1}{p} = \frac{j}{n} + a\left(\frac{1}{r} - \frac{m}{n}\right) + \frac{1-a}{q}, \\ 1 \le q, \quad r \le \infty, \quad 0 \le j < m, \quad \frac{j}{m} \le a \le 1, \end{gathered} \tag{29}$$

and the Young's inequality

$$\begin{gathered} ab \le \frac{\varepsilon}{p}a^p + \frac{1}{q}\varepsilon^{(-q/b)}b^q, \quad a, b, \varepsilon > 0,\ 1 < p, \\ q < \infty, \quad \frac{1}{p} + \frac{1}{q} = 1. \end{gathered} \tag{30}$$

Theorem 10. *Assume $w_1(t) = (u_1(t), v_1(t))$, and $w_2(t) = (u_2(t), v_2(t))$ are two solutions of problem (1)-(2) with initial values $w_{10} = (u_{10}, v_{10})$, $w_{20} = (u_{20}, v_{20}) \in B = H^2 \times H^2$; then one has*

$$\left\|w_1(t) - w_2(t)\right\|_{V_2} \le \exp\left(2C_0 t\right)\left\|w_{10} - w_{20}\right\|_{V_2}. \tag{31}$$

Proof. Letting $h(t) = u_1(t) - u_2(t)$, $g(t) = v_1(t) - v_2(t)$, from (1)-(2), we have

$$ih_t + \gamma_2\Delta h + i\gamma h + f\left(u_1, u_2\right) + g = 0, \tag{32}$$

$$ig_t + \gamma_2\Delta g + \left(i\Gamma - \chi\right) g + h = 0, \tag{33}$$

with periodic initial value

$$\begin{gathered} h(x, t) = h(x + D, t), \qquad g(x, t) = g(x + D, t), \\ x \in R, \quad t > 0, \end{gathered} \tag{34}$$

$$\begin{gathered} h(x, 0) = u_{10}(x) - u_{20}(x), \qquad g(x, 0) = v_{10}(x) - v_{20}(x), \\ x \in R, \end{gathered} \tag{35}$$

where

$$f\left(u_1, u_2\right) = \sigma_1\left(\left|u_1\right|^2 u_1 - \left|u_2\right|^2 u_2\right) + i\sigma_2\left(\left|u_1\right|^4 u_1 - \left|u_2\right|^4 u_2\right). \tag{36}$$

Taking $\phi_1(u) = |u|^2$ and $\phi_2(u) = |u|^4$, then we get

$$\phi_1'(\xi)\, h = |u_1|^2 - |u_2|^2, \tag{37}$$

$$\phi_2'(\eta)\, h = |u_1|^4 - |u_2|^4. \tag{38}$$

Substituting (37) and (38) into (36), we get

$$\begin{aligned} f(u_1, u_2) &= \sigma_1 \left(|u_1|^2 u_1 - |u_1|^2 u_2 + |u_1|^2 u_2 - |u_2|^2 u_2\right) \\ &\quad + i\sigma_2 \left(|u_1|^4 u_1 - |u_1|^4 u_1 + |u_1|^4 u_2 - |u_2|^4 u_2\right) \\ &= \sigma_1 h \left(\phi_1(u_1) + u_2 \phi_1'(\xi)\right) \\ &\quad + i\sigma_2 h \left(\phi_2(u_1) + u_2 \phi_2'(\eta)\right). \end{aligned} \tag{39}$$

Substituting (39) into (32), we obtain

$$\begin{aligned} &ih_t + \gamma_2 \Delta h + i\gamma h + \sigma_1 h \left(\phi_1(u_1) + u_2 \phi_1'(\xi)\right) \\ &\quad + i\sigma_2 h \left(\phi_2(u_1) + u_2 \phi_2'(\eta)\right) + g = 0, \end{aligned} \tag{40}$$

$$ig_t + \gamma_2 \Delta g + (i\Gamma - \chi)\, g + h = 0. \tag{41}$$

To prove the Theorem 4, we take the following four steps.

Step 1. Taking the inner product of (40) with $\overline{h}$ and (41) with $\overline{g}$, respectively, we have

$$\begin{aligned} &\left(ih_t, \overline{h}\right) + \left(\gamma_2 \Delta h, \overline{h}\right) + \left(i\gamma h, \overline{h}\right) \\ &\quad + \left(\sigma_1 h \left(\phi_1(u_1) + u_2 \phi_1'(\xi)\right), \overline{h}\right) \\ &\quad + \left(i\sigma_2 h \left(\phi_2(u_1) + u_2 \phi_2'(\eta)\right), \overline{h}\right) + \left(g, \overline{h}\right) = 0, \end{aligned} \tag{42}$$

$$\left(ig_t, \overline{g}\right) + \left(\gamma_2 \Delta g, \overline{g}\right) + \left((i\Gamma - \chi)\, g, \overline{g}\right) + \left(h, \overline{g}\right) = 0, \tag{43}$$

using

$$\begin{aligned} \frac{d}{dt} \int_\Omega |u|^2 dx &= \frac{d}{dt} \int_\Omega u\overline{u}\, dx = \int_\Omega \left(u_t \overline{u} + u\overline{u_t}\right) dx \\ &= 2 \operatorname{Re} \int_\Omega u_t \overline{u}\, dx. \end{aligned} \tag{44}$$

Thus,

$$\begin{aligned} &\operatorname{Im}\left(i \int_\Omega u_t \overline{u}\, dx\right) = \frac{1}{2} \frac{d}{dt} \int_\Omega |u|^2 dx, \\ &\left(\gamma_2 \Delta h, \overline{h}\right) = -\gamma_2 \|h_x\|^2, \qquad \left(i\gamma h, \overline{h}\right) = i\gamma \|h\|^2, \end{aligned} \tag{45}$$

then taking the imaginary part of (42) and (43), respectively,

$$\begin{aligned} &\frac{1}{2} \frac{d}{dt} \|h\|^2 + \gamma \|h\|^2 + \sigma_1 \operatorname{Im} \int_\Omega u_2 \phi_1'(\xi)\, |h|^2 dx \\ &\quad + \sigma_2 \operatorname{Im} \int_\Omega \phi_2(u_1)\, |h|^2 dx \\ &\quad + \sigma_2 \operatorname{Re} \int_\Omega \phi_2'(\eta)\, |h|^2 dx + \operatorname{Im} \int_\Omega g\overline{h}\, dx = 0, \end{aligned} \tag{46}$$

$$\frac{1}{2} \frac{d}{dt} \|g\|^2 + \Gamma \|g\|^2 + \operatorname{Im} \int_\Omega h\overline{g}\, dx = 0, \tag{47}$$

by using the extend Hölder inequality, we can obtain

$$\begin{aligned} &\left|\operatorname{Im} \int_\Omega g\overline{h}\, dx\right| \le \frac{1}{2}\left(\|g\|^2 + \|h\|^2\right), \\ &\left|\sigma_1 \operatorname{Im} \int_\Omega u_2 \phi_1'(\xi)\, |h|^2 dx\right| \le |\sigma_1| \int_\Omega |u_2|\, \phi_1'(\xi)\, |h|^2 dx \\ &\qquad \le |\sigma_1|\, \|h\|^2 \|u_2\|_\infty \left\|\phi_1'(\xi)\right\|_\infty \\ &\qquad \le C\|h\|^2, \\ &\left|\sigma_2 \operatorname{Re} \int_\Omega u_2 \phi_2'(\eta)\, |h|^2 dx\right| \le |\sigma_2| \int_\Omega |u_2|\, \phi_2'(\xi)\, |h|^2 dx \\ &\qquad \le |\sigma_2|\, \|h\|^2 \|u_2\|_\infty \left\|\phi_2'(\eta)\right\|_\infty \\ &\qquad \le C\|h\|^2. \end{aligned} \tag{48}$$

Combining (46) and (47), then we infer that

$$\begin{aligned} &\frac{1}{2} \frac{d}{dt} \left(\|h\|^2 + \|g\|^2\right) + \gamma \|h\|^2 + \gamma \|g\|^2 \\ &\quad + \sigma_2 \int_\Omega \phi_2(u_1)\, |h|^2 dx \le C\|h\|^2 + \|g\|^2. \end{aligned} \tag{49}$$

Step 2. Taking the inner product of (40) with $-\overline{h_{xx}}$ and (41) with $-\overline{g_{xx}}$, respectively, we have

$$\begin{aligned} &\left(ih_t, \overline{h_{xx}}\right) + \left(\gamma_2 \Delta h, -\overline{h_{xx}}\right) + \left(i\gamma h, -\overline{h_{xx}}\right) \\ &\quad + \left(\sigma_1 h \left(\phi_1(u_1) + u_2 \phi_1'(\xi)\right), -\overline{h_{xx}}\right) \\ &\quad + \left(i\sigma_2 h \left(\phi_2(u_1) + u_2 \phi_2'(\eta)\right), -\overline{h_{xx}}\right) \\ &\quad + \left(g, -\overline{h_{xx}}\right) = 0, \end{aligned} \tag{50}$$

$$\begin{aligned} &\left(ig_t, -\overline{g_{xx}}\right) + \left(\gamma_2 \Delta g, -\overline{g_{xx}}\right) + \left((i\Gamma - \chi)\, g, -\overline{g_{xx}}\right) \\ &\quad + \left(h, -\overline{g_{xx}}\right) = 0. \end{aligned} \tag{51}$$

Note that

$$\begin{aligned} &\left(ih_t, -\overline{h_{xx}}\right) = i \int_\Omega h_{xt} \overline{h_x}\, dx, \\ &\left(g, -\overline{h_{xx}}\right) = \int_\Omega g_x \overline{h_x}\, dx, \\ &\left(\gamma_2 \Delta h, -\overline{h_{xx}}\right) = \|\Delta h\|^2, \\ &\left(i\gamma h, -\overline{h_{xx}}\right) = i\gamma \|h_x\|^2, \end{aligned}$$

$$\begin{aligned}
&\left(\sigma_1 h\left(\phi_1(u_1)+u_2\phi_1'(\xi)\right),-\overline{h_{xx}}\right)\\
&\quad=\sigma_1\int_\Omega\left[|h_x|^2\left(\phi_1(u_1)+u_2\phi_1'(\xi)\right)\right.\\
&\qquad\left.+h\overline{h_x}\left(\phi_1(u_1)+u_2\phi_1'(\xi)\right)_x\right]dx,\\
&\left(i\sigma_2 h\left(\phi_2(u_1)+u_2\phi_2'(\eta)\right),-\overline{h_{xx}}\right)\\
&\quad=i\sigma_2\int_\Omega\left[|h_x|^2\left(\phi_2(u_1)+u_2\phi_2'(\eta)\right)\right.\\
&\qquad\left.+h\overline{h_x}\left(\phi_2(u_1)+u_2\phi_2'(\eta)\right)_x\right]dx,
\end{aligned}\tag{52}$$

then taking the imaginary part of (50) and (51), respectively,

$$\begin{aligned}
&\frac{1}{2}\frac{d}{dt}\|h_x\|^2+\gamma\|h_x\|^2\\
&\quad+\sigma_1\operatorname{Im}\int_\Omega\left(u_2\phi_1'(\xi)|h_x|^2\right.\\
&\qquad\left.+h\overline{h_x}\left(\phi_1(u_1)+u_2\phi_1'(\xi)\right)_x\right)dx\\
&\quad+\sigma_2\operatorname{Im}\int_\Omega\phi_2(u_1)|h_x|^2dx\\
&\quad+\sigma_2\operatorname{Re}\int_\Omega\left(u_2\phi_2'(\eta)|h_x|^2\right.\\
&\qquad\left.+h\overline{h_x}\left(\phi_2(u_1)+u_2\phi_2'(\eta)\right)_x\right)dx\\
&\quad+\operatorname{Im}\int_\Omega g_x\overline{h_x}dx=0,
\end{aligned}\tag{53}$$

$$\frac{1}{2}\frac{d}{dt}\|g\|^2+\Gamma\|g\|^2+\operatorname{Im}\int_\Omega h\overline{g}\,dx=0.\tag{54}$$

Note the following inequalities:

$$\begin{aligned}
&\left|\sigma_1\operatorname{Im}\int_\Omega\left(u_2\phi_1'(\xi)|h_x|^2+h\overline{h_x}\left(\phi_1(u_1)+u_2\phi_1'(\xi)\right)_x\right)dx\right|\\
&\le|\sigma_1|\operatorname{Im}\int_\Omega\left(|u_2|\left|\phi_1'(\xi)\right||h_x|^2\right.\\
&\qquad+|h|\left|\overline{h_x}\right|\left(\left|\phi_1(u_1)_x\right|+|u_{2x}|\left|\phi_1'(\xi)\right|\right.\\
&\qquad\left.\left.+|u_2|\left|\phi_1'(\xi)_x\right|\right)\right)dx\\
&\le C\|h_x\|^2+|\sigma_1|\,\|h\|\left\|\overline{h_x}\right\|\left(\left\|\phi_1(u_1)_x\right\|_\infty+\|u_{2x}\|_\infty\left\|\phi_1'(\xi)\right\|_\infty\right.\\
&\qquad\left.+\|u_2\|_\infty\left\|\phi_1'(\xi)_x\right\|_\infty\right),\\
&\le C\|h_x\|^2+c\|h\|^2,\\
&\sigma_2\operatorname{Re}\int_\Omega\left(u_2\phi_2'(\eta)|h_x|^2+h\overline{h_x}\left(\phi_2(u_1)+u_2\phi_2'(\eta)\right)_x\right)dx\\
&\le C\|h_x\|^2+c\|h\|^2,
\end{aligned}\tag{55}$$

Combining (53) and (54), one can obtain

$$\begin{aligned}
&\frac{1}{2}\frac{d}{dt}\left(\|h_x\|^2+\|g_x\|^2\right)+\gamma\|h_x\|^2+\gamma\|g_x\|^2\\
&\quad+\sigma_2\int_\Omega\phi_2(u_1)|h_x|^2dx\le C\|h_x\|^2+\|g_x\|^2+c\|h\|^2.
\end{aligned}\tag{56}$$

Step 3. Taking the inner product of (40) with $\overline{h_{xxxx}}$ and (41) with $\overline{g_{xxxx}}$, respectively, we have

$$\begin{aligned}
&\left(ih_t,\overline{h_{xxxx}}\right)+\left(\gamma_2\Delta h,\overline{h_{xxxx}}\right)+\left(i\gamma h,\overline{h_{xxxx}}\right)\\
&\quad+\left(\sigma_1 h\left(\phi_1(u_1)+u_2\phi_1'(\xi)\right),\overline{h_{xxxx}}\right)\\
&\quad+\left(i\sigma_2 h\left(\phi_2(u_1)+u_2\phi_2'(\eta)\right),\overline{h_{xxxx}}\right)\\
&\quad+\left(g,\overline{h_{xxxx}}\right)=0,\\
&\left(ig_t,\overline{g_{xxxx}}\right)+\left(\gamma_2\Delta g,\overline{g_{xxxx}}\right)+\left((i\Gamma-\chi)g,\overline{g_{xxxx}}\right)\\
&\quad+\left(h,\overline{g_{xxxx}}\right)=0,
\end{aligned}\tag{57}$$

using

$$\begin{aligned}
&\left(ih_t,\overline{h_{xxxx}}\right)=i\int_\Omega h_{xxt}\overline{h_{xx}}dx,\\
&\left(g,\overline{h_{xxxx}}\right)=\int_\Omega g_{xx}\overline{h_{xx}}dx,\\
&\left(\gamma_2\Delta h,\overline{h_{xxxx}}\right)=\|h_{xxx}\|^2,\\
&\left(i\gamma h,\overline{h_{xxxx}}\right)=i\gamma\|h_{xx}\|^2,\\
&\left(\sigma_1 h\left(\phi_1(u_1)+u_2\phi_1'(\xi)\right),\overline{h_{xxxx}}\right)\\
&\quad=\sigma_1\left(\left(h\left(\phi_1(u_1)+u_2\phi_1'(\xi)\right)\right)_{xx},\overline{h_{xx}}\right)\\
&\quad=\sigma_1\left(h_{xx}\phi_1(u_1)+\psi_1,\overline{h_{xx}}\right),\\
&\left(i\sigma_2 h\left(\phi_2(u_1)+u_2\phi_2'(\eta)\right),\overline{h_{xxxx}}\right)\\
&\quad=i\sigma_2\left(\left(h\left(\phi_2(u_1)+u_2\phi_2'(\eta)\right)\right)_{xx},\overline{h_{xx}}\right)\\
&\quad=i\sigma_2\left(h_{xx}\phi_2(u_1)+\psi_2,\overline{h_{xx}}\right),
\end{aligned}\tag{58}$$

where

$$\begin{aligned}
\psi_1&=h_{xx}u_2\phi_1'(\xi)\\
&\quad+2h_x\left(\phi_1(u_1)_x+u_{2x}\phi_1'(\xi)+u_2\phi_1'(\xi)_x\right)\\
&\quad+h\left(\phi_1(u_1)_{xx}+u_{2xx}\phi_1'(\xi)+2u_{2x}\phi_1'(\xi)_x\right.\\
&\qquad\left.+u_2\phi_1'(\xi)_{xx}\right),
\end{aligned}$$

$$\begin{aligned}\psi_2 = {} & h_{xx}u_2\phi_2'(\eta) \\ & + 2h_x\left(\phi_2(u_1)_x + u_{2x}\phi_2'(\eta) + u_2\phi_2'(\eta)_x\right) \\ & + h\left(\phi_2(u_1)_{xx} + u_{2xx}\phi_2'(\eta) + 2u_{2x}\phi_2'(\eta)_x \right.\\ & \left. + u_2\phi_2'(\eta)_{xx}\right),\end{aligned} \tag{59}$$

then taking the imaginary part of (50) and (51), respectively,

$$\begin{aligned}\frac{1}{2}\frac{d}{dt}\|h_{xx}\|^2 + \gamma\|h_{xx}\|^2 + \sigma_1 \operatorname{Im}\left(\psi_1, \overline{h_{xx}}\right) & \\ + \sigma_2\left(h_{xx}\phi_2(u_1), \overline{h_{xx}}\right) + \sigma_2 \operatorname{Re}\left(\psi_2, \overline{h_{xx}}\right) & \\ + \operatorname{Im}\int_\Omega g_{xx}\overline{h_{xx}}dx = 0, &\end{aligned} \tag{60}$$

$$\frac{1}{2}\frac{d}{dt}\|g_{xx}\|^2 + \Gamma\|g_{xx}\|^2 + \operatorname{Im}\int_\Omega h_{xx}\overline{g_{xx}}dx = 0. \tag{61}$$

Note the following inequalities:

$$\left|\operatorname{Im}\left(\psi_1, \overline{h_{xx}}\right)\right| \le C\|h\|_{H^2}^2, \qquad \left|\sigma_2 \operatorname{Re}\left(\psi_2, \overline{h_{xx}}\right)\right| \le C\|h\|_{H^2}^2. \tag{62}$$

Combining (60) and (61), one can obtain

$$\begin{aligned}\frac{1}{2}\frac{d}{dt}\left(\|h_{xx}\|^2 + \|g_{xx}\|^2\right) + \gamma\|h_{xx}\|^2 + \Gamma\|g_{xx}\|^2 & \\ + \sigma_2\int_\Omega \phi_2(u_1)|h_{xx}|^2dx \le C\|h\|_{H^2}^2 + \|g_{xx}\|^2. &\end{aligned} \tag{63}$$

Step 4. Combining (49), (56) and (63), we get

$$\begin{aligned}\frac{1}{2}\frac{d}{dt}\left(\|h\|_{H^2}^2 + \|g\|_{H^2}^2\right) + \gamma\|h\|_{H^2}^2 + \gamma\|g\|_{H^2}^2 & \\ + \sigma_2\int_\Omega \phi_2(u_1)\left(|h|^2 + |h_x|^2 + |h_{xx}|^2\right)dx & \\ \le C\left(\|h\|^2 + \|h_x\|^2 + \|h\|_{H^2}^2\right) + \|g\|^2 + \|g_x\|^2 + \|g_{xx}\|^2. &\end{aligned} \tag{64}$$

Taking $\mu = \min(\Gamma, \gamma)$,$C_0 = \max(C, 1)$ and noting that

$$\sigma_2\int_\Omega\left(|h|^2 + |h_x|^2 + |h_{xx}|^2\right)dx \ge 0, \tag{65}$$

so (64) can be reduced to

$$\begin{aligned}\frac{1}{2}\frac{d}{dt}\left(\|h\|_{H^2}^2 + \|g\|_{H^2}^2\right) + \mu\left(\|h\|_{H^2}^2 + \|g\|_{H^2}^2\right) & \\ \le C_0\left(\|h\|_{H^2}^2 + \|g\|_{H^2}^2\right). &\end{aligned} \tag{66}$$

By Gronwall's inequality

$$\|h\|_{H^2}^2 + \|g\|_{H^2}^2 \le \exp(2C_0t)\left(\|h(0)\|_{H^2}^2 + \|g(0)\|_{H^2}^2\right), \tag{67}$$

that is,

$$\|w_1(t) - w_2(t)\|_{V_2} \le \exp(2C_0t)\|w_{10} - w_{20}\|_{V_2}. \tag{68}$$

Meanwhile, it indicates that the Lipschitz constant $l(t) \le \exp(2C_0t)$. This completes the proof.

Now, we intend to show the squeezing property for semigroup $S(t)$. To this end, we introduce the operator $A = -(\partial/\partial x^2)$ from $D(A)$ to H with domain

$$D(A) = \left\{u \in H^2(\Omega)\right\}. \tag{69}$$

Obviously, A is an unbounded self-adjoint positive operator and the inverse A^{-1} is compact. Thus, there exists an orthonormal basis $\{w_i\}_{i=1}^\infty$ $i = 1$ of H consisting of eigenvectors of A such that

$$\begin{gathered}Aw_i = \lambda_iw_i, \\ 0 \le \lambda_1 < \lambda_1 \cdots \lambda_i < \cdots \longrightarrow +\infty, \quad \text{when } i \longrightarrow \infty.\end{gathered} \tag{70}$$

For all N denote by $P = P_n : H \rightarrow \operatorname{span}\{w_1, w_2, \ldots, w_n\}$ the projector $Q = Q_N = I - P_N$. In the following, we will use

$$\begin{gathered}\left\|A^{(1/2)}u\right\| = \left\|\frac{\partial u}{\partial x}\right\|, \\ \left\|A^{(1/2)}u\right\| \ge \lambda_{N+1}^{(1/2)}, \quad u \in Q_NH, \\ \|Q_Nu\| \le \|u\|, \quad u \in H, \\ \|AQ_Nu\| = \|Q_NAu\| \le \|Au\|, \quad u \in D(A).\end{gathered} \tag{71}$$

Decompose h, g as

$$h = Ph + Qh, \qquad g = Pg + Qg. \tag{72}$$

Applying Q to (32) and (33) we find that

$$iQh_t + \gamma_2\Delta Qh + i\gamma h + Qf(u_1, u_2) + Qg = 0, \tag{73}$$

$$iQg_t + \gamma_2\Delta Qg + (i\Gamma - \chi)Qg + Qh = 0. \tag{74}$$

Take the inner product of (73) with $\overline{Qh}$ and (74) with $\overline{Qg}$, respectively. Then like Step 1, we can get

$$\begin{aligned}\frac{1}{2}\frac{d}{dt}\left(\|Qh\|^2 + \|Qg\|^2\right) + \gamma\|Qh\|^2 + \Gamma\|Qg\|^2 & \\ + \sigma_2\int_\Omega Q\phi_2(u_1)|Qh|^2dx & \\ \le C\|Qh\|^2 + \|Qg\|^2. &\end{aligned} \tag{75}$$

Take the inner product of (73) with $-\overline{Qh_{xx}}$ and (74) with $-\overline{Qg_{xx}}$, respectively. Then like Step 2, we can get

$$\begin{aligned}\frac{1}{2}\frac{d}{dt}\left(\|Qh_x\|^2 + \|Qg_x\|^2\right) + \gamma\|Qh_x\|^2 + \Gamma\|Qg_x\|^2 & \\ + \sigma_2\int_\Omega Q\phi_2(u_1)|Qh_x|^2dx & \\ \le C\|Qh_x\|^2 + \|Qg_x\|^2 + c\|Qh\|^2. &\end{aligned} \tag{76}$$

Take the inner product of (73) with $\overline{Qh_{xxxx}}$ and (74) with $\overline{Qg_{xxxx}}$, respectively. Then like Step 3, we can get

$$\begin{aligned}\frac{1}{2}\frac{d}{dt}\left(\left\|Qh_{xx}\right\|^2+\left\|Qg_{xx}\right\|^2\right)+\gamma\left\|Qh_{xx}\right\|^2+\Gamma\left\|Qg_{xx}\right\|^2 \\ +\sigma_2\int_\Omega Q\phi_2\left(u_1\right)\left|Qh_{xx}\right|^2dx \\ \leq C\|Qh\|_{H^2}^2+\left\|Qg_{xx}\right\|^2.\end{aligned}\tag{77}$$

Combining (75), (76), and (77), we get

$$\begin{aligned}\frac{1}{2}\frac{d}{dt}\left(\|Qh\|_{H^2}^2+\|Qg\|_{H^2}^2\right)+\mu\left(\|Qh\|_{H^2}^2+\|Qg\|_{H^2}^2\right) \\ \leq C_0\left(\|Qh\|_{H^2}^2+\|Qg\|_{H^2}^2\right).\end{aligned}\tag{78}$$

Using the G-N inequality

$$\left\|u_x\right\|^2\leq\|u\|\left\|u_{xx}\right\|\leq\frac{1}{2}\left(\|u\|^2+\left\|u_{xx}\right\|^2\right),\tag{79}$$

from (78), we have

$$\begin{aligned}&\frac{1}{2}\frac{d}{dt}\left(\|Qh\|_{H^2}^2+\|Qg\|_{H^2}^2\right)+\mu\left(\|Qh\|_{H^2}^2+\|Qg\|_{H^2}^2\right)\\ &\leq\frac{3C_0}{2}\left(\|Qh\|+\left\|Qh_{xx}\right\|+\|Qg\|+\left\|Qg_{xx}\right\|\right)\\ &\leq\frac{3C_0}{2}\lambda_{N+1}^{-1}\left(\left\|Qh_{xx}\right\|+\left\|Qg_{xx}\right\|\right)\\ &\leq\frac{3C_0}{2}\lambda_{N+1}^{-1}\left(\|Qh\|_{H^2}^2+\|Qg\|_{H^2}^2\right)\\ &\leq\frac{3C_0}{2}\lambda_{N+1}^{-1}\exp\left(2C_0t\right)\left(\|h(0)\|_{H^2}^2+\|g(0)\|_{H^2}^2\right).\end{aligned}\tag{80}$$

By Gronwall lemma we get

$$\begin{aligned}&\|Qh\|_{H^2}^2+\|Qg\|_{H^2}^2\\ &\leq\left(\|h(0)\|_{H^2}^2+\|g(0)\|_{H^2}^2\right)\exp(-2\mu t)\\ &\quad+\overline{C}\lambda_{N+1}^{-1}\exp\left(2C_0t\right)\left(\|h(0)\|_{H^2}^2+\|g(0)\|_{H^2}^2\right)\\ &\leq\left[\exp(-2\mu t)+\overline{C}\lambda_{N+1}^{-1}\exp\left(2C_0t\right)\right]\\ &\quad\times\left(\|h(0)\|_{H^2}^2+\|g(0)\|_{H^2}^2\right).\end{aligned}\tag{81}$$

Letting $t_*>0$ be fixed we take $w(t)=w_1(t)-w_2(t)=(h(t),g(t))$ and assume that

$$\exp\left(-2\mu t_*\right)\leq\frac{1}{256}.\tag{82}$$

Then we choose N large enough so that

$$\overline{C}\lambda_{N+1}^{-1}\exp\left(2C_0t\right)\leq\frac{1}{256},\tag{83}$$

that is,

$$\lambda_{N+1}\geq256\overline{C}\exp\left(2C_0t\right).\tag{84}$$

From (82) and (84), we obtain

$$\|Qh\|_{H^2}^2+\|Qg\|_{H^2}^2\leq\frac{1}{128}\left(\|h(0)\|_{H^2}^2+\|g(0)\|_{H^2}^2\right).\tag{85}$$

This shows that when $t_*>0$ is fixed, Lipschitz constant for $S(t)$ in B is equal to $\exp(2C_0t_*)$ and N satisfies

$$\lambda_{N+1}\geq256\overline{C}\exp\left(2C_0t_*\right).\tag{86}$$

We have

$$\|Qw\|_{V_2}\leq\|Qw(0)\|_{V_2}.\tag{87}$$

So when

$$\begin{aligned}\left\|Qw\left(t_*\right)\right\|_{V_2}&>\left\|Pw\left(t_*\right)\right\|_{V_2},\\ \left\|w\left(t_*\right)\right\|_{V_2}&=\left\|Qw\left(t_*\right)\right\|_{V_2}+\left\|Pw\left(t_*\right)\right\|_{V_2}\\ &<2\left\|Qw\left(t_*\right)\right\|_{V_2}\leq\frac{1}{64}\|Qw(0)\|_{V_2}\\ &\leq\frac{1}{64}\|w(0)\|_{V_2}.\end{aligned}\tag{88}$$

This completes the proof of Theorem 4. □

Theorem 11. *The semigroup $S(t)$ associated with problem* (1)-(2) *is squeezing in B. Now we conclude this section by giving our main result.*

Theorem 12. *Suppose that problem* (1)-(2) *satisfies Theorem 9; there exist $t_*\geq(1/2\mu)\ln(256)$ and N large enough such that*

$$\lambda_{N+1}\geq256\overline{C}\exp\left(2C_0t_*\right).\tag{89}$$

Then for the nonlinear semigroup $S(t)$ defined in (4) *and* (5), *$S(t)_{t\leq0}$; B admits an exponential attractor M in V_2 and*

$$\begin{aligned}d_F(M)&\leq1+CN_0,\\ \operatorname{dist}_{V_2}(S(t)B,M)&\leq C_0\exp\left(-C_1t\right),\end{aligned}\tag{90}$$

where C_0, C_1, C are constants independent of the solution of the equation.

4. Conclusions

In this paper, we have studied the coupled Ginzburg-Landau equations which describe Bose-Einstein condensates and nonlinear optical waveguides and cavities with periodic initial boundary; the existence of the exponential attractors is obtained by showing Lipschitz continuity and the squeezing property. For exponential attractor, N is only large enough such that

$$\lambda_{N+1}\geq256\overline{C}\exp\left(2C_0t_*\right).\tag{91}$$

Acknowledgment

This work was supported by Chinese Natural Science Foundation Grant no. 11061028.

References

[1] I. S. Aranson and L. Kramer, "The world of the complex Ginzburg-Landau equation.," *Reviews of Modern Physics*, vol. 74, no. 1, pp. 99–143, 2002.

[2] B. A. Malomed, "Complex Ginzburg-Landau equation," in *Encyclopedia of Nonlinear Science*, A. Scott, Ed., pp. 157–160, Routledge, New York, NY, USA, 2005.

[3] A. Eden, C. Foias, B. Nicolaenko, and K. Temam, *Exponential Attractors for Dissipative Evolution Equations*, vol. 37, John Wiley, New York, NY, USA, 1994.

[4] Z. Dai and B. Guo, "Inertial fractal sets for dissipative Zakharov system," *Acta Mathematicae Applicatae Sinica*, vol. 13, no. 3, pp. 279–288, 1997.

[5] Z. Dai and B. Guo, *Inertial ManiFolds and Approximate Inertial Mani-Folds*, Science Press, Beijing, China, 2000.

[6] Z. Dai, Y. Huang, and X. Sun, "Long-time behavior of solution for coupled Ginzburg-Landau equations describing Bose-Einstein condensates and nonlinear optical waveguides and cavities," *Journal of Mathematical Analysis and Applications*, vol. 362, no. 1, pp. 125–139, 2010.

[7] H. Sakaguchi and B. A. Malomed, "Stable solitons in coupled Ginzburg-Landau equations describing Bose-Einstein condensates and nonlinear optical waveguides and cavities," *Physica D*, vol. 183, no. 3-4, pp. 282–292, 2003.

Hindawi Publishing Corporation
Abstract and Applied Analysis
Volume 2013, Article ID 487810, 10 pages
http://dx.doi.org/10.1155/2013/487810

Research Article

Allee-Effect-Induced Instability in a Reaction-Diffusion Predator-Prey Model

Weiming Wang,[1] Yongli Cai,[2] Yanuo Zhu,[1] and Zhengguang Guo[1]

[1] *College of Mathematics and Information Science, Wenzhou University, Wenzhou 325035, China*
[2] *School of Mathematics and Computational Science, Sun Yat-Sen University, Guangzhou 510275, China*

Correspondence should be addressed to Weiming Wang; weimingwang2003@163.com

Received 25 December 2012; Revised 28 February 2013; Accepted 9 March 2013

Academic Editor: Lan Xu

We investigate the spatiotemporal dynamics induced by Allee effect in a reaction-diffusion predator-prey model. In the case without Allee effect, there is nonexistence of diffusion-driven instability for the model. And in the case with Allee effect, the positive equilibrium may be unstable under certain conditions. This instability is induced by Allee effect and diffusion together. Furthermore, via numerical simulations, the model dynamics exhibits both Allee effect and diffusion controlled pattern formation growth to holes, stripes-holes mixture, stripes, stripes-spots mixture, and spots replication, which shows that the dynamics of the model with Allee effect is not simple, but rich and complex.

1. Introduction

In 1952, Turing published one paper [1] on the subject called "pattern formation"—one of the central issues in ecology [2], putting forth the Turing hypothesis of diffusion-driven instability. Pattern formation in mathematics refers to the process that, by changing a bifurcation parameter, the spatially homogeneous steady states lose stability to spatially inhomogeneous perturbations, and stable inhomogeneous solutions arise [3]. Turing's revolutionary idea was that passive diffusion could interact with the chemical reaction in such a way that even if the reaction by itself has no symmetry-breaking capabilities, diffusion can destabilize the symmetry, so that the system with diffusion can have them [4]. From then on, pattern formation has become a very active area of research, motivated in part by the realization that there are many common aspects of patterns formed by diverse physical, chemical, and biological systems and by cellular automata and reaction-diffusion equations [5–7]. And the appearance and evolution of these patterns have been a focus of recent research activity across several disciplines [8–15].

Segel and Jackson [16] were the first to call attention to the Turing's ideas that would be also applicable in population dynamics. At the same time, Gierer and Meinhardt [17] gave a biologically justified formulation of a Turing model and studied its properties by employing numerical simulation. Levin and Segel [18, 19] suggested this scenario of spatial pattern formation as a possible origin of planktonic patchiness.

The understanding of patterns and mechanisms of spatial dispersal of interacting species is an issue of significant current interest in conservation biology, ecology, and biochemical reactions [20–22]. The spatial component of ecological interaction has been identified as an important factor in how ecological communities are shaped. Empirical evidence suggests that the spatial scale and structure of environment can influence population interactions [23]. A significant amount of work has been done by using this idea in the field of mathematical biology by Murray [20], Okubo and Levin [21], Cantrell and Cosner [23], and others [3, 24–27].

In general, assume that the species prey and predator move randomly on spatial domain, and the spatial movement of the individuals is modeled by diffusion with diffusion coefficients $d_1 > 0$, $d_2 > 0$ for the prey u and predator v, respectively. As an example, a prototypical predator-prey interaction model with logistic growth rate of the prey in the absence of predation is of the following form [28, 29]:

$$\frac{\mathrm{d}u}{\mathrm{d}t} = u(\alpha - \beta u) - f(u)g(v) + d_1 \Delta u,$$
$$\frac{\mathrm{d}v}{\mathrm{d}t} = \sigma f(u)g(v) - z(v) + d_2 \Delta v, \tag{1}$$

where $u(t)$ and $v(t)$ are the densities of the prey and predator at time $t > 0$, respectively. And $\Delta = \partial^2/\partial x^2 + \partial^2/\partial y^2$ is the Laplacian operator in two-dimensional space.

In recent years, many studies, for example, [30–40] and the references therein, show that the reaction-diffusion predator-prey model (e.g., model (1)) is an appropriate tool for investigating the fundamental mechanism of complex spatiotemporal predation dynamics. Of them, Alonso et al. [30] studied how diffusion affects the stability of predator-prey coexistence equilibria and show a new difference between ratio- and prey-dependent models; that is, the prey-dependent models cannot give rise to spatial structures through diffusion-driven instabilities; however, predator-dependent models with the same degree of complexity can. Baurmann et al. [31] investigated the emergence of spatiotemporal patterns in a generalized predator-prey system, derived the conditions for Hopf and Turing instabilities without specifying the predator-prey functional responses discussed their biological implications, identified the codimension-2 Turing-Hopf bifurcation and the codimension-3 Turing-Takens-Bogdanov bifurcation, and found that these bifurcations give rise to complex pattern formation processes in their neighborhood. And Banerjee and Petrovskii [36] studied possible scenarios of pattern formation in a ratio-dependent predator-prey system and found that the emerging patterns are stationary in the large time limit and exhibit only an insignificant spatial irregularity, and spatiotemporal chaos can indeed be observed but only for parameters well inside the Turing-Hopf parameter domain, away from the bifurcation point. Rodrigues et al. [40] paid their attentions to system properties in a vicinity of the Turing-Hopf bifurcation of the predator-prey and found that the asymptotical stationary pattern arises as a sudden transition between two different patterns.

On the other hand, in the research of population dynamics, Allee effect in the population growth has been studied extensively. Allee effect, named after ecologist Allee [41], is a phenomenon in biology characterized by a positive correlation between population size or density and the mean individual fitness (often times measured as per capita population growth rate) of a population or species [42] and may occur under several mechanisms, such as difficulties in finding mates when population density is low, social dysfunction at small population sizes, and increased predation risk due to failing flocking or schooling behavior [43–45]. In an ecological point of view, Allee effect has been modeled into strong and weak cases. The strong Allee effect introduces a population threshold, and the population must surpass this threshold to grow. In contrast, a population with a weak Allee effect does not have a threshold. It has been attracting much more attention recently owing to its strong potential impact on the population dynamics of many plants and animal species [46]. Detailed investigations relating to Allee effect may be found in [47–59].

In most predation models, it has been considered that Allee effect influences only the prey population. For instance, in model (1), corresponding to the function of prey growth rate of the prey $u(\alpha - \beta u)$, to express Allee effect, the most usual continuous growth of the equation that is given as:

$$G(u) = u\left(\alpha - \beta u - \frac{q}{u+b}\right), \tag{2}$$

is called additive Allee effect, which was first deduced in [43] and applied in [60–62]. Here, $qu/(u+b)$ is the term of additive Allee effect and $b \in (0,1)$ and $q \in (0,1)$ are Allee-effect constants. If $q < b\alpha$, then $G(0) = 0$, $G'(0) > 0$, and $G(u)$ is called weak Allee effect; if $q > b\alpha$, then $G(0) = 0$, $G'(0) < 0$, and $G(u)$ is strong Allee effect.

Corresponding to model (1), a prototypical predator-prey interaction model with Allee effect on the prey is given by

$$\frac{\mathrm{d}u}{\mathrm{d}t} = u\left(\alpha - \beta u - \frac{q}{u+b}\right) - f(u)g(v) + d_1 \Delta u,$$
$$\frac{\mathrm{d}v}{\mathrm{d}t} = \sigma f(u)g(v) - z(v) + d_2 \Delta v. \tag{3}$$

According to Turing's idea [1], for model (1)—the special case of model (3) without Allee effect (i.e., $q = 0$)—if the positive equilibrium point $E^* = (u^*, v^*)$ is stable in the case $d_1 = d_2 = 0$ (the nonspatial model) but unstable with respect to solutions in the cases $d_1 > 0$ and $d_2 > 0$ (the spatial model), then E^* is called diffusion-driven instability (i.e., Turing instability or Turing bifurcation), and model (1) may exhibit Turing pattern formation. In contrast, if $E^* = (u^*, v^*)$ is stable in the cases $d_1 > 0$ and $d_2 > 0$, then there is nonexistence of diffusion-driven instability for model (1), and the model cannot exhibit any pattern formation. And in this situation, for model (3), with Allee effect on the prey, there comes a question: is there any instability of the positive equilibrium occurring? Or, is there any diffusion-driven instability of the positive equilibrium occurring? In addition, does model (3) exhibit any pattern formation controlled by Allee effect?

The goal of this paper is to make an insight into the instability induced by the Allee effect in model (3). Our main interest is to check whether the Allee effect is a plausible mechanism of developing spatiotemporal pattern in the model.

The paper is organized as follows. In the next section, we give the model and stability of the equilibria. In Section 3, we discuss the stability/instability of the spatial model with/without Allee effect, derive the conditions for the occurrence of Allee-diffusion-driven instability of the case with Allee effect, and illustrate typical Turing patterns via numerical simulations. Finally, conclusions and remarks are presented in Section 4.

2. The Model System

In model (1), the product $f(u)g(v)$ gives the rate at which prey is consumed. The prey consumed per predator, $f(u)g(v)/v$, was termed as the functional response by Solomon [63]. These functions can be defined in different ways. In this paper, following Lotka [64], we adopt

$$f(u) = cu, \tag{4}$$

which is a linear functional response without saturation, where $c > 0$ denotes the capture rate [65]. And following Harrison [28, 29], we set

$$g(v) = \frac{v}{mv+1}, \tag{5}$$

where $m > 0$ represents a reduction in the predation rate at high predator densities due to mutual interference among the predators while searching for food.

The proportionality constant σ is the rate of prey consumption. And the function $z(v)$ is given by

$$z(v) = \gamma v + l v^2, \quad \gamma > 0,\ l \geq 0, \tag{6}$$

where γ denotes the natural death rate of the predator, and $l > 0$ can be used to model predator intraspecific competition that is not the direct competition for food, such as some type of territoriality [28]. In this paper, we will discuss the case $l = 0$, which is used in a much more traditional case.

Based on the previous discussions, we can establish the following predation model of two partial differential equations with additive Allee effect on prey:

$$\begin{aligned}\frac{\partial u}{\partial t} &= u\left(\alpha - \beta u - \frac{q}{u+b}\right) - \frac{cuv}{mv+1} + d_1\Delta u,\\ \frac{\partial v}{\partial t} &= v\left(-\gamma + \frac{su}{mv+1}\right) + d_2\Delta v,\end{aligned} \tag{7}$$

with the positive initial conditions:

$$\begin{gathered} u(x,y,0) > 0, \qquad v(x,y,0) > 0,\\ (x,y)\in\Omega = (0,L)\times(0,L),\end{gathered} \tag{8}$$

and the zero-flux boundary conditions:

$$\frac{\partial u}{\partial \boldsymbol{v}} = \frac{\partial v}{\partial \boldsymbol{v}} = 0, \quad (x,y)\in\partial\Omega, \tag{9}$$

where s denotes conversion rate, and Ω is a bounded open domain in $\mathbb{R}_+^2$ with boundary $\partial\Omega$. $\boldsymbol{v}$ is the outward unit normal vector on $\partial\Omega$, and zero-flux conditions reflect the situation where the population cannot move across the boundary of the domain.

The main purpose of this paper is to focus on the impacts of diffusion or/and Allee effect on the model system about the positive equilibrium, especially for the instability and pattern formation.

3. Stability Analysis

3.1. The Case without Allee Effect. We first consider the stability of the positive equilibria of model (7) without Allee effect; that is, $q = 0$, and the model is given by

$$\begin{aligned}\frac{\partial u}{\partial t} &= u(\alpha - \beta u) - \frac{cuv}{mv+1} + d_1\Delta u,\\ \frac{\partial v}{\partial t} &= v\left(-\gamma + \frac{su}{mv+1}\right) + d_2\Delta v.\end{aligned} \tag{10}$$

Easy to know that model (10) has a unique positive equilibrium $E^* = (u^*, v^*)$ with $s\alpha > \beta\gamma$, where

$$\begin{aligned} u^* &= \frac{ms\alpha - cs + \sqrt{s^2(m\alpha - c)^2 + 4cms\beta\gamma}}{2ms\beta},\\ v^* &= \frac{su^* - \gamma}{m\gamma},\end{aligned} \tag{11}$$

which is locally asymptotically stable. Next, we will discuss the effect of diffusion on E^*.

Set $U_1 = u - u^*$, $V_1 = v - v^*$, and the linearized system (10) around $E^* = (u^*, v^*)$ is as follows:

$$\begin{aligned}\frac{\partial U_1}{\partial t} &= d_1\Delta U_1 - \beta u^* U_1 - \frac{cu^*}{(mv^*+1)^2}U_2,\\ \frac{\partial U_2}{\partial t} &= d_2\Delta U_2 + \frac{sv^*}{mv^*+1}U_1 - \frac{msu^*v^*}{(mv^*+1)^2}U_2,\\ &\left.\frac{\partial U_1}{\partial v}\right|_{\partial\Omega} = \left.\frac{\partial U_2}{\partial v}\right|_{\partial\Omega} = 0.\end{aligned} \tag{12}$$

Following Malchow et al. [66], we know that any solution of system (12) can be expanded into a Fourier series as follows:

$$\begin{aligned} U_1(\mathbf{r},t) &= \sum_{n,m=0}^{\infty} u_{nm}(\mathbf{r},t) = \sum_{n,m=0}^{\infty} \alpha_{nm}(t)\sin \mathbf{kr},\\ U_2(\mathbf{r},t) &= \sum_{n,m=0}^{\infty} v_{nm}(\mathbf{r},t) = \sum_{n,m=0}^{\infty} \beta_{nm}(t)\sin \mathbf{kr},\end{aligned} \tag{13}$$

where $\mathbf{r} = (x,y)$ and $0 < x < L$, $0 < y < L$. $\mathbf{k} = (k_n, k_m)$ and $k_n = n\pi/L$, $k_m = m\pi/L$ are the corresponding wavenumbers.

Having substituted u_{nm} and v_{nm} into (12), we obtain

$$\begin{aligned}\frac{d\alpha_{nm}}{dt} &= \left(-\beta u^* - d_1k^2\right)\alpha_{nm} + -\frac{cu^*}{(mv^*+1)^2}\beta_{nm},\\ \frac{d\beta_{nm}}{dt} &= \frac{sv^*}{mv^*+1}\alpha_{nm} + \left(-\frac{msu^*v^*}{(mv^*+1)^2} - d_2k^2\right)\beta_{nm},\end{aligned} \tag{14}$$

where $k^2 = k_n^2 + k_m^2$.

A general solution of (14) has the form $C_1\exp(\lambda_1 t) + C_2\exp(\lambda_2 t)$, where the constants C_1 and C_2 are determined by the initial conditions (8) and the exponents λ_1, λ_2 are the eigenvalues of the following matrix:

$$J_{E^*} = \begin{pmatrix} -\beta u^* - d_1 k^2 & -\dfrac{cu^*}{(mv^*+1)^2} \\ \dfrac{sv^*}{mv^*+1} & -\dfrac{msu^*v^*}{(mv^*+1)^2} - d_2 k^2 \end{pmatrix}. \tag{15}$$

Correspondingly, λ_i $(i = 1, 2)$ arises as the solution of following equation:

$$\lambda_i^2 - \operatorname{tr}(J_{E^*})\lambda_i + \det(J_{E^*}) = 0, \tag{16}$$

where the trace and determinant of J_{E^*} are, respectively,

$$\begin{aligned} \operatorname{tr}(J_{E^*}) &= -(d_1 + d_2)k^2 - \beta u^* - \frac{msu^*v^*}{(mv^*+1)^2}, \\ \det(J_{E^*}) &= d_1 d_2 k^4 + \left(d_2 \beta u^* + \frac{d_1 msu^*v^*}{(mv^*+1)^2}\right)k^2 \\ &\quad + \frac{bm\beta u^{*2}v^*}{(mv^*+1)^2} + \frac{bcu^*v^*}{(mv^*+1)^3}. \end{aligned} \tag{17}$$

It is easy to know that $\operatorname{tr}(J_{E^*}) < 0$ and $\det(J_{E^*}) > 0$. Hence, the positive equilibrium E^* of model (10) is uniformly asymptotically stable.

Obviously, there is no effect on the stability of the positive equilibrium whether model (10) with diffusion or not. That is to say, there is nonexistence of diffusion-driven instability in model (10), which is the special case of model (7) without Allee effect.

3.2. The Case with Allee Effect

3.2.1. Allee-Diffusion-Driven Instability. In this subsection, we restrict ourselves to the stability analysis of spatial model (7), which is in the presence of Allee effect on prey.

For the sake of learning the effect of Allee effect on the positive equilibrium of model (7), we first give a definition called Allee-diffusion-driven instability as follows.

Definition 1. If a positive equilibrium is uniformly asymptotically stable in the reaction-diffusion model without Allee-effect (e.g., model (10)) but unstable with respect to solutions of the reaction-diffusion model with Allee effect (e.g., model (7)), then this instability is called Allee-diffusion-driven instability.

Next, we will only investigate the stability of the positive equilibrium of model (7). For simplicity, we take the weak Allee effect case $(0 < q < b\alpha)$ as an example, and the unique positive equilibrium is named $E_w = (u_w, v_w) = (u_w, (su_w - \gamma)/m\gamma)$. We first give the stability of E_w in the case without diffusion as follows that is, $d_1 = d_2 = 0$ in model (7):

$$\begin{aligned} \frac{\mathrm{d}u}{\mathrm{d}t} &= u\left(\alpha - \beta u - \frac{q}{u+b}\right) - \frac{cuv}{mv+1} \triangleq f(u,v), \\ \frac{\mathrm{d}v}{\mathrm{d}t} &= v\left(-\gamma + \frac{su}{mv+1}\right) \triangleq g(u,v). \end{aligned} \tag{18}$$

The Jacobian matrix of (18) evaluated in the positive equilibrium E_w takes the form:

$$J_{E_w} = \begin{pmatrix} -\beta u_w + \dfrac{qu_w}{(u_w+b)^2} & -\dfrac{c\gamma^2}{s^2 u_w} \\ \dfrac{su_w - \gamma}{mu_w} & \dfrac{(\gamma - su_w)\gamma}{su_w} \end{pmatrix}. \tag{19}$$

Suppose that $(u_w + b)^2(c\gamma + ms\beta u_w^2) - mqsu_w^2 > 0$, and set

$$q^{[u_w]} = \left(\beta u_w - \frac{(\gamma - su_w)\gamma}{su_w}\right)\frac{(u_w+b)^2}{u_w}. \tag{20}$$

By some computational analysis, we obtain $\operatorname{tr}(J_{E_w}) < 0$, $\det(J_{E_w}) > 0$. Hence $E_w = (u_w, (su_w - \gamma)/m\gamma)$ is locally asymptotically stable.

And the Jacobian matrix of model (7) at $E_w = (u_w, v_w)$ is given by

$$\widetilde{J}_{E_w} = \begin{pmatrix} \left(-\beta + \dfrac{q}{(u_w+b)^2}\right)u_w - d_1 k^2 & -\dfrac{c\gamma^2}{s^2 u_w} \\ \dfrac{su_w - \gamma}{mu_w} & -\dfrac{\gamma(su_w - \gamma)}{su_w} - d_2 k^2 \end{pmatrix} \tag{21}$$

and the characteristic equation of $\widetilde{J}_{E_w}$ at E_w is

$$\lambda^2 - \operatorname{tr}(\widetilde{J}_{E_w})\lambda + \det(\widetilde{J}_{E_w}) = 0, \tag{22}$$

where

$$\begin{aligned} \operatorname{tr}(\widetilde{J}_{E_w}) &= \operatorname{tr}(J_{E_w}) - (d_1 + d_2)k^2, \\ \det(\widetilde{J}_{E_w}) &= \det(J_{E_w}) + d_1 d_2 k^4 \\ &\quad + \left(\frac{d_1\gamma(su_w - \gamma)}{su_w} + \left(\beta - \frac{q}{(u_w+b)^2}\right)d_2 u_w\right)k^2. \end{aligned} \tag{23}$$

And the instability sets in when at least $\operatorname{tr}(\widetilde{J}_{E_w}) > 0$ or $\det(\widetilde{J}_{E_w}) < 0$ is violated.

Since $\operatorname{tr}(J_{E_w}) < 0$,

$$\operatorname{tr}(\widetilde{J}_{E_w}) = \operatorname{tr}(J_{E_w}) - (d_1 + d_2)k^2 < 0 \tag{24}$$

is always true. Hence, only violation of $\det(\widetilde{J}_{E_w}) < 0$ gives rise to Allee-diffusion-driven instability, which leads to

$$\frac{d_1\gamma(su_w - \gamma)}{su_w} + \left(\beta - \frac{q}{(u_w+b)^2}\right)d_2 u_w \triangleq \Theta < 0, \tag{25}$$

otherwise, $\det(\widetilde{J}_{E_w}) > 0$ for all k if $\det(J_{E_w}) > 0$.

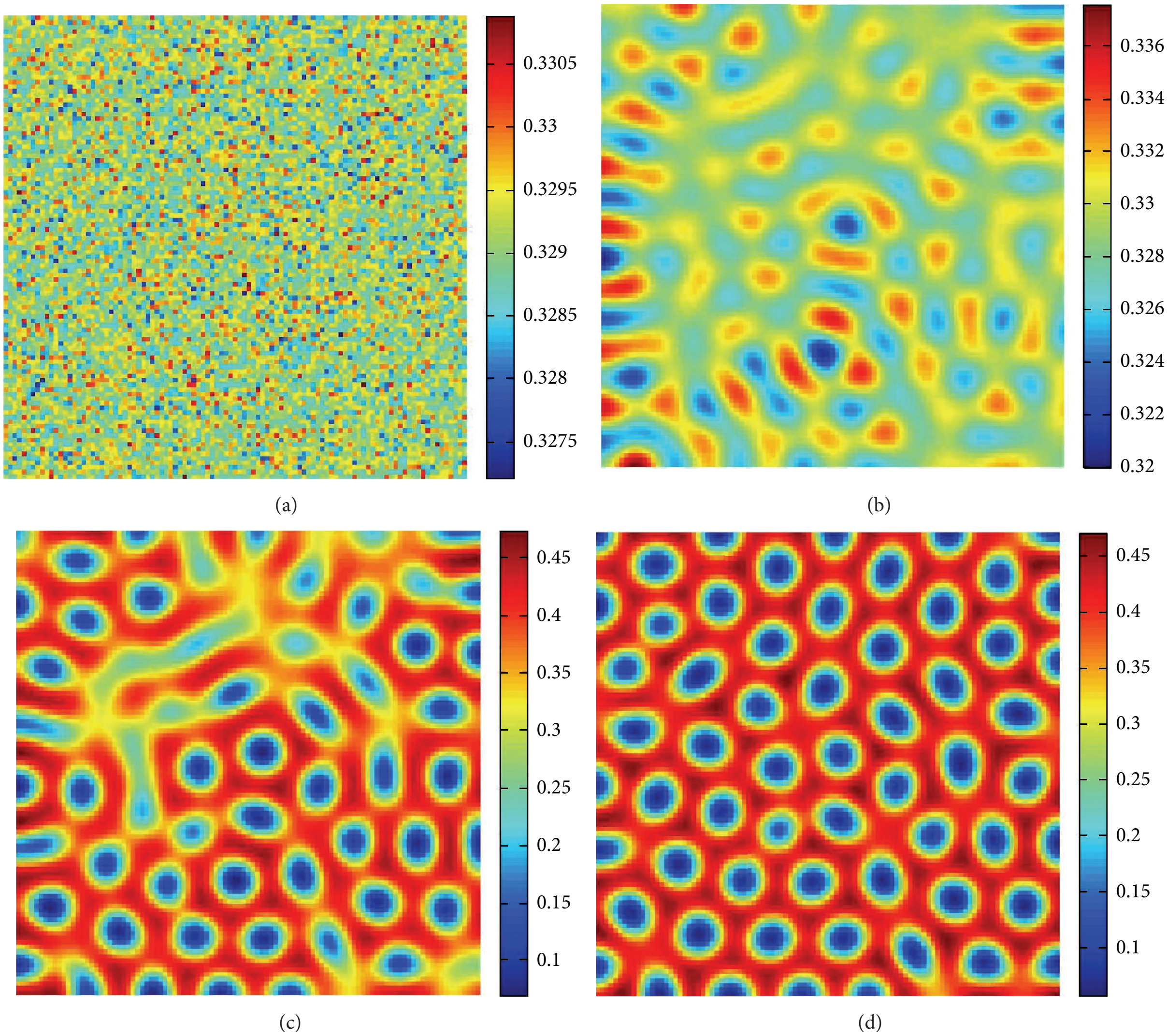

FIGURE 1: Typical Turing patterns of u in model (7) with parameters $\alpha = 1$, $\beta = 0.3$, $\gamma = 0.3$, $b = 0.5$, $c = 0.6$, $m = 0.6$, $q = 0.35$, $s = 1.75$, $d_1 = 0.015$, and $d_2 = 1$. Times: (a) 0; (b) 50; (c) 250; (d) 2500.

Notice that $\det(\widetilde{J}_{E_w})$ achieves its minimum

$$\min_k \det\left(\widetilde{J}_{E_w}\right) = \frac{4d_1d_2 \det\left(J_{E_w}\right) - \Theta^2}{4d_1d_2} \qquad (26)$$

at the critical value $k^{*2} > 0$ where

$$k^{*2} = -\frac{\Theta}{2d_1d_2}. \qquad (27)$$

And $\Theta < 0$ is equivalent to

$$\left(\frac{d_1\gamma\left(su_w - \gamma\right)}{d_2su_w^2} + \beta\right)\left(u_w + b\right)^2 < q < b\alpha, \qquad (28)$$

where $\min_k \det(\widetilde{J}_{E_w}) < 0$ is equivalent to $4d_1d_2 \det(J_{E_w}) - \Theta^2 < 0$, which is equivalent to

$$q > \left(u_w + b\right)^2\left(\beta + \frac{d_1\gamma\left(su_w - \gamma\right)}{d_2su_w^2} + \frac{2\sqrt{d_1d_2 \det\left(J_{E_w}\right)}}{d_2u_w}\right). \qquad (29)$$

And from $\det(\widetilde{J}_{E_w}) = 0$, we can determine k_1 and k_2 as

$$k_1^2 = \frac{-\Theta + \sqrt{\Theta^2 - 4d_1d_1 \det\left(J_{E_w}\right)}}{2d_1d_2},$$
$$k_2^2 = \frac{-\Theta - \sqrt{\Theta^2 - 4d_1d_1 \det\left(J_{E_w}\right)}}{2d_1d_2}. \qquad (30)$$

In conclusion, if $k_1^2 < k^2 < k_2^2$, then $\det(\widetilde{J}_{E_w}) < 0$, and the positive equilibrium E_w of model (7) is unstable. That's to say,

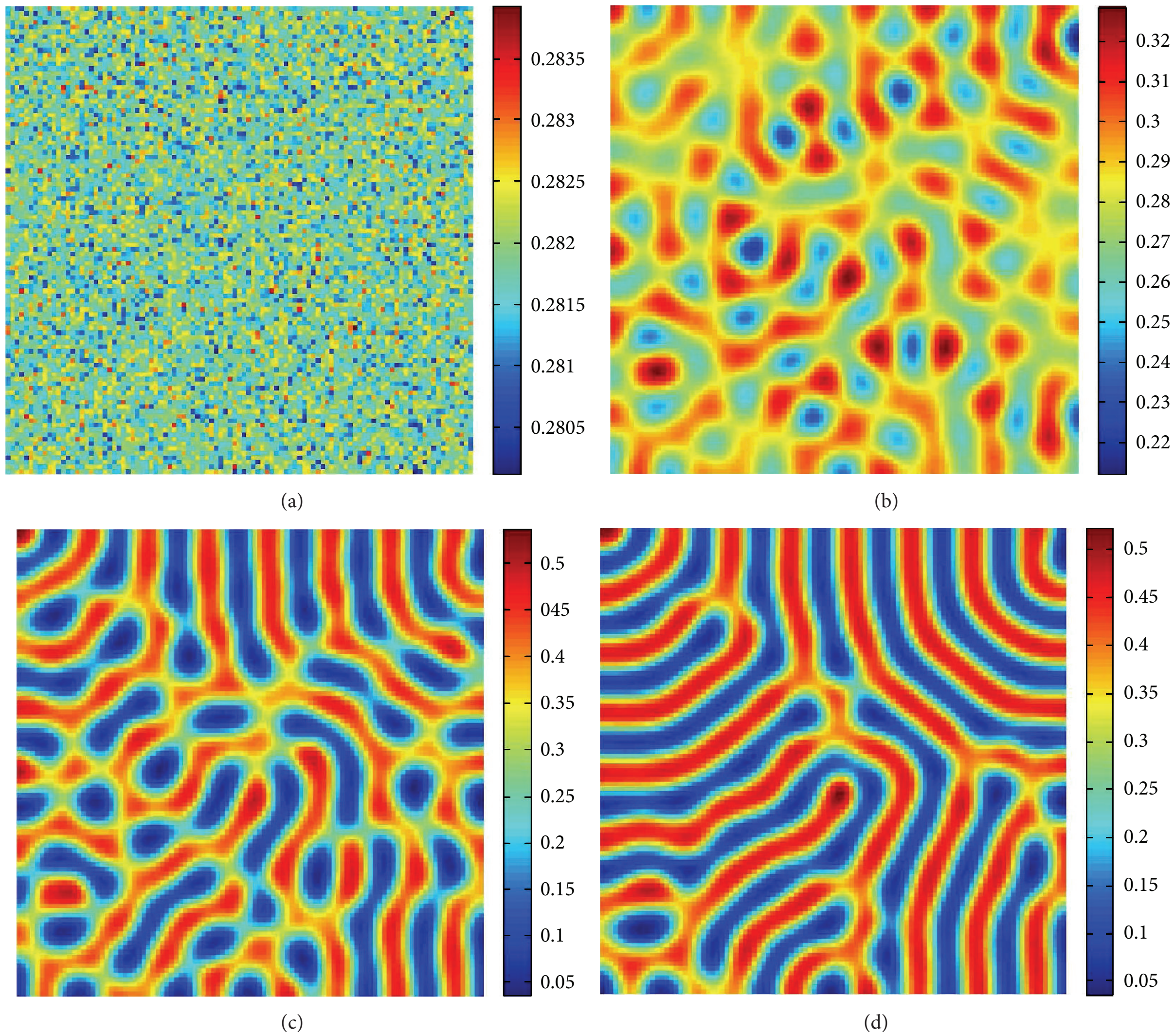

Figure 2: Typical Turing patterns of u in model (7) with parameters $\alpha = 1$, $\beta = 0.3$, $\gamma = 0.3$, $b = 0.5$, $c = 0.6$, $m = 0.6$, $q = 0.35$, $s = 2$, $d_1 = 0.015$, and $d_2 = 1$. Times: (a) 0; (b) 50; (c) 250; (d) 2500.

Allee-diffusion-driven instability occurs, and model (7) may exhibit Turing pattern formation.

3.2.2. Pattern Formation. In this subsection, in two-dimensional space, we perform extensive numerical simulations of the spatially extended model (7) in the case with weak Allee effect and show qualitative results. All of the numerical simulations employ the zero-flux boundary conditions (9) with a system size of 200×200. Other parameters are fixed as $\alpha = 1$, $\beta = 0.3$, $\gamma = 0.3$, $b = 0.5$, $c = 0.6$, $m = 0.6$, $q = 0.35$, $d_1 = 0.015$, and $d_2 = 1$.

The numerical integration of model (7) is performed by using an explicit Euler method for the time integration [67] with a time step size $\Delta t = 1/100$ and the standard five-point approximation [68] for the $2D$ Laplacian with the zero-flux boundary conditions. The initial conditions are always a small amplitude random perturbation around the positive constant steady state solution E_w. After the initial period during which the perturbation spreads, the model goes into either a time-dependent state or an essentially steady state solution (time-independent state).

In the numerical simulations, different types of dynamics can be observed, and it is found that the distributions of predator and prey are always of the same type. Consequently, we can restrict our analysis of pattern formation to one distribution. We only show the distribution of prey u as an instance.

In Figure 1, with $s = 1.75$, there is a pattern consisting of blue hexagons (minimum density of u) in a red (maximum density of u) background, that is, isolated zones with low population densities. We call this pattern as "holes."

When increasing s to $s = 2$, the model dynamics exhibits a transition from stripes-holes growth to stripes replication; that is, holes decay and the stripes pattern emerges (c.f., Figure 2).

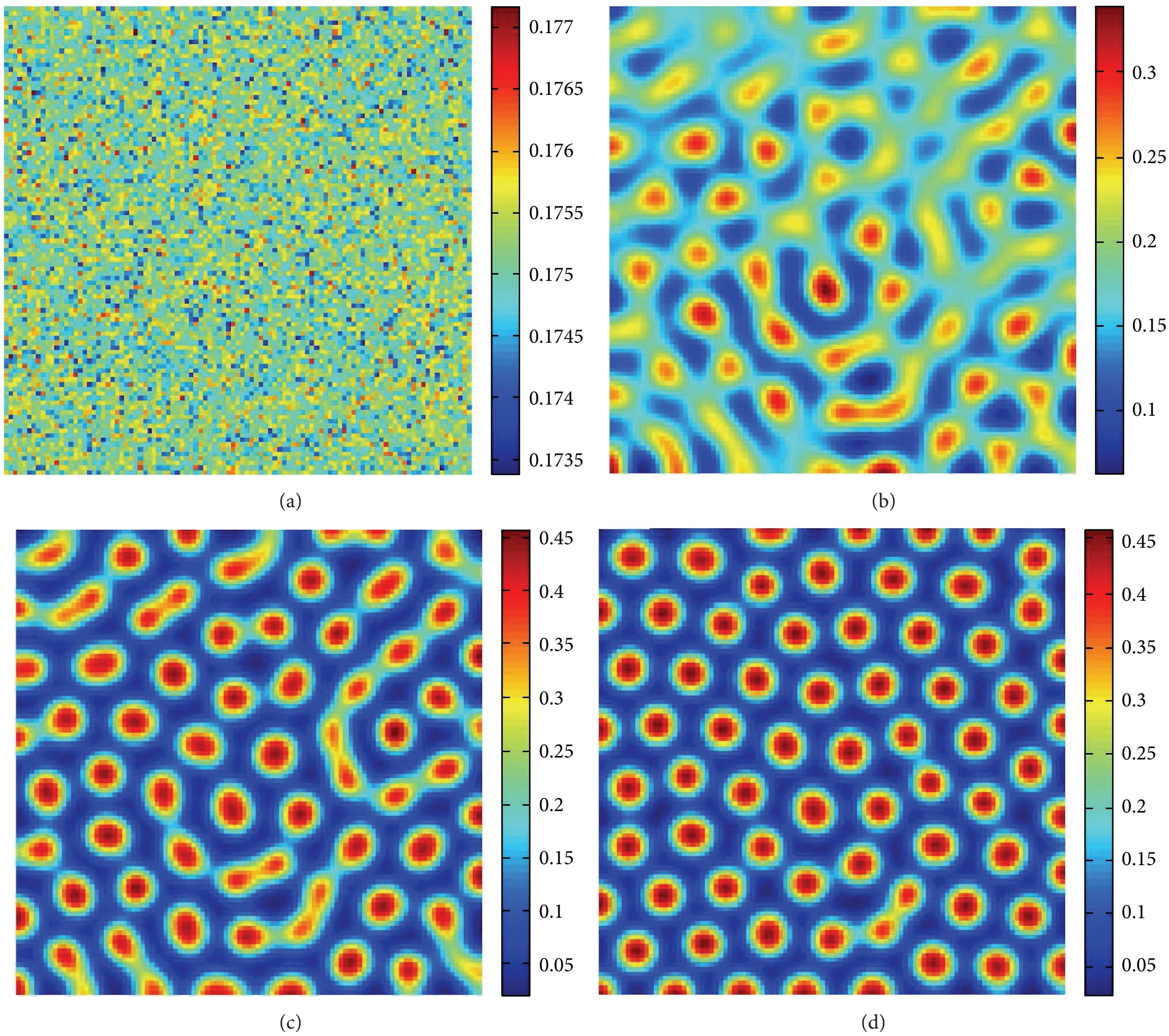

Figure 3: Typical Turing patterns of u in model (7) with parameters $\alpha = 1$, $\beta = 0.3$, $\gamma = 0.3$, $b = 0.5$, $c = 0.6$, $m = 0.6$, $q = 0.35$, $s = 3.0$, $d_1 = 0.015$, and $d_2 = 1$. Times: (a) 0; (b) 50; (c) 250; (d) 2500.

When s increasing to $s = 3.0$, the later random perturbations make these stripes decay, end with the time-independent regular spots (c.f., Figure 3), which is isolated zones with high prey densities.

In Figure 4, we show patterns of time-independent stripes-holes and stripes-spots mixture obtained with model (7). These two patterns are similar to each other. With $s = 1.9$ (c.f., Figure 4(a)), the stripes-holes mixture pattern is at relatively low prey densities, while $s = 2.45$ (c.f., Figure 4(b)), at high prey densities.

From Figures 1 to 4, one can see that, on increasing the control parameter s, the pattern sequence "holes → stripes-holes mixture → stripes → stripes-spots mixture → spots" is observed.

From the viewpoint of population dynamics, "spots" pattern (c.f., Figure 3) shows that the prey population is driven by predator to a very low level in those regions. The final result is the formation of patches of high prey density surrounded by areas of low prey densities [30]. That is to say, under the control of these parameters, the prey is predominant in the domain. In contrast, "holes" pattern (c.f., Figure 1) indicates that the predator is predominant in the domain.

4. Conclusions and Remarks

In summary, in this paper, we have investigated the spatiotemporal dynamics of a predator-prey model that involves Allee effect on prey analytically and numerically.

For model (7), in the case without Allee effect, there is no effect on the stability of the positive equilibrium whether with diffusion or not. That is to say, there is nonexistence of diffusion-driven instability in the model without Allee effect. More precisely, the distribution of species converge to a spatially homogeneous steady state which varies in time.

And in the case with Allee effect, the positive equilibrium may be unstable. This instability is induced by Allee effect and diffusion together, so we give a new definition called "Allee-diffusion-driven instability" and present the analysis of this

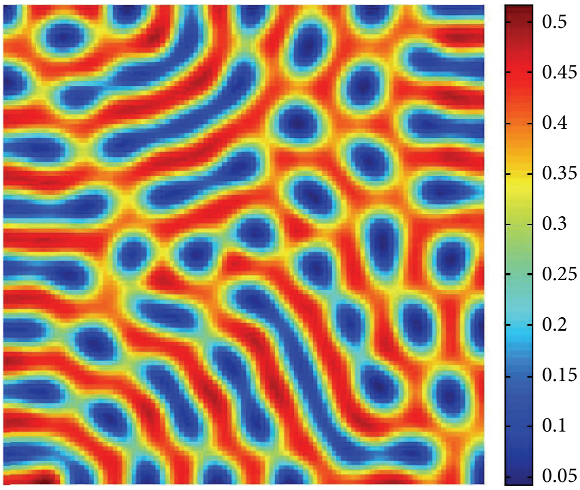

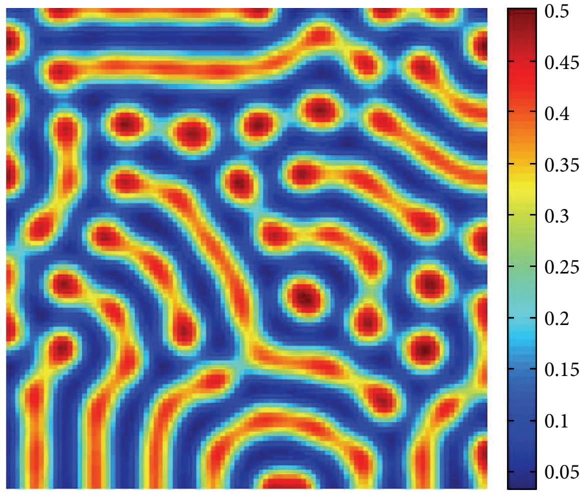

FIGURE 4: Typical Turing patterns of u in model (7) with parameters $\alpha = 1$, $\beta = 0.3$, $\gamma = 0.3$, $b = 0.5$, $c = 0.6$, $m = 0.6$, $q = 0.35$, $d_1 = 0.015$, and $d_2 = 1$. (a) $s = 1.9$; (b) $s = 2.45$.

instability of the model in details. To the best of our knowledge, this is the first reported case. Furthermore, via numerical simulations, it is found that the model dynamics exhibits both Allee effect and diffusion controlled pattern formation growth to holes, stripes-holes mixtures, stripes, stripes-spots mixtures, and spots replication. That is to say, the distribution of species is aggregation. This indicates that the pattern formation of the model with Allee effect is not simple, but rich and complex.

In fact, for a predator-prey system, Okubo and Levin [21] noted Allee effect on the functional response, and a density-dependent death rate of the predator is necessary to generate spatial patterns. And in this paper, we show that a predator-prey system with Allee effect on prey can generate complex Turing spatial patterns, which may be a supplementary to [21].

It is needed to note that, in this paper, we investigate the dynamics of localized patterns in model (7). Such patterns are characterized by a highly spatially heterogeneous solutions and are far from the spatially uniform state. These patterns occur in two-component systems when the ratio of the two diffusion coefficients are very large. In the numerical simulations, we take the diffusivity ratio as $1/0.015 \gg 1$, and so we are close to the regime of localized patterns. And the existence of these spatial patterns can be rigorously proved using tools from nonlinear functional analysis such as Liapunov-Schmidt reduction and fixed-point theorems [13, 14], this is desirable in future studies.

Acknowledgments

The authors would like to thank the anonymous referee for very helpful suggestions and comments which led to improvements of our original paper. This research was supported by Natural Science Foundation of Zhejiang Province (LY12A01014 and LQ12A01009) and the National Basic Research Program of China (2012 CB 426510).

References

[1] A. Turing, "The chemical basis of morphogenesis," *Philosophical Transactions of the Royal Society B*, vol. 237, pp. 37–72, 1952.

[2] S. Levin, "The problem of pattern and scale in ecology," *Ecology*, vol. 73, no. 6, pp. 1943–1967, 1992.

[3] Z. A. Wang and T. Hillen, "Classical solutions and pattern formation for a volume filling chemotaxis model," *Chaos*, vol. 17, no. 3, Article ID 037108, 2007.

[4] N. F. Britton, *Essential Mathematical Biology*, Springer, 2003.

[5] M. C. Cross and P. H. Hohenberg, "Pattern formation outside of equilibrium," *Reviews of Modern Physics*, vol. 65, no. 3, pp. 851–1112, 1993.

[6] K. J. Lee, W. D. McCormick, Q. Ouyang, and H. L. Swinney, "Pattern formation by interacting chemical fronts," *Science*, vol. 261, no. 5118, pp. 192–194, 1993.

[7] A. B. Medvinsky, S. V. Petrovskii, I. A. Tikhonova, H. Malchow, and B.-L. Li, "Spatiotemporal complexity of plankton and fish dynamics," *SIAM Review*, vol. 44, no. 3, pp. 311–370, 2002.

[8] W.-M. Ni and M. Tang, "Turing patterns in the Lengyel-Epstein system for the CIMA reaction," *Transactions of the American Mathematical Society*, vol. 357, no. 10, pp. 3953–3969, 2005.

[9] R. B. Hoyle, *Pattern Formation: An Introduction to Methods*, Cambridge University Press, Cambridge, UK, 2006.

[10] M. J. Ward and J. Wei, "The existence and stability of asymmetric spike patterns for the Schnakenberg model," *Studies in Applied Mathematics*, vol. 109, no. 3, pp. 229–264, 2002.

[11] M. J. Ward, "Asymptotic methods for reaction-diffusion systems: past and present," *Bulletin of Mathematical Biology*, vol. 68, no. 5, pp. 1151–1167, 2006.

[12] J. Wei, "Pattern formations in two-dimensional Gray-Scott model: existence of single-spot solutions and their stability," *Physica D*, vol. 148, no. 1-2, pp. 20–48, 2001.

[13] J. Wei and M. Winter, "Stationary multiple spots for reaction-diffusion systems," *Journal of Mathematical Biology*, vol. 57, no. 1, pp. 53–89, 2008.

[14] W. Chen and M. J. Ward, "The stability and dynamics of localized spot patterns in the two-dimensional Gray-Scott model,"

SIAM Journal on Applied Dynamical Systems, vol. 10, no. 2, pp. 582–666, 2011.

[15] R. McKay and T. Kolokolnikov, "Stability transitions and dynamics of mesa patterns near the shadow limit of reaction-diffusion systems in one space dimension," *Discrete and Continuous Dynamical Systems B*, vol. 17, no. 1, pp. 191–220, 2012.

[16] L Segel and J. Jackson, "Dissipative structure: an explanation and an ecological example," *Journal of Theoretical Biology*, vol. 37, no. 3, pp. 545–559, 1972.

[17] A. Gierer and H. Meinhardt, "A theory of biological pattern formation," *Biological Cybernetics*, vol. 12, no. 1, pp. 30–39, 1972.

[18] S. Levin and L. Segel, "Hypothesis for origin of planktonic patchiness," *Nature*, vol. 259, no. 5545, p. 659, 1976.

[19] S. A. Levin and L. A. Segel, "Pattern generation in space and aspect," *SIAM Review A*, vol. 27, no. 1, pp. 45–67, 1985.

[20] J. D. Murray, *Mathematical Biology*, Springer, 2003.

[21] A. Okubo and S. A. Levin, *Diffusion and Ecological Problems: Modern Perspectives*, Springer, New York, NY, USA, 2nd edition, 2001.

[22] C. Neuhauser, "Mathematical challenges in spatial ecology," *Notices of the American Mathematical Society*, vol. 48, no. 11, pp. 1304–1314, 2001.

[23] R. S. Cantrell and C. Cosner, *Spatial Ecology via Reaction-Diffusion Equations*, John Wiley & Sons, West Sussex, UK, 2003.

[24] T. K. Callahan and E. Knobloch, "Pattern formation in three-dimensional reaction-diffusion systems," *Physica D*, vol. 132, no. 3, pp. 339–362, 1999.

[25] A. Bhattacharyay, "Spirals and targets in reaction-diffusion systems," *Physical Review E*, vol. 64, no. 1, Article ID 016113, 2001.

[26] T. Leppänen, M. Karttunen, K. Kaski, and R. Barrio, "Dimensionality effects in Turing pattern formation," *International Journal of Modern Physics B*, vol. 17, no. 29, pp. 5541–5553, 2003.

[27] J. He, "Asymptotic methods for solitary solutions and compactons," *Abstract and Applied Analysis*, vol. 2012, Article ID 916793, 130 pages, 2012.

[28] G. W. Harrison, "Multiple stable equilibria in a predator-prey system," *Bulletin of Mathematical Biology*, vol. 48, no. 2, pp. 137–148, 1986.

[29] G. W. Harrison, "Comparing predator-prey models to Luckinbill's experiment with didinium and paramecium," *Ecology*, vol. 76, no. 2, pp. 357–374, 1995.

[30] D. Alonso, F. Bartumeus, and J. Catalan, "Mutual interference between predators can give rise to Turing spatial patterns," *Ecology*, vol. 83, no. 1, pp. 28–34, 2002.

[31] M. Baurmann, T. Gross, and U. Feudel, "Instabilities in spatially extended predator-prey systems: spatio-temporal patterns in the neighborhood of Turing-Hopf bifurcations," *Journal of Theoretical Biology*, vol. 245, no. 2, pp. 220–229, 2007.

[32] W. Wang, Q.-X. Liu, and Z. Jin, "Spatiotemporal complexity of a ratio-dependent predator-prey system," *Physical Review E*, vol. 75, no. 5, Article ID 051913, p. 9, 2007.

[33] W. Wang, L. Zhang, H. Wang, and Z. Li, "Pattern formation of a predator-prey system with Ivlev-type functional response," *Ecological Modelling*, vol. 221, no. 2, pp. 131–140, 2010.

[34] R. K. Upadhyay, W. Wang, and N. K. Thakur, "Spatiotemporal dynamics in a spatial plankton system," *Mathematical Modelling of Natural Phenomena*, vol. 5, no. 5, pp. 102–122, 2010.

[35] J. Wang, J. Shi, and J. Wei, "Dynamics and pattern formation in a diffusive predator-prey system with strong Allee effect in prey," *Journal of Differential Equations*, vol. 251, no. 4-5, pp. 1276–1304, 2011.

[36] M. Banerjee and S. Petrovskii, "Self-organised spatial patterns and chaos in a ratiodependent predator–prey system," *Theoretical Ecology*, vol. 4, no. 1, pp. 37–53, 2011.

[37] M. Banerjee, "Spatial pattern formation in ratio-dependent model: higher-order stability analysis," *Mathematical Medicine and Biology*, vol. 28, no. 2, pp. 111–128, 2011.

[38] M. Banerjee and S. Banerjee, "Turing instabilities and spatio-temporal chaos in ratio-dependent Holling-Tanner model," *Mathematical Biosciences*, vol. 236, no. 1, pp. 64–76, 2012.

[39] S. Fasani and S. Rinaldi, "Factors promoting or inhibiting Turing instability in spatially extended prey–predator systems," *Ecological Modelling*, vol. 222, no. 18, pp. 3449–3452, 2011.

[40] L. A. D. Rodrigues, D. C. Mistro, and S. Petrovskii, "Pattern formation, long-term transients, and the Turing-Hopf bifurcation in a space- and time-discrete predator-prey system," *Bulletin of Mathematical Biology*, vol. 73, no. 8, pp. 1812–1840, 2011.

[41] W. C. Allee, *Animal Aggregations: A Study in General Sociology*, AMS Press, 1978.

[42] F. Courchamp, J. Berec, and J. Gascoigne, *Allee Effects in Ecology and Conservation*, Oxford University Press, New York, NY, USA, 2008.

[43] B. Dennis, "Allee effects: population growth, critical density, and the chance of extinction," *Natural Resource Modeling*, vol. 3, no. 4, pp. 481–538, 1989.

[44] M. A. McCarthy, "The Allee effect, finding mates and theoretical models," *Ecological Modelling*, vol. 103, no. 1, pp. 99–102, 1997.

[45] G. Wang, X. G. Liang, and F. Z. Wang, "The competitive dynamics of populations subject to an Allee effect," *Ecological Modelling*, vol. 124, no. 2, pp. 183–192, 1999.

[46] M. A. Burgman, S. Ferson, H. R. Akçakaya et al., *Risk Assessment in Conservation Biology*, Chapman & Hall, London, UK, 1993.

[47] M. Lewis and P. Kareiva, "Allee dynamics and the spread of invading organisms," *Theoretical Population Biology*, vol. 43, no. 2, pp. 141–158, 1993.

[48] P. A. Stephens and W. J. Sutherland, "Consequences of the Allee effect for behaviour, ecology and conservation," *Trends in Ecology and Evolution*, vol. 14, no. 10, pp. 401–405, 1999.

[49] P. A. Stephens, W. J. Sutherland, and R. P. Freckleton, "What is the Allee effect?" *Oikos*, vol. 87, no. 1, pp. 185–190, 1999.

[50] T. H. Keitt, M. A. Lewis, and R. D. Holt, "Allee effects, invasion pinning, and Species' borders," *American Naturalist*, vol. 157, no. 2, pp. 203–216, 2002.

[51] S. R. Zhou, Y. F. Liu, and G. Wang, "The stability of predator–prey systems subject to the Allee effects," *Theoretical Population Biology*, vol. 67, no. 1, pp. 23–31, 2005.

[52] S. Petrovskii, A. Morozov, and B.-L. Li, "Regimes of biological invasion in a predator-prey system with the Allee effect," *Bulletin of Mathematical Biology*, vol. 67, no. 3, pp. 637–661, 2005.

[53] J. Shi and R. Shivaji, "Persistence in reaction diffusion models with weak Allee effect," *Journal of Mathematical Biology*, vol. 52, no. 6, pp. 807–829, 2006.

[54] A. Morozov, S. Petrovskii, and B.-L. Li, "Spatiotemporal complexity of patchy invasion in a predator-prey system with the Allee effect," *Journal of Theoretical Biology*, vol. 238, no. 1, pp. 18–35, 2006.

[55] L. Roques, A. Roques, H. Berestycki, and A. Kretzschmar, "A population facing climate change: joint influences of Allee effects and environmental boundary geometry," *Population Ecology*, vol. 50, no. 2, pp. 215–225, 2008.

[56] C. Çelik and O. Duman, "Allee effect in a discrete-time predator-prey system," *Chaos, Solitons and Fractals*, vol. 40, no. 4, pp. 1956–1962, 2009.

[57] J. Zu and M. Mimura, "The impact of Allee effect on a predator-prey system with Holling type II functional response," *Applied Mathematics and Computation*, vol. 217, no. 7, pp. 3542–3556, 2010.

[58] J. Wang, J. Shi, and J. Wei, "Predator-prey system with strong Allee effect in prey," *Journal of Mathematical Biology*, vol. 62, no. 3, pp. 291–331, 2011.

[59] E. González-Olivares, H. Meneses-Alcay, B. González-Yañez, J. Mena-Lorca, A. Rojas-Palma, and R. Ramos-Jiliberto, "Multiple stability and uniqueness of the limit cycle in a Gause-type predator-prey model considering the Allee effect on prey," *Nonlinear Analysis: Real World Applicationsl*, vol. 12, no. 6, pp. 2931–2942, 2011.

[60] P. Aguirre, E. González-Olivares, and E. Sáez, "Two limit cycles in a Leslie-Gower predator-prey model with additive Allee effect," *Nonlinear Analysis. Real World Applications*, vol. 10, no. 3, pp. 1401–1416, 2009.

[61] P. Aguirre, E. González-Olivares, and E. Sáez, "Three limit cycles in a Leslie-Gower predator-prey model with additive Allee effect," *SIAM Journal on Applied Mathematics*, vol. 69, no. 5, pp. 1244–1262, 2009.

[62] Y. Cai, W. Wang, and J. Wang, "Dynamics of a diffusive predator-prey model with additive Allee effect," *International Journal of Biomathematics*, vol. 5, no. 2, Article ID 1250023, 2012.

[63] M. E. Solomon, "The natural control of animal populations," *The Journal of Animal Ecology*, vol. 18, no. 1, pp. 1–35, 1949.

[64] A. J. Lotka, *Elements of Physical Biology*, Williams and Wilkins, 1925.

[65] C. Jost, *Comparing Predator–Prey Models Qualitatively and Quantitatively with Ecological Time-Series Data*, Institut National Agronomique, Paris-Grignon, 1998.

[66] H. Malchow, S. V. Petrovskii, and E. Venturino, *Spatiotemporal Patterns in Ecology and Epidemiology*, Chapman & Hall, Boca Raton, Fla, USA, 2008.

[67] M. R. Garvie, "Finite-difference schemes for reaction-diffusion equations modeling predator-prey interactions in MATLAB," *Bulletin of Mathematical Biology*, vol. 69, no. 3, pp. 931–956, 2007.

[68] A. Munteanu and R. Solé, "Pattern formation in noisy self-replicating spots," *International Journal of Bifurcation and Chaos*, vol. 16, no. 12, pp. 3679–3683, 2006.

Hindawi Publishing Corporation
Abstract and Applied Analysis
Volume 2013, Article ID 158140, 5 pages
http://dx.doi.org/10.1155/2013/158140

Research Article

Various Heteroclinic Solutions for the Coupled Schrödinger-Boussinesq Equation

Murong Jiang[1] and Zhengde Dai[2]

[1] *School of Information Science and Engineering, Yunnan University, Kunming 650091, China*
[2] *School of Mathematics and Statistics, Yunnan University, Kunming 650091, China*

Correspondence should be addressed to Zhengde Dai; zhddai2004@yahoo.com.cn

Received 31 December 2012; Accepted 21 February 2013

Academic Editor: Peicheng Zhu

Various closed-form heteroclinic breather solutions including classical heteroclinic, heteroclinic breather and Akhmediev breathers solutions for coupled Schrödinger-Boussinesq equation are obtained using two-soliton and homoclinic test methods, respectively. Moreover, various heteroclinic structures of waves are investigated.

1. Introduction

The existence of the homoclinic and heteroclinic orbits is very important for investigating the spatiotemporal chaotic behavior of the nonlinear evolution equations (NEEs). In recent years, exact homoclinic and heterclinic solutions were proposed for some NEEs like nonlinear Schrödinger equation, Sine-Gordon equation, Davey-Stewartson equation, Zakharov equation, and Boussinesq equation [1–7].

The coupled Schrödinger-Boussinesq equation is considered as

$$\begin{aligned} &iE_t + E_{xx} + \beta_1 E - NE = 0, \\ &3N_{tt} - N_{xxxx} + 3\left(N^2\right)_{xx} + \beta_2 N_{xx} - \left(|E|^2\right)_{xx} = 0, \end{aligned} \tag{1}$$

with the periodic boundary condition

$$E(x,t) = E(x+l,t), \qquad N(x,t) = N(x+l,t), \tag{2}$$

where l, β_1, β_2 are real constants, $E(x,t)$ is a complex function, and $N(x,t)$ is a real function. Equation (1) has also appeared in [8] as a special case of general systems governing the stationary propagation of coupled nonlinear upper-hybrid and magnetosonic waves in magnetized plasma. The complete integrability of (1) was studied by Chowdhury et al. [9], and N-soliton solution, homoclinic orbit solution, and rogue solution were obtained by Hu et al. [10], Dai et al. [11–13], and Mu and Qin [14].

2. Linear Stability Analysis

It is easy to see that $(e^{i\theta_0}, \beta_1)$ is a fixed point of (1), and θ_0 is an arbitrary constant. We consider a small perturbation of the form

$$E = e^{i\theta_0}(1+\epsilon), \qquad N = \beta_1(1+\phi), \tag{3}$$

where $|\epsilon(x,t)| \ll 1$, $|\phi(x,t)| \ll 1$. Substituting (3) into (1), we get the linearized equations

$$\begin{aligned} &i\epsilon_t + \epsilon_{xx} - \beta_1\phi = 0, \\ &3\phi_{tt} - \phi_{xxxx} + \left(\beta_2 + 2\beta_1^2\right)\phi_{xx} - \epsilon_{xx} - \bar{\epsilon}_{xx} = 0. \end{aligned} \tag{4}$$

Assume that ϵ and ϕ have the following forms:

$$\begin{aligned} &\epsilon = Ge^{i\mu_n x + \sigma_n t} + He^{-i\mu_n x + \sigma_n t}, \\ &\phi = C\left(e^{i\mu_n x + \sigma_n t} + e^{-i\mu_n x + \sigma_n t}\right), \end{aligned} \tag{5}$$

where G, H are complex constants, and C is a real number; $\mu_n = 2\pi n/l$, and σ_n is the growth rate of the nth modes.

Substituting (5) into (4), we have

$$\begin{aligned} &G\left(i\sigma_n-\mu_n^2\right)=\beta_1 C,\\ &H\left(i\sigma_n-\mu_n^2\right)=\beta_1 C,\\ &\left(3\sigma_n^2-\mu_n^4-\mu_n^2\left(\beta_2+2\beta_1^2\right)\right)C=-\left(G+\overline{H}\right)\nu_n^2,\\ &\left(3\sigma_n^2-\mu_n^4-\mu_n^2\left(\beta_2+2\beta_1^2\right)\right)C=-\left(H+\overline{G}\right)\mu_n^2. \end{aligned} \tag{6}$$

Solving (6), we obtain that

$$\sigma_n^2=\frac{\mu_n^2\left(\beta_2+2\beta_1^2\right)-2\mu_n^4\pm\sqrt{\Delta}}{6}, \tag{7}$$

with

$$\begin{aligned} \Delta&=4\mu_n^8+\mu_n^4\left(\beta_2+2\beta_1^2\right)^2-4\mu_n^6\left(\beta_2+2\beta_1^2\right)\\ &+12\mu_n^4\left(\mu_n^4+\mu_n^2\left(\beta_2+2\beta_1^2\right)-2\beta_1\right). \end{aligned} \tag{8}$$

Obviously, (7) implies that $\mu_n^2(\beta_2+2\beta_1^2)-2\mu_n^4>0$; then,

$$\mu_n^2<\frac{\beta_2+2\beta_1^2}{2}. \tag{9}$$

3. Various Heterclinic Breather Solutions

Set

$$E(x,t)=e^{-iat}u(x,t), \qquad N(x,t)=v_0+v(x,t). \tag{10}$$

Substituting (10) into (1), we get

$$\begin{aligned} &iu_t+u_{xx}+\left(a+\beta_1-v_0\right)u=uv,\\ &3v_{tt}-v_{xxxx}+\left(6v_0+\beta_2\right)v_{xx}+3\left(v^2\right)_x x=\left(|u|^2\right)_{xx}. \end{aligned} \tag{11}$$

We can choose a, v_0 such that $a+\beta_1-v_0=0$.

By using the following transformation

$$u=\frac{g(x,t)}{f(x,t)}, \qquad v=-2(\ln\, f(x,t))_{xx}. \tag{12}$$

Equation (11) can be reduced into the following bilinear form:

$$\begin{aligned} &\left(iD_t+D_x^2\right)g\cdot f=0,\\ &\left(3D_t^2+\left(6v_0+\beta_2\right)D_x^2-D_x^4-\lambda\right)f\cdot f+gg^*=0, \end{aligned} \tag{13}$$

where $g(x,t)$ is an unknown complex function and $f(x,t)$ is a real function, g^* is conjugate function of $g(x,t)$, and λ is an integration constant. The Hirota bilinear operators $D_x^m D_t^n$ are defined by

$$\begin{aligned} &D_x^m D_t^n f(x,t)\cdot g(x,t)\\ &=\left(\frac{\partial}{\partial x}-\frac{\partial}{\partial x'}\right)^m\left(\frac{\partial}{\partial t}-\frac{\partial}{\partial t'}\right)^n\left[f(x,t)\,g\left(x',t'\right)\right]_{x'=x,\,t'=t}. \end{aligned} \tag{14}$$

We use three test functions to investigate the variation of the heterclinic solution for the coupled Schrödinger-Boussinesq equation (1). (1) We seek the following forms of the heterclinic solution:

$$\begin{aligned} &g=1+b_1\cos(px)\,e^{\Omega t+\gamma}+b_2e^{2\Omega t+2\gamma},\\ &f=1+b_3\cos(px)\,e^{\Omega t+\gamma}+b_4e^{2\Omega t+2\gamma}, \end{aligned} \tag{15}$$

where b_1, b_2 are complex numbers and b_3, b_4 are real numbers. b_i $(i=1,2,3,4)$, p, Ω, γ will be determined later.

Choosing $v_0=\beta_1$, then $a=0$. Substituting (15) into the (13), we have the following relations among these constants:

$$\begin{aligned} &\lambda=1, \qquad b_1=\frac{i\Omega+p^2}{i\Omega-p^2}b_3,\\ &b_2=\left(\frac{i\Omega+p^2}{i\Omega-p^2}\right)^2 b_4, \qquad b_4=\frac{\Omega^2+p^4}{4\Omega^2}b_3^2,\\ &\left(3\Omega^2-p^4-\left(6\beta_1+\beta_2\right)p^2\right)\left(\Omega^2+p^4\right)=2p^4. \end{aligned} \tag{16}$$

Therefore, we have the heterclinic solution for (1) as:

$$\begin{aligned} E(x,t)&=\frac{e^{\Omega t+\gamma}+b_1\cos(px)+b_2e^{\Omega t+\gamma}}{\sqrt{b_4}\left(2\cosh\left(\Omega t+\gamma+\ln\sqrt{b_4}\right)+b_3\cos(px)\right)},\\ N(x,t)&\\ &=\beta_1+\frac{2b_3p^2\left(2\sqrt{b_4}\cos(px)\cosh\left(\Omega t+\gamma+\ln\sqrt{b_4}\right)+b_3\right)}{b_4\left(2\cosh\left(\Omega t+\gamma+\ln\sqrt{b_4}\right)+b_3\cos(px)\right)^2}. \end{aligned} \tag{17}$$

It is easy to see that $(E,N)\to(1,\beta_1)$ as $t\to-\infty$ and $(E,N)\to(((i\Omega+p^2)/(i\Omega-p^2))^2,\beta_1)$ as $t\to+\infty$. After giving some constants in (17), we find that the shape of the heterclinic orbit for Schrödinger-Boussinesq equation likes the hook, and the orbits are heterclinic to two different fixed points (see Figure 1 with $\beta_1=1$, $\beta_2=-2$, $p=1$, and $\gamma=1$).

(2) We take ansatz of extended homoclinic test approach for (13) as follows:

$$\begin{aligned} f(x,t)&=e^{-p_1(x-\alpha t)-\eta_0}+b_3\cos\left(p\left(x+\alpha t\right)+\eta_1\right)\\ &\quad+b_4e^{p_1(x-\alpha t)+\eta_0},\\ g(x,t)&=e^{-i\theta}\left(e^{-p_1(x-\alpha t)-\eta_0}+b_1\cos\left(p\left(x+\alpha t\right)+\eta_1\right)\right.\\ &\quad\left.+b_2e^{p_1(x-\alpha t)+\eta_0}\right), \end{aligned} \tag{18}$$

where the parameters $p, p_1, \alpha, \eta_0, \eta_1, b_s$ $(s=1,2,3,4)$ will be determined later, b_1 and b_2 are complex numbers, and b_3 and b_4 are real numbers. Substituting (18) into (13) and choosing $v_0=\beta_1$, we get the following relations among the parameters:

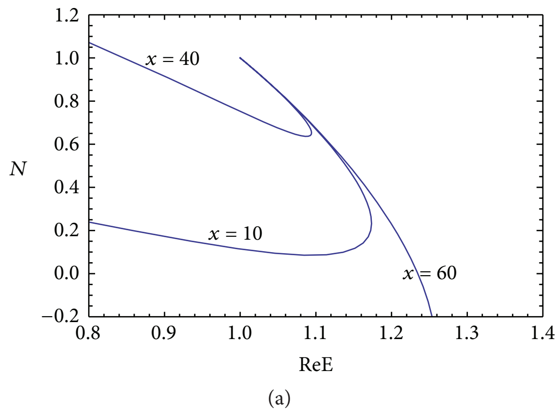

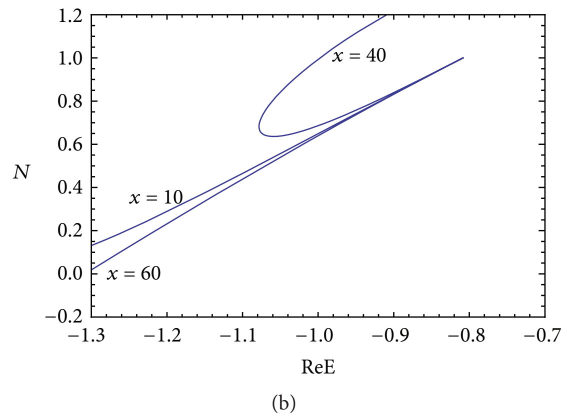

FIGURE 1: Hook heteroclinic orbits for Schrödinger-Boussinesq equation as $t \to -\infty$ (a) and $t \to +\infty$ (b).

$$
\begin{gathered}
p^2 = 3p_1^2, \qquad \lambda = 1, \\
p_1^2 = \frac{3}{4}\alpha^2 - \frac{1}{4}\beta_2 - \frac{3}{2}\beta_1, \qquad \alpha^2 = \frac{(\beta_2 + 6\beta_1)^2 - 2}{4(\beta_2 + 6\beta_1)}, \\
b_1 = \frac{b_3(i\alpha - 2p_1)}{i\alpha + 2p_1}, \qquad b_2 = \frac{b_4(i\alpha - 2p_1)^2}{(i\alpha + 2p_1)^2}, \\
b_3 = \pm\frac{2p_1\sqrt{(3\alpha^2 - 4p_1^2)b_4}}{p\sqrt{\alpha^2 + 4p_1^2}}.
\end{gathered} \tag{19}
$$

From (19), we get the restrictive conditions with

$$
-\sqrt{2} < \beta_2 + 6\beta_1 < 0, \qquad b_4 < 0. \tag{20}
$$

Denote that $(i\alpha - 2p_1)/(i\alpha + 2p_1) = e^{i\theta_0}$. Then, substituting (10) into (1) and employing (19), we obtain the solution of the coupled Schrödinger-Boussinesq equation as follows:

$$
\begin{aligned}
E(x,t) &= e^{i(\theta_0-\theta)}\frac{2\sqrt{-b_4}\sinh\left(p_1(x-\alpha t)+\eta_0+\ln\left(\sqrt{-b_4}\right)+i\theta_0\right)-b_3\cos\left(p(x+\alpha t)+\eta_1\right)}{2\sqrt{-b_4}\sinh\left(p_1(x-\alpha t)+\eta_0+\ln\left(\sqrt{-b_4}\right)\right)-b_3\cos\left(p(x+\alpha t)+\eta_1\right)}, \\
N(x,t) &= \beta_1 - \frac{8\sqrt{-b_4}b_3p_1^2\sinh\left(p_1(x-\alpha t)+\eta_0+\ln\left(\sqrt{-b_4}\right)\right)\cos\left(p(x+\alpha t)+\eta_1\right)}{\left(2\sqrt{-b_4}\sinh\left(p_1(x-\alpha t)+\eta_0+\ln\left(\sqrt{-b_4}\right)\right)-b_3\cos\left(p(x+\alpha t)+\eta_1\right)\right)^2} \\
&\quad - \frac{2\left(-4\sqrt{-b_4}pp_1b_3\cosh\left(p_1(x-\alpha t)+\eta_0+\ln\sqrt{-b_4}\right)\sin\left(p(x+\alpha t)+\eta_1\right)+\left(4b_4-3b_3^2\right)p_1^2\right)}{\left(2\sqrt{-b_4}\sinh\left(p_1(x-\alpha t)+\eta_0+\ln\left(\sqrt{-b_4}\right)\right)-b_3\cos\left(p(x+\alpha t)+\eta_1\right)\right)^2},
\end{aligned} \tag{21}
$$

where η_0, η_1 are arbitrary numbers.

Solution in (21) is a heteroclinic breather wave solution. It is easy to see that $(E, N) \to (e^{-i(\theta+2\theta_0)}, \beta_1)$ as $t \to -\infty$ and $(E, N) \to (e^{-i\theta}, \beta_1)$ as $t \to +\infty$. Given some constants in (21), this kind of the heterclinic orbit likes a spiral, and it is heterclinic to the points $(e^{-i(\theta+2\theta_0)}, \beta_1)$ and $(e^{-i\theta}, \beta_1)$ (see Figure 2 with $\beta_1 = -1.5$, $\beta_2 = 8$, and $b_4 = -4$).

Note that $(e^{-i(\theta+2\theta_0)}, \beta_1)$ and $(e^{-i\theta}, \beta_1)$ are two different fixed points of (21), which is a heteroclinic solution (see Figure 3). This wave also contains the periodic wave, and its amplitude periodically oscillates with the evolution of time, which shows that this wave has breather effect. The previous results combined with (21) show that interaction between a solitary wave and a periodic wave with the same velocity α and opposite propagation direction can form a heteroclinic breather flow. This is a new phenomenon of physics in the stationary propagation of coupled nonlinear upper-hybrid and magnetosonic waves in magnetized plasma.

(3) Use the following forms of the heterclinic solution [14]:

$$
\begin{gathered}
g = b_1\cosh(\alpha t) + b_2\cos(px) + b_3\sinh(\alpha t), \\
f = b_4\cosh(\alpha t) + b_5\cos(px),
\end{gathered} \tag{22}
$$

where b_1, b_2, b_3 are complex numbers and b_4, b_5 are real numbers. b_i $(i = 1, 2, 3, 4, 5)$, p, α will be determined later.

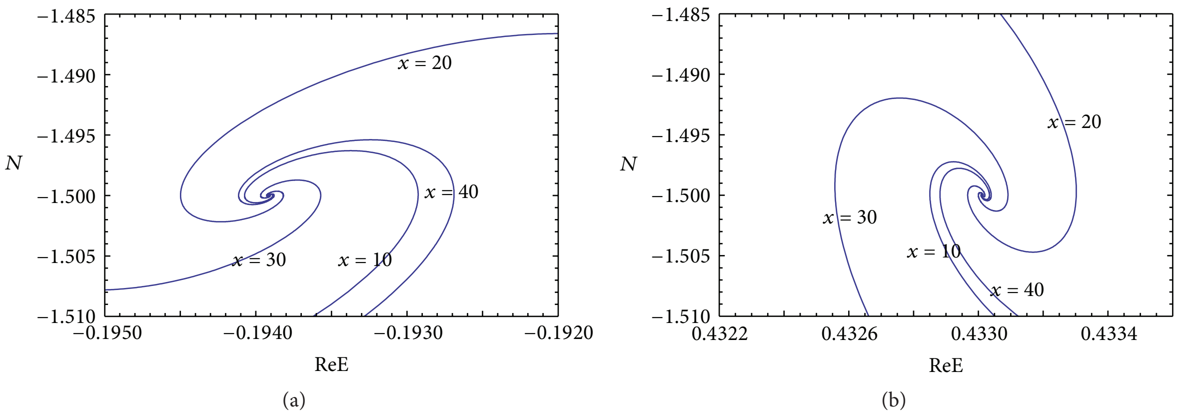

Figure 2: Spiral heteroclinic orbits for Schrödinger-Boussinesq equation as $t \to -\infty$ (a) and $t \to +\infty$ (b).

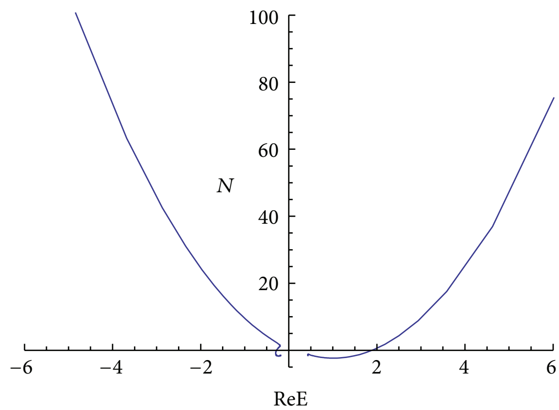

Figure 3: One heteroclinic orbit for Schrödinger-Boussinesq equation as $x = 0$.

We also choose $v_0 = \beta_1$ and substitute (22) into (13). We have the following relations among these constants:

$$
\begin{gathered}
ib_3 b_4 \alpha = b_2 b_5 p^2, \\
b_5 (b_1 + b_3)(i\alpha - p^2) = b_2 b_4 (i\alpha + p^2), \\
b_2 b_4 (i\alpha - p^2) = b_5 (b_1 - b_3)(i\alpha + p^2), \\
- b_4^2 + 12\alpha^2 b_4^2 - 2b_5^2 \cos^2(px) - 16 b_5^2 p^4 - 4 b_5^2 p^2 (6\beta_1 + \beta_2) \\
+ b_1 b_1^* - b_3 b_3^* + 2 b_2 b_2^* \cos^2(px) = 0.
\end{gathered} \tag{23}
$$

Solving (23), we get

$$
\begin{gathered}
b_1 = \frac{(p^4 - \alpha^2) b_2}{\alpha\sqrt{2(\alpha^2 + p^4)}}, \qquad b_3 = \pm i \frac{\sqrt{2} p^2 b_2}{\sqrt{\alpha^2 + p^4}}, \\
b_4^2 = \frac{(\alpha^2 + p^4) b_5^2}{2\alpha^2}.
\end{gathered} \tag{24}
$$

Therefore, we have the heterclinic solution for (1) as

$$
\begin{aligned}
E(x,t) &= \frac{b_1 \cosh(\alpha t) + b_2 \cos(px) + b_3 \sinh(\alpha t)}{b_4 \cosh(\alpha t) + b_5 \cos(px)}, \\
N(x,t) &= \beta_1 + 2 \frac{b_5 p^2 (b_4 \cos(px) \cosh(\alpha t) + b_5)}{(b_4 \cosh(\alpha t) + b_5 \cos(px))^2}.
\end{aligned} \tag{25}
$$

Giving some special parameters in (25), we see that the shape of the heterclinic orbits likes the arc (see Figure 4 with $\beta_1 = 1$, $\alpha = \sqrt{3}$, and $p = \sqrt{2}$). The fixed points are $(E, N) \to ((b_1 - b_3)/b_4, \beta_1)$ as $t \to -\infty$ and $(E, N) \to ((b_1 + b_3)/b_4, \beta_1)$ as $t \to +\infty$.

4. Conclusion

In this work, by using three special test functions in two-soliton method and homoclinic test method, we obtain three families of heteroclinic breather wave solution heteroclinic to two different fixed points, respectively. Moreover, we investigate different structures of these wave solutions. These results show that the Schrödinger-Boussinesq equation has the variety of heteroclinic structure. As the further work, we

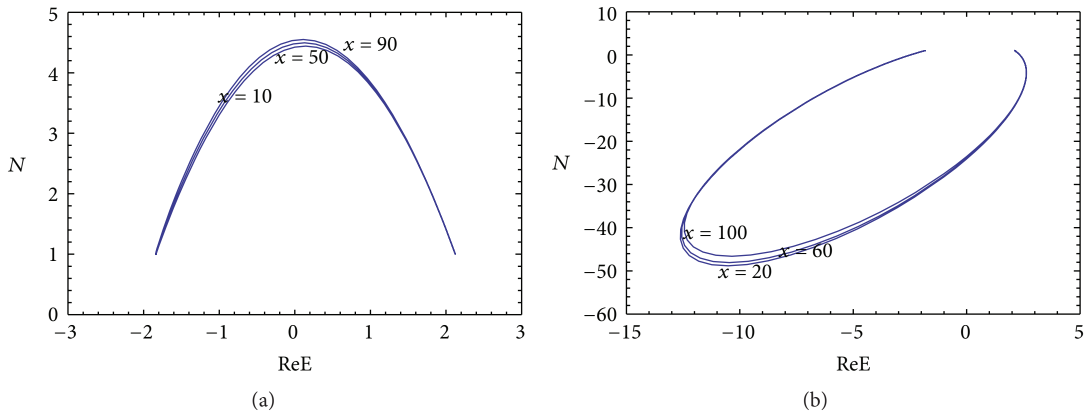

FIGURE 4: Arc Heteroclinic orbit for Schrödinger-Boussinesq equation as $t \to \pm\infty$ at $x = 10 * (2k + 1)$ (a) and $x = 10 * (4k + 2)$ (b), where $k = 0, 1, 2, \ldots$.

will consider whether there exist the spatiotemporal chaos for the coupled Schrödinger-Boussinesq equation or not.

Acknowledgments

This work was supported by Chinese Natural Science Foundation Grant nos. 11161055 and 11061028, as well as Yunnan NSF Grant no. 2008PY034.

References

[1] M. J. Ablowitz and B. M. Herbst, "On homoclinic structure and numerically induced chaos for the nonlinear Schrödinger equation," *SIAM Journal on Applied Mathematics*, vol. 50, no. 2, pp. 339–345, 1990.

[2] N. Ercolani, M. G. Forest, and D. W. McLaughlin, "Geometry of the modulational instability. III. Homoclinic orbits for the periodic sine-Gordon equation," *Physica D*, vol. 43, no. 2-3, pp. 349–384, 1990.

[3] Z. Dai and J. Huang, "Homoclinic tubes for the Davey-Stewartson II equation with periodic boundary conditions," *Chinese Journal of Physics*, vol. 43, no. 2, pp. 349–360, 2005.

[4] Z. Dai, J. Huang, M. Jiang, and S. Wang, "Homoclinic orbits and periodic solitons for Boussinesq equation with even constraint," *Chaos, Solitons and Fractals*, vol. 26, no. 4, pp. 1189–1194, 2005.

[5] Z. Dai, J. Huang, and M. Jiang, "Explicit homoclinic tube solutions and chaos for Zakharov system with periodic boundary," *Physics Letters A*, vol. 352, no. 4-5, pp. 411–415, 2006.

[6] N. N. Rao, "Near-magnetosonic envelope upper-hybrid waves," *Journal of Plasma Physics*, vol. 39, no. 3, pp. 385–392, 1988.

[7] Y. Hase and J. Satsuma, "An N-soliton solution for the nonlinear Schrödinger equation coupled to the Boussinesq equation," *Journal of the Physical Society of Japan*, vol. 57, no. 3, pp. 679–682, 1988.

[8] R. Conte and M. Mussete, "Link between solitary waves and Riccati equation," *Journal of Physics A*, vol. 25, pp. 5600–5615, 1992.

[9] A. R. Chowdhury, B. Dasgupta, and N. N. Rao, "Painléve analysis and Backlund transformations for coupled generalized Schrödinger-Boussinesq system," *Chaos, Solitons and Fractals*, vol. 9, no. 10, pp. 1747–1753, 1998.

[10] X. B. Hu, B. L. Guo, and H. W. Tam, "Homoclinic orbits for the coupled Schrödinger-Boussinesq equation and coupled higgs equation," *Journal of the Physical Society of Japan*, vol. 72, no. 1, pp. 189–190, 2003.

[11] Z. D. Dai, Z. J. Liu, and D. L. Li, "Exact periodic solitary-wave solution for KdV equation," *Chinese Physics Letters*, vol. 25, no. 5, pp. 1531–1534, 2008.

[12] Z. Dai, J. Liu, and D. Li, "Applications of HTA and EHTA to YTSF equation," *Applied Mathematics and Computation*, vol. 207, no. 2, pp. 360–364, 2009.

[13] Z. Dai, Z. Li, Z. Liu, and D. Li, "Exact homoclinic wave and soliton solutions for the 2D Ginzburg-Landau equation," *Physics Letters A*, vol. 372, no. 17, pp. 3010–3014, 2008.

[14] G. Mu and Z. Qin, "Rogue waves for the coupled Schrödinger-Boussinesq equation and the coupled Higgs equation," *Journal of the Physical Society of Japan*, vol. 81, Article ID 084001, 2012.

Hindawi Publishing Corporation
Abstract and Applied Analysis
Volume 2013, Article ID 573782, 5 pages
http://dx.doi.org/10.1155/2013/573782

Research Article

Variational Iteration Method for the Magnetohydrodynamic Flow over a Nonlinear Stretching Sheet

Lan Xu[1,2] and Eric W. M. Lee[3]

[1] *National Engineering Laboratory for Modern Silk, College of Textile and Engineering, Soochow University, 199 Ren-ai Road, Suzhou, Jiangsu 215123, China*
[2] *Nantong Textile Institute of Soochow University, 58 Chong-chuan Road, Nantong, Jiangsu 226018, China*
[3] *Department of Civil and Architectural Engineering, City University of Hong Kong, 83 Tat Chee Avenue, Kowloon Tong, Kowloon, Hong Kong*

Correspondence should be addressed to Eric W. M. Lee; ericlee@cityu.edu.hk

Received 10 December 2012; Accepted 22 February 2013

Academic Editor: de Dai

The variational iteration method (VIM) is applied to solve the boundary layer problem of magnetohydrodynamic flow over a nonlinear stretching sheet. The combination of the VIM and the Padé approximants is shown to be a powerful method for solving two-point boundary value problems consisting of systems of nonlinear differential equations. And the comparison of the obtained results with other available results shows that the method is very effective and convenient for solving boundary layer problems.

1. Introduction

It is well known that most of the phenomena that arise in mathematical physics and engineering fields can be described by partial differential equations. Recent advances of partial differential equations are stimulated by new examples of applications in fluid mechanics, viscoelasticity, mathematical biology, electrochemistry, and physics. There are many traditional and recently developed methods to give numerical and analytical approximate solutions of nonlinear differential equations such as Euler method, Runge-Kutta method, Taylor series method, Adomian decomposition method [1], Variational iteration method [2, 3], Hankel-Padé method [4], DTM-Padé method [5], homotopy perturbation method [6], and Hamiltonian method [7].

In this paper, we consider the model proposed by authors in [1] describing the problem of the boundary layer flow of an incompressible viscous fluid over a nonlinear stretching sheet. The boundary layer flow is often encountered in many engineering and industrial processes. Such processes include the aerodynamic extrusion of plastic sheets, hot rolling, glass fiber production, and so on [1, 4, 5]. And various aspects of the stretching flow problem were discussed by various investigators. Chiam [8] analyzed the MHD flow of a viscous fluid bounded by a stretching surface with power law velocity. He presented the numerical solution of the boundary value problem by utilizing the Runge-Kutta shooting algorithm with Newton iteration. Here, we aim to solve the MHD flow caused by a sheet with nonlinear stretching. The approximate solution of the nonlinear problem is obtained by the variational iteration method.

The variational iteration method [2] is a type of Lagrange multiplier method to find analytical solutions. The method gives the possibility to solve many kinds of non linear equations. In this method, general Lagrange multipliers are introduced to construct correction functional for the problems. The multipliers can be identified optimally via variational theory. It has been used to solve effectively, easily, and accurately a large class of nonlinear problems with approximation [9].

2. Basic Idea of the VIM

The basic idea was systematically illustrated and discussed in [9, 10]. To illustrate the basic idea of the VIM, we consider the following general nonlinear system:

$$L[u(t)] + N[u(t)] = g(t), \tag{1}$$

where L, N, and $g(t)$ are the linear operator, the nonlinear operator, and a given continuous function, respectively. The basic character of the method is to construct a correction functional for the system, which reads

$$u_{n+1}(t) = u_n(t) + \int_0^t \lambda(s)\left[Lu_n(s) + N\tilde{u}_n(s) - g(s)\right] ds, \tag{2}$$

where λ is a Lagrange multiplier which can be identified optimally via the variational theory. The subscript n indicates the nth approximation, and $\tilde{u}_n$ denotes a restricted variation, that is, $\delta\tilde{u}_n = 0$.

3. Problem Statement and Governing Equations

We consider the magnetohydrodynamic (MHD) flow of an incompressible viscous fluid over a stretching sheet at $y = 0$. The fluid is electrically conducting under the influence of an applied magnetic field $B(x)$ normal to the stretching sheet. The induced magnetic field is neglected. The resulting boundary layer equations are as follows [1]:

$$\frac{\partial u}{\partial x} + \frac{\partial v}{\partial y} = 0, \tag{3}$$

$$u\frac{\partial u}{\partial x} + v\frac{\partial u}{\partial y} = \nu\frac{\partial^2 u}{\partial y^2} - \frac{\sigma B^2(x)}{\rho}u, \tag{4}$$

where u and v are the velocity components in the x and y directions, respectively, ν is the kinematic viscosity, ρ is the fluid density, and σ is the electrical conductivity of the fluid. In (4), the external electric field and the polarization effects are negligible, and in [8]

$$B(x) = B_0 x^{(n-1)/2}. \tag{5}$$

The boundary conditions corresponding to the nonlinear stretching of a sheet are

$$\begin{gathered} u(x,0) = cx^n, \qquad v(x,0) = 0, \\ u(x,y) \longrightarrow 0 \quad \text{as } y \longrightarrow \infty. \end{gathered} \tag{6}$$

Upon making use of the following substitutions:

$$\eta = \sqrt{\frac{c(n+1)}{2\nu}}x^{(n-1)/2}y, \qquad u = cx^n f'(\eta), \tag{7}$$

$$v = -\sqrt{\frac{c\nu(n+1)}{2}}x^{(n-1)/2}\left[f(\eta) + \frac{n-1}{n+1}\eta f'(\eta)\right], \tag{8}$$

Substituting (8) into (3)–(6), the resulting nonlinear differential system can be written in the following form:

$$f''' + ff'' - \beta f'^2 - Mf' = 0, \tag{9}$$

$$f(0) = 0, \qquad f'(0) = 1, \qquad f'(\infty) = 0, \tag{10}$$

where

$$\beta = \frac{2n}{1+n}, \qquad M = \frac{2\sigma B_0^2}{\rho c(1+n)}. \tag{11}$$

The parameter β is a measure of the pressure gradient, and M is the magnetic parameter. Positive β denotes the favorable negative pressure gradient, and negative β denotes the unfavorable positive pressure gradient; naturally, $\beta = 0$ denotes the flat plate. For the special case of $\beta = 1$, the exact analytical solution of (9) is [11]

$$f(\eta) = \frac{1 - \exp\left(-\sqrt{1+M}\eta\right)}{\sqrt{1+M}}. \tag{12}$$

4. Approximate Solution by the VIM

In order to obtain VIM solution of (9), we construct a correction functional which reads

$$\begin{aligned} f_{n+1}(\eta) &= f_n(\eta) + \int_0^\eta \lambda(\tau)\left[\frac{\partial^3 f_n(\tau)}{\partial\tau^3} + \tilde{f}_n(\tau)\frac{\partial^2\tilde{f}_n(\tau)}{\partial\tau^2} - \beta \right. \\ &\quad \left. \times\left(\frac{\partial\tilde{f}_n(\tau)}{\partial\tau}\right)^2 - M\frac{\partial\tilde{f}_n(\tau)}{\partial\tau}\right] d\tau, \end{aligned} \tag{13}$$

where $\lambda(\tau)$ is the general Lagrangian multiplier which can be identified optimally via the variational theory. And $\tilde{f}_n(\tau)$ is considered as a restricted variation, that is, $\delta\tilde{f}_n(\tau) = 0$. We omit asterisks for simplicity. Its stationary conditions can be obtained as follows:

$$1 + \lambda''(\tau)\big|_{\tau=\eta} = 0, \qquad \lambda'(\tau)\big|_{\tau=\eta} = 0, \qquad \lambda'''(\tau) = 0. \tag{14}$$

The Lagrange multipliers can be readily identified as the following form:

$$\lambda(\tau) = -\frac{1}{2}(\tau - \eta)^2. \tag{15}$$

As a result, we obtain the following variational iteration formula

$$\begin{aligned} f_{n+1}(\eta) &= f_n(\eta) - \frac{1}{2}\int_0^\eta (\tau-\eta)^2\left[\frac{\partial^3 f_n(\tau)}{\partial\tau^3} + \tilde{f}_n(\tau)\frac{\partial^2\tilde{f}_n(\tau)}{\partial\tau^2} - \beta \right. \\ &\quad \left. \times\left(\frac{\partial\tilde{f}_n(\tau)}{\partial\tau}\right)^2 - M\frac{\partial\tilde{f}_n(\tau)}{\partial\tau}\right] d\tau. \end{aligned} \tag{16}$$

Now, we assume that an initial approximation

$$f_0(\eta) = a + b\eta + c\eta^2. \tag{17}$$

where a, b, and c are unknown constants to be further determined.

By the iteration formula (16) and the initial approximation (17), we can obtain directly the first-order approximate solution as follows:

$$\begin{aligned} f_1(\eta) &= f_0(\eta) - \frac{1}{2}\int_0^\eta (\tau-\eta)^2 \\ &\qquad \times \left[\frac{\partial^3 f_0(\tau)}{\partial\tau^3} + f_0(\tau)\frac{\partial^2 f_0(\tau)}{\partial\tau^2} \right.\\ &\qquad \left. -\beta\left(\frac{\partial f_0(\tau)}{\partial\tau}\right)^2 - M\frac{\partial f_0(\tau)}{\partial\tau}\right] d\tau \\ &= a + b\eta + c\eta^2 - \frac{c^2}{30}\eta^5 + \frac{bM}{6}\eta^3 + \frac{cM}{12}\eta^4\eta^5 \\ &\quad + \frac{\beta b^2}{6}\eta^3 + \frac{\beta c^2}{15} - \frac{ac}{3}\eta^3 - \frac{bc}{12}\eta^4 + \frac{bc\beta}{6}\eta^4 \\ &= a + b\eta + c\eta^2 + \frac{bM + \beta b^2 - 2ac}{6}\eta^3 \\ &\quad + \frac{cM + bc(2\beta-1)}{12}\eta^4 + \frac{(2\beta-1)c^2}{30}\eta^5. \end{aligned} \tag{18}$$

Making use of the initial conditions $f(0) = 0$, $f'(0) = 1$, we can readily obtain the results as follows:

$$a = 0, \qquad b = 1, \qquad c = \frac{1}{2}f''(0), \tag{19}$$

where $f''(0) = \alpha$ will be examined in this work, according the initial condition $f'(\infty) = 0$.

Then,

$$\begin{aligned} f_1(\eta) &= \eta + \frac{1}{2}\alpha\eta^2 + \frac{M+\beta}{6}\eta^3 + \frac{\alpha(M+2\beta-1)}{24}\eta^4 \\ &\quad + \frac{(2\beta-1)\alpha^2}{120}\eta^5. \end{aligned} \tag{20}$$

And the following second-order approximate solution can be obtained

$$\begin{aligned} f_2(\eta) &= f_1(\eta) - \frac{1}{2}\int_0^\eta (\tau-\eta)^2 \\ &\qquad \times \left[\frac{\partial^3 f_1(\tau)}{\partial\tau^3} + f_1(\tau)\frac{\partial^2 f_1(\tau)}{\partial\tau^2} \right.\\ &\qquad \left. -\beta\left(\frac{\partial f_1(\tau)}{\partial\tau}\right)^2 - M\frac{\partial f_1(\tau)}{\partial\tau}\right] d\tau \\ &= \eta + \frac{1}{2}\alpha\eta^2 + \frac{M+\beta}{6}\eta^3 + \frac{\alpha(M+2\beta-1)}{24}\eta^4 \\ &\quad + \left[\frac{(2\beta-1)\alpha^2}{120} + \frac{\beta^2}{60} + \frac{\beta M}{40} - \frac{1}{60} + \frac{M^2}{120} - \frac{M}{60}\right]\eta^5 \\ &\quad + \left(\frac{\beta^2\alpha}{72} + \frac{\beta M\alpha}{72} - \frac{\beta\alpha}{60} + \frac{M^2\alpha}{720} - \frac{M\alpha}{90} + \frac{\alpha}{240}\right)\eta^6 \\ &\quad + \left(\frac{\beta^3}{840} + \frac{\beta^2 M}{420} + \frac{\beta^2\alpha^2}{252} - \frac{\beta^2}{1260} + \frac{\beta M^2}{840} + \frac{\beta M\alpha^2}{504} \right.\\ &\qquad \left. - \frac{\beta M}{630} - \frac{2\beta\alpha^2}{315} - \frac{M^2}{1260} - \frac{M\alpha^2}{630} + \frac{11\alpha^2}{5040}\right)\eta^7 \\ &\quad + \left(\frac{\beta^3\alpha}{1008} + \frac{\beta^2 M\alpha}{672} + \frac{\beta^2\alpha^3}{2016} - \frac{5\beta^2\alpha}{4032} + \frac{\beta M^2\alpha}{2016} \right.\\ &\qquad - \frac{13\beta M\alpha}{8064} - \frac{7\beta\alpha^3}{1260} + \frac{\beta\alpha}{2688} - \frac{M^2\alpha}{2688} + \frac{M\alpha}{2688} \\ &\qquad \left. + \frac{11\alpha^3}{40320}\right)\eta^8 \\ &\quad + \left(\frac{\beta^3\alpha^2}{2592} + \frac{\beta^2 M\alpha^2}{2592} - \frac{37\beta^2\alpha^2}{60480} + \frac{\beta M^2\alpha^2}{18144} \right.\\ &\qquad - \frac{13\beta M\alpha^2}{25920} + \frac{53\beta\alpha^2}{181440} - \frac{M^2\alpha^2}{24192} + \frac{M\alpha^2}{6480} \\ &\qquad \left. - \frac{\alpha^2}{24192}\right)\eta^9 \\ &\quad + \left(\frac{\beta^3\alpha^3}{12960} + \frac{\beta^2 M\alpha^3}{25920} - \frac{\beta^2\alpha^3}{7200} - \frac{13\beta M\alpha^3}{259200} \right.\\ &\qquad \left. + \frac{7\beta\alpha^3}{86400} + \frac{M\alpha^3}{64800} - \frac{\alpha^3}{64800}\right)\eta^{10} \\ &\quad + \left(\frac{\beta^3\alpha^4}{142560} - \frac{\beta^2\alpha^4}{79200} + \frac{7\beta\alpha^4}{950400} - \frac{\alpha^4}{712800}\right)\eta^{11}. \end{aligned} \tag{21}$$

Therefore, according to (13), we can easily obtain higher-order approximate solution as follows:

$$f(\eta) = r_0 + r_1\eta + r_2\eta^2 + r_3\eta^3 + r_4\eta^4 + r_5\eta^5 + \cdots, \tag{22}$$

by using mathematical software such as MATLAB.

It is evident that the main problem for solving (21) is to obtain the value of $f''(0)$, then we can resort to any numerical integration routine to obtain the solution of the problem. For this purpose, we will employ the Padé method to determine this unknown value with high accuracy.

5. Padé Approximation

It is well known that Padé approximations [12] have the advantage of manipulating the polynomial approximation into a rational function of polynomials. This manipulation provides us with more information about the mathematical behavior of the solution. Besides that, power series are not

TABLE 1: Comparison of the values of $f''(0)$ obtained by the variational iteration method and other methods [1] for various values of M when $\beta = 1$.

M	VIM	ADM [1]	Exact [1]
1.0	−1.41421	−1.41421	−1.41421
5.0	−2.44948	−2.44948	−2.44948
10.0	−3.31662	−3.31662	−3.31662
50.0	−7.14142	−7.14142	−7.14142
100.0	−10.04987	−10.04987	−10.04987
500.0	−22.38302	−22.38302	−22.38302

TABLE 2: Comparison of the values of $f''(0)$ obtained by the variational iteration method and the modified Adomian decomposition method [1] for various values of β and M.

M	$\beta = -1.5$		$\beta = 1.5$		$\beta = 5$	
	VIM	ADM [1]	VIM	ADM [1]	VIM	ADM [1]
1.0	−0.6530	−0.6532	−1.5253	−1.5252	−2.1529	−2.1528
5.0	−2.0852	−2.0852	−2.5162	−2.5161	−2.9414	−2.9414
10	−3.0562	−3.0562	−3.3663	−3.3663	−3.6957	−3.6956
50	−7.0239	−7.0239	−7.1647	−7.1647	−7.3256	−7.3256
100	−9.9667	−9.9666	−10.0776	−10.0776	−10.1816	−10.1816
500	−22.3458	−22.3457	−22.3905	−22.3904	−22.4426	−22.4425

useful for large values of η, say $\eta = \infty$. This can be attributed to the possibility that the radius of convergence may not be sufficiently large to contain the boundaries of the domain. Therefore, the combination of the series solution through the decomposition method or any other series solution method with the Padé approximation provides an effective tool for handling boundary value problems on infinite or semi-infinite domains. Furthermore, it is noted that Padé approximants can be easily evaluated by using Matlab.

Therefore, we suppose that the solution $f(\eta)$ can be expanded as a Taylor series about $\eta = 0$

$$f(\eta) = \sum_{j=0}^{\infty} f_j \eta^j. \tag{23}$$

Padé approximant, symbolized by $[S/N]$, is a rational function defined by

$$\left[\frac{S}{N}\right](\eta) = \frac{\sum_{j=0}^{S} p_j \eta^j}{\sum_{j=0}^{N} q_j \eta^j}. \tag{24}$$

If we selected $S = N$, then the approximants $[N/N]$ are called diagonal approximants. More importantly, the diagonal approximants are the most accurate approximants; therefore, we have to construct only diagonal approximants.

Then,

$$\begin{aligned} &\frac{p_0 + p_1\eta + p_2\eta^2 + p_3\eta^3 + \cdots + p_N\eta^N}{q_0 + q_1\eta + q_2\eta^1 + q_3\eta^3 + \cdots + q_N\eta^N} \\ &\quad = r_0 + r_1\eta + r_2\eta^2 + r_3\eta^3 + r_4\eta^4 + \cdots. \end{aligned} \tag{25}$$

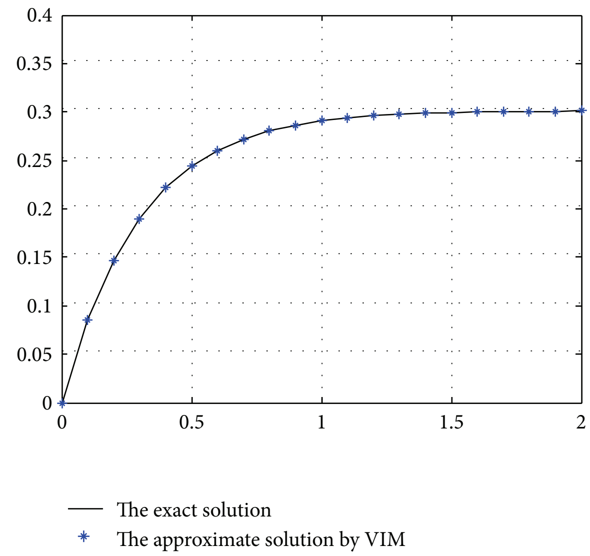

FIGURE 1: Comparison between the approximate solution by the VIM and exact solution for $\beta = 1$ and $M = 10$.

By using cross multiplication in (25), we find

$$\begin{aligned} &p_0 + p_1\eta + p_2\eta^2 + p_3\eta^3 + \cdots + p_N\eta^N \\ &\quad = r_0q_0 + (r_1q_0 + q_1r_0)\eta + (r_2q_0 + q_1r_1 + q_2r_0)\eta^2 \\ &\qquad + (r_3q_0 + q_1r_2 + q_2r_1 + q_3r_0)\eta^3 + \cdots. \end{aligned} \tag{26}$$

Using the boundary condition $f'(\infty) = 0$, the diagonal approximant $[N/N]$ vanishes if the coefficient of η with the highest power in the numerator vanishes. By putting the coefficients of the highest power of η equal to zero, we can easily obtain the values of $f''(0)$ listed in Tables 1 and 2 and Figure 1, using Matlab. The order of Padé approximation [12/12] has sufficient accuracy; on the other hand, if the order of Padé approximation increases, the accuracy of the solution increases.

Substituting (21) and the value of $f''(0)$ into (8), we can easily obtain the second-order approximate solution of (3)-(4).

6. Conclusion

In this paper, the variational iteration method is used to obtain approximate solutions of magnetohydrodynamics boundary layer equations. The analytical solutions of the governing nonlinear boundary layer problem are obtained. Without using the Padé approximation, the analytical solution that were obtained by the VIM cannot satisfy the boundary condition at infinity $f'(\infty) = 0$. The combination of the VIM and the Padé approximants is shown to be a powerful method for solving two-point boundary value problems consisting of systems of nonlinear differential equations. And the obtained solutions are in good agreement with exact values.

Acknowledgments

The work described in this paper was fully supported by a grant from the Research Grants Council of the Hong Kong Special Administrative Region, China (CityU 116308) and Natural Science Foundation of the Jiangsu Higher Education Institutions of China (Grant no. 12KJB130002).

References

[1] T. Hayat, Q. Hussain, and T. Javed, "The modified decomposition method and Padé approximants for the MHD flow over a non-linear stretching sheet," *Nonlinear Analysis: Real World Applications*, vol. 10, no. 2, pp. 966–973, 2009.

[2] J. H. He, "Variational iteration method—a kind of non-linear analytical technique: some examples," *International Journal of Non-Linear Mechanics*, vol. 34, no. 4, pp. 699–708, 1999.

[3] L. Xu, "Variational iteration method for solving integral equations," *Computers & Mathematics with Applications*, vol. 54, no. 7-8, pp. 1071–1078, 2007.

[4] S. Abbasbandy and H. R. Ghehsareh, "Solutions of the magneto-hydrodynamic flow over a nonlinear stretching sheet and nano boundary layers over stretching surfaces," *International Journal for Numerical Methods in Fluids*, vol. 70, pp. 1324–1340, 2012.

[5] M. M. Rashidi, "The modified differential transform method for solving MHD boundary-layer equations," *Computer Physics Communications*, vol. 180, no. 11, pp. 2210–2217, 2009.

[6] J.-H. He, "Homotopy perturbation method with an auxiliary term," *Abstract and Applied Analysis*, vol. 2012, Article ID 857612, 7 pages, 2012.

[7] L. Xu and J. H. He, "Determination of limit cycle by Hamiltonian approach for strongly nonlinear oscillators," *International Journal of Nonlinear Sciences and Numerical Simulation*, vol. 11, no. 12, pp. 1097–1101, 2010.

[8] T. C. Chaim, "Hydromagnetic flow over a surface stretching with a power-law velocity," *International Journal of Engineering Science*, vol. 33, pp. 429–435, 1995.

[9] J.-H. He and X.-H. Wu, "Variational iteration method: new development and applications," *Computers & Mathematics with Applications*, vol. 54, no. 7-8, pp. 881–894, 2007.

[10] J.-H. He, "A short remark on fractional variational iteration method," *Physics Letters A*, vol. 375, no. 38, pp. 3362–3364, 2011.

[11] K. B. Pavlov, "Magnetohydrodynamic flow of an incompressible viscous fluid caused by deformation of a surface," *Magnitnaya Gidrodinamika*, vol. 4, pp. 146–147, 1975.

[12] G. A. Baker, *Essentials of Padé Approximants*, Academic press, London, UK, 1975.

Hindawi Publishing Corporation
Abstract and Applied Analysis
Volume 2013, Article ID 735919, 6 pages
http://dx.doi.org/10.1155/2013/735919

Research Article

Adaptive Wavelet Precise Integration Method for Nonlinear Black-Scholes Model Based on Variational Iteration Method

Huahong Yan

School of Accounting, Capital University of Economics and Business, 121 Zhangjialukou, Huaxiang Fengtai District, Beijing 100070, China

Correspondence should be addressed to Huahong Yan; yanhuahong@263.net

Received 31 December 2012; Revised 14 February 2013; Accepted 17 February 2013

Academic Editor: Lan Xu

An adaptive wavelet precise integration method (WPIM) based on the variational iteration method (VIM) for Black-Scholes model is proposed. Black-Scholes model is a very useful tool on pricing options. First, an adaptive wavelet interpolation operator is constructed which can transform the nonlinear partial differential equations into a matrix ordinary differential equations. Next, VIM is developed to solve the nonlinear matrix differential equation, which is a new asymptotic analytical method for the nonlinear differential equations. Third, an adaptive precise integration method (PIM) for the system of ordinary differential equations is constructed, with which the almost exact numerical solution can be obtained. At last, the famous Black-Scholes model is taken as an example to test this new method. The numerical result shows the method's higher numerical stability and precision.

1. Introduction

The Black-Scholes equation is a mathematical model of a financial market containing certain derivative investment instruments (definition). The idea behind the Black-Scholes model is that the price of an option is determined implicitly by the price of the underlying stock. The Black-Scholes model is a mathematical model based on the notion that prices of stock follow a stochastic process. It is widely employed as a useful approximation, but proper application requires understanding its limitations. Therefore, many nonlinear Black-Scholes equations are proposed in recent years [1, 2]. But it is very difficult to obtain the exact analytical solutions of the nonlinear Black-Scholes models. There are some numerical algorithms that have been proposed based on the difference method to solve those nonlinear problems, but the precision depends on the time step and the discretization in definition domain [3, 4].

Variational iteration method [5–9] proposed by He is a new analytical method to solve nonlinear differential equations, which has been rapidly developed to solve various nonlinear problems of science and engineering as its flexibility and ability to solve nonlinear equations accurately and conveniently [10]. The typical application includes solving free-convective boundary-layer equation [11], q-difference equations [12, 13], and Burgers' flow with fractional derivatives [14, 15]. Comparing with the traditional numerical methods, VIM needs no discretization, linearization, transformation, or perturbation. The wavelet precise integration method (WPIM) is a simple and effective method for linear partial differential equations proposed by Mei [16–20]. For linear steady structural dynamic systems, its numerical results at the integration points are almost equal to that of the exact solution in machine accuracy. But in solving the nonlinear partial differentials, the time step has to be limited to a small value in WPIM for high accuracy.

The main purpose of this paper is to construct a modified VIM for nonlinear Black-Scholes model with combining the VIM with WPIM. According to WPIM, the nonlinear differential equation should be transformed to a system of ordinary differential equations with the multiscales wavelet interpolation operator, and then the nonlinear PDEs become a system of nonlinear ordinary differential equations. So solving the matrix differential equation (MDE) is the key in solving nonlinear PDEs with WPIM. In fact, the matrix differential equation (MDE) is a crucial mathematical foundation of the system engineering and the control theory. But most matrix differential equations do not have precise analytical solutions except linear time-invariant system. In this paper, a coupling technique of He's VIM and WPIM is developed to establish an approximate analytical solution of the matrix differential equations. In contrast to the traditional finite difference approximation, the numerical result obtained with PIM for a set of simultaneous linear time-invariant ODEs approaches the computer precision and is also free from the stiff problem.

2. Fundamental Theory of Coupling Technique of VIM and WPIM

2.1. VIM for Matrix Differential Equation. Consider the nonlinear matrix differential equations as follows:

$$L\left(\dot{\mathbf{V}}, \mathbf{V}, t\right) + N\left(\dot{\mathbf{V}}, \mathbf{V}, t\right) = \mathbf{G}(t), \tag{1}$$

where L is a linear operator, N is a nonlinear operator, $\mathbf{G}(t)$ is an inhomogeneous term, $\mathbf{V}$ is an n-dimensional unknown vector, and dot stands for the differential with respect to time variable t. For convenience, (1) can be rewritten as

$$\dot{\mathbf{V}} - \mathbf{H}\mathbf{V} - \mathbf{F}\left(\dot{\mathbf{V}}, \mathbf{V}, t\right) = 0, \tag{2}$$

where $\mathbf{H}$ is a given $n \times n$ constant matrix, and $\mathbf{F}(\dot{\mathbf{V}}, \mathbf{V}, t)$ is a n-dimensional nonlinear external force vector.

According to VIM, we can write down a correction functional as follows:

$$\begin{aligned}\mathbf{V}_{n+1}(t) &\\ &= \mathbf{V}_n(t) + \int_0^t \lambda \left[\dot{\mathbf{V}}_n(\tau) - \mathbf{H}\mathbf{V}_n(\tau) - \mathbf{F}\left(\dot{\tilde{\mathbf{V}}}_n, \tilde{\mathbf{V}}_n, \tau\right)\right] d\tau,\end{aligned} \tag{3}$$

where λ is a general Lagrange vector multiplier [4, 5, 8] which can be identified optimally via the variational theory. The subscript n denotes the nth approximation, and $\tilde{\mathbf{V}}_n$ is considered as a restricted variation [13–15]; that is, $\delta\tilde{\mathbf{V}}_n = 0$.

Using VIM, the stationary conditions of (3) can be obtained as follows:

$$\begin{gathered}\lambda' + \lambda\mathbf{H} = 0,\\ 1 + \lambda(\tau)|_{\tau=t} = 0.\end{gathered} \tag{4}$$

The Lagrange vector multiplier can therefore be readily identified as follows:

$$\lambda(\tau) = -e^{\mathbf{H}(t-\tau)}. \tag{5}$$

As a result, we obtain the following iteration formula:

$$\begin{aligned}\mathbf{V}_{n+1}(t) = \mathbf{V}_n(t) - \int_0^t e^{\mathbf{H}(t-\tau)} \Big[\dot{\mathbf{V}}_n(\tau)\, \mathbf{H}\mathbf{V}_n(\tau) - &\\ -\mathbf{F}\left(\dot{\tilde{\mathbf{V}}}_n, \tilde{\mathbf{V}}_n, \tau\right)\Big] d\tau.&\end{aligned} \tag{6}$$

According to VIM, we can start with an arbitrary initial approximation that satisfies the initial condition. So we take the exact analytical solution of $\dot{\mathbf{V}} - \mathbf{H}\mathbf{V} = 0$ as the initial approximation; that is,

$$\mathbf{V}_0(t) = e^{\mathbf{H}t}\mathbf{A}, \tag{7}$$

where $\mathbf{A}$ is the given initial value vector.

Substituting (7) into (6) and after simplification, we have

$$\mathbf{V}_{n+1}(t) = \mathbf{V}_n(t) + \int_0^t e^{\mathbf{H}(t-\tau)}\mathbf{F}\left(\dot{\tilde{\mathbf{V}}}_n, \tilde{\mathbf{V}}_n, \tau\right) d\tau. \tag{8}$$

According to the theory of matrices, the analytical expression of the external force $\mathbf{F}(\dot{\tilde{\mathbf{V}}}_n, \tilde{\mathbf{V}}_n, \tau)$ is required now, but it is not always available, except $\mathbf{F}(\dot{\tilde{\mathbf{V}}}_n, \tilde{\mathbf{V}}_n, \tau)$ is a constant vector $\mathbf{f}$; that is,

$$\mathbf{F}\left(\dot{\tilde{\mathbf{V}}}_n, \tilde{\mathbf{V}}_n, \tau\right) = \mathbf{f} \tag{9}$$

the integration term of (8) is

$$\int_0^t e^{\mathbf{H}(t-\tau)}\mathbf{f}\, d\tau = \left(e^{\mathbf{H}t} - \mathbf{I}\right)\mathbf{H}^{-1}\mathbf{f}, \tag{10}$$

where the exponential matrix $e^{\mathbf{H}t}$ can be calculated accurately in PIM and $\mathbf{I}$ is a unit matrix.

Substituting (10) into (8), we obtain the variational iteration formula of the matrix differential equation:

$$\mathbf{V}_{n+1}(t) = \mathbf{V}_n(t) + \left(e^{\mathbf{H}t} - \mathbf{I}\right)\mathbf{H}^{-1}\mathbf{f}. \tag{11}$$

2.2. Coupling Technique of VIM and WPIM for Nonlinear Partial Differential Equation. In most cases, the second-order nonlinear PDEs about the unknown function $u(t, x)$ can be expressed as follows:

$$F\left(u, u_t, u_x, u_{t,x}, u_{xx}\right) = 0. \tag{12}$$

In order to transform the previous nonlinear PDEs into the matrix ODEs form as (1), an adaptive multilevels wavelet interpolation operator should be constructed firstly.

In this section, we take the quasi-Shannon wavelet function as the basis function to approximate the solution function of the nonlinear PDEs. The quasi-Shannon function is defined as follows:

$$\delta_{\Delta\sigma}(x) = \frac{\sin(\pi x/\Delta)}{\pi x/\Delta}\exp\left(-\frac{x^2}{2\sigma^2}\right), \tag{13}$$

where Δ is the discrete step and $\sigma = r\Delta$ (r is a constant) is a parameter relative to the size of the window.

To construct the multilevel interpolation wavelet operator, it is necessary to discretize the wavelet function and the solution function $u(x)$ evenly in the definition domain $[a, b]$. Let the amount of the discrete points be $2^j + 1 (j \in Z)$, and then the discrete points can be defined as

$$x_j^i = a + \frac{i(b-a)}{2^j}. \tag{14}$$

The corresponding discrete basis function can be rewritten as

$$\varphi_j^i(x) = \frac{\sin\left(2^j\pi/(b-a)\right)(x-x_i)}{\left(2^j\pi/(b-a)\right)(x-x_i)} \exp\left(-\frac{2^{2j-1}(x-x_i)^2}{r^2(b-a)^2}\right). \tag{15}$$

The interpolation operator can be defined as

$$u_J(x) = \sum_{i\in Z_\Omega^J} I_i(x)\, u_J^i, \qquad Z_\Omega^J := 0,1,2,\ldots,2^J, \tag{16}$$

where $I_i(x)$ is the interpolation function. According to the wavelet transform theory, function $u(x)$ can be expressed approximately as

$$u_J(x) = \sum_{k_0=0}^{2^{j_0}} u\left(x_{j_0}^{k_0}\right)\varphi_{j_0}^{k_0}(x) + \sum_{j=j_0}^{J-1}\sum_{k\in Z^j}\alpha_j^k\psi_j^k(x), \tag{17}$$

where $Z^j := 0,1,2,\ldots,2^j$ and the interpolation wavelet transform coefficient can be denoted as

$$\begin{aligned}\alpha_j^k &= u\left(x_{j+1}^{2k+1}\right) - \left[\sum_{k_0=0}^{2^{j_0}} u\left(x_{j_0}^{k_0}\right)\varphi_{j_0}^{k_0}\left(x_{j+1}^{2k+1}\right)\right.\\ &\qquad\left. + \sum_{j_1=j_0}^{j-1}\sum_{k_1=0}^{2^{j_1-1}}\alpha_{j_1}^{k_1}\psi_{j_1}^{k_1}\left(x_{j+1}^{2k+1}\right)\right]\\ &= \sum_{n=0}^{2^J}\left[R_{j+1,J}^{2k+1,n} - \sum_{k_0=0}^{2^{j_0}} R_{j_0,J}^{k_0,n}\varphi_{j_0}^{k_0}\left(x_{j+1}^{2k+1}\right)\right]u\left(x_J^n\right)\\ &\quad - \sum_{n=0}^{2^J}\sum_{j_1=j_0}^{j-1}\sum_{k_1=0}^{2^{j_1-1}}\alpha_{j_1}^{k_1}\psi_{j_1}^{k_1}\left(x_{j+1}^{2k+1}\right),\end{aligned} \tag{18}$$

where $0 \le j \le J-1$, $k \in Z^j$, $n \in Z^J$, and R is the restriction operator defined as

$$R_{l,j}^{i,m} = \begin{cases}1, & x_l^i = x_j^m\\ 0, & \text{others.}\end{cases} \tag{19}$$

Suppose that

$$\alpha_j^k = \sum_{n=0}^{2^J} C_{j,J}^{k,n}u\left(x_J^n\right). \tag{20}$$

Substituting (20) into (18), we can obtain

$$\begin{aligned}C_{j,J}^{k,n} &= R_{j+1,J}^{2k+1,n} - \sum_{k_0=0}^{2^{j_0}} R_{j_0,J}^{k_0,n}\varphi_{j_0}^{k_0}\left(x_{j+1}^{2k+1}\right)\\ &\quad - \sum_{j_1=j_0}^{j-1}\sum_{k_1=0}^{2^{j_1-1}} C_{j_1,J}^{k_1,n}\psi_{j_1,k_1}\left(x_{j+1}^{2k+1}\right).\end{aligned} \tag{21}$$

If $j = j_0$, then

$$C_{j,J}^{k,n} = R_{j+1,J}^{2k+1,n} - \sum_{k_0=0}^{2^{j_0}} R_{j_0,J}^{k_0,n}\varphi_{j_0}^{k_0}\left(x_{j+1}^{2k+1}\right). \tag{22}$$

Substituting the restriction operator (19) and the wavelet transform coefficient (20) into (17), the approximate expression of the solution function $u(x)$ can be obtained as

$$\begin{aligned}u_J(x) = \sum_{i\in Z^J}&\left(\sum_{k_0=0}^{2^{j_0}} R_{j_0,J}^{k_0,n}\varphi_{j_0}^{k_0}\left(x_{j+1}^{2k+1}\right)\right.\\ &\left.+\sum_{j_1=j_0}^{j-1}\sum_{k_1=0}^{2^{j_1-1}} C_{j_1,J}^{k_1,n}\psi_{j_1,k_1}\left(x_{j+1}^{2k+1}\right)\right)u\left(x_J^i\right).\end{aligned} \tag{23}$$

According to the definition of the interpolation operator (16), it is easy to obtain the expression of the interpolation operator

$$I_i(x) = \sum_{k_0=0}^{2^{j_0}} R_{j_0,J}^{k_0,i}\varphi_{j_0}^{k_0}(x) + \sum_{j=j_0}^{J-1}\sum_{k\in Z^j} C_{j,J}^{k,i}\psi_j^k(x). \tag{24}$$

The corresponding m-order derivate of the interpolation operator is

$$D_i^{(m)}(x) = \sum_{k_0=0}^{2^{j_0}} R_{j_0,J}^{k_0,i}\varphi_{j_0,k_0}^{(m)}(x) + \sum_{j=j_0}^{J-1}\sum_{k\in Z^j} C_{j,J}^{k,i}\psi_{j,k}^{(m)}(x). \tag{25}$$

Substituting (24) and (25) into (12), the nonlinear PDEs can be changed into an nonlinear ODEs like (1), and then the corresponding analytical solution can be obtained with (11).

In order to solve (1) accurately, the exponential matrix $T(t) = e^{\mathbf{H}t}$ can be calculated accurately by WPIM as follows:

$$T(t) = \exp(\mathbf{H}t) = \left[\exp\left(\frac{\mathbf{H}t}{2^N}\right)\right]^{2^N}. \tag{26}$$

Let $\Delta t = \tau/2^N$, where N is a positive integer (usually take $N = 20$, and then $\Delta t = \tau/1048576$). As τ is a small time step, Δt is a much smaller value, then

$$\begin{aligned}\exp(\mathbf{H}t) &= I + \mathbf{T}_a\\ &= I + \mathbf{H}t + \frac{(\mathbf{H}t)^2\left[I + (\mathbf{H}t)/3 + (\mathbf{H}t)^2/12\right]}{2}\end{aligned} \tag{27}$$

which is the Taylor series expansion of $\exp(\mathbf{H}\Delta t)$. In order to calculate the matrix T more accurately, it is necessary to factorize the matrix T as

$$\mathbf{T}(t) = \left[\exp(\mathbf{H}t)\right]^{2^N} = \left(I + \mathbf{T}_a\right)^{2^{N-1}}\left(I + \mathbf{T}_a\right)^{2^{N-1}}. \tag{28}$$

After doing N times of factorization as mentioned above, a more accurate solution of T can be obtained.

The calculation of the exponent matrix $T(ih)$ at different time steps is needed in solving nonlinear equations through iteration based on the precise integration method, and the algorithm of the matrix $T(ih)$ presented here can obtain all the matrices at different time steps for once.

3. Coupling Technique of VIM and WPIM for the Nonlinear Black-Scholes Model

In order to test the accuracy of the coupling technique of VIM and WPIM for solving nonlinear PDEs, we will consider

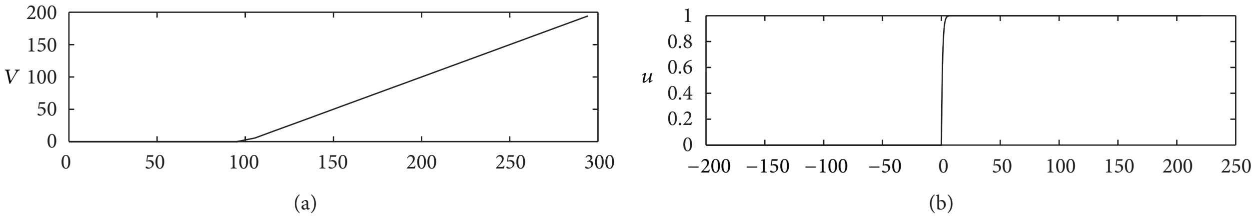

Figure 1: Initial condition of Black-Scholes model.

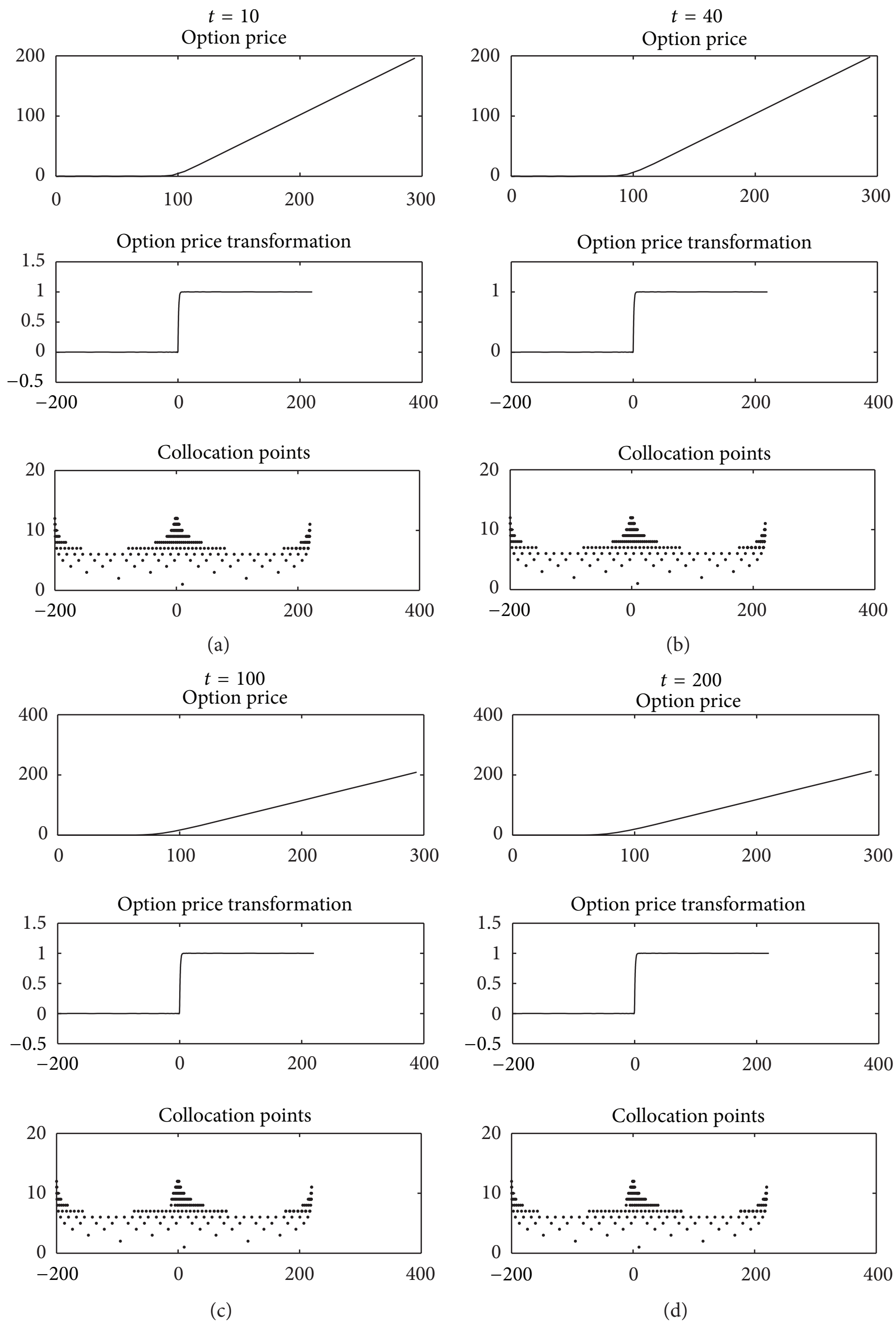

Figure 2: Evolution of the call option price with the parameter t.

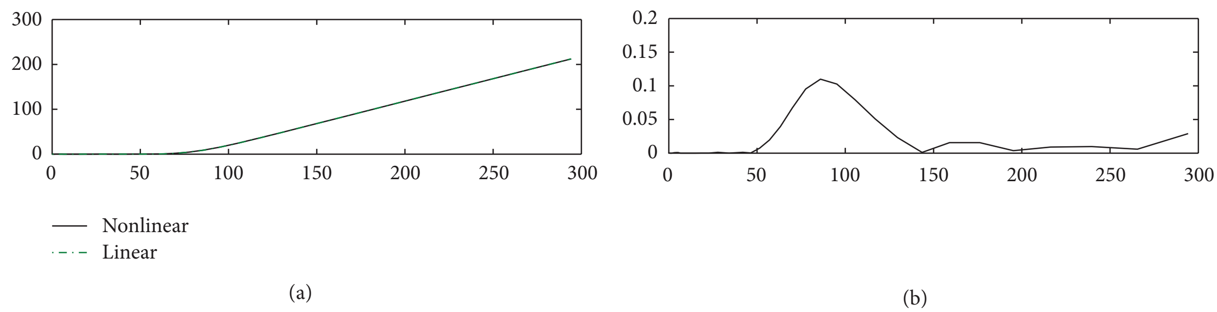

Figure 3: Error of call option price between the linear and nonlinear Black-Scholes models.

the nonlinear Black-Scholes equations which have been increasingly attracting interest over the last two decades, since they provide more accurate values by taking into account more realistic assumptions, such as transaction costs, risks from an unprotected portfolio, large investor's preferences, or illiquid markets, which may have an impact on the stock price, the volatility, the drift, and the option price itself.

Consider the Black-Scholes equation:

$$\frac{\partial V}{\partial t} = rV - \frac{1}{2}\sigma^2 S^2 \frac{\partial^2 V}{\partial S^2} - rS\frac{\partial V}{\partial S}, \quad (29)$$

where $S(t)$ denotes the underlying asset, $t \in (0, T)$, T denotes the expiry date, σ is the volatility (measures the standard deviation of the returns), and r is the riskless interest rate.

In (29), the parameter σ is constant since the transaction cost is taken as zero. Obviously, the σ is not really a constant, and then we can obtain the nonlinear Black-Scholes equation as follows:

$$\frac{\partial V}{\partial t} = rV - \frac{1}{2}\tilde{\sigma}^2\left(t, S, \frac{\partial V}{\partial S}, \frac{\partial^2 V}{\partial S^2}\right) S^2 \frac{\partial^2 V}{\partial S^2} - rS\frac{\partial V}{\partial S}, \quad (30)$$

where $\tilde{\sigma}$ denotes a nonconstant volatility.

In order to solve the problem, it is necessary to perform a variable transformation as follows:

$$x = \ln\left(\frac{S}{K}\right), \quad \tau = \frac{1}{2}\sigma^2 (T - t), \quad u(x, \tau) = e^{-x}\frac{V(s, t)}{K}. \quad (31)$$

Substituting (31) into (30), the following equation can be obtained:

$$\frac{\partial u}{\partial t} = \frac{\tilde{\sigma}^2}{\sigma^2}\left(\frac{\partial^2 u}{\partial x^2} + \frac{\partial u}{\partial x}\right) + D\frac{\partial u}{\partial x}, \quad (32)$$

where

$$D = \frac{2r}{\sigma^2}, \quad x \in R, \ 0 \le \tau \le \tilde{T} = \frac{\sigma^2}{2}. \quad (33)$$

Initial condition

$$u(x, 0) = \left(1 - e^{-x}\right)^+ \quad \text{for } x \in R. \quad (34)$$

Boundary condition

$$\begin{aligned} u(x, \tau) &= 0 \quad \text{as } x \longrightarrow -\infty, \\ u(x, \tau) &\sim 1 - e^{-D\tau - x} \quad \text{as } x \longrightarrow \infty. \end{aligned} \quad (35)$$

The initial condition is shown in Figure 1. According to the transformation relation (31), it is easy to understand that the point $x = 0$ is corresponding to the strike price $S = K$. Obviously, the initial solution curve is smooth in most positions except that near $x = 0$, where a sharp steep wave happened. So, an adaptive numerical method is necessary to this problem.

The evolution of the call option price with the development of the parameter t is illustrated in Figure 2, which shows that the volatility around the strike is greater and there is a sharp shock around it in the transformation form of the option price. The adaptive WPIM and VIM can capture it precisely; that is, there are more collocation points around this place than other places. This is helpful to improve the accuracy and efficiency.

In following, an adaptive interpolation wavelet numerical method is used to solve the nonlinear partial differential equation.

It is well known that the analytical solution of the linear Black-Scholes model for call option price (C) can be obtained as follows:

$$C = S \cdot N(d_1) - Ke^{-rT} N(d2), \quad (36)$$

where

$$d_1 = \frac{\ln(S/K) + \left(r + (1/2)\sigma^2\right)T}{\sigma\sqrt{T}}, \quad d_2 = d_1 - \sigma\sqrt{T}, \quad (37)$$

where C is the call price, S is the underlying asset price, K is the strike price, r is the riskless rate, T is the maturity, σ is the volatility, and $N(d_1)$ expresses the normal distribution.

The error of the call option price between linear and nonlinear Black-Scholes models is shown in Figure 3. It is obvious that the error arising around the strike price, which expresses the nonlinear B-S model, and the coupling technique are effective. With the call option price that is going far away from the strike price, the error is becoming smaller and smaller, which shows that coupling technique is accurate and efficient.

4. Conclusion

The coupling technique of VIM and WPIM developed in this paper can solve nonlinear partial differential equations successfully. Comparison between the numerical results of the linear and nonlinear Black-Scholes models illustrates that the proposed method is an accurate and efficient method for the nonlinear PDEs. In addition, as the coupling technique of VIM and WPIM for matrix differential equations has the uniform analytical solution, it can be easily used to solve various nonlinear problems.

Acknowledgments

The author would like to express his warmest gratitude to Professor Shuli Mei, for his instructive suggestions and valuable comments on the writing of this thesis. Without his invaluable help and generous encouragement, the present thesis would not have been accomplished. At the same time, the author is also grateful to the support of the National Natural Science Foundation of China (no. 41171337), the National Key Technology R and D Program of China (no. 2012BAD35B02), and the Project for Improving Scientific Research Level of Beijing Municipal Commission of Education.

References

[1] J. Wang, J. R. Liang, L. J. Lv, W. Y. Qiu, and F. Y. Ren, "Continuous time Black-Scholes equation with transaction costs in subdiffusive fractional Brownian motion regime," *Physica A*, vol. 391, no. 3, pp. 750–759, 2012.

[2] J. P. N. Bishwal, "Stochastic moment problem and hedging of generalized Black-Scholes options," *Applied Numerical Mathematics*, vol. 61, no. 12, pp. 1271–1280, 2011.

[3] T. K. Jana and P. Roy, "Pseudo Hermitian formulation of the quantum Black-Scholes Hamiltonian," *Physica A*, vol. 391, no. 8, pp. 2636–2640, 2012.

[4] M. K. Kadalbajoo, L. P. Tripathi, and A. Kumar, "A cubic B-spline collocation method for a numerical solution of the generalized Black-Scholes equation," *Mathematical and Computer Modelling*, vol. 55, no. 3-4, pp. 1483–1505, 2012.

[5] J. H. He, "Variational iteration method: a kind of nonlinear analytical technique: some exomples," *International Journal of Non-Linear Mechanics*, vol. 34, no. 4, pp. 699–708, 1999.

[6] J. H. He, "Variational iteration method for autonomous ordinary differential systems," *Applied Mathematics and Computation*, vol. 114, no. 2-3, pp. 115–123, 2000.

[7] J. H. He, X. H. Wu, and F. Austin, "The variational iteration method which should be followed," *Nonlinear Science Letters A*, vol. 1, pp. 1–30, 2007.

[8] J. H. He and X. H. Wu, "Variational iteration method: new development and applications," *Computers & Mathematics with Applications*, vol. 54, no. 7-8, pp. 881–894, 2007.

[9] J. H. He, "Asymptotic methods for solitary solutions and compactons," *Abstract and Applied Analysis*, vol. 2012, Article ID 916793, 130 pages, 2012.

[10] G. C. Wu, "New trends in the variational iteration method," *Communications in Fractional Calculus*, vol. 2, no. 2, pp. 59–75, 2011.

[11] M. S. Tauseef, Y. Ahmet, A. S. Sefa, and U. Muhammad, "Modified variational iteration method for free-convective boundary-layer equation using padé approximation," *Mathematical Problems in Engineering*, vol. 2010, Article ID 318298, 11 pages, 2010.

[12] G. C. Wu, "Variational iteration method for q-difference equations of second order," *Journal of Applied Mathematics*, vol. 2012, Article ID 102850, 5 pages, 2012.

[13] H. Kong and L. L. Huang, "Lagrange multipliers of q-difference equations of third order," *Communications in Fractional Calculus*, vol. 3, no. 1, pp. 30–33, 2012.

[14] G. C. Wu and D. Baleanu, "Variational iteration method for the Burgers' flow with fractional derivatives–new Lagrange multipliers," *Applied Mathematical Modelling*, 2012.

[15] G. C. Wu, "Challenge in the variational iteration method—a new approach to the Lagrange multipliers," *Journal of King Saud University—Science*, 2012.

[16] S. L. Mei, Q. S. Lu, S. W. Zhang, and L. Jin, "Adaptive interval wavelet precise integration method for partial differential equations," *Applied Mathematics and Mechanics*, vol. 26, no. 3, pp. 364–371, 2005.

[17] S. L. Mei, C. J. Du, and S. W. Zhang, "Asymptotic numerical method for multi-degree-of-freedom nonlinear dynamic systems," *Chaos, Solitons and Fractals*, vol. 35, no. 3, pp. 536–542, 2008.

[18] S. L. Mei and S. W. Zhang, "Coupling technique of variational iteration and homotopy perturbation methods for nonlinear matrix differential equations," *Computers & Mathematics with Applications*, vol. 54, no. 7-8, pp. 1092–1100, 2007.

[19] S. L. Mei, C. J. Du, and S. W. Zhang, "Linearized perturbation method for stochastic analysis of a rill erosion model," *Applied Mathematics and Computation*, vol. 200, no. 1, pp. 289–296, 2008.

[20] S. L. Mei, S. W. Zhang, and T. W. Lei, "On wavelet precise time-integration method for Burgers equation," *Chinese Journal of Computational Mechanics*, vol. 20, no. 1, pp. 49–52, 2003.

Hindawi Publishing Corporation
Abstract and Applied Analysis
Volume 2013, Article ID 624352, 5 pages
http://dx.doi.org/10.1155/2013/624352

Research Article

A Lotka-Volterra Competition Model with Cross-Diffusion

Wenyan Chen and Ya Chen

Department of Mathematics, Southeast University, Nanjing 210018, China

Correspondence should be addressed to Wenyan Chen; wychen@seu.edu.cn

Received 9 October 2012; Revised 24 January 2013; Accepted 29 January 2013

Academic Editor: Lan Xu

A Lotka-Volterra competition model with cross-diffusions under homogeneous Dirichlet boundary condition is considered, where cross-diffusions are included in such a way that the two species run away from each other because of the competition between them. Using the method of upper and lower solutions, sufficient conditions for the existence of positive solutions are provided when the cross-diffusions are sufficiently small. Furthermore, the investigation of nonexistence of positive solutions is also presented.

1. Introduction

In this paper, we deal with the following Lotka-Volterra competition model with cross-diffusions:

$$\begin{gathered} -\Delta (u + \alpha v) = u (a - u - cv), \quad x \in \Omega, \\ -\Delta (\beta u + v) = v (b - v - du), \quad x \in \Omega, \\ u = v = 0, \quad x \in \partial\Omega, \end{gathered} \tag{1}$$

where Ω is a bounded domain in $\mathbf{R}^N$ with smooth boundary $\partial\Omega$ and all parameters $a, b, c, d, \alpha, \beta$ are positive constants. u and v stand for the densities of the two competitors; a and b are the intrinsic growth rates of u and v, respectively; c and d are the competitive parameters between the two species; Here α and β are referred to as cross-diffusions. Cross-diffusions express the two species run away from each other because of the competition between them. In this paper, the boundary condition is under homogeneous Dirichlet boundary condition which in biologically means that the boundary is not suitable for both species and they will all die on the boundary, and this is an ideal case.

In order to describe the meaning of cross-diffusions in this model (1) from the biological point, we give the general model with intrinsic diffusion and cross-diffusion:

$$\begin{aligned} \frac{\partial u}{\partial t} &= \operatorname{div} \{k_{11} (u, v) \nabla u + k_{12} (u, v) \nabla v\} + f (u, v), \\ \frac{\partial v}{\partial t} &= \operatorname{div} \{k_{21} (u, v) \nabla u + k_{22} (u, v) \nabla v\} + g (u, v), \end{aligned} \tag{2}$$

where u and v stand for the densities of the two species, intrinsic diffusion parameters $k_{11}(u, v), k_{22}(u, v) > 0$, cross-diffusion parameters $k_{12}(u, v), k_{21}(u, v)$,

$$\begin{aligned} J_u &= - \{k_{11} (u, v) \nabla u + k_{12} (u, v) \nabla v\}, \\ J_v &= - \{k_{21} (u, v) \nabla u + k_{22} (u, v) \nabla v\} \end{aligned} \tag{3}$$

can be seen as the out-flux vector of u and v at x. The cross-diffusion parameters $k_{12}(u, v), k_{21}(u, v) \geq 0$ imply that the two competitors u and v diffuse in the direction of lower contrary of their competitor to avoid each other. $f(u, v)$, $g(u, v)$ are response function and in this paper the classical Logistic Type is considered and $\alpha, \beta \geq 0$. More biological meaning of the system can be seen in [1–3].

The method of upper and lower solutions is a useful tool to study the existence of solutions of elliptic systems. However, there are many difficulties in investigating the existences of positive solutions of strongly coupled elliptic systems. Recently, by changing general strongly coupled elliptic systems into weakly coupled ones, the author in paper [4] gives the method to judge the solutions existence of elliptic systems by using the Schauder theorem. Furthermore, the method can be used to solve the existence of solutions of strongly coupled elliptic systems. In [5] Ko and Ryu investigate Lotka-Volterra prey-predator model with cross-diffusion:

$$\begin{aligned} -\Delta u &= u\left(a_1 - u - b_{12} v\right), \quad x \in \Omega, \\ -D\Delta u - \Delta v &= v\left(a_2 + b_{21} u - v\right), \quad x \in \Omega, \\ u &= v = 0, \quad x \in \partial\Omega. \end{aligned} \tag{4}$$

Here D may be positive or negative. Using the developing method of upper and lower solutions in [4], the author gave a sufficient conditions for the existence of positive solutions to (4). Inspired by the paper [5], we investigate the existence and nonexistence of positive solutions to (1).

The main goal of this paper is to provide sufficient conditions for the existence of positive solutions to (1) when the cross-diffusions α and β are small. More precisely, we have the following theorem. Let $\lambda_1 > 0$ be the principal eigenvalue of $-\Delta$ under homogeneous Dirichlet boundary condition. It is well known that the principal eigenfunction ϕ corresponding to λ_1 does not change sign in Ω and $\|\phi\|_\infty = 1$.

Theorem 1. *If* $\min\{a - cb, b - da\} > \lambda_1$, *then there exist positive constants* $\overline{\alpha} = \overline{\alpha}(a, b, c, d, \Omega)$, $\overline{\beta} = \overline{\beta}(a, b, c, d, \Omega)$, *when* $\alpha < \overline{\alpha}$, $\beta < \overline{\beta}$, (1) *has at least one positive solution.*

For $\alpha = \beta = 0$, (1) is the Lotka-Volterra competition model under homogeneous Dirichlet boundary condition. In [6, 7], the authors use different methods to prove the existence of positive solutions, a sufficient condition for the existence is $\min\{a - cb, b - da\} > \lambda_1$. The conclusion implies that weakly cross-diffusion does not affect the existence of positive solution.

This paper is organized as follows. In Section 2, the existence theorem of solutions for a general class of strongly coupled elliptic systems is presented using the method of upper and lower solutions. In Section 3, sufficient conditions for the existence and nonexistence of positive solutions of (1) are investigated. Moreover, we give the corresponding results simply if the competitive system only has one cross-diffusion.

2. The Existence Theorem of Solutions for a Class of Strongly Coupled Elliptic Systems

In this section, we presented the existence theorem of solutions for a general class of strongly coupled elliptic systems:

$$\begin{aligned} -\Delta A(u, v) &= f_1(u, v), \quad x \in \Omega, \\ -\Delta B(u, v) &= f_2(u, v), \quad x \in \Omega, \\ u &= v = 0, \quad x \in \partial\Omega. \end{aligned} \tag{5}$$

Here let A, B, f_1, f_2 satisfy the following hypotheses conditions.

(H1) U, V are domain in $\mathbf{R}^2$, $(0,0) \in U$. (A, B) is a C^2 function about (u, v) from U to V, $A(0,0) = B(0,0) = 0$, and have a continuous inverse $(A^*, B^*) \in C^2(V, U)$. Then for all $(u, v) \in U$, let

$$w = A(u, v), \qquad z = B(u, v). \tag{6}$$

There exists only one $(w, z) \in V$, satisfying

$$u = A^*(w, z), \qquad v = B^*(w, z). \tag{7}$$

(H2) The function A^* is increasing in w and decreasing in z; B^* is decreasing in w and increasing in z.

(H3) The functions $f_1(u, v)$, $f_2(u, v)$ are Lipschitz continuous in U, and there exist positive constants M_1, M_2 such that for all $(u, v) \in U$, the function $f_1(u, v) + M_1 A(u, v)$ is increasing in u; the function $f_2(u, v) + M_2 B(u, v)$ is increasing in v.

According to the hypothesis (H1), (5) can be rewritten as the following equal PDE equations:

$$\begin{aligned} -\Delta w + M_1 w &= f_1(u, v) + M_1 A(u, v), \quad x \in \Omega, \\ -\Delta z + M_2 z &= f_2(u, v) + M_2 B(u, v), \quad x \in \Omega, \\ u = A^*(w, z), &\quad v = B^*(w, z), \quad x \in \Omega, \\ w &= z = 0, \quad x \in \partial\Omega. \end{aligned} \tag{8}$$

Remark 2. According to the hypothesis (H1), (5) can also be equal to the following weakly coupled elliptic equations:

$$\begin{aligned} -\Delta w &= f_1\left(A^*(w, z), B^*(w, z)\right) := g_1(w, z), \quad x \in \Omega, \\ -\Delta z &= f_2\left(A^*(w, z), B^*(w, z)\right) := g_2(w, z), \quad x \in \Omega, \\ w &= z = 0, \quad x \in \partial\Omega. \end{aligned} \tag{9}$$

In its pure form, (9) is simpler than (8). However, due to the complicity of mixed functions $g_1(w(x), z(x))$ and $g_2(w(x), z(x))$, it is difficult to find the solutions of (9) directly. Therefore, we discuss (8).

Assume functions $\overline{u}$, $\overline{v}$, $\underline{u}$, $\underline{v} \in C(\overline{\Omega})$, $\overline{w}$, $\overline{z}$, $\underline{w}$, $\underline{z} \in C^\alpha(\overline{\Omega}) \bigcap C^2(\Omega)$, the values of functions $(\overline{u}, \overline{v})$ and $(\underline{u}, \underline{v})$ are in V and the values of functions $(\overline{w}, \overline{z})$ and $(\underline{w}, \underline{z})$ are in U. To describe easily, let

$$\begin{aligned} U &= \left\{u \in C\left(\overline{\Omega}\right) : \underline{u}(x) \le u(x) \le \overline{u}(x)\right\}, \\ V &= \left\{u \in C\left(\overline{\Omega}\right) : \underline{v}(x) \le v(x) \le \overline{v}(x)\right\}. \end{aligned} \tag{10}$$

According the definition of upper and lower solutions in [4] and conditions (H1)–(H3), we give the definition of upper and lower solutions of (5).

Definition 3. A pair of functions $((\overline{u}, \overline{v}, \overline{w}, \overline{z}), (\underline{u}, \underline{v}, \underline{w}, \underline{z}))$ are called upper and lower solutions of (9) provided that they satisfy the relation $(\overline{u},\overline{v},\overline{w},\overline{z}) \geq (\underline{u},\underline{v},\underline{w},\underline{z})$, and for all $(u,v) \in U \times V$, satisfy the following inequalities:

$$\begin{aligned}
&-\Delta\overline{w} + M_1\overline{w} \geq f_1(\overline{u},v) + M_1 A(\overline{u},v), \quad x \in \Omega,\\
&-\Delta\overline{z} + M_2\overline{z} \geq f_2(u,\overline{v}) + M_2 B(u,\overline{v}), \quad x \in \Omega,\\
&-\Delta\underline{w} + M_1\underline{w} \leq f_1(\underline{u},v) + M_1 A(\underline{u},v), \quad x \in \Omega,\\
&-\Delta\underline{z} + M_2\underline{z} \leq f_2(u,\underline{v}) + M_2 B(u,\underline{v}), \quad x \in \Omega,\\
&\overline{u} \geq A^*(\overline{w},\underline{z}), \quad \overline{v} \geq B^*(\underline{w},\overline{z}), \quad x \in \Omega,\\
&\underline{u} \leq A^*(\underline{w},\overline{z}), \quad \underline{v} \leq B^*(\overline{w},\underline{z}), \quad x \in \Omega,\\
&\overline{w} \geq 0 \geq \underline{w}, \quad \overline{z} \geq 0 \geq \underline{z}, \quad x \in \partial\Omega.
\end{aligned} \tag{11}$$

We can have the following conclusion from [4, Theorem 2.1].

Proposition 4. *Assume that* (8) *has coupled upper and lower solutions* $((\overline{u},\overline{v},\overline{w},\overline{z}),(\underline{u},\underline{v},\underline{w},\underline{z}))$, *then there exists at least one solution* (u,v,w,z), *satisfying the relation*

$$(\underline{u},\underline{v},\underline{w},\underline{z}) \leq (u,v,w,z) \leq (\overline{u},\overline{v},\overline{w},\overline{z}). \tag{12}$$

Furthermore, (u,v) *is the solution of* (5).

Next, if $\overline{u},\overline{v},\underline{u},\underline{v}$ satisfy

$$\begin{aligned}
&\overline{u} = A^*(\overline{w},\underline{z}), \qquad \overline{v} = B^*(\underline{w},\overline{z}),\\
&\underline{u} = A^*(\underline{w},\overline{z}), \qquad \underline{v} = B^*(\overline{w},\underline{z}),
\end{aligned} \tag{13}$$

then

$$\begin{aligned}
&\overline{w} = A(\overline{u},\underline{v}), \qquad \overline{z} = B(\underline{u},\overline{v}),\\
&\underline{w} = A(\underline{u},\overline{v}), \qquad \underline{z} = B(\overline{u},\underline{v}),
\end{aligned} \tag{14}$$

(11) can be rewritten as

$$\begin{aligned}
&-\Delta A(\overline{u},\underline{v}) + M_1 A(\overline{u},\underline{v}) \geq f_1(\overline{u},v) + M_1 A(\overline{u},v), \quad x \in \Omega,\\
&-\Delta B(\underline{u},\overline{v}) + M_2 B(\underline{u},\overline{v}) \geq f_2(u,\overline{v}) + M_2 B(u,\overline{v}), \quad x \in \Omega,\\
&-\Delta A(\underline{u},\overline{v}) + M_1 A(\underline{u},\overline{v}) \leq f_1(\underline{u},v) + M_1 A(\underline{u},v), \quad x \in \Omega,\\
&-\Delta B(\overline{u},\underline{v}) + M_2 B(\overline{u},\underline{v}) \leq f_2(u,\underline{v}) + M_2 B(u,\underline{v}), \quad x \in \Omega,\\
&A(\overline{u},\underline{v}) \geq 0 \geq A(\underline{u},\overline{v}), \quad B(\underline{u},\overline{v}) \geq 0 \geq B(\overline{u},\underline{v}), \quad x \in \partial\Omega.
\end{aligned} \tag{15}$$

Synthetically, we have the following result.

Theorem 5. *If there is a pair of functions* $((\overline{u},\overline{v}),(\underline{u},\underline{v}))$, *satisfying*

$$(\overline{u},\overline{v},A(\overline{u},\underline{v}),B(\underline{u},\overline{v})) \geq (\underline{u},\underline{v},A(\underline{u},\overline{v}),B(\overline{u},\underline{v})), \tag{16}$$

and for all $(u,v) \in U \times V$, (15) *is satisfied, then* (5) *has at least one solution* (u,v), *satisfying the relation* $(\underline{u},\underline{v}) \leq (u,v) \leq (\overline{u},\overline{v})$.

To make sure the upper and lower solutions reasonable, we give the following two lemmas; more details can be found in [8, 9].

Lemma 6. *If the functions* $u,v \in C^1(\overline{\Omega})$ *satisfy* $u|_{\partial\Omega} = v|_{\partial\Omega} = 0$, $u|_{\Omega} > 0$, $(\partial u/\partial \nu)|_{\partial\Omega} < 0$, ν *is the outer unit normal vector of* $\partial\Omega$, *then there exists positive constant* ε, *such that* $u(x) > \varepsilon v(x)$, *for all* $x \in \Omega$.

For the equation:

$$\begin{aligned}
-\Delta u &= u(a-u), \quad x \in \Omega,\\
u &= 0, \quad x \in \partial\Omega.
\end{aligned} \tag{17}$$

Lemma 7. *If* $a > \lambda_1$, *then* (17) *has a unique positive solution* θ_a *satisfying* $\theta_a \leq a$. *In addition,* θ_a *is increasing with respect to* a.

3. A Lotka-Volterra Competition Model with Two Cross-Diffusions

In this section, the existence of positive solutions of (1) corresponding to $\alpha \geq 0$, $\beta \geq 0$, is investigated by applying Theorem 5 to prove Theorem 1.

Proof. We seek some positive constants $R, K, \delta, R, K > \lambda_1$ sufficiently large and δ sufficiently small, Lemma 6 may guarantee the existence of θ_R and θ_K. It can be easily known from Hopf boundary lemma:

$$\frac{\partial\phi}{\partial\nu}(x) < 0, \quad \frac{\partial\theta_R}{\partial\nu}(x) < 0, \quad \frac{\partial\theta_K}{\partial\nu}(x) < 0, \quad \forall x \in \partial\Omega. \tag{18}$$

Observe that $\min\{a-cb, b-da\} > \lambda_1$, using Lemma 7, we can have R, K, δ, $a < R < (b-\lambda_1)/d$, $b < K < (a-\lambda_1)/c$, satisfying the following three conditions:

(i) $\delta\phi(x) < \theta_R(x)$, $\delta\phi(x) < \theta_K(x)$, for all $x \in \Omega$;
(ii) $(\partial(\theta_R - \delta\phi)/\partial\nu)(x) < 0$, $(\partial(\theta_K - \delta\phi)/\partial\nu)(x) < 0$;
(iii) $\delta < \min\{a - \lambda_1 - cK, b - \lambda_1 - dR\}$.

Let $M_1 = 2R + cK$, $M_2 = 2K + dR$. Using Lemma 7 again, there exist $\overline{\alpha} = \overline{\alpha}(a,b,c,d,\Omega) < 1$, $\overline{\beta} = \overline{\beta}(a,b,c,d,\Omega) < 1$, for all $(\rho,\tau) \in [0,\overline{\alpha}) \times [0,\overline{\beta})$, for all $x \in \Omega$, satisfying

(iv) $\theta_R - \delta\phi > \rho(\theta_K - \delta\phi)$, $\theta_K - \delta\phi > \tau(\theta_R - \delta\phi)$;
(v) $(R-a)\theta_R > \rho[M_1\theta_K - (M_1+\lambda_1)\delta\phi]$, $(K-b)\theta_K > \tau[M_2\theta_R - (M_2+\lambda_1)\delta\phi]$;
(vi) $(a - \lambda_1 - \delta - cK)\delta\phi > \rho[(K + M_1 - \theta_K)\theta_K - M_1\delta\phi]$;
(vii) $(b - \lambda_1 - \delta - dR)\delta\phi > \tau[(R + M_2 - \theta_R)\theta_R - M_2\delta\phi]$.

We will verify $\overline{\alpha}$, $\overline{\beta}$ satisfying Theorem 5. Suppose that $(\alpha,\beta) \in [0,\overline{\alpha}) \times [0,\overline{\beta})$. Then we construct a pair of upper and lower solutions of the form

$$(\overline{u},\overline{v}) = (\theta_R, \theta_K), \qquad (\underline{u},\underline{v}) = (\delta\phi, \delta\phi), \tag{19}$$

where δ satisfies conditions (i)–(iii). Let

$$A(u,v) = u + \alpha v, \qquad B(u,v) = \beta u + v. \tag{20}$$

Then

$$A^*(w,z) = \frac{w-\alpha z}{1-\alpha\beta}, \qquad B^*(w,z) = \frac{z-\beta w}{1-\alpha\beta}. \tag{21}$$

By simply computing, (H1) and (H2) are satisfied, where $U = [0,R]\times[0,K]$, $V = [0, R+\alpha K]\times[0, K+\beta R]$.

Note

$$f_1(u,v) = u(a-u-cv), \qquad f_2(u,v) = v(b-v-du). \tag{22}$$

And for all $(u,v)\in U$, we have

$$\begin{aligned}
\left[f_1(u,v) + M_1 A(u,v)\right]_u &= a - 2u - cv + M_1 \\
&\geq -2R - cK + M_1 = 0, \\
\left[f_2(u,v) + M_2 B(u,v)\right]_v &= b - 2v - du + M_2 \\
&\geq -2K - dR + M_2 = 0.
\end{aligned} \tag{23}$$

So (H3) is satisfied; observer that $\overline{u}|_{\partial\Omega} = \overline{v}|_{\partial\Omega} = \underline{u}|_{\partial\Omega} = \underline{v}|_{\partial\Omega} = 0$, $(\overline{u},\overline{v}) \geq (\underline{u},\underline{v})$ and (iv) and (15) and the boundary conditions of (16) can be checked. Therefore, if we want to obtain the existence of solutions through [4, Theorem 2.1], we should only verify for all $(u,v)\in U\times V$,

$$\begin{aligned}
-\Delta A(\overline{u},\underline{v}) + M_1 A(\overline{u},\underline{v}) &\geq f_1(\overline{u},v) + M_1 A(\overline{u},v), \quad x\in\Omega, \\
-\Delta B(\underline{u},\overline{v}) + M_2 B(\underline{u},\overline{v}) &\geq f_2(u,\overline{v}) + M_2 B(u,\overline{v}), \quad x\in\Omega, \\
-\Delta A(\underline{u},\overline{v}) + M_1 A(\underline{u},\overline{v}) &\leq f_1(\underline{u},v) + M_1 A(\underline{u},v), \quad x\in\Omega, \\
-\Delta B(\overline{u},\underline{v}) + M_2 B(\overline{u},\underline{v}) &\leq f_2(u,\underline{v}) + M_2 B(u,\underline{v}), \quad x\in\Omega.
\end{aligned} \tag{24}$$

Because f_1 is decreasing in v, f_2 is decreasing in u, and $A(u,v)$ is increasing in v, $B(u,v)$ is increasing in u, only to verify the following inequations:

$$\begin{aligned}
-\Delta A(\overline{u},\underline{v}) + M_1 A(\overline{u},\underline{v}) &\geq f_1(\overline{u},\underline{v}) + M_1 A(\overline{u},\overline{v}), \quad x\in\Omega, \\
-\Delta B(\underline{u},\overline{v}) + M_2 B(\underline{u},\overline{v}) &\geq f_2(\underline{u},\overline{v}) + M_2 B(\overline{u},\overline{v}), \quad x\in\Omega, \\
-\Delta A(\underline{u},\overline{v}) + M_1 A(\underline{u},\overline{v}) &\leq f_1(\underline{u},\overline{v}) + M_1 A(\underline{u},\underline{v}), \quad x\in\Omega, \\
-\Delta B(\overline{u},\underline{v}) + M_2 B(\overline{u},\underline{v}) &\leq f_2(\overline{u},\underline{v}) + M_2 B(\underline{u},\underline{v}), \quad x\in\Omega.
\end{aligned} \tag{25}$$

It is easy to check (25) by (v), (vi), and (vii). So from [4, Theorem 2.1], (1) has a solution (u,v), in addition $(\overline{u},\overline{v}) \geq (u,v) \geq (\underline{u},\underline{v}) > (0,0)$. □

In the end, before investigating the nonexistence of positive solutions of (1), we give its priori bound of positive solutions.

Theorem 8. *Any positive solutions (u,v) of (1) have a priori bound; that is*

$$u(x) \leq \frac{b}{d}, \qquad v(x) \leq \frac{a}{c}. \tag{26}$$

Proof. Let $w = u + \alpha v$, $z = \beta u + v$; then

$$u = \frac{w-\alpha z}{1-\alpha\beta}, \qquad v = \frac{z-\beta w}{1-\alpha\beta}. \tag{27}$$

Equation (1) can be rewritten as

$$\begin{gathered}
-\Delta w = \frac{w-\alpha z}{1-\alpha\beta}\left(a - \frac{w-\alpha z}{1-\alpha\beta} - c\frac{z-\beta w}{1-\alpha\beta}\right), \quad x\in\Omega, \\
-\Delta z = \frac{z-\beta w}{1-\alpha\beta}\left(b - \frac{z-\beta w}{1-\alpha\beta} - d\frac{w-\alpha z}{1-\alpha\beta}\right), \quad x\in\Omega, \\
(w,z) = (0,0), \quad x\in\partial\Omega.
\end{gathered} \tag{28}$$

Since $(u,v) > (0,0)$, it easily follows that $w-\alpha z > 0$, $z-\beta w > 0$. Assume that $z(x)$ attains its positive maximum at $x_0\in\Omega$, then

$$\begin{gathered}
a(1-\alpha\beta) - w(x_0) + \alpha z(x_0) - cz(x_0) + c\beta w(x_0) > 0 \\
a(1-\alpha\beta) - cz(x_0) + c\beta\alpha z(x_0) > 0, \\
z(x) \leq z(x_0) \leq \frac{a}{c}
\end{gathered} \tag{29}$$

so that

$$v = z - \beta u \leq z(x_0) \leq \frac{a}{c}. \tag{30}$$

Similarly, we can obtain the desired result

$$u \leq \frac{b}{d}. \tag{31}$$

□

Theorem 9. *If one of the following conditions:*

(i) $b \leq ad$, $\lambda_1 \geq (b + c\beta(b/d))/(1-\alpha\beta)$;

(ii) $(1-(\alpha+\beta)/2)\lambda_1 \geq \max\{a,b\}$;

is satisfied, then (1) with $\alpha < \overline{\alpha}$, $\beta < \overline{\beta}$ has no positive solution.

Proof. Multiplying u and v to the first and second equations in (1), and integrating these equations on Ω, we have

$$\begin{aligned}
\int_\Omega |\nabla u|^2 dx + \alpha\int_\Omega \nabla u\nabla v dx &= \int_\Omega u^2(a-u-cv)\,dx, \\
\alpha\int_\Omega |\nabla v|^2 dx + \int_\Omega \nabla u\nabla v dx &= \int_\Omega uv(a-u-cv)\,dx, \\
\beta\int_\Omega |\nabla u|^2 dx + \int_\Omega \nabla u\nabla v dx &= \int_\Omega uv(b-v-du)\,dx, \\
\int_\Omega |\nabla v|^2 dx + \beta\int_\Omega \nabla u\nabla v dx &= \int_\Omega v^2(b-v-du)\,dx.
\end{aligned} \tag{32}$$

(i) Suppose, by contradiction that (1) has a positive solution (u, v), then the second and fourth equations in (32) yield

$$\int_\Omega v^3 dx + \beta \int_\Omega uv(a-u)\,dx = -(1-\alpha\beta)\int_\Omega |\nabla v|^2 dx + \beta \int_\Omega cuv^2 dx + \int_\Omega v^2(b-du)\,dx. \tag{33}$$

Since $u \le b/d$ by Theorem 8, the left-hand side of (33) must be positive. On the other hand, the Poincare inequality, $\|\nabla v\|_{L^2}^2 \ge \lambda_1 \|v\|_{L^2}^2$, for $v \in W_2^1(\Omega)$ and the given assumption shows the following contradiction:

$$-(1-\alpha\beta)\int_\Omega |\nabla v|^2 dx + \beta\int_\Omega cuv^2 dx + \int_\Omega v^2(b-du)\,dx \le -\left[(1-\alpha\beta)\lambda_1 - c\beta\frac{b}{d} - b\right]\int_\Omega v^2 dx \le 0. \tag{34}$$

(ii) A contraction argument is also used assuming that (1) has a positive solution (u, v). Adding the first equation to the fourth equation, and then subtracting $a\int_\Omega u^2 dx + b\int_\Omega v^2 dx$ from the both sides, the following identity is obtained:

$$\int_\Omega |\nabla u|^2 dx + (\alpha+\beta)\int_\Omega \nabla u \nabla v\,dx + \int_\Omega |\nabla v|^2 dx - a\int_\Omega u^2 dx - b\int_\Omega v^2 dx = -\int_\Omega u^2(u+cv)\,dx - \int_\Omega v^2(v+du)\,dx. \tag{35}$$

Since $2\nabla u \nabla v = |\nabla(u+v)|^2 - |\nabla u|^2 - |\nabla v|^2$ and $(1-(\alpha+\beta)/2)\lambda_1 \ge \max\{a, b\}$, the Poincare inequality shows that the left-hand side of (35) must be nonnegative, more precisely,

$$\begin{aligned}
&\int_\Omega |\nabla u|^2 dx + (\alpha+\beta)\int_\Omega \nabla u\nabla v\,dx + \int_\Omega |\nabla v|^2 dx - a\int_\Omega u^2 dx - b\int_\Omega v^2 dx \\
&= \left(1-\frac{\alpha+\beta}{2}\right)\int_\Omega |\nabla u|^2 dx + \frac{\alpha+\beta}{2}\int_\Omega |\nabla(u+v)|^2 dx \\
&\quad + \left(1-\frac{\alpha+\beta}{2}\right)\int_\Omega |\nabla v|^2 dx - a\int_\Omega u^2 dx - b\int_\Omega v^2 dx \\
&\ge \left[\left(1-\frac{\alpha+\beta}{2}\right)\lambda_1 - a\right]\int_\Omega u^2 dx + \frac{\alpha+\beta}{2} \\
&\quad \cdot \int_\Omega |\nabla(u+v)|^2 dx + \left[\left(1-\frac{\alpha+\beta}{2}\right)\lambda_1 - b\right]\int_\Omega v^2 dx \\
&\ge \left[\left(1-\frac{\alpha+\beta}{2}\right)\lambda_1 - a\right]\int_\Omega u^2 dx \\
&\quad + \left[\left(1-\frac{\alpha+\beta}{2}\right)\lambda_1 - b\right]\int_\Omega v^2 dx \ge 0.
\end{aligned} \tag{36}$$

However, this results in a contradiction since the right-hand side of (35) is clearly strictly negative by the positivity of u and v. □

Remark 10. Before closing this section, more sufficient conditions of the nonexistence of positive solutions of (1) with $\alpha + \beta > 0$, $\alpha\beta = 0$ are investigated. Take $\alpha = 0$, $\beta > 0$ for example, then (1) may be reduced as

$$\begin{aligned}
-\Delta u &= u(a-u-cv), \quad x \in \Omega, \\
-\Delta(\beta u + v) &= v(b-v-du), \quad x \in \Omega, \\
(u, v) &= (0, 0), \quad x \in \partial\Omega.
\end{aligned} \tag{37}$$

Using the same method, we can obtain that (37) has no positive solution, if one of the following conditions is satisfied:

(i) $\lambda_1 \ge b + \beta ca$;

(ii) $\lambda_1 \ge a$;

(iii) $(1-\beta/2)\lambda_1 \ge \max\{a, b\}$;

(iv) $c < 1 < a/b$ and $(1-d)/\beta \le \lambda_1/(b+\beta a) \le 1$.

References

[1] Y. Lou and W.-M. Ni, "Diffusion, self-diffusion and cross-diffusion," *Journal of Differential Equations*, vol. 131, no. 1, pp. 79–131, 1996.

[2] Z. Ling and M. Pedersen, "Coexistence of two species in a strongly coupled cooperative model," *Mathematical and Computer Modelling*, vol. 45, no. 3-4, pp. 371–377, 2007.

[3] Y. Lou and W.-M. Ni, "Diffusion vs cross-diffusion: an elliptic approach," *Journal of Differential Equations*, vol. 154, no. 1, pp. 157–190, 1999.

[4] C. V. Pao, "Strongly coupled elliptic systems and applications to Lotka-Volterra models with cross-diffusion," *Nonlinear Analysis. Theory, Methods & Applications A*, vol. 60, no. 7, pp. 1197–1217, 2005.

[5] W. Ko and K. Ryu, "On a predator-prey system with cross diffusion representing the tendency of predators in the presence of prey species," *Journal of Mathematical Analysis and Applications*, vol. 341, no. 2, pp. 1133–1142, 2008.

[6] A. Leung, "Equilibria and stabilities for competing-species reaction-diffusion equations with Dirichlet boundary data," *Journal of Mathematical Analysis and Applications*, vol. 73, no. 1, pp. 204–218, 1980.

[7] N. Lakoš, "Existence of steady-state solutions for a one-predator—two-prey system," *SIAM Journal on Mathematical Analysis*, vol. 21, no. 3, pp. 647–659, 1990.

[8] L. Li, "Coexistence theorems of steady states for predator-prey interacting systems," *Transactions of the American Mathematical Society*, vol. 305, no. 1, pp. 143–166, 1988.

[9] C. V. Pao, *Nonlinear Parabolic and Elliptic Equations*, Plenum Press, New York, NY, USA, 1992.

Hindawi Publishing Corporation
Abstract and Applied Analysis
Volume 2013, Article ID 230871, 3 pages
http://dx.doi.org/10.1155/2013/230871

Research Article

Analysis of Stability of Traveling Wave for Kadomtsev-Petviashvili Equation

Jun Liu,[1] Xi Liu,[2] Gui Mu,[1] Chunyan Zhu,[1] and Jie Fu[1]

[1] *College of Mathematics and Information Science, Qujing Normal University, Qujing, Yunnan 655011, China*
[2] *College of Information Science and Engineering, Yunnan University, Kunming, Yunnan 650091, China*

Correspondence should be addressed to Jun Liu; liujunxei@126.com

Received 31 January 2013; Accepted 4 February 2013

Academic Editor: de Dai

This paper presents the boundedness and uniform boundedness of traveling wave solutions for the Kadomtsev-Petviashvili (KP) equation. They are discussed by means of a traveling wave transformation and Lyapunov function.

1. Introduction

We consider the Kadomtsev-Petviashvili (KP) equation:

$$u_{tx} + 6u_x u_{xx} + u_{xxxx} + u_{yy} + cu = 0. \tag{1}$$

It is well known that Kadomtsev-Petviashvili equation arises in a number of remarkable nonlinear problems both in physics and mathematics. By using various methods and techniques, exact traveling wave solutions, solitary wave solutions, doubly periodic solutions, and some numerical solutions have been obtained in [1–6].

In this paper, (1) can be changed into an ordinary differential equation by using traveling wave transformation; the boundedness and uniform boundedness of solution for the resulting ordinary differential equation are discussed using the method of Lyapunov function.

2. The Boundedness

Taking a traveling wave transformation $\xi = \alpha x + \beta y + \gamma t$ in (1), then (1) can be transformed into the following form:

$$u^{(4)} + \left(\frac{\gamma}{\alpha^3} + \frac{\beta^2}{\alpha^4} + \frac{6}{\alpha^2}u\right)u'' + \frac{6}{\alpha^2}u'^2 + \frac{c}{\alpha^4}u = 0. \tag{2}$$

In general, we use the following system, which is equivalent to (2):

$$\begin{aligned} u^{(4)} + au''' + f\left(t, u, u''\right) + g\left(u'\right) + du \\ = p\left(t, u, u', u'', u'''\right), \end{aligned} \tag{3}$$

where

$$f\left(t, u, u'\right) = \left(\frac{\gamma}{\alpha^3} + \frac{\beta^2}{\alpha^4} + \frac{6}{\alpha^2}u\right)u'', \qquad g\left(u'\right) = \frac{6}{\alpha^2}u'^2,$$
$$p\left(t, u, u', u'', u'''\right) = -au''', \qquad d = \frac{c}{\alpha^4}. \tag{4}$$

We consider the following system, which is equivalent to (3):

$$\begin{aligned} x_1' = x_2, \qquad x_2' = x_3, \qquad x_3' = x_4, \\ x_4' = -ax_4 - f\left(t, x_1, x_2, x_3\right) - g\left(x_2\right) - dx_1 \\ + p\left(t, x_1, x_2, x_3, x_4\right). \end{aligned} \tag{5}$$

Theorem 1. *If the following conditions hold for the system* (5)*:*

(i) *there are positive constants a, b, d, δ, k, and λ such that*

$$k \le b^2\lambda, \quad ab\frac{g\left(x_2\right)}{x_2} - \left[\frac{g\left(x_2\right)}{x_2}\right]^2 - a^2 d \ge \delta, \quad \left(x_2 \ne 0\right). \tag{6}$$

(ii) $f(t,x_1,x_2,0)=0$, $0\le f(t,x_1,x_2,x_3)/x_3-b\le 2\delta\lambda/k$ $(x_2\neq 0)$.

(iii) $x_3 f'_t(t,x_1,x_2,x_3)+x_2x_3 f'_{x_1}(t,x_1,x_2,x_3)+x_3^2 f'_{x_2}(t,x_1,x_2,x_3)\le 0$.

(iv) $|p(t,x_1,x_2,x_3,x_4)| \le q(t)(x_1^2+x_2^2+x_3^2+x_4^2)^{1/2}$, *where* $q(t)$ *is a nonnegative continuous function and* $\int_0^\infty q(t)dt<\infty$.

Then, all the solutions of system (5) *are bounded.*

Proof. We first construct the Lyapunov function $V=V(t,x_1,x_2,x_3,x_4)$ defined by

$$\begin{aligned}
V &= b^2(2x_4+ax_3+bx_2)^2+2bd(2x_3+ax_2+bx_1)^2\\
&\quad+\left(b^2-4d\right)(ax_4+bx_2)^2+4ab^2\\
&\quad\times\int_0^{x_2}\left[\frac{g(x_2)}{x_2}-\frac{ad}{b}\right]x_2dx_2\\
&\quad+\left[2b\left(b^2-4d\right)+4a^2d\right]x_3^2\\
&\quad+8b^2\int_0^{x_3}\left[\frac{f(t,x_1,x_2,x_3)}{x_3}-b\right]x_3dx_3.
\end{aligned}\tag{7}$$

It follows from conditions (i) and (ii) that

$$\begin{gathered}
b^2-4d\ge 0,\\
0\le\int_0^{x_2}\left[\frac{g(x_2)}{x_2}-\frac{ad}{b}\right]x_2dx_2\le\frac{a\left(b^2-d\right)}{2b}x_2^2,\\
0\le\int_0^{x_3}\left[\frac{f(t,x_1,x_2,x_3)}{x_3}-b\right]x_3dx_3\le\frac{\delta\lambda}{k}x_3^2.
\end{gathered}\tag{8}$$

Summing up the above discussions, we get

$$V\ge 2b\left(b^2-4d\right)x_3^2+4a^2dx_3^2.\tag{9}$$

Thus, we deduce that the function $V(t,x_1,x_2,x_3,x_4)$ defined in (7) is a positive definite function which has infinite inferior limit and infinitesimal upper limit. Hence, there exsits a positive constant $\varepsilon(>0)$ such that

$$V(t,x_1,x_2,x_3,x_4)\ge\varepsilon\left(x_1^2+x_2^2+x_3^2+x_4^2\right).\tag{10}$$

Taking the total derivative of (7) with respect to t along the trajectory of (5), we obtain

$$\begin{aligned}
\frac{dV}{dt} &= -2ab^2\left[x_4+\frac{1}{a}g(x_2)\right]^2\\
&\quad-2b^3x_2x_3\left[\frac{f(t,x_1,x_2,x_3)}{x_3}-b\right]\\
&\quad-2ab^2\left[\frac{f(t,x_1,x_2,x_3)}{x_3}-b\right]x_3^2-\frac{2b^2}{a}\\
&\quad\times\left[ab\frac{g(x_2)}{x_2}-\frac{g^2(x_2)}{x_2^2}-a^2d\right]x_2^2\\
&\quad+4b^2\int_0^{x_3}f'_t(t,x_1,x_2,x_3)\,dx_3\\
&\quad+4b^2x_2\int_0^{x_3}f'_{x_1}(t,x_1,x_2,x_3)\,dx_3\\
&\quad+4b^2x_3\int_0^{x_3}f'_{x_2}(t,x_1,x_2,x_3)\,dx_3\\
&\quad+2b^2(bx_2+ax_3+2x_4)\,p(t,x,x_2,x_3,x_4).
\end{aligned}\tag{11}$$

By using conditions (i) and (iii), it follows that

$$\begin{aligned}
\frac{dV}{dt} &\le -\frac{2b^2\delta}{a}x_2^2-2b^3x_2x_3\left[\frac{f(t,x_1,x_2,x_3)}{x_3}-b\right]\\
&\quad-2ab^2\left[\frac{f(t,x_1,x_2,x_3)}{x_3}-b\right]x_3^2\\
&\quad+2b^2(bx_2+ax_3+2x_4)\,p(t,x,x_2,x_3,x_4).
\end{aligned}\tag{12}$$

According to (ii), we have

$$\begin{aligned}
&2b^3x_2x_3\left[\frac{f(t,x_1,x_2,x_3)}{x_3}-b\right]\\
&\quad+2ab^2\left[\frac{f(t,x_1,x_2,x_3)}{x_3}-b\right]x_3^2\\
&=-\frac{b^4}{2a}\left[\frac{f(t,x_1,x_2,x_3)}{x_3}-b\right]x_2^2\\
&\quad+\frac{2b^2}{a}\left[\frac{f(t,x_1,x_2,x_3)}{x_3}-b\right]\cdot\left(ax_3+\frac{b}{2}x_2\right)^2\\
&\ge-\frac{b^4}{2a}\left[\frac{f(t,x_1,x_2,x_3)}{x_3}-b\right]x_2^2\\
&=-\frac{b^4}{2a}\cdot\frac{2\delta\lambda}{k}x_2^2=-\frac{b^4\delta\lambda}{ak}x_2^2.
\end{aligned}\tag{13}$$

Hence,

$$\begin{aligned}\frac{dV}{dt} \leq &-\frac{2b^2\delta}{a}x_2^2+\frac{b^4\delta\lambda}{ak}x_2^2\\ &+2b^2\left(bx_2+ax_3+2x_4\right)p\left(t,x,x_2,x_3,x_4\right)\\ =&-\frac{b^2\delta}{a}x_2^2+\frac{b^2\delta}{ak}\left(b^2\lambda-k\right)x_2^2\\ &+2b^2\left(4+a^2+b^2\right)^{1/2}\left(x_2^2+x_3^2+x_4^2\right)^{1/2}\\ &\times\left(x_2^2+x_3^2+x_4^2\right)^{1/2}q\left(t\right)\\ \leq&-\frac{b^2\delta}{a}x_2^2+2b^2\left(4+a^2+b^2\right)^{1/2}\left(x_2^2+x_3^2+x_4^2\right)q\left(t\right)\\ \leq&-\frac{b^2\delta}{a}x_2^2+2b^2\left(4+a^2+b^2\right)^{1/2}\cdot q\left(t\right)\cdot\frac{V}{\varepsilon}\\ \leq&\ 2b^2\left(4+a^2+b^2\right)^{1/2}\cdot\frac{q\left(t\right)}{\varepsilon}\cdot V\equiv\varphi\left(V,t\right).\end{aligned} \tag{14}$$

Thus, all the solutions of system (5) are bounded. □

Theorem 2. *Let conditions (i)–(iv) of Theorem 1 be satisfied for the system* (5)*, and let the following condition hold:*

$$\left(4+a^2+b^2\right)^{1/2}\cdot\frac{q\left(t\right)}{\varepsilon}\cdot V-\frac{\delta}{a}x_2^2\leq 0. \tag{15}$$

Then, all the solutions of system (5) *are uniformly bounded.*

Proof. It is clear that the function $V(t,x_1,x_2,x_3,x_4)$ defined in (7) satisfies the conditions (15), therefore, all the solutions of system (5); are uniformly bounded [7]. □

Acknowledgments

This work was financially supported by the Chinese Natural Science Foundation (11061028) and Yunnan Natural Science Foundation (2010CD086).

References

[1] Z. Dai, J. Liu, and Z. Liu, "Exact periodic kink-wave and degenerative soliton solutions for potential Kadomtsev-Petviashvili equation," *Communications in Nonlinear Science and Numerical Simulation*, vol. 15, no. 9, pp. 2331–2336, 2010.

[2] D.-s. Li and H.-q. Zhang, "New soliton-like solutions to the potential Kadomstev-Petviashvili (PKP) equation," *Applied Mathematics and Computation*, vol. 146, no. 2-3, pp. 381–384, 2003.

[3] X. Zeng, Z. Dai, D. Li, S. Han, and H. Zhou, "Some exact periodic soliton solution and resonance for the potential Kadomtsrv-Petviashvili equation," *Chaos, Solitons & Fractals*, vol. 42, pp. 657–661, 2009.

[4] I. E. Inan and D. Kaya, "Some exact solutions to the potential Kadomtsev-Petviashvili equation and to a system of shallow water wave equations," *Physics Letters A*, vol. 355, no. 4-5, pp. 314–318, 2006.

[5] D. Kaya and S. M. El-Sayed, "Numerical soliton-like solutions of the potential Kadomtsev-Petviashvili equation by the decomposition method," *Physics Letters A*, vol. 320, no. 2-3, pp. 192–199, 2003.

[6] Z. Li, Z. Dai, and J. Liu, "New periodic solitary-wave solutions to the 3 + 1-dimensional Kadomtsev-Petviashvili equation," *Mathematical & Computational Applications*, vol. 15, no. 5, pp. 877–882, 2010.

[7] C. Tunç, "On the uniform boundedness of solutions of some non-autonomous differential equations of the fourth order," *Applied Mathematics and Mechanics*, vol. 20, no. 6, pp. 622–628, 1999.

Hindawi Publishing Corporation
Abstract and Applied Analysis
Volume 2013, Article ID 767254, 5 pages
http://dx.doi.org/10.1155/2013/767254

Research Article

The Multisoliton Solutions for the (2 + 1)-Dimensional Sawada-Kotera Equation

Zhenhui Xu,[1] Hanlin Chen,[2] and Wei Chen[3]

[1] *Applied Technology College, Southwest University of Science and Technology, Mianyang 621010, China*
[2] *School of Science, Southwest University of Science and Technology, Mianyang 621010, China*
[3] *School of Mathematics and Computer Science, Mianyang Normal University, Mianyang 621000, China*

Correspondence should be addressed to Zhenhui Xu; xuzhenhui19@163.com

Received 13 November 2012; Revised 19 December 2012; Accepted 1 January 2013

Academic Editor: Lan Xu

Applying bilinear form and extended three-wavetype of ansätz approach on the (2 + 1)-dimensional Sawada-Kotera equation, we obtain new multisoliton solutions, including the double periodic-type three-wave solutions, the breather two-soliton solutions, the double breather soliton solutions, and the three-solitary solutions. These results show that the high-dimensional nonlinear evolution equation has rich dynamical behavior.

1. Introduction

As is well known that the exact solutions of nonlinear evolution equations play an important role in nonlinear science field, especially in nonlinear physical science since they can provide much physical information and more insight into the physical aspects of the problem and thus lead to further applications. The search for exact solutions of nonlinear partial differential equations has long been an interesting and hot topic in nonlinear mathematical physics. Consequently, many methods are available to look for exact solutions of nonlinear evolution equations, such as the inverse scattering method, the Lie group method, the mapping method, Exp-function method, and ansätz technique [1–4]. Very recently, Wang et al. [5] proposed a new technique called extended three-wave approach to seek multiwave solutions for integrable equations, and this method has been used to investigate several equations [6, 7]. In this paper, we consider the following Sawada-Kotera equation:

$$\begin{aligned} u_t = {} & \left(u_{xxxx} + 5uu_{xx} + \frac{5}{3}u^3 + 5u_{xy}\right)_x \\ & - 5\int \left(u_{yy}\right) dx + 5uu_y + 5u_x \int \left(u_y\right) dx. \end{aligned} \tag{1}$$

Equation (1) was derived by B. G. Konopelchenko and V. G. Dubrovsky, and was called the Sawada-Kotera (SK) equation; for example, see [8]. By means of the two-soliton method, the exact periodic soliton solutions, N-soliton solutions, and traveling wave solutions of the SK equation were found [8–10].

In this paper, we discuss further the (2 + 1)-dimensional SK equation, by using bilinear form and extended three-wave type of ansätz approach, respectively [5, 11–15], and some new multisoliton solutions are obtained.

2. The Multisoliton Solutions

We assume

$$u = -2(\ln f)_{xx}, \tag{2}$$

where $f = f(x, y, t)$ is an unknown real function. Substituting (2) into (1), we can reduce (1) into the following equation [8]:

$$\left(D_x^6 + 5D_yD_x^3 - 5D_y^2 + D_xD_t\right) f \cdot f = 0, \tag{3}$$

where the Hirota bilinear operator D is defined by $(n, m \geq 0)$

$$\begin{aligned} D_x^m D_t^n f(x,t) \cdot g(x,t) &= \left(\frac{\partial}{\partial x} - \frac{\partial}{\partial x'}\right)^m \left(\frac{\partial}{\partial t} - \frac{\partial}{\partial t'}\right)^n \\ &\quad \times \left[f(x,t)\, g(x',t')\right]\Big|_{x'=x,t'=t}. \end{aligned} \tag{4}$$

Now we suppose the solution of (3) as

$$f = e^{-\xi} + \delta_1 \cos(\eta) + \delta_2 \cosh(\gamma) + \delta_3 e^{\xi}, \tag{5}$$

where $\xi = a_1 x + b_1 y + c_1 t$, $\eta = a_2 x + b_2 y + c_2 t$, $\gamma = a_3 x + b_3 y + c_3 t$, and a_i, b_i, and c_i $(i = 1,2,3)$ are some constants to be determined later. Substituting (5) into (3) and equating all the coefficients of different powers of e^{ξ}, $e^{-\xi}$, $\sin(\eta)$, $\cos(\eta)$, $\sinh(\gamma)$, $\cosh(\gamma)$, and the constant term to zero, we can obtain a set of algebraic equations for a_i, b_i, c_i, and δ_j $(i = 1,2,3;\ j = 1,2,3)$. Solving the system with the aid of Maple, we get the following results.

Case 1. If $a_2 = 0$, then

$$\begin{gathered} b_1 = -\frac{1}{4} a_1 \left(4a_1^2 + 3a_3^2\right), \qquad b_2 = \frac{3}{2}\, i a_1^2 a_3, \\ b_3 = -\frac{1}{4} a_3 \left(6a_1^2 + a_3^2\right), \qquad \delta_2 = -\frac{\delta_1 a_1^2}{a_1^2 - a_3^2}, \\ \delta_3 = \delta_3, \\ c_1 = \frac{9}{16} a_1 \left(5a_3^4 + 40a_1^2 a_3^2 + 16a_1^4\right), \\ c_2 = -\frac{45}{4}\, i a_1^2 a_3 \left(2a_1^2 + a_3^2\right), \\ c_3 = \frac{9}{16} a_3 \left(a_3^4 + 20a_1^2 a_3^2 + 40a_1^4\right), \end{gathered} \tag{6}$$

where a_1, a_3, δ_1, and δ_3 are free real constants. Substituting (6) into (5) and taking $\delta_3 > 0$, we have

$$\begin{aligned} f_1 &= 2\sqrt{\delta_3} \cosh\left(a_1 x + K_1 y + L_1 t + \frac{1}{2}\ln(\delta_3)\right) \\ &\quad - \delta_1 \cosh(M_1 y + N_1 t) - \frac{\delta_1 a_1^2}{a_1^2 - a_3^2} \\ &\quad \times \cosh(a_3 x - H_1 y + J_1 t), \end{aligned} \tag{7}$$

where $K_1 = (1/4)a_1(4a_1^2 + 3a_3^2)$, $L_1 = (9/16)a_1(5a_3^4 + 40a_1^2 a_3^2 + 16a_1^4)$, $M_1 = -(3/2)a_1^2 a_3$, $N_1 = (45/4)a_1^2 a_3(2a_1^2 + a_3^2)$, $H_1 = (1/4)a_3(6a_1^2 + a_3^2)$, and $J_1 = (9/16)a_3(a_3^4 + 20a_1^2 a_3^2 + 40a_1^4)$. Substituting (7) into (2) yields the three-soliton solution of SK equation as follows:

$$\begin{aligned} u_1 = &-\Bigg(2\Bigg[2\sqrt{\delta_3} a_1^2 \cosh\left(\xi_1 + \frac{1}{2}\ln(\delta_3)\right) - \frac{\delta_1 a_1^2 a_3^2 \cosh(\eta_1)}{a_1^2 - a_3^2}\Bigg]\Bigg) \\ &\times \left(2\sqrt{\delta_3}\cosh\left(\xi_1 + \frac{1}{2}\ln(\delta_3)\right) - \frac{\delta_1 a_1^2 \cosh(\eta_1)}{a_1^2 - a_3^2} - \delta_1 \cosh(\gamma_1)\right)^{-1} \\ &+ \Bigg[\Bigg(2\Bigg(2\sqrt{\delta_3} a_1 \sinh\left(\xi_1 + \frac{1}{2}\ln(\delta_3)\right) - \frac{\delta_1 a_1^2 a_3 \sinh(\eta_1)}{(a_1^2 - a_3^2)}\Bigg)\Bigg) \\ &\times \left(2\sqrt{\delta_3}\cosh\left(\xi_1 + \frac{1}{2}\ln(\delta_3)\right) - \frac{\delta_1 a_1^2 \cosh(\eta_1)}{a_1^2 - a_3^2} - \delta_1 \cosh(\gamma_1)\right)^{-1}\Bigg]^2, \end{aligned} \tag{8}$$

where $\xi_1 = a_1 x + K_1 y + L_1 t$, $\eta_1 = a_3 x - H_1 y + J_1 t$, and $\gamma_1 = M_1 y + N_1 t$.

If taking $a_3 = iA_3$ in (7), then we have

$$\begin{aligned} f_2 &= 2\sqrt{\delta_3}\cosh\left(a_1 x + K_2 y + L_2 t + \frac{1}{2}\ln(\delta_3)\right) \\ &\quad + \delta_1 \cos(M_2 y + N_2 t) \\ &\quad - \frac{\delta_1 a_1^2 \cos(A_3 x - H_2 y + J_2 t)}{a_1^2 + A_3^2}, \end{aligned} \tag{9}$$

where $\delta_3 > 0$, $K_2 = -(1/4)a_1(4a_1^2 - 3A_3^2)$, $L_2 = (9/16)a_1(5A_3^4 - 40a_1^2 A_3^2 + 16a_1^4)$, $M_2 = (3/2)a_1^2 A_3$, $N_2 = -(45/4)a_1^2 A_3(2a_1^2 - A_3^2)$, $H_2 = A_3 x - (1/4)A_3(6a_1^2 - A_3^2)$, and $J_2 = (9/16)A_3(A_3^4 - 20a_1^2 A_3^2 + 40a_1^4)$. Substituting (9) into (2) yields the double breather soliton solution of SK equation as follows:

$$\begin{aligned} u_2 = &-\Bigg(2\Bigg[2a_1^2\sqrt{\delta_3}\cosh\left(\xi_2 + \frac{1}{2}\ln(\delta_3)\right) + \frac{\delta_1 a_1^2 A_3^2 \cos(\eta_2)}{a_1^2 + A_3^2}\Bigg]\Bigg) \\ &\times \left(2\sqrt{\delta_3}\cosh\left(\xi_2 + \frac{1}{2}\ln(\delta_3)\right) + \delta_1 \cos(\gamma_2) - \frac{\delta_1 a_1^2 \cos(\eta_2)}{a_1^2 + A_3^2}\right)^{-1} \end{aligned}$$

$$+2\left[\left(\left(2a_1\sqrt{\delta_3}\sinh\left(\xi_2+\frac{1}{2}\ln(\delta_3)\right)+\frac{\delta_1 a_1^2 A_3\sin(\eta_2)}{a_1^2+A_3^2}\right)\times\left(2\sqrt{\delta_3}\cosh\left(\xi_2+\frac{1}{2}\ln(\delta_3)\right)+\delta_1\cos(\gamma_2)-\frac{\delta_1 a_1^2\cos(\eta_2)}{a_1^2+A_3^2}\right)^{-1}\right]^2, \tag{10}$$

where $\xi_2 = a_1x + K_2y + L_2t$, $\eta_2 = A_3x - H_2y + J_2t$, and $\gamma_2 = M_2y + N_2t$.

Case 2. If $a_2 \neq 0$, then

$$\begin{gathered} b_1 = -a_1^3, \qquad b_2 = a_2^3, \qquad b_3 = -a_3^3, \\ \delta_1 = \delta_1, \qquad \delta_2 = \delta_2, \qquad \delta_3 = \delta_3, \\ c_1 = 9a_1^5, \qquad c_2 = 9a_2^5, \qquad c_3 = 9a_3^5, \end{gathered} \tag{11}$$

where a_1, a_2, a_3, δ_1, δ_2, and δ_3 are free real constants. Substituting (11) into (5) and taking $\delta_3 > 0$, we have

$$\begin{aligned} f_3 &= 2\sqrt{\delta_3}\cosh\left(a_1x - a_1^3y + 9a_1^5t + \frac{1}{2}\ln(\delta_3)\right) \\ &\quad + \delta_1\cos\left(a_2x + a_2^3y + 9a_2^5t\right) \\ &\quad + \delta_2\cosh\left(a_3x - a_3^3y + 9a_3^5t\right). \end{aligned} \tag{12}$$

Substituting (12) into (2) yields the breather two-soliton solution of SK equation as follows:

$$\begin{aligned} u_3 = &-\left(2\left[2\sqrt{\delta_3}a_1^2\cosh\left(\xi_3+\frac{1}{2}\ln(\delta_3)\right)-\delta_1a_2^2\cos(\eta_3)+\delta_2a_3^2\cosh(\gamma_3)\right]\right) \\ &\times\left(2\sqrt{\delta_3}\cosh\left(\xi_3+\frac{1}{2}\ln(\delta_3)\right)+\delta_1\cos(\eta_3)+\delta_2\cosh(\gamma_3)\right)^{-1} \\ &+\left[\left(2\left(2\sqrt{\delta_3}a_1\sinh\left(\xi_3+\frac{1}{2}\ln(\delta_3)\right)-\delta_1a_2\sin(\eta_3)+\delta_2a_3\sinh(\gamma_3)\right)\right)\right. \\ &\left.\times\left(2\sqrt{\delta_3}\cosh\left(\xi_3+\frac{1}{2}\ln(\delta_3)\right)+\delta_1\cos(\eta_3)+\delta_2\cosh(\gamma_3)\right)^{-1}\right]^2, \end{aligned} \tag{13}$$

where $\xi_3 = a_1x - a_1^3y + 9a_1^5t$, $\eta_3 = a_2x + a_2^3y + 9a_2^5t$, and $\gamma_3 = a_3x - a_3^3y + 9a_3^5t$.

The expression (u_3) is the breather two-soliton solution of SK equation which is a periodic wave in x, y and meanwhile is a two-soliton in x, y (refer to Figure 1(b)).

Case 3. If $a_2 = b_1 = 0$, then

$$\begin{gathered} a_1 = 2a_3, \qquad b_2 = \sqrt{21}a_3^3, \qquad b_3 = -\frac{3}{2}a_3^3, \\ c_1 = -\frac{169}{2}a_3^5, \\ c_2 = -20\sqrt{21}a_3^5, \qquad c_3 = -\frac{349}{4}a_3^5, \\ \delta_3 = \frac{5}{152}\delta_2^2 - \frac{7}{228}\delta_1^2, \end{gathered} \tag{14}$$

where a_3, δ_1, and δ_2 are free real constants. Substituting (14) into (5) and taking $\delta_3 > 0$, we have

$$\begin{aligned} f_4 &= 2\sqrt{\frac{5}{152}\delta_2^2 - \frac{7}{228}\delta_1^2} \\ &\quad\times\cosh\left(-2a_3x + \frac{169}{2}a_3^5t - \frac{1}{2}\ln\left(\frac{5}{152}\delta_2^2 - \frac{7}{228}\delta_1^2\right)\right) \\ &\quad + \delta_1\cos\left(-\sqrt{21}a_3^3y + 20\sqrt{21}a_3^5t\right) \\ &\quad + \delta_2\cosh\left(-a_3x + \frac{3}{2}{a_3}^3y + \frac{349}{4}a_3^5t\right), \end{aligned} \tag{15}$$

where $(5/152)\delta_2^2 - (7/228)\delta_1^2 > 0$. Substituting (15) into (2) yields the breather two-soliton solution of SK equation as follows:

$$\begin{aligned} u_4 = &-\left(2\left[8\sqrt{K_4}a_3^2\cosh\left(\xi_4-\frac{1}{2}\ln(K_4)\right)+\delta_2a_3^2\cosh(\eta_4)\right]\right) \\ &\times\left(2\sqrt{K_4}\cosh\left(\xi_4-\frac{1}{2}\ln(K_4)\right)+\delta_1\cos(\gamma_4)+\delta_2\cosh(\eta_4)\right)^{-1} \\ &+2\left[\left(4\sqrt{K_4}a_3\sinh\left(\xi_4-\frac{1}{2}\ln(K_4)\right)+\delta_2a_3\sinh(\eta_4)\right)\right. \\ &\left.\times\left(2\sqrt{K_4}\cosh\left(\xi_4-\frac{1}{2}\ln(K_4)\right)+\delta_1\cos(\gamma_4)+\delta_2\cosh(\eta_4)\right)^{-1}\right]^2, \end{aligned} \tag{16}$$

where $K_4 = (5/152)\delta_2^2 - (7/228)\delta_1^2$, $\xi_4 = -2a_3x + (169/2)a_3^5t$, $\eta_4 = -a_3x + (3/2)a_3^3y + (349/4)a_3^5t$, and $\gamma_4 = -\sqrt{21}a_3^3y + 20\sqrt{21}a_3^5t$.

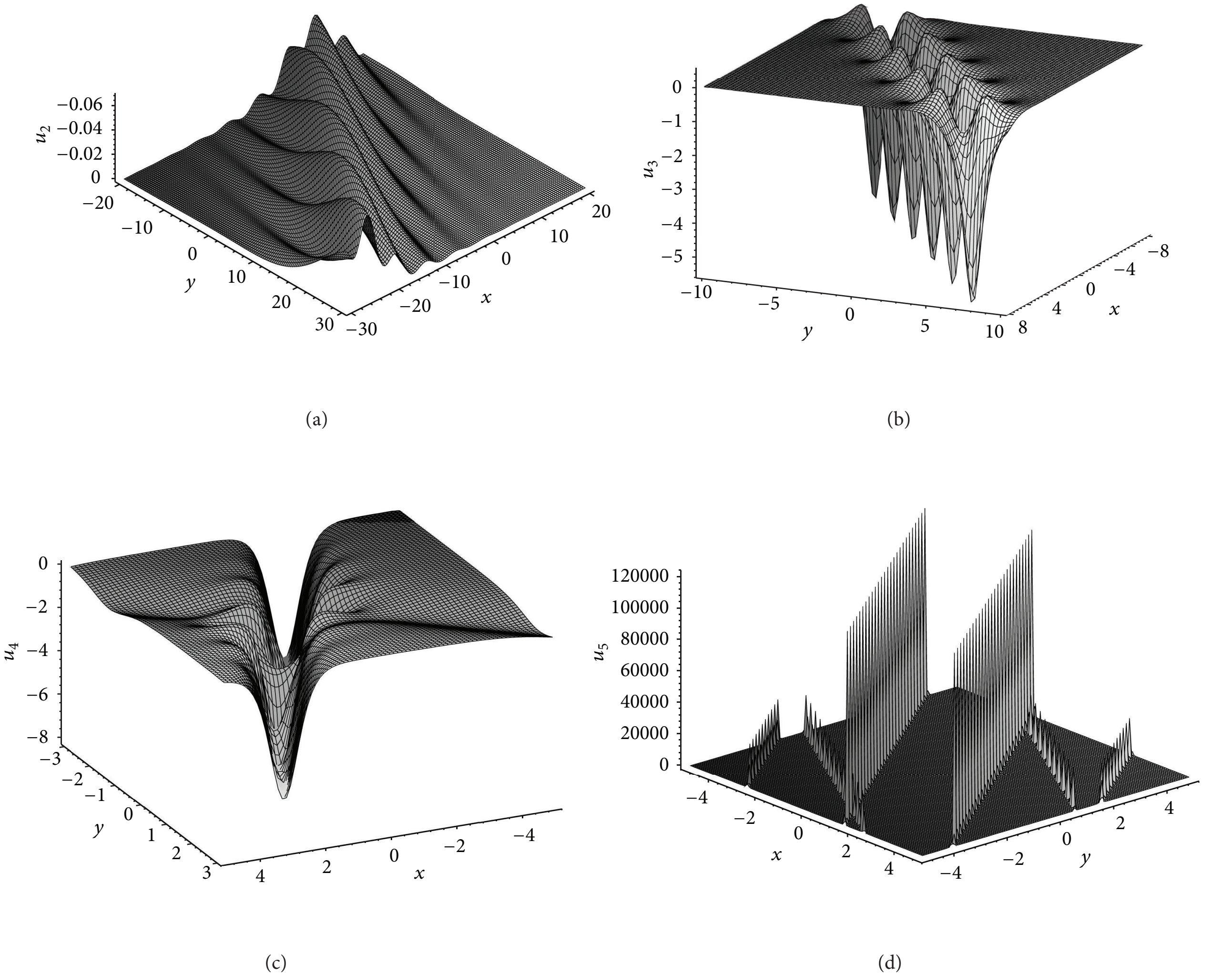

Figure 1: (a) The figure of u_2 as $\delta_1 = 1$, $\delta_3 = 1$, and $t = 1$. (b) The figure of u_3 as $\delta_1 = \sqrt{2}$, $\delta_2 = 1$, and $t = 0$. (c) The figure of u_4 as $\delta_1 = \sqrt{2}$, $\delta_2 = \sqrt{5}$, and $t = 0.005$. (d) The figure of u_5 as $\delta_1 = 1$, $\delta_2 = 1$, and $t = 0$.

The expression (u_4) is the breather two-soliton solution of SK equation which is a periodic wave in y-t and meanwhile is a two-soliton in x, y and in x-t, respectively (refer to Figure 1(c)).

Notice that u_3 and u_4 are also the breather two-soliton solutions, but their structure is different, because the two wave propagation directions are different in the u_3 and u_4, respectively (refer to Figures 1(b) and 1(c)).

If taking $a_1 = iA_1$, $a_3 = iA_3$ in (12), then we have

$$
\begin{aligned}
f_5 = {} & 2\cos\left(A_1 x + A_1^3 y + 9A_1^5 t\right) \\
& + \delta_1 \cos\left(a_2 x + a_2^3 y + 9a_2^5 t\right) \\
& + \delta_2 \cos\left(A_3 x + A_3^3 y + 9A_3^5 t\right),
\end{aligned}
\tag{17}
$$

when $\delta_3 = 1$. Substituting (17) into (2) gives the double-periodic three-wave solution of SK equation as follows:

$$
\begin{aligned}
u_5 = {} & \frac{2\left[2A_1^2\cos(\xi_5) + \delta_1 a_2^2 \cos(\eta_5) + \delta_2 A_3^2 \cos(\gamma_5)\right]}{2\cos(\xi_5) + \delta_1\cos(\eta_5) + \delta_2\cos(\gamma_5)} \\
& + 2\left[\frac{2A_1\sin(\xi_5) + \delta_1 a_2 \sin(\eta_5) + \delta_2 A_3 \sin(\gamma_5)}{2\cos(\xi_5) + \delta_1\cos(\eta_5) + \delta_2\cos(\gamma_5)}\right]^2,
\end{aligned}
\tag{18}
$$

where $\xi_5 = A_1 x + A_1^3 y + 9A_1^5 t$, $\eta_5 = a_2 x + a_2^3 y + 9a_2^5 t$, and $\gamma_5 = A_3 x + A_3^3 y + 9A_3^5 t$.

3. Conclusion

By using bilinear form and extended three-wave type of ansätz approach, we discuss further the (2 + 1)-dimensional

Sawada-Kotera equation and find some new multisoliton solutions. The result shows that the extended three-wave type of ansätz approach may provide us with a straightforward and effective mathematical tool for seeking multiwave solutions of high-dimensional nonlinear evolution equations.

Acknowledgments

This work was supported by Chinese Natural Science Foundation Grant nos. 11061028, 10971169. Sichuan Educational Science Foundation Grant no. 09zc008.

References

[1] M. J. Abolowitz and P. A. Clarkson, *Solitons, Nonlinear Evolution Equations and Inverse Scattering Transform*, Cambridge University Press, Cambridge, UK, 1991.

[2] A. Maccari, "Chaos, solitons and fractals in the nonlinear Dirac equation," *Physics Letters A*, vol. 336, no. 2-3, pp. 117–125, 2005.

[3] Z. Feng, "Comment on "On the extended applications of homogeneous balance method""," *Applied Mathematics and Computation*, vol. 158, no. 2, pp. 593–596, 2004.

[4] X. Q. Liu, H. L. Chen, and Y. Q. Lü, "Explicit solutions of the generalized KdV equations with higher order nonlinearity," *Applied Mathematics and Computation*, vol. 171, no. 1, pp. 315–319, 2005.

[5] C. Wang, Z. Dai, and L. Liang, "Exact three-wave solution for higher dimensional KdV-type equation," *Applied Mathematics and Computation*, vol. 216, no. 2, pp. 501–505, 2010.

[6] Z. Dai, S. Lin, H. Fu, and X. Zeng, "Exact three-wave solutions for the KP equation," *Applied Mathematics and Computation*, vol. 216, no. 5, pp. 1599–1604, 2010.

[7] Z. Li and Z. Dai, "Exact periodic cross-kink wave solutions and breather type of two-solitary wave solutions for the (3 + 1)-dimensional potential-YTSF equation," *Computers and Mathematics with Applications*, vol. 61, no. 8, pp. 1939–1945, 2011.

[8] H. Y. Ruan, "Interactions between two-periodic solitons in the (2 + 1)-dimensional Sawada-Kotera equations," *Acta Physica Sinica*, vol. 53, no. 6, pp. 1618–1622, 2004.

[9] H. M. Fu and Z. D. Dai, "Periodic soliton wave solutions for two-dimension S-K equation," *Journal of Xuzhou Normal University*, vol. 27, no. 4, pp. 20–22, 2009.

[10] Z. Y. Wang and H. L. Lv, "Travelling wave solutions of (2 + 1)-dimensional Sawada-Kotera equation," *Journal of Liaocheng University*, vol. 23, no. 4, 2010.

[11] W. X. Ma and E. Fan, "Linear superposition principle applying to Hirota bilinear equations," *Computers and Mathematics with Applications*, vol. 61, no. 4, pp. 950–959, 2011.

[12] Z. Dai, J. Huang, M. Jiang, and S. Wang, "Homoclinic orbits and periodic solitons for Boussinesq equation with even constraint," *Chaos, Solitons and Fractals*, vol. 26, no. 4, pp. 1189–1194, 2005.

[13] Z. H. Xu, D. Q. Xian, and H. L. Chen, "New periodic solitary-wave solutions for the Benjiamin Ono equation," *Applied Mathematics and Computation*, vol. 215, no. 12, pp. 4439–4442, 2010.

[14] Z. Dai, S. Li, Q. Dai, and J. Huang, "Singular periodic soliton solutions and resonance for the Kadomtsev-Petviashvili equation," *Chaos, Solitons and Fractals*, vol. 34, no. 4, pp. 1148–1153, 2007.

[15] J. H. He, "Asymptotic methods for solitary solutions and compactons," *Abstract and Applied Analysis*, vol. 2012, Article ID 916793, 130 pages, 2012.

Hindawi Publishing Corporation
Abstract and Applied Analysis
Volume 2013, Article ID 784134, 5 pages
http://dx.doi.org/10.1155/2013/784134

Research Article

Symmetry Reduced and New Exact Nontraveling Wave Solutions of (2+1)-Dimensional Potential Boiti-Leon-Manna-Pempinelli Equation

Chen Han-Lin and Xian Da-Quan

School of Sciences, Southwest University of Science and Technology, Mianyang, Sichuan 621010, China

Correspondence should be addressed to Xian Da-Quan; daquanxian@163.com

Received 21 September 2012; Accepted 8 December 2012

Academic Editor: Zhengde Dai

With the aid of Maple symbolic computation and Lie group method, (2+1)-dimensional PBLMP equation is reduced to some (1+1)-dimensional PDE with constant coefficients. Using the homoclinic test technique and auxiliary equation methods, we obtain new exact nontraveling solution with arbitrary functions for the PBLMP equation.

1. Introduction

In this paper, we will consider the potential Boiti-Leon-Manna-Pempinelli (PBLMP) equation

$$u_{yt} + u_{xxxy} - 3u_{xx}u_y - 3u_x u_{xy} = 0, \tag{1}$$

where $u : R_x \times R_y \times R_t^+ \rightarrow R$. By some transformations, the PBLMP equation (1) can be equivalent to the asymmetric Nizhnik-Novikov-Veselov (ANNV) system. In fact, the ANNV equation can be obtained from the inner parameter-dependent symmetry constraint of the KP equation [1] and may be considered as a model for an incompressible fluid [2]. The Painlevé analysis, Lax pair, and some exact solutions have been studied for the PBLMP equation [3]. Tang and Lou obtained the bilinear form of (1) and variable separation solutions including two arbitrary functions by the multilinear variable separation approach [4, 5].

In this paper, by means of Maple symbolic computation, we will use the Lie group method [6, 7], homoclinic test technique [8, 9] and so forth to reduce and solve the PBLMP equation. First, we will derive symmetry of (1). Then we use the symmetry to reduce (1) to some $(1 + 1)$-dimensional PDE with constant coefficients. Finally, solving the reduced PDE by Homoclinic test technique and auxiliary equation methods [10, 11] implies abundant exact nontraveling wave periodic solutions for the PBLMP equation.

2. Symmetry of (1)

This section is devoted to Lie point group symmetries of (1). Let

$$\sigma = \sigma\left(x, y, t, u, u_x, u_y, u_t\right) \tag{2}$$

be the symmetry of (1). Based on Lie group theory [6], σ satisfies the following symmetry equation:

$$\sigma_{yt} + \sigma_{yxxx} - 3u_{xx}\sigma_y - 3u_y\sigma_{xx} - 3u_x\sigma_{xy} - 3u_{xy}\sigma_x = 0. \tag{3}$$

To get some symmetries of (1), we take the function σ in the form

$$\begin{aligned}\sigma = \; & a(x, y, t)\, u_x + b(x, y, t)\, u_y + c(x, y, t)\, u_t \\ & + d(x, y, t)\, u + e(x, y, t),\end{aligned} \tag{4}$$

where a, b, c, d, e are functions of x, y, t to be determined, and $u(x, y, t)$ satisfies (1). Substituting (4) and (1) into (3), one can get

$$\begin{gathered} a = \frac{1}{3}k_1 x + \lambda(t), \qquad b = \mu(y), \\ c = k_1 t + k_2, \qquad d = \frac{1}{3}k_1, \qquad e = \frac{1}{3}\lambda'(t)\, x + \xi(t), \end{gathered} \tag{5}$$

where k_1, k_2 are arbitrary constants. $\lambda(t), \xi(t)$ are arbitrary functions of t. $\mu(y)$ is a arbitrary function of y. Substituting (5) into (4), we obtain the symmetries of (1) as follows:

$$\sigma = \left(\frac{1}{3}k_1 x + \lambda(t)\right) u_x + \mu(y) u_y + (k_1 t + k_2) u_t + \frac{1}{3}k_1 u + \frac{1}{3}\lambda'(t) x + \xi(t). \tag{6}$$

3. Symmetry Reduction of (1)

Based on the integrability of reduced equation of the symmetry (6), we consider the following three cases.

Case 1. Let $k_1 = k_2 = 0$, $\lambda(t) = r$, $\xi(t) = 1$, $\mu(y) = -1/\tau(y)$ in (6), then

$$\sigma = \tau(y)^{-1}\left(r\tau(y) u_x - u_y + \tau(y)\right), \tag{7}$$

where r is an arbitrary nonzero constant, $\tau(y) \neq 0$. Solving the differential equation for $\sigma = 0$, one gets

$$u = \int \tau(y)\, dy + w(\theta, t), \qquad \theta = x + \int r\tau(y)\, dy. \tag{8}$$

Substituting (8) into (1), we get the following $(1+1)$-dimensional nonlinear PDE with constant coefficients:

$$r w_{\theta\theta\theta\theta} - 6 r w_\theta w_{\theta\theta} + r w_{\theta t} - 3 w_{\theta\theta} = 0. \tag{9}$$

Integrating (9) once with respect to θ and taking integration constant to zero yield

$$r w_{\theta\theta\theta} - 3 r w_\theta^2 + r w_t - 3 w_\theta = 0. \tag{10}$$

Case 2. Taking $k_1 = 0$, $k_2 = 1$, $\lambda(t) = 0$, $\xi(t) = 0$, $\mu(y) = 1/\tau(y)$ in (6) yields

$$\sigma = \tau(y)^{-1}\left(u_y + r\tau(y) u_t\right). \tag{11}$$

Solving the differential equation for $\sigma = 0$, one gets

$$u = w(x, \theta), \qquad \theta = t - \int \tau(y)\, dy. \tag{12}$$

Substituting (12) into (1), we have the function $w(x, \theta)$ which must satisfy the following PDE:

$$w_{xxx\theta} - 3 w_{xx} w_\theta - 3 w_x w_{x\theta} + w_{\theta\theta} = 0. \tag{13}$$

Case 3. Let $k_1 = k_2 = 0$, $\lambda(t) = 1$, $\xi(t) = 0$, $\mu(y) = -1/\tau(y)$ in (6), then

$$\sigma = \tau(y)^{-1}\left(\tau(y) u_x - u_y\right). \tag{14}$$

Solving the equation for $\sigma = 0$, we obtain

$$u = w(\theta, t), \qquad \theta = x + \int \tau(y)\, dy. \tag{15}$$

Substituting (15) into (1) yields a reduced PDE of (1) with constant coefficients:

$$w_{\theta\theta\theta\theta} - 6 w_{\theta\theta} w_\theta + w_{\theta t} = 0. \tag{16}$$

Integrating (16) once with respect to θ and taking integration constant to zero yield

$$w_{\theta\theta\theta} - 3 w_\theta^2 + w_t = 0. \tag{17}$$

Combining the above results, we obtain some reduced equations of (1) expressed by (10), (13), and (17), respectively. Meanwhile many new explicit solutions of (1) from these reduced Equations. can be achieved. We omit other cases based on symmetries (6) here.

4. Solve Reduced PDE and Get Exact Nontraveling Wave Solutions of (1)

In this section, we seek exact nontraveling wave solutions of (1) by using some appropriate methods to solve reduced equations (10), (13), and (17).

4.1. Solve Reduced PDE (10). Now, we seek solutions of (10) by auxiliary equation method. Make transformation as follows:

$$w(\theta, t) = \varphi(\xi), \qquad \xi = p\theta + qt, \tag{18}$$

where p, q are nonzero constants. Substituting (18) into (10) obtains an ordinary differential equation for $\varphi(\xi)$ as follows:

$$p^3 r \varphi''' - 3 r p^2 \varphi'^2 + (qr - 3p)\varphi' = 0, \tag{19}$$

where $\varphi' = d\varphi/d\xi$. Let $\varphi' = f$, then (19) can be written as

$$p^3 r f'' - 3 r p^2 f^2 + (qr - 3p) f = 0. \tag{20}$$

This is the fourth type of ellipse equation (12), its solutions are as follows:

$$f = \begin{cases} -\dfrac{3p - qr}{2p^2 r}\operatorname{sech}^2\left[\sqrt{\dfrac{3p - qr}{4p^3 r}}(\xi - \xi_0)\right], & pr(3p - qr) > 0, \\ \dfrac{3p - qr}{2p^2 r}\operatorname{csch}^2\left[\sqrt{\dfrac{3p - qr}{4p^3 r}}(\xi - \xi_0)\right], & pr(3p - qr) > 0, \\ -\dfrac{3p - qr}{2p^2 r}\sec^2\left[\sqrt{-\dfrac{3p - qr}{4p^3 r}}(\xi - \xi_0)\right], & pr(3p - qr) < 0, \end{cases} \tag{21}$$

where ξ_0 is the integration constant. From the result of (21), some new exact solutions u_1 through u_3 of (1) can be obtained:

$$u_1 = \int \tau(y)\,dy - \sqrt{\frac{3p-qr}{pr}} \times \tanh\left[\sqrt{\frac{3p-qr}{4p^3 r}}\left(p\left(x + r\int \tau(y)\,dy\right) + qt - \xi_0\right)\right], \quad pr(3p-qr) > 0,$$

$$u_2 = \int \tau(y)\,dy - \sqrt{\frac{3p-qr}{pr}} \times \coth\left[\sqrt{\frac{3p-qr}{4p^3 r}}\left(p\left(x + r\int \tau(y)\,dy\right) + qt - \xi_0\right)\right], \quad pr(3p-qr) > 0,$$

$$u_3 = \int \tau(y)\,dy - \sqrt{\frac{qr-3p}{pr}} \times \tan\left[\sqrt{\frac{qr-3p}{4p^3 r}}\left(p\left(x + r\int \tau(y)\,dy\right) + qt - \xi_0\right)\right], \quad pr(qr-3p) < 0. \tag{22}$$

Particularly, we assume $p = q = 1$, $r = 2$, $\tau(y) = \sin(y)$, $\xi_0 = 0$, $x = \operatorname{sech}(t)$, then the solution u_1 can be depicted by Figure 1(a). If $p = -1$, $q = 1$, $r = -1$, $\tau(y) = \mp\cos(y)$, $\xi_0 = 0$, $x = \sin(t)$, then u_3 can be depicted by Figures 1(b) and 2(a).

4.2. Solve Reduced PDE (13). Make transformation to (13) as follows:

$$w(x,\theta) = \varphi(\xi), \qquad \xi = kx + c\theta, \tag{23}$$

where k, c are non-zero constants. Substituting (23) into (13) then we have

$$c\varphi' + k^3\varphi''' - 3K^2\varphi'^2 = 0. \tag{24}$$

It is equivalent to (19). Based on the above accordant idea, we can get

$$u_4 = \sqrt{-\frac{c}{2k}} \times \tanh\left[\sqrt{-\frac{c}{2k^3}}\left(kx + c\left(t - \int \tau(y)\,dy\right) - \xi_0\right)\right], \quad kc < 0,$$

$$u_5 = \sqrt{-\frac{c}{2k}} \times \coth\left[\sqrt{-\frac{c}{2k^3}}\left(kx + c\left(t - \int \tau(y)\,dy\right) - \xi_0\right)\right], \quad kc < 0,$$

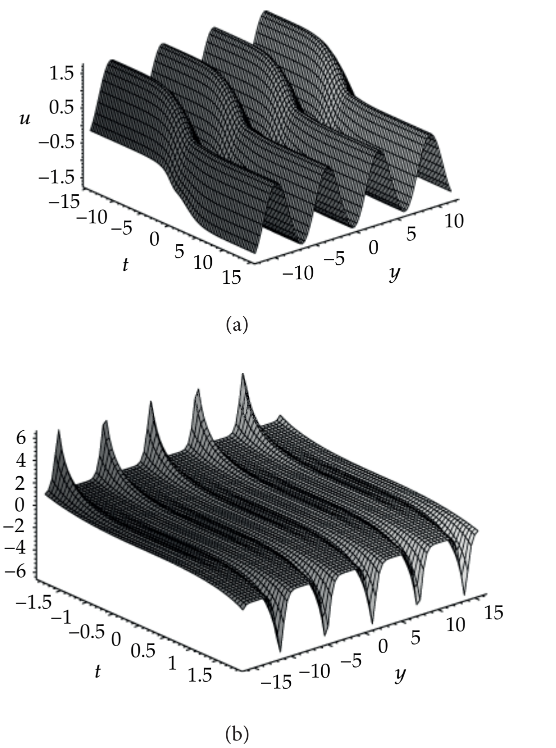

FIGURE 1: (a) The figure of u_1 as $p = 1$, $q = 1$, $r = 2$, $\tau(y) = \sin(y)$, $\xi_0 = 0$, $x = \operatorname{sech}(t)$. (b) The figure of u_3 as $p = -1$, $q = 1$, $r = -1$, $\tau(y) = -\cos(y)$, $\xi_0 = 0$, $x = \sin(t)$.

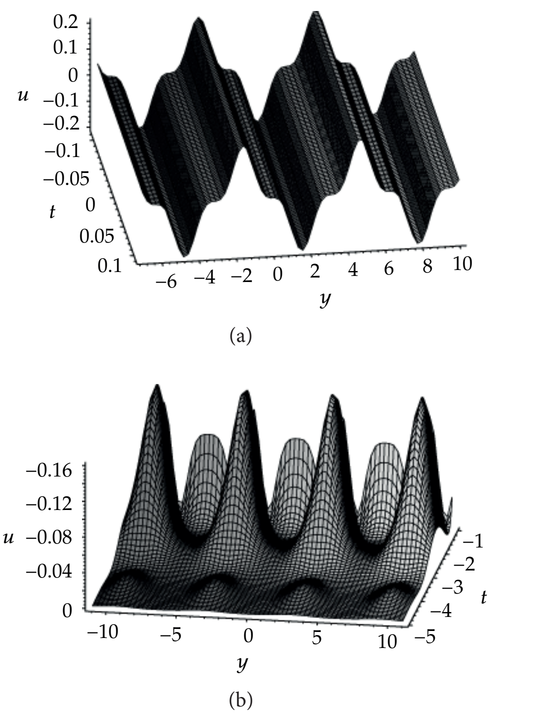

FIGURE 2: (a) The figure of u_3 as $p = -1$, $q = 1$, $r = -1$, $\tau(y) = \cos(y)$, $\xi_0 = 0$, $x = \sin(t)$. (b) The figure of u_9 as $p_1 = 1$, $c_1 = 1$, $p_2 = 1$, $\tau(y) = \sin(y)$, $x = \sin(t)$.

$$u_6 = \sqrt{\frac{c}{2k}} \times \tan\left[\sqrt{\frac{c}{2k^3}}\left(kx+c\left(t-\int \tau(y)\,dy\right)-\xi_0\right)\right], \quad kc>0. \tag{25}$$

4.3. Solve Reduced PDE (17). In this section, we use homoclinic test technique [8, 9] to (17) and transform the unknown function as follows:

$$w(\theta,t) = -2(\ln f(\theta,t))_\theta. \tag{26}$$

Substituting (26) into (17) and using the bilinear form, we can get

$$\left(D_\theta D_t + D_\theta^4\right)(f\cdot f) = 0, \tag{27}$$

where the Hirota operator D is defined in [12]. In this case we choose extended homoclinic test function

$$f = e^{-p_1(\theta-\omega_1 t)} + c_1\cos\left(p_2\left(\theta+\omega_2 t\right)\right) + c_2 e^{p_1(\theta-\omega_1 t)}, \tag{28}$$

where $p_2, \omega_1, \omega_2, c_1$, and c_2 are real constants to be determined. Substituting (28) into (27) yields a set of algebraic equations as follows:

$$\begin{gathered}
p_1 c_1 p_2\left(4\left(p_1^2-p_2^2\right)+\omega_2-\omega_1\right)=0,\\
c_1\left(\left(p_1^4+p_4^4-6p_1^2p_2^2\right)-p_1^2\omega_1-p_2^2\omega_2\right)=0,\\
p_1p_2c_1c_2\left(4\left(p_1^2-p_2^2\right)+\omega_2-\omega_1\right)=0,\\
c_1c_2\left(\left(p_1^4+p_4^4-6p_1^2p_2^2\right)-p_1^2\omega_1-p_2^2\omega_2\right)=0,\\
4\left(4p_1^4c_2+c_1^2p_2^4\right)-4p_1^2\omega_1c_2-c_1^2p_2^2\omega_2=0.
\end{gathered} \tag{29}$$

Solving the above equations (29) yields

$$(1)\begin{cases} p_1 = p_1, \quad p_2 = p_2, \quad c_1 = 0, \quad c_2 = c_2,\\ \omega_1 = 4p_1^2, \quad \omega_2 = \omega_2, \end{cases} \tag{30}$$

$$(2)\begin{cases} p_1 = p_1, \quad p_2 = p_2, \quad c_1 = c_1, \quad c_2 = -\dfrac{c_1^2p_2^2}{p_1^2},\\ \omega_1 = -3p_2^2+p_1^2, \quad \omega_2 = -3p_1^2+p_2^2, \end{cases} \tag{31}$$

$$(3)\begin{cases} p_1 = p_2 i, \quad p_2 = p_2, \quad c_1 = c_1, \quad c_2 = c_2,\\ \omega_1 = -4p_2^2, \quad \omega_2 = 4p_2^2, \end{cases} \tag{32}$$

$$(4)\begin{cases} p_1 = p_2 i, \quad p_2 = p_2, \quad c_1 = c_1, \quad c_2 = \dfrac{1}{4}c_1^2,\\ \omega_1 = \omega_2-8p_2^2, \quad \omega_2 = \omega_2, \end{cases} \tag{33}$$

where $i^2 = -1$. Substituting (30)–(33) into (28) yields the solutions u_7 through u_{11} of (1) as follows:

$$u_7 = -2p_1\tanh\left(p_1\left(x+\int\tau(y)\,dy\right)-4p_1^2t+\frac{1}{2}\ln c_2\right), \tag{34}$$

when $c_2 > 0$ in (30);

$$u_8 = -2p_1\coth\left(p_1\left(x+\int\tau(y)\,dy\right)-4p_1^2t+\frac{1}{2}\ln(-c_2)\right), \tag{35}$$

when $c_2 < 0$ in (30);

$$\begin{aligned}
u_9 &= -2p_1p_2\\
&\quad\times\left(\coth\left(p_1\left(x+\int\tau(y)\,dy\right)-\left(p_1^2-3p_2^2\right)t+\ln\frac{c_1p_2}{p_1}\right)\right.\\
&\quad\left.+\sin\left(p_2\left(x+\int\tau(y)\,dy\right)-\left(3p_1^2-p_2^2\right)t\right)\right)\\
&\quad\times\left(p_2\sinh\left(p_1\left(x+\int\tau(y)\,dy\right)-\left(p_1^2-3p_2^2\right)t+\ln\frac{c_1p_2}{p_1}\right)\right.\\
&\quad\left.+p_1\cos\left(p_2\left(x+\int\tau(y)\,dy\right)-\left(3p_1^2-p_2^2\right)t\right)\right)^{-1},
\end{aligned} \tag{36}$$

when $c_1p_1p_2 > 0$ in (31) (see Figure 2(b));

$$u_{10}(x,y,t) = p_2\tan\left(p_2\left(x+\int\tau(y)\,dy\right)+4p_2^2t\right), \tag{37}$$

when $c_2 = 1$ in (32);

$$\begin{aligned}
u_{11}(x,y,t) &= -2p_2\\
&\quad\times\frac{\sin\left(p_2\left(x+\int\tau(y)\,dy\right)+\left(8p_2^2-\omega_2\right)t\right)+\sin\left(p_2\left(x+\int\tau(y)\,dy\right)+\omega_2t\right)}{\cos\left(p_2\left(x+\int\tau(y)\,dy\right)+\left(8p_2^2-\omega_2\right)t\right)+\cos\left(p_2\left(x+\int\tau(y)\,dy\right)+\omega_2t\right)},
\end{aligned} \tag{38}$$

when $c_1 = 2$ in (33).

Remark 1. If one lets $w_\theta = v$ in (16), then (16) can be written as

$$v_t - 6vv_\theta + v_{\theta\theta\theta} = 0. \tag{39}$$

This is the famous KdV equation.

5. Conclusions

In this paper, a combination of Lie group method and homoclinic test technique and so forth is applied and thus the symmetries (6) are obtained. The (2+1)-dimensional potential Boiti-Leon-Manna-Pempinelli equation (1) is reduced to (1 + 1)-dimensional nonlinear PDE of constant coefficients (10), (13), and (17). Further auxiliary equation method and homoclinic test technique are used and some new exact nontraveling wave solutions are obtained. And they include some special and strange structures to be further studied and other relevant solutions about symmetry (6) will be discussed later in another paper. Our results show that combining the Lie group method with homoclinic test technique and so forth is effective in finding nontraveling wave exact solutions of nonlinear evolution equations.

Acknowledgments

The authors would like to thank Professor Dai Zhengde for his helpful discussions. This work was supported by the Chinese Natural Science Foundation Grant no. 10971169 and the key research projects of Sichuan Provincial Educational Administration, no. 10ZA021.

References

[1] S.-Y. Lou and X.-B. Hu, "Infinitely many Lax pairs and symmetry constraints of the KP equation," *Journal of Mathematical Physics*, vol. 38, no. 12, pp. 6401–6427, 1997.

[2] M. J. Ablowitz and P. A. Clarkson, *Solitons, Nonlinear Evolution Equations and Inverse Scattering*, vol. 149, Cambridge University Press, Cambridge, Mass, USA, 1991.

[3] P. G. Estévez and S. Leble, "A wave equation in 2 + 1 Painlevé analysis and solutions," *Inverse Problems*, vol. 11, no. 4, pp. 925–937, 1995.

[4] X. Y. Tang, *Locallized Excitations and Symmetries of (2+1)-Dimensional Nonlinear Systems*, Shanghai Physics Department, Shanghai Jiao Tong University, Shanghai, China, 2004.

[5] S. Y. Lou and X. Y. Tang, *Methods of Nonlinear Mathematical Physics*, Beling Science Press of China, Beijing, China, 2006.

[6] P. J. Olver, *Applications of Lie Groups to Differential Equations*, vol. 107, Springer, New York, NY, USA, 1986.

[7] D. Q. Xian, "New exact solutions to a class of nonlinear wave equations," *Journal of University of Electronic Science and Technology of China*, vol. 35, no. 6, pp. 977–980, 2006.

[8] Z. Dai and D. Xian, "Homoclinic breather-wave solutions for Sine-Gordon equation," *Communications in Nonlinear Science and Numerical Simulation*, vol. 14, no. 8, pp. 3292–3295, 2009.

[9] Z.-D. Dai, D.-Q. Xian, and D.-L. Li, "Homoclinic breather-wave with convective effect for the (1+1)-dimensional boussinesq equation," *Chinese Physics Letters*, vol. 26, no. 4, Article ID 040203, 2009.

[10] H. L. Chen and D. Q. Xian, "Periodic wave solutions for the Klein-Gordon-Zakharov equation," *Acta Mathematicae Applicatae Sinica*, vol. 29, no. 6, 2006.

[11] S. K. Liu and S. D. Liu, *Nonliner Equations in Physics*, Peking University Press, Beijing, China, 2000.

[12] R. Hirota, "Exact envelope-soliton solutions of a nonlinear wave equation," *Journal of Mathematical Physics*, vol. 14, no. 7, pp. 805–809, 1973.

Hindawi Publishing Corporation
Abstract and Applied Analysis
Volume 2013, Article ID 131207, 8 pages
http://dx.doi.org/10.1155/2013/131207

Research Article

Construction of Target Controllable Image Segmentation Model Based on Homotopy Perturbation Technology

Shu-Li Mei

College of Information and Electrical Engineering, China Agricultural University, Postbox 53, East Campus, 17 Qinghua Donglu Road, Haidian District, Beijing 100083, China

Correspondence should be addressed to Shu-Li Mei; meishuli@163.com

Received 31 December 2012; Revised 4 January 2013; Accepted 6 January 2013

Academic Editor: Lan Xu

Based on the basic idea of the homotopy perturbation method which was proposed by Jihuan He, a target controllable image segmentation model and the corresponding multiscale wavelet numerical method are constructed. Using the novel model, we can get the only right object from the multiobject images, which is helpful to avoid the oversegmentation and insufficient segmentation. The solution of the variational model is the nonlinear PDEs deduced by the variational approach. So, the bottleneck of the variational model on image segmentation is the lower efficiency of the algorithm. Combining the multiscale wavelet interpolation operator and HPM, a semianalytical numerical method can be obtained, which can improve the computational efficiency and accuracy greatly. The numerical results on some images segmentation show that the novel model and the numerical method are effective and practical.

1. Introduction

In general, choosing different parameters in the most common image segmentation methods usually leads to different image segmentation results [1]. In other words, the object segmentation results are uncontrollable by the common methods. To solve the problem, one of the most common strategies is choosing thresholds using prior knowledge or analyzing the distribution of gray values of an image with the gray value histogram. Another method is image enhancement, which can often destroy the contour of the objects.

The variational method on image segmentation is a new image processing technology, which processes lots of better properties in processing medical images such as MRI and CI [2]. In this method, the pictures are taken as continuous energetic fields, and so the corresponding information in digital images such as gradient, divergence, and the curvature of the object contour can be viewed as the differential operators embedded in the variational model on image processing. The traditional complicated image processing such as denoising with texture preserving and exact segmentation can be done by this model. The outstanding work of this field is the energy function for image segmentation proposed by Mumford and Shah, which has been widely used, and its mathematical properties are well analyzed. This is a general approach on image segmentation, where it is assumed that objects can be characterized by smooth surfaces or volumes in three dimensions. In order to solve the Mumford-Shah model with the Euler-Lagrange method, a simplified model was deduced by Chan and Vese, in which the Euclid length was employed instead of the Hausdorff length [3]. So, the simplified model is also called Chan-Vese model. Similar to other image segmentation methods, Chan-Vese model cannot identify the object as well. Multilevel set approach for solving C-V model can segment all the objects in a picture. But it will obviously lead to oversegmentation [4].

In many cases, the purpose of the image segmentation is to get one special single object instead of all the objects in a multiobject image. Therefore, the purpose of this paper is to construct a target controllable image segmentation model based on the basic idea of homotopy perturbation technology (HPM). Using the variational method, the optimal solution of the energy function can be expressed as a nonlinear partial differential equation. So, another task of this study is to construct an effective numerical method on nonlinear PDEs by combining the multiscale wavelet interpolation

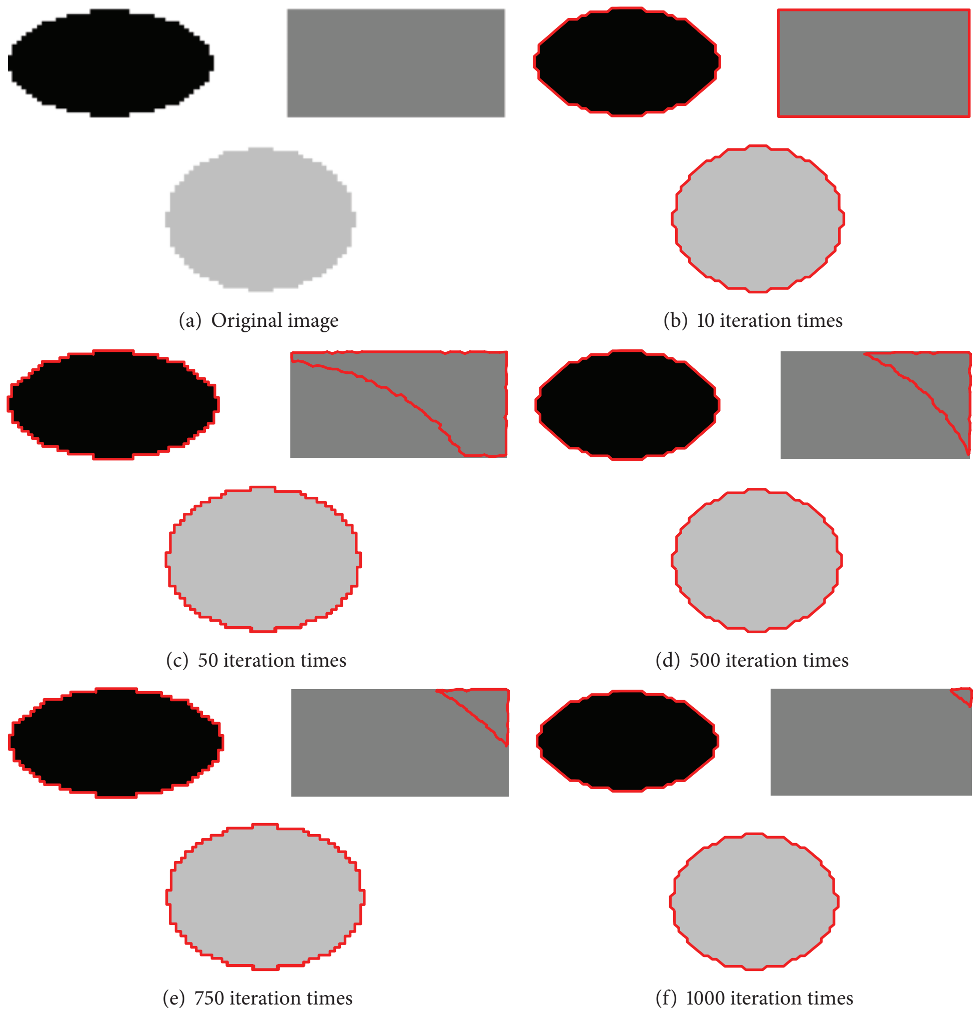

Figure 1: Multiobject image segmentation at $k = 1$ ($\lambda_1 = \lambda_2 = 10$, $\Delta t = 10$).

operator and the homotopy perturbation method. The homotopy perturbation method (HPM) proposed by He [5, 6] is constantly being developed and applied to solve various nonlinear problems by He [7–15] and by others [16–20]. The better improvement is adding an auxiliary parameter into the homotopy equation, which is helpful to eliminate the secular term in the perturbation solution. This can improve the rate of convergence greatly. Unlike analytical perturbation methods, HPM does not depend on small parameter which is difficult to find. The variational iteration method was another simple and effective method for nonlinear equations proposed by He [21–26], which can provide analytical approximations to a rather wide class of nonlinear equations [27–33] without linearization, perturbation, or discretization which can result in massive numerical computation. In order to solve the nonlinear PDEs, it is necessary to introduce the wavelet numerical algorithm [34–37] into HPM.

2. Construction of Target Controllable Image Segmentation Model

In order to solve the Mumford-Shah model with the Euler-Lagrange method, a simplified model was deduced by Chan and Vese, in which the Euclid length was employed instead of the Hausdorff length. This simplified model can also be called the Chan-Vese model, which can be expressed as follows:

$$E^{CV}(c_1, c_2, C) = \lambda_1 \int_{\Omega_1} (I_0 - c_1)^2 dxdy + \lambda_2 \int_{\Omega_2} (I_0 - c_2)^2 dxdy + \nu |C|, \qquad (1)$$

$$c_i = \operatorname{mean}_{\Omega_i}(u_0) = \frac{\int_{\Omega_i} u_0(x, y)\, dxdy}{\operatorname{Area}(\Omega_i)}, \quad i = 1, 2,$$

where λ_1 and λ_2 are positive constants and c_1 and c_2 are the average gray level values inside (Ω_1) and outside (Ω_2) of the object contour, respectively. I_0 denotes the image to process, $|C|$ is the length of the object contour, and ν is the weight parameter. According to the level set method, the contour curves of the objects should be embedded into the level set function as follows:

$$C = \{(x, y) \mid (x, y) \in \Omega, \phi(x, y) = 0\},$$
$$\Omega_1 = \{(x, y) \mid (x, y) \in \Omega, \phi(x, y) > 0\}, \tag{2}$$
$$\Omega_2 = \{(x, y) \mid (x, y) \in \Omega, \phi(x, y) < 0\}.$$

Then, the level set-based C-V model can be rewritten as follows:

$$\begin{aligned} E(c_1, c_2, \phi) = {} & \lambda_1 \int_\Omega |I_0 - c_1|^2 H(\phi)\, dxdy \\ & + \lambda_2 \int_\Omega |I_0 - c_2|^2 (1 - H(\phi))\, dxdy \\ & + \nu \int_\Omega |H(\phi)|\, dxdy, \end{aligned} \tag{3}$$

$$H(\phi) = \begin{cases} 1, & \phi \geq 0, \\ 0, & \phi < 0, \end{cases} \qquad \delta_\varepsilon = \frac{\varepsilon}{\pi(\varepsilon^2 + \phi^2)}.$$

Using the variational method, the PDEs with respect to the variable ϕ can be obtained as follows:

$$\frac{\partial\phi}{\partial t} = \delta_\varepsilon(\phi)\left[\nu \operatorname{div}\left(\frac{\nabla\phi}{|\nabla\phi|}\right) - \lambda_1|I_0 - c_1|^2 + \lambda_2|I_0 - c_2|^2\right]. \tag{4}$$

Obviously, $\operatorname{div}(\nabla\phi/|\nabla\phi|)$ is the curvature of the level set function ϕ, and $\delta_\varepsilon(\phi)$ is used to constrain the growth of the level set function.

The solution of (4) is the level set function $\phi(x, y, t)$ at time t. The zero level set is the object contour curve, which can be obtained by solving $\phi(x, y, t) = 0$.

In the following, what we are talking about is how to construct the target controllable image segmentation model based on the basic idea of HPM. It is easy to understand that the function of the curvature in C-V model is just to preserve the smoothness of the object contour. Neglecting the curvature in (4), the simplified model can be obtained as follows:

$$\frac{\partial\phi}{\partial t} = \delta_\varepsilon(\phi)\left[-\lambda_1|I_0 - c_1|^2 + \lambda_2|I_0 - c_2|^2\right]. \tag{5}$$

In solving the C-V model with HPM and iteration method, the average gray level values inside and outside of the contour curves c_1 and c_2 vary with the evolution of the level set function. This evolution will end up with that the contour curve coincides with the object boundary. Then, c_1 and c_2 become constants, and the right hand of (5) should equal zero; that is,

$$\frac{\lambda_1}{\lambda_2} = \frac{|I_0 - c_2|^2}{|I_0 - c_1|^2}. \tag{6}$$

In general, λ_1 and λ_2 are constant, which are correlated to c_1 and c_2 obviously.

It is easy to understand that the segmentation results and the values of c_1/c_2 are in one-to-one correspondence with each other. So, the object segmentation can be controlled by the value of (λ_1/λ_2). Let $k = \lambda_1/\lambda_2$, $m = c_1/c_2$, and substitute k, m into (5), we can obtain

$$\frac{\partial\phi}{\partial t} = \delta_\varepsilon(\phi)\left[(1 - k) I_0^2 - 2I_0c_2(1 - km) + c_2^2\left(1 - km^2\right)\right]. \tag{7}$$

Let

$$F(I_0) = (1 - k) I_0^2 - 2I_0c_2(1 - km) + c_2^2\left(1 - km^2\right). \tag{8}$$

It is obviously that $F(I_0) = 0$ is the necessary condition for the functional extremum problem about C-V model. The solution of the necessary condition is

$$\begin{aligned} I_0 &= \frac{2c_2(1 - km) \pm \sqrt{4c_2^2(1 - km)^2 - 4(1 - k)c_2^2(1 - km^2)}}{2(1 - k)} \\ &= \frac{(c_2 - kc_1) \pm (c_2 - c_1)\sqrt{k}}{1 - k}. \end{aligned} \tag{9}$$

In the end of the image segmentation processing, the gray level value I_0 of the pixel inside the object contour equals c_2; that is, $I_0 = c_2$ (in Ω_2). Then, the relation between the parameter k and the average gray level value of the image can be expressed as

$$k = \left(\frac{c_1}{c_2 - c_1}\right)^2 \quad \text{or} \quad k = \left(\frac{2c_2 - c_1}{c_2 - c_1}\right)^2. \tag{10}$$

In the end of the image segmentation procedure, the final c_1 and c_2 should be coincident with average gray level values inside and outside of the segmentation target, respectively. They can be determined in advance by the priori knowledge. But in the beginning of the image segmentation processing, c_1 and c_2 are the average gray level values inside and outside of the zero level set, respectively. They are determined by the position of the level set function, which is random in most cases. It is easy to understand that there is a continuous map between the two cases, that is, the connection between the two cases can be set up by the HPM. In other words, the parameter k in (10) can be taken as the homotopy parameter; then, a linear homotopy function for (4) can be constructed as

$$\begin{aligned} & \frac{\partial\phi}{\partial t} - \delta_\varepsilon(\phi)\left[\nu \operatorname{div}\left(\frac{\nabla\phi}{|\nabla\phi|}\right) - |I_0 - c_1|^2\right] + p\delta_\varepsilon(\phi)|I_0 - c_2|^2 \\ & \quad + \alpha p(1 - p)\phi = 0, \end{aligned} \tag{11}$$

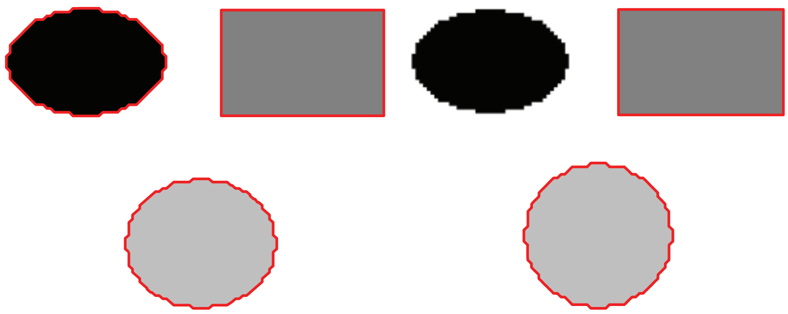

(a) 10 iteration times

(b) 1000 iteration times

Figure 2: Multitarget image segmentation with target controllable model.

where the homotopy parameter $p \in [1, k]$, k is determined by the final c_1 and c_2 based on the priori knowledge in advance and ν is a weight parameter. α is an auxiliary parameter, which can be identified by eliminating the secular term in the perturbation analytical solution.

Equation (11) is the target controllable image segmentation model. It should be pointed out that the auxiliary parameter α appearing in this model is set to zero, as there is no any secular term in the perturbation analytical solution.

3. HPM on Nonlinear System Based on the Multilevel Wavelet Analysis

3.1. Wavelet Numerical Discretization Schemes on C-V Model. The definition domain of the image is defined as $(x_{\min}, x_{\max}) \times (y_{\min}, y_{\max})$, which should be divided evenly into $2^j \times 2^j$ (j is the level number) subdomains according to the wavelet collocation method. The connection nodes between two adjoining subdomains are the discretization points defined as $(x^j_{k_1}, y^j_{k_2})$, where

$$x^j_{k_1} = x_{\min} + k_1 \frac{x_{\max} - x_{\min}}{2^j}, \qquad y^j_{k_1} = y_{\min} + k_2 \frac{y_{\max} - y_{\min}}{2^j}. \tag{12}$$

In addition, $w^{j(m,n)}_{k1,k2}(x, y)$ denotes the multiscale wavelet function and the corresponding mth and nth derivatives with respect to x and y, respectively. The level set function $\phi(x, y, t)$ and the corresponding derivative function can be descretized as follows:

$$\begin{aligned}\phi^{J(m,n)}(x, y, t) &= \sum_{k_{01}=0}^{1} \sum_{k_{02}=0}^{1} \phi\left(x^0_{k_{01}}, y^0_{k_{02}}\right) w^{0(m,n)}_{k_{01},k_{02}}(x, y) \\ &+ \sum_{j=0}^{J-1} \sum_{k_{11}=0}^{2^j-1} \sum_{k_{12}=0}^{2^j-1} \left[\alpha^1_{j,k_{11},k_{12}}(t)\, w^{j+1(m,n)}_{2k_{11}+1,2k_{12}}(x, y)\right. \\ &\quad + \alpha^2_{j,k_{11},k_{12}}(t)\, w^{j+1(m,n)}_{2k_{11},2k_{12}+1}(x, y) \\ &\quad \left. + \alpha^3_{j,k_{11},k_{12}}(t)\, w^{j+1(m,n)}_{2k_{11}+1,2k_{12}+1}(x, y)\right],\end{aligned} \tag{13}$$

where j and J are constants, which denote the wavelet scale number and the maximum of the scale number, respectively. $\alpha^1_{j,k_{11},k_{12}}$, $\alpha^2_{j,k_{11},k_{12}}$, and $\alpha^3_{j,k_{11},k_{12}}$ are the wavelet coefficients at the discretization point $(x^j_{k_1}, y^j_{k_2})$.

According to above definitions, the curvature of the level set $\phi(x, y, t)$ can be expressed approximately as

$$\begin{aligned}\operatorname{div}\left(\frac{\nabla\phi}{|\nabla\phi|}\right) &\approx \operatorname{div}\left(\frac{\nabla\phi^J}{|\nabla\phi^J|}\right) \phi^{J(2,0)}(x, y, t)\left(\phi^{J(0,1)}(x, y, t)\right)^2 \\ &\quad + \phi^{J(0,2)}(x, y, t)\left(\phi^{J(1,0)}(x, y, t)\right)^2 \\ &= \left(-2\phi^{J(0,1)}(x, y, t)\,\phi^{J(1,0)}(x, y, t)\,\phi^{J(1,1)}\right. \\ &\qquad \left.\times (x, y, t)\right) \\ &\quad \times \left(\left(\phi^{J(0,1)}(x, y, t)\right)^2\right. \\ &\qquad \left. + \left(\phi^{J(1,0)}(x, y, t)\right)^2\right)^{-3/2}.\end{aligned} \tag{14}$$

Substituting (14) and (13) into (11), we obtain

$$\begin{aligned}&\frac{\partial\phi^J(x, y, t)}{\partial t} - \delta_\varepsilon\left(\phi^J(x, y, t)\right) \\ &\quad \times \left[\nu \operatorname{div}\left(\frac{\nabla\phi^J(x, y, t)}{|\nabla\phi^J(x, y, t)|}\right) - |I_0 - c_1|^2\right] \\ &\quad + p\delta_\varepsilon\left(\phi^J(x, y, t)\right)|I_0 - c_2|^2 = 0.\end{aligned} \tag{15}$$

Obviously, (15) is a nonlinear ordinary differential equation.

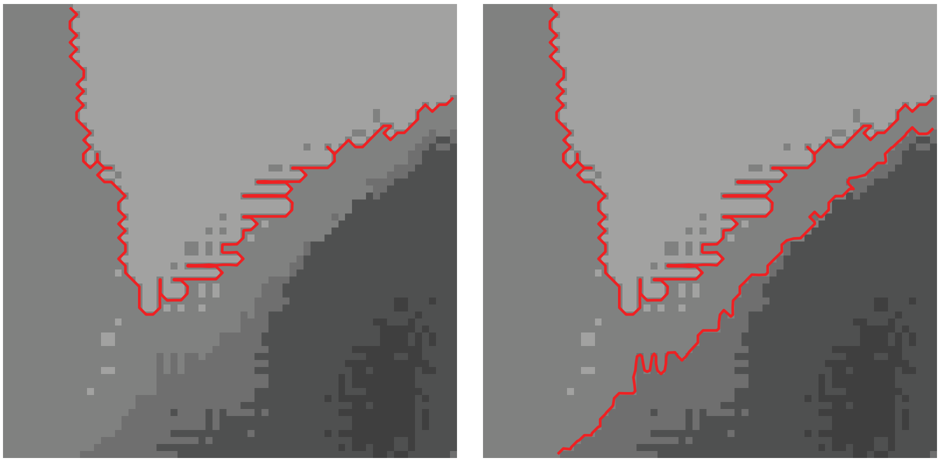

(a) C-V model (b) Target controllable model

FIGURE 3: Special object segmentation.

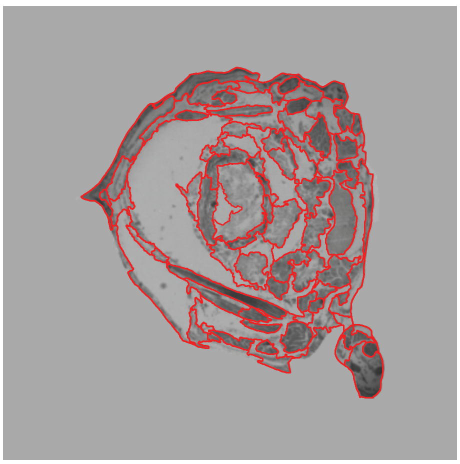

FIGURE 4: Locust's coelom image segmentation results by the target controllable model.

3.2. HPM on Discretization Format of C-V Model. There are various ways to construct a homotopy function. For (15), a linear homotopy function can be constructed as

$$\frac{d\phi^J(x,y,t)}{dt} = (1-\varepsilon)F_n + \varepsilon F_{n+1}, \quad t \in [t_n, t_{n+1}], \tag{16}$$

where

$$F_n = \delta_\varepsilon(\phi^J(x,y,t_n))\left[\nu \operatorname{div}\left(\frac{\nabla\phi^J(x,y,t_n)}{|\nabla\phi^J(x,y,t_n)|}\right) - |I_0 - c_1|^2 + p|I_0 - c_2|^2\right], \quad n \in \mathbb{Z}, \tag{17}$$

where ν is the weight parameter. According to the perturbation theory, the solution of (16) can be expressed as the power series expansion of p

$$\phi^J(x,y,t) = \phi_0^J(x,y,t) + \varepsilon\phi_1^J(x,y,t) + \varepsilon^2\phi_2^J(x,y,t) + \cdots. \tag{18}$$

Substituting (18) into (16) and rearranging based on powers of ε-terms, we have

$$\begin{aligned} \varepsilon^0 &: \frac{d\phi_0^J(x,y,t)}{dt} = F_n \\ \varepsilon^1 &: \frac{d\phi_1^J(x,y,t)}{dt} = f_1 \\ \varepsilon^2 &: \frac{d\phi_2^J(x,y,t)}{dt} = f_2 \\ &\vdots, \end{aligned} \tag{19}$$

where f_1 and f_2 are functions with respect to ε^1 and ε^2, respectively. It is easy to identify the homotopy parameter as

$$\varepsilon(t) = \frac{t-t_n}{t_{n+1}-t_n}, \quad t \in [t_n, t_{n+1}]. \tag{20}$$

Thus, based on the definition of the Taylor series, $\phi_1^J(x,y,t)$ can be identified as $(t_{n+1}-t_n)F_n$, and f_1 can be identified as

$$f_1 = (t_{n+1}-t_n) \times \frac{d}{dt}\left\{\delta_\varepsilon(\phi^J(x,y,t))\left[\nu \operatorname{div}\left(\frac{\nabla\phi^J(x,y,t)}{|\nabla\phi^J(x,y,t)|}\right) - |I_0-c_1|^2 + p|I_0-c_2|^2\right]\right\}. \tag{21}$$

Substituting $\phi_0^J(x,y,t)$ and $\phi_1^J(x,y,t)$ into (18) and assuming $\varepsilon = 1$, the numerical solution of (16) can be obtained subsequently:

$$\phi^J(x,y,t_{n+1}) = \phi_0^J(x,y,t_n) + \phi_1^J(x,y,t_n). \quad (22)$$

Then, the wavelet coefficient can be obtained as follows:

$$\begin{aligned}
\alpha^1_{j,k1,k2}(t_{n+1}) &= \phi^J\left(x^{j+1}_{2k1+1}, y^{j+1}_{2k2}, t_{n+1}\right) \\
&\quad - \Bigg[\sum_{k01=0}^{1}\sum_{k02=0}^{1}\phi^J\left(x^0_{k01}, y^0_{k02}, t_{n+1}\right) \times w^0_{k01,k02}\left(x^{j+1}_{2k1+1}, y^{j+1}_{2k2}\right) \\
&\quad + \sum_{j1=0}^{j-1}\sum_{k11=0}^{2^{j1}}\sum_{k12=0}^{2^{j2}}\Big(\alpha^1_{j1,k11,k12} w^{j1+1}_{2k11+1,2k12} \times \left(x^{j+1}_{2k1+1}, y^{j+1}_{2k2}\right) \\
&\quad + \alpha^2_{j1,k11,k12} w^{j1+1}_{2k11,2k12+1} \times \left(x^{j+1}_{2k1+1}, y^{j+1}_{2k2}\right) \\
&\quad + \alpha^3_{j1,k11,k12} \times w^{j1+1}_{2k11+1,2k12+1} \times \left(x^{j+1}_{2k1+1}, y^{j+1}_{2k2}\right)\Big)\Bigg], \\
\alpha^2_{j,k1,k2}(t_{n+1}) &= \phi^J\left(x^{j+1}_{2k1}, y^{j+1}_{2k2+1}, t_{n+1}\right) \\
&\quad - \Bigg[\sum_{k01=0}^{1}\sum_{k02=0}^{1}\phi^J\left(x^0_{k01}, y^0_{k02}, t_{n+1}\right) \times w^0_{k01,k02}\left(x^{j+1}_{2k1}, y^{j+1}_{2k2+1}\right) \\
&\quad + \sum_{j1=0}^{j-1}\sum_{k11=0}^{2^{j1}}\sum_{k12=0}^{2^{j2}}\Big(\alpha^1_{j1,k11,k12} w^{j1+1}_{2k11+1,2k12} \times \left(x^{j+1}_{2k1}, y^{j+1}_{2k2+1}\right) \\
&\quad + \alpha^2_{j1,k11,k12} w^{j1+1}_{2k11,2k12+1} \times \left(x^{j+1}_{2k1}, y^{j+1}_{2k2+1}\right) \\
&\quad + \alpha^3_{j1,k11,k12} \times w^{j1+1}_{2k11+1,2k12+1} \times \left(x^{j+1}_{2k1}, y^{j+1}_{2k2+1}\right)\Big)\Bigg], \\
\alpha^3_{j,k1,k2}(t_{n+1}) &= \phi^J\left(x^{j+1}_{2k1+1}, y^{j+1}_{2k2+1}, t_{n+1}\right) \\
&\quad - \Bigg[\sum_{k01=0}^{1}\sum_{k02=0}^{1}\phi^J\left(x^0_{k01}, y^0_{k02}, t_{n+1}\right) \times w^0_{k01,k02}\left(x^{j+1}_{2k1+1}, y^{j+1}_{2k2+1}\right) \\
&\quad + \sum_{j1=0}^{j-1}\sum_{k11=0}^{2^{j1}}\sum_{k12=0}^{2^{j2}}\Big(\alpha^1_{j1,k11,k12} w^{j1+1}_{2k11+1,2k12} \times \left(x^{j+1}_{2k1+1}, y^{j+1}_{2k2+1}\right) \\
&\quad + \alpha^2_{j1,k11,k12} w^{j1+1}_{2k11,2k12+1} \times \left(x^{j+1}_{2k1+1}, y^{j+1}_{2k2+1}\right) \\
&\quad + \alpha^3_{j1,k11,k12} \times w^{j1+1}_{2k11+1,2k12+1} \times \left(x^{j+1}_{2k1+1}, y^{j+1}_{2k2+1}\right)\Big)\Bigg],
\end{aligned} \quad (23)$$

where

$$x^j_k = x_{\min} + \frac{x_{\max} - x_{\min}}{2^j}, \qquad y^j_k = y_{\min} + \frac{y_{\max} - y_{\min}}{2^j}. \quad (24)$$

$w^j_{k1,k2}(x,y)$ is the quasi-Shannon wavelet function; that is,

$$\begin{aligned}
w^j_{k1,k2}(x,y) &= \frac{\sin\left[(\pi/\Delta j_1)\left(x - x^j_{k1}\right)\right]}{(\pi/\Delta\Delta j_1)\left(x - x^j_{k1}\right)} \\
&\quad \times \frac{\sin\left[(\pi/\Delta j_2)\left(y - y^j_{k2}\right)\right]}{(\pi/\Delta j_2)\left(y - y^j_{k2}\right)} \\
&\quad \times \exp\left(-\frac{1}{2r^2}\frac{\left(x - x^j_{k1}\right)^2}{\left(\Delta j_1\right)^2}\right) \\
&\quad \times \exp\left(-\frac{1}{2r^2}\frac{\left(y - y^j_{k2}\right)^2}{\left(\Delta j_2\right)^2}\right),
\end{aligned} \quad (25)$$

$$\Delta j_1 = \frac{x_{\max} - x_{\min}}{2^j}, \qquad \Delta j_2 = \frac{y_{\max} - y_{\min}}{2^j}.$$

Substituting the three wavelet coefficients into (16), $\phi^{J(m,n)}(x, y, t_{n+1})$ can be obtained; then we can obtain F_{n+1} as follows:

$$F_{n+1} = \delta_\varepsilon\left(\phi^J\left(x, y, t_{n+1}\right)\right) \times \left[\nu \operatorname{div}\left(\frac{\nabla\phi^J\left(x, y, t_{n+1}\right)}{\left|\nabla\phi^J\left(x, y, t_{n+1}\right)\right|}\right) - \left|I_0 - c_1\right|^2 + p\left|I_0 - c_2\right|^2\right], \quad n \in \mathbb{Z}. \tag{26}$$

At last, we can obtain the image segmentation result expressed in the level set as follows:

$$\phi^J\left(x, y, t_{n+1}\right) = \phi^J\left(x, y, t_n\right) + \frac{t_{n+1} - t_n}{2}\left(F_n + F_{n+1}\right). \tag{27}$$

4. Numerical Experiences and Discussion

In this section, we take some multiobject images as examples to illustrate the efficiency of the target controllable image segmentation model compared with the C-V model. The original image showed in Figure 1 consisted of three geometrical solid objects. The color of the background is white, and whole area is 1. The gray level values and the areas of the three objects are showed in Table 1. The image segmentation aims to get the circular and the rectangular objects. In other words, we want to take the black elliptical object as the background.

The segmentation results of C-V model are showed in Figure 1. With the increasing of the iteration times, the rectangular object becomes a part of the background gradually instead of the elliptical object, which does not meet our requirement obviously.

The segmentation results with the target controllable model are showed in Figure 2. The final $c_1 = 255 \times 0.7976/(0.7976 + 0.0568) = 238.05$, and $c_2 = (163 \times 0.0723 + 7 \times 0.0733)/(0.0723 + 0.0733) = 86.464$. It should be pointed out that the final c_1 and c_2 can be obtained by priori knowledge in most cases. At the beginning of the segmentation, all the three objects are obtained as the foreground. With the increasing of the iteration times, the black object is gradually pushed into the background and out of the object region.

Figure 3 is an enlarged local image of the locust body cavity. The objects have an irregular shape with a slightly serrated border which can introduce over an insufficient segmentation. So it is difficult to segment with other methods. Using the target controllable model, we can get the right object easily. This example shows that the novel model and the corresponding numerical method are practical. Indeed, the novel model has been used to segment the locust's coelom images (Figure 4).

5. Conclusions

C-V model is a kind of the modified Mumford-Shah model which has been widely used in medical images, and its mathematical properties are well analyzed. But the segmentation result is usually uncontrollable. The target controllable image segmentation model proposed in this paper is based on the idea of HPM. The numerical experiences show that the novel model and the corresponding numerical algorithm are effective and practical. It meets the requirement of the medical images segmentation.

Table 1: The gray level values and areas of all objects.

	Ellipse	Circle	Squareness	Background
Gray level value	0	163	7	255
Area	0.0568	0.0723	0.0733	0.7976

Acknowledgment

This work is supported by the National Natural Science Foundation of China under Grant no. 41171337 and National Key Technologies R & D Program of China under Grant no. 2012BAD35B02.

References

[1] O. Wirjadi, "Survey of 3rd image segmentation methods," Berichte Des Fraunhofer ITWM 123, 2007.

[2] L. A. Vese and T. F. Chan, "A multiphase level set framework for image segmentation using the Mumford and Shah model," *International Journal of Computer Vision*, vol. 50, no. 3, pp. 271–293, 2002.

[3] T. F. Chan, S. Esedoglu, and M. Nikolova, "Algorithms for finding global minimizers of image segmentation and denoising models," UCLA Report, 2004.

[4] T. Goldstein, X. Bresson, and S. Osher, "Geometric applications of the split Bregman method: segmentation and surface reconstruction," *Journal of Scientific Computing*, vol. 45, no. 1–3, pp. 272–293, 2010.

[5] J.-H. He, "A coupling method of a homotopy technique and a perturbation technique for non-linear problems," *International Journal of Non-Linear Mechanics*, vol. 35, no. 1, pp. 37–43, 2000.

[6] J.-H. He, "Homotopy perturbation technique," *Computer Methods in Applied Mechanics and Engineering*, vol. 178, no. 3-4, pp. 257–262, 1999.

[7] J.-H. He, "Asymptotology by homotopy perturbation method," *Applied Mathematics and Computation*, vol. 156, no. 3, pp. 591–596, 2004.

[8] J.-H. He, "Homotopy perturbation method: a new nonlinear analytical technique," *Applied Mathematics and Computation*, vol. 135, no. 1, pp. 73–79, 2003.

[9] J. H. He, "Limit cycle and bifurcation of nonlinear problems," *Chaos, Solitons and Fractals*, vol. 26, no. 3, pp. 827–833, 2005.

[10] J. H. He, "Application of homotopy perturbation method to nonlinear wave equations," *Chaos, Solitons and Fractals*, vol. 26, no. 3, pp. 695–700, 2005.

[11] J.-H. He, "Periodic solutions and bifurcations of delay-differential equations," *Physics Letters A*, vol. 347, no. 4–6, pp. 228–230, 2005.

[12] J.-H. He, "The homotopy perturbation method nonlinear oscillators with discontinuities," *Applied Mathematics and Computation*, vol. 151, no. 1, pp. 287–292, 2004.

[13] J. H. He, "Homotopy perturbation method for bifurcation of nonlinear problems," *International Journal of Nonlinear Sciences and Numerical Simulation*, vol. 6, no. 2, pp. 207–208, 2005.

[14] J.-H. He, "Asymptotic methods for solitary solutions and compactons," *Abstract and Applied Analysis*, vol. 2012, Article ID 916793, 130 pages, 2012.

[15] J.-H. He, "New interpretation of homotopy perturbation method," *International Journal of Modern Physics B*, vol. 20, no. 18, pp. 2561–2568, 2006.

[16] L. Cveticanin, "Homotopy-perturbation method for pure nonlinear differential equation," *Chaos, Solitons and Fractals*, vol. 30, no. 5, pp. 1221–1230, 2006.

[17] S. Abbasbandy, "Application of He's homotopy perturbation method for Laplace transform," *Chaos, Solitons and Fractals*, vol. 30, no. 5, pp. 1206–1212, 2006.

[18] M. Rafei and D. D. Ganji, "Explicit solutions of Helmholtz equation and fifth-order KdV equation using homotopy perturbation method," *International Journal of Nonlinear Sciences and Numerical Simulation*, vol. 7, no. 3, pp. 321–328, 2006.

[19] A. M. Siddiqui, R. Mahmood, and Q. K. Ghori, "Thin film flow of a third grade fluid on a moving belt by he's homotopy perturbation method," *International Journal of Nonlinear Sciences and Numerical Simulation*, vol. 7, no. 1, pp. 7–14, 2006.

[20] A. M. Siddiqui, M. Ahmed, and Q. K. Ghori, "Couette and poiseuille flows for non-newtonian fluids," *International Journal of Nonlinear Sciences and Numerical Simulation*, vol. 7, no. 1, pp. 15–26, 2006.

[21] J.-H. He, "Variational iteration method: a kind of non-linear analytical technique: some examples," *International Journal of Non-Linear Mechanics*, vol. 34, no. 4, pp. 699–708, 1999.

[22] J.-H. He, "Variational iteration method for autonomous ordinary differential systems," *Applied Mathematics and Computation*, vol. 114, no. 2-3, pp. 115–123, 2000.

[23] J.-H. He and X.-H. Wu, "Construction of solitary solution and compacton-like solution by variational iteration method," *Chaos, Solitons & Fractals*, vol. 29, no. 1, pp. 108–113, 2006.

[24] J.-H. He, "Approximate analytical solution for seepage flow with fractional derivatives in porous media," *Computer Methods in Applied Mechanics and Engineering*, vol. 167, no. 1-2, pp. 57–68, 1998.

[25] J.-H. He, "Approximate solution of nonlinear differential equations with convolution product nonlinearities," *Computer Methods in Applied Mechanics and Engineering*, vol. 167, no. 1-2, pp. 69–73, 1998.

[26] J.-H. He, "Asymptotic methods: the next frontier towards nonlinear science," *Computers & Mathematics with Applications*, vol. 61, no. 8, pp. 1907–1908, 2011.

[27] M. A. Abdou and A. A. Soliman, "Variational iteration method for solving Burger's and coupled Burger's equations," *Journal of Computational and Applied Mathematics*, vol. 181, no. 2, pp. 245–251, 2005.

[28] A. A. Soliman, "A numerical simulation and explicit solutions of KdV-Burgers' and Lax's seventh-order KdV equations," *Chaos, Solitons and Fractals*, vol. 29, no. 2, pp. 294–302, 2006.

[29] E. M. Abulwafa, M. A. Abdou, and A. A. Mahmoud, "The solution of nonlinear coagulation problem with mass loss," *Chaos, Solitons & Fractals*, vol. 29, no. 2, pp. 313–330, 2006.

[30] S. Momani and S. Abuasad, "Application of He's variational iteration method to Helmholtz equation," *Chaos, Solitons & Fractals*, vol. 27, no. 5, pp. 1119–1123, 2006.

[31] N. Bildik and A. Konuralp, "The use of variational iteration method, differential transform method and adomian decomposition method for solving different types of nonlinear partial differential equations," *International Journal of Nonlinear Sciences and Numerical Simulation*, vol. 7, no. 1, pp. 65–70, 2006.

[32] Z. M. Odibat and S. Momani, "Application of variational iteration method to nonlinear differential equations of fractional order," *International Journal of Nonlinear Sciences and Numerical Simulation*, vol. 7, no. 1, pp. 27–34, 2006.

[33] J.-H. He, "Some asymptotic methods for strongly nonlinear equations," *International Journal of Modern Physics B*, vol. 20, no. 10, pp. 1141–1199, 2006.

[34] Z. Wan-Xie, "On precise integration method," *Journal of Computer and Applied Mathematics*, vol. 163, no. 1, pp. 59–78, 2004.

[35] D.-C. Wan and G.-W. Wei, "The study of quasi wavelets based numerical method applied to Burgers' equations," *Applied Mathematics and Mechanics*, vol. 21, no. 10, pp. 991–1001, 2000.

[36] G. W. Wei, "Quasi wavelets and quasi interpolating wavelets," *Chemical Physics Letters*, vol. 296, no. 3-4, pp. 253–258, 1998.

[37] S.-L. Mei, C. J. Du, and S. W. Zhang, "Asymptotic numerical method for multi-degree-of-freedom nonlinear dynamic systems," *Chaos, Solitons and Fractals*, vol. 35, no. 3, pp. 536–542, 2008.

Hindawi Publishing Corporation
Abstract and Applied Analysis
Volume 2013, Article ID 578942, 11 pages
http://dx.doi.org/10.1155/2013/578942

Research Article

A Novel Method for Solving KdV Equation Based on Reproducing Kernel Hilbert Space Method

Mustafa Inc,[1] Ali Akgül,[2] and Adem Kiliçman[3]

[1] *Department of Mathematics, Science Faculty, Firat University, 23119 Elaziğ, Turkey*
[2] *Department of Mathematics, Education Faculty, Dicle University, 21280 Diyarbakır, Turkey*
[3] *Department of Mathematics and Institute for Mathematical Research, University Putra Malaysia (UPM), Selangor, 43400 Serdang, Malaysia*

Correspondence should be addressed to Adem Kiliçman; akilicman@putra.upm.edu.my

Received 19 September 2012; Revised 17 December 2012; Accepted 23 December 2012

Academic Editor: Lan Xu

We propose a reproducing kernel method for solving the KdV equation with initial condition based on the reproducing kernel theory. The exact solution is represented in the form of series in the reproducing kernel Hilbert space. Some numerical examples have also been studied to demonstrate the accuracy of the present method. Results of numerical examples show that the presented method is effective.

1. Introduction

In this paper, we consider the Korteweg-de Vries (KdV) equation of the form

$$u_t(x,t) + \varepsilon u(x,t)\, u_x(x,t) + u_{xxx}(x,t) = 0, \qquad -\infty < x < \infty,\ t > 0, \tag{1}$$

with initial condition

$$u(x,0) = f(x). \tag{2}$$

The constant factor ε is just a scaling factor to make solutions easier to describe. Most of the authors chose ε to be *one* or *six*. Some mathematicians and physicians investigated the exact solution of the KdV equation without having either initial conditions or boundary conditions [1], while others studied its numerical solution [2, 3].

The numerical solution of KdV equation is of great importance because it is used in the study of nonlinear dispersive waves. This equation is used to describe many important physical phenomena. Some of these studies are the shallow water waves and the ion acoustic plasma waves [4]. It represents the long time evolution of wave phenomena, in which the effect of nonlinear terms uu_x is counterbalanced by the dispersion u_{xxx}. Thus it has been found to model many wave phenomena such as waves in enharmonic crystals, bubble liquid mixtures, ion acoustic wave, and magnetohydrodynamic waves in a warm plasma as well as shallow water waves [5, 6].

The KdV equation exhibits solutions such as solitary waves, solitons and recurrence [7]. Goda [8] and Vliegenthart [9] used the finite difference method to obtain the numerical solution of KdV equation. Soliman [2] used the collocation solution with septic splines to obtain the solution of the KdV equation. Numerical solutions of KdV equation were obtained by the variational iteration method, finite difference method [3, 10], and by using the meshless based on the collocation with radial basis functions [11]. Wazwaz presented the Adomian decomposition method for KdV equation with different initial conditions [12]. Syam [13] worked the ADM for solving the nonlinear KdV equation with appropriate initial conditions.

In present work, we use the following equation:

$$v(x,t) = u(x,t) - u(x,0), \tag{3}$$

by transformation for homogeneous initial condition of (1) and (2), we get the following:

$$v_t(x,t) + A(x,t)\,v(x,t) + B(x,t)\,v_x(x,t) + v_{xxx}(x,t) = f\left(x,t,v(x,t),v_x(x,t)\right), \quad v(x,0) = 0, \tag{4}$$

where

$$\begin{aligned} A(x,t) &= \varepsilon f'(x), \\ B(x,t) &= \varepsilon f(x), \\ f\left(x,t,v(x,t),v_x(x,t)\right) &= -\varepsilon v(x,t)\,v_x(x,t) - \varepsilon f(x)\,f'(x) - f'''(x). \end{aligned} \tag{5}$$

In this paper, we solve (1) and (2) by using reproducing kernel method. The nonlinear problem is solved easily and elegantly without linearizing the problem by using RKM. The technique has many advantages over the classical techniques; mainly, it avoids linearization to find analytic and approximate solutions of (1) and (2). It also avoids discretization and provides an efficient numerical solution with high accuracy, minimal calculation, and avoidance of physically unrealistic assumptions. In the next section, we will describe the procedure of this method.

The theory of reproducing kernels was used for the first time at the beginning of the 20th century by Zaremba in his work on boundary value problems for harmonic and biharmonic functions [14]. Reproducing kernel theory has important application in numerical analysis, differential equations, probability and statistics [14, 15]. Recently, using the RKM, some authors discussed fractional differential equation, nonlinear oscillator with discontinuity, singular nonlinear two-point periodic boundary value problems, integral equations, and nonlinear partial differential equations [14, 15].

The efficiency of the method was used by many authors to investigate several scientific applications. Geng and Cui [16] applied the RKHSM to handle the second-order boundary value problems. Yao and Cui [17] and Wang et al. [18] investigated a class of singular boundary value problems by this method and the obtained results were good. Zhou et al. [19] used the RKHSM effectively to solve second-order boundary value problems. In [20], the method was used to solve nonlinear infinite-delay-differential equations. Wang and Chao [21], Li and Cui [22], and Zhou and Cui [23] independently employed the RKHSM to variable-coefficient partial differential equations. Geng and Cui [24] and Du and Cui [25] investigated to the approximate solution of the forced Duffing equation with integral boundary conditions by combining the homotopy perturbation method and the RKHSM. Lv and Cui [26] presented a new algorithm to solve linear fifth-order boundary value problems. In [27, 28], authors developed a new existence proof of solutions for nonlinear boundary value problems. Cui and Du [29] obtained the representation of the exact solution for the nonlinear Volterra-Fredholm integral equations by using the reproducing kernel space. Wu and Li [30] applied iterative reproducing kernel method to obtain the analytical approximate solution of a nonlinear oscillator with discontinuities. Inc et al. [15] used this method for solving Telegraph equation.

The paper is organized as follows. Section 2 introduces several reproducing kernel spaces and a linear operator. The representation in $W(\Omega)$ is presented in Section 3. Section 4 provides the main results. The exact and approximate solutions of (1) and (2) and an iterative method are developed for the kind of problems in the reproducing kernel space. We have proved that the approximate solution uniformly converges to the exact solution. Some numerical experiments are illustrated in Section 5. We give some conclusions in Section 6.

2. Preliminaries

2.1. Reproducing Kernel Spaces. In this section, we define some useful reproducing kernel spaces.

Definition 1 (reproducing kernel). Let E be a nonempty abstract set. A function $K : E \times E \to C$ is a reproducing kernel of the Hilbert space H if and only if

(a) for all $t \in E$, $K(\cdot,t) \in H$,

(b) for all $t \in E$, $\varphi \in H$, $\langle \varphi(\cdot), K(\cdot,t)\rangle = \varphi(t)$. This is also called "the reproducing property": the value of the function φ at the point t is reproduced by the inner product of φ with $K(\cdot,t)$.

Then we need some notation that we use in the development of the paper. In the next we define several spaces with inner product over those spaces. Thus the space is defined as

$$W_2^4[0,1] = \left\{ \begin{array}{c} v(x) \mid v(x), v'(x), v''(x), v'''(x) \\ \text{are absolutely continuous in } [0,1], \\ v^{(4)}(x) \in L^2[0,1],\ x \in [0,1] \end{array} \right\}. \tag{6}$$

The inner product and the norm in $W_2^4[0,1]$ are defined, respectively, by

$$\begin{aligned} \langle v(x), g(x)\rangle_{W_2^4} &= \sum_{i=0}^{3} v^{(i)}(0)\,g^{(i)}(0) + \int_0^1 v^{(4)}(x)\,g^{(4)}(x)\,dx, \quad v(x), g(x) \in W_2^4[0,1], \\ \|v\|_{W_2^4} &= \sqrt{\langle v, v\rangle_{W_2^4}}, \quad v \in W_2^4[0,1]. \end{aligned} \tag{7}$$

The space $W_2^4[0,1]$ is a reproducing kernel space, that is, for each fixed $y \in [0,1]$ and any $v(x) \in W_2^4[0,1]$, there exists a function $R_y(x)$ such that

$$v(y) = \left\langle v(x), R_y(x)\right\rangle_{W_2^4}. \tag{8}$$

Similarly, we define the space

$$W_2^2[0,T]=\left\{\begin{array}{c} v(t)\mid v(t),v'(t)\\ \text{are absolutely continuous in } [0,T],\\ v''(t)\in L^2[0,T],\ t\in[0,T],\ v(0)=0\end{array}\right\}. \tag{9}$$

The inner product and the norm in $W_2^2[0,T]$ are defined, respectively, by

$$\begin{aligned}\langle v(t),g(t)\rangle_{W_2^2} &= \sum_{i=0}^{1} v^{(i)}(0)\,g^{(i)}(0)\\ &\quad+\int_0^T v''(t)\,g''(t)\,dt,\quad v(t),g(t)\in W_2^2[0,T],\end{aligned} \tag{10}$$

$$\|v\|_{W_1}=\sqrt{\langle v,v\rangle_{W_2^2}},\quad v\in W_2^2[0,T].$$

Thus the space $W_2^2[0,T]$ is also a reproducing kernel space and its reproducing kernel function $r_s(t)$ can be given by

$$r_s(t)=\begin{cases} st+\dfrac{s}{2}t^2-\dfrac{1}{6}t^3, & t\le s,\\ st+\dfrac{t}{2}s^2-\dfrac{1}{6}s^3, & t>s,\end{cases} \tag{11}$$

and the space

$$W_2^2[0,1]=\left\{\begin{array}{c} v(x)\mid v(x),v'(x)\\ \text{are absolutely continuous in } [0,1],\\ v''(x)\in L^2[0,1],\ x\in[0,1]\end{array}\right\}, \tag{12}$$

where the inner product and and the norm in $W_2^2[0,1]$ are defined, respectively, by

$$\langle v(t),g(t)\rangle_{W_2^2}=\sum_{i=0}^{1} v^{(i)}(0)\,g^{(i)}(0)+\int_0^T v''(t)\,g''(t)\,dt,$$

$$v(t),g(t)\in W_2^2[0,1],$$

$$\|v\|_{W_2}=\sqrt{\langle v,v\rangle_{W_2^2}},\quad v\in W_2^2[0,1]. \tag{13}$$

The space $W_2^2[0,1]$ is a reproducing kernel space, and its reproducing kernel function $Q_y(x)$ is given by

$$Q_y(x)=\begin{cases} 1+xy+\dfrac{y}{2}x^2-\dfrac{1}{6}x^3, & x\le y,\\ 1+xy+\dfrac{x}{2}y^2-\dfrac{1}{6}y^3, & x>y.\end{cases} \tag{14}$$

Similarly, the space $W_2^1[0,T]$ is defined by

$$W_2^1[0,T]=\left\{\begin{array}{c} v(t)\mid v(t)\ \text{is absolutely continuous in } [0,T],\\ v(t)\in L^2[0,T],\ t\in[0,T]\end{array}\right\}. \tag{15}$$

The inner product and the norm in $W_2^1[0,T]$ are defined, respectively, by

$$\langle v(t),g(t)\rangle_{W_2^1}=v(0)\,g(0)+\int_0^T v'(t)\,g'(t)\,dt,$$

$$v(t),g(t)\in W_2^1[0,T], \tag{16}$$

$$\|v\|_{W_2^1}=\sqrt{\langle v,v\rangle_{W_2^1}},\quad v\in W_2^1[0,T].$$

The space $W_2^1[0,T]$ is a reproducing kernel space and its reproducing kernel function $q_s(t)$ is given by

$$q_s(t)=\begin{cases} 1+t, & t\le s,\\ 1+s, & t>s.\end{cases} \tag{17}$$

Further we define the space $W(\Omega)$ as

$$W(\Omega)=\left\{\begin{array}{c} v(x,t)\mid \dfrac{\partial^4 v}{\partial x^3\partial t},\ \text{is completely continuous,}\\ \text{in } \Omega=[0,1]\times[0,T],\\ \dfrac{\partial^6 v}{\partial x^4\partial t^2}\in L^2(\Omega),\ v(x,0)=0\end{array}\right\}, \tag{18}$$

and the inner product and the norm in $W(\Omega)$ are defined, respectively, by

$$\begin{aligned}\langle v(x,t),g(x,t)\rangle_W &= \sum_{i=0}^{3}\int_0^T\left[\frac{\partial^2}{\partial t^2}\frac{\partial^i}{\partial x^i}v(0,t)\,\frac{\partial^2}{\partial t^2}\frac{\partial^i}{\partial x^i}g(0,t)\right]dt\\ &\quad+\sum_{j=0}^{1}\left\langle\frac{\partial^j}{\partial t^j}v(x,0),\frac{\partial^j}{\partial t^j}g(x,0)\right\rangle_{W_2^4}\\ &\quad+\int_0^T\int_0^1\left[\frac{\partial^4}{\partial x^4}\frac{\partial^2}{\partial t^2}v(x,t)\,\frac{\partial^4}{\partial x^4}\frac{\partial^2}{\partial t^2}g(x,t)\right]dx\,dt,\end{aligned} \tag{19}$$

$$\|v\|_W=\sqrt{\langle v,v\rangle_W},\quad v\in W(\Omega).$$

Now we have the following theorem.

Theorem 2. *The space $W_2^4[0,1]$ is a complete reproducing kernel space and, its reproducing kernel function $R_y(x)$ can be denoted by*

$$R_y(x)=\begin{cases}\displaystyle\sum_{i=1}^{8}c_i(y)\,x^{i-1}, & x\le y,\\ \displaystyle\sum_{i=1}^{8}d_i(y)\,x^{i-1}, & x>y,\end{cases} \tag{20}$$

where

$$c_1(y)=1,\quad c_2(y)=y,\quad c_3(y)=\frac{1}{4}y^2,$$
$$c_4(y)=\frac{1}{36}y^3,\quad c_5(y)=\frac{1}{144}y^3,\quad c_6(y)=-\frac{1}{240}y^2,$$
$$c_7(y)=\frac{1}{720}y,\quad c_8(y)=-\frac{1}{5040},$$
$$d_1(y)=1-\frac{1}{5040}y^7,\quad d_2(y)=y+\frac{1}{720}y^6,$$
$$d_3(y)=\frac{1}{4}y^2-\frac{1}{240}y^5,\quad d_4(y)=\frac{1}{36}y^3+\frac{1}{144}y^4,$$
$$d_5(y)=0,\quad d_6(y)=0,\quad d_7(y)=0,\quad d_8(y)=0. \tag{21}$$

Proof. Since

$$\begin{aligned}\langle v(x),R_y(x)\rangle_{W_2^4} &= \sum_{i=0}^{3} v^{(i)}(0)R_y^{(i)}(0)+\int_0^1 v^{(4)}(x)R_y^{(4)}(x)\,dx,\\ &\quad (v(x),R_y(x)\in W_2^4[0,1])\end{aligned} \tag{22}$$

through iterative integrations by parts for (22) we have

$$\begin{aligned}\langle v(x),R_y(x)\rangle_{W_2^4} &= \sum_{i=0}^{3} v^{(i)}(0)\left[R_y^{(i)}(0)-(-1)^{(3-i)}R_y^{(7-i)}(0)\right]\\ &\quad+\sum_{i=0}^{3}(-1)^{(3-i)}v^{(i)}(1)R_y^{(7-i)}(1)\\ &\quad+\int_0^1 v(x)R_y^{(8)}(x)\,dx.\end{aligned} \tag{23}$$

Note that property of the reproducing kernel

$$\langle v(x),R_y(x)\rangle_{W_2^4}=v(y). \tag{24}$$

If

$$\begin{aligned}&R_y(0)+R_y^{(7)}(0)=0,\\ &R_y'(0)-R_y^{(6)}(0)=0,\\ &R_y''(0)+R_y^{(5)}(0)=0,\\ &R_y'''(0)-R_y^{(4)}(0)=0,\\ &R_y^{(4)}(1)=0,\\ &R_y^{(5)}(1)=0,\\ &R_y^{(6)}(1)=0,\\ &R_y^{(7)}(1)=0,\end{aligned} \tag{25}$$

then by (23) we obtain the following equation:

$$R_y^{(8)}(x)=\delta(x-y), \tag{26}$$

when $x\neq y$,

$$R_y^{(8)}(x)=0; \tag{27}$$

therefore

$$R_y(x)=\begin{cases}\displaystyle\sum_{i=1}^{8}c_i(y)x^{i-1}, & x\leq y,\\ \displaystyle\sum_{i=1}^{8}d_i(y)x^{i-1}, & x>y.\end{cases} \tag{28}$$

Since

$$R_y^{(8)}(x)=\delta(x-y), \tag{29}$$

we have

$$\partial^k R_{y^+}(y)=\partial^k R_{y^-}(y),\quad k=0,1,2,3,4,5,6, \tag{30}$$

$$\partial^7 R_{y^+}(y)-\partial^7 R_{y^-}(y)=1. \tag{31}$$

From (25)–(31), the unknown coefficients $c_i(y)$ ve $d_i(y)$ $(i=1,2,\ldots,8)$ can be obtained. Thus $R_y(x)$ is given by

$$R_y(x)=\begin{cases}1+yx+\frac{1}{4}y^2x^2+\frac{1}{36}y^3x^3+\frac{1}{144}y^3x^4\\ \quad-\frac{1}{240}y^2x^5+\frac{1}{720}yx^6-\frac{1}{5040}x^7, & x\leq y,\\ 1+xy+\frac{1}{4}x^2y^2+\frac{1}{36}x^3y^3+\frac{1}{144}x^3y^4\\ \quad-\frac{1}{240}x^2y^5+\frac{1}{720}xy^6-\frac{1}{5040}y^7, & x>y.\end{cases} \tag{32}$$

□

Theorem 3. *The $W(\Omega)$ is a reproducing kernel space, and its reproducing kernel function is*

$$K_{(y,s)}(x,t)=R_y(x)r_s(t), \tag{33}$$

such that for any $v(x,t)\in W(\Omega)$,

$$\begin{aligned}v(y,s)&=\langle v(x,t),K_{(y,s)}(x,t)\rangle_W,\\ K_{(y,s)}(x,t)&=K_{(x,t)}(y,s),\end{aligned} \tag{34}$$

where $R_y(x)$, $r_s(t)$ are the reproducing kernel functions of $W_2^4[0,1]$ and $W_2^2[0,T]$, respectively.

Similarly, the space $\widehat{W}(\Omega)$ is defined as

$$\widehat{W}(\Omega)=\left\{\begin{array}{c}v(x,t)\mid \dfrac{\partial v}{\partial x}\text{ is completely continuous}\\ \text{in }\Omega=[0,1]\times[0,T],\\ \dfrac{\partial^3 v}{\partial x^2\partial t}\in L^2(\Omega)\end{array}\right\}. \tag{35}$$

The inner product and the norm in $\widehat{W}(\Omega)$ are defined, respectively, by

$$\begin{aligned}
&\langle v(x,t), g(x,t)\rangle_{\widehat{W}} \\
&= \sum_{i=0}^{1}\int_0^T \left[\frac{\partial}{\partial t}\frac{\partial^i}{\partial x^i}v(0,t)\frac{\partial}{\partial t}\frac{\partial^i}{\partial x^i}g(0,t)\right]dt \\
&\quad + \langle v(x,0), g(x,0)\rangle_{W_2^2} \\
&\quad + \int_0^T\int_0^1 \left[\frac{\partial^2}{\partial x^2}\frac{\partial}{\partial t}v(x,t)\frac{\partial^2}{\partial x^2}\frac{\partial}{\partial t}g(x,t)\right]dx\,dt, \\
&\|v\|_{\widehat{W}} = \sqrt{\langle v, v\rangle_{\widehat{W}}}, \quad v \in \widehat{W}(\Omega).
\end{aligned} \tag{36}$$

Then the space $\widehat{W}(\Omega)$ is a reproducing kernel space and its reproducing kernel function $G_{(y,s)}(x,t)$ is

$$G_{(y,s)}(x,t) = Q_y(x)\,Q_s(t). \tag{37}$$

3. Solution Representation in $W(\Omega)$

On defining the linear operator $L : W(\Omega) \to \widehat{W}(\Omega)$ as

$$\begin{aligned}
Lv &= v_t(x,t) - 24\left(\operatorname{sech}^3 x\right)(\sinh x)\,v(x,t) \\
&\quad + 12\left(\operatorname{sech}^2 x\right)v_x(x,t) + v_{xxx}(x,t),
\end{aligned} \tag{38}$$

model problem (1) changes to the following problem:

$$\begin{aligned}
&Lv(x,t) = f(x,t,v,v_x), \quad (x,t) \in [0,1]\times[0,T] \subset \mathbb{R}^2, \\
&v(x,0) = 0.
\end{aligned} \tag{39}$$

Lemma 4. *The operator L is a bounded linear operator.*

Proof. We have

$$\begin{aligned}
\|Lv\|_{\widehat{W}}^2 &= \sum_{i=0}^{1}\int_0^T\left[\frac{\partial}{\partial t}\frac{\partial^i}{\partial x^i}Lv(0,t)\right]^2 dt \\
&\quad + \langle Lv(x,0), Lv(x,0)\rangle_{W_2} \\
&\quad + \int_0^T\int_0^1\left[\frac{\partial^2}{\partial x^2}\frac{\partial}{\partial t}Lv(x,t)\right]^2 dx\,dt \\
&= \sum_{i=0}^{1}\int_0^T\left[\frac{\partial}{\partial t}\frac{\partial^i}{\partial x^i}Lv(0,t)\right]^2 dt \\
&\quad + \sum_{i=0}^{1}\left[\frac{\partial^i}{\partial x^i}Lv(0,0)\right]^2 + \int_0^1\left[\frac{\partial^2}{\partial x^2}Lv(x,0)\right]^2 \\
&\quad + \int_0^T\int_0^1\left[\frac{\partial^2}{\partial x^2}\frac{\partial}{\partial t}Lv(x,t)\right]^2 dx\,dt,
\end{aligned} \tag{40}$$

since

$$\begin{aligned}
v(x,t) &= \langle v(\xi,\eta), K_{(x,t)}(\xi,\eta)\rangle_W, \\
Lv(x,t) &= \langle v(\xi,\eta), LK_{(x,t)}(\xi,\eta)\rangle_W,
\end{aligned} \tag{41}$$

on using the the continuity of $K_{(x,t)}(\xi,\eta)$, we have

$$|Lv(x,t)| \le \|v\|_W \left\|LK_{(x,t)}(\xi,\eta)\right\|_W \le a_0\|v\|_W. \tag{42}$$

Similarly for $i = 0, 1$,

$$\begin{aligned}
\frac{\partial^i}{\partial x^i}Lv(x,t) &= \left\langle v(\xi,\eta), \frac{\partial^i}{\partial x^i}LK_{(x,t)}(\xi,\eta)\right\rangle_W, \\
\frac{\partial}{\partial t}\frac{\partial^i}{\partial x^i}Lv(x,t) &= \left\langle v(\xi,\eta), \frac{\partial}{\partial t}\frac{\partial^i}{\partial x^i}LK_{(x,t)}(\xi,\eta)\right\rangle_W,
\end{aligned} \tag{43}$$

and then

$$\begin{aligned}
\left|\frac{\partial^i}{\partial x^i}Lv(x,t)\right| &\le e_i\|v\|_W, \\
\left|\frac{\partial}{\partial t}\frac{\partial^i}{\partial x^i}Lv(x,t)\right| &\le f_i\|v\|_W.
\end{aligned} \tag{44}$$

Therefore

$$\|Lv(x,t)\|_{\widehat{W}}^2 \le \sum_{i=0}^{1}\left(e_i^2 + f_i^2\right)\|v\|_W^2 \le a^2\|v\|_W^2. \tag{45}$$

□

Now, choose a countable dense subset $\{(x_1,t_1),(x_2,t_2),\ldots\}$ in $\Omega = [0,1]\times[0,T]$ and define

$$\Phi_i(x,t) = G_{(x_i,t_i)}(x,t), \qquad \Psi_i(x,t) = L^*\Phi_i(x,t), \tag{46}$$

where L^* is the adjoint operator of L. The orthonormal system $\{\widehat{\Psi}_i(x,t)\}_{i=1}^{\infty}$ of $W(\Omega)$ can be derived from the process of Gram-Schmidt orthogonalization of $\{\Psi_i(x,t)\}_{i=1}^{\infty}$ as

$$\widehat{\Psi}_i(x,t) = \sum_{k=1}^{i}\beta_{ik}\Psi_k(x,t). \tag{47}$$

Theorem 5. *Suppose that $\{(x_i,t_i)\}_{i=1}^{\infty}$ is dense in Ω; then $\{\Psi_i(x,t)\}_{i=1}^{\infty}$ is complete system in $W(\Omega)$ and*

$$\Psi_i(x,t) = L_{(y,s)}K_{(y,s)}(x,t)\Big|_{(y,s)=(x_i,t_i)}. \tag{48}$$

Proof. We have

$$\begin{aligned}
\Psi_i(x,t) &= \left(L^*\Phi_i\right)(x,t) = \left\langle\left(L^*\Phi_i\right)(y,s), K_{(x,t)}(y,s)\right\rangle_W \\
&= \left\langle\Phi_i(y,s), L_{(y,s)}K_{(x,t)}(y,s)\right\rangle_{\widehat{W}} \\
&= L_{(y,s)}K_{(x,t)}(y,s)\Big|_{(y,s)=(x_i,t_i)} \\
&= L_{(y,s)}K_{(y,s)}(x,t)\Big|_{(y,s)=(x_i,t_i)}.
\end{aligned} \tag{49}$$

Clearly $\Psi_i(x,t) \in W(\Omega)$. For each fixed $v(x,t) \in W(\Omega)$, if

$$\langle v(x,t), \Psi_i(x,t)\rangle_W = 0, \quad i = 1,2,\ldots \tag{50}$$

then

$$\begin{aligned}\langle v(x,t),(L^*\Phi_i)(x,t)\rangle_W &= \langle Lv(x,t),\Phi_i(x,t)\rangle_{\widehat{W}} \\ &= (Lv)(x_i,t_i)=0,\quad i=1,2,\ldots.\end{aligned} \tag{51}$$

Note that $\{(x_i,t_i)\}_{i=1}^{\infty}$ is dense in $W(\Omega)$, hence, $(Lv)(x,t)=0$. It follows that $v=0$ from the existence of L^{-1}. So the proof is complete. □

Theorem 6. *If $\{(x_i,t_i)\}_{i=1}^{\infty}$ is dense in Ω, then the solution of (39) is*

$$v(x,t)=\sum_{i=1}^{\infty}\sum_{k=1}^{i}\beta_{ik}f(x_k,t_k,v(x_k,t_k),\partial_x v(x_k,t_k))\widehat{\Psi}_i(x,t). \tag{52}$$

Proof. Since $\{\Psi_i(x,t)\}_{i=1}^{\infty}$ is complete system in $W(\Omega)$, we have

$$\begin{aligned}v(x,t) &= \sum_{i=1}^{\infty}\left\langle v(x,t),\widehat{\Psi}_i(x,t)\right\rangle_W\widehat{\Psi}_i(x,t) \\ &= \sum_{i=1}^{\infty}\sum_{k=1}^{i}\beta_{ik}\langle v(x,t),\Psi_k(x,t)\rangle_W\widehat{\Psi}_i(x,t) \\ &= \sum_{i=1}^{\infty}\sum_{k=1}^{i}\beta_{ik}\langle v(x,t),L^*\Phi_k(x,t)\rangle_W\widehat{\Psi}_i(x,t) \\ &= \sum_{i=1}^{\infty}\sum_{k=1}^{i}\beta_{ik}\langle Lv(x,t),\Phi_k(x,t)\rangle_{\widehat{W}}\widehat{\Psi}_i(x,t) \\ &= \sum_{i=1}^{\infty}\sum_{k=1}^{i}\beta_{ik}\left\langle Lv(x,t),G_{(x_k,t_k)}(x,t)\right\rangle_{\widehat{W}}\widehat{\Psi}_i(x,t) \\ &= \sum_{i=1}^{\infty}\sum_{k=1}^{i}\beta_{ik}Lu(x_k,t_k)\widehat{\Psi}_i(x,t) \\ &= \sum_{i=1}^{\infty}\sum_{k=1}^{i}\beta_{ik}f(x_k,t_k,v(x_k,t_k),\partial_x v(x_k,t_k))\widehat{\Psi}_i(x,t).\end{aligned} \tag{53}$$

□

Now the approximate solution $v_n(x,t)$ can be obtained from the n-term intercept of the exact solution $v(x,t)$ and

$$v_n(x,t)=\sum_{i=1}^{n}\sum_{k=1}^{i}\beta_{ik}f(x_k,t_k,v(x_k,t_k),\partial_x v(x_k,t_k))\widehat{\Psi}_i(x,t). \tag{54}$$

Obviously

$$\|v_n(x,t)-v(x,t)\|\longrightarrow 0,\quad (n\longrightarrow\infty). \tag{55}$$

4. The Method Implementation

If we write

$$A_i=\sum_{k=1}^{i}\beta_{ik}f(x_k,t_k,v(x_k,t_k),\partial_x v(x_k,t_k)), \tag{56}$$

then (52) can be written as

$$v(x,t)=\sum_{i=1}^{\infty}A_i\widehat{\Psi}_i(x,t). \tag{57}$$

Now let $(x_1,t_1)=0$; then from the initial conditions of (39), $v(x_1,t_1)$ is known. We put $v_0(x_1,t_1)=v(x_1,t_1)$ and define the n-term approximation to $v(x,t)$ by

$$v_n(x,t)=\sum_{i=1}^{n}B_i\widehat{\Psi}_i(x,t), \tag{58}$$

where

$$B_i=\sum_{k=1}^{i}\beta_{ik}f(x_k,t_k,v_{k-1}(x_k,t_k),\partial_x v_{k-1}(x_k,t_k)). \tag{59}$$

In the sequel, we verify that the approximate solution $v_n(x,t)$ converges to the exact solution, uniformly. First the following lemma is given.

Lemma 7. *If $v_n \xrightarrow{\|\cdot\|} \hat{v}$, $(x_n,t_n)\rightarrow(y,s)$, and $f(x,t,v(x,t),v_x(x,t))$ is continuous, then*

$$\begin{aligned}&f(x_n,t_n,v_{n-1}(x_n,t_n),\partial_x v_{n-1}(x_n,t_n)) \\ &\quad\longrightarrow f(y,s,\hat{v}(y,s),\partial_x\hat{v}(y,s)).\end{aligned} \tag{60}$$

Proof. Since

$$\begin{aligned}&|v_{n-1}(x_n,t_n)-\hat{v}(y,s)| \\ &\quad=|v_{n-1}(x_n,t_n)-v_{n-1}(y,s)+v_{n-1}(y,s)-\hat{v}(y,s)| \\ &\quad\le|v_{n-1}(x_n,t_n)-v_{n-1}(y,s)|+|v_{n-1}(y,s)-\hat{v}(y,s)|.\end{aligned} \tag{61}$$

From the definition of the reproducing kernel, we have

$$\begin{aligned}v_{n-1}(x_n,t_n) &= \left\langle v_{n-1}(x,t),K_{(x_n,t_n)}(x,t)\right\rangle_W, \\ v_{n-1}(y,s) &= \left\langle v_{n-1}(x,t),K_{(y,s)}(x,t)\right\rangle_W.\end{aligned} \tag{62}$$

It follows that

$$\begin{aligned}&|v_{n-1}(x_n,t_n)-v_{n-1}(y,s)| \\ &\quad=\left|\left\langle v_{n-1}(x,t),K_{(x_n,t_n)}(x,t)-K_{(y,s)}(x,t)\right\rangle\right|.\end{aligned} \tag{63}$$

From the convergence of $v_{n-1}(x,t)$, there exists a constant M, such that

$$\|v_{n-1}(x,t)\|_W\le N\|\hat{v}(y,s)\|_W,\quad\text{as } n\ge M. \tag{64}$$

At the same time, we can prove

$$\left\|K_{(x_n,t_n)}(x,t)-K_{(y,s)}(x,t)\right\|_W \longrightarrow 0, \quad \text{as } n\longrightarrow\infty \tag{65}$$

using Theorem 3. Hence

$$v_{n-1}(x_n,t_n)\longrightarrow \widehat{v}(y,s), \quad \text{as } (x_n,t_n)\longrightarrow (y,s). \tag{66}$$

In a similiar way it can be shown that

$$\partial_x v_{n-1}(x_n,t_n)\longrightarrow \partial_x\widehat{v}(y,s), \quad \text{as } (x_n,t_n)\longrightarrow (y,s). \tag{67}$$

So

$$\begin{aligned} &f(x_n,t_n,v_{n-1}(x_n,t_n),\partial_x v_{n-1}(x_n,t_n)) \\ &\quad\longrightarrow f(y,s,\widehat{v}(y,s),\partial_x\widehat{v}(y,s)). \end{aligned} \tag{68}$$

This completes the proof. □

Theorem 8. *Suppose that $\|v_n\|$ is a bounded in* (58) *and* (39) *has a unique solution. If $\{(x_i,t_i)\}_{i=1}^{\infty}$ is dense in Ω, then the n-term approximate solution $v_n(x,t)$ derived from the above method converges to the analytical solution $v(x,t)$ of* (39) *and*

$$v(x,t)=\sum_{i=1}^{\infty}B_i\widehat{\Psi}_i(x,t), \tag{69}$$

where B_i is given by (59).

Proof. First, we prove the convergence of $v_n(x,t)$. From (58), we infer that

$$v_{n+1}(x,t)=v_n(x,t)+B_{n+1}\widehat{\Psi}_{n+1}(x,t). \tag{70}$$

The orthonormality of $\{\widehat{\Psi}_i\}_{i=1}^{\infty}$ yields that

$$\left\|v_{n+1}\right\|^2=\left\|v_n\right\|^2+B_{n+1}^2=\sum_{i=1}^{n+1}B_i^2. \tag{71}$$

In terms of (71), it holds that $\|v_{n+1}\| > \|v_n\|$. Due to the condition that $\|v_n\|$ is bounded, $\|v_n\|$ is convergent and there exists a constant c such that

$$\sum_{i=1}^{\infty}B_i^2=c. \tag{72}$$

This implies that

$$\{B_i\}_{i=1}^{\infty}\in l^2. \tag{73}$$

If $m>n$, then

$$\begin{aligned} &\left\|v_m-v_n\right\|^2 \\ &\quad=\left\|v_m-v_{m-1}+v_{m-1}-v_{m-2}+\cdots+v_{n+1}-v_n\right\|^2 \\ &\quad=\left\|v_m-v_{m-1}\right\|^2+\left\|v_{m-1}-v_{m-2}\right\|^2+\cdots+\left\|v_{n+1}-v_n\right\|^2. \end{aligned} \tag{74}$$

On account of

$$\left\|v_m-v_{m-1}\right\|^2=B_m^2, \tag{75}$$

consequently

$$\left\|v_m-v_n\right\|^2=\sum_{l=n+1}^{m}B_l^2\longrightarrow 0, \quad \text{as } n\longrightarrow\infty. \tag{76}$$

The completeness of $W(\Omega)$ shows that $v_n \to \widehat{v}$ as $n\to\infty$. Now, let we prove that $\widehat{v}$ is the solution of (39). Taking limits in (58) we get

$$\widehat{v}(x,t)=\sum_{i=1}^{\infty}B_i\widehat{\Psi}_i(x,t). \tag{77}$$

Note that

$$\begin{aligned} (L\widehat{v})(x,t)&=\sum_{i=1}^{\infty}B_iL\widehat{\Psi}_i(x,t), \\ (L\widehat{v})(x_l,t_l)&=\sum_{i=1}^{\infty}B_iL\widehat{\Psi}_i(x_l,t_l) \\ &=\sum_{i=1}^{\infty}B_i\left\langle L\widehat{\Psi}_i(x,t),\Phi_l(x,t)\right\rangle_{\widehat{W}} \\ &=\sum_{i=1}^{\infty}B_i\left\langle \widehat{\Psi}_i(x,t),L^*\Phi_l(x,t)\right\rangle_{W} \\ &=\sum_{i=1}^{\infty}B_i\left\langle \widehat{\Psi}_i(x,t),\Psi_l(x,t)\right\rangle_{W}. \end{aligned} \tag{78}$$

Therefore

$$\begin{aligned} \sum_{l=1}^{i}\beta_{il}(L\widehat{v})(x_l,t_l)&=\sum_{i=1}^{\infty}B_i\left\langle \widehat{\Psi}_i(x,t),\sum_{l=1}^{i}\beta_{il}\Psi_l(x,t)\right\rangle_W \\ &=\sum_{i=1}^{\infty}B_i\left\langle \widehat{\Psi}_i(x,t),\widehat{\Psi}_l(x,t)\right\rangle_W=B_l. \end{aligned} \tag{79}$$

In view of (71), we have

$$L\widehat{v}(x_l,t_l)=f(x_l,t_l,u_{l-1}(x_l,t_l),\partial_x u_{l-1}(x_l,t_l)). \tag{80}$$

Since $\{(x_i,t_i)\}_{i=1}^{\infty}$ is dense in Ω, for each $(y,s)\in\Omega$, there exists a subsequence $\{(x_{n_j},t_{n_j})\}_{j=1}^{\infty}$ such that

$$\left(x_{n_j},t_{n_j}\right)\longrightarrow (y,s), \quad j\longrightarrow\infty. \tag{81}$$

We know that

$$L\widehat{v}\left(x_{n_j},t_{n_j}\right)=f\left(x_{n_j},t_{n_j},u_{n_{j-1}}\left(x_{n_j},t_{n_j}\right),\partial_x u_{n_{j-1}}\left(x_{n_j},t_{n_j}\right)\right). \tag{82}$$

Let $j\to\infty$; by Lemma 7 and the continuity of f, we have

$$(L\widehat{v})(y,s)=f(y,s,\widehat{v}(y,s),\partial_x\widehat{v}(y,s)), \tag{83}$$

which indicates that $\widehat{v}(x,t)$ satisfy (39). This completes the proof. □

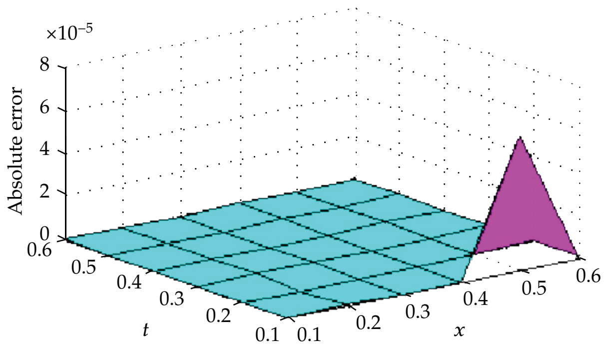

Figure 1: The absolute error for Example 10 at $0.1 \leq x,\ t \leq 0.6$.

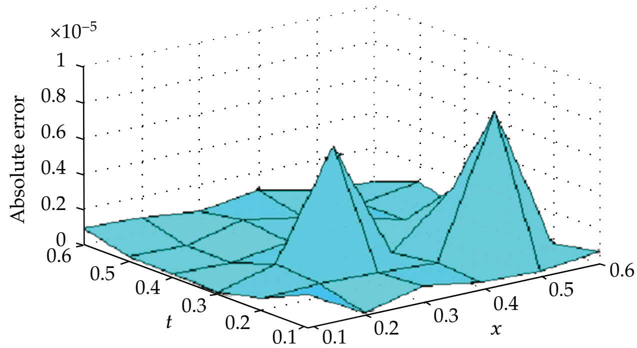

Figure 2: The absolute error for Example 11 at $0.1 \leq x,\ t \leq 0.6$.

Remark 9. In a same manner, it can be proved that

$$\left\| \frac{\partial v_n(x,t)}{\partial x} - \frac{\partial v(x,t)}{\partial x} \right\| \longrightarrow 0, \quad \text{as } n \longrightarrow \infty, \tag{84}$$

where

$$\begin{aligned} \frac{\partial v(x,t)}{\partial x} &= \sum_{i=1}^{\infty} B_i \frac{\partial \widehat{\Psi}_i(x,t)}{\partial x}, \\ \frac{\partial v_n(x,t)}{\partial x} &= \sum_{i=1}^{n} B_i \frac{\partial \widehat{\Psi}_i(x,t)}{\partial x}, \end{aligned} \tag{85}$$

where B_i is given by (59).

5. Numerical Results

In this section, two numerical examples are provided to show the accuracy of the present method. All computations are performed by Maple 16. Results obtained by the method are compared with exact solution and the ADM [13] of each example are found to be in good agreement with each others. The RKM does not require discretization of the variables, that is, time and space, it is not effected by computation round off errors and one is not faced with necessity of large computer memory and time. The accuracy of the RKM for the KdV equation is controllable and absolute errors are very small with present choice of x and t (see Tables 1, 2, 3, and 4 and Figures 1, 2, and 3). The numerical results that we obtained justify the advantage of this methodology.

Example 10 (see [13]). Consider the following KdV equation with initial condition

$$\begin{aligned} &u_t(x,t) + \varepsilon u(x,t) u_x(x,t) \\ &\quad + u_{xxx}(x,t) = 0, \quad -\infty < x < \infty,\ t > 0, \\ &u(x,0) = 2\operatorname{sech}^2 x, \quad -\infty < x < \infty \end{aligned} \tag{86}$$

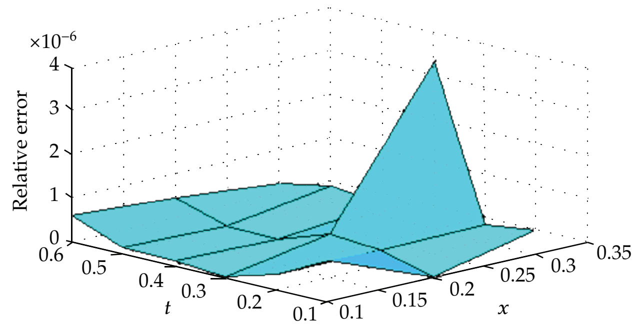

Figure 3: The relative error for Example 11 at $0.1 \leq x,\ t \leq 0.6$.

with $\varepsilon = 6$. The exact solution is $u(x,t) = 2\operatorname{sech}^2(x - 4t)$. If we apply (3) to (86), then the following (87) is obtained

$$\begin{aligned} &v_t(x,t) - 24\operatorname{sech}^3 x \sinh x v(x,t) \\ &\quad + 12\operatorname{sech}^2 x v_{xx}(x,t) + v_{xxx}(x,t) \\ &\quad = -6v(x,t) v_x(x,t) - 32\frac{\sinh x}{\cosh^3 x} \\ &\quad + 48\frac{\sinh^3 x}{\cosh^5 x} + 48\operatorname{sech}^5 x \sinh x, \\ &v(x,0) = 0. \end{aligned} \tag{87}$$

Example 11 (see [13]). We now consider the KdV equation with initial condition

$$\begin{aligned} &u_t(x,t) + \varepsilon u(x,t) u_x(x,t) \\ &\quad + u_{xxx}(x,t) = 0, \quad -\infty < x < \infty,\ t > 0, \\ &u(x,0) = 6\operatorname{sech}^2 x, \quad -\infty < x < \infty. \end{aligned} \tag{88}$$

Table 1: The exact solution of Example 10 for initial condition at $0.1 \leq x, t \leq 0.6$.

x/t	0.1	0.2	0.3	0.4	0.5	0.6
0.1	1.830273924	1.269479180	0.718402632	0.36141327	0.17121984	0.07882210
0.2	1.922085966	1.423155525	0.839948683	0.43230491	0.20711674	0.09585068
0.3	1.980132581	1.572895466	0.973834722	0.51486639	0.25001974	0.11644607
0.4	2	1.711277572	1.118110335	0.61003999	0.30105415	0.14130164
0.5	1.980132581	1.830273924	1.269479180	0.71840263	0.36141327	0.17121984
0.6	1.922085966	1.922085966	1.423155525	0.83994868	0.43230491	0.20711674

Table 2: The approximate solution of Example 10 for initial condition at $0.1 \leq x, t \leq 0.6$.

x/t	0.1	0.2	0.3	0.4	0.5	0.6
0.1	1.830273864	1.269478141	0.718402628	0.36141327	0.17128272	0.07883011
0.2	1.922085928	1.423155537	0.839948629	0.43230491	0.20711710	0.09585155
0.3	1.980132606	1.572896076	0.973834717	0.51486633	0.25001974	0.11644677
0.4	2.000000027	1.711278098	1.118110380	0.61004008	0.30105468	0.14130128
0.5	1.980133013	1.830274266	1.269479288	0.71840299	0.36141338	0.17122050
0.6	1.922086667	1.922086057	1.423155510	0.83994874	0.43230465	0.20711669

Table 3: The absolute error of Example 11 for initial condition at $0.1 \leq x, t \leq 0.6$.

x/t	0.1	0.2	0.3	0.4	0.5	0.6
0.1	1.78×10^{-6}	3.01×10^{-9}	8.55×10^{-7}	3.49×10^{-7}	2.85×10^{-7}	6.28×10^{-7}
0.2	6.38×10^{-7}	6.98×10^{-7}	6.52×10^{-7}	4.51×10^{-7}	8.33×10^{-6}	2.42×10^{-7}
0.3	2.2×10^{-8}	9.09×10^{-7}	6.88×10^{-6}	1.35×10^{-7}	2.97×10^{-6}	1.69×10^{-7}
0.4	1.70×10^{-7}	1.03×10^{-7}	5.38×10^{-7}	1.20×10^{-6}	3.98×10^{-7}	1.68×10^{-7}
0.5	2.26×10^{-7}	1.29×10^{-7}	8.74×10^{-7}	3.13×10^{-7}	4.02×10^{-7}	9.63×10^{-7}
0.6	8.94×10^{-7}	7.83×10^{-7}	4.34×10^{-7}	9.79×10^{-7}	2.77×10^{-7}	1.45×10^{-8}

Table 4: The relative error of Example 11 for initial condition at $0.1 \leq x, t \leq 0.6$.

x/t	0.1	0.2	0.3	0.4	0.5	0.6
0.1	9.201×10^{-7}	5.113×10^{-10}	5.707×10^{-7}	3.868×10^{-7}	6.06×10^{-7}	2.76×10^{-6}
0.2	3.441×10^{-7}	3.498×10^{-7}	3.968×10^{-7}	4.320×10^{-7}	1.48×10^{-6}	8.84×10^{-7}
0.3	1.255×10^{-8}	4.555×10^{-7}	3.881×10^{-6}	1.132×10^{-7}	4.49×10^{-6}	5.13×10^{-7}
0.4	1.032×10^{-7}	5.264×10^{-8}	2.862×10^{-7}	8.964×10^{-7}	5.13×10^{-7}	4.27×10^{-7}
0.5	1.460×10^{-7}	6.857×10^{-8}	4.469×10^{-7}	2.089×10^{-7}	4.44×10^{-7}	2.04×10^{-6}
0.6	6.079×10^{-7}	4.410×10^{-7}	2.175×10^{-7}	5.958×10^{-7}	2.65×10^{-7}	2.58×10^{-8}

The exact solution is $u(x,t) = 12((3 + 4\cosh(2x - 8t) + \cosh(4x - 64t))/[3\cosh(x - 28t) + \cosh(3x - 36t)]^2)$. If we apply (3) to (88), then the following (89) is obtained:

$$\begin{aligned} v_t(x,t) &- 72\operatorname{sech}^3 x \sinh x v(x,t) \\ &+ 36\operatorname{sech}^2 x v_{xx}(x,t) + v_{xxx}(x,t) \\ &= -6v(x,t)\, v_x(x,t) - 96\frac{\sinh x}{\cosh^3 x} \\ &+ 144\frac{\sinh^3 x}{\cosh^5 x} + 432\operatorname{sech}^5 x \sinh x, \\ v(x,0) &= 0. \end{aligned} \tag{89}$$

Using our method we choose 36 points on $[0,1]$. We replace v with u for simplicity. In Tables 3 and 4, we compute the absolute errors $|u(x,t) - u_n(x,t)|$ and the relative errors $|u(x,t) - u_n(x,t)|/|u(x,t)|$ at the points $\{(x_i, t_i) : x_i = t_i = i,\ i = 0.1, \ldots, 0.6\}$.

Remark 12. The problem discussed in this paper has been solved with Adomian method [13] and Homotopy analysis method [31]. In these studies, even though the numerical results give good results for large values of x, these methods give away values from the analytical solution for small values of x and t. However, the method is used in our study for large and small values of x and t, results are very close to the analytical solutions can be obtained. In doing so, it is possible to refine the result by increasing the intensive points.

6. Conclusion

In this paper, we introduce an algorithm for solving the KdV equation with initial condition. For illustration purposes, we chose two examples which were selected to show the computational accuracy. It may be concluded that the RKM is very powerful and efficient in finding exact solution for wide classes of problem. The approximate solution obtained by the present method is uniformly convergent.

Clearly, the series solution methodology can be applied to much more complicated nonlinear differential equations and boundary value problems. However, if the problem becomes nonlinear, then the RKM does not require discretization or perturbation and it does not make closure approximation. Results of numerical examples show that the present method is an accurate and reliable analytical method for the KdV equation with initial or boundary conditions.

Acknowledgment

A. Kiliçman gratefully acknowledge that this paper was partially supported by the University Putra Malaysia under the ERGS Grant Scheme having project no. 5527068 and Ministry of Science, Technology and Inovation (MOSTI), Malaysia under the Science Fund 06-01-04-SF1050.

References

[1] P. G. Drazin and R. S. Johnson, *Solitons: An Introduction*, Cambridge University Press, Cambridge, UK, 1989.

[2] A. A. Soliman, "Collucation solution of the KdV equation using septic splines," *International Journal of Computer Mathematics*, vol. 81, pp. 325–331, 2004.

[3] A. A. Soliman, A. H. A. Ali, and K. R. Raslan, "Numerical solution for the KdV equation based on similarity reductions," *Applied Mathematical Modelling*, vol. 33, no. 2, pp. 1107–1115, 2009.

[4] N. J. Zabusky, "A synergetic approach to problem of nonlinear dispersive wave propagation and interaction," in *Proceeding of Symposium Nonlinear PDEs*, W. Ames, Ed., pp. 223—-258, Academic Press, New York, NY, USA, 1967.

[5] D. J. Korteweg-de Vries and G. de Vries, "On the change in form of long waves advancing in rectangular canal and on a new type of long stationary waves," *Philosophical Magazine*, vol. 39, pp. 422–443, 1895.

[6] C. Gardner and G. K. Marikawa, "The effect of temperature of the width of a small amplitude solitary wave in a collision free plasma," *Communications on Pure and Applied Mathematics*, vol. 18, pp. 35–49, 1965.

[7] R. K. Dodd, J. C. Eilbeck, J. D. Gibbon, and H. C. Morris, *Solitons and Nonlinear Wave Equations*, Academic Press, New York, NY, USA, 1982.

[8] K. Goda, "On stability of some finite difference schemes for the KdV equation," *Journal of the Physical Society of Japan*, vol. 39, pp. 229–236, 1975.

[9] A. C. Vliengenthart, "On finite difference methods for KdV equation," *Journal of Engineering Mathematics*, vol. 5, pp. 137–155, 1971.

[10] M. Inc, "Numerical simulation of KdV and mKdV equations with initial conditions by the variational iteration method," *Chaos, Solitons and Fractals*, vol. 34, no. 4, pp. 1075–1081, 2007.

[11] I. Dağ and Y. Dereli, "Numerical solution of KdV equation using radial basis functions," *Applied Mathematical Modelling*, vol. 32, pp. 535–546, 2008.

[12] A. M. Wazwaz, *Partial Differential Equations and Solitary Waves Theory*, Higher Education Press, Springer, London, UK, 2009.

[13] M. I. Syam, "Adomian decomposition method for approximating the solution of the KdV equation," *Applied Mathematics and Computation*, vol. 162, pp. 1465–1473, 2005.

[14] N. Aronszajn, "Theory of reproducing kernels," *Transactions of the American Mathematical Society*, vol. 68, pp. 337–404, 1950.

[15] M. Inc, A. Akgül, and A. Kilicman, "Explicit solution of telegraph equation based on reproducing Kernel method," *Journal of Function Spaces and Applications*, vol. 2012, Article ID 984682, 23 pages, 2012.

[16] F. Geng and M. Cui, "Solving a nonlinear system of second order boundary value problems," *Journal of Mathematical Analysis and Applications*, vol. 327, pp. 1167–1181, 2007.

[17] H. Yao and M. Cui, "A new algorithm for a class of singular boundary value problems," *Applied Mathematics and Computation*, vol. 186, pp. 1183–1191, 2007.

[18] W. Wang, M. Cui, and B. Han, "A new method for solving a class of singular two-point boundary value prolems," *Applied Mathematics and Computation*, vol. 206, pp. 721—-727, 2008.

[19] Y. Zhou, Y. Lin, and M. Cui, "An efficient computational method for second order boundary value problemsof nonlinear diffierential equations," *Applied Mathematics and Computation*, vol. 194, pp. 357–365, 2007.

[20] X. Lü and M. Cui, "Analytic solutions to a class of nonlinear infinite-delay-differential equations," *Journal of Mathematical Analysis and Applications*, vol. 343, pp. 724–732, 2008.

[21] Y. L. Wang and L. Chao, "Using reproducing kernel for solving a class of partial differential equation with variable-coefficients," *Applied Mathematics and Mechanics*, vol. 29, pp. 129–137, 2008.

[22] F. Li and M. Cui, "A best approximation for the solution of one-dimensional variable-coefficient Burger's equation," *Numerical Methods for Partial Differential Equations*, vol. 25, pp. 1353–1365, 2009.

[23] S. Zhou and M. Cui, "Approximate solution for a variable-coefficient semilinear heat equation with nonlocal boundary conditions," *International Journal of Computer Mathematics*, vol. 86, pp. 2248–2258, 2009.

[24] F. Geng and M. Cui, "New method based on the HPM and RKHSM for solving forced Duffing equations with integral boundary conditions," *Journal of Computational and Applied Mathematics*, vol. 233, no. 2, pp. 165–172, 2009.

[25] J. Du and M. Cui, "Solving the forced Duffing equations with integral boundary conditions in the reproducing kernel space," *International Journal of Computer Mathematics*, vol. 87, pp. 2088–2100, 2010.

[26] X. Lv and M. Cui, "An efficient computational method for linear fifth-order two-point boundary value problems," *Journal of Computational and Applied Mathematics*, vol. 234, no. 5, pp. 1551–1558, 2010.

[27] W. Jiang and M. Cui, "Constructive proof for existence of nonlinear two-point boundary value problems," *Applied Mathematics and Computation*, vol. 215, no. 5, pp. 1937–1948, 2009.

[28] J. Du and M. Cui, "Constructive proof of existence for a class of fourth-order nonlinear BVPs," *Computers and Mathematics with Applications*, vol. 59, no. 2, pp. 903–911, 2010.

[29] M. Cui and H. Du, "Representation of exact solution for the nonlinear Volterra-Fredholm integral equations," *Applied*

Mathematics and Computation, vol. 182, no. 2, pp. 1795–1802, 2006.

[30] B. Y. Wu and X. Y. Li, "Iterative reproducing kernel method for nonlinear oscillator with discontinuity," *Applied Mathematics Letters*, vol. 23, no. 10, pp. 1301–1304, 2010.

[31] H. Jafari and M. A. Firoozjaee, "Homotopy analysis method for KdV equation," *Surveys in Mathematics and Its Applications*, vol. 5, pp. 89–98, 2010.

Hindawi Publishing Corporation
Abstract and Applied Analysis
Volume 2013, Article ID 696074, 7 pages
http://dx.doi.org/10.1155/2013/696074

Research Article

Saddle-Node Heteroclinic Orbit and Exact Nontraveling Wave Solutions for (2+1)D KdV-Burgers Equation

Da-Quan Xian

School of Sciences, Southwest University of Science and Technology, Mianyang 621010, China

Correspondence should be addressed to Da-Quan Xian; daquanxian@163.com

Received 21 September 2012; Accepted 8 December 2012

Academic Editor: de Dai

We have undertaken the fact that the periodic solution of (2+1)D KdV-Burgers equation does not exist. The Saddle-node heteroclinic orbit has been obtained. Using the Lie group method, we get two-(1+1)-dimensional PDE, through symmetric reduction; and by the direct integral method, spread F-expansion method, and (G'/G)-expansion method, we obtain exact nontraveling wave solutions, for the (2+1)D KdV Burgers equation, and find out some new strange phenomenons of sympathetic vibration to evolution of nontraveling wave.

1. Introduction

We consider the (2+1)-dimensional Korteweg-de Vries Burgers ((2+1)D KdV Burgers) equation

$$(u_t + uu_x - \beta u_{xx} + \alpha u_{xxx})_x + \gamma u_{yy} = 0, \qquad (1)$$

where $u : R_x \times R_y \times R_t^+ \rightarrow R, \alpha, \beta$, and γ are real parameters. Equation (1) is model equation for wide class of nonlinear wave models in an elastic tube, liquid with small bubbles, and turbulence [1–3]. Much attention has been put on the study of their exact solutions by some methods [4], such as, a complex line soliton by extended tanh method with symbolic computation [5], exact traveling wave solutions including solitary wave solutions, periodic wave and shock wave solutions by extended mapping method, and homotopy perturbation method [6, 7].

It is well known that the investigation of exact solutions of nonlinear evolution equations plays an important role in the study of nonlinear physical phenomena. Many effective methods have been presented [7–22], such as functional variable separation method [8, 9], homotopy perturbation method [12], F-expansion method [7, 13], Lie group method [14, 15], variational iteration method [16], homoclinic test method [17–19], Exp-function method [20, 21], and homogeneous balance method [22]. Practically, there is no unified method that can be used to handle all types of nonlinearity.

In this paper, we will discuss the existence of periodic traveling wave solution and seek the Saddle-Node heteroclinic orbit, and further use the Lie group method with the aid of the symbolic computation system Maple to construct the non-traveling wave solutions for (1).

2. Existence of Periodic Traveling Wave Solution of (1)

Introducing traveling wave transformation in this form

$$u(x, y, t) = u(\xi), \quad \xi = px + qy - ct \qquad (2)$$

permits us to convert (1) into an ODE for $u = u(\xi)$

$$p\left(puu_\xi - \beta p^2 u_{\xi\xi} + \alpha p^3 u_{\xi\xi\xi}\right)_\xi - ru_{\xi\xi} = 0, \qquad (3)$$

where $r = pc - q^2\gamma$, Integrating (3) with respect to ξ twice and taking integration constant to A yields

$$2\alpha p^4 u_{\xi\xi} - 2\beta p^3 u_\xi + p^2 u^2 - 2ru = A. \qquad (4)$$

Letting $u_\xi = v$, thus nonlinear ordinary differential equation (4) is equivalent to the autonomous dynamic system as follows:

$$\frac{du}{d\xi} = v, \qquad (5)$$

$$\frac{dv}{d\xi} = \frac{1}{2\alpha p^4}\left(2\beta p^3 v - p^2 u^2 + 2ru + A\right). \qquad (6)$$

The dynamic system (5) has two balance points:

$$P_1(u_1, v_1) = \left(\frac{r + \sqrt{r^2 + p^2 A}}{p^2}, 0\right),$$
$$P_2(u_2, v_2) = \left(\frac{r - \sqrt{r^2 + p^2 A}}{p^2}, 0\right). \tag{7}$$

The Jacobi matrixes at the balance points for the right-hand side of (5) are obtained as follows, respectively:

$$J_1 = \begin{pmatrix} 0 & 1 \\ -\dfrac{\sqrt{r^2 + p^2 A}}{p^4 \alpha} & \dfrac{\beta}{p\alpha} \end{pmatrix},$$
$$J_2 = \begin{pmatrix} 0 & 1 \\ \dfrac{\sqrt{r^2 + p^2 A}}{p^4 \alpha} & \dfrac{\beta}{p\alpha} \end{pmatrix}. \tag{8}$$

Their latent equations are expressed, respectively, as,

$$p^3\lambda(p\alpha\lambda - \beta) + \sqrt{r^2 + p^2 A} = 0,$$
$$p^3\lambda(p\alpha\lambda - \beta) - \sqrt{r^2 + p^2 A} = 0. \tag{9}$$

Relevant latent roots are as follows respectively:

$$\lambda_1 = \frac{p\beta \pm \sqrt{p^2\beta^2 - 4\alpha\sqrt{r^2 + p^2 A}}}{2p^2\alpha},$$
$$\lambda_2 = \frac{p\beta \pm \sqrt{p^2\beta^2 + 4\alpha\sqrt{r^2 + p^2 A}}}{2p^2\alpha}. \tag{10}$$

Obviously, if $p^2\beta^2 > 4\alpha\sqrt{r^2 + p^2 A}$, then λ_1 are two positive real roots, therefore P_1 is a nonsteady node point. If $0 < p^2\beta^2 < 4\alpha\sqrt{r^2 + p^2 A}$, then λ_1 are conjugate complex roots and real part is positive, so P_1 is a nonsteady focus point. And λ_2 is a positive and minus real root, thus P_2 is a saddle point. From (5), we know the phase trajectory on the phase plane satisfies

$$\frac{dv}{du} = \frac{2\beta p^3 v - p^2 u^2 + 2ru + A}{2\alpha p^4 v}. \tag{11}$$

Integrating (11), we can obtain

$$H(u, v) = Au + ru^2 - \frac{1}{3}p^2 u^3 + 2\beta p^3 uv - \alpha p^4 v^2, \tag{12}$$

where $H(u, v)$ is a total energy or Hamilton function of system (4). Apparently

$$u_\xi \neq -\frac{\partial H}{\partial v}, \qquad v_\xi \neq \frac{\partial H}{\partial u}. \tag{13}$$

Consequently, the system expressed in (12) is not a conservative one, then periodic traveling wave solution of (1) does not exist.

We conclude the above analysis in the following theorem.

Theorem 1. *Under the traveling wave transformation, the periodic solution of (2+1)-dimensional KdV-Burgers equation does not exist.*

But, saddle-node heteroclinic orbits and nontraveling periodic solution do exist, which will be discussed later in this paper.

3. Saddle-Node Heteroclinic Orbits of KdV-Burgers Equation

First, we assume the solutions of (4) in the form

$$u(\xi) = \frac{r + \sqrt{r^2 + p^2 A}}{p^2} + \frac{b}{(1 + e^{a\xi})^2}. \tag{14}$$

Substituting (14) into (4) yields

$$\begin{aligned} &2\left(4\alpha p^4 a^2 + \sqrt{r^2 + p^2 A} + 2\beta p^3 a\right)e^{2a\xi} \\ &\quad - 4\left(\alpha p^4 a^2 - \sqrt{r^2 + p^2 A} - \beta p^3 a\right)e^{a\xi} \\ &\quad + 2\sqrt{r^2 + p^2 A} + p^2 b = 0. \end{aligned} \tag{15}$$

Then we get

$$\begin{aligned} &4\alpha p^4 a^2 + \sqrt{r^2 + p^2 A} + 2\beta p^3 a = 0, \\ &\alpha p^4 a^2 - \sqrt{r^2 + p^2 A} - \beta p^3 a = 0, \\ &2\sqrt{r^2 + p^2 A} + p^2 b = 0. \end{aligned} \tag{16}$$

Solving the system (16) gets

$$a = -\frac{\beta}{5\alpha p}, \qquad b = -\frac{12\beta^2}{25\alpha}, \qquad \sqrt{r^2 + p^2 A} = \frac{6p^2\beta^2}{25\alpha}. \tag{17}$$

Substituting (17) into (14) obtains

$$\begin{aligned} u(\xi) &= \frac{r + \sqrt{r^2 + p^2 A}}{p^2} - \frac{12\beta^2}{25\alpha}\frac{1}{\left(1 + e^{-(\beta/5\alpha p)\xi}\right)^2} \\ &= u_1 - \frac{3\beta^2}{25\alpha}\left(1 + \tanh\frac{\beta}{20\alpha}\xi\right)^2. \end{aligned} \tag{18}$$

Evidently, $\xi \to -\infty \Rightarrow u(\xi) \to u_1$, $\xi \to +\infty \Rightarrow u(\xi) \to u_1 - (6\beta^2/25\alpha) = u_2$. Thus (18) is a saddle-node heteroclinic orbit through nonsteady node point P_1 and saddle point P_2 [23].

Ecumenic, taking the Hamiliton function $H(u,v) = B$, we obtain

$$\frac{du}{d\xi} = v = \frac{3p\beta u \pm \sqrt{3u\left[3A\alpha + 3\left(p^2\beta^2 + r\alpha\right)u - p^2\alpha u^2\right] - 9B\alpha}}{3\alpha p^2}, \tag{19}$$

where B is an arbitrary constant. Integrating (19) with respect to ξ we have

$$\int^{u(\xi)} \frac{3\alpha p^2}{3p\beta s \pm \sqrt{3s\left[3A\alpha + 3\left(p^2\beta^2 + r\alpha\right)s - p^2\alpha s^2\right] - 9B\alpha}} ds = \xi + \xi_0, \tag{20}$$

where ξ_0 is an arbitrary constant. We can see that (4) has the general solution (20) and all partial cases as include above result can be found from the general solution of (20). Example, take $\alpha\sqrt{r^2 + p^2 A} - p^2\beta^2 = 0$, $3B\alpha + A\beta^2 = 0$, $r\alpha + p^2\beta^2 = 0$ in (20), we find a solution of (4) as follows:

$$u(\xi) = -\frac{3\beta^2}{4\alpha}\left[1 + \tanh\left(\frac{\beta}{4p\alpha}\xi + \xi_0\right)\right]^2. \tag{21}$$

It is a heteroclinic orbit too.

4. Li Symmetry of (1)

This section devotes to Li symmetry of (1) [14, 15]. Let

$$\sigma = \sigma\left(x, y, t, u, u_t, u_x, u_y, \ldots\right). \tag{22}$$

be the Li symmetry of (1). From Lie group theory, σ satisfies the following equation

$$\sigma_{xt} + 2u_x\sigma_x + u\sigma_{xx} + \sigma u_{xx} - \beta\sigma_{x^3} + \alpha\sigma_{x^4} + \gamma\sigma_{yy} = 0. \tag{23}$$

We take the function σ in the form

$$\sigma = a_1 u_x + a_2 u_y + a_3 u_t + a_4 u + a_5, \tag{24}$$

where $a_i = a_i(x,y,t) : R_x \times R_y \times R_t^+ \rightarrow R$ $(i = 1,\ldots,5)$ are functions to be determined later. Substituting (3) into (2) yields

$$a_1 = -\frac{1}{2\gamma}k_2'(t)\,y + k_1(t), \qquad a_2 = k_2(t),$$
$$a_3 = c, \qquad a_4 = 0, \qquad a_5 = \frac{1}{2\gamma}k_2''(t)\,y - k_1'(t), \tag{25}$$

where $k_j(t)$ $(j = 1,2)$ are arbitrary functions of t, c is an arbitrary constant. Substituting (25) into (24), we obtain the Li symmetries of (1) as follows:

$$\sigma = \left[-\frac{1}{2\gamma}k_2'(t)\,y + k_1(t)\right]u_x + k_2(t)\,u_y + cu_t + \frac{1}{2\gamma}k_2''(t)\,y - k_1'(t). \tag{26}$$

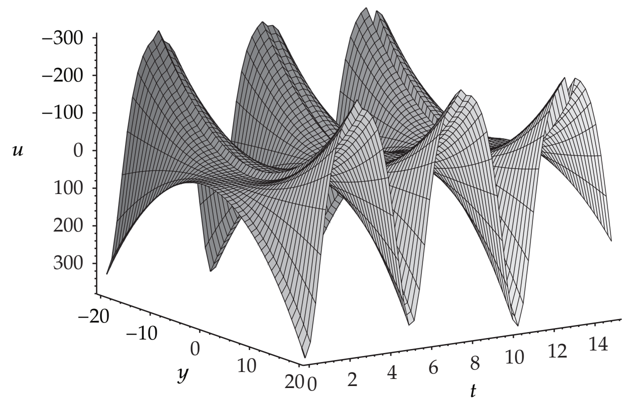

Figure 1: The strange phenomenon which is a sympathetic vibration of periodicity on the t-axis and paraboloid on y-axis for $u_1(x,y,t)$ as $x = 1$.

5. Symmetry Reduction and Solutions of (1)

Based on the integrability of reduced equation of symmetry (26), we are to consider the following three cases.

Case 1. Taking $k_2(t) = 0$ and $c = 0$ in (26) yields

$$\sigma = k_1(t)\,u_x - k_1'(t). \tag{27}$$

The solution of the differential equation $\sigma = 0$ is

$$u = \frac{k_1'(t)}{k_1(t)}x + F(y,t), \quad F(y,t) : R_y \times R_t^+ \rightarrow R. \tag{28}$$

Substituting (28) into (1) yields the function $F(y,t)$ which satisfies the following linear PDE:

$$\frac{k_1''}{k_1} + \gamma\frac{\partial^2 F}{\partial y^2} = 0. \tag{29}$$

By integrating both sides, we find out the following result:

$$F(y,t) = -\frac{k_1''}{2\gamma k_1}y^2 + k_3(t)\,y + k_4(t), \tag{30}$$

where $k_3(t)$, $k_4(t)$ are new arbitrary functions of t. Substituting (30) into (28), we can get the solutions of (1) as follows:

$$u_1(x,y,t) = \frac{k_1'(t)}{k_1(t)}x - \frac{k_1''}{2\gamma k_1}y^2 + k_3(t)\,y + k_4(t). \tag{31}$$

(1) Given $k_i(t) = \mathrm{cn}(t, 0.95)$ $(i = 1,3,4)$, $x = 1$, $\gamma = 0.6$ in (31), the local structure of u_1 is obtained (Figure 1). Where $\mathrm{cn}(t, 0.95)$ is an Jacobian elliptic cosine function.

(2) Given $k_1(t) = \mathrm{sech}(t)$, $k_3(t) = \sin(t)$, $k_4(t) = \mathrm{cn}(t, 0.1)$, $y = 1$, $\gamma = 0.6$ in (31), the local structure of u_1 is obtained (Figure 2).

Case 2. Take $k_1(t) = t$, $k_2(t) = 1$ and $c = 0$ in (26), then

$$\sigma = tu_x + u_y - 1. \tag{32}$$

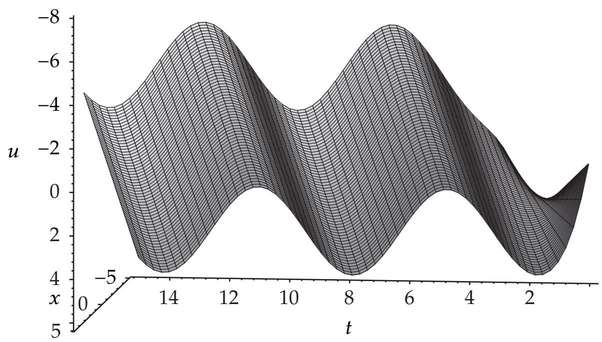

FIGURE 2: The periodic solution which is a periodic nontraveling wave traveling on the t-axis for $u_1(x, y, t)$ as $y = 1$.

Solving the differential equation $\sigma = 0$, we can get

$$u = y + F(t, \xi), \quad \xi = x - ty. \tag{33}$$

Substituting (33) into (1) and integrating once with respect to ξ yield

$$F_t + FF_\xi + \gamma t^2 F_\xi - \beta F_{\xi\xi} + \alpha F_{\xi\xi\xi} = 0. \tag{34}$$

Again, further using the transformation of dependent variable to (34),

$$F(t, \xi) = F(\theta), \quad \theta = k\left(t - \frac{1}{3}\gamma t^3 + \xi\right). \tag{35}$$

Substituting (35) into (34) and integrating once with respect to θ yield

$$2k^2\alpha F'' - 2k\beta F' + F^2 + 2F + A = 0, \tag{36}$$

where A is an integration constant, $F' = dF(\theta)/d\theta$. We assume that the solution of (36) can be expressed in the form

$$F(\theta) = a_0 + a_1 w(\theta) + a_2 w(\theta)^2, \tag{37}$$

where a_i $(i = 0, 1, 2)$ are constants to be determined later, $w(\theta)$ satisfies the following auxiliary equation

$$w' = p + qw^2. \tag{38}$$

Substituting (37) and (38) into (36) and equating the coefficients of all powers of w to zero yield a set of algebra equations for a_0, a_1, a_2, and A as follows.

$$\begin{aligned}
&w^4: a_2\left(a_2 + 12\alpha k^2 q^2\right) = 0,\\
&w^3: -4\beta k a_2 q + 2a_1 a_2 + 4\alpha k^2 a_1 q^2 = 0,\\
&w^2: a_1^2 + 16\alpha k^2 a_2 qp - 2\beta k a_1 q + 2a_2 + 2a_2 a_0 = 0,\\
&w^1: 2a_1 a_0 - 4\beta k a_2 p + 2a_1 + 4\alpha k^2 a_1 qp = 0,\\
&w^0: 2a_0 + A + 4\alpha k^2 a_2 p^2 + a_0^2 - 2\beta k a_1 p = 0.
\end{aligned} \tag{39}$$

Solving the system of function equations with the aid of Maple, we obtain

$$a_0 = \frac{3\beta^2 - 25\alpha}{25\alpha}, \qquad a_1 = \frac{6\beta^2 q}{25s\alpha}, \qquad a_2 = \frac{3\beta^2 q}{25\alpha p}. \tag{40}$$

when $k = \beta/10s\alpha$, $pq < 0$, $A = (625\alpha^2 - 36\beta^4)/625\alpha^2$, where $s = \sqrt{-pq}$.

It is known that solutions of (38) are as follows [24]:

$$w(\theta) = -s\tanh(s\theta), \qquad w(\theta) = -s\coth(s\theta). \tag{41}$$

Substituting (41), (40), (37), and (35) into (33), we obtain solutions of (1) as follows:

$$\begin{aligned}
&u_2(x, y, t)\\
&\quad = \frac{1}{25\alpha}\left\{3\beta^2 - 25\alpha - 3q\beta^2\right.\\
&\qquad \times\left[\tanh\left(\frac{\beta}{10s\alpha}\left(x - ty + t - \frac{\gamma}{3}t^3\right)\right)\right.\\
&\qquad \left.\left. - 2pq\tanh^2\left(\frac{\beta}{10s\alpha}\left(x - ty + t - \frac{\gamma}{3}t^3\right)\right)\right]\right\}\\
&\quad + y,\\
&u_3(x, y, t)\\
&\quad = \frac{1}{25\alpha}\left\{3\beta^2 - 25\alpha - 3q\beta^2\right.\\
&\qquad \times\left[\coth\left(\frac{\beta}{10s\alpha}\left(x - ty + t - \frac{\gamma}{3}t^3\right)\right)\right.\\
&\qquad \left.\left. - 2pq\coth^2\left(\frac{\beta}{10s\alpha}\left(x - ty + t - \frac{\gamma}{3}t^3\right)\right)\right]\right\}\\
&\quad + y.
\end{aligned} \tag{42}$$

(see Figures 3 and 4).

Remark 2. If we direct assume that the solution of (34) can be expressed in the form

$$F(t, \xi) = a_0(t) + a_1(t) w(\theta) + a_2(t) w(\theta)^2, \tag{43}$$

where $\theta = f(t)\xi + g(t)$, $f(t)$, and $g(t)$ are continuous functions of t to be determined later. $w(\theta)$ satisfies the auxiliary equation (38). Substituting (43) and (38) into (34), equating the coefficients of all powers of w to zero yields a set of

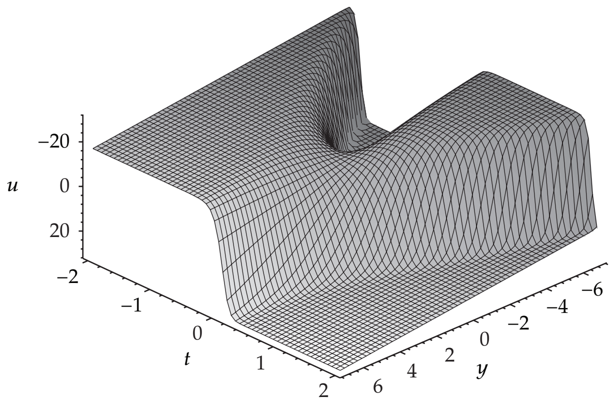

FIGURE 3: Local structure of $u_2(x, y, t)$ is shown as $x = 1$, $\alpha = 1$, $\beta = 10$, $p = -1$, $q = 1$, and $\gamma = 6$.

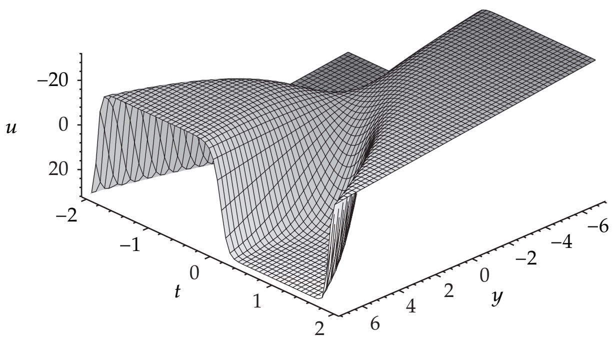

FIGURE 4: Local structure of $u_3(x, y, t)$ is shown as $x = 1$, $\alpha = 1$, $\beta = 10$, $p = -1$, $q = 1$, $\gamma = 6$.

function equations for $a_0(t)$, $a_1(t)$, $a_2(t)$, $f(t)$, and $g(t)$ as follows:

$$\begin{aligned}
&w^5:\ 2fa_2q\left(12f^2q^2\alpha + a_2\right) = 0,\\
&w^4:\ -3fq\left(-2a_1q^2f^2\alpha + 2qfa_2\beta - a_1a_2\right) = 0,\\
&w^3:\ -2\beta a_1f^2q^2 + 2a_2^2fp + 40\alpha a_2f^3q^2p + 2a_2g'q\\
&\qquad + 2a_0a_2fq + a_1^2fq + 2a_2f'\xi q + 2\gamma t^2a_2fq = 0,\\
&w^2:\ -8\beta a_2f^2pq + a_1g'q + a_2' + a_0a_1fq + \gamma t^2a_1fq\\
&\qquad + 8\alpha a_1f^3pq^2 + a_1f'\xi q + 3a_1a_2fq = 0,\\
&w^1:\ a_1^2fp + 16\alpha a_2f^3p^2q + a_1' + 2\gamma t^2a_2fp + 2a_0a_2fp\\
&\qquad + 2a_2g'p + 2a_2f'\xi p - 2\beta a_1f^2pq = 0,\\
&w^0:\ a_1g'p + a_1f'\xi p + a_0a_1fp - 2\beta a_2f^2p^2 + a_0'\\
&\qquad + 2\alpha a_1f^3p^2q + \gamma t^2a_1fp = 0.
\end{aligned} \tag{44}$$

Solving the system of function equations, we obtain

$$\begin{gathered}
a_0(t) = \frac{3\beta^2}{25\alpha}, \qquad a_1(t) = \pm\frac{6\beta^2q}{25s\alpha},\\
a_2(t) = \frac{3\beta^2q}{25\alpha p}, \qquad f(t) = \pm\frac{\beta}{10s\alpha}, \qquad g(t) = \mp\frac{\beta\gamma}{30s\alpha}t^3.
\end{gathered} \tag{45}$$

This result indicate the idea is equivalent to idea of Case 2 above.

Case 3. Take $k_2(t) = 0$ and $c = 1$ in (26), then

$$\sigma = k_1(t)u_x + u_t - k_1(t). \tag{46}$$

Solving the differential equation $\sigma = 0$, we obtain

$$u = k_1(t) + F(\xi, y), \quad \xi = x - \int k_1(t)\,dt. \tag{47}$$

Substituting (47) into (1) yield

$$\alpha F_{\xi\xi\xi\xi} - \beta F_{\xi\xi\xi} + FF_{\xi\xi} + F_\xi^2 + \gamma F_{yy} = 0. \tag{48}$$

Using the transformation $F(\xi, y) = F(\eta)$, $\eta = k\xi - cy$ and integrating the resulting equation with respect to η we have

$$k^2F^2 + 2\gamma c^2F + 2k^4\alpha F'' - 2k^3\beta F' + A = 0, \tag{49}$$

where A is an arbitrary constant, $F' = dF/d\eta$. Suppose that the solution of ODE (49) can be expressed by a polynomial in (G'/G) as follows:

$$F(\eta) = b_n\left(\frac{G'}{G}\right)^n + \cdots, \tag{50}$$

where $G = G(\eta)$ satisfies the second-order LODE in the form [25]

$$G'' + \lambda G' + \mu G = 0. \tag{51}$$

Balancing F'' with F^2 in (49) gives $n = 2$. So that

$$F(\eta) = b_2\left(\frac{G'}{G}\right)^2 + b_1\left(\frac{G'}{G}\right) + b_0, \quad b_2 \neq 0, \tag{52}$$

where b_i $(i = 0, 1, 2)$ and μ are constants to be determined later. Substituting (52) and (51) into (49). Setting these coefficients of the G'/G to zero, yields a set of algebraic equations as follows:

$$\begin{aligned}
&k^2b_2\left(12\alpha k^2 + b_2\right) = 0,\\
&2k^2\left(10\alpha k^2b_2\lambda + b_1b_2 + 2\alpha k^2b_1 + 2\beta kb_2\right) = 0,\\
&8\alpha k^4b_2\lambda^2 + 2\beta k^3b_1 + k^2b_1^2 + 16\alpha k^4b_2\mu + 2k^2b_2b_0\\
&\qquad + 6\alpha k^4b_1\lambda + 4\beta k^3b_2\lambda + 2\gamma c^2b_2 = 0,\\
&2k^2b_1b_0 + 4\beta k^3b_2\mu + 4\alpha k^4b_1\mu + 2\gamma c^2b_1 + 2\alpha k^4b_1\lambda^2\\
&\qquad + 2\beta k^3b_1\lambda + 12\alpha k^4b_2\lambda\mu = 0,\\
&2\gamma c^2b_0 + 2\alpha k^4b_1\lambda\mu + A + 2\beta k^3b_1\mu + 4\alpha k^4b_2\mu^2 + k^2b_0^2 = 0.
\end{aligned} \tag{53}$$

Solving the algebraic equations above yields

$$b_0 = \frac{15k^3\lambda\alpha\left(5k\lambda\alpha + 2\beta\right) - 3k^2\beta^2 + 25c^2\alpha\gamma}{25k^2\alpha},$$
$$b_1 = -\frac{12k\left(5k\alpha\lambda + \beta\right)}{5}, \qquad b_2 = -12k^2\alpha. \tag{54}$$

when $25k^2\alpha^2(4\mu - \lambda^2) + \beta^2 = 0$ and $625\alpha^2(Ak^2 - c^2\gamma^2) + 36k^4\beta^4 = 0$. Consequently, we obtain the following solution of (1) for $\lambda^2 - 4\mu > 0$:

$$\begin{aligned} u_4(x,y,t) = {} & -12k^2\alpha\tau^2 \\ & \times \Bigg[\left(C_1 \sinh\tau\left(k\left(x - \int k_1(t)\,dt\right) - cy\right)\right. \\ & \qquad \left. + C_2 \cosh\tau\left(k\left(x - \int k_1(t)\,dt\right) - cy\right)\right) \\ & \qquad \times \left(C_1 \cosh\tau\left(k\left(x - \int k_1(t)\,dt\right) - cy\right)\right. \\ & \qquad\quad + C_2 \sinh\tau \\ & \qquad\quad \left.\times\left(k\left(x - \int k_1(t)\,dt\right) - cy\right)\right)^{-1}\Bigg]^2 \\ & + \left(12k^2\lambda\alpha\tau - \frac{12k\left(5k\alpha\lambda + \beta\right)}{5}\right) \\ & \times \Bigg[\left(C_1 \sinh\tau\left(k\left(x - \int k_1(t)\,dt\right) - cy\right)\right. \\ & \qquad \left. + C_2 \cosh\tau\left(k\left(x - \int k_1(t)\,dt\right) - cy\right)\right) \\ & \qquad \times \left(C_1 \cosh\tau\left(k\left(x - \int k_1(t)\,dt\right) - cy\right)\right. \\ & \qquad\quad + C_2 \sinh\tau \\ & \qquad\quad \left.\times\left(k\left(x - \int k_1(t)\,dt\right) - cy\right)\right)^{-1}\Bigg]^2 \\ & + \frac{15k^3\lambda\alpha\left(5k\lambda\alpha + 2\beta\right) - 3k^2\beta^2 + 25c^2\alpha\gamma}{25k^2\alpha} \\ & + \frac{\lambda^2}{4}, \end{aligned} \tag{55}$$

where $\tau = (1/2)\sqrt{\lambda^2 - 4\mu}$.

6. Conclusions

Based on the fact that the periodic solution of (2+1)D KdV-Burgers equation does not exist, we have obtained Saddle-node Heteroclinic Orbits. By applying the Lie group method, we reduce the (2+1)D KdV Burgers equation to (1+1)-dimensional equations including the (1+1)-dimensional linear partial differential equation with constants coefficients (29), (48) and (1+1)-dimensional nonlinear partial differential equation with variable coefficients (34). By solving the equations (29), (34), and (48), we obtain some new exact solutions and discover the strange phenomenon of sympathetic vibration to evolution of nontraveling wave soliton for the (2+1)D KdV Burgers equation. Our results show that the unite of Lie group method with others is effective to search simultaneously exact solutions for nonlinear evolution equations. Other structures of solutions with symmetry (26) are to be further studied.

Acknowledgments

The authors would like to thank professor S. Y. Lou for the helpful discussions. This work was supported by key research projects of Sichuan Provincial Educational Administration no. 10ZA021 and Chinese Natural Science Foundation Grant no. 10971169.

References

[1] R. S. Johnson, "A non-linear equation incorporating damping and dispersion," *Journal of Fluid Mechanics*, vol. 42, pp. 49–60, 1970.

[2] L. van Wijngaarden, "One-dimensional flow of liquids containing small gas bubbles," *Annual Review of Fluid Mechanics*, vol. 4, pp. 369–396, 1972.

[3] G. Gao, "A theory of interaction between dissipation and dispersion of turbulence," *Scientia Sinica A*, vol. 28, no. 6, pp. 616–627, 1985.

[4] W. X. Ma, "An exact solution to two-dimensional Korteweg-de Vries-Burgers equation," *Journal of Physics A*, vol. 26, no. 1, pp. L17–L20, 1993.

[5] Z. B. Li and M. L. Wang, "Travelling wave solutions to the two-dimensional KdV-Burgers equation," *Journal of Physics A*, vol. 26, no. 21, pp. 6027–6031, 1993.

[6] J. Zhang, "Soliton-like solutions for the (2 + 1)-dimensional nonlinear evolution equation," *Communications in Theoretical Physics*, vol. 32, no. 2, pp. 315–318, 1999.

[7] E. G. Fan and H. Q. Zhang, "A note on the homogeneous balance method," *Physics Letters A*, vol. 246, pp. 403–406, 1998.

[8] S. Y. Lou and G. J. Ni, "The relations among a special type of solutions in some (D + 1)-dimensional nonlinear equations," *Journal of Mathematical Physics*, vol. 30, no. 7, pp. 1614–1620, 1989.

[9] X.-Y. Tang and S.-Y. Lou, "Folded solitary waves and foldons in (2 + 1) dimensions," *Communications in Theoretical Physics*, vol. 40, no. 1, pp. 62–66, 2003.

[10] E. J. Parkes and B. R. Duffy, "Travelling solitary wave solutions to a compound KdV-Burgers equation," *Physics Letters A*, vol. 229, no. 4, pp. 217–220, 1997.

[11] A. Elgarayhi and A. Elhanbaly, "New exact traveling wave solutions for the two-dimensional KdV-Burgers and Boussinesq equations," *Physics Letters A*, vol. 343, no. 1–3, pp. 85–89, 2005.

[12] A. Molabahrami, F. Khani, and S. Hamedi-Nezhad, "Soliton solutions of the two-dimensional KdV-Burgers equation by homotopy perturbation method," *Physics Letters A*, vol. 370, no. 5-6, pp. 433–436, 2007.

[13] H. L. Chen and D. Q. Xian, "Periodic wave solutions for the Klein-Gordon-Zakharov equations," *Acta Mathematicae Applicatae Sinica. Yingyong Shuxue Xuebao*, vol. 29, no. 6, pp. 1139–1144, 2006.

[14] D. Q. Xian, "New exact solutions to a class of nonlinear wave equations," *Journal of University of Electronic Science and Technology of China*, vol. 35, no. 6, pp. 977–980, 2006.

[15] D.-Q. Xian and H.-L. Chen, "Symmetry reduced and new exact non-traveling wave solutions of potential Kadomtsev-Petviashvili equation with p-power," *Applied Mathematics and Computation*, vol. 217, no. 4, pp. 1340–1349, 2010.

[16] J.-H. He, "Periodic solutions and bifurcations of delay-differential equations," *Physics Letters A*, vol. 347, no. 4–6, pp. 228–230, 2005.

[17] Z. Dai and D. Xian, "Homoclinic breather-wave solutions for Sine-Gordon equation," *Communications in Nonlinear Science and Numerical Simulation*, vol. 14, pp. 3292–3295, 2009.

[18] Z. Dai, D. Xian, and D. Li, "Homoclinic breather-wave with convective effect for the (1 + 1)- dimensional boussinesq equation," *Chinese Physics Letters*, vol. 26, no. 4, Article ID 040203, 2009.

[19] Z. Dai, Z. Li, Z. Liu, and D. Li, "Exact homoclinic wave and soliton solutions for the 2D Ginzburg-Landau equation," *Physics Letters A*, vol. 372, no. 17, pp. 3010–3014, 2008.

[20] D. Xian and Z. Dai, "Application of exp-function method to potential kadomtsev-petviashvili equation," *Chaos, Solitons and Fractals*, vol. 42, pp. 2653–2659, 2009.

[21] G.-C. Xiao, D.-Q. Xian, and X.-Q. Liu, "Application of exp-function method to Dullin-Gottwald-Holm equation," *Applied Mathematics and Computation*, vol. 210, no. 2, pp. 536–541, 2009.

[22] X.-Q. Liu and S. Jiang, "The $\sec_q$-$\tanh_q$-method and its applications," *Physics Letters A*, vol. 298, no. 4, pp. 253–258, 2002.

[23] S. K. Liu and S. D. Liu, *Solitary wave and turbulence*, Shanghai Scientifc and Technological Education, Shanghai, China, 1994.

[24] S. K. Liu and S. D. Liu, *Nonliner Equations in Physics*, Peking University, Beijing, China, 2000.

[25] M. Wang, X. Li, and J. Zhang, "The (G'/G)-expansion method and travelling wave solutions of nonlinear evolution equations in mathematical physics," *Physics Letters A*, vol. 372, no. 4, pp. 417–423, 2008.

Hindawi Publishing Corporation
Abstract and Applied Analysis
Volume 2013, Article ID 934060, 8 pages
http://dx.doi.org/10.1155/2013/934060

Research Article

Homotopy Perturbation Method for Fractional Gas Dynamics Equation Using Sumudu Transform

Jagdev Singh,[1] Devendra Kumar,[2] and A. Kılıçman[3]

[1] *Department of Mathematics, Jagannath University, Rampura, Chaksu, Jaipur, Rajasthan 303901, India*
[2] *Department of Mathematics, Jagannath Gupta Institute of Engineering & Technology, Jaipur, Rajasthan 302022, India*
[3] *Department of Mathematics and Institute for Mathematical Research, University Putra Malaysia (UPM), 43400 Serdang, Selangor, Malaysia*

Correspondence should be addressed to A. Kılıçman; akilicman@putra.upm.edu.my

Received 12 September 2012; Revised 19 November 2012; Accepted 6 December 2012

Academic Editor: Lan Xu

A user friendly algorithm based on new homotopy perturbation Sumudu transform method (HPSTM) is proposed to solve nonlinear fractional gas dynamics equation. The fractional derivative is considered in the Caputo sense. Further, the same problem is solved by Adomian decomposition method (ADM). The results obtained by the two methods are in agreement and hence this technique may be considered an alternative and efficient method for finding approximate solutions of both linear and nonlinear fractional differential equations. The HPSTM is a combined form of Sumudu transform, homotopy perturbation method, and He's polynomials. The nonlinear terms can be easily handled by the use of He's polynomials. The numerical solutions obtained by the proposed method show that the approach is easy to implement and computationally very attractive.

1. Introduction

Fractional calculus is a field of applied mathematics that deals with derivatives and integrals of arbitrary orders. During the last decade, fractional calculus has found applications in numerous seemingly diverse fields of science and engineering. Fractional differential equations are increasingly used to model problems in fluid mechanics, acoustics, biology, electromagnetism, diffusion, signal processing, and many other physical processes [1–19].

There exists a wide class of literature dealing with the problems of approximate solutions to fractional differential equations with various different methodologies, called perturbation methods. The perturbation methods have some limitations; for example, the approximate solution involves series of small parameters which poses difficulty since the majority of nonlinear problems have no small parameters at all. Although appropriate choices of small parameters sometimes lead to ideal solution, in most of the cases unsuitable choices lead to serious effects in the solutions. Therefore, an analytical method is welcome which does not require a small parameter in the equation modeling the phenomenon.

Recently, there is a very comprehensive literature review in some new asymptotic methods for the search for the solitary solutions of nonlinear differential equations, nonlinear differential-difference equations, and nonlinear fractional differential equations; see [20]. The homotopy perturbation method (HPM) was first introduced by He [21]. The HPM was also studied by many authors to handle linear and nonlinear equations arising in various scientific and technological fields [22–32]. The Adomian decomposition method (ADM) [33] and variational iteration method (VIM) [34] have also been applied to study the various physical problems.

In a recent paper, Singh et al. [35] have paid attention to study the solutions of linear and nonlinear partial differential equations by using the homotopy perturbation Sumudu transform method (HPSTM). The HPSTM is a combination of Sumudu transform, HPM, and He's polynomials and is mainly due to Ghorbani and Saberi-Nadjafi [36] and Ghorbani [37].

In this paper, we consider the following nonlinear time-fractional gas dynamics equation of the form

$$D_t^{\alpha} U + \frac{1}{2}\left(U^2\right)_x - U(1-U) = 0, \quad t > 0,\ 0 < \alpha \leq 1, \tag{1}$$

with the initial condition

$$U(x,0) = e^{-x}, \tag{2}$$

where α is a parameter describing the order of the fractional derivative. The function $U(x,t)$ is the probability density function, t is the time, and x is the spatial coordinate. The derivative is understood in the Caputo sense. The general response expression contains a parameter describing the order of the fractional derivative that can be varied to obtain various responses. In the case of $\alpha = 1$ the fractional gas dynamics equation reduces to the classical gas dynamics equation. The gas dynamics equations are based on the physical laws of conservation, namely, the laws of conservation of mass, conservation of momentum, conservation of energy, and so forth. The nonlinear fractional gas dynamics has been studied previously by Das and Kumar [38].

Further, we apply the HPSTM and ADM to solve the nonlinear time-fractional gas dynamics equation. The objective of the present paper is to extend the application of the HPSTM to obtain analytic and approximate solutions to the time-fractional gas dynamics equation. The advantage of the HPSTM is its capability of combining two powerful methods for obtaining exact and approximate analytical solutions for nonlinear equations. It provides the solutions in terms of convergent series with easily computable components in a direct way without using linearization, perturbation, or restrictive assumptions. It is worth mentioning that the HPSTM is capable of reducing the volume of the computational work as compared to the classical methods while still maintaining the high accuracy of the numerical result; the size reduction amounts to an improvement of the performance of the approach.

2. Sumudu Transform

In the early 90's, Watugala [39] introduced a new integral transform, named the Sumudu transform and applied it to the solution of ordinary differential equation in control engineering problems. The Sumudu transform, is defined over the set of functions

$$\begin{aligned} A = \{ & f(t) \mid \exists\, M, \tau_1, \tau_2 > 0, |f(t)| \\ & < M e^{|t|/\tau_j}, \text{if } t \in (-1)^j \times [0,\infty) \} \end{aligned} \tag{3}$$

by the following formula:

$$\begin{aligned} \overline{f}(u) &= S[f(t)] \\ &= \int_0^\infty f(ut) e^{-t} dt, \quad u \in (-\tau_1, \tau_2). \end{aligned} \tag{4}$$

Some of the properties were established by Weerakoon in [40, 41]. In [42], by Aşiru, further fundamental properties of this transform were also established. Similarly, this transform was applied to the one-dimensional neutron transport equation in [43] by Kadem. In fact it was shown that there is a strong relationship between Sumudu and other integral transforms; see Kılıçman et al. [44]. In particular the relation between Sumudu transform and Laplace transforms was proved in Kılıçman and Gadain [45].

Further, in Eltayeb et al. [46], the Sumudu transform was extended to the distributions and some of their properties were also studied in Kılıçman and Eltayeb [47]. Recently, this transform is applied to solve the system of differential equations; see Kılıçman et al. in [48].

Note that a very interesting fact about Sumudu transform is that the original function and its Sumudu transform have the same Taylor coefficients except the factor n; see Zhang [49]. Thus if $f(t) = \sum_{n=0}^{\infty} a_n t^n$ then $F(u) = \sum_{n=0}^{\infty} n! a_n u^n$; see Kılıçman et al. [44]. Similarly, the Sumudu transform sends combinations, $C(m,n)$, into permutations, $P(m,n)$, and hence it will be useful in the discrete systems.

3. Basic Definitions of Fractional Calculus

In this section, we mention the following basic definitions of fractional calculus which are used further in the present paper.

Definition 1. The Riemann-Liouville fractional integral operator of order $\alpha > 0$, of a function $f(t) \in C_\mu$, and $\mu \geq -1$ is defined as [5]

$$J^\alpha f(t) = \frac{1}{\Gamma(\alpha)} \int_0^t (t-\tau)^{\alpha-1} f(\tau)\, d\tau, \quad (\alpha > 0), \tag{5}$$

$$J^0 f(t) = f(t). \tag{6}$$

For the Riemann-Liouville fractional integral, we have

$$J^\alpha t^\gamma = \frac{\Gamma(\gamma+1)}{\Gamma(\gamma+\alpha+1)} t^{\alpha+\gamma}. \tag{7}$$

Definition 2. The fractional derivative of $f(t)$ in the Caputo sense is defined as [10]

$$\begin{aligned} D_t^\alpha f(t) &= J^{m-\alpha} D^n f(t) \\ &= \frac{1}{\Gamma(n-\alpha)} \int_0^t (t-\tau)^{m-\alpha-1} f^{(m)}(\tau)\, d\tau, \end{aligned} \tag{8}$$

for $m-1 < \alpha \leq m$, $m \in N$, $t > 0$.

For the Riemann-Liouville fractional integral and the Caputo fractional derivative, we have the following relation:

$$J_t^\alpha D_t^\alpha f(t) = f(t) - \sum_{k=0}^{m-1} f^{(k)}(0+) \frac{t^k}{k!}. \tag{9}$$

Definition 3. The Sumudu transform of the Caputo fractional derivative is defined as follows [50]:

$$\begin{aligned} S[D_t^\alpha f(t)] &= u^{-\alpha} S[f(t)] \\ &\quad - \sum_{k=0}^{m-1} u^{-\alpha+k} f^{(k)}(0+), \quad (m-1 < \alpha \leq m). \end{aligned} \tag{10}$$

4. Solution by Homotopy Perturbation Sumudu Transform Method (HPSTM)

4.1. Basic Idea of HPSTM. To illustrate the basic idea of this method, we consider a general fractional nonlinear nonhomogeneous partial differential equation with the initial condition of the form

$$D_t^{\alpha}U(x,t) + RU(x,t) + NU(x,t) = g(x,t), \tag{11}$$

$$U(x,0) = f(x), \tag{12}$$

where $D_t^{\alpha}U(x,t)$ is the Caputo fractional derivative of the function $U(x,t)$, R is the linear differential operator, N represents the general nonlinear differential operator, and $g(x,t)$ is the source term.

Applying the Sumudu transform (denoted in this paper by S) on both sides of (11), we get

$$S\left[D_t^{\alpha}U(x,t)\right] + S\left[RU(x,t)\right] + S\left[NU(x,t)\right] = S\left[g(x,t)\right]. \tag{13}$$

Using the property of the Sumudu transform, we have

$$\begin{aligned} S\left[U(x,t)\right] = {} & f(x) + u^{\alpha}S\left[g(x,t)\right] \\ & - u^{\alpha}S\left[RU(x,t) + NU(x,t)\right]. \end{aligned} \tag{14}$$

Operating with the Sumudu inverse on both sides of (14) gives

$$U(x,t) = G(x,t) - S^{-1}\left[u^{\alpha}S\left[RU(x,t) + NU(x,t)\right]\right], \tag{15}$$

where $G(x,t)$ represents the term arising from the source term and the prescribed initial conditions. Now we apply the HPM:

$$U(x,t) = \sum_{n=0}^{\infty} p^n U_n(x,t), \tag{16}$$

and the nonlinear term can be decomposed as

$$NU(x,t) = \sum_{n=0}^{\infty} p^n H_n(U), \tag{17}$$

for some He's polynomials $H_n(U)$ [37] that are given by

$$\begin{aligned} & H_n(U_0, U_1, \dots, U_n) \\ & \quad = \frac{1}{n!}\frac{\partial^n}{\partial p^n}\left[N\left(\sum_{i=0}^{\infty} p^i U_i\right)\right]_{p=0}, \quad n = 0, 1, 2, \dots. \end{aligned} \tag{18}$$

Substituting (16) and (17) in (15), we get

$$\begin{aligned} & \sum_{n=0}^{\infty} p^n U_n(x,t) \\ & \quad = G(x,t) \\ & \qquad - p\left(S^{-1}\left[u^{\alpha}S\left[R\sum_{n=0}^{\infty} p^n U_n(x,t) + \sum_{n=0}^{\infty} p^n H_n(U)\right]\right]\right), \end{aligned} \tag{19}$$

which is the coupling of the Sumudu transform and the HPM using He's polynomials. Comparing the coefficients of like powers of p, the following approximations are obtained:

$$\begin{aligned} p^0 &: U_0(x,t) = G(x,t), \\ p^1 &: U_1(x,t) = -S^{-1}\left[u^{\alpha}S\left[RU_0(x,t) + H_0(U)\right]\right], \\ p^2 &: U_2(x,t) = -S^{-1}\left[u^{\alpha}S\left[RU_1(x,t) + H_1(U)\right]\right], \\ p^3 &: U_3(x,t) = -S^{-1}\left[u^{\alpha}S\left[RU_2(x,t) + H_2(U)\right]\right], \\ & \vdots \end{aligned} \tag{20}$$

Proceeding in this same manner, the rest of the components $U_n(x,t)$ can be completely obtained and the series solution is thus entirely determined. Finally, we approximate the analytical solution $U(x,t)$ by truncated series:

$$U(x,t) = \lim_{N\to\infty}\sum_{n=0}^{N} U_n(x,t). \tag{21}$$

The above series solutions generally converge very rapidly.

4.2. Solution of the Problem. Consider the following nonlinear time-fractional gas dynamics equation:

$$D_t^{\alpha}U + \frac{1}{2}\left(U^2\right)_x - U(1-U) = 0, \quad 0 < \alpha \le 1, \tag{22}$$

with the initial condition

$$U(x,0) = e^{-x}. \tag{23}$$

Applying the Sumudu transform on both sides of (22), subject to the initial condition (23), we have

$$S\left[U(x,t)\right] = e^{-x} - u^{\alpha}S\left[\frac{1}{2}\left(U^2\right)_x - U(1-U)\right]. \tag{24}$$

The inverse Sumudu transform implies that

$$U(x,t) = e^{-x} - S^{-1}\left[u^{\alpha}S\left[\frac{1}{2}\left(U^2\right)_x - U(1-U)\right]\right]. \tag{25}$$

Now applying the HPM, we get

$$\begin{aligned} & \sum_{n=0}^{\infty} p^n U_n(x,t) \\ & \quad = e^{-x} - p\left(S^{-1}\left[u^{\alpha}S\left[\frac{1}{2}\left(\sum_{n=0}^{\infty} p^n H_n(U)\right)\right.\right.\right. \\ & \qquad\qquad - \left(\sum_{n=0}^{\infty} p^n U_n(x,t)\right) \\ & \qquad\qquad \left.\left.\left. + \left(\sum_{n=0}^{\infty} p^n H_n'(U)\right)\right]\right]\right), \end{aligned} \tag{26}$$

where $H_n(U)$ and $H'_n(U)$ are He's polynomials [37] that represent the nonlinear terms. So, the He's polynomials are given by

$$\sum_{n=0}^{\infty} p^n H_n(U) = \left(U^2\right)_x. \tag{27}$$

The first few components of He's polynomials are given by

$$\begin{gathered} H_0(U) = \left(U_0^2\right)_x, \\ H_1(U) = 2\left(U_0 U_1\right)_x, \\ H_1(U) = \left(U_1^2 + 2U_0 U_2\right)_x, \\ \vdots \end{gathered} \tag{28}$$

and for $H'_n(U)$, we find that

$$\begin{gathered} \sum_{n=0}^{\infty} p^n H'_n(U) = U^2, \\ H'_0(U) = U_0^2, \\ H'_1(U) = 2U_0 U_1, \\ H'_2(U) = U_1^2 + 2U_0 U_2, \\ \vdots \end{gathered} \tag{29}$$

Comparing the coefficients of like powers of p, we have

$$\begin{aligned} p^0 &: U_0(x,t) = e^{-x}, \\ p^1 &: U_1(x,t) = -S^{-1}\left[u^\alpha S\left[\frac{1}{2}H_0(U) - U_0 + H'_0(U)\right]\right] \\ &= e^{-x}\frac{t^\alpha}{\Gamma(\alpha+1)}, \\ p^2 &: U_2(x,t) = -S^{-1}\left[u^\alpha S\left[\frac{1}{2}H_1(U) - U_1 + H'_1(U)\right]\right] \\ &= e^{-x}\frac{t^{2\alpha}}{\Gamma(2\alpha+1)}, \\ p^3 &: U_3(x,t) = -S^{-1}\left[u^\alpha S\left[\frac{1}{2}H_2(U) - U_2 + H'_2(U)\right]\right] \\ &= e^{-x}\frac{t^{3\alpha}}{\Gamma(3\alpha+1)}, \\ &\vdots \end{aligned} \tag{30}$$

Therefore, the series solution is

$$\begin{aligned} U(x,t) \\ = e^{-x}\left[1 + \frac{t^\alpha}{\Gamma(\alpha+1)} + \frac{t^{2\alpha}}{\Gamma(2\alpha+1)} + \frac{t^{3\alpha}}{\Gamma(3\alpha+1)} + \cdots\right]. \end{aligned} \tag{31}$$

Setting $\alpha = 1$ in (31), we reproduce the solution of the problem as follows:

$$U(x,t) = e^{-x}\left(1 + t + \frac{t^2}{2!} + \frac{t^3}{3!} + \cdots\right). \tag{32}$$

This solution is equivalent to the exact solution in closed form:

$$U(x,t) = e^{t-x}. \tag{33}$$

Now, we calculate numerical results of the probability density function $U(x,t)$ for different time-fractional Brownian motions $\alpha = 1/3, 2/3, 1$ and for various values of t and x. The numerical results for the approximate solution (31) obtained by using HPSTM and the exact solution (33) for various values of t, x, and α are shown in Figures 1(a)–1(d) and those for different values of t and α at $x = 1$ are depicted in Figure 2.

It is observed from Figures 1 and 2 that $U(x,t)$ increases with the increase in t and decreases with the increase in α. Figures 1(c) and 1(d) clearly show that, when $\alpha = 1$, the approximate solution (31) obtained by the present method is very near to the exact solution. It is to be noted that only the third-order term of the HPSTM was used in evaluating the approximate solutions for Figures 1 and 2. It is evident that the efficiency of the present method can be dramatically enhanced by computing further terms of $U(x,t)$ when the HPSTM is used.

5. Solution by Adomian Decomposition Method (ADM)

5.1. Basic Idea of ADM. To illustrate the basic idea of ADM [51, 52], we consider a general fractional nonlinear nonhomogeneous partial differential equation with the initial condition of the form

$$D_t^\alpha U(x,t) + RU(x,t) + NU(x,t) = g(x,t), \tag{34}$$

where $D_t^\alpha U(x,t)$ is the Caputo fractional derivative of the function $U(x,t)$, R is the linear differential operator, N represents the general nonlinear differential operator, and $g(x,t)$ is the source term.

Applying the operator J_t^α on both sides of (34) and using result (9), we have

$$\begin{aligned} U(x,t) = &\sum_{k=0}^{m-1}\left(\frac{\partial^k U}{\partial t^k}\right)_{t=0}\frac{t^k}{k!} \\ &+ J_t^\alpha g(x,t) - J_t^\alpha\left[RU(x,t) + NU(x,t)\right]. \end{aligned} \tag{35}$$

Next, we decompose the unknown function $U(x,t)$ into sum of an infinite number of components given by the decomposition series

$$U = \sum_{n=0}^{\infty} U_n, \tag{36}$$

and the nonlinear term can be decomposed as

$$NU = \sum_{n=0}^{\infty} A_n, \tag{37}$$

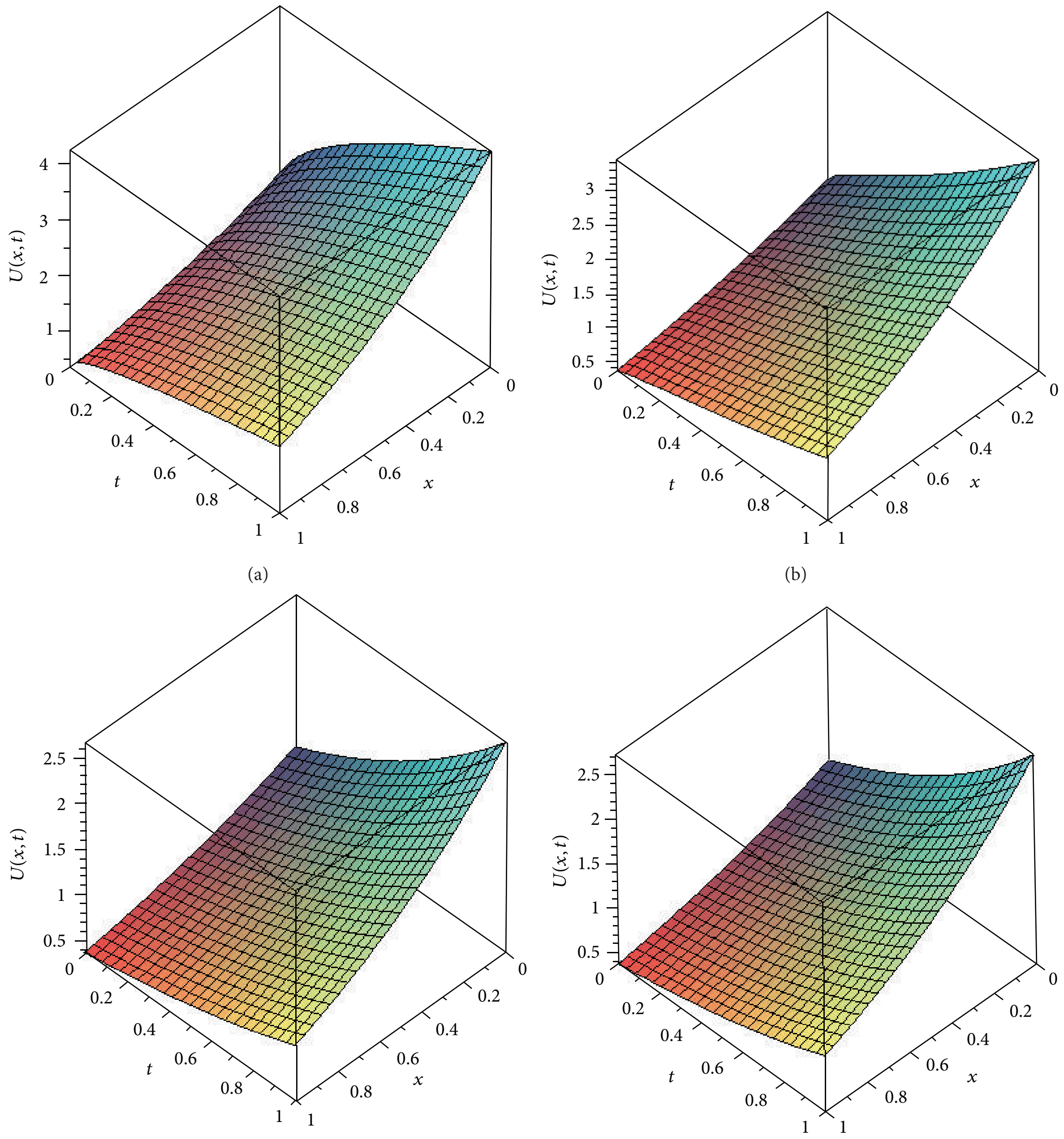

(a) (b) (c) (d)

FIGURE 1: The behaviour of the $U(x,t)$ w.r.t. x and t are obtained when (a) $\alpha = 1/3$, (b) $\alpha = 2/3$, (c) $\alpha = 1$, and (d) exact solution.

where A_n are Adomian polynomials that are given by

$$A_n = \frac{1}{n!}\left[\frac{d^n}{d\lambda^n} N\left(\sum_{i=0}^{n} \lambda^i U_i\right)\right]_{\lambda=0}, \quad n = 0, 1, 2, \ldots \tag{38}$$

The components $U_0, U_1, U_2, \ldots$ are determined recursively by substituting (36) and (37) into (34) leading to

$$\begin{aligned}\sum_{n=0}^{\infty} U_n = &\sum_{k=0}^{m-1}\left(\frac{\partial^k U}{\partial t^k}\right)_{t=0}\frac{t^k}{k!} \\ &+ J_t^{\alpha} g(x,t) - J_t^{\alpha}\left[R\left(\sum_{n=0}^{\infty} U_n\right) + \sum_{n=0}^{\infty} A_n\right].\end{aligned} \tag{39}$$

This can be written as

$$\begin{aligned}U_0 + U_1 + U_2 + \cdots = &\sum_{k=0}^{m-1}\left(\frac{\partial^k U}{\partial t^k}\right)_{t=0}\frac{t^k}{k!} + J_t^{\alpha} g(x,t) \\ &- J_t^{\alpha}\left[R\left(U_0 + U_1 + U_2 + \cdots\right)\right. \\ &\left.+ \left(A_0 + A_1 + A_2 + \cdots\right)\right].\end{aligned} \tag{40}$$

Adomian method uses the formal recursive relations as

$$\begin{aligned}U_0 &= \sum_{k=0}^{m-1}\left(\frac{\partial^k U}{\partial t^k}\right)_{t=0}\frac{t^k}{k!} + J_t^{\alpha} g(x,t), \\ U_{n+1} &= -J_t^{\alpha}\left[R\left(U_n\right) + A_n\right], \quad n \geq 0.\end{aligned} \tag{41}$$

Table 1: Comparison study between HPSTM, ADM, and the exact solution when $\alpha = 1$.

x	t	HPSTM	ADM	Exact solution
0	0.1	1.221333333	1.221333333	1.221402758
0.2	0.1	0.9999431595	0.9999431595	1.000000000
0.4	0.1	0.8186842160	0.8186842160	0.8187307531
0.6	0.1	0.6702819447	0.6702819447	0.6703200460
0.8	0.1	0.5487804413	0.5487804413	0.5488116361
1.0	0.1	0.4493037263	0.4493037263	0.4493289641

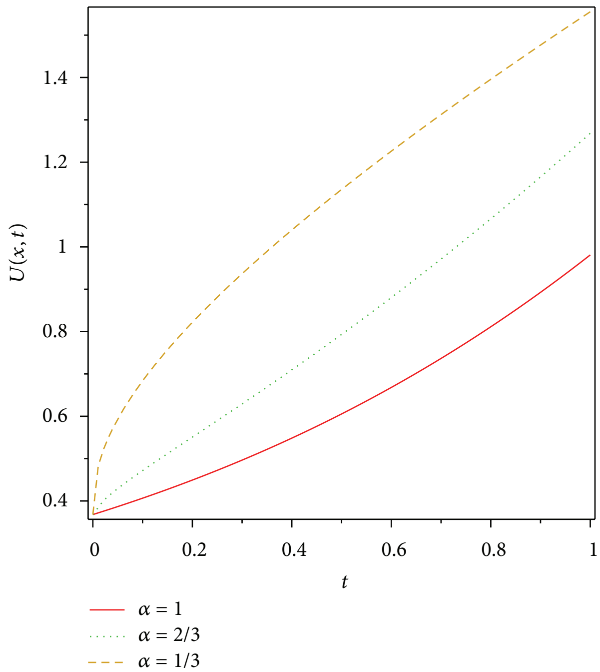

Figure 2: Plots of $U(x,t)$ versus t at $x = 1$ for different values of α.

5.2. Solution of the Problem. Consider the following nonlinear time-fractional gas dynamics equation:

$$D_t^\alpha U + \frac{1}{2}\left(U^2\right)_x - U(1-U) = 0, \quad 0 < \alpha \le 1, \tag{42}$$

with the initial condition

$$U(x,0) = e^{-x}. \tag{43}$$

Applying the operator J_t^α on both sides of (42) and using result (9), we have

$$U = \sum_{k=0}^{1-1} \frac{t^k}{k!}\left[D_t^k U\right]_{t=0} - J_t^\alpha\left[\frac{1}{2}\left(U^2\right)_x - U + U^2\right]. \tag{44}$$

This gives the following recursive relations using (41):

$$U_0 = \sum_{k=0}^{0} \frac{t^k}{k!}\left[D_t^k U\right]_{t=0},$$
$$U_{n+1} = -J_t^\alpha\left[A_n - U_n\right], \quad n = 0,1,2,\dots, \tag{45}$$

where

$$A_n = \frac{1}{n!}\left[\left(\frac{1}{2}\frac{\partial}{\partial x} + 1\right)\frac{d^n}{d\lambda^n}\left(\sum_{i=0}^{n}\lambda^i U_i\right)^2\right]_{\lambda=0}, \quad n = 0,1,2,\dots \tag{46}$$

which using the results (7), (5), and (43) gives

$$\begin{aligned}
U_0(x,t) &= e^{-x}, \\
A_0 &= 0, \\
U_1(x,t) &= e^{-x}\frac{t^\alpha}{\Gamma(\alpha+1)}, \\
A_1 &= 0, \\
U_2(x,t) &= e^{-x}\frac{t^{2\alpha}}{\Gamma(2\alpha+1)}, \\
A_2 &= 0, \\
U_3(x,t) &= e^{-x}\frac{t^{3\alpha}}{\Gamma(3\alpha+1)}, \\
&\vdots
\end{aligned} \tag{47}$$

Therefore, the decomposition series solution is

$$U(x,t) = e^{-x}\left[1 + \frac{t^\alpha}{\Gamma(\alpha+1)} + \frac{t^{2\alpha}}{\Gamma(2\alpha+1)} + \frac{t^{3\alpha}}{\Gamma(3\alpha+1)} + \cdots\right], \tag{48}$$

which is the same solution as obtained by using HPSTM.

From Table 1, it is observed that the values of the approximate solution at different grid points obtained by the HPSTM and ADM are close to the values of the exact solution with high accuracy at the third-term approximation. It can also be noted that the accuracy increases as the order of approximation increases.

The comparison between the third iteration solution of the HPSTM and the second iteration solution of the ADM is given in Figure 3.

It is observed that for $x = 1$ and $\alpha = 1$, there is a good agreement between the two methods.

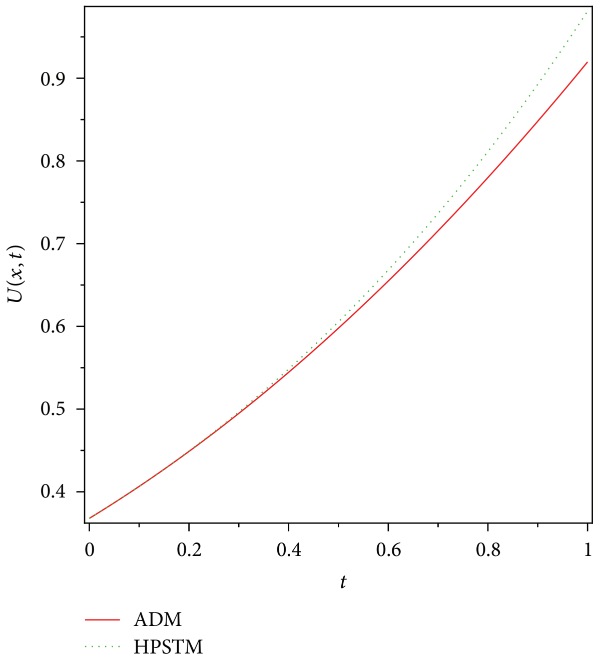

Figure 3: Comparison of the HPSTM and the ADM when $x = 1$ and $\alpha = 1$.

6. Conclusions

In this paper, the homotopy perturbation Sumudu transform method (HPSTM) and the Adomian decomposition method (ADM) are successfully applied for solving nonlinear time-fractional gas dynamics equation. The numerical solutions show that there is a good agreement between the two methods. Therefore, these two methods are very powerful and efficient techniques for solving different kinds of linear and nonlinear fractional differential equations arising in different fields of science and engineering. However, the HPSTM has an advantage over the ADM which is that it solves the nonlinear problems without using Adomian polynomials. In conclusion, the HPSTM and the ADM may be considered as a nice refinement in existing numerical techniques and might find the wide applications.

Acknowledgment

The authors are grateful to the referees for their invaluable suggestions and comments for the improvement of the paper.

References

[1] H. Beyer and S. Kempfle, "Definition of physically consistent damping laws with fractional derivatives," *Zeitschrift für Angewandte Mathematik und Mechanik*, vol. 75, no. 8, pp. 623–635, 1995.

[2] J. H. He, "Some applications of nonlinear fractional differential equations and their approximations," *Bulletin of Science, Technology & Society*, vol. 15, no. 2, pp. 86–90, 1999.

[3] J.-H. He, "Approximate analytical solution for seepage flow with fractional derivatives in porous media," *Computer Methods in Applied Mechanics and Engineering*, vol. 167, no. 1-2, pp. 57–68, 1998.

[4] R. Hilfer, "Fractional time evolution," in *Applications of Fractional Calculus in Physics*, pp. 87–130, World Scientific, River Edge, NJ, USA, 2000.

[5] I. Podlubny, *Fractional Differential Equations: An Introduction to Fractional Derivatives, Fractional Differential Equations, to Methods of Their Solution and some of Their Applications*, vol. 198 of *Mathematics in Science and Engineering*, Academic Press, San Diego, Calif, USA, 1999.

[6] F. Mainardi, Y. Luchko, and G. Pagnini, "The fundamental solution of the space-time fractional diffusion equation," *Fractional Calculus & Applied Analysis*, vol. 4, no. 2, pp. 153–192, 2001.

[7] S. Z. Rida, A. M. A. El-Sayed, and A. A. M. Arafa, "On the solutions of time-fractional reaction-diffusion equations," *Communications in Nonlinear Science and Numerical Simulation*, vol. 15, no. 12, pp. 3847–3854, 2010.

[8] A. Yıldırım, "He's homotopy perturbation method for solving the space- and time-fractional telegraph equations," *International Journal of Computer Mathematics*, vol. 87, no. 13, pp. 2998–3006, 2010.

[9] L. Debnath, "Fractional integral and fractional differential equations in fluid mechanics," *Fractional Calculus & Applied Analysis*, vol. 6, no. 2, pp. 119–155, 2003.

[10] M. Caputo, *Elasticita E Dissipazione*, Zani-Chelli, Bologna, Italy, 1969.

[11] K. S. Miller and B. Ross, *An Introduction to the Fractional Calculus and Fractional Differential Equations*, John Wiley & Sons, New York, NY, USA, 1993.

[12] K. B. Oldham and J. Spanier, *The Fractional Calculus: Theory and Applications of Differentiation and Integration to Arbitrary Order, With an Annotated Chronological Bibliography by Bertram Ross, Mathematics in Science and Engineering*, vol. 111, Academic Press, New York, NY, USA, 1974.

[13] A. A. Kilbas, H. M. Srivastava, and J. J. Trujillo, *Theory and Applications of Fractional Differential Equations*, vol. 204 of *North-Holland Mathematics Studies*, Elsevier Science B.V., Amsterdam, The Netherlands, 2006.

[14] X. J. Yang, *Advanced Local Fractional Calculus and Its Applications*, World Science Publisher, New York, NY, USA, 2012.

[15] X. J. Yang, "Local fractional integral transforms," *Progress in Nonlinear Science*, vol. 4, pp. 1–225, 2011.

[16] X. J. Yang, *Local Fractional Functional Analysis and Its Applications*, Asian Academic, Hong Kong, China, 2011.

[17] X. J. Yang, "Heat transfer in discontinuous media," *Advances in Mechanical Engineering and Its Applications*, vol. 1, no. 3, pp. 47–53, 2012.

[18] X. J. Yang, "Local fractional partial differential equations with fractal boundary problems," *Advances in Computational Mathematics and Its Applications*, vol. 1, no. 1, pp. 60–63, 2012.

[19] D. Q. Zeng and Y. M. Qin, "The Laplace-Adomian-Pade technique for the seepage flows with the Riemann-Liouville derivatives," *Communications in Fractional Calculus*, vol. 3, no. 1, pp. 26–29, 2012.

[20] J. H. He, "Asymptotic methods for solitary solutions and compactons," *Abstract and Applied Analysis*, vol. 2012, Article ID 916793, 130 pages, 2012.

[21] J.-H. He, "Homotopy perturbation technique," *Computer Methods in Applied Mechanics and Engineering*, vol. 178, no. 3-4, pp. 257–262, 1999.

[22] J.-H. He, "Homotopy perturbation method: a new nonlinear analytical technique," *Applied Mathematics and Computation*, vol. 135, no. 1, pp. 73–79, 2003.

[23] J.-H. He, "New interpretation of homotopy perturbation method. Addendum: 'some asymptotic methods for strongly nonlinear equations'," *International Journal of Modern Physics B*, vol. 20, no. 18, pp. 2561–2568, 2006.

[24] D. D. Ganji, "The application of He's homotopy perturbation method to nonlinear equations arising in heat transfer," *Physics Letters A*, vol. 355, no. 4-5, pp. 337–341, 2006.

[25] A. Yildirim, "An algorithm for solving the fractional nonlinear Schrödinger equation by means of the homotopy perturbation method," *International Journal of Nonlinear Sciences and Numerical Simulation*, vol. 10, no. 4, pp. 445–450, 2009.

[26] D. D. Ganji and M. Rafei, "Solitary wave solutions for a generalized Hirota-Satsuma coupled KdV equation by homotopy perturbation method," *Physics Letters A*, vol. 356, no. 2, pp. 131–137, 2006.

[27] M. M. Rashidi, D. D. Ganji, and S. Dinarvand, "Explicit analytical solutions of the generalized Burger and Burger-Fisher equations by homotopy perturbation method," *Numerical Methods for Partial Differential Equations*, vol. 25, no. 2, pp. 409–417, 2009.

[28] H. Aminikhah and M. Hemmatnezhad, "An efficient method for quadratic Riccati differential equation," *Communications in Nonlinear Science and Numerical Simulation*, vol. 15, no. 4, pp. 835–839, 2010.

[29] S. H. Kachapi and D. D. Ganji, *Nonlinear Equations: Analytical Methods and Applications*, Springer, 2012.

[30] H. Jafari, A. M. Wazwaz, and C. M. Khalique, "Homotopy perturbation and variational iteration methods for solving fuzzy differential equations," *Communications in Fractional Calculus*, vol. 3, no. 1, pp. 38–48, 2012.

[31] Y. M. Qin and D. Q. Zeng, "Homotopy perturbation method for the q-diffusion equation with a source term," *Communications in Fractional Calculus*, vol. 3, no. 1, pp. 34–37, 2012.

[32] M. Javidi and M. A. Raji, "Combination of Laplace transform and homotopy perturbation method to solve the parabolic partial differential equations," *Communications in Fractional Calculus*, vol. 3, no. 1, pp. 10–19, 2012.

[33] J. S. Duan, R. Rach, D. Buleanu, and A. M. Wazwaz, "A review of the Adomian decomposition method and its applications to fractional differential equations," *Communications in Fractional Calculus*, vol. 3, no. 2, pp. 73–99, 2012.

[34] D. D. Ganji, "A semi-Analytical technique for non-linear settling particle equation of motion," *Journal of Hydro-Environment Research*, vol. 6, no. 4, pp. 323–327, 2012.

[35] J. Singh, D. Kumar, and Sushila, "Homotopy perturbation Sumudu transform method for nonlinear equations," *Advances in Applied Mathematics and Mechanics*, vol. 4, pp. 165–175, 2011.

[36] A. Ghorbani and J. Saberi-Nadjafi, "He's homotopy perturbation method for calculating adomian polynomials," *International Journal of Nonlinear Sciences and Numerical Simulation*, vol. 8, no. 2, pp. 229–232, 2007.

[37] A. Ghorbani, "Beyond Adomian polynomials: he polynomials," *Chaos, Solitons and Fractals*, vol. 39, no. 3, pp. 1486–1492, 2009.

[38] S. Das and R. Kumar, "Approximate analytical solutions of fractional gas dynamic equations," *Applied Mathematics and Computation*, vol. 217, no. 24, pp. 9905–9915, 2011.

[39] G. K. Watugala, "Sumudu transform—a new integral transform to solve differential equations and control engineering problems," *Mathematical Engineering in Industry*, vol. 6, no. 4, pp. 319–329, 1998.

[40] S. Weerakoon, "Application of Sumudu transform to partial differential equations," *International Journal of Mathematical Education in Science and Technology*, vol. 25, no. 2, pp. 277–283, 1994.

[41] S. Weerakoon, "Complex inversion formula for Sumudu transform," *International Journal of Mathematical Education in Science and Technology*, vol. 29, no. 4, pp. 618–621, 1998.

[42] M. A. Aşiru, "Further properties of the Sumudu transform and its applications," *International Journal of Mathematical Education in Science and Technology*, vol. 33, no. 3, pp. 441–449, 2002.

[43] A. Kadem, "Solving the one-dimensional neutron transport equation using Chebyshev polynomials and the Sumudu transform," *Analele Universitatii din Oradea*, vol. 12, pp. 153–171, 2005.

[44] A. Kılıçman, H. Eltayeb, and K. A. M. Atan, "A note on the comparison between Laplace and Sumudu transforms," *Iranian Mathematical Society*, vol. 37, no. 1, pp. 131–141, 2011.

[45] A. Kılıçman and H. E. Gadain, "On the applications of Laplace and Sumudu transforms," *Journal of the Franklin Institute*, vol. 347, no. 5, pp. 848–862, 2010.

[46] H. Eltayeb, A. Kılıçman, and B. Fisher, "A new integral transform and associated distributions," *Integral Transforms and Special Functions*, vol. 21, no. 5-6, pp. 367–379, 2010.

[47] A. Kılıçman and H. Eltayeb, "A note on integral transforms and partial differential equations," *Applied Mathematical Sciences*, vol. 4, no. 1–4, pp. 109–118, 2010.

[48] A. Kılıçman, H. Eltayeb, and R. P. Agarwal, "On Sumudu transform and system of differential equations," *Abstract and Applied Analysis*, Article ID 598702, 11 pages, 2010.

[49] J. Zhang, "A Sumudu based algorithm for solving differential equations," *Academy of Sciences of Moldova*, vol. 15, no. 3, pp. 303–313, 2007.

[50] V. B. L. Chaurasia and J. Singh, "Application of Sumudu transform in Schödinger equation occurring in quantum mechanics," *Applied Mathematical Sciences*, vol. 4, no. 57–60, pp. 2843–2850, 2010.

[51] G. Adomian, *Solving Frontier Problems of Physics: The Decomposition Method*, vol. 60 of *Fundamental Theories of Physics*, Kluwer Academic, Dordrecht, The Netherlands, 1994.

[52] Z. Odibat and S. Momani, "Numerical methods for nonlinear partial differential equations of fractional order," *Applied Mathematical Modelling*, vol. 32, no. 1, pp. 28–39, 2008.

Hindawi Publishing Corporation
Abstract and Applied Analysis
Volume 2013, Article ID 270191, 12 pages
http://dx.doi.org/10.1155/2013/270191

Research Article

Complex Dynamics of a Diffusive Holling-Tanner Predator-Prey Model with the Allee Effect

Zongmin Yue, Xiaoqin Wang, and Haifeng Liu

Faculty of Science, Shaanxi University of Science and Technology, Xi'an, Shaanxi 710021, China

Correspondence should be addressed to Zongmin Yue; joanna_yzm@163.com

Received 2 August 2012; Revised 9 December 2012; Accepted 21 December 2012

Academic Editor: Lan Xu

We investigate the complex dynamics of a diffusive Holling-Tanner predation model with the Allee effect on prey analytically and numerically. We examine the existence of the positive equilibria and the related dynamical behaviors of the model and find that when the model is with weak Allee effect, the solutions are local and global stability for some conditions around the positive equilibrium. In contrast, when the model is with strong Allee effect, this may lead to the phenomenon of bistability; that is to say, there is a separatrix curve that separates the behavior of trajectories of the system, implying that the model is highly sensitive to the initial conditions. Furthermore, we give the conditions of Turing instability and determine the Turing space in the parameters space. Based on these results, we perform a series of numerical simulations and find that the model exhibits complex pattern replication: spots, spots-stripes mixtures, and stripes patterns. The results show that the impact of the Allee effect essentially increases the models spatiotemporal complexity.

1. Introduction

Recently, there has been a great interest in studying nonlinear difference/differential equations and systems [1–6]. One of the reasons for this is a necessity for some techniques which can be used in investigating equations arising in mathematical models describing real-life situations in population biology, economy, probability theory, genetics, psychology, sociology, and so forth. And the bases for analyzing the dynamics of complex ecological systems are the interactions between two species, particularly the dynamical relationship between predators and their preys [7]. From the Lotka-Volterra model [8, 9], several alternatives for modeling continuous time consumer-resource interactions have been proposed. In recent years, one of the important predator-prey models is Holling-Tanner model, which was described by May [10]. This model reads as follows:

$$\begin{aligned} \frac{dH}{dt} &= r_1 H\left(1 - \frac{H}{K}\right) - \frac{c_1 HP}{k_1 + H}, \\ \frac{dP}{dt} &= s_1 P\left(1 - \frac{P}{\delta H}\right), \end{aligned} \tag{1}$$

where H and P represent prey and predator population densities at time t, respectively. r, K, c_1, k_1, s_1, and δ are positive constants. r_1 and s_1 are the intrinsic growth rate of prey and predator, respectively. K is the carrying capacity of the prey, and δ takes on the role of the prey-dependent carrying capacity for the predator. The rate at which the predator consumes the prey, $c_1 HP/(k_1 + H)$, is known as the Holling type-II functional response [11]. The parameter c_1 is the maximum number of the prey that can be eaten per predator per time, and k_1 is the saturation value that corresponds to the number of the preys necessary to achieve one half of the maximum rate c_1.

The dynamics of model (1) has been considered in many articles. For example, Hsu and Huang [12] obtained some results on the global stability of the positive equilibrium. More precise, under the conditions which local stability of the positive equilibrium implies its global stability. Gasull and coworkers [13] investigated the conditions of the asymptotic stability of the positive equilibrium which does not imply global stability. Sáez and González-Olivares [14] showed the asymptotic stability of a positive equilibrium and gave a qualitative description of the bifurcation curve.

On the other hand, in population dynamics, any mechanism that can lead to a positive relationship between a component of individual fitness and either the number or density of conspecifics constitutes what is usually called an Allee effect [15–24], starting with the pioneer work of Allee [25]. The outflux of prey to constant rate can be considered as Allee effect because a change on interaction dynamics is provoked, for instance, due to difficulty of encountering mates [17]. Nowadays, it is widely accepted that the Allee effect greatly increases the likelihood of local and global extinction [18] and can lead to a rich variety of dynamical effects.

From an ecological point of view, the Allee effect has been denominated in different ways [19–22] and modeled into strong and weak ones [15, 16, 19], depending on the degree of positive density dependence. Mathematically speaking, if $H = H(t)$ indicates the population size, we assume that the growth function $G(H)$ satisfies the following:

(i) if $G(0) = 0$, $G'(0) > 0$, $G(H)$ is called weak Allee effect;

(ii) if $G(0) = 0$, $G'(0) < 0$, $G(H)$ is called strong Allee effect.

The most common mathematical form describing this phenomenon for a single species is given by

$$G(H) = H(1-H)(H-m), \tag{2}$$

where $0 < m < 1$ or $-1 < m \le 0$, which is named the multiplicative Allee effect; here, a threshold value m is incorporated such that population growth is negative below m. When $m < H < 1$, the per capita growth rate is positive.

Furthermore, Boukal et al. [22] proposed that the prey exhibits a demographic Allee effect at low population densities due to reasons other than predation by the focal predator as follows:

$$G(H) = AH(1-H)\left(1-\frac{b+c}{H+c}\right), \tag{3}$$

where b is the Allee threshold, and c is an auxiliary parameter ($c > 0$ and $b \ge -c$). The auxiliary parameter c affects the overall shape of the per capita growth curve of the prey. When c is fixed, the unit growth rate of the species is only in connection with the Allee threshold.

For model (1), we make a change of variables as follows:

$$(H, P, t) = \left(K\widetilde{H}, K\widetilde{P}, \frac{\widetilde{t}}{r_1}\right). \tag{4}$$

For the sake of convenience, we still use variables H and P instead of $\widetilde{H}$ and $\widetilde{P}$.

(H1) The basic model is a Holling-Tanner type as the form

$$\begin{aligned}\frac{dH}{dt} &= H(1-H) - \frac{aHP}{1+H},\\ \frac{dP}{dt} &= rP\left(1-\frac{P}{\delta H}\right),\end{aligned} \tag{5}$$

where $a = c_1/K$, $k_1 = K$, and $r = s_1/r$.

(H2) Following Boukal et al. [22], in Allee effect equation (3), we choose the auxiliary parameter $c = 1$, and $b+1 \equiv m$ is the Allee threshold. That is, prey H has the population growth function

$$G(H) = H(1-H)\left(1-\frac{m}{H+1}\right). \tag{6}$$

Obviously, we have the following:

(i) if $0 < m \le 1$, $G(0) = 0$, $G'(0) > 0$, the Allee effect (6) is the weak one;

(ii) if $m > 1$, $G(0) = 0$, $G'(0) < 0$, the Allee effect (6) is the strong one;

(iii) if $m = 0$, the Allee effect will disappear.

And we can get the following model with the Allee effect on prey:

$$\begin{aligned}\frac{dH}{dt} &= H(1-H)\left(1-\frac{m}{H+1}\right) - \frac{aHP}{1+H},\\ \frac{dP}{dt} &= rP\left(1-\frac{P}{\delta H}\right).\end{aligned} \tag{7}$$

(H3) Assume that the individuals in populations H and P move randomly described as Brownian random motion [26]. We can get a simple spatial model corresponding to model (7) as follows:

$$\begin{aligned}\frac{\partial H}{\partial t} &= H(1-H)\left(1-\frac{m}{H+1}\right) - \frac{aHP}{1+H} + d_1\nabla^2 H,\\ \frac{\partial P}{\partial t} &= rP\left(1-\frac{P}{\delta H}\right) + d_2\nabla^2 P,\\ H(x,y,0) &= H_0 > 0, \quad P(x,y,0) = P_0 > 0,\\ &(x,y) \in \Omega = (0,L)\times(0,L).\end{aligned} \tag{8}$$

Here, the nonnegative constants d_1 and d_2 are the diffusion coefficients of $H(t)$ and $P(t)$, respectively. $\nabla^2 = \partial^2/\partial x^2 + \partial^2/\partial y^2$ is the Laplacian operator in two-dimensional space, which describes the random moving. The initial distribution of species N_0 and P_0 are continuous functions. And the boundary condition is assumed to be zero-flux one as follows:

$$\frac{\partial H}{\partial n} = \frac{\partial P}{\partial n} = 0, \quad (x,y) \in \partial\Omega. \tag{9}$$

L indicates the size of the model in the directions of x and y, respectively, and n is the outward unit normal vector of the boundary $\partial\Omega$. The main reason for choosing such boundary conditions is that we are interested in the self-organization of pattern, and the zero-flux boundary conditions imply that no external input is imposed form exterior [27].

There are some excellent works on a Holling-Tanner model considering the diffusion [28–33] and the references therein. In [28], Guan and co-workers studied the spatiotemporal dynamics of a modified version of the Leslie-Gower predator-prey model incorporating a prey refuge and showed that the model dynamics exhibits complex Turing pattern replication: stripes, cold/hot spots-stripes coexistence, and cold/hot spots patterns. Without the Allee effect, Peng and Wang [29, 30] analyzed the global stability of the unique positive constant steady state and established some results for the existence and nonexistence of positive nonconstant steady states. Wang et al. [31] considered the Turing and Hopf bifurcations of the equilibrium solutions. Liu and Xue [32] investigated the pattern formation and found that spots, black-eye, and labyrinthine patterns can be observed in the model. Chen and Shi [33] proved global stability of the unique constant equilibrium.

However, the research about the influence of Allee effect on pattern formation of diffusive Holling-Tanner model seems rare. The main purpose of this paper is to study dynamical behaviors of a Holling-Tanner predator-prey model with the Allee effect. We will determine how the Allee effect affects the dynamics of the model and focus on the stability of the positive steady state and bifurcation mechanism and patterns formation analysis of the model.

The rest of the paper is organized as follows. In Sections 2 and 3, we present our main results about the stability and bifurcation analysis of the nonspatial model (7) and the spatial model (8), respectively. Especially, in regards to the spatial model (8) in Section 3, we will give the conditions of the Turing instability and determine the Turing space, and by performing a series of numerical simulations, we illustrate the emergence of different patterns. Finally, in Section 4, some conclusions and remarks are given.

2. Dynamics Analysis of the Nonspatial Model (7)

2.1. Boundedness. Now, we prove that all solutions are eventually bounded.

Theorem 1. *All the solutions of model* (7) *which are initiated in* $\mathbb{R}_+^2$ *are uniformly bounded.*

Proof. Let $H(t)$ and $P(t)$ be any solution of model (7) with initial conditions $(H(0), P(0)) = (H_0, P_0)$ such that $H_0 > 0$, $P_0 > 0$. From the first equation of model (7), we have

$$\frac{dH}{dt} \le H(1-H); \tag{10}$$

a standard comparison theorem shows that

$$\limsup_{t\to\infty} H(t) \le 1. \tag{11}$$

Then, from the second equation of model (7), we get $dP/dt \le rP(1-(P/\delta))$, which implies that

$$\limsup_{t\to\infty} P(t) \le \delta. \tag{12}$$

Define the function $W(t) = H(t) + P(t)$, differentiating both sides with respect to t; we get

$$\begin{aligned}\frac{dW}{dt} &= \frac{dH}{dt} + \frac{dP}{dt} \le H(1-H) + rP\left(1-\frac{P}{\delta}\right)\\ &\le \frac{1}{4} + rP\left(1-\frac{P}{\delta}\right).\end{aligned} \tag{13}$$

Then,

$$\begin{aligned}\frac{dW}{dt} + W &\le \frac{1}{4} + rP\left(1-\frac{P}{\delta}\right) + H + P\\ &\le \frac{5}{4} + P\left(1 + r - \frac{rP}{\delta}\right) \le \frac{5}{4} + \frac{\delta(r+1)^2}{4r} \triangleq M.\end{aligned} \tag{14}$$

Using the theory of differential inequality, for all $t \ge T \ge 0$, we have

$$0 \le W(t) \le M - (M - W(T))\, e^{-(t-T)}. \tag{15}$$

Hence, $\limsup_{t\to\infty} (H(t) + P(t)) \le M$. This completes the proof. □

Remark 2. In fact, if $m \ge 2$, $dH/dt < 0$ always holds, which means that the prey and predator will extinct. Hence, we will later only focus on the case of $0 \le m < 2$.

Next, we will investigate the existence of equilibria and their local and global stability with respect to model (7).

2.2. Equilibria Analysis in the Case of the Strong Allee Effect (i.e., $1 < m < 2$). In this subsection, we consider the existence and stability of the equilibrium of model (7) with strong Allee effect; that is, $1 < m < 2$.

We note that model (7) is not defined at the P-axis, particularly at the point $(0, 0)$, but both isoclines pass through this point, and in this case, it is a point of particular interest [34]. The character of $(0, 0)$ can be obtained after rescaling the time in model (7) by $t = \tau H(1 + H)$ as follows:

$$\begin{aligned}\frac{dH}{d\tau} &= H^2(1-H)(1+H-m) - aH^2P,\\ \frac{dP}{d\tau} &= r(1+H)P\left(H - \frac{P}{\delta}\right).\end{aligned} \tag{16}$$

Lemma 3. *The point* $(0, 0)$ *of model* (16) *has a hyperbolic and a parabolic sector [20, 35] determined for the line* $P = (\delta(m-1+r)/r)H$. *That is, there exists a separatrix curve in the phase plane that divides the behavior of trajectories; the point* $(0, 0)$ *is then an attractor point for certain trajectories and a saddle point for others.*

Proof. As the Jacobian matrix of the point $(0, 0)$ for model (16) is the zero matrix, we follow the methodology used in [20, 35] given by the function $\varphi(u, v) = (uv, v) = (H, P)$. Then, we have that

$$\frac{du}{d\tau} = \frac{1}{v}\left(\frac{dH}{d\tau} - u\frac{dP}{d\tau}\right), \quad \frac{dv}{d\tau} = \frac{dP}{d\tau}, \tag{17}$$

and rescaling the time by $T = v\tau$, it becomes

$$\begin{aligned}\frac{du}{dT} &= u\Bigg(((1-uv)(uv+1-m) - av)\,u\\ &\qquad - r(1+uv)\left(u - \frac{1}{\delta}\right)\Bigg),\\ \frac{dv}{dT} &= r(1+uv)\,v\left(u - \frac{1}{\delta}\right).\end{aligned} \tag{18}$$

Clearly, if $v = 0$, then $dv/dT = 0$. Moreover, $du/dT = u((1-m)u - r(u-(1/\delta)))$.

The singularities of model (18) are $(0,0)$ and $(r/(\delta(m-1+r)),0)$; that is, a separatrix straight exists in the phase plane uv, given by $u = r/(\delta(m-1+r))$. The Jacobian matrixes of $(0,0)$ and $(r/(\delta(m-1+r)),0)$ for model (18) are

$$J_{(0,0)} = \begin{pmatrix} \dfrac{r}{\delta} & 0 \\ 0 & -\dfrac{r}{\delta} \end{pmatrix},$$

$$J_{(r/(\delta(m-1+r)),0)} = \begin{pmatrix} -\dfrac{r}{\delta} & -\dfrac{r^2(-2rm + a\delta(m-1+r)+r)}{\delta^3(m-1+r)^3} \\ 0 & -\dfrac{r(m-1)}{\delta(m-1+r)} \end{pmatrix}. \tag{19}$$

Then, $(0,0)$ is a hyperbolic saddle point, and $(r/(\delta(m-1+r)),0)$ is an attractor point. Using the blowing down, the point $(0,0)$ is a saddle node in model (16), and the line $P = ((\delta(m-1+r))/r)H$ divides the behavior of trajectories on the phase plane. The proof is completed. □

Moreover, it is easy to verify that model (7) always has two boundary equilibria $E_0 = (m-1,0)$ and $E_1 = (1,0)$. And the behavior of model (7) around E_0 and E_1 is found as follows.

The Jacobian matrix of model (7) at the equilibrium $E_0 = (m-1,0)$ takes the form

$$J_{E_1} = \begin{pmatrix} \dfrac{(m-1)(2-m)}{m} & \dfrac{a(m-1)}{m} \\ 0 & r \end{pmatrix}. \tag{20}$$

Hence, the equilibrium $E_0 = (m-1,0)$ is an unstable node point (nodal source).

The Jacobian matrix of model (7) at the equilibrium $E_0 = (1,0)$ takes the form

$$J_{E_0} = \begin{pmatrix} \dfrac{m}{2}-1 & -\dfrac{a}{2} \\ 0 & r \end{pmatrix}. \tag{21}$$

Hence, the equilibrium $E_1 = (1,0)$ is a saddle point.

And model (7) has a positive equilibrium $E = (H, \delta H)$, where H satisfies

$$H^2 - (m - a\delta)H - (1-m) = 0. \tag{22}$$

For simplicity, we consider $A = m - a\delta$ and $B = \sqrt{(m-a\delta)^2 + 4(1-m)}$; then, the two roots of (22) are given by

$$H_+ = \frac{1}{2}(A+B), \qquad H_- = \frac{1}{2}(A-B). \tag{23}$$

Lemma 4.

(i) *Suppose that $m - a\delta > 0$ and $1 < m < 2$.*

(a) *If $B^2 > 0$ holds, model (7) has two positive equilibria $E_+ = (H_+, \delta H_+)$ and $E_- = (H_-, \delta H_-)$.*

(b) *If $B^2 = 0$ holds, model (7) has a unique positive equilibrium $E_e = (H_e, \delta H_e)$. Note that in this case $H_e = H_+ = H_- = A/2 = \sqrt{m-1}$.*

(c) *If $B^2 < 0$, model (7) has no positive equilibrium.*

(ii) *If $m - a\delta \le 0$, model (7) has no positive equilibrium.*

Let $E = (N,P)$ be an arbitrary positive equilibrium. The Jacobian matrix of model (7) at the positive equilibrium $E = (H, \delta H)$ takes the form

$$J_E = \begin{pmatrix} \dfrac{H\left(a\delta H + 2m - (1+H)^2\right)}{(1+H)^2} & -\dfrac{aH}{1+H} \\ r\delta & -r \end{pmatrix}. \tag{24}$$

Then, we can get

$$\det(J_E) = \frac{rH\left(H^2 + 2H + 1 + a\delta - 2m\right)}{(H+1)^2},$$
$$\operatorname{tr}(J_E) = \frac{H\left(a\delta H + 2m - (1+H)^2\right)}{(1+H)^2} - r. \tag{25}$$

We can see that the sign of $\det(J_E)$ is determined by

$$F(H) \triangleq H^2 + 2H + 1 + a\delta - 2m = H^2 + 2H + 1 - A - m. \tag{26}$$

Thus, we can obtain

$$F(H_+) = \frac{(A+B)^2}{4} + B - m + 1 = B\left(1 + \frac{A}{2}\right) + \frac{1}{2}B^2 > 0;$$
$$F(H_-) = \frac{(A-B)^2}{4} - B - m + 1 = -\frac{1}{2}B(A-B) - B < 0;$$
$$F(H_e) = \frac{A}{4} + 1 - m = 0. \tag{27}$$

Hence, we obtain $\det(J_{E_+}) > 0$, $\det(J_{E_-}) < 0$, and $\det(J_{E_e}) = 0$. And the positive equilibrium $E_- = (H_-, \delta H_-)$ is a saddle point. The nature of the equilibrium point E_+ is dependent on the sign of the trace of the Jacobian matrix evaluated in this point. Whether E_+ is a node or a focus depends on the sign of $(\operatorname{tr}(J_{E_+}))^2 - 4\det(J_{E_+})$.

In the following results, we study the stability of the positive equilibrium E_+ and the unique positive equilibria E_e.

Theorem 5. *Define*

$$r_+ = \frac{H_+}{(1+H_+)^2}\left(a\delta H_+ + 2m - (1+H_+)^2\right). \tag{28}$$

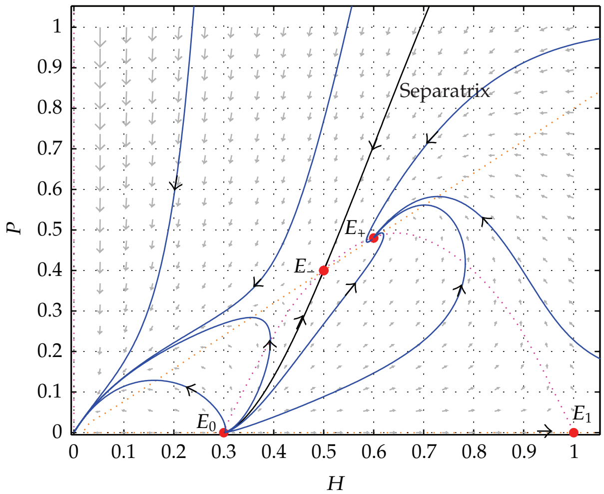

Figure 1: The phase portrait of model (7) with the strong Allee effect. The parameters are taken as $a = 0.25$, $\delta = 0.8$, $m = 1.3$ and $r = 0.15$. In this case, $E_0 = (0.3, 0)$ is an unstable node point, $E_1 = (1, 0)$ and $E_- = (0.5, 0.4)$ are saddle points; the positive equilibrium $E_+ = (0.6, 0.48)$ is local asymptotically stable. There exists a separatrix curve determined by the stable manifold of the equilibrium point E_-. The dotted curves are the nullclines.

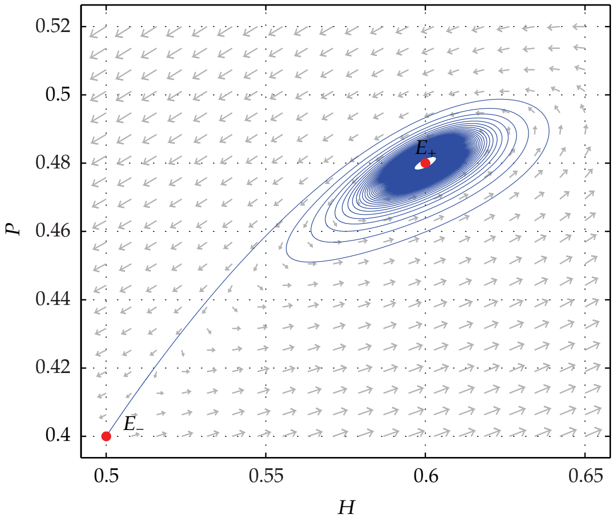

Figure 2: The phase portrait of model (7) with the strong Allee effect. The parameters are taken as $a = 0.25$, $\delta = 0.8$, $m = 1.3$, and $r = 0.0375$. The model enters into a Hopf bifurcation around $E_+ = (0.6, 0.48)$ at $r = r_+$.

(a) *If $r > r_+$, the positive equilibrium $E_+ = (H_+, \delta H_+)$ is a locally asymptotically stable point;*

(a1) *if $(r_+ - r)^2 < 4\det(J_{E_+})$, then E_+ is a stable focus,*

(a2) *if $(r_+ - r)^2 > 4\det(J_{E_+})$, then E_+ is a stable node point.*

(b) *If $r < r_+$, the positive equilibrium $E_+ = (H_+, \delta H_+)$ is an unstable point;*

(b1) *if $(r_+ - r)^2 < 4\det(J_{E_+})$, then E_+ is an unstable focus surrounded by a stable limit cycle,*

(b2) *if $(r_+ - r)^2 > 4\det(J_{E_+})$, then E_+ is an unstable node and the limit cycle disappears.*

(c) *A Hopf bifurcation occurs at $r = r_+$ around the positive equilibrium $E_+ = (H_+, \delta H_+)$. That is to say, model* (7) *has at least one positive periodic orbit.*

Proof. Here, we only give the proof of the existence of Hopf bifurcation. It is easy to see that

(i) $\mathrm{tr}(J(E_+))|_{r=r_+} = 0$ holds,

(ii) the characteristic equation is $\lambda^2 + \det(J(E_+))|_{r=r_+} = 0$, whose roots are purely imaginary,

(iii) $(d/dr)[\mathrm{tr}(J(E_+))]_{r=r_+} = -1 \neq 0$.

From the Poincaré-Andronov-Hopf Bifurcation Theorem [36], we know that model (7) undergoes a Hopf bifurcation at E_+ as r passes through the value r_+. The proof is completed. □

Figure 1 illustrates the local stability of the positive equilibrium E_+ and the separatrix curve generated by the stable manifold of the positive equilibrium E_-. The orbits initiating the right of the separatrix curve tend to E_+, while the orbits initiating the left of the separatrix curve tend to $(0, 0)$ that represents the extinction of the population. Figure 2 illustrates a Hopf bifurcation situation of the model around E_+. The parameter values are given in the figures.

Theorem 6. *The unique equilibrium point $E_e = (\sqrt{m-1}, (1/\delta)\sqrt{m-1})$ is*

(i) *a nonhyperbolic attractor node, if and only if $r > \sqrt{m-1}(1-\sqrt{m-1})^2/(1+\sqrt{m-1})$;*

(ii) *a nonhyperbolic repellor node, if and only if $r > \sqrt{m-1}(1-\sqrt{m-1})^2/(1+\sqrt{m-1})$;*

(iii) *a cusp point, if and only if $r = \sqrt{m-1}(1-\sqrt{m-1})^2/(1+\sqrt{m-1})$, and in this case, there exists a unique trajectory which attains the point E_e. And in this case, the point $(0, 0)$ is a global attractor.*

Proof. We have

$$\mathrm{tr}\left(J_{E_e}\right) = \frac{\sqrt{m-1}\left(1-\sqrt{m-1}\right)^2}{1+\sqrt{m-1}} - r. \qquad (29)$$

Hence (i) and (ii) hold.

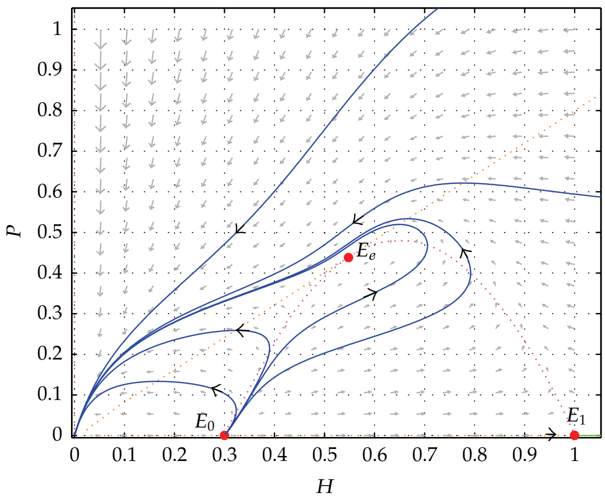

FIGURE 3: The phase portrait of model (7) with the strong Allee effect. The parameters are taken as $a = 0.2556936062$, $\delta = 0.8$, $m = 1.3$, and $r = 0.07238979895$. $E_0 = (0.3, 0)$ is an unstable node point; $E_1 = (1, 0)$ is saddle point; the positive equilibrium $E_2 = (0.2, 0.4)$ is a cusp point. In this case, the point $(0, 0)$ is globally asymptotically stable. The dotted curves are the nullclines.

Moreover, $\mathrm{tr}(J_{E_e}) = 0$, if and only if $r = \sqrt{m-1}(1-\sqrt{m-1})^2/(1-\sqrt{m+1})$. In this case, we obtain the Jacobian matrix of (16) as follows:

$$\begin{aligned}
&\tilde{J}\left(\sqrt{m-1}, \frac{1}{\delta}\sqrt{m-1}\right) \\
&= \begin{pmatrix} (m-1)\left(1-\sqrt{m-1}\right)^2 & -(m-1)\left(1-\sqrt{m-1}\right)^2 \\ (m-1)\left(1-\sqrt{m-1}\right)^2 & -(m-1)\left(1-\sqrt{m-1}\right)^2 \end{pmatrix} \\
&= (m-1)\left(1-\sqrt{m-1}\right)^2 \begin{pmatrix} 1 & -1 \\ 1 & -1 \end{pmatrix};
\end{aligned} \tag{30}$$

and the associate Jordan matrix is

$$\begin{pmatrix} 0 & -(m-1)\left(1-\sqrt{m-1}\right)^2 \\ 0 & 0 \end{pmatrix}. \tag{31}$$

Then, the singularity $(\sqrt{m-1}, (1/\delta)\sqrt{m-1})$ is a cusp point, since it is a point of codimension 2, and we have a Bogdanov-Takens bifurcation [37]. □

The cusp point is shown in Figure 3.

2.3. Equilibria Analysis in the Case of the Weak Allee Effect (i.e., $0 < m \le 1$). In this subsection, we consider the stability of the equilibrium of model (7) with weak Allee effect ($0 < m \le 1$).

It is easy to verify that model (7) always has one boundary equilibrium $E_0 = (1, 0)$ which is a saddle point and a positive equilibrium $E^* = (H^*, \delta H^*)$, where

$$H^* = \frac{m - a\delta + \sqrt{(m-a\delta)^2 + 4(1-m)}}{2}. \tag{32}$$

From (24), we have

$$\begin{aligned}
\det\left(J_{E^*}\right) &= \frac{rH^*\left(H^{*2} + 2H^* + 1 + a\delta - 2m\right)}{(H^*+1)^2} > 0, \\
\mathrm{tr}\left(J_{E^*}\right) &= \frac{H^*\left(a\delta H^* + 2m - (1+H^*)^2\right)}{(1+H^*)^2} - r.
\end{aligned} \tag{33}$$

Hence, we have the following results on the stability of the positive equilibrium $E^* = (H^*, \delta H^*)$.

Theorem 7. *Define*

$$r^* = \frac{H^*\left(a\delta H^* + 2m - (1+H^*)^2\right)}{(1+H^*)^2}. \tag{34}$$

(a) *If $r > r^*$, the positive equilibrium $E^* = (H^*, \delta H^*)$ is a locally asymptotically stable point, and*

(a1) *if $(r^* - r)^2 < 4\det(J_{E^*})$, then E^* is a stable focus;*

(a2) *if $(r^* - r)^2 > 4\det(J_{E^*})$, then E^* is a stable node point.*

(b) *If $r < r^*$, the positive equilibrium $E^* = (H^*, \delta H^*)$ is an unstable point, and*

(b1) *if $(r^* - r)^2 < 4\det(J_{E^*})$, then E^* is an unstable focus surrounded by a stable limit cycle;*

(b2) *if $(r^* - r)^2 > 4\det(J_{E^*})$, then E^* is an unstable node and the limit cycle disappears.*

(c) *A Hopf bifurcation occurs at $r = r^*$ around the positive equilibrium $E^* = (H^*, \delta H^*)$. That is to say, model (7) has at least one positive periodic orbit.*

In the following theorem, we study the global behavior of the positive equilibrium E^*.

Theorem 8. *If $0 < m < 1/(1 + a\delta)$, the positive equilibrium $E^* = (H^*, \delta H^*)$ is globally asymptotically stable.*

Proof. Construct the following Lyapunov function:

$$V(H, P) = \int_{H^*}^{H} \frac{\xi - H_+}{\xi\phi(\xi)} d\xi + \frac{1}{r}\int_{\delta H^*}^{P} \frac{\eta - \delta H^*}{\eta} d\eta, \tag{35}$$

where

$$\phi(H) = \frac{aH}{H+1}. \tag{36}$$

Then,

$$\frac{dV}{dt} = \frac{H - H^*}{H\phi(H)}\frac{dH}{dt} + \frac{P - \delta H^*}{rP}\frac{dP}{dt}. \tag{37}$$

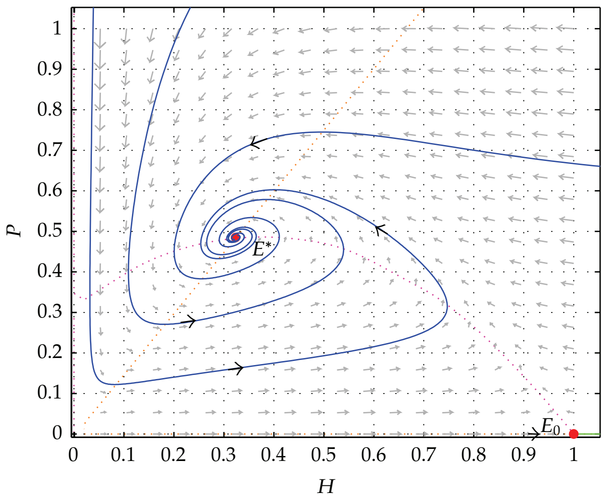

FIGURE 4: The phase portrait of model (7) with the weak Allee effect. The parameters are taken as $a = 0.25$, $\delta = 0.8$, $m = 1.3$, and $r = 0.1$. In this case, $E_0 = (1, 0)$ is saddle point; the positive equilibrium $E^* = (0.3232928050, 0.4849392075)$ is globally asymptotically stable. The dotted curves are the nullclines.

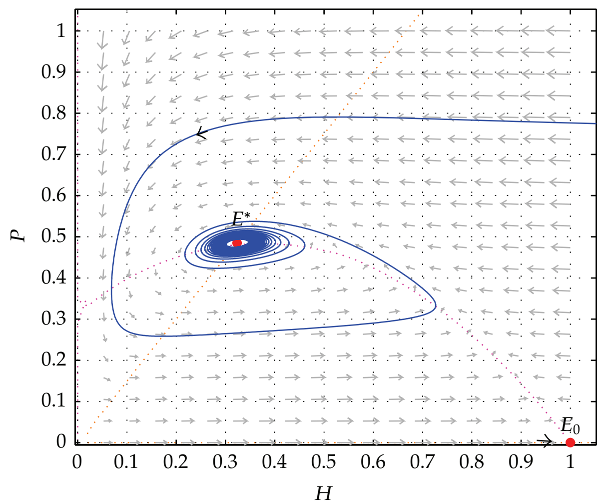

FIGURE 5: The phase portrait of model (7) with the weak Allee effect. The parameters are taken as $a = 0.25$, $\delta = 0.8$, $m = 1.3$, and $r = 0.025265$. The model enters into a Hopf bifurcation around $E^* = (0.3232928050, 0.4849392075)$ at $r = r^*$.

Substituting the value of dH/dt and dP/dt from the model of (7), we obtained

$$\begin{aligned}\frac{dV}{dt} &= \frac{H - H^*}{aH}\left[(1 - H)(1 + H - m) - a\delta H^*\right] \\ &\quad - \frac{\delta}{H}(P - \delta H^*)^2.\end{aligned} \tag{38}$$

Note that $a\delta H^* = H^*(1 - H^*)(1 + H^* - m)$; we obtain

$$\frac{dV}{dt} = -\frac{(H - H^*)^2}{aH}(H + H^* - m) - \frac{\delta}{H}(P - \delta H^*)^2. \tag{39}$$

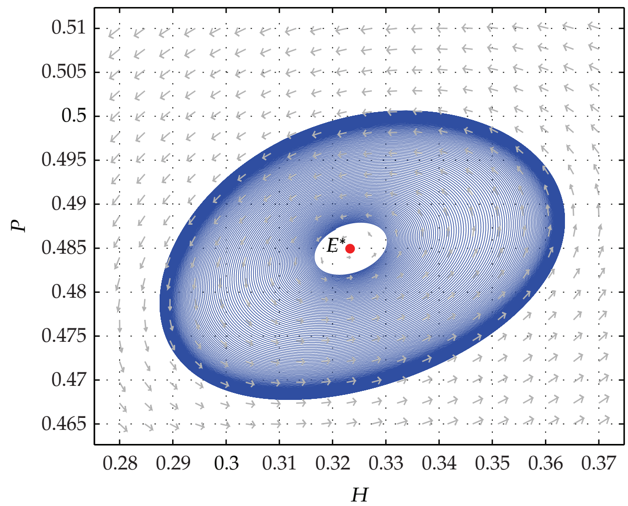

FIGURE 6: The phase portrait of model (7) with the weak Allee effect. The parameters are taken as $a = 0.8$, $\delta = 1.5$, $m = 0.75$, and $r = 0.025$. The positive equilibrium $E^* = (0.3232928050, 0.4849392075)$ is an unstable focus surrounded by a stable limit cycle.

Hence, if $0 < m < 1/(1 + a\delta)$, $H^* - m > 0$ which is equivalent to $dV/dt < 0$.

Hence, the positive equilibrium $E^* = (H^*, \delta H^*)$ is globally asymptotically stable. This completes the proof. □

Figure 4 demonstrates the global stability situation of model (7) around E^*. Figure 5 illustrates a Hopf bifurcation situation of the model around E^*. Figure 6 shows a stable limit cycle around E^* which is an unstable focus. The parameter values are given in the figures.

3. Dynamics of the Spatial Model (8)

In this section, we will investigate the dynamics of the spatial model (8). As an example, we only focus on the positive equilibrium point $E^* = (H^*, \delta H^*)$ in the case of weak Allee effect ($0 < m < 1$).

3.1. Turing Instability. Mathematically speaking, an equilibrium is Turing instability (diffusion-driven instability) means that it is an asymptotically stable equilibrium E^* of model (7) but is unstable with respect to the solutions of reaction-diffusion model (8).

In the presence of diffusion, we will introduce small perturbations $U_1 = H - H^*$, $U_2 = P - \delta H^*$, where $|U_1|, |U_2| \ll 1$. To study the effect of diffusion on the model, we have considered the linearized form of model as follows:

$$\begin{aligned}\frac{\partial U_1}{\partial t} &= r^* U_1 - \frac{aH^*}{1 + H^*}U_2 + d_1\nabla^2 U_1, \\ \frac{\partial U_2}{\partial t} &= r\delta U_1 - rU_2 + d_2\nabla^2 U_2,\end{aligned} \tag{40}$$

where r^* is defined as (34).

Following Malchow et al. [38], we can know that any solution of model (40) can be expanded into a Fourier series so that

$$U_1(\mathbf{r},t)=\sum_{n,m=0}^{\infty}u_{nm}(\mathbf{r},t)=\sum_{n,m=0}^{\infty}\alpha_{nm}(t)\sin\mathbf{kr},$$
$$U_2(\mathbf{r},t)=\sum_{n,m=0}^{\infty}v_{nm}(\mathbf{r},t)=\sum_{n,m=0}^{\infty}\beta_{nm}(t)\sin\mathbf{kr},\tag{41}$$

where $\mathbf{r}=(x,y)$, and $0<x<L$ and $0<y<L$. $\mathbf{k}=(k_n,k_m)$, and $k_n=n\pi/L$ and $k_m=m\pi/L$ are the corresponding wavenumbers.

Having substituted u_{nm} and v_{nm} into (40), we obtain

$$\frac{d\alpha_{nm}}{dt}=\left(r^*-d_1k^2\right)\alpha_{nm}-\frac{aH^*}{1+H^*}\beta_{nm},$$
$$\frac{d\beta_{nm}}{dt}=r\delta\alpha_{nm}-\left(r+d_2k^2\right)\beta_{nm},\tag{42}$$

where $k^2=k_n^2+k_m^2$.

A general solution of (42) has the form $C_1\exp(\lambda_1 t)+C_2\exp(\lambda_2 t)$, where the constants C_1 and C_2 are determined by the initial conditions (3), and the exponents λ_1 and λ_2 are the eigenvalues of the following matrix:

$$\widetilde{D}=\begin{pmatrix} r^*-d_1k^2 & -\dfrac{aH^*}{1+H^*}\\ r\delta & -r-d_2k^2\end{pmatrix}.\tag{43}$$

Correspondingly, λ_1 and λ_2 are the solutions of the following equation:

$$\lambda^2-\operatorname{tr}\left(\widetilde{D}\right)\lambda+\det\left(\widetilde{D}\right)=0,\tag{44}$$

where

$$\operatorname{tr}\left(\widetilde{D}\right)=r^*-r-(d_1+d_2)k^2,$$
$$\det\left(\widetilde{D}\right)=d_1d_2k^4+(rd_1-r^*d_2)k^2+\det\left(J\left(E^*\right)\right).\tag{45}$$

Summarizing the previous discussions, we can get the following theorem immediately.

Theorem 9. *(i) The positive equilibrium E^* of model* (8) *is locally asymptotically stable if $r>\max\{r^*,r^*d_2/d_1\}$ holds.*

(ii) If the positive equilibrium E^* of model (7) *is globally asymptotically stable, then the corresponding steady state E^* of model* (8) *is also globally asymptotically stable.*

Proof. (i) Using Routh-Hurwitz criteria, we can know that the positive equilibrium E^* is locally asymptotically stable, if and only if $\operatorname{tr}(\widetilde{D})<0$ and $\det(\widetilde{D})>0$. So, we obtain $r>\max\{r^*,r^*d_2/d_1\}$.

(ii) We select the Lyapunov function for model (8) as follows:

$$V_2(t)=\iint_\Omega V(H,P)\,dx\,dy,\tag{46}$$

where $V(H,P)$ is the same as defined in (35). So,

$$\frac{dV_2}{dt}=\iint_\Omega\frac{dV}{dt}dx\,dy+\iint_\Omega\left\{\frac{\partial V}{\partial H}d_1\nabla^2H+\frac{\partial V}{\partial P}d_2\nabla^2P\right\}dx\,dy.\tag{47}$$

Using Green's first identity in the plane,

$$\iint_\Omega F\nabla^2G\,dx\,dy=\int_{\partial\Omega}F\frac{\partial G}{\partial n}ds-\iint_\Omega(\nabla F\cdot\nabla G)\,dx\,dy.\tag{48}$$

Considering the zero-flux boundary conditions, one can show that

$$\iint_\Omega\frac{\partial V}{\partial H}d_1\nabla^2H\,dx\,dy=-d_1\iint_\Omega\frac{\partial^2V}{\partial H^2}\left[\left(\frac{\partial H}{\partial x}\right)^2+\left(\frac{\partial H}{\partial y}\right)^2\right]dx\,dy\le 0,$$
$$\iint_\Omega\frac{\partial V}{\partial P}d_2\nabla^2P\,dx\,dy=-d_2\iint_\Omega\frac{\partial^2V}{\partial P^2}\left[\left(\frac{\partial P}{\partial x}\right)^2+\left(\frac{\partial P}{\partial y}\right)^2\right]dx\,dy\le 0.\tag{49}$$

From the previous analysis, we note that $dV_2/dt<0$ is valid if $dV/dt<0$ is true. This implies that the equilibrium E^* of both model (7) and model (8) is globally asymptotically stable if $0<m<1/(1+a\delta)$ holds. This ends the proof. □

On the other hand, Turing instability sets in when at least one of the conditions is either $\operatorname{tr}(\widetilde{D})<0$ or $\det(\widetilde{D})>0$. It is evident that the condition $\operatorname{tr}(\widetilde{D})<0$ is not violated when the requirement $r^*-r<0$ is met [39]. Hence, only violation of condition $\det(\widetilde{D})>0$ gives rise to diffusion instability. Then, the condition for diffusive instability is given by

$$G\left(k^2\right)\equiv d_1d_2k^4+(rd_1-r^*d_2)k^2+\det\left(J\left(E^*\right)\right)<0.\tag{50}$$

$G(\cdot)$ is quadratic in k^2, and the graph of $G(k^2)=0$ is a parabola. The minimum of $G(k^2)$ occurs at $k^2=k_m^2$, where

$$k_m^2=\frac{r^*d_2-rd_1}{2d_1d_2}>0.\tag{51}$$

The critical wave number k_c of the first perturbations to grow is found by evaluating k_m from (51).

Thus, a sufficient condition for Turing instability is that $G(k_m^2)$ is negative. Therefore,

$$G\left(k_m^2\right)=\det\left(J\left(E^*\right)\right)-\frac{\left(rd_1-r^*d_2\right)^2}{4d_1d_2}<0.\tag{52}$$

Combination of (51) and (52) leads to the following final criterion for diffusive instability:

$$\left(rd_1-r^*d_2\right)^2>4d_1d_2\det\left(J\left(E^*\right)\right).\tag{53}$$

Summarizing the previous discussions, we can obtain the following theorem.

Theorem 10. *If $rd_1/d_2 < r^* < r$ and $r^* d_2 - rd_1 > 2\sqrt{d_1 d_2 \det(J(E^*))}$ hold, the criterion for Turing instability for model* (8) *emerges, and the critical wave number $k_c = \sqrt{(r^* d_2 - rd_1)/2d_1 d_2}$.*

The Turing instability (or bifurcation) breaks spatial symmetry, leading to the formation of patterns that are stationary in time and oscillatory in space [40, 41]. We adopt the intrinsic growth rates of predator r as the bifurcation parameter, and the linear stability analysis yields the bifurcation diagram shown in Figure 7. The Turing bifurcation curve separates the parametric space into two domains. Above the curve, the solutions of model (8) are stable for all pairs of (m, r); that is, there is no Turing instability. While below the curve, the solutions of model (8) are unstable for (m, r) and diffusive instability emerges; that is, Turing patterns emerge. This domain is called the Turing space.

3.2. Pattern Formation. In this subsection, we performed extensive numerical simulations of the spatially extended model (8) in two-dimension spaces, and the qualitative results are shown here. All our numerical simulations employ the zero-flux boundary conditions with a model size of $L \times L$, with $L = 100$ discretized through $x \to (x_0, x_1, x_2, \ldots, x_n)$ and $y \to (y_0, y_1, y_2, \ldots, y_n)$, with $n = 200$. Other parameters are fixed as $a = 0.8$, $\delta = 1.75$, $r = 0.15$, $d_1 = 0.01$, and $d_2 = 1$.

The numerical integration of model (8) is performed by using a finite difference approximation for the spatial derivatives and an explicit Euler method for the time integration [42] with a time stepsize of $\tau = 1/100$. The initial condition is always a small amplitude random perturbation around the positive constant steady state solution E^*. After the initial period during which the perturbation spread, either the model goes into a time-dependent state or to an essentially steady state solution (time independent).

More precisely, the concentrations $(H_{i,j}^{n+1}, P_{i,j}^{n+1})$ at the moment $(n+1)\tau$ at the mesh position (i, j) are given by

$$\begin{aligned} H_{i,j}^{n+1} &= H_{i,j}^{n} + \tau d_1 \Delta_h H_{i,j}^{n} + \tau f\left(H_{i,j}^{n}, P_{i,j}^{n}\right), \\ P_{i,j}^{n+1} &= P_{i,j}^{n} + \tau d_2 \Delta_h P_{i,j}^{n} + \tau g\left(H_{i,j}^{n}, P_{i,j}^{n}\right), \end{aligned} \tag{54}$$

with the Laplacian defined by

$$\Delta_h H_{i,j}^{n} = \frac{H_{i+1,j}^{n} + H_{i-1,j}^{n} + H_{i,j+1}^{n} + H_{i,j-1}^{n} - 4H_{i,j}^{n}}{h^2}, \tag{55}$$

where $f(H, P) = H(1 - H)(1 - m/(H + 1)) - aHP/(1 + H)$, $g(H, P) = rP(1 - P/\delta H)$, and the space stepsize $h = 1/3$.

In the numerical simulations, different types of dynamics are observed, and it is found that the distributions of predator and prey are always of the same type. Consequently, we can restrict our analysis of pattern formation to one distribution. In this section, we show the distribution of prey H, for instance.

Figure 8 shows the evolution of the spatial pattern of prey H at $t = 0, 500, 1000, 2000$, with small random perturbation of the stationary solution E^* of the spatially homogeneous systems when m is located in "Turing space."

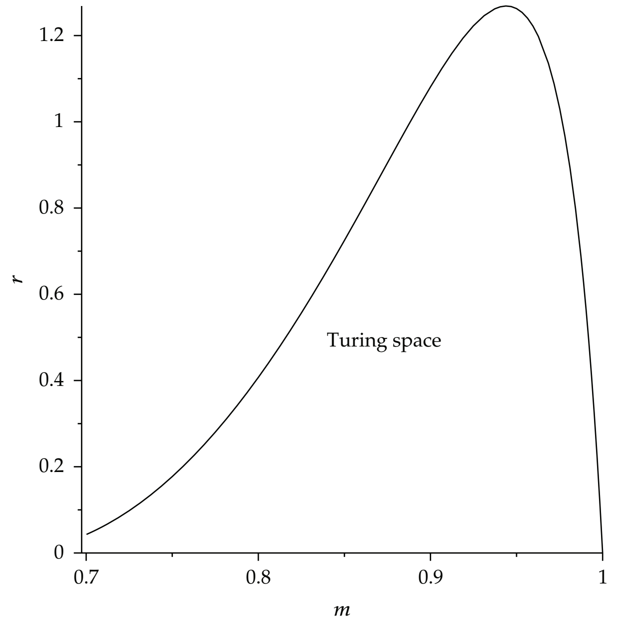

Figure 7: Turing bifurcation diagram for model (8) using m and r as parameters. Other parameters are taken as $a = 0.8$, $\delta = 1.75$, $d_1 = 0.01$, and $d_2 = 1$. Above the curve, the positive equilibrium E^* is the only stable solution of model (3). Below the curve, the positive equilibrium E^* loses its stability with respect to model (3), and Turing instability occurs; this domain is called the Turing space.

In this case, one can see that for model (8), the random initial distribution leads to the formation of a strongly irregular transient pattern in the domain. After the irregular pattern is formed (c.f., Figures 8(b) and 8(c)), it grows slightly and jumps alternately for a certain time, and finally spots patterns, which are isolated zones with low prey densities, prevail over the whole domain, and the dynamics of the model does not undergo any further changes (c.f., Figure 8(d)).

Figure 9 shows stripe patterns are interlaced stripes of high and low population densities of prey H for the parameter $m = 0.78$ at $t = 1000$. In Figure 10, with the parameter $m = 0.85$, the spot-stripe mixtures pattern is time independent with low prey densities.

4. Concluding Remarks

In this paper, we are concerned with the complex dynamics in a diffusive Holling-Tanner predator-prey model with the Allee effect on prey. The value of this study lies in two folds. First, the local asymptotic stability conditions for coexisting equilibrium and conditions for Hopf bifurcation are described briefly for the model with the weak and strong Allee effects. Second, it gives the analysis of Turing instability which determines the Turing space in the spatial domain and meanwhile illustrates the Turing pattern formation close to the onset Turing bifurcation via numerical simulations, which shows that the model dynamics exhibits complex pattern replication.

We note that in the analyzed models, a big difference between the dynamics of model with strong or weak Allee

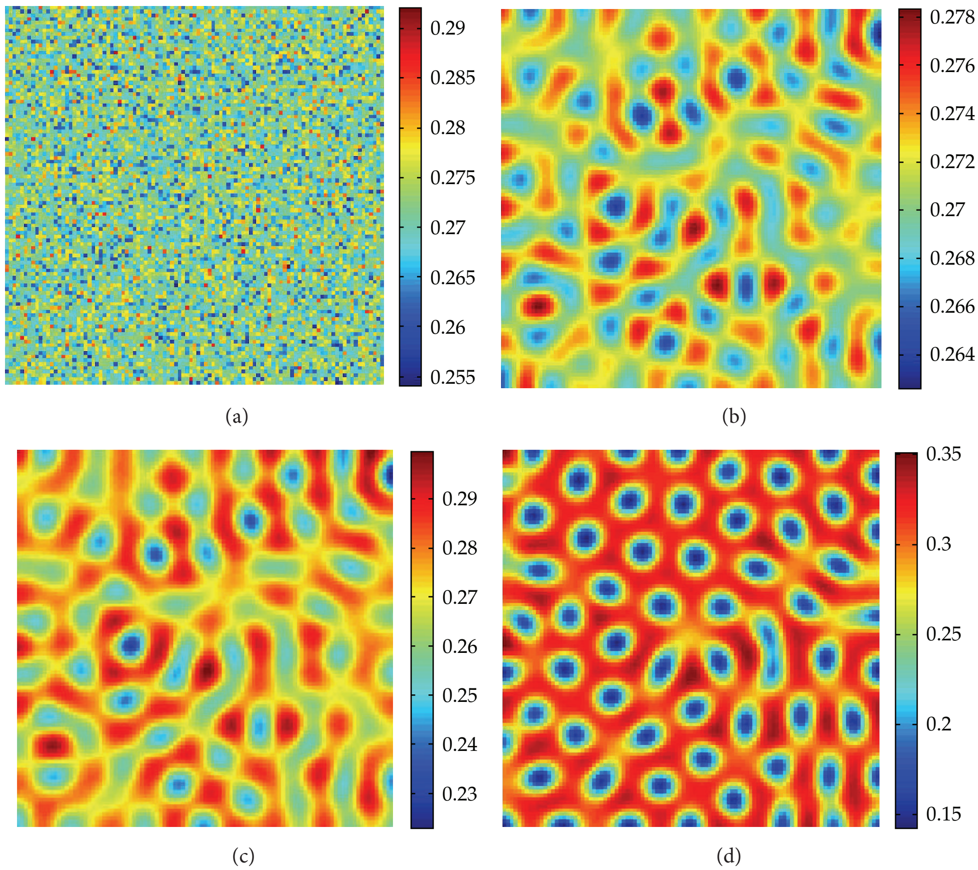

Figure 8: Spots pattern of H in model (8) for $m = 0.75$. Times: (a) 0, (b) 500, (c) 1000, and (d) 2000.

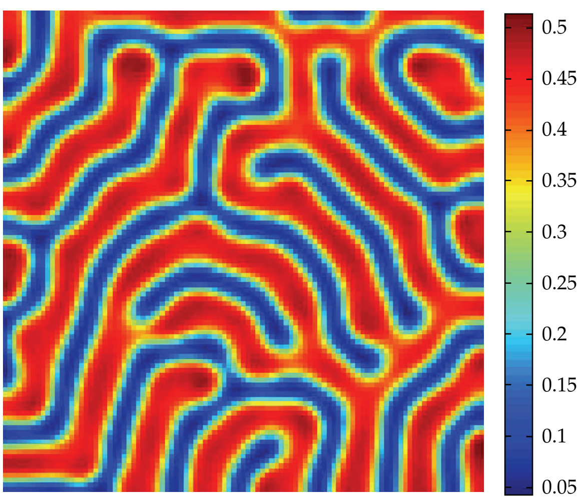

Figure 9: Stripes pattern of H in model (8) for $m = 0.78$ at $t = 1000$.

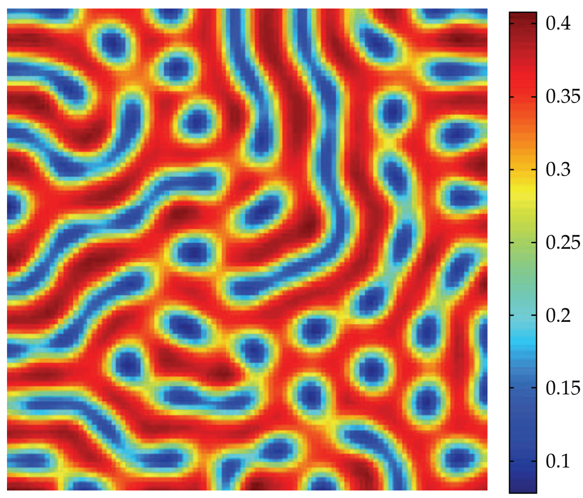

Figure 10: Spot-stripe mixtures pattern of H in model (8) for $m = 0.85$ at $t = 1000$.

effect exists. In the case of strong Allee effect, two positive equilibria can coexist for a subset of parameters with a varied dynamics but different to other Holling-Tanner models analyzed earlier [12–14]. We have shown that one of these equilibria is always a saddle point and proved the existence of a separatrix curve. And there is no global asymptotically stable positive equilibrium. In this case, the point $(0, 0)$ is an attractor in addition to locally stable positive equilibrium E_+ for determined parameter values, which leads to the existence of a bistability phenomenon. The dynamics of the model is determined by the initial conditions; the predator and prey may be extinction or coexistence. This means that the strong Allee effect could easily lead to the risk of population extinction. Nevertheless, in the case of weak Allee effect, model (7) can only have one unique positive equilibrium, which is globally asymptotically stable under some conditions. Therefore, the predators and preys can coexist in stable conditions.

Furthermore, we have investigated the conditions for the predator-prey model which experiences spatial patterns through diffusion-driven instability. We have derived the conditions of Turing instability in terms of our model parameters analytically. In addition, to get a deeper insight into the model's dynamics behaviour, we select the different values of parameter m. An increase of m, from the numerical results, one can see that our model has rich and complex spatiotemporal behavior. We find three typical Turing patterns, that is, spots pattern, stripes pattern, and spots-stripes mixtures pattern. To the best of our knowledge, the Turing pattern we illustrate here is the first reported case to our model. And our complete analysis of the spatial model will give new suggestion to the models with the Allee effect.

Acknowledgments

The authors would like to thank the anonymous referee for very helpful suggestions and comments which led to improvements of their original paper. And this work is supported by the Cooperative Project of Yulin City (2011).

References

[1] J. D. Murray, *Mathematical Biology. II: Spatial Models and Biomedical Applications*, vol. 18 of *Interdisciplinary Applied Mathematics*, Springer, New York, NY, USA, 3rd edition, 2003.

[2] S. Stević, "A short proof of the Cushing-Henson conjecture," *Discrete Dynamics in Nature and Society*, Article ID 37264, 5 pages, 2006.

[3] S. Stević, "Asymptotic behavior of a class of nonlinear difference equations," *Discrete Dynamics in Nature and Society*, Article ID 47156, 10 pages, 2006.

[4] M. De La Sen and S. Alonso-Quesada, "Model-matching-based control of the Beverton-Holt equation in ecology," *Discrete Dynamics in Nature and Society*, Article ID 793512, 21 pages, 2008.

[5] M. De la Sen and S. Alonso-Quesada, "A control theory point of view on Beverton-Holt equation in population dynamics and some of its generalizations," *Applied Mathematics and Computation*, vol. 199, no. 2, pp. 464–481, 2008.

[6] J. He, "Asymptotic methods for solitary solutions and compactons," *Abstract and Applied Analysis*, vol. 2012, Article ID 916793, 130 pages, 2012.

[7] Y. Li and D. Xiao, "Bifurcations of a predator-prey system of Holling and Leslie types," *Chaos, Solitons & Fractals*, vol. 34, no. 2, pp. 606–620, 2007.

[8] A. J. Lotka, *Elements of Physical Biology*, Williams and Wilkins, Baltimore, Md, USA, 1925.

[9] V. Volterra, "Fluctuations in the abundance of a species considered mathematically," *Nature*, vol. 118, no. 2972, pp. 558–560, 1926.

[10] R. M. May, *Stability and Complexity in Model Ecosystems*, Princeton University Press, Princeton, NJ, USA, 1974.

[11] C. S. Holling, "The components of predation as revealed by a study of small-mammal predation of the European Pine Sawfly," *The Canadian Entomologist*, vol. 91, no. 5, pp. 293–320, 1959.

[12] S. B. Hsu and T. W. Huang, "Global stability for a class of predator-prey systems," *SIAM Journal on Applied Mathematics*, vol. 55, no. 3, pp. 763–783, 1995.

[13] A. Gasull, R. E. Kooij, and J. Torregrosa, "Limit cycles in the Holling-Tanner model," *Publicacions Matematiques*, vol. 41, no. 1, pp. 149–167, 1997.

[14] E. Sáez and E. González-Olivares, "Dynamics of a predator-prey model," *SIAM Journal on Applied Mathematics*, vol. 59, no. 5, pp. 1867–1878, 1999.

[15] G. Wang, X. G. Liang, and F. Z. Wang, "The competitive dynamics of populations subject to an Allee effect," *Ecological Modelling*, vol. 124, no. 2-3, pp. 183–192, 1999.

[16] A. Kent, C. P. Doncaster, and T. Sluckin, "Consequences for predators of rescue and Allee effects on prey," *Ecological Modelling*, vol. 162, no. 3, pp. 233–245, 2003.

[17] E. Gonzalez-Olivares, J. Mena-Lorca, H. Meneses-Alcay, B. Gonzalez-Yanez, and J. D. Flores, "Allee effect, emigration and immigration in a class of predator-prey models," *Biophysical Reviews and Letters*, vol. 3, pp. 195–251, 2008.

[18] S. R. Zhou, Y. F. Liu, and G. Wang, "The stability of predator-prey systems subject to the Allee effects," *Theoretical Population Biology*, vol. 67, no. 1, pp. 23–31, 2005.

[19] J. Wang, J. Shi, and J. Wei, "Predator-prey system with strong Allee effect in prey," *Journal of Mathematical Biology*, vol. 62, no. 3, pp. 291–331, 2011.

[20] E. González-Olivares, J. Mena-Lorca, A. Rojas-Palma, and J. D. Flores, "Dynamical complexities in the Leslie-Gower predator-prey model as consequences of the Allee effect on prey," *Applied Mathematical Modelling*, vol. 35, no. 1, pp. 366–381, 2011.

[21] P. Aguirre, E. González-Olivares, and E. Sáez, "Three limit cycles in a Leslie-Gower predator-prey model with additive Allee effect," *SIAM Journal on Applied Mathematics*, vol. 69, no. 5, pp. 1244–1262, 2009.

[22] D. S. Boukal, M. W. Sabelis, and L. Berec, "How predator functional responses and Allee effects in prey affect the paradox of enrichment and population collapses," *Theoretical Population Biology*, vol. 72, no. 1, pp. 136–147, 2007.

[23] Y. Cai, W. Wang, and J. Wang, "Dynamics of a diffusive predator-prey model with additive Allee effect," *International Journal of Biomathematics*, vol. 5, no. 2, Article ID 1250023, 2012.

[24] A. Morozov, S. Petrovskii, and B. L. Li, "Bifurcations and chaos in a predator-prey system with the Allee effect," *Proceedings of the Royal Society B*, vol. 271, no. 1546, pp. 1407–1414, 2004.

[25] W. C. Allee, *Animal Aggregations: A Study in General Sociology*, University of Chicago Press, Chicago, Ill, USA, 1931.

[26] R. S. Cantrell and C. Cosner, *Spatial Ecology via Reaction-Diffusion Equations*, Wiley Series in Mathematical and Computational Biology, John Wiley & Sons, Chichester, UK, 2003.

[27] J. D. Murray, "Discussion: turing's theory of morphogenesis-its influence on modelling biological pattern and form," *Bulletin of Mathematical Biology*, vol. 52, no. 1-2, pp. 119–132, 1990.

[28] X. Guan, W. Wang, and Y. Cai, "Spatiotemporal dynamics of a Leslie-Gower predator-prey model incorporating a prey refuge," *Nonlinear Analysis: Real World Applications*, vol. 12, no. 4, pp. 2385–2395, 2011.

[29] R. Peng and M. Wang, "Positive steady states of the Holling-Tanner prey-predator model with diffusion," *Proceedings of the Royal Society of Edinburgh A*, vol. 135, no. 1, pp. 149–164, 2005.

[30] R. Peng and M. Wang, "Global stability of the equilibrium of a diffusive Holling-Tanner prey-predator model," *Applied Mathematics Letters*, vol. 20, no. 6, pp. 664–670, 2007.

[31] W. Wang, Y. Lin, L. Zhang, F. Rao, and Y. Tan, "Complex patterns in a predator-prey model with self and cross-diffusion," *Communications in Nonlinear Science and Numerical Simulation*, vol. 16, no. 4, pp. 2006–2015, 2011.

[32] P. Liu and Y. Xue, "Spatiotemporal dynamics of a predator-prey model," *Nonlinear Dynamics*, vol. 69, no. 1-2, pp. 71–77, 2012.

[33] S. Chen and J. Shi, "Global stability in a diffusive Holling-Tanner predator-prey model," *Applied Mathematics Letters*, vol. 25, no. 3, pp. 614–618, 2012.

[34] J. Mena-Lorca, E. Gonzalez-Olivares, and B. Gonzalez-Yanez, "The Leslie-Gower predator-prey model with Allee effect on prey: a simple model with a rich and interesting dynamiscs," in *Proceedings of the International Symposium on Mathematical and Computational Biology*, pp. 105–132, 2006.

[35] E. Sáez and E. González-Olivares, "Dynamics of a predator-prey model," *SIAM Journal on Applied Mathematics*, vol. 59, no. 5, pp. 1867–1878, 1999.

[36] S. Wiggins, *Introduction to Applied Nonlinear Dynamical Systems and Chaos*, vol. 2 of *Texts in Applied Mathematics*, Springer, New York, NY, USA, 1990.

[37] F. Dumortier, J. Llibre, and J. C. Artés, *Qualitative Theory of Planar Differential Systems*, Universitext, Springer, Berlin, Germany, 2006.

[38] H. Malchow, S. V. Petrovskii, and E. Venturino, *Spatiotemporal Patterns in Ecology and Epidemiology: Theory, Models, and Simulation*, Chapman & Hall/CRC Mathematical and Computational Biology Series, Chapman & Hall/CRC, Boca Raton, Fla, USA, 2008.

[39] A. Okubo and S. A. Levin, *Diffusion and Ecological Problems: Modern Perspectives*, vol. 14 of *Interdisciplinary Applied Mathematics: Mathematical Biology*, Springer, New York, NY, USA, 2nd edition, 2001.

[40] W. Wang, Q.-X. Liu, and Z. Jin, "Spatiotemporal complexity of a ratio-dependent predator-prey system," *Physical Review E*, vol. 75, no. 5, Article ID 051913, 2007.

[41] W. Wang, L. Zhang, H. Wang, and Z. Li, "Pattern formation of a predator-prey system with Ivlev-type functional response," *Ecological Modelling*, vol. 221, no. 2, pp. 131–140, 2010.

[42] M. R. Garvie, "Finite-difference schemes for reaction-diffusion equations modeling predator-prey interactions in MATLAB," *Bulletin of Mathematical Biology*, vol. 69, no. 3, pp. 931–956, 2007.

Hindawi Publishing Corporation
Abstract and Applied Analysis
Volume 2013, Article ID 891914, 3 pages
http://dx.doi.org/10.1155/2013/891914

Research Article

Nonlinear Response of Strong Nonlinear System Arisen in Polymer Cushion

Jun Wang,[1,2] Li-xin Lu,[1,2] Huan-xin Jiang,[1,2] and Yong Zhu[3]

[1] *Key Laboratory of Food Packaging Techniques and Safety of China National Packaging Corporation, Wuxi, Jiangsu 214122, China*
[2] *Department of Packaging Engineering, Jiangnan University, Wuxi, Jiangsu 214122, China*
[3] *Packaging Engineering Research Institute, Jinan University, Zhuhai, Guandong 519070, China*

Correspondence should be addressed to Jun Wang; wangj_1982@jiangnan.edu.cn

Received 14 December 2012; Revised 30 December 2012; Accepted 30 December 2012

Academic Editor: Lan Xu

A dynamic model is proposed for a polymer foam-based nonlinear cushioning system. An accurate analytical solution for the nonlinear free vibration of the system is derived by applying He's variational iteration method, and conditions for resonance are obtained, which should be avoided in the cushioning design.

1. Introduction

Packaged products can be potentially damaged by dropping. In order to prevent any damage, a product and a cushioning packaging are always included in a packaging system [1, 2], and it is very important to investigate the condition for resonance. However, the oscillation in the packaging system is of inherent nonlinearity [3–5], and it remains a problem to obtain the resonance condition for nonlinear packaging system. Polymer foams, especially EPS (expanded polystyrene), are widely used for cushion or protective packaging, and the governing equations can be expressed as

$$\begin{gathered} m\ddot{x} + \beta_3 th(\beta_1 x) + \beta_4 \tan(\beta_2 x) \\ + \beta_5 \tan^3(\beta_2 x) = 0, \\ x(0) = 0, \\ \dot{x}(0) = \sqrt{2gh}. \end{gathered} \tag{1}$$

Here, the coefficient m denotes the mass of the packaged product, while β_i denote, respectively, the characteristic constants of polymer foams which could be obtained by compression test, and h is the dropping height.

By introducing these parameters: $T_0 = \sqrt{m/\beta_1\beta_3}$, $L = 1/\beta_1$ and let $X = x/L$, $T = t/T_0$, $\lambda_1 = \beta_2/\beta_1$, $\lambda_2 = \beta_4/\beta_3$, and $\lambda_3 = \beta_5/\beta_3$, (1) can be written in the following forms

$$\begin{gathered} \ddot{X} + thX + \lambda_2 \tan(\lambda_1 X) \\ + \lambda_3 \tan^3(\lambda_1 X) = 0, \\ X(0) = 0, \\ \dot{X}(0) = V = \frac{T_0}{L}\sqrt{2gh} = \sqrt{\frac{2\beta_1 mgh}{\beta_3}}. \end{gathered} \tag{2}$$

By using Taylor series for $\sin X$ and $\tan X$, (2) can be equivalently written as

$$\begin{gathered} \ddot{X} + \omega_{01}^2 X + \left(-\frac{1}{3} + \lambda_3\lambda_1^3 + \frac{1}{3}\lambda_2\lambda_1^3\right)X^3 \\ + \left(\frac{2}{15} + \frac{2}{15}\lambda_2\lambda_1^5 + \lambda_3\lambda_1^5\right)X^5 + \frac{11}{15}\lambda_3\lambda_1^7 X^7 = 0, \\ X(0) = 0, \\ \dot{X}(0) = V = \frac{T_0}{L}\sqrt{2gh} = \sqrt{\frac{2\beta_1 mgh}{\beta_3}}, \end{gathered} \tag{3}$$

where

$$\omega_{01} = \sqrt{1+\lambda_1\lambda_2}. \tag{4}$$

2. Variational Iteration Method

The variational iteration method [6–13] has been widely applied in solving many different kinds of nonlinear equations [6–16], and is especially effective in solving nonlinear vibration problems with approximations [17–20]. Applying the variational iteration method [6–13], the following iteration formulae can be constructed:

$$\begin{aligned} X_1 = X_0 &+ \frac{1}{\omega_{01}} \\ &\times \int_0^t \sin\omega_{01}(s-t)\left\{\ddot{X}_0 + \omega_{01}^2 X_0\right. \\ &\qquad + \left(-\frac{1}{3}+\lambda_3\lambda_1^3+\frac{1}{3}\lambda_2\lambda_1^3\right)X_0^3 \\ &\qquad + \left(\frac{2}{15}+\frac{2}{15}\lambda_2\lambda_1^5+\lambda_3\lambda_1^5\right)X_0^5 \\ &\qquad \left.+\frac{11}{15}\lambda_3\lambda_1^7X_0^7\right\}ds. \end{aligned} \tag{5}$$

Beginning with the initial solutions,

$$X_0 = A\sin(\Omega t). \tag{6}$$

We have

$$\begin{aligned} X_1 = A\sin(\Omega t) &- \frac{1}{\omega_{01}(\Omega^2-\omega_{01}^2)} \\ &\times\left(aA+\frac{3}{4}bA^3+\frac{5}{256}cA^5-\frac{637}{1024}dA^7\right) \\ &(\Omega\sin(\omega_{01}t)+\omega_{01}\sin(\Omega t)) \\ &-\frac{1}{4\omega_{01}(9\Omega^2-\omega_{01}^2)}\left(bA^3+\frac{5}{64}cA^5-\frac{189}{256}dA^7\right) \\ &(3\Omega\sin(\omega_{01}t)+\omega_{01}\sin(3\Omega t)) \\ &+\frac{1}{16\omega_{01}(25\Omega^2-\omega_{01}^2)}\left(cA^5+\frac{7}{4}dA^7\right) \\ &(5\Omega\sin(\omega_{01}t)+\omega_{01}\sin(5\Omega t)) \\ &-\frac{dA^7}{64\omega_{01}(49\Omega^2-\omega_{01}^2)} \\ &\times(7\Omega\sin(\omega_{01}t)+\omega_{01}\sin(7\Omega t)), \end{aligned} \tag{7}$$

where

$$\begin{aligned} a &= 1+\lambda_1\lambda_2, \\ b &= -\frac{1}{3}+\frac{1}{3}\lambda_2\lambda_1^3+\lambda_3\lambda_1^3, \\ c &= \frac{2}{15}+\frac{2}{15}\lambda_2\lambda_1^5+\lambda_3\lambda_1^5, \\ d &= \frac{11}{15}\lambda_3\lambda_1^7. \end{aligned} \tag{8}$$

3. Resonance

The resonance can be expected when one of the following conditions is met:

$$\begin{aligned} \Omega &= \omega_{01}, \\ \Omega &= \frac{1}{3}\omega_{01}, \\ \Omega &= \frac{1}{5}\omega_{01}, \\ \Omega &= \frac{1}{7}\omega_{01}. \end{aligned} \tag{9}$$

These conditions should be avoided during the cushioning packaging design procedure.

4. Conclusion

The conditions for resonance, which should be avoided in the cushioning packaging design procedure, can be easily obtained using the variational iteration method.

Acknowledgments

This work was supported by the National Natural Science Foundation of China (Grant no.: 51205167), the Research Fund of Young Scholars for the Doctoral Program of Higher Education of China (Grant no.: 20120093120014), and the Fundamental Research Funds for the Central Universities (Grant no.: JUSRP51302A).

References

[1] R. E. Newton, *Fragility Assessment Theory and Practice*, Monterey Research Laboratory, Monterey, Calif, USA, 1968.

[2] G. J. Burgess, "Product fragility and damage boundary theory," *Packaging Technology and Science*, vol. 1, no. 1, pp. 5–10, 1988.

[3] J. Wang and Z. W. Wang, "Damage boundary surface of a tangent nonlinear packaging system with critical component," *Journal of Vibration and Shock*, vol. 27, no. 2, pp. 166–167, 2008.

[4] J. Wang, Z. W. Wang, L. X. Lu, Y. Zhu, and Y. G. Wang, "Three-dimensional shock spectrum of critical component for nonlinear packaging system," *Shock and Vibration*, vol. 18, no. 3, pp. 437–445, 2011.

[5] J. Wang, J. H. Jiang, L. X. Lu, and Z. W. Wang, "Dropping damage evaluation for a tangent nonlinear system with a critical component," *Computers and Mathematics with Applications*, vol. 61, no. 8, pp. 1979–1982, 2011.

[6] J.-H. He, "Variational iteration method—a kind of non-linear analytical technique: some examples," *International Journal of Non-Linear Mechanics*, vol. 34, no. 4, pp. 699–708, 1999.

[7] J.-H. He, "Variational iteration method-Some recent results and new interpretations," *Journal of Computational and Applied Mathematics*, vol. 207, no. 1, pp. 3–17, 2007.

[8] J.-H. He and X. H. Wu, "Variational iteration method: new development and applications," *Computers and Mathematics with Applications*, vol. 54, no. 7-8, pp. 881–894, 2007.

[9] J.-H. He, "Some asymptotic methods for strongly nonlinear equations," *International Journal of Modern Physics B*, vol. 20, no. 10, pp. 1141–1199, 2006.

[10] G.-C. Wu, "Laplace transform overcoming principal drawbacks in application of the variational iteration method to fractional heat equations," *Thermal Science*, vol. 6, no. 4, pp. 1257–1261, 2012.

[11] J.-H. He, "Asymptotic methods for solitary solutions and compactons," *Abstract and Applied Analysis*, vol. 2012, Article ID 916793, 130 pages, 2012.

[12] J.-H. He, "An elementary introduction to recently developed asymptotic methods and nanomechanics in textile engineering," *International Journal of Modern Physics B*, vol. 22, no. 21, pp. 3487–3578, 2008.

[13] J.-H. He, "Notes on the optimal variational iteration method," *Applied Mathematics Letters*, vol. 25, no. 10, pp. 1579–1581, 2012.

[14] J. Singh, P. K. Gupta, and K. Nath Rai, "Variational iteration method to solve moving boundary problem with temperature dependent physical properties," *Thermal Science*, vol. 15, supplement 2, pp. S229–S239, 2011.

[15] J. Wang, Y. Khan, R. H. Yang, L. X. Lu, Z. W. Wang, and N. Faraz, "A mathematical modelling of inner-resonance of tangent nonlinear cushioning packaging system with critical components," *Mathematical and Computer Modelling*, vol. 54, no. 11-12, pp. 2573–2576, 2011.

[16] S. T. Mohyud-Din, M. A. Noor, and K. I. Noor, "Variational iteration method for Burgers' and coupled Burgers' equations using He's polynomials," *Zeitschrift für Naturforschung Section A*, vol. 65, no. 4, pp. 263–267, 2010.

[17] L. N. Zhang and J.-H. He, "Resonance in Sirospun yarn spinning using a variational iteration method," *Computers and Mathematics with Applications*, vol. 54, no. 7-8, pp. 1064–1066, 2007.

[18] L. Xu, "Dynamics of two-strand yarn spinning in forced vibration," *Nonlinear Analysis, Theory, Methods and Applications*, vol. 71, no. 12, pp. e827–e829, 2009.

[19] D. H. Shou, "He's variational iteration method for two-strand yarn spinning," *Nonlinear Analysis: Theory, Methods and Applications*, vol. 71, no. 12, pp. e830–e833, 2009.

[20] R. H. Yang and S. Y. Wang, "Resonance in a rotor-spun composite yarn spinning process obtained using the variational iteration method," *Computers and Mathematics with Applications*, vol. 58, no. 11-12, pp. 2486–2488, 2009.

Hindawi Publishing Corporation
Abstract and Applied Analysis
Volume 2012, Article ID 350287, 7 pages
doi:10.1155/2012/350287

Research Article

Exact Solutions of ϕ^4 Equation Using Lie Symmetry Approach along with the Simplest Equation and Exp-Function Methods

Hossein Jafari,[1,2] Nematollah Kadkhoda,[1] and Chaudry Masood Khalique[2]

[1] *Department of Mathematics Science, University of Mazandaran, P.O. Box 47416-95447, Babolsar, Iran*
[2] *International Institute for Symmetry Analysis and Mathematical Modelling, Department of Mathematical Sciences, North-West University, Mafikeng Campus, Private Bag X 2046, Mmabatho 2735, South Africa*

Correspondence should be addressed to Hossein Jafari, jafari_h@math.com

Received 21 August 2012; Revised 22 October 2012; Accepted 9 November 2012

Academic Editor: Lan Xu

This paper obtains the exact solutions of the ϕ^4 equation. The Lie symmetry approach along with the simplest equation method and the Exp-function method are used to obtain these solutions. As a simplest equation we have used the equation of Riccati in the simplest equation method. Exact solutions obtained are travelling wave solutions.

1. Introduction

The research area of nonlinear equations has been very active for the past few decades. There are several kinds of nonlinear equations that appear in various areas of physics and mathematical sciences. Much effort has been made on the construction of exact solutions of nonlinear equations as they play an important role in many scientific areas, such as, in the study of nonlinear physical phenomena [1, 2]. Nonlinear wave phenomena appear in various scientific and engineering fields, such as fluid mechanics, plasma physics, optical fiber, biology, oceanology [3], solid state physics, chemical physics, and geometry. In recent years, many powerful and efficient methods to find analytic solutions of nonlinear equation have drawn a lot of interest by a diverse group of scientists. These methods include, the tanh-function method, the extended tanh-function method [2, 4, 5], the sine-cosine method [6], and the (G'/G)-expansion method [7, 8].

In this paper, we study the φ^4 equation, namely,

$$\phi_{tt} - \phi_{xx} - \phi + \phi^3 = 0. \tag{1.1}$$

The purpose of this paper is to use the Lie symmetry method along with the simplest equation method (SEM) and the Exp-function method to obtain exact solutions of the φ^4 equation. The simplest equation method was developed by Kudryashov [9–12] on the basis of a procedure analogous to the first step of the test for the Painlevé property. The Exp-function method is a very powerful method for solving nonlinear equations. This method was introduced by He and Wu [13] and since its appearance in the literature it has been applied by many researchers for solving nonlinear partial differential equations. See for example, [14, 15].

The outline of this paper is as follows. In Section 2 we discuss the methodology of Lie symmetry analysis and obtain the Lie point symmetries of the φ^4 equation. We then use the translation symmetries to reduce this equation to an ordinary differential equation (ODE). In Section 3 we describe the SEM and then we obtain the exact solutions of the reduced ODE using SEM. In Section 4 we explain the basic idea of the Exp-function method and obtain exact solutions of the reduced ODE using the Exp-function method. Concluding remarks are summarized in Section 5.

2. Lie Symmetry Analysis

We recall that a Lie point symmetry of a partial differential equation (PDE) is an invertible transformation of the independent and dependent variables that keep the equation invariant. In general determining all the symmetries of a partial differential equation is a daunting task. However, Sophus Lie (1842–1899) noticed that if we confine ourselves to symmetries that depend continuously on a small parameter and that form a group (continuous one-parameter group of transformations), one can linearize the symmetry condition and end up with an algorithm for calculating continuous symmetries [16–19].

The symmetry group of (1.1) will be generated by the vector field of the form

$$X = \tau(t,x,\phi)\frac{\partial}{\partial t} + \xi(t,x,\phi)\frac{\partial}{\partial x} + \eta(t,x,\phi)\frac{\partial}{\partial \phi}. \tag{2.1}$$

Applying the second prolongation $X^{[2]}$ to (1.1) we obtain

$$X^{[2]}\left(\phi_{tt} - \phi_{xx} - \phi + \phi^3\right)\Big|_{(1.1)} = 0, \tag{2.2}$$

where

$$\begin{gathered}
X^{[2]} = X + \zeta_1\frac{\partial}{\partial \phi_t} + \zeta_2\frac{\partial}{\partial \phi_x} + \zeta_{11}\frac{\partial}{\partial \phi_{tt}} + \zeta_{12}\frac{\partial}{\partial \phi_{tx}} + \zeta_{22}\frac{\partial}{\partial \phi_{xx}}, \\
\zeta_1 = D_t(\eta) - \phi_t D_t(\tau) - \phi_x D_t(\xi), \\
\zeta_2 = D_x(\eta) - \phi_t D_x(\tau) - \phi_x D_x(\xi), \\
\zeta_{11} = D_t(\zeta_1) - \phi_{tt} D_t(\tau) - \phi_{tx} D_t(\xi),
\end{gathered}$$

$$\begin{aligned}
\zeta_{12} &= D_x(\zeta_1) - \phi_{tt} D_x(\tau) - \phi_{tx} D_x(\xi), \\
\zeta_{22} &= D_x(\zeta_2) - \phi_{tx} D_t(\tau) - \phi_{xx} D_t(\xi), \\
D_t &= \frac{\partial}{\partial t} + \phi_t \frac{\partial}{\partial \phi} + \phi_{tx} \frac{\partial}{\partial \phi_x} + \phi_{tt} \frac{\partial}{\partial \phi_t} + \cdots, \\
D_x &= \frac{\partial}{\partial x} + \phi_x \frac{\partial}{\partial \phi} + \phi_{xx} \frac{\partial}{\partial \phi_x} + \phi_{tx} \frac{\partial}{\partial \phi_t} + \cdots.
\end{aligned} \tag{2.3}$$

Expanding the (2.2) we obtain the following overdetermined system of linear partial differential equations:

$$\begin{gathered}
\eta - \eta_{tt} + \eta_{xx} = 0, \qquad \eta_u - 2\tau_t = 0, \qquad 2\eta_{tu} - \tau_{tt} + \tau_{xx} = 0, \qquad \tau_t - \xi_x = 0, \\
\eta_{uu} - 2\tau_{tu} = 0, \qquad \tau_u = 0, \qquad \xi_{tt} + 2\eta_{xu} - \xi_{xx} = 0, \qquad \tau_{uu} = 0, \qquad \xi_t - \tau_x = 0, \\
\xi_{tu} - \tau_{xu} = 0, \\
\xi_{uu} = 0, \\
\xi_u = 0, \\
\eta_{uu} - 2\xi_{xu} = 0.
\end{gathered} \tag{2.4}$$

Solving the above system we obtain the following infinitesimal generators:

$$X_1 = \frac{\partial}{\partial t}, \qquad X_2 = \frac{\partial}{\partial x}, \qquad X_3 = x\frac{\partial}{\partial t} + t\frac{\partial}{\partial x}. \tag{2.5}$$

We now use a linear combination of the translation symmetries X_1 and X_2, namely, $X = X_1 + cX_2$ and reduce (1.1) to an ordinary differential equation. The symmetry X yields the following two invariants:

$$\chi = x - ct, \qquad u = \phi, \tag{2.6}$$

which gives a group invariant solution $u = u(\chi)$ and consequently using these invariants (1.1) is transformed into the second-order nonlinear ODE

$$\left(c^2 - 1\right)u'' - u + u^3 = 0. \tag{2.7}$$

3. Solution of (2.7) Using the Simplest Equation Method

We now use the simplest equation method to solve (2.7). The simplest equation that will be used is the Ricatti equation

$$G'(\chi) = bG(\chi) + dG(\chi)^2, \tag{3.1}$$

where b and d are arbitrary constants. This equation is a well-known nonlinear ordinary differential equation which possess exact solutions given by elementary functions. The solutions can be expressed as

$$G(\chi) = \frac{b\exp[b(\chi + C)]}{1 - d\exp[b(\chi + C)]}, \tag{3.2}$$

for the case when $d < 0$, $b > 0$, and

$$G(\chi) = -\frac{b\exp[b(\chi + C)]}{1 + d\exp[b(\chi + C)]}, \tag{3.3}$$

for $d > 0$, $b < 0$. Here C is a constant of integration.

Let us consider the solution of (2.7) of the form

$$u(\chi) = \sum_{i=0}^{M} A_i (G(\chi))^i, \tag{3.4}$$

where $G(\chi)$ satisfies the Riccati equation (3.1), M is a positive integer that can be determined by balancing procedure, and $A_0, A_1, A_2, \ldots, A_M$ are parameters to be determined.

The balancing procedure yields $M = 1$, so the solution of (2.7) is of form

$$u(\chi) = A_0 + A_1 G(\chi). \tag{3.5}$$

3.1. Solution of (2.7) *When* $d < 0$ *and* $b > 0$

Substituting (3.5) into (2.7) and making use of the Ricatti equation (3.1) and then equating all coefficients of the functions G^i to zero, we obtain an algebraic system of equations in terms of A_0 and A_1. Solving these algebraic equations, with the aid of Mathematica, we obtain the following values of A_0 and A_1.

Case 1. $A_0 = -1$, $A_1 = -bd + bc^2 d$, $b = \pm\sqrt{2}/\sqrt{1 - c^2}$, $1 - c^2 \neq 0$.

Case 2. $A_0 = 1$, $A_1 = bd - bc^2 d$, $b = \pm\sqrt{2}/\sqrt{1 - c^2}$, $1 - c^2 \neq 0$.

Therefore, when $d < 0$, $b > 0$ the solution of (2.7) and hence the solution of (1.1) for Case 1 is given by

$$\phi_1(x, t) = -1 + \frac{b^2 d(c^2 - 1)\exp[b(x - ct + C)]}{1 - d\exp[b(x - ct + C)]}, \tag{3.6}$$

and the solution of (1.1) for Case 2 is given by

$$\phi_2(x, t) = 1 - \frac{b^2 d(c^2 - 1)\exp[b(x - ct + C)]}{1 - d\exp[b(x - ct + C)]}. \tag{3.7}$$

3.2. Solution of (2.7) *When* $d > 0$ *and* $b < 0$

If $d > 0$, $b < 0$, substituting (3.5) into (2.7) and making use of (3.1) and then proceeding as above, we obtain the following values of A_0 and A_1.

Case 3. $A_0 = -1$, $A_1 = -bd + bc^2d$, $b = \pm\sqrt{2}/\sqrt{1-c^2}$, $1-c^2 \neq 0$.

Case 4. $A_0 = 1$, $A_1 = bd - bc^2d$, $b = \pm\sqrt{2}/\sqrt{1-c^2}$, $1-c^2 \neq 0$.

Therefore, when $d > 0$, $c < 0$ the solution of (2.7) and hence the solution of (1.1) for Case 3 is given by

$$\phi_3(x,t) = -1 - \frac{b^2 d(c^2-1)\exp[b(x-ct+C)]}{1+d\exp[b(x-ct+C)]}, \tag{3.8}$$

and the solution of (1.1) for Case 4 is given by

$$\phi_4(x,t) = 1 + \frac{b^2 d(c^2-1)\exp[b(x-ct+C)]}{1+d\exp[b(x-ct+C)]}. \tag{3.9}$$

4. Solution of (2.7) Using the Exp-Function Method

In this section we use the Exp-function method for solving (2.7). According to the Exp-function method [13–15], we consider solutions of (2.7) in the form

$$u(\chi) = \frac{\sum_{n=-b}^{d} a_n \exp(n\chi)}{\sum_{m=-p}^{q} b_m \exp(m\chi)}, \tag{4.1}$$

where b, d, p, and q are positive integers which are unknown to be further determined, a_n and b_m are unknown constants. By the balancing procedure of the Exp-function method, we obtain $p = b$ and $q = d$. Furthermore, for simplicity, we set $p = b = 1$ and $q = d = 1$, so (4.1) reduces to

$$u(\chi) = \frac{a_{-1}\exp(-\chi) + a_0 + a_1\exp(\chi)}{b_{-1}\exp(-\chi) + b_0 + b_1\exp(\chi)}. \tag{4.2}$$

Substituting (4.2) into (2.7) and by the help of Mathematica, we obtain

$$\begin{gathered} c = \pm\sqrt{2}, \quad a_{-1} = 0, \quad a_1 = 0, \\ b_{-1} = \frac{a_0^2}{8}, \quad b_0 = 0, \quad b_1 = 1, \end{gathered} \tag{4.3}$$

where a_0 is a free parameter. Substituting these results into (4.2), we obtain the exact solution

$$u(\chi) = \frac{a_0\exp(\chi)}{(a_0^2/8) + \exp(2\chi)}, \tag{4.4}$$

of (2.7). Consequently, if we choose that $a_0 = \sqrt{8}$ then this solution, in terms of the variables x and t becomes

$$\phi(x,t) = \sqrt{2}\operatorname{sech}\left(\sqrt{\frac{1}{c^2-1}}(x-ct)\right), \tag{4.5}$$

which is a soliton solution of our φ^4 equation (1.1).

5. Conclusion

In this paper, Lie symmetry analysis in conjunction with the simplest equation method and the Exp-function method have been successfully used to obtain exact solutions of the φ^4 equation. As a simplest equation, we have used the Riccati equation. The solutions obtained were travelling wave solutions. In particular, a soliton solution was also obtained.

References

[1] M. Duranda and D. Langevin, "Physicochemical approach to the theory of foam drainage," *The European Physical Journal E*, vol. 7, pp. 35–44, 2002.
[2] E. Fan, "Extended tanh-function method and its applications to nonlinear equations," *Physics Letters A*, vol. 277, no. 4-5, pp. 212–218, 2000.
[3] L. A. Ostrovsky, "Nonlinear internal waves in a rotating ocean," *Oceanology*, vol. 18, pp. 119–125, 1978.
[4] A.-M. Wazwaz, "The tanh-coth method for solitons and kink solutions for nonlinear parabolic equations," *Applied Mathematics and Computation*, vol. 188, no. 2, pp. 1467–1475, 2007.
[5] A.-M. Wazwaz, "The tanh method: solitons and periodic solutions for the Dodd-Bullough-Mikhailov and the Tzitzeica-Dodd-Bullough equations," *Chaos, Solitons & Fractals*, vol. 25, no. 1, pp. 55–63, 2005.
[6] A.-M. Wazwaz, "The sine-cosine method for obtaining solutions with compact and noncompact structures," *Applied Mathematics and Computation*, vol. 159, no. 2, pp. 559–576, 2004.
[7] R. Abazari, "Application of (G'/G)-expansion method to travelling wave solutions of three nonlinear evolution equation," *Computers & Fluids*, vol. 39, no. 10, pp. 1957–1963, 2010.
[8] E. Salehpour, H. Jafari, and N. Kadkhoda, "Application of, (G'/G)-expansion method to nonlinear Lienard equation," *Indian Journal of Science and Technology*, vol. 5, pp. 2554–2556, 2012.
[9] H. Jafari, N. Kadkhoda, and C. M. Khalique, "Travelling wave solutions of nonlinear evolution equations using the simplest equation method," *Computers & Mathematics with Applications*, vol. 64, no. 6, pp. 2084–2088, 2012.
[10] N. A. Kudryashov, "Simplest equation method to look for exact solutions of nonlinear differential equations," *Chaos, Solitons & Fractals*, vol. 24, no. 5, pp. 1217–1231, 2005.
[11] N. A. Kudryashov and N. B. Loguinova, "Extended simplest equation method for nonlinear differential equations," *Applied Mathematics and Computation*, vol. 205, no. 1, pp. 396–402, 2008.
[12] N. K. Vitanov, "Application of simplest equations of Bernoulli and Riccati kind for obtaining exact traveling-wave solutions for a class of PDEs with polynomial nonlinearity," *Communications in Nonlinear Science and Numerical Simulation*, vol. 15, no. 8, pp. 2050–2060, 2010.
[13] J.-H. He and X.-H. Wu, "Exp-function method for nonlinear wave equations," *Chaos, Solitons & Fractals*, vol. 30, no. 3, pp. 700–708, 2006.
[14] X.-H. Wu and J.-H. He, "EXP-function method and its application to nonlinear equations," *Chaos, Solitons & Fractals*, vol. 38, no. 3, pp. 903–910, 2008.
[15] X. W. Zhou, Y. X. Wen, and J. H. He, "Exp-function method to solve the non-linear dispersive K(m,n) equations," *International Journal of Nonlinear Science and Numerical Simulation*, vol. 9, pp. 301–306, 2008.
[16] G. W. Bluman and S. Kumei, *Symmetries and Differential Equations*, vol. 81 of *Applied Mathematical Sciences*, Springer, New York, NY, USA, 1989.
[17] N. H. Ibragimov, *CRC Handbook of Lie Group Analysis of Differential Equations*, vol. 1–3, CRC Press, Boca Raton, Fla, USA, 19941996.

[18] A. G. Johnpillai and C. M. Khalique, “Lie group classification and invariant solutions of mKdV equation with time-dependent coefficients,” *Communications in Nonlinear Science and Numerical Simulation*, vol. 16, no. 3, pp. 1207–1215, 2011.

[19] P. J. Olver, *Applications of Lie Groups to Differential Equations*, vol. 107 of *Graduate Texts in Mathematics*, Springer, Berlin, Germany, 2nd edition, 1993.

Hindawi Publishing Corporation
Abstract and Applied Analysis
Volume 2012, Article ID 567401, 15 pages
doi:10.1155/2012/567401

Research Article

Local Fractional Fourier Series with Application to Wave Equation in Fractal Vibrating String

Ming-Sheng Hu,[1] Ravi P. Agarwal,[2] and Xiao-Jun Yang[3]

[1] *Institute of Software Science, Zhengzhou Normal University, Zhengzhou 450044, China*
[2] *Department of Mathematics, Texas A and M University, Kingsville, TX 78363-8202, USA*
[3] *Department of Mathematics and Mechanics, China University of Mining and Technology, Jiangsu, Xuzhou 221008, China*

Correspondence should be addressed to Xiao-Jun Yang, dyangxiaojun@163.com

Received 14 August 2012; Revised 25 October 2012; Accepted 8 November 2012

Academic Editor: Lan Xu

We introduce the wave equation in fractal vibrating string in the framework of the local fractional calculus. Our particular attention is devoted to the technique of the local fractional Fourier series for processing these local fractional differential operators in a way accessible to applied scientists. By applying this technique we derive the local fractional Fourier series solution of the local fractional wave equation in fractal vibrating string and show the fundamental role of the Mittag-Leffler function.

1. Introduction

Fractional calculus arises in many problems of physics, continuum mechanics, visco-elasticity, and quantum mechanics, and other branches of applied mathematics and nonlinear dynamics have been studied [1–7]. In general, the fractional analogues are obtained by changing the classical time derivative by a fractional one, which can be Riemann-Liouville, Caputo, or another one. Many classical partial differential equations possess a fractional analogue, like the fractional diffusion-wave equation [8–12], the fractional diffusion equation [13–16], the fractional wave equation [17, 18], the fractional Schrödinger equation [19, 20], the fractional heat equation [21], the fractional KdV equation [22], the fractional Fokker-Planck equations [23], the fractional Fick's law [24], the fractional evolution equation [25], the Fractional Heisenberg equation [26], the fractional Ginzburg-Landau equation [27], Fractional hydrodynamic equation [28], the fractional seepage flow equation [29], and the fractional KdV-Burgers equation [30].

There also are other methods for solving fractional differential equations, for example, the fractional variational iteration method [31, 32] and the fractional complex transform [33–37]. In all of the methods mentioned above, the solutions of the fractional differential equations should be analytical if the fractional derivative is in the Caputo or Riemann-Liouville sense. However, some solutions to ordinary and partial differential equations are fractal curves. As a result, we cannot employ the classical Fourier series, which requires that the defined functions should be differentiable, to describe some solutions to ordinary and partial differential equations in fractal space. However, based on the modified Riemann-Liouville derivative, Jumarie structured a Jumurie's calculus of fractional order [38] (which is one of useful tools to deal with everywhere continuous but nowhere differentiable functions) and its applications were taken into account in Probability calculus of fractional order [39], Laplace transform of fractional order via the Mittag-Leffler function (in convenient Hilbert space) [40], and adomian decomposition method for nonsmooth initial value problems [41]. Local fractional calculus is revealed as one of useful tools to deal with everywhere continuous but nowhere differentiable functions in areas ranging from fundamental science to engineering [42–57]. For these merits, local fractional calculus was successfully applied in the local fractional Laplace problems [53, 54], local fractional Fourier analysis [53, 54], local fractional short time transform [53, 54], local fractional wavelet transform [53–55], fractal signal [55, 56], and local fractional variational calculus [57].

In this paper we introduce a local fractional wave equation in fractal vibrating string which is described as

$$\frac{\partial^{2\alpha}u(x,t)}{\partial t^{2\alpha}} + a^{2\alpha}\frac{\partial^{2\alpha}u(x,t)}{\partial x^{2\alpha}} = 0, \tag{1.1}$$

with fractal boundary conditions

$$\begin{gathered} u(0,t) = u(l,t) = 0, \\ u(0,t) = \frac{\partial^{\alpha}u(l,t)}{\partial x^{\alpha}} = 0, \\ u(x,0) = f(x), \\ \frac{\partial^{\alpha}u(l,0)}{\partial x^{\alpha}} = g(x), \end{gathered} \tag{1.2}$$

where $\partial^{2\alpha}u(x,t)/\partial t^{2\alpha}$, $\partial^{2\alpha}u(x,t)/\partial x^{2\alpha}$, $\partial^{\alpha}u(l,0)/\partial x^{\alpha}$, and $\partial^{\alpha}u(l,t)/\partial x^{\alpha}$ are local fractional partial differential operator, and where $u(x,t)$ is local fractional continuous (for more details, see [53, 54]). We study the technique of the local fractional Fourier series for treating the local fractional wave equation in fractal vibrating string. This paper is organized as follows. In Section 2, we specify and investigate the concepts of local fractional calculus and local fractional Fourier series. In Section 3, we present the solving process for local fractional wave equation with local fractional derivative. In Section 4, we study the expression solution with Mittag-Leffler functions in fractal space. Finally, Section 5 is conclusions.

2. Preliminaries

In this section we start with local fractional continuity of functions, and we introduce the notions of local fractional calculus and local fractional Fourier series.

2.1. Local Fractional Continuity of Functions

In order to discuss the local fractional continuity of nondifferential functions on fractal sets, we first consider the following results.

Lemma 2.1 (see [57]). *Let F be a subset of the real line and be a fractal. If $f:(F,d)\rightarrow(\Omega',d')$ is a bi-Lipschitz mapping, then there are for constants $\rho,\tau>0$, and $F\subset R$,*

$$\rho^{s}H^{s}(F)\leq H^{s}(f(F))\leq\tau^{s}H^{s}(F),\tag{2.1}$$

such that for all $x_1,x_2\in F$,

$$\rho^{\alpha}|x_1-x_2|^{\alpha}\leq|f(x_1)-f(x_2)|\leq\tau^{\alpha}|x_1-x_2|^{\alpha}.\tag{2.2}$$

As a direct result of Lemma 2.1, we have, [57],

$$|f(x_1)-f(x_2)|\leq\tau^{\alpha}|x_1-x_2|^{\alpha},\tag{2.3}$$

such that

$$|f(x_1)-f(x_2)|<\varepsilon^{\alpha},\tag{2.4}$$

where α is fractal dimension of F. The result that is directly deduced from fractal geometry is related to fractal coarse-grained mass function $\gamma^{\alpha}[F,a,b]$, which reads, [57],

$$\gamma^{\alpha}[F,a,b]=\frac{H^{\alpha}(F\cap(a,b))}{\Gamma(1+\alpha)},\tag{2.5}$$

with

$$H^{\alpha}(F\cap(a,b))=(b-a)^{\alpha},\tag{2.6}$$

where H^{α} is α dimensional Hausdorff measure.

Notice that we consider the dimensions of any fractal spaces (e.g., Cantor spaces or like-Cantor spaces) as a positive number. It looks like Euclidean space because its dimension is also a positive number. The detailed results had been considered in [53, 54, 57].

Definition 2.2. If there exists, [53, 57],

$$|f(x)-f(x_0)|<\varepsilon^{\alpha},\tag{2.7}$$

with $|x - x_0| < \delta$, for $\varepsilon, \delta > 0$ and $\varepsilon, \delta \in R$, then $f(x)$ is called local fractional continuous at $x = x_0$, denoted by $\lim_{x \to x_0} f(x) = f(x_0)$. $f(x)$ is called local fractional continuous on the interval (a, b), denoted by

$$f(x) \in C_\alpha(a, b), \tag{2.8}$$

if (2.7) is valid for $x \in (a, b)$.

Definition 2.3. If a function $f(x)$ is called a nondifferentiable function of exponent α, $0 < \alpha \le 1$, which satisfies Hölder function of exponent α, then for $x, y \in X$ such that, [54, 57],

$$\left| f(x) - f(y) \right| \le C \left| x - y \right|^\alpha. \tag{2.9}$$

Definition 2.4. A function $f(x)$ is called to be continuous of order α, $0 < \alpha \le 1$, or shortly α continuous, when we have that, [54, 57],

$$f(x) - f(x_0) = o\left((x - x_0)^\alpha\right). \tag{2.10}$$

Remark 2.5. Compared with (2.10), (2.7) is standard definition of local fractional continuity. Here (2.9) is unified local fractional continuity [57].

2.2. Local Fractional Derivatives and Integrals

Definition 2.6 (let $f(x) \in C_\alpha(a, b)$). Local fractional derivative of $f(x)$ of order α at $x = x_0$ is given, [53–57],

$$f^{(\alpha)}(x_0) = \left. \frac{d^\alpha f(x)}{dx^\alpha} \right|_{x = x_0} = \lim_{x \to x_0} \frac{\Delta^\alpha \left(f(x) - f(x_0) \right)}{(x - x_0)^\alpha}, \tag{2.11}$$

where $\Delta^\alpha (f(x) - f(x_0)) \cong \Gamma(1 + \alpha) \Delta (f(x) - f(x_0))$.

For any $x \in (a, b)$, there exists, [53–57],

$$f^{(\alpha)}(x) = D_x^{(\alpha)} f(x), \tag{2.12}$$

denoted by

$$f(x) \in D_x^{(\alpha)}(a, b). \tag{2.13}$$

Local fractional derivative of high order is derived as, [57],

$$f^{(k\alpha)}(x) = \overbrace{D_x^{(\alpha)} \cdots D_x^{(\alpha)}}^{k \text{ times}} f(x), \tag{2.14}$$

and local fractional partial derivative of high order, [57],

$$\frac{\partial^{k\alpha} f(x)}{\partial x^{k\alpha}} = \overbrace{\frac{\partial^{\alpha}}{\partial x^{\alpha}} \cdots \frac{\partial^{\alpha}}{\partial x^{\alpha}}}^{k \text{ times}} f(x). \tag{2.15}$$

Definition 2.7 (let $f(x) \in C_\alpha(a,b)$). Local fractional integral of $f(x)$ of order α in the interval $[a,b]$ is given by, [53–57],

$${}_aI_b^{(\alpha)} f(x) = \frac{1}{\Gamma(1+\alpha)} \int_a^b f(t)(dt)^\alpha = \frac{1}{\Gamma(1+\alpha)} \lim_{\Delta t \to 0} \sum_{j=0}^{j=N-1} f(t_j)(\Delta t_j)^\alpha, \tag{2.16}$$

where $\Delta t_j = t_{j+1} - t_j$, $\Delta t = \max\{\Delta t_1, \Delta t_2, \Delta t_j, \ldots\}$, and $[t_j, t_{j+1}]$, $j = 0, \ldots, N-1$, $t_0 = a$, $t_N = b$, is a partition of the interval $[a,b]$.

For convenience, we assume that

$${}_aI_a^{(\alpha)} f(x) = 0 \quad \text{if } a = b, \qquad {}_aI_b^{(\alpha)} f(x) = -{}_bI_a^{(\alpha)} f(x) \quad \text{if } a < b. \tag{2.17}$$

For any $x \in (a,b)$, we get, [53, 54, 57],

$${}_aI_x{}^{(\alpha)} f(x), \tag{2.18}$$

denoted by

$$f(x) \in I_x^{(\alpha)}(a,b). \tag{2.19}$$

Remark 2.8. If $f(x) \in D_x^{(\alpha)}(a,b)$, or $I_x^{(\alpha)}(a,b)$, we have that, [46, 47, 50],

$$f(x) \in C_\alpha(a,b). \tag{2.20}$$

2.3. Special Functions in Fractal Space

Definition 2.9. The Mittag-Leffler function in fractal space is defined by, [53, 57],

$$E_\alpha(x^\alpha) := \sum_{k=0}^{\infty} \frac{x^{\alpha k}}{\Gamma(1+k\alpha)}, \quad x \in R,\ 0 < \alpha \le 1. \tag{2.21}$$

Definition 2.10. The sine function in fractal space is given by the expression, [54, 57],

$$\sin_\alpha x^a := \sum_{k=0}^{\infty} (-1)^k \frac{x^{\alpha(2k+1)}}{\Gamma[1+\alpha(2k+1)]}, \quad x \in R,\ 0 < \alpha \le 1. \tag{2.22}$$

Definition 2.11. The cosine function in fractal space is given, [54, 57],

$$\cos_\alpha x^a := \sum_{k=0}^{\infty}(-1)^k \frac{x^{2\alpha k}}{\Gamma(1+2\alpha k)}, \quad x \in R,\ 0 < \alpha \le 1. \tag{2.23}$$

The following rules hold [54, 57]:

$$\begin{gathered}
E_\alpha(x^\alpha)E_\alpha(y^\alpha) = E_\alpha((x+y)^\alpha), \qquad E_\alpha(x^\alpha)E_\alpha(-y^\alpha) = E_\alpha((x-y)^\alpha), \\
E_\alpha(i^\alpha x^\alpha)E_\alpha(i^\alpha y^\alpha) = E_\alpha(i^\alpha(x+y)^\alpha), \qquad E_\alpha(i^\alpha x^\alpha) = \cos_\alpha x^\alpha + i^\alpha \sin_\alpha x^\alpha, \\
\sin_\alpha x^\alpha = \frac{E_\alpha(i^\alpha x^\alpha) - E_\alpha(-i^\alpha x^\alpha)}{2i^\alpha}, \qquad \cos_\alpha x^\alpha = \frac{E_\alpha(i^\alpha x^\alpha) + E_\alpha(-i^\alpha x^\alpha)}{2}, \\
\cos_\alpha(-x)^\alpha = \cos_\alpha x^\alpha, \qquad \sin_\alpha(-x)^\alpha = -\sin_\alpha x^\alpha, \\
\cos_\alpha^2 x^\alpha + \sin^2{}_\alpha x^\alpha = 1, \qquad \sin_\alpha^2 x^\alpha = \frac{1-\cos_\alpha(2x)^\alpha}{2}, \\
\cos_\alpha^2 x^\alpha = \frac{1+\cos_\alpha(2x)^\alpha}{2}, \qquad \tan_\alpha x^\alpha = \frac{\sin_\alpha(2x)^\alpha}{1+\cos_\alpha(2x)^\alpha} = \frac{1-\cos_\alpha(2x)^\alpha}{\sin_\alpha(2x)^\alpha}, \\
\sin_\alpha(2x)^\alpha = 2\sin_\alpha x^\alpha \cos_\alpha x^\alpha, \qquad \cos_\alpha(2x)^\alpha = \cos_\alpha^2 x^\alpha - \sin_\alpha^2 x^\alpha, \\
\tan_\alpha(2y)^\alpha = \frac{2\tan_\alpha y^\alpha}{1+\tan_\alpha^2 x^\alpha}, \qquad \sin_\alpha(2x)^\alpha = \frac{2\tan_\alpha x^\alpha}{1+\tan_\alpha^2 x^\alpha}, \\
\cos_\alpha(2x)^\alpha = \frac{1-\tan_\alpha^2 x^\alpha}{1+\tan_\alpha^2 x^\alpha}, \qquad \tan_\alpha(x+y)^\alpha = \frac{\tan_\alpha x^\alpha + \tan_\alpha y^\alpha}{1+\tan_\alpha x^\alpha \tan_\alpha y^\alpha}, \\
\cos_\alpha x^\alpha + \cos_\alpha y^\alpha = 2\cos_\alpha\left(\frac{x+y}{2}\right)^\alpha \cos_\alpha\left(\frac{x-y}{2}\right)^\alpha, \\
\cos_\alpha x^\alpha - \cos_\alpha y^\alpha = -2\sin_\alpha\left(\frac{x+y}{2}\right)^\alpha \sin_\alpha\left(\frac{x-y}{2}\right)^\alpha, \\
\sin_\alpha x^\alpha + \sin_\alpha y^\alpha = 2\sin_\alpha\left(\frac{x+y}{2}\right)^\alpha \cos_\alpha\left(\frac{x-y}{2}\right)^\alpha, \\
\sin_\alpha x^\alpha - \sin_\alpha y^\alpha = 2\cos_\alpha\left(\frac{x+y}{2}\right)^\alpha \sin_\alpha\left(\frac{x-y}{2}\right)^\alpha, \\
\cos_\alpha(x+y)^\alpha = \cos_\alpha x^\alpha \cos_\alpha y^\alpha - \sin_\alpha x^\alpha \sin_\alpha y^\alpha, \\
\cos_\alpha(x-y)^\alpha = \cos_\alpha x^\alpha \cos_\alpha y^\alpha + \sin_\alpha x^\alpha \sin_\alpha y^\alpha, \\
\sin_\alpha(x+y)^\alpha = \sin_\alpha x^\alpha \cos_\alpha y^\alpha + \cos_\alpha x^\alpha \sin_\alpha y^\alpha, \\
\cos_\alpha x^\alpha \cos_\alpha y^\alpha = \frac{\cos_\alpha(x+y)^\alpha + \cos_\alpha(x-y)^\alpha}{2},
\end{gathered}$$

$$\begin{aligned}
&\sin_\alpha x^\alpha \sin_\alpha y^\alpha = -\frac{\cos_\alpha (x+y)^\alpha - \cos_\alpha (x-y)^\alpha}{2},\\
&\sin_\alpha x^\alpha \cos_\alpha y^\alpha = \frac{\sin_\alpha (x+y)^\alpha + \sin_\alpha (x-y)^\alpha}{2},\\
&\sin_\alpha (mx)^\alpha \sin_\alpha (nx)^\alpha = \frac{\cos_\alpha ((m-n)x)^\alpha - \cos_\alpha ((m+n)x)^\alpha}{2},\\
&\cos_\alpha (nx)^\alpha \sin_\alpha (mx)^\alpha = \frac{\sin_\alpha ((m+n)x)^\alpha - \sin_\alpha ((m-n)x)^\alpha}{2},\\
&E_\alpha\left(i^\alpha (nx)^\alpha\right) = \left(\cos_\alpha (nx)^\alpha + i^\alpha \sin_\alpha (nx)^\alpha\right)^n,\\
&\sum_{k=1}^{n} \sin_\alpha (nx)^\alpha = \frac{\sin_\alpha (nx/2)^\alpha}{\sin_\alpha (x/2)^\alpha} \sin_\alpha \left(\frac{(n+1)x}{2}\right)^\alpha, \quad \sin_\alpha \left(\frac{x}{2}\right)^\alpha \neq 0,\\
&\sum_{k=1}^{n} \cos_\alpha (nx)^\alpha = \frac{\sin_\alpha (nx/2)^\alpha}{\sin_\alpha (x/2)^\alpha} \cos_\alpha \left(\frac{(n+1)x}{2}\right)^\alpha, \quad \sin_\alpha \left(\frac{x}{2}\right)^\alpha \neq 0,\\
&\frac{1}{2} + \sum_{k=1}^{n} \cos_\alpha (nx)^\alpha = \frac{\sin_\alpha ((2n+1)x/2)^\alpha}{2\sin_\alpha (x/2)^\alpha}, \quad \sin_\alpha \left(\frac{x}{2}\right)^\alpha \neq 0.
\end{aligned} \tag{2.24}$$

Remark 2.12. i^α is fractal imaginary unit, for more details, see [53–57].

2.4. Local Fractional Fourier Series

Definition 2.13. Suppose that $f(x) \in C_\alpha(-\infty, \infty)$ and $f(x)$ be $2l$-periodic. For $k \in Z$, local fractional Fourier series of $f(x)$ is defined as, [53–55],

$$f(x) = \frac{a_0}{2} + \sum_{k=1}^{\infty} \left(a_n \cos_\alpha \frac{\pi^\alpha (kx)^\alpha}{l^\alpha} + b_n \sin_\alpha \frac{\pi^\alpha (kx)^\alpha}{l^\alpha} \right), \tag{2.25}$$

where

$$\begin{aligned}
a_k &= \frac{1}{l^\alpha} \int_{-l}^{l} f(x) \cos_\alpha \frac{\pi^\alpha (kx)^\alpha}{l^\alpha} (dx)^\alpha,\\
b_k &= \frac{1}{l^\alpha} \int_{-l}^{l} f(x) \sin_\alpha \frac{\pi^\alpha (kx)^\alpha}{l^\alpha} (dx)^\alpha
\end{aligned} \tag{2.26}$$

are the local fractional Fourier coefficients.

For local fractional Fourier series (2.25), the weights of the fractional trigonometric functions are calculated as

$$a_k = \frac{\int_{-l+t_0}^{l+t_0} f(x)\cos_\alpha\left(\pi^\alpha (kx)^\alpha / l^\alpha\right)(dx)^\alpha}{\int_{-l+t_0}^{l+t_0} \cos_\alpha^2\left(\pi^\alpha (kx)^\alpha / l^\alpha\right)(dx)^\alpha},$$
$$a_k = \frac{\int_{-l+t_0}^{l+t_0} f(x)\sin_\alpha\left(\pi^\alpha (kx)^\alpha / l^\alpha\right)(dx)^\alpha}{\int_{-l+t_0}^{l+t_0} \sin_\alpha^2\left(\pi^\alpha (kx)^\alpha / l^\alpha\right)(dx)^\alpha}. \tag{2.27}$$

Definition 2.14. Suppose that $f(x) \in C_\alpha(-\infty, \infty)$ and $f(x)$ be $2l$-periodic. For $k \in Z$, complex generalized Mittag-Leffler form of local fractional Fourier series of $f(x)$ is defined as, [53, 54],

$$f(x) = \sum_{k=-\infty}^{\infty} C_k E_\alpha\left(\frac{\pi^\alpha i^\alpha (kx)^\alpha}{l^\alpha}\right), \tag{2.28}$$

where the local fractional Fourier coefficients is

$$C_k = \frac{1}{(2l)^\alpha} \int_{-l}^{l} f(x) E_\alpha\left(\frac{-\pi^\alpha i^\alpha (kx)^\alpha}{l^\alpha}\right)(dx)^\alpha \quad \text{with } k \in Z. \tag{2.29}$$

The above generalized forms of local fractional series are valid and are also derived from the generalized Hilbert space [53, 54].

For local fractional Fourier series (2.28), the weights of the Mittag-Leffler functions are written in the form

$$C_k = \frac{\left(1/(2l)^\alpha\right) \int_{-l+t_0}^{l+t_0} f(x) E_\alpha\left(-\pi^\alpha i^\alpha (kx)^\alpha / l^\alpha\right)(dx)^\alpha}{\left(1/(2l)^\alpha\right) \int_{-l+t_0}^{l+t_0} E_\alpha\left(-\pi^\alpha i^\alpha (kx)^\alpha / l^\alpha\right) \overline{E_\alpha\left(-\pi^\alpha i^\alpha (kx)^\alpha / l^\alpha\right)}(dx)^\alpha}. \tag{2.30}$$

Above is generalized to calculate local fractional Fourier series.

3. Solutions to Wave Equation with Fractal Vibrating String

Now we look for particular solutions of the form

$$u(x,t) = \phi(x) T(t), \tag{3.1}$$

and arrive at the equations

$$\phi^{(2\alpha)} + \lambda^{2\alpha}\phi = 0, \tag{3.2}$$

$$T^{(2\alpha)} + a^{2\alpha}\lambda^{2\alpha} T = 0, \tag{3.3}$$

with the boundary conditions

$$\phi(0) = \phi^{(\alpha)}(l) = 0. \tag{3.4}$$

Equation has the solution

$$\phi(x) = C_1 \cos_\alpha \lambda^\alpha x^\alpha + C_2 \sin_\alpha \lambda^\alpha x^\alpha \quad (C_1 = \cos t,\ C_2 = \cos t). \tag{3.5}$$

According to (3.4), for $x = 0$ and $x = l$ we derive as

$$\begin{gathered} \phi(0) = C_1 = 0, \\ \phi(l) = \phi(x)\big|_{x=l} = C_2 \sin_\alpha \lambda^\alpha l^\alpha = 0. \end{gathered} \tag{3.6}$$

Assuming that $C_2 \neq 0$, since otherwise $\phi(x)$ is identically zero, we find that

$$\lambda_n^\alpha l^\alpha = n^\alpha \pi^\alpha, \tag{3.7}$$

where n is an integer; we write

$$\begin{gathered} \lambda_n^\alpha = \left(\frac{n\pi}{l}\right)^\alpha \quad (n = 0, 1, 2, \ldots), \\ \phi_n(x) = \sin_\alpha \lambda_n^\alpha x^\alpha = \sin_\alpha n^\alpha \left(\frac{\pi x}{l}\right)^\alpha = 0 \quad (n = 0, 1, 2, \ldots). \end{gathered} \tag{3.8}$$

For $\lambda^\alpha = \lambda_n^\alpha$ equation (3.3) leads to

$$T_n(t) = A_n \cos_\alpha a^\alpha \lambda_n^\alpha t^\alpha + B_n \sin_\alpha a^\alpha \lambda_n^\alpha t^\alpha \quad (n = 0, 1, 2, \ldots), \tag{3.9}$$

and therefore

$$u_n(x,t) = (A_n \cos_\alpha a^\alpha \lambda_n^\alpha t^\alpha + B_n \sin_\alpha a^\alpha \lambda_n^\alpha t^\alpha) \sin_\alpha n^\alpha \left(\frac{\pi x}{l}\right)^\alpha \quad (n = 0, 1, 2, \ldots). \tag{3.10}$$

To solve our problem, we form the local fractional Fourier series

$$\begin{aligned} u(x,t) &= \sum_{n=1}^{\infty} u_n(x,t) \\ &= \sum_{n=1}^{\infty} (A_n \cos_\alpha a^\alpha \lambda_n^\alpha t^\alpha + B_n \sin_\alpha a^\alpha \lambda_n^\alpha t^\alpha) \sin_\alpha n^\alpha \left(\frac{\pi x}{l}\right)^\alpha, \end{aligned} \tag{3.11}$$

and require that

$$\begin{aligned}
u(x,0) &= \sum_{n=1}^{\infty} u_n(x,0) = \sum_{n=1}^{\infty} A_n \sin_\alpha n\left(\frac{\pi x}{l}\right)^\alpha = f(x),\\
\frac{\partial^\alpha u(l,0)}{\partial x^\alpha} &= \sum_{n=1}^{\infty}\left(-A_n a^\alpha \lambda_n^\alpha \sin_\alpha a^\alpha \lambda_n^\alpha t^\alpha + B_n a^\alpha \lambda_n^\alpha \cos_\alpha a^\alpha \lambda_n^\alpha t^\alpha\right)\sin_\alpha n\left(\frac{\pi x}{l}\right)^\alpha \Bigg|_{t=0}\\
&= \sum_{n=1}^{\infty} B_n a^\alpha \lambda_n^\alpha \sin_\alpha n\left(\frac{\pi x}{l}\right)^\alpha\\
&= g(x).
\end{aligned} \tag{3.12}$$

A calculation of local fractional Fourier coefficients of $f(x)$ and $g(x)$ with respect to the system $\{\sin_\alpha n^\alpha (\pi x/l)^\alpha\}$ is given by

$$A_n = \frac{\int_0^l f(x)\sin_\alpha n^\alpha (\pi x/l)^\alpha (dx)^\alpha}{\int_0^l \sin_\alpha^2 n^\alpha (\pi x/l)^\alpha (dx)^\alpha} \quad (n = 0, 1, 2, \ldots), \tag{3.13}$$

$$B_n a^\alpha \lambda_n^\alpha = \frac{\int_0^l g(x)\sin_\alpha n^\alpha (\pi x/l)^\alpha (dx)^\alpha}{\int_0^1 \sin_\alpha^2 n^\alpha (\pi x/l)^\alpha (dx)^\alpha} \quad (n = 0, 1, 2, \ldots). \tag{3.14}$$

But $\int_0^l \sin_\alpha^2 n^\alpha (\pi x/l)^\alpha (dx)^\alpha = l^\alpha/2$ and therefore

$$A_n = \frac{2}{l^\alpha}\int_0^l f(x)\sin_\alpha \lambda_n^\alpha x^\alpha (dx)^\alpha \quad (n = 0, 1, 2, \ldots), \tag{3.15}$$

$$B_n = \frac{2}{a^\alpha \lambda_n^\alpha l^\alpha}\int_0^l g(x)\sin_\alpha \lambda_n^\alpha x^\alpha (dx)^\alpha \quad (n = 0, 1, 2, \ldots). \tag{3.16}$$

Thus, the solution of our problem is given by formula (3.11), where local fractional Fourier coefficients are determined. From (3.14) and (3.16), we get the harmonic vibrations

$$u_n(x,t) = \left(A_n \cos_\alpha a^\alpha \lambda_n^\alpha t^\alpha + B_n \sin_\alpha a^\alpha \lambda_n^\alpha t^\alpha\right)\sin_\alpha \lambda_n^\alpha x^\alpha, \tag{3.17}$$

where

$$\begin{aligned}
A_n &= \frac{2}{l^\alpha}\int_0^l f(x)\sin_\alpha \lambda_n^\alpha x^\alpha (dx)^\alpha \quad (n = 0, 1, 2, \ldots),\\
B_n &= \frac{1}{2/a^\alpha \lambda_n^\alpha l^\alpha}\int_0^l g(x)\sin_\alpha \lambda_n^\alpha x^\alpha (dx)^\alpha \quad (n = 0, 1, 2, \ldots).
\end{aligned} \tag{3.18}$$

4. Expression Solutions with Mittag-Leffler Functions in Fractal Space

Taking into account the relations, [57],

$$\begin{aligned}\sin_\alpha x^\alpha &= \frac{E_\alpha(i^\alpha x^\alpha) - E_\alpha(-i^\alpha x^\alpha)}{2i^\alpha},\\ \cos_\alpha x^\alpha &= \frac{E_\alpha(i^\alpha x^\alpha) + E_\alpha(-i^\alpha x^\alpha)}{2},\end{aligned} \tag{4.1}$$

we obtain the harmonic vibration with the Mittag-Leffler functions in fractal space

$$\begin{aligned}u_n(x,t) &= \left(A_n \frac{E_\alpha(i^\alpha a^\alpha \lambda_n^\alpha t^\alpha) + E_\alpha(-i^\alpha a^\alpha \lambda_n^\alpha t^\alpha)}{2} + B_n \frac{E_\alpha(i^\alpha a^\alpha \lambda_n^\alpha t^\alpha) - E_\alpha(-i^\alpha a^\alpha \lambda_n^\alpha t^\alpha)}{2i^\alpha}\right)\\ &\quad\times \frac{E_\alpha(i^\alpha \lambda_n^\alpha x^\alpha) - E_\alpha(-i^\alpha \lambda_n^\alpha x^\alpha)}{2i^\alpha}\\ &= \left[\frac{A_n + B_n}{2} E_\alpha(i^\alpha a^\alpha \lambda_n^\alpha t^\alpha) + \frac{A_n - B_n}{2} E_\alpha(-i^\alpha a^\alpha \lambda_n^\alpha t^\alpha)\right]\\ &\quad\times \frac{E_\alpha(i^\alpha \lambda_n^\alpha x^\alpha) - E_\alpha(-i^\alpha \lambda_n^\alpha x^\alpha)}{2i^\alpha}\\ &= \frac{A_n + B_n}{4i^\alpha}\left\{E_\alpha\left[i^\alpha \lambda_n^\alpha (at+x)^\alpha\right] - E_\alpha\left[i^\alpha \lambda_n^\alpha (at-x)^\alpha\right]\right\}\\ &\quad+ \frac{A_n - B_n}{4i^\alpha}\left\{E_\alpha\left[i^\alpha \lambda_n^\alpha (x-at)^\alpha\right] - E_\alpha\left[-i^\alpha \lambda_n^\alpha (at+x)^\alpha\right]\right\},\end{aligned} \tag{4.2}$$

where its coefficients are

$$\begin{aligned}A_n &= \frac{2}{l^\alpha}\int_0^l f(x)\sin_\alpha \lambda_n^\alpha x^\alpha (dx)^\alpha\\ &= \frac{2}{l^\alpha}\int_0^l f(x)\frac{E_\alpha(i^\alpha \lambda_n^\alpha x^\alpha) - E_\alpha(-i^\alpha \lambda_n^\alpha x^\alpha)}{2i^\alpha}(dx)^\alpha\\ &= \frac{1}{i^\alpha l^\alpha}\int_0^l f(x)\left(E_\alpha(i^\alpha \lambda_n^\alpha x^\alpha) - E_\alpha(-i^\alpha \lambda_n^\alpha x^\alpha)\right)(dx)^\alpha \quad (n = 0,1,2,\ldots),\\ B_n &= \frac{2}{a^\alpha \lambda_n^\alpha l^\alpha}\int_0^l g(x)\sin_\alpha \lambda_n^\alpha x^\alpha (dx)^\alpha\\ &= \frac{2}{a^\alpha \lambda_n^\alpha l^\alpha}\int_0^l g(x)\frac{E_\alpha(i^\alpha \lambda_n^\alpha x^\alpha) - E_\alpha(-i^\alpha \lambda_n^\alpha x^\alpha)}{2i^\alpha}(dx)^\alpha\\ &= \frac{1}{a^\alpha \lambda_n^\alpha l^\alpha i^\alpha}\int_0^l g(x)\left(E_\alpha(i^\alpha \lambda_n^\alpha x^\alpha) - E_\alpha(-i^\alpha \lambda_n^\alpha x^\alpha)\right)(dx)^\alpha \quad (n = 0,1,2,\ldots).\end{aligned} \tag{4.3}$$

Hereby, we always find that

$$\left|f(x) - f(x_0)\right| < \varepsilon^{\alpha}, \qquad \left|g(x) - g(x_0)\right| < \varepsilon^{\alpha} \tag{4.4}$$

with $|x - x_0| < \delta$, for $\varepsilon, \delta > 0$ and $\varepsilon, \delta \in R$.

Hence the boundary conditions are fractal and solution with Mittag-Leffler functions in fractal space is given by

$$\begin{aligned} u(x,t) &= \sum_{n=1}^{\infty} u_n(x,t) \\ &= \sum_{n=1}^{\infty} \frac{A_n + B_n}{4i^{\alpha}} \left\{ E_{\alpha}\left[i^{\alpha}\lambda_n^{\alpha}(at + x)^{\alpha}\right] - E_{\alpha}\left[i^{\alpha}\lambda_n^{\alpha}(at - x)^{\alpha}\right] \right\} \\ &\quad + \sum_{n=1}^{\infty} \frac{A_n - B_n}{4i^{\alpha}} \left\{ E_{\alpha}\left[i^{\alpha}\lambda_n^{\alpha}(x - at)^{\alpha}\right] - E_{\alpha}\left[-i^{\alpha}\lambda_n^{\alpha}(at + x)^{\alpha}\right] \right\}, \end{aligned} \tag{4.5}$$

where its coefficients are derived as

$$\begin{aligned} A_n &= \frac{1}{i^{\alpha} l^{\alpha}} \int_0^l f(x)\left(E_{\alpha}(i^{\alpha}\lambda_n^{\alpha}x^{\alpha}) - E_{\alpha}(-i^{\alpha}\lambda_n^{\alpha}x^{\alpha})\right)(dx)^{\alpha} \quad (n = 0, 1, 2, \ldots), \\ B_n &= \frac{1}{a^{\alpha}\lambda_n^{\alpha} l^{\alpha} i^{\alpha}} \int_0^l g(x)\left(E_{\alpha}(i^{\alpha}\lambda_n^{\alpha}x^{\alpha}) - E_{\alpha}(-i^{\alpha}\lambda_n^{\alpha}x^{\alpha})\right)(dx)^{\alpha} \quad (n = 0, 1, 2, \ldots). \end{aligned} \tag{4.6}$$

5. Conclusions

We applied the technique of the local fractional Fourier series to treat with the local fractional wave equation in fractal vibrating string. When contrasted with other analytical methods, such as the heat-balance integral method, the homotopy perturbation method [11], the variational iteration method [29], the exp-function method [58], the fractional variational iteration method [31, 32], the fractional complex method [33–37], and others [59–61], the present method combines the following two advantages. The boundary conditions to the governing equations are local fractional continuous (the functions are nondifferential functions in fractal space) because we employ the local fractional Fourier series, derived from local fractional calculus, to deal with them. The governing equations with fractal behaviors in media are structured based on the local fractional calculus. The way plays a crucial role in local fractional calculus. This technique is efficient for the applied scientists to process these differential equations with the local fractional differential operators in fractal space. This paper that is an outstanding example of application of local fractional Fourier series to the local fractional differential operators is given to elucidate the solution processes and reliable results.

Acknowledgments

This paper is sponsored by the National Natural Science Foundation of China (NSFC, Grant U1204703), the Key Scientific and Technological Project of Henan Province (122102310004), the Fundamental Research Funds for the Central Universities (HUST: 2012QN087, 2012QN088), and the Innovation Scientists and Technicians Troop Construction Projects of Zhengzhou City (10LJRC190, 121PRKXF658-4).

References

[1] R. Hilfe, *Applications of Fractional Calculus in Physics*, World Scientific, River Edge, NJ, USA, 2000.
[2] J. Sabatier, O. P. Agrawal, and J. A. Tenreiro, *Machado, Advances in Fractional Calculus: Theoretical Developments and Applications in Physics and Engineering*, Springer, New York, NY, USA, 2007.
[3] K. B. Oldham and J. Spanier, *The Fractional Calculus*, Academic Press, London, UK, 1974.
[4] K. S. Miller and B. Ross, *An Introduction To the Fractional Calculus and Fractional Differential Equations*, John Wiley & Sons, New York, NY, USA, 1993.
[5] I. Podlubny, *Fractional Differential Equations*, vol. 198, Academic Press, San Diego, Calif, USA, 1999.
[6] S. G. Samko, A. A. Kilbas, and O. I. Marichev, *Fractional Integrals and Derivatives*, Gordon and Breach Science Publishers, Yverdon, Switzerland, 1993.
[7] A. A. Kilbas, H. M. Srivastava, and J. J. Trujillo, *Theory and Applications of Fractional Differential Equations*, vol. 204, Elsevier, Amsterdam, The Netherlands, 2006.
[8] W. R. Schneider and W. Wyss, "Fractional diffusion and wave equations," *Journal of Mathematical Physics*, vol. 30, no. 1, pp. 134–144, 1989.
[9] O. P. Agrawal, "Solution for a fractional diffusion-wave equation defined in a bounded domain," *Nonlinear Dynamics*, vol. 29, no. 1–4, pp. 145–155, 2002.
[10] A. M. A. El-Sayed, "Fractional-order diffusion-wave equation," *International Journal of Theoretical Physics*, vol. 35, no. 2, pp. 311–322, 1996.
[11] H. Jafari and S. Seifi, "Homotopy analysis method for solving linear and nonlinear fractional diffusion-wave equation," *Communications in Nonlinear Science and Numerical Simulation*, vol. 14, no. 5, pp. 2006–2012, 2009.
[12] Y. Povstenko, "Non-axisymmetric solutions to time-fractional diffusion-wave equation in an infinite cylinder," *Fractional Calculus and Applied Analysis*, vol. 14, no. 3, pp. 418–435, 2011.
[13] F. Mainardi and G. Pagnini, "The Wright functions as solutions of the time-fractional diffusion equation," *Applied Mathematics and Computation*, vol. 141, no. 1, pp. 51–62, 2003.
[14] Y. Luchko, "Some uniqueness and existence results for the initial-boundary-value problems for the generalized time-fractional diffusion equation," *Computers & Mathematics with Applications*, vol. 59, no. 5, pp. 1766–1772, 2010.
[15] M. M. Meerschaert, D. A. Benson, H.-P. Scheffler, and B. Baeumer, "Stochastic solution of space-time fractional diffusion equations," *Physical Review E*, vol. 65, no. 4, Article ID 041103, 4 pages, 2002.
[16] S. D. Eidelman and A. N. Kochubei, "Cauchy problem for fractional diffusion equations," *Journal of Differential Equations*, vol. 199, no. 2, pp. 211–255, 2004.
[17] T. Sandev and Ž. Tomovski, "The general time fractional wave equation for a vibrating string," *Journal of Physics A*, vol. 43, no. 5, Article ID 055204, 2010.
[18] T. M. Atanackovic and B. Stankovic, "Generalized wave equation in nonlocal elasticity," *Acta Mechanica*, vol. 208, no. 1-2, pp. 1–10, 2009.
[19] J. Dong and M. Xu, "Space-time fractional Schrödinger equation with time-independent potentials," *Journal of Mathematical Analysis and Applications*, vol. 344, no. 2, pp. 1005–1017, 2008.
[20] S. Z. Rida, H. M. El-Sherbiny, and A. A. M. Arafa, "On the solution of the fractional nonlinear Schrödinger equation," *Physics Letters A*, vol. 372, no. 5, pp. 553–558, 2008.
[21] R. Scherer, S. L. Kalla, L. Boyadjiev, and B. Al-Saqabi, "Numerical treatment of fractional heat equations," *Applied Numerical Mathematics*, vol. 58, no. 8, pp. 1212–1223, 2008.
[22] S. Momani, "An explicit and numerical solutions of the fractional KdV equation," *Mathematics and Computers in Simulation*, vol. 70, no. 2, pp. 110–118, 2005.
[23] R. Metzler and T. F. Nonnenmacher, "Space- and time-fractional diffusion and wave equations, fractional Fokker-Planck equations, and physical motivation," *Chemical Physics*, vol. 84, pp. 67–90, 2002.
[24] P. Paradisi, R. Cesari, F. Mainardi, and F. Tampieri, "The fractional Fick's law for non-local transport processes," *Physica A*, vol. 293, no. 1-2, pp. 130–142, 2001.

[25] Y. Zhou and F. Jiao, “Nonlocal Cauchy problem for fractional evolution equations,” *Nonlinear Analysis*, vol. 11, no. 5, pp. 4465–4475, 2010.
[26] V. E. Tarasov, “Fractional Heisenberg equation,” *Physics Letters A*, vol. 372, no. 17, pp. 2984–2988, 2008.
[27] V. E. Tarasov and G. M. Zaslavsky, “Fractional Ginzburg-Landau equation for fractal media,” *Physica A*, vol. 354, no. 15, pp. 249–261, 2005.
[28] V. E. Tarasov, “Fractional hydrodynamic equations for fractal media,” *Annals of Physics*, vol. 318, no. 2, pp. 286–307, 2005.
[29] J.-H. He, “Approximate analytical solution for seepage flow with fractional derivatives in porous media,” *Computer Methods in Applied Mechanics and Engineering*, vol. 167, no. 1-2, pp. 57–68, 1998.
[30] Q. Wang, “Numerical solutions for fractional KdV-Burgers equation by Adomian decomposition method,” *Applied Mathematics and Computation*, vol. 182, no. 2, pp. 1048–1055, 2006.
[31] G. C. Wu and E. W. M. Lee, “Fractional variational iteration method and its application,” *Physics Letters A*, vol. 374, no. 25, pp. 2506–2509, 2010.
[32] J.-H. He, “A short remark on fractional variational iteration method,” *Physics Letters A*, vol. 375, no. 38, pp. 3362–3364, 2011.
[33] Z.-B. Li and J.-H. He, “Fractional complex transform for fractional differential equations,” *Mathematical & Computational Applications*, vol. 15, no. 5, pp. 970–973, 2010.
[34] J.-H. He, S. K. Elagan, and Z. B. Li, “Geometrical explanation of the fractional complex transform and derivative chain rule for fractional calculus,” *Physics Letters A*, vol. 376, no. 4, pp. 257–259, 2012.
[35] Z. B. Li and J. H. He, “Application of the fractional complex transform to fractional differential equations,” *Nonlinear Science Letters A*, vol. 2, no. 3, pp. 121–126, 2011.
[36] Z. B. Li, W. H. Zhu, and J. H. He, “Exact solutions of time-fractional heat conduction equation by the fractional complex transform,” *Thermal Science*, vol. 16, no. 2, pp. 335–338, 2012.
[37] Q. L. Wang, J. H. He, and Z. B. Li, “Fractional model for heat conduction in polar bear hairs,” *Thermal Science*, vol. 16, no. 2, pp. 339–342, 2012.
[38] G. Jumarie, “On the representation of fractional Brownian motion as an integral with respect to $(dt)^a$,” *Applied Mathematics Letters*, vol. 18, no. 7, pp. 739–748, 2005.
[39] G. Jumarie, “Probability calculus of fractional order and fractional Taylor’s series application to Fokker-Planck equation and information of non-random functions,” *Chaos, Solitons and Fractals*, vol. 40, no. 3, pp. 1428–1448, 2009.
[40] G. Jumarie, “Laplace’s transform of fractional order via the Mittag-Leffler function and modified Riemann-Liouville derivative,” *Applied Mathematics Letters*, vol. 22, no. 11, pp. 1659–1664, 2009.
[41] G.-C. Wu, “Adomian decomposition method for non-smooth initial value problems,” *Mathematical and Computer Modelling*, vol. 54, no. 9-10, pp. 2104–2108, 2011.
[42] K. M. Kolwankar and A. D. Gangal, “Local fractional Fokker-Planck equation,” *Physical Review Letters*, vol. 80, no. 2, pp. 214–217, 1998.
[43] A. Carpinter and A. Sapora, “Diffusion problems in fractal media defined on Cantor sets,” *ZAMM Journal of Applied Mathematics and Mechanics*, vol. 90, no. 3, pp. 203–210, 2010.
[44] K. M. Kolwankar and A. D. Gangal, “Fractional differentiability of nowhere differentiable functions and dimensions,” *Chaos*, vol. 6, no. 4, pp. 505–513, 1996.
[45] X. R. Li, *Fractional calculus, fractal geometry, and stochastic processes [Ph.D. thesis]*, University of Western Ontario, Ontario, Canada, 2003.
[46] A. Babakhani and V. D. Gejji, “On calculus of local fractional derivatives,” *Journal of Mathematical Analysis and Applications*, vol. 270, no. 1, pp. 66–79, 2002.
[47] A. Parvate and A. D. Gangal, “Calculus on fractal subsets of real line. I. Formulation,” *Fractals*, vol. 17, no. 1, pp. 53–81, 2009.
[48] F. Ben Adda and J. Cresson, “About non-differentiable functions,” *Journal of Mathematical Analysis and Applications*, vol. 263, no. 2, pp. 721–737, 2001.
[49] A. Carpinteri, B. Chiaia, and P. Cornetti, “The elastic problem for fractal media: basic theory and finite element formulation,” *Computers & Structures*, vol. 82, no. 6, pp. 499–508, 2004.
[50] A. Carpinteri and P. Cornetti, “A fractional calculus approach to the description of stress and strain localization in fractal media,” *Chaos, Solitons, Fractals*, vol. 13, no. 1, pp. 85–94, 2002.
[51] Y. Chen, Y. Yan, and K. Zhang, “On the local fractional derivative,” *Journal of Mathematical Analysis and Applications*, vol. 362, no. 1, pp. 17–33, 2010.
[52] A. Carpinteri, B. Chiaia, and P. Cornetti, “On the mechanics of quasi-brittle materials with a fractal microstructure,” *Engineering Fracture Mechanics*, vol. 70, no. 6, pp. 2321–2349, 2003.

[53] X. J. Yang, "Local fractional integral transforms," *Progress in Nonlinear Science*, vol. 4, pp. 1–225, 2011.
[54] X. J. Yang, *Local Fractional Functional Analysis and Its Applications*, Asian Academic Publisher, Hong Kong, 2011.
[55] X. J. Yang, "Local fractional calculus and its applications," in *Proceedings of the 5th IFAC Workshop Fractional Differentiation and Its Applications, (FDA '12)*, pp. 1–8, Nanjing, China, 2012.
[56] X. J. Yang, M. K. Liao, and J. W. Chen, "A novel approach to processing fractal signals using the Yang-Fourier transforms," *Procedia Engineering*, vol. 29, pp. 2950–2954, 2012.
[57] X. J. Yang, *Advanced Local Fractional Calculus and Its Applications*, World Science Publisher, New York, NY, USA, 2012.
[58] S. Zhang and H.-Q. Zhang, "Fractional sub-equation method and its applications to nonlinear fractional PDEs," *Physics Letters A*, vol. 375, no. 7, pp. 1069–1073, 2011.
[59] J. H. He, "Analytical methods for thermal science—an elementary introduction," *Thermal Science*, vol. 15, pp. S1–S3, 2011.
[60] J. H. He, "A new fractal derivation," *Thermal Science*, vol. 15, pp. S145–S147, 2011.
[61] J. H. He, "Asymptotic methods for solitary solutions and compactons," *Abstract and Applied Analysis*, vol. 2012, Article ID 916793, 130 pages, 2012.

Hindawi Publishing Corporation
Abstract and Applied Analysis
Volume 2012, Article ID 327682, 9 pages
doi:10.1155/2012/327682

Research Article

Soliton Solutions for the Wick-Type Stochastic KP Equation

Y. F. Guo,[1,2] L. M. Ling,[2] and D. L. Li[1]

[1] *Department of Information and Computation of Science, Guangxi University of Technology, Liuzhou, Guangxi 545006, China*
[2] *Institute of Applied Physics and Computational Mathematics, P.O. Box 8009, Beijing 100088, China*

Correspondence should be addressed to Y. F. Guo, guoyan_feng@yahoo.com.cn

Received 10 September 2012; Accepted 28 November 2012

Academic Editor: Peicheng Zhu

The Wick-type stochastic KP equation is researched. The stochastic single-soliton solutions and stochastic multisoliton solutions are shown by using the Hermite transform and Darboux transformation.

1. Introduction

In recent decades, there has been an increasing interest in taking random effects into account in modeling, analyzing, simulating, and predicting complex phenomena, which have been widely recognized in geophysical and climate dynamics, materials science, chemistry biology, and other areas, see [1, 2]. If the problem is considered in random environment, the stochastic partial differential equations (SPDEs) are appropriate mathematical models for complex systems under random influences or noise. So far, we know that the random wave is an important subject of stochastic partial differential equations.

In 1970, while studying the stability of the KdV soliton-like solutions with small transverse perturbations, Kadomtsev and Petviashvili [3] arrived at the two-dimensional version of the KdV equation:

$$u_{tx} = (u_{xxx} + 6uu_x)_x + 3\alpha^2 u_{yy}, \tag{1.1}$$

which is known as *Kadomtsev-Petviashvili* (KP) equation. The KP equation appears in physical applications in two different forms with $\alpha = 1$ and $\alpha = i$, usually referred to as the KP-I and the KP-II equations. The number of physical applications for the KP equation is even larger than the number of physical applications for the KdV equation. It is well known that homogeneous balance method [4, 5] has been widely applied to derive the nonlinear transformations and exact solutions (especially the solitary waves) and Darboux transformation [6], as well as the similar reductions of nonlinear PDEs in mathematical physics. These subjects have been researched by many authors.

For SPDEs, in [7], Holden et al. gave white noise functional approach to research stochastic partial differential equations in Wick versions, in which the random effects are taken into account. In this paper, we will use their theory and method to investigate the stochastic soliton solutions of Wick-type stochastic KP equation, which can be obtained in the influence of the random factors.

The Wick-type stochastic KP equation in white noise environment is considered as the following form:

$$U_{tx} = \left(f(t)\Diamond U_{xxx} + 6g(t)\Diamond U\Diamond U_x\right)_x^{\Diamond} + 3\alpha^2 f(t)\Diamond U_{yy} + W(t)\Diamond R^{\Diamond}\left(U, U_x, U_{xx}, U_{xxxx}, U_{yy}\right), \tag{1.2}$$

which is the perturbation of the KP equation with variable coefficients:

$$u_{tx} = \left(f(t)u_{xxx} + 6g(t)uu_x\right)_x + 3\alpha^2 f(t)u_{yy}, \tag{1.3}$$

by random force $W(t)\Diamond R^{\Diamond}(U, U_x, U_{xx}, U_{xxxx}, U_{yy})$, where $\Diamond$ is the Wick product on the Hida distribution space $(S(\mathbb{R}^d))^*$ which is defined in Section 2, $f(t)$ and $g(t)$ are functions of t, $W(t)$ is Gaussian white noise, that is, $W(t) = \dot{B}(t)$ and $B(t)$ is a Brownian motion, $R(u, u_x, u_{xx}, u_{xxxx}, u_{yy}) = \beta u_{xxxx} + 6\gamma u_x^2 + 6\gamma u u_{xx} + 3\alpha^2\beta u_{yy}$ is a function of $u, u_x, u_{xx}, u_{xxxx}, u_{yy}$ for some constants β, γ, and $R^{\Diamond}$ is the Wick version of the function R.

This paper is organized as follows. In Section 2, the work function spaces are given. In Section 3, we present the single-soliton solutions of stochastic KP equation (1.2). Section 4 is devoted to investigate the multisoliton solutions of stochastic KP equation (1.2).

2. SPDEs Driven by White Noise

Let $(S(\mathbb{R}^d))$ and $(S(\mathbb{R}^d))^*$ be the Hida test function and the Hida distribution space on $\mathbb{R}^d$, respectively. The collection $\xi^n = e^{(-x^2/2)h_n(\sqrt{2}x)/(\pi(n-1)!)^{1/2}}$, $n \geq 1$ constitutes an orthogonal basis for $L^2(\mathbb{R})$, where $h_n(x)$ is the d-order Hermite polynomials. The family of tensor products $\xi_\alpha = \xi_{\alpha_1,\ldots,\alpha_d} = \xi_{\alpha_1} \otimes \cdots \otimes \xi_{\alpha_1}$ $(\alpha \in \mathbb{N}^d)$ forms an orthogonal basis for $L^2(\mathbb{R}^d)$, where $\alpha = (\alpha_1, \ldots, \alpha_d)$ is d-dimensional multi-indices with $\alpha_1, \ldots, \alpha_d \in \mathbb{N}$. The multi-indices $\alpha = (\alpha_1, \ldots, \alpha_d)$ are defined as elements of the space $\mathcal{J} = (\mathbb{N}_0^{\mathbb{N}})_c$ of all sequences $\alpha = (\alpha_1, \alpha_2, \ldots)$ with elements $\alpha_i \in \mathbb{N}_0$ and with compact support, that is, with only finite many $\alpha_i \neq 0$. For $\alpha = (\alpha_1, \alpha_2, \ldots)$, we define

$$H_\alpha(\omega) = \prod_{i=1}^{\infty} h_{\alpha_i}\left(\langle \omega, \eta_i \rangle\right), \quad \omega \in \left(S\left(\mathbb{R}^d\right)\right)^*. \tag{2.1}$$

If $n \in \mathbb{N}$ is fixed, let $(S)_1^n$ consist of those $x = \sum_\alpha c_\alpha H_\alpha \in \oplus_{k=1}^n L^2(\mu)$ with $c_\alpha \in \mathbb{R}^n$ such that $\|x\|_{1,k}^2 = \sum_\alpha c_\alpha^2 (\alpha!)^2 (2\mathbb{N})^{k\alpha} < \infty$ for all $k \in \mathbb{N}$ with $c_\alpha^2 = |c_\alpha|^2 = \sum_{k=1}^n (c_\alpha^{(k)})^2$ if $c_\alpha = (c_\alpha^{(1)}, \ldots, c_\alpha^{(n)}) \in \mathbb{R}^n$, where μ is the white noise measure on $(S^*(\mathbb{R}), \mathcal{B}(S^*(\mathbb{R})))$, $\alpha! = \prod_{k=1}^{\infty} \alpha_k!$ and $(2\mathbb{N})^\alpha = \prod_j (2j)^{\alpha_j}$ for $\alpha = (\alpha_1, \alpha_2, \ldots) \in \mathcal{J}$. The space $(S)_{-1}^n$ can be regarded as the dual of

$(S)_1^n$. $(S)_{-1}^n$ consisting of all formal expansion $X = \sum_\alpha b_\alpha H_\alpha$ with $b_\alpha \in \mathbb{R}^n$ such that $\|X\|_{-1,-q} = \sum_\alpha b_\alpha^2 (2\mathbb{N})^{-q\alpha} < \infty$ for some $q \in \mathbb{N}$, by the action $\langle X, x\rangle = \sum_\alpha (b_\alpha, c_\alpha)\alpha!$ and (b_α, c_α) is the usual inner product in $\mathbb{R}^n$.

$X \Diamond Y = \sum_{\alpha,\beta}(a_\alpha, b_\beta)H_{\alpha+\beta}$ is called the Wick product of X and Y, for $X = \sum_\alpha a_\alpha H_\alpha$, $Y = \sum_\alpha b_\alpha H_\alpha \in (S)_{-1}^n$ with $a_\alpha, b_\alpha \in \mathbb{R}^n$. We can prove that the spaces $(S(\mathbb{R}^d))$, $(S(\mathbb{R}^d))^*(S)_1^n$, and $(S)_{-1}^n$ are closed under Wick products.

For $X = \sum_\alpha a_\alpha H_\alpha \in (S)_{-1}^n$ with $a_\alpha \in \mathbb{R}^n$, $\mathscr{H}(X)$ or $\widetilde{X}$ is defined as the Hermite transform of X by $\mathscr{H}(X)(z) = \widetilde{X}(z) = \sum_\alpha a_\alpha z^\alpha \in \mathbb{C}^n$ (when convergent), where $z = (z_1, z_2, \ldots) \in \mathbb{C}^{\mathbb{N}}$ (the set of all sequences of complex numbers) and $z^\alpha = z_1^{\alpha_1} z_2^{\alpha_2} \cdots z_n^{\alpha_n} \cdots$ for $\alpha = (\alpha_1, \alpha_2, \ldots) \in \mathcal{J}$. For $X, Y \in (S)_{-1}^N$, by this definition we have $\widetilde{X \Diamond Y}(z) = \widetilde{X}(z) \cdot \widetilde{Y}(z)$ for all z such that $\widetilde{X}(z)$ and $\widetilde{Y}(z)$ exist. The product on the right-hand side of the above formula is the complex bilinear product between two elements of $\mathbb{C}^N$ defined by $(z_1^1, \ldots, z_n^1) \cdot (z_1^2, \ldots, z_n^2) = \sum_{k=1}^n z_k^1 z_k^2$, where $z_k^i \in \mathbb{C}$. Let $X = \sum_\alpha a_\alpha H_\alpha \in (S)_{-1}^n$. Then the vector $c_0 = \widetilde{X}(0) \in \mathbb{R}^n$ is called the generalized expectation of X denoted by $\mathbb{E}(X)$. Suppose that $f : V \to \mathbb{C}^n$ is an analytic function, where V is a neighborhood of $\mathbb{E}(X)$. Assume that the Taylor series of f around $\mathbb{E}(X)$ has coefficients in $\mathbb{R}^n$. Then the Wick version $f^\Diamond(X) = \mathscr{H}^{-1}(f \circ \widetilde{X}) \in (S)_{-1}^n$.

Suppose that modeling considerations lead us to consider the SPDE expressed formally as $A(t, x, \partial_t, \nabla_x, U, \omega) = 0$, where A is some given function, $U = U(t, x, \omega)$ is the unknown generalized stochastic process, and the operators $\partial_t = \partial/\partial_t$, $\nabla_x = (\partial/\partial_{x_1}, \ldots, \partial/\partial_{x_d})$ when $x = (x_1, \ldots, c_d) \in \mathbb{R}^d$. If we interpret all products as wick products and all functions as their Wick versions, we have

$$A^\Diamond(t, x, \partial_t, \nabla_x, U, \omega) = 0. \tag{2.2}$$

Taking the Hermite transform of (2.2), the Wick product is turned into ordinary products (between complex numbers), and the equation takes the form

$$\widetilde{A}\left(t, x, \partial_t, \nabla_x, \widetilde{U}, z_1, z_2, \ldots\right) = 0, \tag{2.3}$$

where $\widetilde{U} = \mathscr{H}(U)$ is the Hermite transform of U and $z_1, z_2, \ldots$ are complex numbers. Suppose that we can find a solution $u = u(t, x, z)$ of (2.3) for each $z = (z_1, z_2, \ldots) \in \mathbb{K}_q(r)$ for some q, r, where $\mathbb{K}_q(r) = z = (z_1, z_2, \ldots) \in \mathbb{C}^{\mathbb{N}}$ and $\sum_{\alpha \neq 0} |z^\alpha|^2 (2\mathbb{N})^{q\alpha} < r^2$. Then under certain conditions, we can take the inverse Hermite transform $U = \mathscr{H}^{-1} u \in (S)_{-1}$ and thereby obtain a solution U of the original Wick equation (2.2). We have the following theorem, which was proved by Holden et al. in [7].

Theorem 2.1. *Suppose that $u(t, x, z)$ is a solution (in the usual strong, pointwise sense) of* (2.3) *for (t, x) in some bounded open set $G \subset \mathbb{R} \times \mathbb{R}^d$ and $z \in \mathbb{K}_q(r)$ for some q, r. Moreover, suppose that $u(t, x, z)$ and all its partial derivatives, which are involved in* (2.3)*, are bounded for $(t, x, z) \in G \times \mathbb{K}_q(r)$, continuous with respect to $(t, x) \in G$ for all $z \in \mathbb{K}_q(r)$, and analytic with respect to $z \in \mathbb{K}_q(r)$ for all $(t, x) \in G$. Then there exists $U(t, x) \in (S)_{-1}$ such that $u(t, x, z) = (\widetilde{U}(t, x))(z)$ for all $(t, x, z) \in G \times \mathbb{K}_q(r)$ and $U(t, x)$ solves (in the strong sense in $(S)_{-1}$)* (2.2) *in $(S)_{-1}$.*

3. Single-Soliton Solution of Stochastic KP Equation

In this section, we investigate the single-soliton solutions of the Wick-type stochastic KP equation (1.2). Using the similar idea of the Darboux transformation about the determinant nonlinear partial differential equations, we can obtain the soliton solutions of (1.2), which can be seen in the following theorem.

Theorem 3.1. *For the Wick-type stochastic KP equation* (1.2) *in white noise environment, one has the single-soliton solution* $U[1] \in (S)_{-1}$ *for KP-I:*

$$U[1] = \frac{\lambda^2}{2k}\left(\operatorname{sech}\left(\frac{\overline{\Phi}}{2}\right)\right)^2, \quad when\ \alpha = 1 \tag{3.1}$$

and for KP-II:

$$U[1] = \frac{2a^2}{k}\operatorname{sech}^2\left(\overline{\Phi}_1(t,x,y)\right), \quad when\ \alpha = i, \tag{3.2}$$

where $\overline{\Phi}(t,x,y) = \lambda x + \lambda^2 y + 4\lambda^3\int_0^t f(s)ds + 4\lambda^3\beta B(t) - 2\lambda^3\beta t^2$ *and*

$$\overline{\Phi}_1(t,x,y) = ax - 2aby + 4\left(a^3 - 3ab^2\right)\int_0^t f(s)ds + 4\beta\left(a^3 - 3ab^2\right)\left(B(t) - \frac{1}{2}t^2\right). \tag{3.3}$$

Proof. Taking the Hermite transform of (1.2), the equation (1.2) can be changed into

$$\widetilde{U}_{tx} = \left[f(t) + \beta\widetilde{W}(t,z)\right]\widetilde{U}_{xxxx} + 6\left[g(t) + \gamma\widetilde{W}(t,z)\right]\left(\widetilde{U}\widetilde{U}_x\right)_x + 3\alpha^2\left[f(t) + \beta\widetilde{W}(t,z)\right]\widetilde{U}_{yy}, \tag{3.4}$$

where $\widetilde{U}$ is the Hermite transform of U; the Hermite transform of $W(t)$ is defined by $\widetilde{W}(t,z) = \sum_{k=1}^{\infty}\eta_k(t)z_k$ where $z = (z_1, z_2, \ldots) \in (\mathbb{C}^{\mathbb{N}})_c$ is parameter.

Suppose that $g(t)+\gamma\widetilde{W}(t,z) = k[f(t)+\beta\widetilde{W}(t,z)]$. Let $u = k\widetilde{U}$. From (3.4), we can obtain

$$u_{tx} = \left[f(t) + \beta\widetilde{W}(t,z)\right](u_{xxx} + 6uu_x)_x + 3\alpha^2\left[f(t) + \beta\widetilde{W}(t,z)\right]u_{yy}. \tag{3.5}$$

Let $F(t,z) = f(t) + \beta\widetilde{W}(t,z)$; then (3.5) can be changed into

$$u_{tx} = F(t,z)(u_{xxx} + 6uu_x)_x + 3\alpha^2 F(t,z)u_{yy}. \tag{3.6}$$

Now we consider the soliton solutions of (3.6) using Darboux transform. It is more convenient to consider the compatibility condition of the following linear system of partial differential equations, that is, Lax pair of (3.6):

$$\begin{aligned}\phi_y &= \alpha^{-1}\phi_{xx} + \alpha^{-1}u\phi,\\ \phi_t &= 4F(t,z)\phi_{xxx} + 6F(t,z)u\phi_x + 3F(t,z)(\alpha v_y + u_x)\phi.\end{aligned} \tag{3.7}$$

Then we can obtain the Wick-type Lax pair of (1.2):

$$\begin{aligned}\phi_y &= \alpha^{-1}\phi_{xx} + \alpha^{-1}u\Diamond\phi,\\ \phi_t &= 4\big(f(t)+\beta W(t)\big)\Diamond\phi_{xxx} + 6\big(f(t)+\beta W(t)\big)\Diamond u\Diamond\phi_x\\ &\quad + 3\big(f(t)+\beta W(t)\big)\Diamond\big(\alpha v_y + u_x\big)\Diamond\phi.\end{aligned} \tag{3.8}$$

Let ϕ_1 be a given solution of (3.8). Using the idea of the Darboux transformation about the determinant nonlinear partial differential equations, by direct computation, it is easy to know that if supposing that $\phi[1] = \phi_x - (\phi_{1x}\Diamond{\phi_1}^{\Diamond(-1)})\Diamond\phi$, where ϕ is an arbitrary solution of (3.8), then $\phi[1]$ satisfies the following equations:

$$\begin{aligned}\phi_y[1] &= \alpha^{-1}\phi_{xx}[1] + \alpha^{-1}u[1]\Diamond\phi[1],\\ \phi_t[1] &= 4\big(f(t)+\beta W(t)\big)\Diamond\phi_{xxx}[1] + 6\big(f(t)+\beta W(t)\big)\Diamond u[1]\phi_x[1]\\ &\quad + 3\big(f(t)+\beta W(t)\big)\Diamond\big(\alpha v_y[1] + u_x[1]\big)\Diamond\phi[1],\end{aligned} \tag{3.9}$$

where $u[1] = u + 2(\phi_{1x}\Diamond{\phi_1}^{\Diamond(-1)})_x^{\Diamond}$, $v[1] = v + 2(\phi_{1x}\Diamond{\phi_1}^{\Diamond(-1)})$.

Since (3.6) is nonlinear, it is difficult to solve it in general. In particular, taking $u = 0$ and $v = 0$, then from (3.8), we have

$$\begin{aligned}\phi_y &= \alpha^{-1}\phi_{xx},\\ \phi_t &= 4\big(f(t)+\beta W(t)\big)\Diamond\phi_{xxx}.\end{aligned} \tag{3.10}$$

If $\alpha = 1$, (3.10) have the exponential function solution

$$\phi_1(t,x,y,z) = \exp^{\Diamond}\{\varphi(t,x,y,z)\} + 1, \tag{3.11}$$

where

$$\varphi = \lambda x + \lambda^2 y + 4\lambda^3\left(\int_0^t f(s)ds + \beta B(t)\right), \tag{3.12}$$

and λ is an arbitrary real parameter. Then we can obtain the single-soliton solution of (3.6). By (3.11) and (3.12) there exists a stochastic single-solitary solution of (1.2) as following:

$$U[1] = \frac{2}{k}\left(\phi_{1x}\Diamond{\phi_1}^{\Diamond(-1)}\right)\Diamond\phi = \frac{\lambda^2}{2k}\left(\operatorname{sech}^{\Diamond}\left(\frac{\Phi}{2}\right)\right)^2, \tag{3.13}$$

where

$$\Phi(t,x,y) = \lambda x + \lambda^2 y + 4\lambda^3\int_0^t f(s)ds + 4\lambda^3\beta B(t). \tag{3.14}$$

Since $\exp^{\diamond}\{B(t)\} = \exp\{B(t) - (1/2)t^2\}$ (see Lemma 2.6.16 in [7]), (1.2) has the single-soliton solution

$$U[1] = \frac{\lambda^2}{2k}\left(\operatorname{sech}\left(\frac{\overline{\Phi}}{2}\right)\right)^2, \tag{3.15}$$

where

$$\overline{\Phi}(t,x,y) = \lambda x + \lambda^2 y + 4\lambda^3 \int_0^t f(s)ds + 4\lambda^3 \beta B(t) - 2\lambda^3 \beta t^2. \tag{3.16}$$

In particular, when $f(s) = 1$ we can obtain the solution of (2.2), respectively, as follows:

$$U[1] = \frac{\lambda^2}{2k}\operatorname{sech}^2\left(\frac{1}{2}\left(\lambda x + \lambda^2 y + 4\lambda^3 t + 4\lambda^3 \beta B(t) - 2\lambda^3 \beta t^2\right)\right). \tag{3.17}$$

If $\alpha = i$, (3.10) have the exponential function solution

$$\phi_1(t,x,y,z) = \exp^{\diamond}\{\varphi_1(t,x,y,z)\} + \exp^{\diamond}\{-\overline{\varphi}_1(t,x,y,z)\}, \tag{3.18}$$

where

$$\varphi_1(t,x,y,z) = \lambda x + i\lambda^2 y + 4\lambda^3\left(\int_0^t f(s)ds + \beta B(t)\right), \tag{3.19}$$

$\overline{\varphi}_1$ is the conjugation of $\overline{\varphi}_1$ and λ is an arbitrary complex parameter. Let $\lambda = a+ib$, according to (3.9), from (3.18) and (3.19) there exists a stochastic single-solitary solution of (1.2) as follows:

$$U[1] = \frac{2}{k}\left(\phi_{1x}\diamond\phi_1^{\diamond(-1)}\right)\diamond\phi = \frac{2a^2}{k}\left(\operatorname{sech}^{\diamond}(\Phi_1(t,x,y))\right)^2, \tag{3.20}$$

where

$$\Phi_1(t,x,y) = ax - 2aby + 4\left(a^3 - 3ab^2\right)\int_0^t f(s)ds + 4\left(a^3 - 3ab^2\right)\beta B(t). \tag{3.21}$$

Same as the former case, since $\exp^{\diamond}\{B(t)\} = \exp\{B(t) - (1/2)t^2\}$, (1.2) has the single-soliton solution

$$U[1] = \frac{2a^2}{k}\operatorname{sech}^2\left(\overline{\Phi}_1(t,x,y)\right), \tag{3.22}$$

where

$$\overline{\Phi}_1(t,x,y) = ax - 2aby + 4\left(a^3 - 3ab^2\right)\int_0^t f(s)ds + 4\beta\left(a^3 - 3ab^2\right)\left(B(t) - \frac{1}{2}t^2\right). \tag{3.23}$$

In particular, when $f(s)=1$ we can obtain the solution of (2.2) as follows:

$$U[1]=\frac{2a^2}{k}\operatorname{sech}^2\left(ax-2aby+4\left(a^3-3ab^2\right)\left(t-\frac{\beta}{2}t^2+\beta B(t)\right)\right). \tag{3.24}$$

□

4. Multisoliton Solutions of Stochastic KP Equation

At the same time, the multisoliton solutions of stochastic KP equation can be also considered. It is evident that the Darboux transformation can be applied to (3.9) again. This operation can be repeated arbitrarily. For the second step of this procedure we have

$$\phi[2]=\left(\frac{\partial}{\partial x}-\frac{\phi_{2x}[1]}{\phi_2[1]}\right)\left(\frac{\partial}{\partial x}-\frac{\phi_{1x}}{\phi_1}\right)\phi, \tag{4.1}$$

where $\phi_2[1]$ is the fixed solution of (3.9), which is generated by some fixed solution ϕ_2 of (3.8) and independent of ϕ_1. We know that

$$\phi_2[1]=\phi_{2x}-\frac{\phi_{1x}}{\phi_1}\phi_2, \tag{4.2}$$

$$u[2]=u+2\frac{\partial^2}{\partial x^2}\ln W(\phi_1,\phi_2). \tag{4.3}$$

By using N-times Darboux transformation, the formula (4.3) can be generalized to obtain the solutions of the initial equations (3.8) without any use of the solutions related to the intermediate iterations of the process.

Let $\phi_1,\phi_2,\ldots,\phi_N$ be different and independent solutions of (3.8). We define the Wronski determinant W of functions $f_1,\ldots,f_m$ as

$$W(f_1,\ldots,f_m)=\det A,\qquad A_{ij}=\frac{d^{i-1}f_j}{dx^{i-1}},\quad i,j=1,2,\ldots,m. \tag{4.4}$$

Theorem 4.1. *For the Wick-type stochastic KP equation* (1.2) *in white noise environment, one has the N-soliton solution $U[N]\in(S)_{-1}$ satisfying*

$$U[N]=\frac{2}{k}\frac{\partial^2}{\partial x^2}\ln^{\diamond}W^{\diamond}(\phi_1,\ldots,\phi_N). \tag{4.5}$$

Proof. From [6], it is easy to see that the function

$$\phi[N]=\frac{W(\phi_1,\ldots,\phi_N,\phi)}{W(\phi_1,\ldots,\phi_N)} \tag{4.6}$$

satisfies the following equations:

$$\begin{aligned}\phi_y[N] &= \alpha^{-1}\phi_{xx}[N] + \alpha^{-1}u[N]\phi[N],\\ \phi_t[N] &= 4F(t,z)\phi_{xxx}[N] + 6F(t,z)u[N]\phi_x[N]\\ &\quad + 3F(t,z)\left(\alpha v_y[N] + u_x[N]\right)\phi[N],\end{aligned} \tag{4.7}$$

where $u[N] = u + 2(\partial^2/\partial x^2)\ln W(\phi_1,\ldots,\phi_N)$ and $v[N] = v + 2(\partial/\partial x)\ln W(\phi_1,\ldots,\phi_N)$.

Then we have the Wick-type form

$$\phi[N] = \frac{W^{\Diamond}(\phi_1,\ldots,\phi_N,\phi)}{W^{\Diamond}(\phi_1,\ldots,\phi_N)} \tag{4.8}$$

satisfying the following equations:

$$\begin{aligned}\phi_y[N] &= \alpha^{-1}\phi_{xx}[N] + \alpha^{-1}u[N]\Diamond\phi[N],\\ \phi_t[N] &= 4\left(f(t) + W(t)\right)\Diamond\phi_{xxx}[N] + 6\left(f(t) + W(t)\right)\Diamond u[N]\Diamond\phi_x[N]\\ &\quad + 3\left(f(t) + W(t)\right)\Diamond\left(\alpha v_y[N] + u_x[N]\right)\Diamond\phi[N],\end{aligned} \tag{4.9}$$

where $u[N] = u + 2(\partial^2/\partial x^2)\ln^{\Diamond} W^{\Diamond}(\phi_1,\ldots,\phi_N)$.

In particular, taking $u = 0$, $v = 0$, we can obtain the N-soliton solution of (1.2):

$$U[N] = \frac{2}{k}\frac{\partial^2}{\partial x^2}\ln^{\Diamond} W^{\Diamond}(\phi_1,\ldots,\phi_N). \tag{4.10}$$

When $\alpha = 1$ and $\alpha = i$, $\phi_1,\ldots,\phi_N$ are represented by the corresponding forms (3.11) and (3.18), where λ, a, b take the different constants. □

Remark 4.2. However, in generally, in the view of the modeling point, one can consider the situations where the noise has a different nature. It turns out that there is a close mathematical connection between SPDEs driven by Gaussian and Poissonian noise at least for Wick-type equations. It is well known that there is a unitary map to the solution of the corresponding Gaussian SPDE, see [7]. Hence, if the coefficient $f(t)$ is perturbed by Poissonian white noise in (1.2), the stochastic single-soliton solution and stochastic multisoliton solutions also can be obtained by the same discussion.

Acknowledgments

This paper is supported by National Natural Science Foundation of China (no. 11061003) and Foundation of Ph.D. of Guangxi University of Technology (no. 03081587).

References

[1] E. Weinan, X. Li, and E. Vanden-Eijnden, "Some recent progress in multiscale modeling," in *Multiscale Modelling and Simulation*, vol. 39 of *Lecture Notes in Computational Science and Engineering*, pp. 3–21, Springer, Berlin, Germany, 2004.

[2] P. Imkeller and A. H. Monahan, "Conceptual stochastic climate models," *Stochastics and Dynamics*, vol. 2, no. 3, pp. 311–326, 2002.

[3] B. B. Kadomtsev and V. I. Petviashvili, "Stability of combined waves in weakly dispersing media," *Doklady Akademii Nauk SSSR*, vol. 192, no. 4, pp. 753–756, 1970.

[4] R. Hirota, *The Direct Method in Soliton Theory*, Cambridge University Press, Cambridge, UK, 2004.

[5] Z. Dai, Y. Huang, X. Sun, D. Li, and Z. Hu, "Exact singular and non-singular solitary-wave solutions for Kadomtsev-Petviashvili equation with p-power of nonlinearity," *Chaos, Solitons and Fractals*, vol. 40, no. 2, pp. 946–951, 2009.

[6] V. B. Matveev and M. A. Salle, *Darboux Transformations and Solitons*, Springer, Berlin, Germany, 1991.

[7] H. Holden, B. Øksendal, J. Ubøe, and T. Zhang, *Stochastic Partial Differential Equations: A Modeling, White Noise Functional Approach*, Birkhäuser, Basel, Switzerland, 1996.

Hindawi Publishing Corporation
Abstract and Applied Analysis
Volume 2012, Article ID 964974, 2 pages
doi:10.1155/2012/964974

Letter to the Editor

Comment on "Variational Iteration Method for Fractional Calculus Using He's Polynomials"

Ji-Huan He

National Engineering Laboratory for Modern Silk, College of Textile and Engineering, Soochow University, 199 Ren-ai Road, Suzhou 215123, China

Correspondence should be addressed to Ji-Huan He, hejihuan@suda.edu.cn

Received 17 November 2012; Accepted 1 December 2012

Recently Liu applied the variational homotopy perturbation method for fractional initial boundary value problems. This note concludes that the method is a modified variational iteration method using He's polynomials. A standard variational iteration algorithm for fractional differential equations is suggested.

1. Introduction

The variational iteration method [1, 2] has been shown to solve a large class of nonlinear differential problems effectively, easily, and accurately with the approximations converging rapidly to accurate solutions. In 1998, the method was first adopted to solve fractional differential equations [2]. Recently Liu applied the variational homotopy perturbation method for fractional initial boundary value problems [3]; however, the method is nothing but a modified variational iteration method.

2. Liu's Work

Liu used the following example to elucidate the solution process [3]:

$$\frac{\partial^{\alpha} u}{\partial t^{\alpha}} - \frac{1}{2} x^2 \frac{\partial^2 u}{\partial x^2} = 0. \tag{2.1}$$

The classical variational iteration algorithm reads [4]

$$u_{n+1}(x,t) = u_n(x,t) - \int_0^t \left\{ \frac{\partial^\alpha u_n(x,s)}{\partial s^\alpha} - \frac{1}{2}x^2 \frac{\partial^2 u_n(x,s)}{\partial x^2} \right\} \mathrm{d}s, \tag{2.2}$$

which is exactly the same as that in Liu's work [3], where the nonlinear term is expanded into He's polynomials [5]. So what Liu used is exactly the variational iteration method using He's polynomials, which has been widely used for solving various nonlinear problems [6–8].

3. Conclusion

The so-called variational homotopy perturbation method is nothing but the variational iteration method using He's polynomials. A standard variational iteration algorithm using He's polynomials is suggested to follow Guo and Mei's work [9], and the variational iteration algorithm using Adomian's polynomials was given in [10].

Acknowledgment

The work is supported by PAPD (a project funded by the Priority Academic Program Development of Jiangsu Higher Education Institutions).

References

[1] J.-H. He, "Some asymptotic methods for strongly nonlinear equations," *International Journal of Modern Physics B*, vol. 20, no. 10, pp. 1141–1199, 2006.
[2] J.-H. He, "Approximate analytical solution for seepage flow with fractional derivatives in porous media," *Computer Methods in Applied Mechanics and Engineering*, vol. 167, no. 1-2, pp. 57–68, 1998.
[3] Y. Liu, "Variational homotopy perturbation method for solving fractional initial boundary value problems," *Abstract and Applied Analysis*, vol. 2012, Article ID 727031, 10 pages, 2012.
[4] J. H. He, "Asymptotic methods for solitary solutions and compactons," *Abstract and Applied Analysis*, vol. 2012, Article ID 916793, 130 pages, 2012.
[5] A. Ghorbani, "Beyond Adomian polynomials: He polynomials," *Chaos, Solitons and Fractals*, vol. 39, no. 3, pp. 1486–1492, 2009.
[6] M. A. Noor and S. T. Mohyud-Din, "Variational iteration method for solving higher-order nonlinear boundary value problems using He's polynomials," *The International Journal of Nonlinear Sciences and Numerical Simulation*, vol. 9, pp. 141–156, 2008.
[7] S. T. Mohyud-Din, "Solving heat and wave-like equations using He's polynomials," *Mathematical Problems in Engineering*, vol. 2009, Article ID 427516, 12 pages, 2009.
[8] M. A. Noor and S. T. Mohyud-Din, "Variational iteration method for fifth-order boundary value problems using He's polynomials," *Mathematical Problems in Engineering*, vol. 2008, Article ID 954794, 12 pages, 2008.
[9] S. Guo and L. Mei, "The fractional variational iteration method using He's polynomials," *Physics Letters A*, vol. 375, no. 3, pp. 309–313, 2011.
[10] J. Ji, J. Zhang, and Y. Dong, "The fractional variational iteration method improved with the Adomian series," *Applied Mathematics Letters*, vol. 25, no. 12, pp. 2223–2226, 2012.

Hindawi Publishing Corporation
Abstract and Applied Analysis
Volume 2012, Article ID 962789, 11 pages
doi:10.1155/2012/962789

Research Article

Exact Travelling Wave Solutions for Isothermal Magnetostatic Atmospheres by Fan Subequation Method

Hossein Jafari,[1,2] Maryam Ghorbani,[1] and Chaudry Masood Khalique[2]

[1] *Department of Mathematics, Faculty of Mathematical Sciences, University of Mazandaran, P.O. Box 47416-95447, Babolsar, Iran*

[2] *International Institute for Symmetry Analysis and Mathematical Modelling, Department of Mathematical Sciences, North-West University, Mafikeng Campus, Private Bag X2046, Mmabatho 2735, South Africa*

Correspondence should be addressed to Hossein Jafari, jafari_h@math.com

Received 1 September 2012; Revised 14 November 2012; Accepted 15 November 2012

Academic Editor: Lan Xu

The equations of magnetohydrostatic equilibria for a plasma in a gravitational field are investigated analytically. An investigation of a family of isothermal magnetostatic atmospheres with one ignorable coordinate corresponding to a uniform gravitational field in a plane geometry is carried out. These equations transform to a single nonlinear elliptic equation for the magnetic vector potential u. This equation depends on an arbitrary function of u that must be specified. With choices of the different arbitrary functions, we obtain analytical solutions of elliptic equation using the Fan subequation method.

1. Introduction

The equations of magnetostatic equilibria have been used extensively to model the solar magnetic structure [1–4]. An investigation of a family of isothermal magnetostatic atmospheres with one ignorable coordinate corresponding to a uniform gravitational field in a plane geometry is carried out. The force balance consists of the $J \wedge B$ force (B is the magnetic field induction and J is the electric current density), the gravitational force, and gas pressure gradient force. However, in many models, the temperature distribution is specified a priori and direct reference to the energy equations is eliminated. In solar physics, the equations of magnetostatic have been used to model diverse phenomena, such as the slow evolution stage of solar flares, or the magnetostatic support of prominences [5, 6]. The nonlinear equilibrium problem has been solved in several cases [7–9].

Recently, Fan and Hon [10] developed an algebraic method, belonging to the sub-equation method to seek more new solutions of nonlinear partial differential equations (NLPDEs) that can be expressed as polynomial in an elementary function which satisfies a more general sub-equation, called Fan sub-equation, than other sub-equations like Riccati equation, auxiliary ordinary equation, elliptic equation, and generalized Riccati equation. As we know, the more general analytical exact solutions of the sub-equation are proposed, the more general corresponding exact solutions of NLPDEs will be obtained. Thus, it is very important how to obtain more new solutions to the sub-equation. Fortunately, the Fan sub-equation method can construct more general exact solutions to the sub-equation that can capture all the solutions of the Riccati equation, auxiliary ordinary equation, elliptic equation, and generalized Riccati equation. Some works using the Fan's technique are presented in [1, 11–16].

In this paper, we obtain the exact travelling wave solutions for the Liouville and sinh-Poisson equations using the Fan sub-equation method. These two models are special cases of magnetostatic atmospheres model. Also in these cases there is force balance between differents forces.

2. The Basic Idea of Fan Subequation Method

In this section, we outline the main steps of Fan sub-equation method [11].

Step 1. For a given nonlinear partial differential equation

$$N(u, u_t, u_x, u_{tt}, u_{xx}, \ldots) = 0 \tag{2.1}$$

we consider its travelling wave solutions $u(x,t) = u(\xi)$, $\xi = x - ct$, then (2.1) is reduced to a nonlinear ordinary differential equation

$$N\left(u(\xi), -cu'(\xi), u'(\xi), c^2u''(\xi), u''(\xi), \ldots\right) = 0, \tag{2.2}$$

where a prime denotes the derivative with respect to the variable ξ.

Step 2. Expand the solution of (2.2) in the form

$$u(\xi) = \sum_{i=0}^{n} A_i \phi^i, \quad A_n \neq 0, \tag{2.3}$$

where A_i $(i = 0, 1, \ldots, n)$ are constants to be determined later and the new variable ϕ satisfies the Fan sub-equation

$$\phi'(\xi) = \epsilon \sqrt{\sum_{j=0}^{4} w_j \phi^j}, \tag{2.4}$$

where $\epsilon = \pm 1$ and w_j $(j = 0, \ldots, 4)$ are constants.

Thus, the derivatives with respect to the variable ξ become the derivatives with respect to the variable ϕ as follows:

$$\frac{du}{d\xi} = \epsilon \sqrt{\sum_{j=0}^{4} w_j \phi^j} \frac{du}{d\phi}, \qquad \frac{d^2u}{d\xi^2} = \frac{1}{2} \sqrt{\sum_{j=1}^{4} j w_j \phi^{j-1}} \frac{du}{d\phi} + \sum_{j=0}^{4} w_j \phi^j \frac{d^2u}{d\phi^2}. \tag{2.5}$$

Step 3. Determine n by substituting (2.3) with (2.4) into (2.2) and balancing the linear term of the highest order with the nonlinear term in (2.2).

Step 4. Substituting (2.3) and (2.4) into (2.2) again and collecting all coefficients of ϕ^i $(i = 0, 1, 2, \ldots, n)$, then setting these coefficients to zero will give a set of algebraic equations with respect to A_i $(i = 0, 1, \ldots, n)$.

Step 5. Solve these algebraic equations to obtain A_i $(i = 0, 1, 2, \ldots, n)$. Substituting these results into (2.3) yields the general form of travelling wave solutions.

Step 6. For each solution to (2.4) which depends on the special conditions chosen for the w_0, w_1, w_2, w_3, and w_4, it follows from (2.3) obtained from the above steps that the corresponding exact solution of (2.2) can be constructed.

3. Basic Equations

The relevant magnetohydrostatic equations consist of the equilibrium equation

$$J \wedge B - \rho \nabla \Phi - \nabla P = 0, \tag{3.1}$$

which is coupled with Maxwells equations

$$J = \frac{\nabla \wedge B}{\mu}, \qquad \nabla \cdot B = 0, \tag{3.2}$$

where P, ρ, μ, and Φ are the gas pressure, the mass density, the magnetic permeability, and the gravitational potential, respectively. It is assumed that the temperature is uniform in space and that the plasma is an ideal gas with equation of state $p = \rho R_0 T_0$, where R_0 is the gas constant and T_0 is the temperature. Then the magnetic field B can be written as

$$B = \nabla u \wedge e_x + B_x e_x = \left(B_x, \frac{\partial u}{\partial z}, \frac{-\partial u}{\partial y} \right). \tag{3.3}$$

The form of (3.3) for B ensures that $\nabla \cdot B = 0$ and there is no mono pole or defect structure.

Equation (3.1) requires the pressure and density to be of the form [4]

$$P(y,z) = P(u)e^{-z/h}, \qquad \rho(y,z) = \frac{1}{(gh)} P(u)e^{-z/h}, \tag{3.4}$$

where $h = R_0 T_0 / g$ is the scale height. Substituting (3.2)–(3.4) into (3.1), we obtain

$$\nabla^2 u + f(u)e^{-z/h} = 0, \tag{3.5}$$

where

$$f(u) = \mu \frac{dP}{du}. \tag{3.6}$$

Equation (3.6) gives

$$P(u) = P_0 + \frac{1}{\mu} \int f(u)du, \tag{3.7}$$

where P_0 is constant. Substituting (3.7) into (3.4), we obtain

$$\begin{aligned} P(y,z) &= \left(P_0 + \frac{1}{\mu} \int f(u)du \right) e^{-z/h}, \\ \rho(y,z) &= \frac{1}{gh} \left(P_0 + \frac{1}{\mu} \int f(u)du \right) e^{-z/h}. \end{aligned} \tag{3.8}$$

Using transformation $x_1 + ix_2 = e^{-z/l} e^{iy/l}$, (3.5) reduces to

$$\frac{\partial^2 u}{\partial x_1^2} + \frac{\partial^2 u}{\partial x_2^2} + l^2 f(u) e^{(2/l - 1/h)z} = 0. \tag{3.9}$$

These equations have been given in [2].

4. Applications of the Fan Subequation Method

In this section, we will employ the Fan sub-equation method for solving (3.9) for specific forms of the function $f(u)$.

4.1. Liouville Equation

We first consider Liouville equation, which is a special case of (3.9), namely,

$$u_{xx} + u_{tt} - \alpha^2 l^2 e^{-2u} = 0. \tag{4.1}$$

In order to apply the Fan sub-equation method, we use the wave transformation $u(x,t) = u(\xi)$, $\xi = x - ct$ and transform (4.1) into the form

$$\left(1 + c^2\right) u'' = \alpha^2 l^2 e^{-2u}. \tag{4.2}$$

We next use the transformation $v = e^{-2u}$ and obtain the nonlinear ordinary differential equation

$$\left(1 + c^2\right) v v'' - \left(1 + c^2\right) v'^2 + 2\alpha^2 l^2 v^3 = 0. \tag{4.3}$$

Using Step 3 given above, we get $n = 2$, therefore the solution of (4.3) can be expressed as

$$v(\xi) = A_0 + A_1 \phi + A_2 \phi^2. \tag{4.4}$$

Following Step 4, we obtain a system of nonlinear algebraic equations for A_0, A_1, and A_2:

$$\begin{aligned}
&2\alpha^2 l^2 {A_0}^3 - \epsilon^2 {A_1}^2 w_0 - c^2 \epsilon^2 {A_1}^2 w_0 + 2\epsilon^2 A_0 w_0 + 2c^2 \epsilon^2 A_0 A_2 w_0 \\
&\quad + \frac{1}{2}\epsilon^2 A_0 A_1 w_1 + \frac{1}{2} c^2 \epsilon^2 A_0 A_1 w_1 = 0, \\
&6\alpha l^2 {A_0}^2 A_1 - 2\epsilon^2 A_1 A_2 w_0 - 2c^2 \epsilon^2 A_1 A_2 w_0 - \frac{1}{2}\epsilon^2 {A_1}^2 w_1 + 3\epsilon^2 A_0 A_2 w_1 \\
&\quad + 3c^2 \epsilon^2 A_0 {A_1}^2 + \epsilon^2 A_0 A_1 w_2 + c^2 \epsilon^2 A_0 A_1 w_2 = 0, \\
&6\alpha^2 l^2 A_0 {A_1}^2 + 6\alpha^2 l^2 {A_0}^2 A_2 - 2\epsilon^2 {A_2}^2 w_0 - \frac{1}{2}\epsilon^2 A_1 A_2 w_1 - \frac{1}{2} c^2 \epsilon^2 A_1 A_2 w_1 \\
&\quad + 4\epsilon^2 A_0 A_2 w_2 + 4c^2 \epsilon^2 A_0 A_2 w_2 + \frac{3}{2}\epsilon^2 A_0 A_1 w_3 + \frac{3}{2} c^2 \epsilon^2 A_0 A_1 w_3 = 0, \\
&2\alpha^2 l^2 {A_1}^3 + 12\alpha^2 l^2 A_0 A_1 A_2 - \epsilon^2 {A_2}^2 w_1 - c^2 \epsilon^2 {A_2}^2 w_1 + \epsilon^2 A_1 A_2 w_2 + c^2 \epsilon^2 A_1 A_2 w_2 \\
&\quad + \frac{1}{2}\epsilon^2 {A_1}^2 w_3 + \frac{1}{2} c^2 \epsilon^2 {A_1}^2 w_3 + 5\epsilon^2 A_0 A_2 w_3 + 5c^2 \epsilon^2 A_0 A_2 w_3 \\
&\quad + 2\epsilon^2 A_0 A_1 w_4 + 2c^2 \epsilon^2 A_0 A_1 w_4 = 0,
\end{aligned}$$

$$
\begin{aligned}
&6\alpha^2 l^2 {A_1}^2 A_2 + 6\alpha^2 l^2 A_0 {A_2}^2 + \frac{5}{2}\epsilon^2 A_1 A_2 w_3 + \frac{5}{2}\epsilon^2 c^2 A_1 A_2 w_3 + \epsilon^2 {A_1}^2 w_4 \\
&\quad + c^2\epsilon^2 {A_1}^2 w_4 + 6\epsilon^2 A_0 A_2 w_4 + 6c^2\epsilon^2 A_0 A_2 w_4 = 0, \\
&6\alpha^2 l^2 A_1 {A_2}^2 + \epsilon^2 {A_2}^2 w_3 + c^2\epsilon^2 {A_2}^2 w_1 + \epsilon^2 A_1 A_2 w_2 + c^2\epsilon^2 {A_2}^2 w_3 \\
&\quad + 4\epsilon^2 A_1 A_2 w_4 + 4c^2\epsilon^2 A_1 A_2 w_4 = 0, \\
&2\alpha^2 l^2 {A_2}^3 + 2\epsilon^2 {A_2}^2 w_4 + 2c^2\epsilon^2 {A_2}^2 w_4 = 0.
\end{aligned}
\tag{4.5}
$$

Case 1. When $w_0 = w_1 = w_3 = 0$, $w_2 > 0$, $w_4 < 0$, (2.4) admits a hyperbolic function solution

$$\phi = \sqrt{-\frac{w_2}{w_4}}\ \operatorname{sech}\left(\sqrt{w_2}\ \xi\right). \tag{4.6}$$

Thus (4.4) yields the following new solitary wave solution of (2.1) of bell-type

$$v_1(\xi) = \frac{(1+c^2)w_2}{\alpha^2 l^2}\operatorname{sech}^2\left(\sqrt{w_2}\ \xi\right), \tag{4.7}$$

where $w_2 > 0$, $w_4 < 0$, $\alpha \neq 0$, $l \neq 0$, and c are arbitrary constants. Reverting back to the original variables x and t, we obtain the solution of (4.1) in the form

$$u_1(x,t) = -\frac{1}{2}\ln\left[\frac{(1+c^2)w_2}{\alpha^2 l^2}\operatorname{sech}^2\left\{\sqrt{w_2}\ (x-ct)\right\}\right]. \tag{4.8}$$

Case 2. When $w_1 = w_3 = 0$, $w_0 = {w_2}^2/4w_4$, $w_2 < 0$, $w_4 > 0$, (2.4) admits two hyperbolic function solutions

$$\phi = \pm\sqrt{-\frac{w_2}{2w_4}}\ \tanh\left(\sqrt{\frac{-w_2}{2}}\ \xi\right), \tag{4.9}$$

and so (4.4) yields one family of solitary travelling wave solutions of (4.1) given by

$$u_2(x,t) = -\frac{1}{2}\ln\left[-\frac{(1+c^2)w_2}{2\alpha^2 l^2} + \frac{(1+c^2)w_2}{\alpha^2 l^2}\tanh^2\left(\sqrt{-\frac{w_2}{2}}\ (x-ct)\right)\right], \tag{4.10}$$

where $w_2 < 0$, $w_4 > 0$, $\alpha \neq 0$, $l \neq 0$, and c are arbitrary constants.

Case 3. When $w_0 = w_1 = 0$, $w_3 = \pm 2\sqrt{w_2 w_4}$, $w_2 > 0$, $w_4 > 0$, (2.4) has two kinds of exact solutions:

$$\phi = -\frac{\sqrt{w_2 w_4}}{2w_4}\ \operatorname{sign}(w_3)\left[1 + \tanh\left(\frac{\sqrt{w_2}}{2}\ \xi\right)\right], \tag{4.11}$$

and (4.4) yields one family of solitary travelling wave solutions of (4.1) given by

$$u_3(x,t) = -\frac{1}{2}\ln\left[\pm\frac{(1+c^2)w_2}{\alpha^2 l^2}\operatorname{sign}(w_3)\left[1+\tanh\left(\frac{\sqrt{w_2}}{2}(x-ct)\right)\right]\right.$$
$$\left.-\frac{(1+c^2)w_2}{4\alpha^2 l^2}\left[1+\tanh\left(\frac{\sqrt{w_2}}{2}(x-ct)\right)\right]^2\right], \tag{4.12}$$

where $w_2 > 0$, $w_4 > 0$, $\alpha \neq 0$, $l \neq 0$, and c are arbitrary constants.

Case 4. When $w_1 = w_3 = 0$, (2.4) admits three Jacobian elliptic doubly periodic solutions

$$\begin{aligned}
\phi &= \sqrt{\frac{-w_2k^2}{w_4(2k^2-1)}}\ \operatorname{cn}\left(\sqrt{\frac{w_2}{2k^2-1}}\ \xi, k\right), \quad \text{for } w_0 = \frac{{w_2}^2k^2(k^2-1)}{w_4(2k^2-1)^2},\ w_2>0, w_4<0,\\
\phi &= \sqrt{\frac{-w_2}{w_4(2-k^2)}}\ \operatorname{dn}\left(\sqrt{\frac{w_2}{2-k^2}}\ \xi, k\right), \quad \text{for } w_0 = \frac{{w_2}^2(1-k^2)}{w_4(k^2-2)^2},\ w_2>0, w_4<0,\\
\phi &= \pm\sqrt{\frac{-w_2k^2}{w_4(k^2+1)}}\ \operatorname{sn}\left(\sqrt{\frac{-w_2}{k^2+1}}\ \xi, k\right), \quad \text{for } w_0 = \frac{{w_2}^2k^2}{w_4(k^2+1)^2},\ w_2<0, w_4>0,
\end{aligned} \tag{4.13}$$

and (4.4), respectively, yields two families of Jacobian elliptic doubly periodic wave solutions

$$u_4(x,t) = -\frac{1}{2}\ln\left[-\frac{(1+c^2)w_2}{2\alpha^2 l^2} + \frac{(1+c^2)w_2(2k^2-1)}{4\alpha^2 l^2(k^2-1)}\ \operatorname{cn}^2\left(\sqrt{\frac{w_2}{2k^2-1}}(x-ct), k\right)\right], \tag{4.14}$$

with $w_2 > 0$, $w_4 < 0$, $\alpha \neq 0$, $l \neq 0$, $k \in (\sqrt{2}/2, 1)$, and c being arbitrary constants. Similarly, from (4.4), respectively, we can obtain two families of Jacobian elliptic doubly periodic wave solutions

$$u_5(x,t) = -\frac{1}{2}\ln\left[-\frac{(1+c^2)w_2}{2\alpha^2 \beta^2} + \frac{(1+c^2)w_2(k^2-2)}{4\alpha^2 l^2(1-k^2)}\ \operatorname{dn}^2\left(\sqrt{\frac{w_2}{2-k^2}}(x-ct), k\right)\right], \tag{4.15}$$

with $w_2 > 0$, $w_4 < 0$, $\alpha \neq 0$, $l \neq 0$, $k \in (0,1)$, and c being arbitrary constants. Similarly, from (4.4), respectively, we can obtain two families of Jacobian elliptic doubly periodic wave solutions

$$u_6(x,t) = -\frac{1}{2}\ln\left[-\frac{(1+c^2)w_2}{2\alpha^2 l^2} + \frac{(1+c^2)w_2(k^2+1)}{4\alpha^2 l^2}\ \operatorname{sn}^2\left(\sqrt{-\frac{w_2}{k^2+1}}(x-ct), k\right)\right] \tag{4.16}$$

with $w_2 < 0$, $w_4 > 0$, $\alpha \neq 0$, $l \neq 0$, $k \in (0,1)$, and c being arbitrary constants.

4.2. *The* sinh*-Poisson Equation*

Secondly, we consider sinh-Poisson equation which plays an important role in soliton model with BPS Bound. Also, this equation is a special case of (3.9) and is given by

$$u_{xx} + u_{tt} = \beta^2 \sinh(u). \tag{4.17}$$

In order to apply the Fan sub-equation method, we use the wave transformation $\xi = x - ct$ and convert (4.17) into the form

$$\left(1 + c^2\right)u'' = \beta^2 \sinh(u). \tag{4.18}$$

We next use the transformation $v = e^u$ and obtain the equation

$$2\left(1 + c^2\right)vv'' - 2\left(1 + c^2\right)v'^2 - \beta^2\left(v^3 - v\right) = 0. \tag{4.19}$$

Applying Step 3, we get $n = 2$, therefore the solution of (4.19) can be expressed as

$$v(\xi) = A_0 + A_1\phi + A_2\phi^2. \tag{4.20}$$

Then using Step 4, we obtain a system of nonlinear algebraic equations for A_0, A_1, and A_2:

$$\begin{aligned}
&- l^2 {A_0}^3 - 2\epsilon^2 {A_1}^2 w_0 - 2c^2\epsilon^2 {A_1}^2 w_0 + 4\epsilon^2 A_0 A_2 w_0 + 4c^2\epsilon^2 A_0 A_2 w_0 \\
&\qquad + \epsilon^2 A_0 A_1 w_1 + c^2\epsilon^2 A_0 A_1 w_1 = 0, \\
&- 3l^2 {A_0}^2 A_1 - 4\epsilon^2 A_1 A_2 w_0 - 4c^2\epsilon^2 A_1 A_2 w_0 - \epsilon^2 {A_1}^2 w_1 - c^2\epsilon^2 {A_1}^2 w_1 + 6\epsilon^2 A_0 A_2 w_1 \\
&\qquad + 6c^2\epsilon^2 A_0 A_2 w_1 + 2\epsilon^2 A_0 A_1 w_2 + 2c^2\epsilon^2 A_0 A_1 w_2 = 0, \\
&- 3l^2 A_0 {A_1}^2 - 3l^2 {A_0}^2 A_2 - 4\epsilon^2 {A_2}^2 w_0 - 4c^2\epsilon^2 {A_2}^2 w_0 - \epsilon^2 A_1 A_2 w_1 - c^2\epsilon^2 A_1 A_2 w_1 \\
&\qquad + 8\epsilon^2 A_0 A_2 w_2 + 8c^2\epsilon^2 A_0 A_2 w_2 + 3\epsilon^2 A_0 A_1 w_3 + 3c^2\epsilon^2 A_0 A_1 w_3 = 0, \\
&- l^2 {A_1}^3 - 6l^2 A_0 A_1 A_2 - 2\epsilon^2 {A_2}^2 w_1 - 2c^2\epsilon^2 {A_2}^2 w_1 + 2\epsilon^2 A_1 A_2 w_2 + 2c^2\epsilon^2 A_1 A_2 w_2 \\
&\qquad + \epsilon^2 {A_1}^2 w_3 + c^2\epsilon^2 {A_1}^2 w_3 + 10\epsilon^2 A_0 A_2 w_3 + 10c^2\epsilon^2 A_0 A_2 w_3 \\
&\qquad + 4\epsilon^2 A_0 A_1 w_4 + 4c^2\epsilon^2 A_0 A_1 w_4 = 0, \\
&- 3l^2 {A_1}^2 A_2 - 3l^2 A_0 {A_2}^2 + 5\epsilon^2 A_1 A_2 w_3 + 5c^2\epsilon^2 A_1 A_2 w_3 + 2\epsilon^2 {A_1}^2 w_4 + 2c^2\epsilon^2 {A_1}^2 w_4 \\
&\qquad + 12\epsilon^2 A_0 A_2 w_4 + 12c^2\epsilon^2 A_0 A_2 w_4 = 0, \\
&- 3l^2 A_1 {A_2}^2 + 2\epsilon^2 {A_2}^2 w_3 + 2c^2\epsilon^2 {A_2}^2 w_3 + 8\epsilon^2 A_1 A_2 w_4 + 8c^2\epsilon^2 A_1 A_2 w_4 = 0, \\
&- l^2 {A_2}^3 + 4\epsilon^2 {A_2}^2 w_4 + 4c^2\epsilon^2 {A_2}^2 w_4 = 0.
\end{aligned} \tag{4.21}$$

Case 1. When $w_0 = w_1 = w_3 = 0$, $w_2 > 0$, $w_4 < 0$, (2.4) admits a hyperbolic function solution

$$\phi = \sqrt{-\frac{w_2}{w_4}}\,\operatorname{sech}\left(\sqrt{w_2}\,\xi\right) \tag{4.22}$$

and (4.20) yields the following new solitary wave solution of (4.17) of bell-type

$$u_1(x,t) = \ln\left[-\frac{4(1+c^2)w_2}{l^2}\operatorname{sech}^2\left(\sqrt{w_2}\,(x-ct)\right)\right], \tag{4.23}$$

where $w_2 > 0$, $w_4 < 0$, $l \neq 0$, and c are arbitrary constants.

Case 2. When $w_1 = w_3 = 0$, $w_0 = w_2{}^2/4w_4$, $w_2 < 0$, $w_4 > 0$, (2.4) admits two hyperbolic function solutions

$$\phi = \pm\sqrt{-\frac{w_2}{2w_4}}\,\tanh\left(\sqrt{\frac{-w_2}{2}}\,\xi\right), \tag{4.24}$$

and (4.20) yields one family of solitary travelling wave solutions of (4.17) given by

$$u_2(x,t) = \ln\left[\frac{2(1+c^2)w_2}{l^2} - \frac{2(1+c^2)w_2}{l^2}\tanh^2\left(\sqrt{-\frac{w_2}{2}}(x-ct)\right)\right], \tag{4.25}$$

where $w_2 < 0$, $w_4 > 0$, $l \neq 0$, and c are arbitrary constants.

Case 3. When $w_0 = w_1 = 0$, $w_3 = \pm 2\sqrt{w_2 w_4}$, $w_2 > 0$, $w_4 > 0$, (2.4) has two kinds of exact solutions

$$\phi = -\frac{\sqrt{w_2 w_4}}{2w_4}\operatorname{sign}(w_3)\left[1 + \tanh\left(\frac{\sqrt{w_2}}{2}\xi\right)\right], \tag{4.26}$$

and (4.20) yields one family of solitary travelling wave solutions solitary travelling wave solutions of (4.17) given by

$$\begin{aligned} u_3(x,t) = \ln\Bigg[&\pm\frac{2(1+c^2)w_2}{l^2}\operatorname{sign}(w_3)\left[1 + \tanh\left(\frac{\sqrt{w_2}}{2}(x-ct)\right)\right] \\ &-\frac{(1+c^2)w_2}{l^2}\left[1 + \tanh\left(\frac{\sqrt{w_2}}{2}(x-ct)\right)\right]^2\Bigg], \end{aligned} \tag{4.27}$$

where $w_2 > 0, w_4 > 0$, $l \neq 0$ and c are arbitrary constants.

Case 4. When $w_1 = w_3 = 0$, (2.4) admits three Jacobian elliptic doubly periodic solutions

$$\begin{aligned}
\phi &= \sqrt{\frac{-w_2 k^2}{w_4(2k^2-1)}}\ \mathrm{cn}\left(\sqrt{\frac{w_2}{2k^2-1}}\ \xi, k\right), \quad \text{for } w_0 = \frac{{w_2}^2 k^2 (k^2-1)}{w_4(2k^2-1)^2}, \ w_2 > 0, w_4 < 0, \\
\phi &= \sqrt{\frac{-w_2}{w_4(2-k^2)}}\ \mathrm{dn}\left(\sqrt{\frac{w_2}{2-k^2}}\ \xi, k\right), \quad \text{for } w_0 = \frac{{w_2}^2 (1-k^2)}{w_4(k^2-2)^2}, \ w_2 > 0, w_4 < 0, \\
\phi &= \pm\sqrt{\frac{-w_2 k^2}{w_4(k^2+1)}}\ \mathrm{sn}\left(\sqrt{\frac{-w_2}{k^2+1}}\ \xi, k\right), \quad \text{for } w_0 = \frac{{w_2}^2 k^2}{w_4(k^2+1)^2}, \ w_2 < 0, w_4 > 0,
\end{aligned} \tag{4.28}$$

and (4.20), respectively, yields two families of Jacobian elliptic doubly periodic wave solutions

$$u_4(x,t) = \ln\left[\frac{2(1+c^2)w_2}{l^2} + \frac{2(1+c^2)(2k^2-1)w_2}{l^2(k^2-1)}\ \mathrm{cn}^2\left(\sqrt{\frac{w_2}{2k^2-1}}(x-ct), k\right)\right], \tag{4.29}$$

with $w_2 > 0$, $w_4 < 0$, $l \neq 0$, $k \in (\sqrt{2}/2, 1)$, and c being arbitrary constants. Similarly, from (4.20), respectively, we can obtain two families of Jacobian elliptic doubly periodic wave solutions

$$u_5(x,t) = \ln\left[\frac{2(1+c^2)w_2}{l^2} - \frac{2(1+c^2)w_2(2-k^2)}{l^2(1-k^2)}\ \mathrm{dn}^2\left(\sqrt{\frac{w_2}{2-k^2}}(x-ct), k\right)\right], \tag{4.30}$$

with $w_2 > 0$, $w_4 < 0$, $\alpha \neq 0$, $l \neq 0$, $k \in (0,1)$, and c being arbitrary constants. Likewise, from (4.20), respectively, we can get two families of Jacobian elliptic doubly periodic wave solutions

$$u_6(x,t) = \ln\left[\frac{2(1+c^2)w_2}{l^2} - \frac{2(1+c^2)w_2(k^2+1)}{l^2}\ \mathrm{sn}^2\left(\sqrt{-\frac{w_2}{k^2+1}}(x-ct), k\right)\right], \tag{4.31}$$

with $w_2 < 0$, $w_4 > 0$, $\alpha \neq 0$, $l \neq 0$, $k \in (0,1)$, and c being arbitrary constants.

5. Concluding Remarks

In this paper, the Fan sub-equation method has been successfully used to obtain some exact travelling wave solutions for the Liouville and sinh-Poisson equations. These exact solutions include the hyperbolic function solutions, trigonometric function solutions. When the parameters are taken as special values, the solitary wave solutions are derived from the hyperbolic function solutions. Thus, this study shows that the Fan sub-equation method is quite efficient and practically well suited for use in finding exact solutions for nonlinear partial differential equations. The reliability of the method and the reduction in the size of computational domain give this method a wider applicability.

References

[1] A. H. Khater, M. A. El-Attary, M. F. El-Sabbagh, and D. K. Callebaut, "Two-dimensional magnetohydrodynamic equilibria," *Astrophysics and Space Science*, vol. 149, no. 2, pp. 217–223, 1988.

[2] A. H. Khater, D. K. Callebaut, and O. H. El-Kalaawy, "Bäcklund transformations and exact solutions for a nonlinear elliptic equation modelling isothermal magnetostatic atmosphere," *IMA Journal of Applied Mathematics*, vol. 65, no. 1, pp. 97–108, 2000.

[3] I. Lerche and B. C. Low, "Some nonlinear problems in astrophysics," *Physica D. Nonlinear Phenomena*, vol. 4, no. 3, pp. 293–318, 1981/82.

[4] B. C. Low, "Evolving force-free magnetic elds. I—the development of the pre are stage," *The Astrophysical Journal*, vol. 212, pp. 234–242, 1977.

[5] X.-H. Wu and J.-H. He, "Solitary solutions, periodic solutions and compacton-like solutions using the Exp-function method," *Computers & Mathematics with Applications*, vol. 54, no. 7-8, pp. 966–986, 2007.

[6] W. Zwingmann, "Theoretical study of onset conditions for solar eruptive processes," *Solar Physics*, vol. 111, pp. 309–331, 1987.

[7] I. Lerche and B. C. Low, "On the equilibrium of a cylindrical plasma supported horizontally by magneticelds in uniform gravity," *Solar Physics*, vol. 67, pp. 229–243, 1980.

[8] G. M. Webb, "Isothermal magnetostatic atmospheres. II—similarity solutions with current proportional to the magnetic potential cubed," *The Astrophysical Journal*, vol. 327, pp. 933–949, 1988.

[9] G. M. Webb and G. P. Zank, "Application of the sine-Poisson equation in solar magnetostatics," *Solar Physics*, vol. 127, pp. 229–252, 1990.

[10] E. G. Fan and Y. C. Hon, "A series of travelling wave solutions for two variant Boussinesq equations in shallow water waves," *Chaos, Solitons & Fractals*, vol. 15, no. 3, pp. 559–566, 2003.

[11] D. Feng and K. Li, "Exact traveling wave solutions for a generalized Hirota-Satsuma coupled KdV equation by Fan sub-equation method," *Physics Letters A*, vol. 375, no. 23, pp. 2201–2210, 2011.

[12] S. A. El-Wakil and M. A. Abdou, "The extended Fan sub-equation method and its applications for a class of nonlinear evolution equations," *Chaos, Solitons and Fractals*, vol. 36, no. 2, pp. 343–353, 2008.

[13] E. Yomba, "The modified extended Fan sub-equation method and its application to the (2 + 1)-dimensional Broer-Kaup-Kupershmidt equation," *Chaos, Solitons and Fractals*, vol. 27, no. 1, pp. 187–196, 2006.

[14] E. Yomba, "The extended Fan's sub-equation method and its application to KdV-MKdV, BKK and variant Boussinesq equations," *Physics Letters A*, vol. 336, no. 6, pp. 463–476, 2005.

[15] S. Zhang and H.-Q. Zhang, "Fan sub-equation method for Wick-type stochastic partial differential equations," *Physics Letters A*, vol. 374, no. 41, pp. 4180–4187, 2010.

[16] S. Zhang and T. Xia, "A further improved extended Fan sub-equation method and its application to the (3 + 1)-dimensional Kadomstev-Petviashvili equation," *Physics Letters A*, vol. 356, no. 2, pp. 119–123, 2006.